University of Southampton

Faculty of MEDICINE

CLINICAL AND EXPERIMENTAL SCIENCES

A SYSTEMS IMMUNOLOGY APPROACH TO UNDERSTANDING HUMAN LANGERHANS CELL TOLEROGENIC FUNCTION

by

JAMES DAVID DAVIES

Thesis for the degree of DOCTOR OF PHILOSOPHY

AUGUST 2020

University of Southampton

Abstract

Faculty of MEDICINE

CLINICAL AND EXPERIMENTAL SCIENCES

Doctor of Philosophy

A SYSTEMS IMMUNOLOGY APPROACH TO UNDERSTANDING HUMAN LANGERHANS CELL TOLEROGENIC FUNCTION

by

James David Davies

Langerhans cells (LC) maintain skin homeostasis through orchestrating immunogenic and tolerogenic immune responses in steady-state epidermis and at local lymph nodes after migration. While the mechanisms promoting activation of immune responses has been elucidated, little is known about the molecular mechanisms underpinning LC induced tolerance. We hypothesised that heterogeneous human LC populations existed *in situ*, which specialised in regulation of immunogenic vs tolerogenic regulation in healthy skin. Within the transcriptome of tolerance regulating LC, we sought to identify key molecular mediators of tolerogenic programming.

Previously published transcriptomic data containing a wide selection of DC subpopulations, including LC was analysed. Here, core mechanisms of tolerogenic programming across DCs was investigated. Overall, LC transcriptomic programming was largely distinct, although common pathways of suppression of stimuli responsiveness were identified in steady-state LCs.

The Drop-seq scRNA-seq protocol was optimised and implemented on steady-state and migrated LCs, to explore heterogeneity amongst populations and identify key molecular regulators of tolerogenic programming. This identified tolerogenic programmes (including *IDO1*) to be upregulated in migrated LCs, alongside enhanced immunocompetent programming compared to steady-state LCs. The latter populations were split into two subpopulations defined by immaturity and immunocompetency. Transcription factors (TFs) that correlated with enhanced migrated LC tolerogenic programmes included *IRF4* and *RELB*.

Using *in vitro* experimentation, the importance of LC immunocompetency for mediation of Treg induction was revealed in steady-state LC populations (Immunocompetent/CD86High and Immature/CD86Low). Furthermore, immunocompetent migrated LCs displayed enhanced induction of functionally suppressive Tregs. Inhibition of *IDO1* reduced migrated LC tolerogenic potential, revealing the criticalness of tolerogenic programming for LC tolerogenicity.

Mathematical modelling using TFs identified from analyses thought to control immunogenic (*IRF1*$\perp$*IRF4*) vs tolerogenic (*IRF4, MAP3K14, RELB)* programming reflected observations from previous studies in which unstimulated migrated LC display both immunogenic and tolerogenic potential whilst, inflammatory stimuli (TNFα) increases favouring of immunogenic responses.

Overall, our analysis identified critical mechanisms which equip LCs with tolerogenic function and revealed potential mechanisms by which immunogenic vs tolerogenic responses are initiated.

Table of Contents

Table of Tables

Table of Figures

Research Thesis: Declaration of Authorship

Print name: JAMES DAVID DAVIES

Title of thesis: A SYSTEM IMMUNOLOGY APPROACH TO UNDERSTANDING HUMAN LANGERHANS CELL TOLEROGENIC FUNCTION

I declare that this thesis and the work presented in it are my own and has been generated by me as the result of my own original research.

I confirm that:

1. This work was done wholly or mainly while in candidature for a research degree at this University;
2. Where any part of this thesis has previously been submitted for a degree or any other qualification at this University or any other institution, this has been clearly stated;
3. Where I have consulted the published work of others, this is always clearly attributed;
4. Where I have quoted from the work of others, the source is always given. With the exception of such quotations, this thesis is entirely my own work;
5. I have acknowledged all main sources of help;
6. Where the thesis is based on work done by myself jointly with others, I have made clear exactly what was done by others and what I have contributed myself;
7. Parts of this work have been published as:-

   Davies, J. *et al.* (2019) 'Single cell transcriptomic analysis indentifies Langerhans cells immunocompetency is critical for IDO1- dependent ability to induce tolerogenic T cells', *bioRxiv*. Cold Spring Harbor Laboratory, p. 2019.12.20.884130. doi: 10.1101/2019.12.20.884130.

Signature: ..... Date: 20/08/2020

Acknowledgements

Firstly, I would like to thank my Primary Supervisor Dr Marta E Polak, for her constant invaluable support throughout my project. Her experience, guidance and reassurance has been fundamental to my development as a scientist. She has been incredibly inspiring and I feel extremely grateful and proud to have completed my PhD in the Systems Immunology Group (SIG) under her supervision.

I will always feel indebted to Dr Sofia Sirvent and Dr Andres Vallejo Pulido for sharing their extensive knowledge in both experimental and computational analysis. Their patience and enthusiasm have been invaluable and I couldn't have hoped for better role models and teachers in the lab. I also thank Kalum Clayton for sharing the highs and lows of the PhD journey with me and for providing lots of laughter. I thank everyone else in the SIG too, including Gemma Porter, Dr Ying Teo and Gabriela Barbetta. Together, everyone has made my time in Southampton so enjoyable and I will look back on these times with great affection.

I am also very grateful to Dr Ben MacArthur for his supervision over the last 4 years and for sharing his extensive experience and knowledge of mathematics. It has been amazing to be part of the Quantitative Biomedicine group and I would like thank everyone in the group for being so welcoming and helpful in expanding my understanding of maths.

I would like to say thank you to every else who has helped me on my PhD journey. This includes everyone on Level E, who have provided such a warm and friendly atmosphere to work in. Everyone has been so helpful, generous with their time and encouraging. I particularly thank Dr Jane Collins for her supervision during my Year 1 rotation project and for being so supportive throughout my PhD. I also thank Professor Donna Davies for her supervision.

My family and friends have always been extremely encouraging throughout my studies and I thank them for all their support.

I am also very grateful to Wellcome Trust and MRC UK for funding this project.

Definitions and Abbreviations

Ag ..... Antigen

AICE ..... AP-1-IRF composite elements

AP-1 ..... Activator protein 1

APC ..... Antigen presenting cell

BMP-7 ..... Bone morphogenetic protein 7

BrdU..... Bromodeoxyuridine

BSA ..... Bovine serum albumin

BH ..... Benjamini Hochberg

CD207 ..... Langerin

CsA..... Cyclosporin A

CCR7 ..... C-C chemokine receptor type 7

CCL19..... Chemokine (C-C motif) ligand 19

CCL21..... Chemokine (C-C motif) ligand 21

cDNA..... Complimentary DNA

CHS ..... Contact hypersensitivity

CPTT..... Counts per ten thousand

CRISPR..... Clustered regularly interspaced short palindromic repeats

CTLA-4..... Cytotoxic T-lymphocyte-associated protein 4

Dsg3..... Desmoglein 3

EDTA ..... Ethylenediaminetetraacetic acid

EICE..... ETS-IRF composite element

EPAC ..... Epacadostat

ETS..... E26 transformation-specific transcription factor

FACS..... Fluorescence associated cell sorting

DC..... Dendritic cell

DDC..... Dermal dendritic cell

DEG ..... Differentially expressed gene

DN-DDC ..... CD14-CD141- DDC

DNA ..... Deoxyribonucleic acid

dNTPs ..... Deoxyribonucleotide triphosphate

FACS ..... Fluorescence-activated cell sorting

FAO ..... Fatty acid oxidation

FBS ..... Foetal bovine serum

FcR ..... Fc-gamma receptor

FOXP3 ..... Forkhead box protein P3

GEO ..... Gene expression omnibus

GM-CSF ..... Granulocyte monocyte colony stimulating factor

GRN ..... Gene regulatory network

GVHD ..... Graft versus host disease

HIV ..... Human immunodeficiency virus

HLA-DR ..... MHC II receptor

HMOX1 ..... Haem oxygenase 1

HSV ..... Herpes simplex virus

IDO ..... Indoleamine 2,3-dioxygenase

IFNγ ..... Interferon gamma

IL-10 ..... Interleukin 10

IL-10R ..... Interleukin 10 receptor

IL-12 ..... Interleukin 12

IL-13 ..... Interleukin 13

IL-17 ..... Interleukin 17

IL-1α ..... Interleukin 1 alpha

IL-2 ..... Interleukin 2

IL-35 ..... Interleukin 35

IL-4 ..... Interleukin 4

IL-5 ..... Interleukin 5

IL-6 ..... Interleukin 6

IL-8 ..... Interleukin 8

IL10MoDC ..... IL-10 stimulated MoDC

IRF ..... Interferon regulatory factor

IRF-GRN ..... Interferon regulatory factor gene regulatory network

ISRE ..... interferon-stimulated response element

KC ..... Keratinocyte

LC ..... Langerhans cell

LPS ..... Lipopolysaccharide

LPSMoDC ..... LPS stimulated MoDC

LPS-IL10MoDC ..... LPS stimulated IL10MoDC

LPS-TolMoDC ..... LPS stimulated TolMoDC

MAST ..... Model-based Analysis of Single Cell Transcriptomics

MCL ..... Markov clustering alogrithm

mEPN ..... Modified Edinburgh Pathway Notation

MHC I ..... Major histocompatibility complex I

MHC II ..... Major histocompatibility complex II

MoDC ..... Monocyte derived dendritic cell

MPLA ..... Monophosphoryl lipid A

MYC ..... MYC Proto-Oncogene, BHLH Transcription Factor

NFκB ..... Nuclear factor kappa light chain enhancer of activate B cells

NK cell ..... Natural killer cell

NOD ..... Nucleotide binding oligomerisation

ODE ..... Ordinary differential equation

OVA ..... Ovalbumin

OXPHOS ..... Oxidative phosphorylation

PAGA ..... Partition-based graph abstraction

PAMP..... Pathogen associated molecular pattern

PBMC..... Peripheral blood mononuclear cell

PBS ..... Phosphate buffer saline

PC ..... Principle component

PCA..... principle component analysis

PCR ..... Polymerase chain reaction

pDC..... Plasmacytoid dendritic cell

PD-L1 ..... Programmed death ligand 1

PD-L2 ..... Programmed death ligand 2

PFO..... Perfluoro-1-octanol

PlaDC..... Placental DC

PRR..... Pattern recognition receptor

qPCR..... Quantitative polymerase chain reaction

RANK ..... Receptor activator of NFκB

RANKL..... Receptor activator of NFκB ligand

RELA ..... Nuclear factor NF-kappa-B p65 subunit

RMA ..... Robust multi-array average

RNA ..... Ribonucleic acid

RNA-seq..... RNA sequencing

RUNX3 ..... Runt-related transcription factor 3

RT ..... Reverse transcription

SCENIC..... Single-cell regulatory network inference and clustering

scRNA-seq..... Single cell RNA sequencing

SDS ..... Sodium dodecyl sulphate

SLE..... Systemic lupus erythematosus

SPN..... Signalling Petri-net

SSC ..... Saline-sodium citrate

STAMP..... Single transcriptome attached to microparticle

TCR ..... T cell receptor

TF ..... Transcription factor

TGF-β ..... Transforming growth factor beta

Th1 ..... T helper cell type 1

Th17 ..... T helper cell type 17

Th2 ..... T helper cell type 2

TLR ..... Toll like receptor

TNFα ..... Tumour necrosis factor alpha

TolMoDC ..... Dexamethasone and VitD3 stimulated MoDC

Treg ..... Regulatory T cell

TRM ..... Tissue resident memory T cell

TSLP ..... Thymic stromal lymphopoietin

TSO ..... Template switch oligo

TW ..... Tween 20

UMAP ..... Uniform manifold approximation and projection

UMI ..... Unique molecular identifier

UVB ..... Type B ultraviolet radiation

UVR ..... Ultraviolet radiation

VitD3 ..... 1,25-dihydroxyvitamin D

Chapter 1 Introduction/Literature review

Our bodies constantly encounter foreign material and stimuli that can be either 'safe' or 'dangerous' for the maintenance of health. Peripheral locations of the body, such as the skin, which are continuously challenged by diverse antigen and stimuli, are sites at which the body's ability to distinguish 'safe' from dangerous' is essential (Nagl *et al.*, 2002). The immune system has therefore evolved mechanisms by which appropriate responses are induced. Key to distinguishing between harmful and non-harmful stimuli are dendritic cells (DCs), professional antigen-presenting cells (APCs) of the innate immune system which prime, mediate and augment immune responses (Stockwin *et al.*, 2000)(Lewis and Reizis, 2012). At the human epidermis, the most peripheral layer of the skin, resides a unique subclass of DC called the Langerhans cell (LC). Interestingly, whilst the role for LC immune regulation at the skin has been widely explored since their discovery in 1868, definitive understanding of LC biological function and their vital role at the epidermis is an ongoing area of research (Valladeau and Saeland, 2005).

1.1 Regulation of the innate and adaptive immune system

The human body's immune system prevents the establishment of infection from pathogenic agents such as bacteria, viruses and parasites (Chaplin, 2010). It can be split into two distinct divisions, the innate and the adaptive immune system, which together provide complete immunological protection (**Figure 1**). The innate immune system is characterised by its speed and widespread activity to target many types of pathogen indiscriminately. The innate immune system includes various physical, chemical and anatomical barriers, as well as professional innate leukocytes (Chaplin, 2010)(Madigan *et al.*, 2012). Professional innate leukocytes include monocytes, macrophages, mast cells, neutrophils, eosinophils, basophils, NK cells and DCs. Present in both the blood and peripheral tissues of the body, innate leukocytes are specialised in mediating rapid counteractive measures against diverse immunological threats. This includes pathogen scavenging, ingestion and destruction by phagocytic DCs, macrophages and neutrophils, as well as the production of potent pathogen killing enzymes and toxins by granulocytes, such as mast cells, basophils, eosinophils and neutrophils (Savina and Amigorena, 2007)(Madigan *et al.*, 2012). Innate immune cells also secrete a plethora of cytokines and chemokines, molecules fundamental for orchestrating inflammation, cell communication and the directing of immune responses (Lacy and Stow, 2011). Structural cells at the environmental interfaces of the body, such as skin epidermal keratinocytes (KC) and gut epithelial cells, also provide innate immune function through the production of antimicrobial peptides and inflammatory cytokines and chemokines (Bernard *et al.*,

2012)(Dommett *et al.*, 2005). Cross talk and interaction between innate immune cells and structural barrier cells are therefore vital to provide efficient protection.

The speed of innate immune cell activity is achieved through the expression of a panel of receptors which recognise molecular structures conserved across many different microbes (Turvey and Broide, 2010). These receptors are called pattern recognition receptors (PRRs) and recognise highly conserved pathogen associated molecular patterns (PAMPs). PRRs include Toll-like receptors (TLRs), found on cell surface and endosomal membranes and NOD-like receptors, present within the cell cytoplasm(Takeuchi and Akira, 2010). The most characterised class of PRRs are the TLRs, consisting of ten different members (TLR1-TLR10). Each member recognises molecular structures common across broad types of microorganism. TLR4 for example, recognise lipopolysaccharide (LPS), a cell membrane structure present on all gram-negative bacteria, whilst TLR3 recognises double stranded RNA, which is produced during viral replication and not usually found within human cells (Akira, 2003). Once a PAMP has been recognised, innate immune cells initiate pathways resulting in inflammation and ultimately destruction of the invading microorganism.

Whilst the innate immune system is effective at clearing infectious microorganisms indiscriminately and rapidly, the adaptive immune response is required in order for the body to develop microorganism-specific responses and memory. The body is therefore protected from repeated infections from pathogens that have already been encountered. The adaptive immune response consists of T and B cells, which differ in their mechanism to clear infection, but are similar in their capacity to provide specificity and long-term immunological memory and protection. DCs are critical important for the induction of both B cell and T cell activation and memory. Newly emergent naïve T cells from the thymus differentiate into effector T cell populations after encounter with antigen presented on major histocompatibility complexes (MHC) by a DC (Pennock *et al.*, 2013)(Charles A Janeway *et al.*, 2001). T cells can broadly be split into two main classes, CD4 helper T cells and CD8 cytotoxic T cells. CD4 helper T cells, as their name suggests, assist in the activity and coordination of the immune response to achieve full effectivity. They produce inflammatory cytokines that assist in macrophage mediated microbial killing, cytotoxic T cell activity and antibody production from B cells (Smith-Garvin, Koretzky and Jordan, 2009). CD4 helper T cells can come in a variety of subtypes that have unique phenotypes and produce different immune response outcomes. Th1 T cells produce IFNγ and IL-2, contributing to intracellular pathogen destruction. Th2 cytokines include IL-4, IL-5 and IL-13, which induce protective responses against parasites. Th17 cells produce larger quantities of IL-17, which leads to the clearance of extracellular pathogens and are therefore important for protecting areas of the body readily exposed to pathogens, including the skin (Chakravarti *et al.*, 2009)(Weaver *et al.*, 2013). However, not all immune regulation pathways induced by CD4 helper T cells results in immunogenic and inflammatory responses.

Regulatory T cells (Tregs) for example, are critically responsible for dampening immune responses, preventing uncontrolled inflammation and promoting tolerance to self (Broere *et al.*, 2011). In a more direct approach to alleviating infection, CD8 cytotoxic T cells actively mediate destruction of infected or cancerous cells to prevent pathogen replication and the spread of infection or malignancy. B cells, which emerge from the bone marrow, regulate immune protection through the production of antibodies. Antibodies are protein complexes which bind specific antigen leading to immobilisation of pathogens and mediating their inactivation and clearance (Alberts *et al.*, 2002a). Follicular DCs are fundamental to support germinal centre organisation, in which B cell proliferation occurs and engage with B cells to prime responses and promote survival (Heesters, Myers and Carroll, 2014). The trade-off for the specificity that is developed during adaptive immunity is the amount of time in which it takes to develop. There is therefore a delay in which adaptive immune responses are activated after the initial infection. Protection during this period is provided by the rapid responses of the innate immune system. After the adaptive immune response develops, it supports the innate immune response and ultimately leads to clearance of infection and long term memory against particular pathogens to prevent reinfection (Alberts *et al.*, 2002b). The combined power that both divisions of the immune system provide in protecting our bodies form infection, demonstrates why the ability to link the activation of both responses, through DC activity, is fundamental for health.

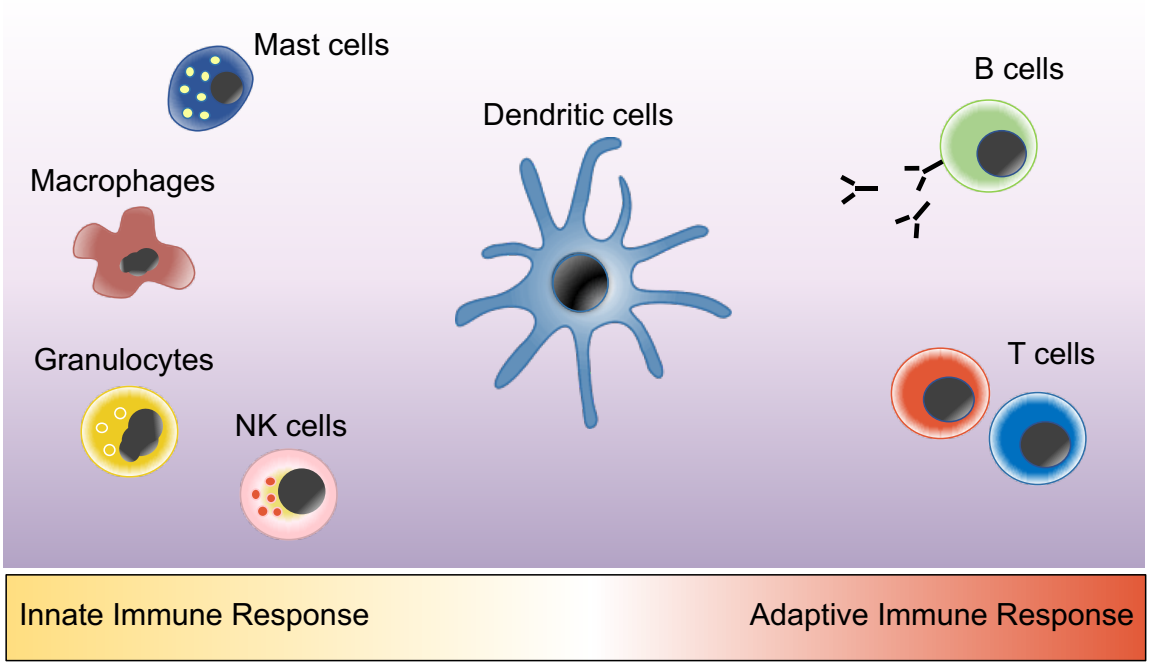

Figure 1. DCs bridge the gap between innate and adaptive immunity. Innate immune cells (left) include macrophages, mast cells, NK cells, Granulocytes (Neutrophils, Basophils, Eosinophils) and DCs. DCs are antigen presenting cells and can mediate the activation of adaptive immunity, which induces the activation of B cells and T cells (right).

1.2 DC regulation of immunity

DCs are unique components of the immune system, as they are critically responsible for linking innate immune responses to the activation of adaptive immune responses (**Figure 1**). Whilst macrophage and B cells are also classed as APCs, DC antigen presenting capabilities are the most potent, providing unparalleled capacity to initiate adaptive immune responses (Steinman, 1991). Furthermore, DCs appear to be the most equipped innate immune cell for PAMP recognition, as the broadest range of PRRs are expressed on their surface (Kaisho and Akira, 2001). For antigen presenting function, DCs must be able to engulf extracellular structures once recognised and are therefore equipped with endocytic, phagocytic and macropinocytotic function (Savina and Amigorena, 2007)(ten Broeke, Wubbolts and Stoorvogel, 2013). Within DCs, captured extracellular complexes are transported within cytoplasmic endosomes and phagosomes (Banchereau and Steinman, 1998). Inside the cytoplasmic compartments, proteases cleave the antigen into peptides, which can then be incorporated onto MHC, which are transported to the cell surface via exocytosis for presentation to T cells (ten Broeke, Wubbolts and Stoorvogel, 2013). MHC complexes are essential for the activation of adaptive immune responses because T cells cannot recognise antigen in its unprocessed and unpresented form (Banchereau and Steinman, 1998).

T cells interact with MHC complexes via surface T cell receptors (TCRs), which are fundamental for their ability to recognise antigen and become activated. Individual naïve T cells during development in the thymus are equipped with TCRs specific for certain MHC and antigen complex structures. After engagement of TCR and MHC complexes, T cell clonal amplification occurs leading to the production of large numbers of T cells able to clear infection (Zhan *et al.*, 2017). The diversity of TCRs that allows them to recognise the huge array of different antigen and MHC complex structures which can occur, is a result of V(D)J recombination (Clambey *et al.*, 2014)(Charles A Janeway *et al.*, 2001)(Madigan *et al.*, 2012). Here, the many non-contiguous gene segments which code for the TCRα and TCRβ chains are genetically recombined in various ways, which along with editing of individual nucleotides at joining regions, leads to the generation of an estimated 10^{15} different heterodimeric TCRs (Nikolich-Žugich, Slifka and Messaoudi, 2004).

MHC come in class I and class II forms, which differ in their structure, presence on different cell types, the origin of the peptide antigens they present and the class of T cell they interact with (Wieczorek *et al.*, 2017)(Madigan *et al.*, 2012). MHC II are heterodimeric structures composed of α and β chains expressed form the MHC II gene region. Whilst MHC I are also heterodimers, they are composed of a single MHC gene region expressed protein, the class I α chain, which is attached to β-microglobulin (Madigan *et al.*, 2012). MHC I complexes classically interact with CD8 T cells, whilst MHC II complexes typically interact with CD4 T cells. MHC I present antigens from an intracellular

origin and can be expressed by all nucleated cells in the human body. MHC I interaction with T cells frequently occurs due to virally infected cells presenting viral antigen on cell surface MHC I, to induce both cell and virus destruction. In contrast, MHC II present antigen from an extracellular origin and therefore its expression is predominantly restricted to professional APCs, such as DCs. MHC II interaction however can steer T cell immune responses to either an activated or inhibitory state, as well as controlling the potency of these responses (Steinman, Hawiger and Nussenzweig, 2003). Efficient activation of T cells by DCs occurs via a combination of 3 signals (**Figure 2**). The first signal occurs through initial MHC II and TCR interaction. This alone however is not enough to prime T cell activation. In response to PAMPs, DCs initiate a critical transition from immaturity to maturity, with an increase in costimulatory molecules and cytokines being produced to prime them for adaptive immune response activation (Banchereau and Steinman, 1998)(López, Yount and Moran, 2006). The second signal of activation therefore comes through co stimulatory molecules expressed on DC surfaces. Costimulatory molecules include CD80 and CD86, ligands for both CD28 and CTLA4 receptors on T cells. Costimulatory molecules are important for controlling both the strength and outcome of T cell immune response. Interaction between CD80/CD86 and CD28 for example, leads to T cell activation, whereas in contrast, interaction with CTLA4 leads to T cell inhibition (Hubo *et al.*, 2013). The increase in CD80/CD86 molecules induced by DC maturation is crucial for inducing immunogenic T cell responses, as at low levels, overriding tolerogenic ICOS signalling induce stable IL10R expression, the receptor for anti-inflammatory IL-10 (Hubo *et al.*, 2013). The third signal comes from cytokines, that influence cellular activity. In the context of T cell and DC interaction, CD40L interaction with CD40 on DCs, induces the production of inflammatory cytokines, including IL-12, that mediate Th1 and CD8 cytotoxic T cell immune responses, as well as promoting T cell survival (Habib *et al.*, 2007)(Lapteva *et al.*, 2007)(Henry *et al.*, 2008)(Banchereau and Steinman, 1998). In summary, the regulation of DC mediated adaptive T cell immune response activation is a multi-step process which allows specificity and tight regulation.

Critical for interactions between DC and T cells to occur is DC ability to migrate out of peripheral tissues to local lymph nodes. Progenitors or newly differentiated DCs circulate in the blood and can be summoned to target peripheral tissues at which antigen acquisition can occur. After antigen encounter and to initiate novel adaptive immune responses, DCs must the extricate back into the bloodstream to carry the antigenic cargo to the lymph nodes for interaction with naïve T cells (Alvarez, Vollmann and von Andrian, 2008)(**Figure 2**). Fundamental to trafficking ability is the detachment of cellular connections, cellular motility and the expression of CCR7, a chemokine receptor for CCL19 and CCL21, which homes DCs to the lymph nodes (Alvarez, Vollmann and von Andrian, 2008)(Hampton and Chtanova, 2019).

The ability to tightly regulate the induction and outcome of MHC interaction with T cells is an important feature of DCs, as not all extracellular antigens they process and present are from harmful sources (Steinman, 2007). In the context of the skin for example, antigens encountered here can be derived from both pathogenic and commensal microorganisms, as well as noxious chemicals and inert materials, thus highlighting the requirement for diverse immune response outcomes (Clayton *et al.*, 2017)(Doebel, Voisin and Nagao, 2017). It is well established that in response to self-antigens or antigens from 'non-harmful' sources, DCs downregulate inflammatory immune responses in favour of promoting immunological tolerance (Steinman, Hawiger and Nussenzweig, 2003)(Steinman *et al.*, 2003). Maintenance of self-tolerance is fundamental for immune homeostasis and the prevention of uncontrolled destructive autoimmunity. Thus, mechanisms controlling self-tolerance in the body derive from two regulatory levels in which DCs are indispensable: central tolerance and peripheral tolerance. Critical in mechanisms of DC induced tolerance are Tregs, the immunosuppressive subclass of T cell. In central tolerance, DCs inspect the pool of developing T cells within the thymus for self-reactivity (Banchereau and Steinman, 1998). Here, along with medullary thymic epithelial cells (MTECs), migratory DCs can present a panel of self-antigen to T cells. Any T cells possessing TCRs with high affinity to MHC self-antigen complexes are induced to undergo apoptosis (Audiger *et al.*, 2017)(Ardouin *et al.*, 2016). The second layer of protection, peripheral tolerance filters out any self-reactive T cells which escape deletion within the thymus and also promotes tolerance to newly acquired antigen attained by DCs at the periphery of the body (Ardouin *et al.*, 2016). In cases when autoreactive T cell interact with self-antigen presenting DCs, Treg differentiation or the induction of T cell apoptosis can occur. Tregs are distinguished by CD25 expression and the activity of the FOXP3 transcription factor(Paust and Cantor, 2005). Tregs are equipped to down regulate inflammatory immune responses through the inactivation of inflammatory Th1, Th2 and Th17 T cell responses (Ohkura, Kitagawa and Sakaguchi, 2013). For example, the production of anti-inflammatory cytokines IL-10, IL-35 and TGFβ, can induce tolerogenic conditions, whilst the release of perforin and granzyme can actively destroy effector T cells. Furthermore, high CD25 expression leads to IL-2 consumption that starves other T cells, preventing activation (Schmidt, Nino-Castro and Schultze, 2012). Without DC mediated tolerogenic responses, the body loses its ability to distinguish between self and non-self, leading to inflammatory responses and autoimmune disease. The importance of DC tolerogenic responses is highlighted in mice studies, where induced DC depletion results in autoimmune disease and uncontrolled Th1 and Th17 responses (Audiger *et al.*, 2017). Also, dysregulated DC immunogenic responses in systemic lupus erythematosus (SLE), driven by augmented type 1 interferon signalling, promotes autoreactive T cell proliferation and loss of tolerance (Mbongue *et al.*, 2014). Furthermore, the importance Treg induction for the prevention of autoimmunity is seen in immunodysregulation polyendocrinopathy enteropathy X-linked (IPEX) syndrome, in which

mutation of the *FOXP3* gene leads to fatal systemic autoimmune disease (Paust and Cantor, 2005). Tolerogenic responses are particularly critical at the mucosal surfaces and environmentally exposed sites like the skin. In the gastrointestinal tract or lungs of children, tolerance to most food antigen and aeroallergen develops through age, although lack of tolerance to these antigens can lead to potentially lethal allergic responses (Kucuksezer *et al.*, 2013). Allergen specific immunotherapies, in which allergic patients are exposed to minor amounts of antigen that can be delivered subcutaneously, sublingually or epicutaneously, have been utilised to train and tolerise the immune system, with the role of Tregs in this process emphasised (Kucuksezer *et al.*, 2013). However, dysregulated tolerance which occurs in tumour microenvironments leads to enhanced disease and metastases, due to the evasion of immune surveillance. Here, the release of immunomodulatory molecules such as IL-10, TGF-β and IDO1, promotes tolerogenic DC differentiation and absent anti-tumour responses (Fricke and Gabrilovich, 2006). Intriguingly, specific 'immune privileged' sites in the body, such as the hair follicles, brain, corneal tissue and placenta, are characterised by increased tolerogenicity, mediated partly through the restriction of APC function (Bertolini *et al.*, 2020). Additionally, 'immune privilige' in the gut lumen, promoted through the secretion of immunomodulatory molecules that preferentially promote tolerogenic responses are critical to mediate tolerance to hugely diverse luminal antigen and microbiotic flora (Iweala and Nagler, 2006).

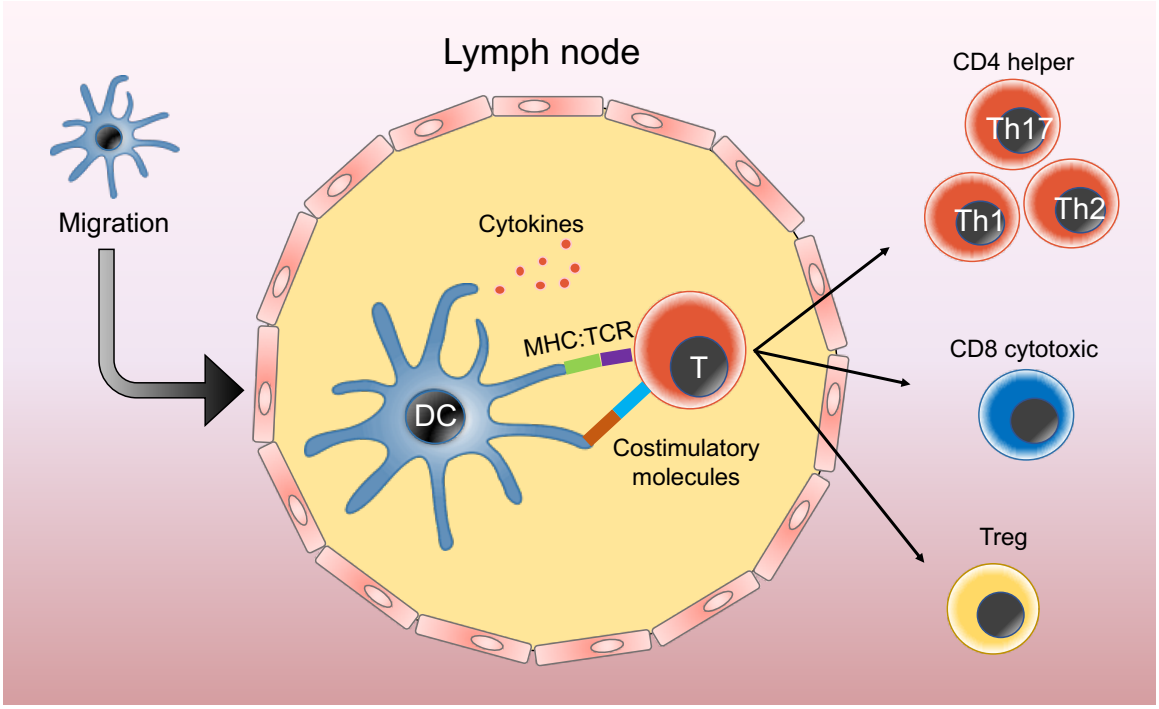

Figure 2. DC migration to the lymph nodes mediates diverse T cell responses. During maturation, DC migrate out of peripheral tissues towards the lymph nodes. Here, antigen in MHC complexes expressed on DC surfaces interact with TCRs on T cells. Depending on the expression of co-stimulatory molecules (CD80/CD86-CD28/CTLA4) and cytokines, T cells can be differentiation towards immunogenic CD4 helper T cells (Th1, Th2 and Th17) and CD8 cytotoxic T cells or immunosuppressive Tregs.

The ability of DC to induce both inflammatory and tolerogenic immune responses has created speculation as to how immune response outcomes are decided. Currently there are varying theories hypothesised and divergent results from functional studies as to what critically regulates DC tolerogenicity. Initially proposed by Ralph Steinman, is the theory that the status of DC activation is the most critical factor which determines DC immune responses. Here, immature DCs are anticipated to be responsible for mediating tolerance and defining 'self', through steady-state trafficking and self-antigen presentation to T cells to suppress their activation. They then lose tolerogenic capacity and become immunogenic after maturation (Steinman *et al.*, 2000)(Banchereau and Steinman, 1998)(Steinman *et al.*, 2003)(Mellman and Steinman, 2001)(Audiger *et al.*, 2017). However, the priming of tolerogenic immune responses by mature DC has been demonstrated in numerous studies. Antigen loaded DC ability to stimulate CD4+CD25+ T cells correlates with increased maturation (Yamazaki *et al.*, 2003). Furthermore, $CD83^{high}$CCR7+HLA-DR^{high} IL-10DC are phenotypically mature and can induce more highly suppressive Tregs than those induced by phenotypically immature $CD83^{low}$CCR7-HLA-DR^{low} IL-10DC (Kryczanowsky *et al.*, 2016).

Additionally, the expression of tolerogenic mediators (indoleamine 2,3-dioxygenase, IDO) by phenotypically mature human CD123+ monocyte derived DCs (MoDCs), potently inhibit T cell proliferation *in vitro* (Munn *et al.*, 2002). Alternatively, Steinman also proposed that DC populations are heterogenous with sub populations of DCs dedicated towards either immunogenic and tolerogenic responses which could be influenced by residency or migratory capacity (Banchereau and Steinman, 1998). Specific subpopulations of DC attributed to tolerance regulation have been identified across different tissues. In the spleen, $CD11c^{Low}CD45RB^{HIgh}$ DCs display enhanced Treg induction through IL-10 production, in comparison to $CD11c^{High}CD45RB^{-}$ DCs, which are highly primed for immunogenic Th1 responses through IFNγ production (Wakkach *et al.*, 2003). A specific $CD103^{+}$ expressing DC population in the gut are also strongly associated with tolerance regulation (Scott, Aumeunier and Mowat, 2011)(Coombes and Powrie, 2008). Furthermore, in the dermis, specific CD141+CD14+ subpopulations of dermal DCs (DDCs) are attributed to tolerogenic mechanisms, such as Treg induction and IL-10 production, which suppress pathology induced in mouse models of allogenic induced inflammation (Haniffa, Gunawan and Jardine, 2015)(Chu *et al.*, 2012).

Skin, and in particular epidermis, its outermost layer, is a site critical for maintenance of peripheral tolerance. However, it is not fully understood how the immune homeostasis is controlled in human epidermis. LCs are a unique population of DCs residing in this compartment, capable of inducing both immunogenic and tolerogenic responses. Therefore, we set to investigate what molecular mechanisms allow human LCs to promote immune homeostasis.

1.3 LC characteristics and ontogeny

The DC family consists of conventional DCs, plasmacytoid DCs (pDCs), monocyte-like DCs and LCs (Collin, McGovern and Haniffa, 2013). LCs are unique to other DC types in that they exclusively colonise the skin epidermis, as well as the foreskin, oral and vaginal epithelium(Hussain, Lehner and Thomas, 1995)(Zhou *et al.*, 2011)(Lombardi, Hauser and Budtz-Jorgensen, 1993). LCs are widely conserved across the skin of mammals, birds and reptiles(Doebel, Voisin and Nagao, 2017). Like other DC types, LCs are characterised by their ability to process and present antigen for initiating adaptive immunogenic T cell responses, as well as homeostatic regulation and tolerance. First described by Paul Langerhans in 1868, LCs were initially believed to have a role in the nervous system due to their long cellular projections (Kashem, Haniffa and Kaplan, 2017). In the 1970s, their immunological role was first described, with the finding that they express immune receptors and have the ability to activate T cell responses through antigen presentation (Katz, Tamaki and Sachs, 1979)(Rowden, Lewis and Sullivan, 1977). LCs are however distinguishable from other DC subtypes through unique gene expression and developmental origin.

LCs can typically be distinguished from other DC types due to high co-expression of CD1a and the C-type lectin receptor CD207, or langerin (Romani, Clausen and Stoitzner, 2010)(Collin, McGovern and Haniffa, 2013). In human LCs, CD207/langerin is specifically found on LCs, whilst dermal DC subsets expressing CD207/langerin can also be observed in mice (Doebel, Voisin and Nagao, 2017). Within the cytoplasm of LCs, CD207/langerin form tennis racket shaped organelles called Birbeck granules, which are uniquely found in LCs. Although these organelles are believed to play a role in antigen capture and the endosome pathway, their definite role and importance for LC function is largely unknown (Kissenpfennig *et al.*, 2005)(Mc Dermott *et al.*, 2002). Like other DC types, LCs express high levels of the MHC II receptor HLA-DR, key to peptide antigen presentation function (Collin, McGovern and Haniffa, 2013). The structurally similar CD1a also conveys antigen presentation function, although specifically for lipids (Amagai, 2016). LCs are therefore well equipped to process and present antigen from a variety of sources they encounter at the epidermis.

Whilst conventional DCs arise from bone marrow precursors, the developmental origin of LCs is debated with discrepancy between studies. Early studies on LC ontogeny propose a bone marrow precursor is responsible for LC population maintenance, which is supported by *in vitro* studies showing LC differentiation from the myeloid and lymphoid CD34+ haematopoietic progenitor cells (Katz, Tamaki and Sachs, 1979)(Caux *et al.*, 1999). However, influx of leukocytes is infrequently observed in the steady state uninflamed epidermis (Chorro *et al.*, 2009). Furthermore, LCs develop entirely independently of the cytokine receptor FMS-like tyrosine kinase-3 (Flt3), supporting evidence for a developmental origin different from conventional DCs (Deckers, Hammad and Hoste, 2018). Interestingly, clinical studies involving human monocytopenia patients, who lack conventional DC populations, show no changes to LC or macrophage populations (Bigley *et al.*, 2011). Thus, other studies propose a LC progenitor residing in the epidermis that maintains the population throughout life with self-replicating capabilities, a property similar to tissue resident macrophages (Hoeffel *et al.*, 2012)(Collin and Milne, 2016). Supportive of self-replicative capacity is the observation that BrdU labelled human LCs transplanted onto mice increased by ~70% 5 days post transplantation (Czernielewski and Demarchez, 1987). Also, after human hand transplantation, LCs of donor origin have been shown to be maintained in the allograft four years post-transplantation (Kanitakis, Petruzzo and Dubernard, 2004). Instead LCs are believed to follow a similar ontogeny pathway to tissue resident macrophages (Ginhoux and Merad, 2010)(West and Bennett, 2018)(Kaplan, 2017)(Doebel, Voisin and Nagao, 2017). During early embryonic development it is proposed that an initial wave of myeloid progenitors from the yolk sac seed the epidermis, establishing a population of resident LCs. Later on in embryonic development, LCs derived from monocytes of the foetal liver become the dominant population at the epidermis (Hoeffel *et al.*, 2012)(Merad *et al.*, 2013). Supporting murine studies of LCs during neonatal

development show that LC seeding of the epidermis occurs prior to birth. Two days after birth, mass expansion of the LC population is observed with LC turnover still occurring even one week after birth (Chorro *et al.*, 2009). Phenotypically and ontogenically, LCs therefore appear situated somewhere in between classical DCs and macrophages, with potent antigen presentation and migratory capacity similar DCs, but ontogeny, self-renewal and tissue residency features similar to macrophages (Doebel, Voisin and Nagao, 2017)(Deckers, Hammad and Hoste, 2018)(**Figure 3**). Environmental factors however also heavily influence LC origin and constitution. In severe inflammatory settings for example, LCs can derive from blood monocytes to replenish and support the tissue resident LC population (Seré *et al.*, 2012). Murine graft versus host disease (GVHD) models, in which the resident LC population has been destroyed, show reconstitution from monocyte precursors that over time become indistinguishable to embryo derived LCs (Ferrer *et al.*, 2019). Overall, the unique features of LC gene expression, development and residence suggest they have a niche role specifically required at the epidermal environmental interface, unparalleled by other DC types and macrophages.

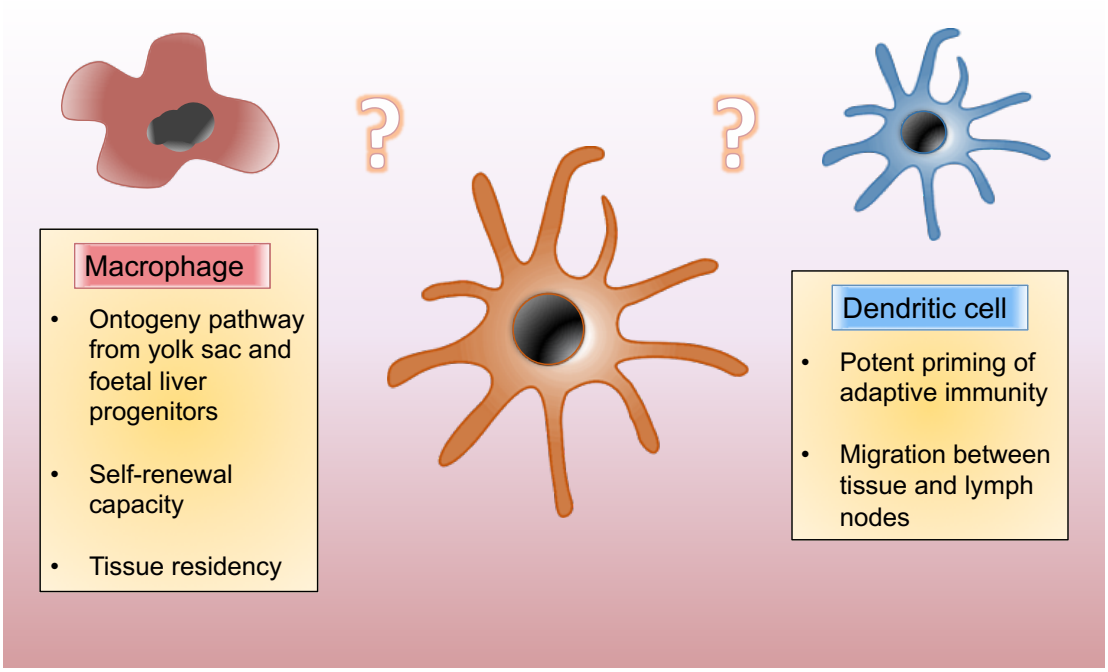

Figure 3. LCs share similarities to both macrophages and DCs. LCs share several qualities similar to macrophages, including ontogeny pathway, ability to self-renew themselves without relying on bone marrow precursors and long-term residency within tissues. However, like DCs, they have high capacity for antigen processing and presentation to prime adaptive immunity and can migrate from the peripheral tissues to the lymph nodes.

1.4 Skin biology and regulation of LCs

The skin is the largest organ of the human body, providing protection from damage and infection as well as forming a sensory interface with the external environment. As discussed, the human immune system consists of innate and adaptive arms of immunity. Immediate and non-specific innate protection from pathogen infection is provided by the physical barriers of the body, such as the skin (Turvey and Broide, 2010). Skin can be divided into 3 layers, each equipping the organ its protective and sensory abilities. The cushioning subcutaneous layer of fat is covered by the dermis, which is largely composed of connective tissue, with an array of interspersed immune cells, including dermal DCs (DDCs), lymphocytes and macrophages (Di Meglio, Perera and Nestle, 2011). The most superficial layer of the skin, the epidermis, is constituted by a thick epithelium of KCs with interspersed LCs and melanocytes. The epidermis contains 4 distinguishable layers. From the most basal layer outwards, the epidermis is constituted by the stratum basale, stratum spinosum, stratum granulosum and the stratum corneum, with each layer comprising KCs in different stages of differentiation (Di Meglio, Perera and Nestle, 2011)(Baroni *et al.*, 2012). The most superficial layer, the stratum corneum contains corneocytes, terminally differentiated KCs which provide a thick barrier to the external environment. The dry acidic environment of the stratum corneum also restricts microbe residence (Elias, 2007). Between the tightly packed KCs, LC protrude dendritic extensions to increase their capacity for antigen capture (Heath and Carbone, 2013). Within the epidermis, LC frequency is low, constituting just 2-5% of the total cell population (Deckers, Hammad and Hoste, 2018)(Seré *et al.*, 2012). In the steady-state, LC turnover in the skin is also incredibly slow, with around 1-2% replicating at any given time (Ginhoux and Merad, 2010). Despite this, LCs likely stand as the most peripheral sentinels of the body and are therefore responsible for initiating the bodies first response to invading pathogens at the skin. Antigens encountered by LCs not only originate from invading microbes, but also molecular structures from apoptotic cells (Mutyambizi, Berger and Edelson, 2009). LCs are therefore important regulators of immunological self-tolerance to suppress inflammatory responses.

The human skin is a very active immune organ due to its exposure to a diverse variety of both harmful and non-harmful antigenic stimuli in the environment (Nestle *et al.*, 2009). This includes factors from both the external environment (UV radiation, microbes, chemicals and medicines) and epidermal microenvironment (nutrients, cytokines, chemokines and danger signals), with the resulting signalling environment therefore incredibly complex (Clayton *et al.*, 2017)(**Figure 4**). After encountering antigen, LCs must adopt the most appropriate response to its source, either immunogenic or tolerogenic responses. The highly influential effects tissue microenvironments have on cellular transcriptomes has been described in mouse macrophages, where macrophage populations from different tissue compartments display distinct gene expression programmes

(Lavin *et al.*, 2014). The signalling context within epidermal tissue therefore likely profoundly shapes LC behaviour and immunological outcomes.

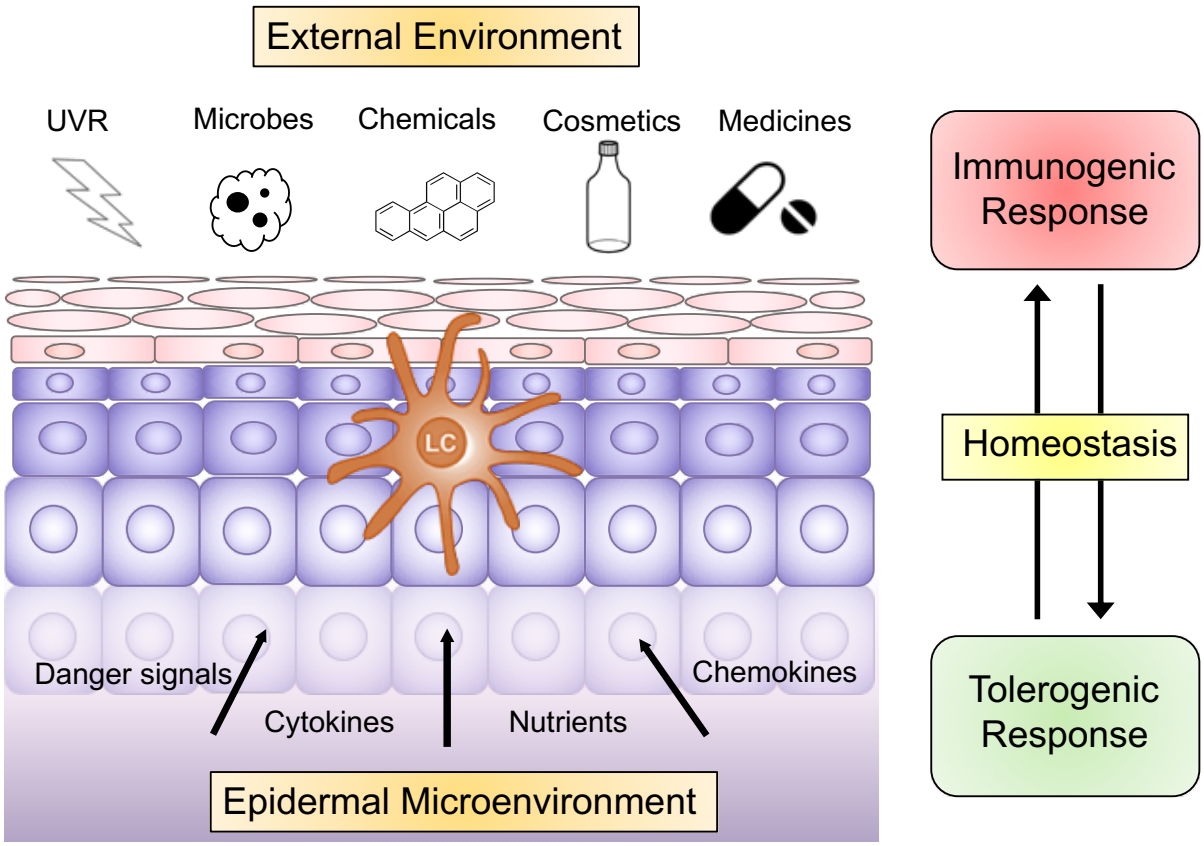

Figure 4. LC regulation of immune responses is determined by the external microenvironment and epidermal microenvironment. In the epidermis, LCs transduce signalling from both the external environment (e.g. UV radiations (UVR), microbes, chemicals, cosmetics and medicines) and epidermal microenvironment (Danger signals, cytokines, chemokines and nutrients). Depending on the context of the signalling they encounter (harmful or safe), LCs can mediate either immunogenic or tolerogenic responses to maintain tissue homeostasis.

1.5 LC immune activation

Consistent with the initiation of immunity by conventional DCs, adaptive immune responses initiated by LCs against pathogens begin after engagement of PRRs with PAMPs expressed by epidermal microbes (Deckers, Hammad and Hoste, 2018). After antigen capture and maturation, LC cease to phagocytose and instead upregulate expression of T cell stimulatory molecules (Reis e Sousa, Stahl and Austyn, 1993)(Clayton *et al.*, 2017). This primes LCs with the capacity to induce T cell immune responses, before beginning the migration process to local lymph nodes (Banchereau and Steinman, 1998). For migration to occur, connections to neighbouring KCs are broken through

down regulation of the adhesion molecule E-cadherin (Cumberbatch, Dearman, Griffiths, *et al.*, 2000). The migration process out of the epidermis is indicated to be a critical process to induce full LC activation. Meta-analysis performed by us (Clayton et al 2017.), of enzymatically digested LC at the steady state and LCs left to migrate out of epidermis fragments in culture, identified distinct gene expression programmes of each state. Migrated LCs were characterised by an increase in antigen processing and presentation as compared to steady state LCs, demonstrating how the migration process equips LCs with the capacity to prime T cell stimulation at the local lymph nodes. The expression of T cell co-stimulatory molecules are also further enhanced during the migration process (Cumberbatch, Dearman, Griffiths, *et al.*, 2000).

Whilst the mechanisms of maturation between different DC cell types follows a similar series of cellular events, the precise T cell responses that are induced can differ (Pulendran *et al.*, 1997). For example, LCs contrast from CD14+ dermal DCs (DDCs) through their heightened ability to induce Th2 CD4 T cells and cytotoxic CD8 T cell activity (Klechevsky *et al.*, 2008). LCs also mediate superior antigen cross-presentation and CD8 T cell activation compared to CD11c+ DDC, which is dependent on caveolin expression (Polak *et al.*, 2014)(Polak *et al.*, 2012). Interaction between LCs and T cells direct diverse outcomes of immune responses and are highly specific to the context of the initiating stimuli. LCs mediate these different responses through expression of cytokines and costimulatory molecules. Cytokines produced by LCs, in response to bacterial and fungal pathogen at the epidermis, induce Th17 T cell differentiation, which mediates killing of extracellular pathogens, such as *Candida Albicans* and *Porphyromonas ginigvalis* (Igyártó *et al.*, 2011)(Bittner-Eddy *et al.*, 2016). *Staphylococcus aureus*, a common coloniser of the skin, also triggers the release of Th1 and Th17 inducing cytokines from LCs during infection (van Dalen *et al.*, 2017). The increased ability for LCs to induce CD8 T cell activity, as compared to DDCs, is also attributed to increased expression of CD70, giving example of how changes in costimulatory expression can effect LC mediated T cell response outcomes (Polak *et al.*, 2012). The unique balance of T cell responses induced by LCs are likely to be specific to responses required for maintenance of human skin health and could explain their biological niche at the epidermis. The unique collection of receptors expressed on LC cell membrane surfaces also heavily influences LC capacity to respond to different antigenic stimuli. High expression of CD1a for example, provides enhanced ability to activate lipid specific CD1a-restricted T cells, which secrete large amounts of IL-22 and IL-17 (West and Bennett, 2018). Whilst a negative role of CD1a-restricted T cells involving contact dermatitis to poison ivy has been identified, CD1a mediated presentation of *Mycobacterium Leprae* antigen to CD1a-restricted T cells appears to be important for disease resolution (Kim *et al.*, 2016)(Hunger *et al.*, 2004). As leprosy wounds manifest at the epidermis, high levels of LC CD1a expression would therefore be highly protective to disease manifestation. CD207 is implicated in both the restriction and permissiveness

to infection of HIV. Whilst some studies postulate that CD207 expression by LC mediates transmission to T cells, others identify an important role of CD207 and birbeck granules in mediating HIV degradation and infection prevention (de Witte *et al.*, 2007)(Ribeiro *et al.*, 2016). In summary, the cell surface receptor profile of LCs and the array of cytokines they release, direct and define LC mediated immune responses at the epidermis.

The close proximity between KCs and LCs in the epidermis leads to a convergence and intimate relationship to their function and regulation of immune responses (**Figure 5**). Whilst LCs are the signature antigen presenting immune cells of the epidermis, KCs themselves have antigen presenting function and the ability to regulate T cell responses (Nickoloff *et al.*, 1995). Like LCs, KCs rapidly induce the secretion of inflammatory mediators during interaction with pathogens (Bourke *et al.*, 2015). These mediators are critical for optimal LC immune function. KC detection of the PAMP CpG through TLR9 for example, induces KC secretion of IL-1α, GM-CSF and TNFα, increasing the activation of LC antigen presentation pathways(Sugita *et al.*, 2007). TNFα is a powerful immunomodulatory cytokine expressed by KCs which is widely known for its augmentative effects on LC immune function (Clayton *et al.*, 2017)ˏ(Théry and Amigorena, 2001)ˏ(Cumberbatch and Kimber, 1992)ˏ(Polak *et al.*, 2014)(Sirvent *et al.*, 2020). TNFα stimulated LCs for example, display enhanced antigen cross presentation to potently activate CD8 cytotoxic T cells (Sirvent *et al.*, 2020). Furthermore, TNFα stimulation enhances LC mediation of Th1 and Th2 T cell skin homing via chemokine production. Also, KC secretion of TSLP, which is associated with atopic dermatitis, also modulates LC function to more proallergic/atopic phenotypes and impairs CD8 T cell activation (Ebner *et al.*, 2007)(Polak *et al.*, 2017). However, not all KC derived signalling leads to the activation of inflammatory immune responses. In response to non-inflammatory signalling, or even tolerogenic signalling such as TGFβ, inflammatory CD4 and CD8 T cells are suppressed and instead regulatory T cells (Treg) are induced (Shklovskaya *et al.*, 2011)ˏ(Gorvel *et al.*, 2014)ˏ(Schmidt, Nino-Castro and Schultze, 2012). Through restricting inflammatory immune responses against harmful sources only, LCs ensure the body is well protected from pathogens, whilst preventing uncontrolled and widespread tissue damage. TGFβ signalling is also crucial for maintaining integrin connections between LC and KCs that prevent migration out of the epidermis (Mohammed *et al.*, 2016). Models of TGFβ inhibition cause a depletion in the epidermal LC population (Kel *et al.*, 2010). Furthermore, BMP7, a TGFβ superfamily member, has been demonstrated to be critical for LC population maintenance at the epidermis in BMP7 knockout mice (Yasmin *et al.*, 2013). LCs are therefore highly dependent on KCs for inducing appropriate immune responses and for maintaining their presence at the epidermis.

Overall, LCs orchestrate the balance between immunity and tolerance and respond to all the milieu of stimulatory signals in the epidermal environment before deciding on the most appropriate direction of immune responses. However, despite the importance of their function for skin and systemic homeostasis, the precise molecular mechanisms that determine whether LCs induce either immunogenic or tolerogenic responses, although well studied, are not completely understood.

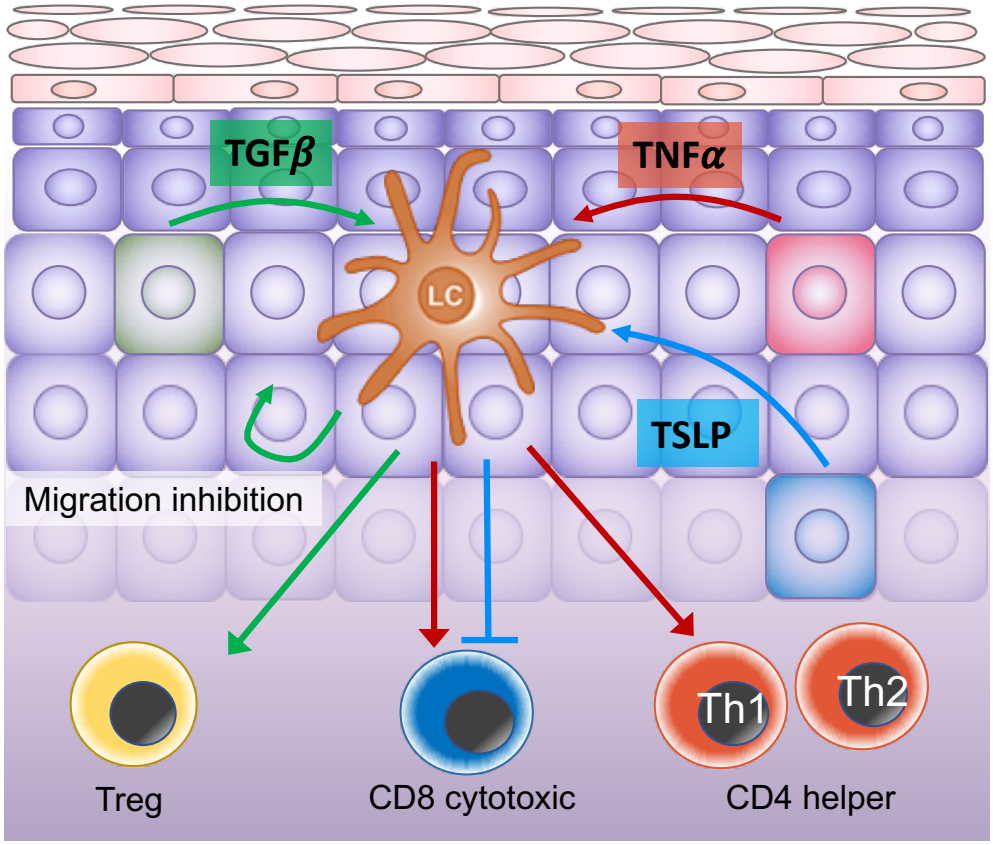

Figure 5. LC immune responses are directed by KCs. Cytokines secreted by KCs produce differential T cell responses and outcomes. TGFβ secretion causes the retention of LC within the epidermis and the induction of Tregs. Proinflammatory TNFα induces potent LC antigen presentation function to induce CD8 cytotoxic T cells responses and the promotion of Th1 and Th2 CD4 helper T cell homing to the skin. Proallergic TSLP associated with atopic dermatitis, inhibits CD8 cytotoxic T cell induction by LC.

1.6 LCs, homeostasis and tolerance

LCs in the steady-state are positioned at the epidermis ready for antigen encounter, extending and retracting dendritic extensions between keratinocytes (Clausen and Stoitzner, 2015). The environmental stimuli LCs encounter direct immune responses towards immunogenic or tolerogenic pathways (Banchereau and Steinman, 1998). Whilst the ability of LCs to potently induce

adaptive immune responses is well established, an emerging understanding of LC immunology is that steady-state immune responses may in fact be preferentially sided towards tolerance and immunoregulation over immunogenic responses (Lutz, Döhler and Azukizawa, 2010)(**Figure 6**). Evidence for a reduced inflammatory capacity of LC is shown in studies demonstrating an absence of LC mediated inflammatory responses to pathogenic stimuli. Studies on Leishmaniasis have found LC function is redundant during infection, with LCs unable to induce *Leishmania major* specific T cell responses (Ritter *et al.*, 2004). Ablation of LCs in *L. major* infection also results in reduced activation of Tregs and an increased ability to clear the disease (Kautz-Neu *et al.*, 2011). Similarly, LCs also fail to induce cytotoxic T cell responses to herpes simplex virus 1 (HSV) (Allan *et al.*, 2003). Investigations into antigen processing and presentation potential in certain contexts, similarly reveal limitations in LC mediated immunity. Chimeric mouse models involving LC specific antigen presentation fail to induce effector T cell responses and T cell survival (Shklovskaya *et al.*, 2011). LC co-culture with splenic DCs and ovalbumin (OVA) protein, inhibit T cell responses which are induced by splenic DC culture alone (Imai *et al.*, 2008). In some contexts, LCs therefore appear to actively disrupt the development of immunogenic responses.

Studies directly comparing epidermal LCs to closely situated DDCs show reduced expression of inflammatory cytokines by LCs. DDCs isolated from primary skin samples display greater expression of IL-6 and IL-8 than LC counterparts after exposure to TNFα (Polak *et al.*, 2012). Through comparing affinity to induce NK cell mediated cytotoxicity, LCs required supplementary IL-2 and IL-12 stimuli, as non-supplemented LC were unable to produce adequate amounts of IL-12p70 and IL-15R-α for direct NK cell stimulation (Mü Nz *et al.*, 2005). LCs also appear to have an increased capacity to maintain tolerance to bacterial flora on the skin. In comparison to DDCs, LCs lack expression of TLR2, TLR4 and TLR5, limiting their capacity to mature after bacterial encounter (van der Aar *et al.*, 2013). The different skin compartments in which these two skin DC types are found could explain why they differ in their inflammatory properties. As LCs are positioned within the peripheral epidermal barrier, high reactivity to all encountered stimuli could be unnecessary and lead to unwarranted inflammation. Below the protective epidermal barrier in the dermis, DDCs may need to react more effectively to pathogen invasion to prevent establishment of infection (van der Aar *et al.*, 2013). Overall this could emphasise the more highly regulated and context driven responses established by LCs.

With evidence showing a reduced role of LCs for inducing inflammatory immune responses during T-cell interaction, the principal role of LCs is believed to lie in their homeostatic potential. In the steady state, LCs phagocytose nearby apoptotic cells, such as KCs and melanocytes, removing environmental self-antigen to prevent the initiation of damage responses and the release of inflammatory cytokines (West and Bennett, 2018)(Larregina and Falo, 2005). The processing rate

of self-antigen by LC has been tracked in murine studies by measuring the amount of melanin protein transported to local skin draining lymph nodes (Hemmi *et al.*, 2001). This processing rate remains unchanged even during inflammation, indicating self-antigen processing and presentation to T-cells is an integral LC process (Yoshino *et al.*, 2006). Whilst antigen presentation to T cells is a fundamental LC process, which occurs in both inflammation and steady state homeostasis, the context in which it occurs highly influences immune response outcomes. Antigen processing and presentation provides the first signal for the induction of inflammatory T cell immune responses, but the lack of PRR stimulation, in the context of self-antigen, prevents an increase in costimulatory receptors and cytokines to pass a threshold of activation (Mutyambizi, Berger and Edelson, 2009)·(Berger *et al.*, 2006). Instead LC interaction with T cells results in skewed differentiation pathways towards Tregs. In mouse models, LC mediated presentation of the keratinocyte associated protein desmoglein 3 (Dsg3) leads to the proliferation of Dsg3 specific Treg cells that suppress self-reactive immune responses (Kitashima *et al.*, 2018).

The induction of Tregs by LC appears to be critical for both systemic and epidermal tolerance regulation. Using human donor derived LCs, it was shown that steady state LCs expand functional skin resident Treg populations in the epidermis to promote tolerance (Seneschal *et al.*, 2012). Furthermore, in the absence of maturation stimuli (IL-1β and TNFα), LCs highly induce the differentiation of S*taphylococcus aureus* and *Escherichia coli* antigen specific autologous Tregs, as compared to DDCs (van der Aar *et al.*, 2013). A crucial role for LC induced Tregs for tolerance regulation can be seen in epicutaneous immunotherapy desensitised OVA-sensitive mice, in which the induction of Tregs prevents systemic immune activation (Dioszeghy *et al.*, 2018). Interestingly, LC induction of Tregs after ionising radiation treatment is implicated in the exacerbation of tumour growth through tumour evasion of immunity (Price *et al.*, 2015). Overall, this corroborates the pivotal role of LCs for maintaining and inducing self-tolerance at the epidermis.

Like immunogenic responses, tolerogenic responses by LCs are influenced by signalling from the external environment and epidermal microenvironment. As discussed above, KC are highly regulatory towards LCs. Tolerogenic stimuli such as TGF-β and IL-10 are produced by epidermal KCs (Enk and Katz, 1992), which prevent LC maturation and the migration out of the epidermis (Kel *et al.*, 2010), as well as inhibiting antigen presentation and the induction of pro-inflammatory Th1 T cell responses (Cumberbatch *et al.*, 2005). TGF-β is produced by LCs themselves, which can act in an autocrine and paracrine fashion to support their own regulation (Deckers, Hammad and Hoste, 2018). Interestingly, UV-B exposure to the skin also drives LC towards tolerogenic function, preventing Th1 T cell induction (Simon *et al.*, 1991). Furthermore, exposure of LCs to supernatants

from keratinocyte cultures exposed to UV-B restricts LC mediated inflammatory responses, with high concentrations of IL-10 secreted by KCs shown to drive this effect (Beissert *et al.*, 1995).

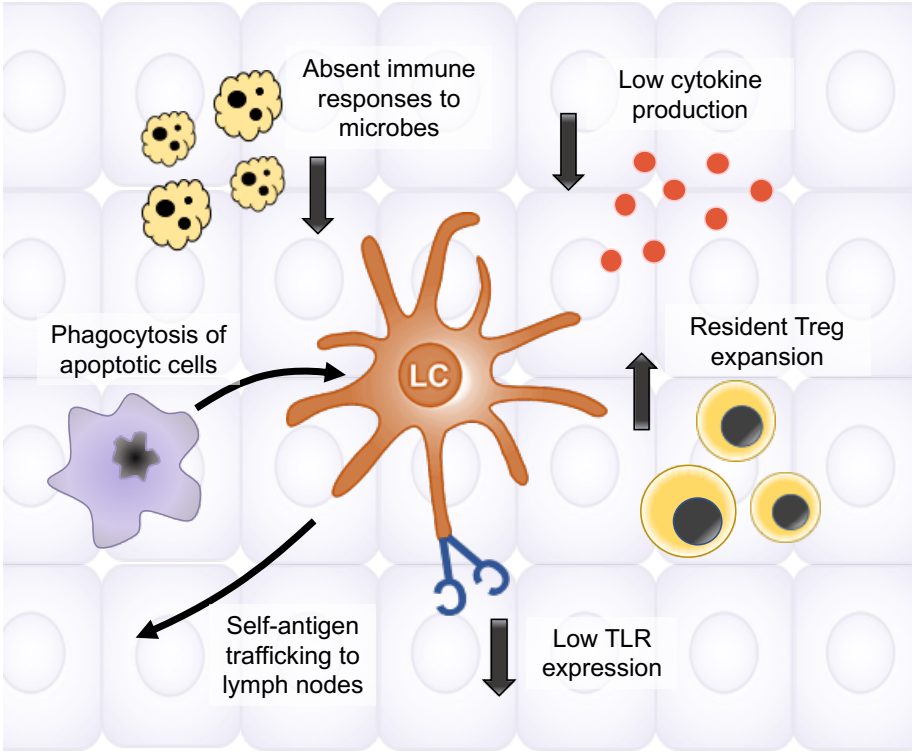

Figure 6. LCs are equipped for a tolerogenic role at the epidermis. LCs exhibit several features which are important for homeostasis and tolerogenic potential. This includes absent immune responses to certain pathogens (*L. major,* HSV), along with low TLR expression and microbe sensing. LC also display low cytokine production compared to DDCs. LC can also expand resident memory Treg populations in the steady-state and phagocytose apoptotic cells for self-antigen tracking to the lymph nodes to induce Tregs.

To further understand LC tolerogenic function, studies have amplified tolerogenic function through immunosuppressive drugs or molecules. This includes dexamethasone and lactoferrin which inhibit the migration process and therefore interfere with the activation of adaptive immune responses (Cumberbatch, Dearman and Kimber, 1999)؛(Cumberbatch, Dearman, Uribe-Luna, *et al.*, 2000). TGF-β an important cytokine for development and maintenance of the LC population at the epidermis also prevents LC migration out of the tissue, whilst 1,25-dihydroxyvitamin D3 (VitD3) treatment of LCs results in suppression of antigen presentation capabilities (Dam *et al.*, 1996)؛(Bobr *et al.*, 2012)؛(Worthington *et al.*, 2012). Cyclosporin A (CsA) is a strong immunosuppressant drug used to prevent skin tissue transplant rejection. Human skin culture with CsA has been shown to inhibit LC antigen presenting function (Dupuy *et al.*, 1991). Whilst these studies focus on the cellular phenotypes of LC tolerance, research into the transcriptomic programmes and gene regulatory networks underlying tolerogenic function remains largely unexplored.

1.7 Gene expression and transcriptional regulation underlying tolerogenic LCs

In order to mediate tolerogenic responses DCs must differentially regulate gene expression to express tolerance pathways genes (Vendelova *et al.*, 2018). Mechanism of DC tolerance induction include the production of anti-inflammatory cytokines (IL-10, IL-35 and TGFβ), T cell modulatory surface ligands (PD-L1, Fas-L) and immunomodulatory enzymes (IDO and HMOX1) (Domogalla *et al.*, 2017)(Obregon *et al.*, 2017)(Marín, Cuturi and Moreau, 2018). Some of these mechanisms have been proven to be actively displayed by LCs. The expression of IDO, an enzyme involved in tryptophan metabolism, which restricts T cell activation, is commonly induced during tolerance across many DC subtypes, to inhibit inflammatory CD4 and CD8 T cell responses and induce Treg differentiation (Munn and Mellor, 2013)(Manches *et al.*, 2012). In LCs, IDO1 is rapidly induced in response to IFNγ to downregulate T cell activation (von Bubnoff *et al.*, 2004). Upregulation of IDO expression can also be triggered by UV-B radiation through the activation of aryl hydrocarbon receptors on LC surfaces (Koch *et al.*, 2017). The cell surface ligands PD-L1 and PD-L2 have also been demonstrated to mediate T cell tolerance by DCs (Keir *et al.*, 2008). In LC, PD-L1 and PD-L2 expression after migration is associated with the dampening of T cell activation (Pẽa-Cruz *et al.*, 2010). Glycan binding proteins, such as Galectin-1, also downregulate immunogenic DC activation and the activation of cytotoxic CD8 T cells, instead favouring Treg induction (Martínez Allo *et al.*, 2020).

Changes in cellular gene expression are modulated by transcription factors (TFs). In DCs, key TFs have been identified which influence both development and immune response regulation (Clayton *et al.*, 2017)(Lin *et al.*, 2015)(Vander Lugt *et al.*, 2014). The effects of external stimuli which drive the differentiation of different LC responses, presumably including tolerance, are therefore translated intracellularly through changes in TF regulation. For LC gene regulation, the interferon regulatory factor (IRF) and NFκB family of TFs have been critically implicated in immunity, whilst the TGFβ-PU.1-RUNX3 transcription axis has implications for LC development and the steady-state (Polak *et al.*, 2017)(Clayton *et al.*, 2017)(Chopin and Nutt, 2015)(**Figure 7**).

TF regulation of LC is important for development and population maintenance. As demonstrated by Chopin et al., the effects of TGFβ on LCs is mediated through PU.1 activation, which subsequently activates RUNX3 (Chopin *et al.*, 2013). The importance of RUNX3 for LC development and the steady-state at the epidermis is demonstrated in LCs that lack PU.1, but can maintain their epidermal population through ectopic RUNX3 expression. The homeostatic effects and suppression of immune activation induced by TGFβ signalling therefore appears to be mediated by PU.1-RUNX3 TFs. Importantly, PU.1 also plays a role in the induction of LC maturation (Chopin and Nutt, 2015).

The NFκB TF family is strongly associated with immune cell regulation of inflammatory responses, including DCs (Oeckinghaus and Ghosh, 2009)(Amit *et al.*, 2009)(Clayton *et al.*, 2017). Furthermore, its importance for the regulation of LC immune responses has been explored (Kraft *et al.*, 2002). Interestingly, a role of NFκB for tolerance regulation and homeostasis has also been identified. Stimulation of LC expressed receptor activator of NFκB (RANK) by its ligand RANKL, presented by KCs, is important for maintenance of the LC epidermal population and tolerogenic activity. Murine studies of RANKL deletion show abrogated LC proliferation and therefore reduced numbers of epidermal LCs (Barbaroux *et al.*, 2008). RANKL stimulated LCs also upregulate IL-10 secretion and have been demonstrated to increase CD4+ CD25+ Treg cells, which drive anti-inflammatory immune responses (Yoshiki *et al.*, 2010)(Schöppl *et al.*, 2015). Similarly, NFκB is implicated in immunogenic LC regulation (Peiser *et al.*, 2008)(Mutyambizi, Berger and Edelson, 2009). TLR stimulation activates NFκB and amplifies LC antigen presentation capacity through increased expression of costimulatory molecules and MHC II (Mutyambizi, Berger and Edelson, 2009). Furthermore, LC TLR ligation leads to NFκB mediated CCR7, CD86, CD83, TNFα and IL-6 production (Peiser *et al.*, 2008). Interestingly there is disparity in the activity of different NFκB pathways. NFκB is constituted by two divisions, the canonical and non-canonical pathways (Oeckinghaus and Ghosh, 2009) and RelB,, the main TF component of the non-canonical NFκB pathway, is not expressed in steady-state tissue residing epidermal LC or trypsin extracted LC (Clark *et al.*, 1999). Furthermore, *RELB* is not activated in LCs in response to potent antigenic stimuli (Shklovskaya *et al.*, 2011). Differential regulation of NFκB components therefore appears to be critical for LC regulation of both immunogenic and tolerogenic responses.

The importance of the IRF TF family for the regulation of LC function has also been shown in recent years (Clayton *et al.*, 2017)(Polak *et al.*, 2017)(Sirvent *et al.*, 2020). In LC, the interactions between *IRF1*, *IRF4* and *IRF8* have been demonstrated to be important for the regulation of immunogenic LC responses, such as phagocytosis, MHC I and II regulation and Th1, Th2 and Th17 T cell induction (Polak *et al.*, 2017). Importantly, *IRF4* has been demonstrated to be critical for the genomic programming and gene regulation associated with antigen processing and presentation in LCs (Polak *et al.*, 2017)(Sirvent *et al.*, 2020). Interestingly however, *IRF4* has also been linked with the restriction of inflammatory cytokine responsive genes in human *IRF4* CRISPR-Cas9 knockout LCs, suggesting an immunoregulatory role (Sirvent *et al.*, 2020). Furthermore, in bone marrow DCs, IRF4 has been demonstrated to be central for the induction of both effector T cells and Tregs (Vander Lugt, Riddell, Aly A Khan, *et al.*, 2017). Therefore, similar to NFκB, IRF regulation of LC appear to influence both tolerogenic and immunogenic responses.

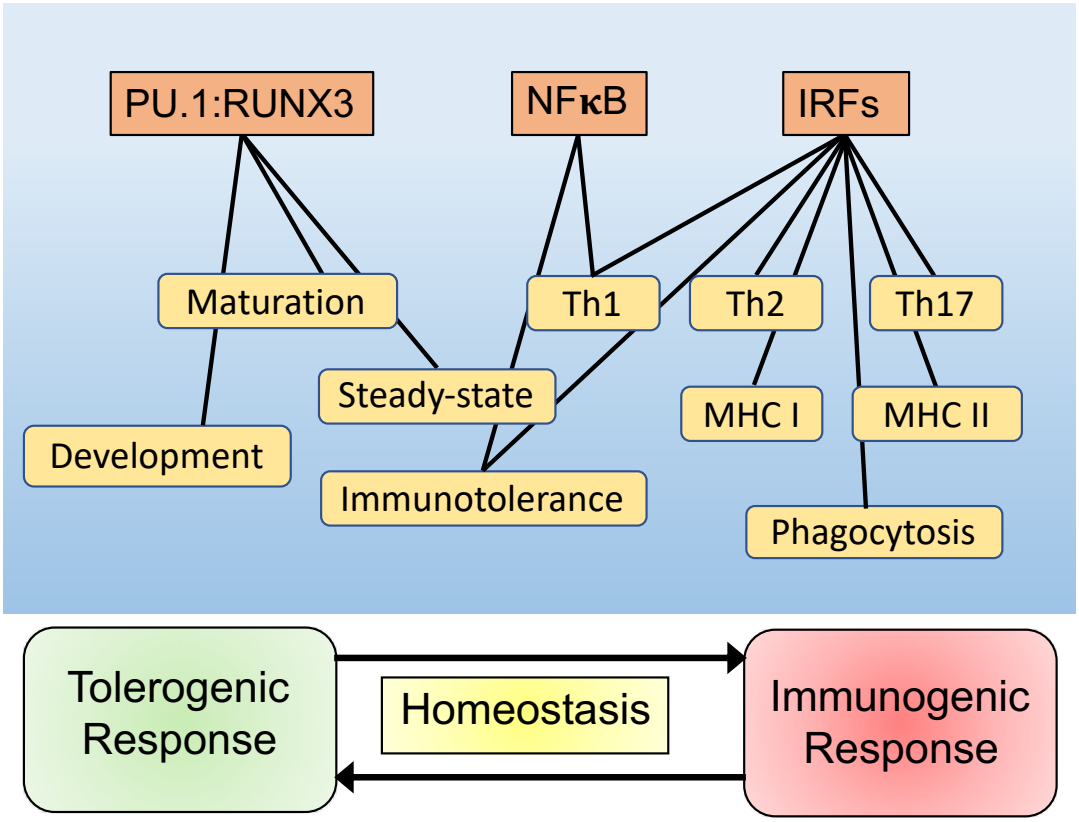

Figure 7. Transcriptional programs regulated by key TFs in LCs. The PU.1:RUNX3 transcription axis is important in LC development and the maintenances of the steady-state. NFκB is implicated in the regulation of both immunogenic and tolerogenic responses in LCs. Furthermore, the IRF TF family is highly associated with LC activation and immunogenic responses, but are also implicated in the regulation of immunotolerance. Figure adapted from Clayton et al. 2017.

1.8 LC transcriptomics

All cells in an individual organism possess the same DNA, yet each cell in an organism carries out a specific function and can respond to unique biological context at any one time. These differences are a result of changes in gene regulation, which create different expression patterns of mRNA transcripts and therefore unique transcriptomic programmes. The development of high throughput sequencing methods to measure cellular gene expression provides insight into the transcriptomic programmes that define different cell types and cellular responses. These methods have therefore greatly expanded the potential to understand cellular and molecular biology in steady state, modulated and diseased cells and tissues.

Methods of transcriptomic measurement converge with the basic principles of quantifying gene transcript abundance, with the requirement to first extract mRNA from cell cultures or tissues, before converting it into stable cDNA for measurement. The precise methods for measuring and quantifying cDNA however can differ between techniques. The DNA microarray, one of the first techniques which allowed large scale transcriptomic measurement, was developed in the mid 1990s (Cieślik and Chinnaiyan, 2017). Microarrays include a panel of DNA probes complimentary to specific genes attached to their surface. DNA probes targeting a specific gene are localised together on the microarray chip. Fluorescently labelled sample cDNA is applied to the chip and hybridisation of the labelled sample to the probes allows the number of transcripts from a particular gene to be quantified through detecting the level of fluorescence. The expression level of thousands of genes can therefore be simultaneously measured on one microarray chip. A drawback of this method however is the requirement for prior knowledge of the gene sequences printed on the chip and this therefore limits the ability to detect novel transcripts and splice variants. More recently, in the mid 2000s, a sequencing by synthesis approach called RNA-seq was first published, allowing quantitative measurements of gene transcripts with an unrestricted exploratory potential to discover new transcripts and splice variants (Bainbridge *et al.*, 2006)(Kukurba and Montgomery, 2015). mRNA is first reverse transcribed into cDNA before amplification and ligation of specific adaptor sequences which enable sequencing (Kukurba and Montgomery, 2015). Biotechnology companies have adapted the basics of RNA-seq, opting for different sequencing approaches of the prepared cDNA libraries, producing different efficiencies and outputs (Buermans and den Dunnen, 2014). As an example, Illumina, one of the leading sequencing companies, adopt a bridge amplification method in which single cDNA transcripts are clonally amplified on a flow cell, creating transcript clusters. Terminating deoxynucleotide bases (A, C, T and G) with attached fluorophores, are one by one hybridised to the sequence. After each hybridisation, the deoxynucleotide base that was added is determined through laser excitation of the fluorophore (Bentley *et al.*, 2008). The whole sequence is therefore deduced after consequential base addition and fluorophore detection. Using bioinformatic tools, the base sequences are aligned to a reference genome in order to identify the corresponding genes the sequences are derived from. The expression level of a gene transcript is quantified by the number of sequences aligned to that gene.

Transcriptomic data analysis has been applied to address many biological questions related to LC/DC function and development, that would otherwise be difficult and extensive to explore *in vitro*. This includes the deconvolution of lineage relationships between LCs and other immune cells, including closely located DDCs (**Figure 8**). As discussed, the common ontogeny pathway between LC and macrophage development and their self-renewal qualities has led to speculation that LCs are a specialised subset of tissue resident macrophage that possess DC qualities, such as potent

antigen presenting function. Transcriptomic analysis comparing LCs to both DDCs and dermal macrophages through hierarchical clustering of whole transcriptome data, has revealed the highly unique gene expression displayed by LCs (Clayton *et al.*, 2017). Principle component analysis (PCA) using skin DC whole transcriptome microarray data, shows the distinct gene expression programmes displayed by LCs compared to CD14+ and CD141+ DDC subtypes, demonstrating the divergent genomic programming influenced by habitancy in epidermal and dermal skin compartments (Artyomov *et al.*, 2015). Furthermore, using microarray, the distinct gene expression programmes displayed by LCs and DDCs after TNFα stimulation have been revealed (Polak *et al.*, 2014). Here, sample to sample clustering of whole transcriptomic data revealed that DDCs display a more dramatic change in gene expression in response to stimuli, characterised by upregulation of inflammatory cytokines and chemokines. In contrast, LC transcriptomic changes were more subtle and included upregulation of genes encoding metabolic processes and antigen capture. The phenotypic differences observed between LCs and DDCs are therefore underlined by unique transcriptomic profiles. LCs extracted from different locations of the body have also been explored to study tissue heterogeneity. Interestingly, skin LCs and vaginal epithelium LCs display heterogenous gene regulation, but both show a convergence towards a more regulatory (*IDO1* expression) and Th2 inducing transcriptomic programme compared to the more pro-inflammatory Th1 associated expression profiles of CD14+ DDCs (Duluc *et al.*, 2014). Furthermore, comparisons between transcriptomes of multiple DC subtypes isolated from human blood and skin using hierarchical clustering shows DCs cluster by location of residence, further highlighting the importance of tissue microenvironments on DC programming (Harman *et al.*, 2013). Gene regulation underlying divergent immunogenic and tolerogenic DC function has also been explored using transcriptomics. For examples, tailored responses to specific pathogens can be observed in the transcriptomes of DCs (Huang *et al.*, 2001). Inflammatory and non-inflammatory DCs can be distinguished by their specific gene expression profiles (Torri *et al.*, 2010). MoDCs stimulated with tolerogenic stimuli dexamethasone and VitD3 show an increased metabolic capacity, with increased expression of genes associated with mitochondrial and fatty acid oxidation pathways (Malinarich *et al.*, 2015). VitD3 stimulated DCs also show reduced expression of antigen presenting HLA class II and CD1 genes, whilst increasing the expression of inhibitory receptors, such as LILRB1 (ILT2) and immunosuppressive molecules, such as TGFβ (Széles *et al.*, 2009).

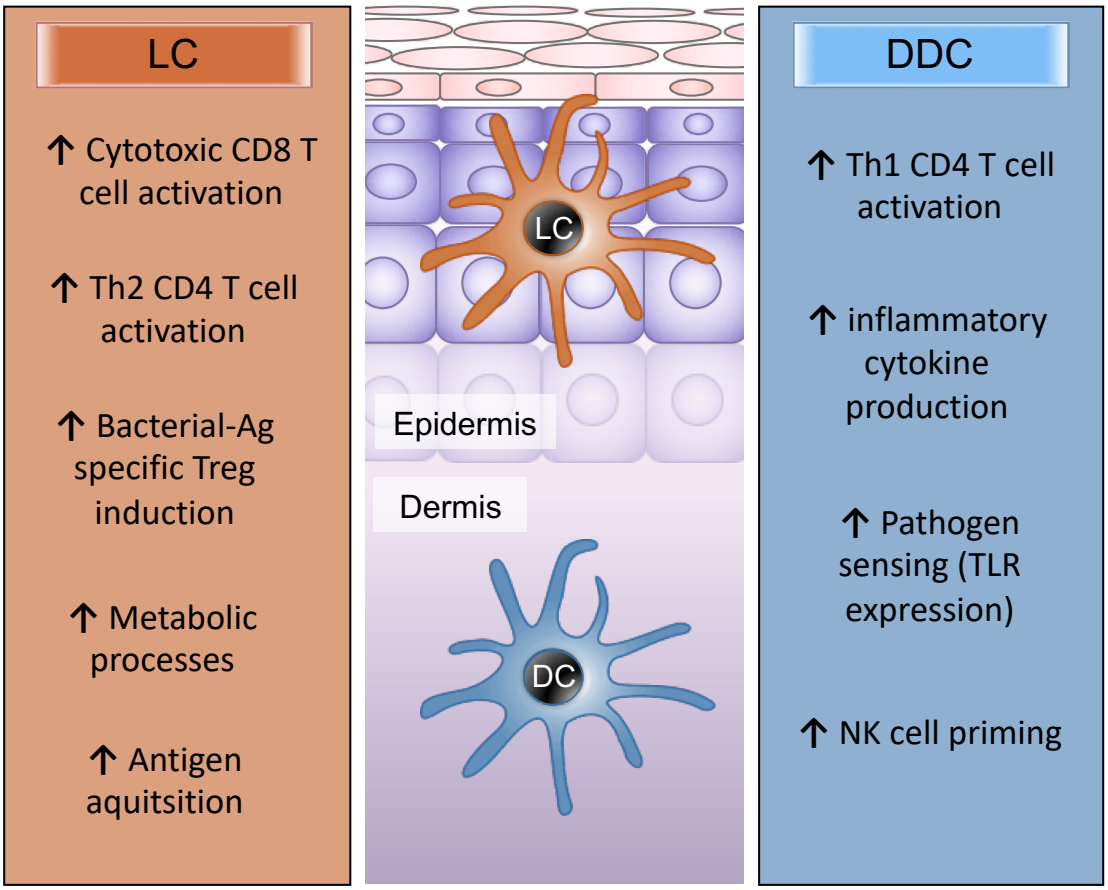

Figure 8. Transcriptomic and functional *in vitro* have studies have together revealed the different phenotypes exhibited by LCs and DDCs. Extensive studies investigating LCs and DDCs have revealed differences between cellular phenotypes. Functionally, LCs are characterised by increased CD8 cytotoxic T cell, CD4 Th2 T cell and bacterial-Ag specific Treg induction. At the transcriptome level they exhibited elevated expression of metabolic and antigen acquisition genes. DDCs, display increased inflammatory cytokine production at both the protein and transcriptomic level, which are associated with CD4 Th1 T cell activation and NK cell priming. They also display elevated expression of pathogen sensing molecules, such as TLRs.

From conducting analysis of transcriptomic data, the underlying gene expression patterns can infer the interaction and relationship between cellular molecules. This can allow the identification of molecular networks, constituted by multiple regulatory TFs and their targets. Therefore, not only the specific expression profile certain cellular phenotypes can be understood, but also the intracellular mechanisms that induce and regulate them. Complex regulatory networks are increasingly being revealed to underlie cellular processes, such as immune regulation and responses to stimuli (Loriaux and Hoffmann, 2012)(Hoffmann, 2016)(Xue *et al.*, 2014)(Mabbott *et al.*, 2013). Regulatory networks controlling cellular gene expression programmes are termed 'gene regulatory networks' (GRNs) (Singh, Khan and Dinner, 2014)(Clayton *et al.*, 2017). GRNs can include

interactions between DNA regulatory elements and transcription factors which mediate specific transcriptomic profiles/programmes and cell functions (Macneil and Walhout, 2011)(Polak *et al.*, 2017). Due to the complexity of GRNs it is near impossible to achieve complete understanding of their regulation under different conditions using *in vitro* procedures. To attain better knowledge of GRN dynamics at the steady state and after network perturbation, translation of *in vitro* data into computational modelling methodologies are necessary. Thus, TF GRNs can be constructed through combining observations from *cis*-regulatory (predicted TF binding sites in target genes) and *trans*-regulatory (correlation between TF and target gene expression) methods, as well as functional perturbations of network components *in vitro* (Amit *et al.*, 2009). GRN models have been applied to DCs to identify convergent and divergent TF expression during DC differentiation and development pathways (Lin *et al.*, 2015). More specifically, insights into specific gene expression profiles and GRNs regulating immunogenic LC function have been made. Immunostimulatory cytokines such as TNFα and TSLP for example, modulate an interferon regulatory factor (IRF) GRN (IRF-GRN) controlling LC antigen processing and activation (Polak *et al.*, 2017). Using a signalling Petri net framework, the LC IRF-GRN was reconstructed for modelling *in silico*. Containing directional transitions between network components, the addition of *in vitro* derived TF expression data into the model can produce *in silico* prediction of corresponding immune output genes. Using this model, the predicted outcomes of TNFα and TSLP stimulation produced *in silico* correctly matched outcomes of experimental *in vitro* data. This included an enhanced capability for LCs to induce cross-presentation to CD8+ T cells in response to TNFα and reduced function in response to TSLP, which has likely implications for reduced antiviral response capacity in atopic skin. With GRNs underlying LC immunogenic responses, we hypothesised that similarly, a unique GRN regulates LC tolerogenic responses.

Conventional RNA-seq and microarrays methods use bulk populations of cells and tissues to acquire mRNA for transcriptomic analysis. Therefore, mRNA expression measured is an average across the whole cell population. The importance of cellular heterogeneity to mediating diverse phenotypic functions in a cell population is becoming more and more recognised (Altschuler *et al.*, 2010). Heterogeneity may influence how cells respond to different stimuli and interact with other cells in the environment. If we are to address differences between cell types in a tissue and heterogeneity within cell populations, sequencing resolution at the single cell level is therefore required. Recently, a number of methods have been developed to perform RNA-seq at the single cell level, including Smart-seq, 10x, CEL-seq, MARS-seq and Seq-well (Picelli *et al.*, 2014)ˌ(Zheng *et al.*, 2017)ˌ(Hashimshony *et al.*, 2012)ˌ(Deng *et al.*, 2014)ˌ(Gierahn *et al.*, 2017). All single cell RNA-seq (scRNA-seq) methods converge in the requirement for isolation of single cells, although this can be achieved through various mechanism, such as fluorescence-activated cell sorting (FACS),

microfluidics and equal distribution of precise cell concentrations through gravitational sorting. Drop-seq, a novel approach of scRNA-seq, uses microfluidics to isolate single cells (Macosko *et al.*, 2015). In a high throughput and cost-efficient manner, a microfluidic device is flushed with primer coated microparticle beads and cells in aqueous solution. The device is also flushed with oil creating droplet encapsulation events at the aqueous phase and oil phase interface. Effective encapsulation events crate droplets containing one single cell and microparticle bead. Each bead is coated with uniquely barcoded poly(dT) oligo primers and when a cell and bead are encapsulated into the same droplet, the cell is lysed and its mRNA is captured by its poly(A) tail to the beads surface. The unique barcodes allow each transcript to be tracked back to its cell of origin and therefore whole transcriptome data originating from single cells can be produced. The oligo primers also consist of a unique molecular identifier (UMI), which is exclusive to each primer on each bead. UMIs are therefore distinct for each captured transcript and allow adjustment for amplification biases induced during cDNA library preparation.

The resolution provided through single cell transcriptomic analysis has allowed identification of previously undescribed cell subtypes. For example, scRNA-seq has been used to define heterogeneity within the blood DC and monocyte compartment and resulted in the describing of new subtype of blood DC and monocytes not previously recognised (Villani *et al.*, 2017). Here, the new DC subpopulation, termed DC5, can be identified through high expression of *AXL, SIGLEC1* and *SIGLEC6* and expressed gene profiles comparable to both pDC and conventional DCs. Additionally, the field of single cell analysis is constantly evolving with the appearance of updated and enhanced methods. This includes targeted sequencing approaches (Constellation Drop-seq, BD Rhapsody, DART-seq) and methods which integrate sequencing with cell surface protein expression profiling (CITE-seq, REAP-seq), to overall improve the effectivity of single cell analysis for different investigative contexts (Vallejo *et al.*, 2019)(Shum *et al.*, 2019)(Saikia *et al.*, 2019)(Peterson *et al.*, 2017).

In the skin, scRNA-seq has been used to investigate the cell population present in the human epidermis to characterise genomic programming during the steady state and during inflammation (Cheng *et al.*, 2018). Additionally, scRNA-seq has been utilised to characterise heterogeneity and differentiation pathways in murine epidermal cell populations, including the hair follicles, in the steady-state and during wound healing (Joost *et al.*, 2016)(Joost *et al.*, 2018). Furthermore, the power of single cell analysis on skin has been demonstrated during its application on healthy and lupus nephritis skin and renal tissue (Der *et al.*, 2019). Here, disease biomarkers have been identified that can be traced in the skin, with implications for personalised medicine. In human LCs, Drop-seq single cell analysis on migrated populations has revealed cellular differentiation of maturation, which involves transitional programming of oxidative phosphorylation and antigen

processing and presentation pathways (Sirvent *et al.*, 2020). Furthermore, applications of scRNA-seq to CRISPR-Cas9 *IRF4* knockout human LCs has allowed investigation and exploration of gene editing at the single cell level (Sirvent *et al.*, 2020). Thus far, only few studies have specifically investigated the transcriptomes of human LC populations at the single cell level. Undoubtedly, further application of scRNA-seq analysis on human LC will reveal the level of heterogeneity present amongst different LC populations and provide insight into how different LC immune responses are coordinated and regulated.

1.9 Therapeutics of tolerogenic LCs

It is well described that loss of tolerance can lead to inflammatory diseases and autoimmunity in which our own immune system is unable to correctly distinguish between 'self' and 'non-self', leading to disease, characterised by the self-destruction of tissues (Mackay, 2000). Here, the inherent diversity of TCR generation can lead to the generation of lymphocytes which are reactive to self-antigen or antigen from innocuous agents, that should in non-diseased circumstances be removed during central and peripheral tolerance (Horton, Shanmugarajah and Fairchild, 2017). The expansion in the understanding of tolerance and the characterisation of cells which mediate tolerogenic responses, has therefore sparked interest into their application therapeutically. Tolerogenic DCs and Tregs are well known for their tolerogenic properties and ability to regulate and suppress inflammatory responses (Schmidt, Nino-Castro and Schultze, 2012). The ability to harness DC tolerogenic ability however is particularly promising therapeutically due to their multiple mechanisms of tolerance mediation, including T cell anergy induction, the stimulation of multiple lymphocyte sub types, including Tregs and potent antigen acquisition and processing function, which could have implications for targeted immunoregulation (Obregon *et al.*, 2017)(Domogalla *et al.*, 2017)(Hasegawa and Matsumoto, 2018)(Horton, Shanmugarajah and Fairchild, 2017). Reintroducing and maintaining long term tolerance using tolerogenic DCs would therefore be the desired outcome.

In the study of tolerogenic DC capacity, several studies have utilised immunomodulatory stimuli, including VitD3, dexamethasone, TGFβ, rapamycin and co-stimulatory molecule (CD80/CD86) inhibitors, to amplify tolerogenic function for analysis *in vitro* (Marín, Cuturi and Moreau, 2018)(Domogalla *et al.*, 2017). Signature phenotypes induced in tolerogenic DCs include downregulation of costimulatory molecule (CD80, CD86) and MHC expression and the upregulation of immunosuppressive surface markers (PD-L1, ILT3) and secretory molecules (IDO, IL-10, IL-6) (Domogalla *et al.*, 2017). The application of induced tolerogenic DCs to treat autoimmune disorders has been tested, including for Type 1 diabetes, rheumatoid arthritis, Crohn's disease and multiple sclerosis (Phillips *et al.*, 2017). Most treatments are currently in the early stages of clinical trials to

assess their safety for therapeutic administration into patients. In a Phase I trial for Type 1 diabetes, isolated monocytes from patients were differentiated into MoDCs, and cultured with inhibitors of CD40, CD80 and CD86 costimulatory molecule expression (Giannoukakis *et al.*, 2011)(Phillips *et al.*, 2017). Injection of these DCs in the skin near the anatomical site of the pancreas resulted in patients displaying increased populations of B cells with potential regulatory properties and signs of recovery of functional beta cell recovery, identified through the detection of C-peptide markers. Similarly, a phase I clinical trial for rheumatoid arthritis therapy, involving MoDCs cultured with self-antigen re-administration into inflamed knees of the patients, proved to be safe but had minor effects in the alleviation of patient symptoms (Bell *et al.*, 2017). However, the group has further demonstrated *in vitro,* that VitD3 and dexamethasone stimulated MoDCs can dampen activation of CD4+ T cells from rheumatoid arthritis patients (Anderson *et al.*, 2017). Overall, the modest success of tolerogenic DCs in clinical trials highlights the importance in continued expansion in our understanding of DC tolerogenic responses.

The human skin is no different in its susceptibility for inflammatory and autoimmune disorders which can develop in individuals who lose tolerogenic function. Such disorders, include atopic dermatitis, psoriasis and contact allergies to antigen. The accessibility of the human skin to treatment gives unprecedented opportunities for studying the effects of tolerogenic DC in the alleviation of inflammatory and autoimmune disorders. With LC being the prime candidate for regulating tolerance at the epidermis, understanding the key features of their regulation could be pivotal in inducing long term disease alleviation of inflammatory skin disorders. In murine models of SLE, LC ablation resulted in an increased number of self-reactive antibodies to skin antigen, but no difference in the number of antibodies detected against systemic targets, suggesting LC tolerance regulation may be more localised to the skin (King *et al.*, 2015). In contact hypersensitivity (CHS) responses, the depletion of LC populations, in LC ablated mice or as a result of epidermal steroid exposure, leads to worsening of CHS, thus highlighting a regulatory role for LC (Kaplan *et al.*, 2005)(Grabbe *et al.*, 1995). Furthermore, in murine models of CHS, antigen processing and presentation by LCs downregulates local and systemic immune responses and promotes Treg expansion (Dioszeghy *et al.*, 2011)(Dioszeghy *et al.*, 2018). Like conventional DCs, enhancement of LC tolerogenic programmes, through immunomodulatory molecules such as steroids and VitD3, is also implicated in enhancing tolerogenic LC function to resolve inflammatory skin conditions (Chu, Di Meglio and Nestle, 2011). Whilst LC function is associated in the resolution of skin disease, it is equally implicated to be dysregulated in disease settings. Dysregulation of LC immune responses for example can contribute to disease and is caused by an unbalance in cytokines such as TSLP, in the inflamed skin microenvironment (Dubrac, Schmuth and Ebner, 2010). LC function is also abnormal in psoriasis, with surrounding KCs and immune cells stimulating inflammatory LC activity

(Cumberbatch *et al.*, 2006)·(Eidsmo and Martini, 2018). Thus, this highlights the importance/key role for correct LC tolerogenic regulation for the maintenance of skin health.

Overall, whilst LC are implicated in homeostatic and tolerogenic regulation at the epidermis, the precise mechanisms and gene regulation (including GRNs) which underlie these responses are currently unknown. As LCs are central coordinators of skin immune regulation, they are prime targets for restoring tolerance in disease. The extensive and diverse mechanisms exhibited by DCs in the regulation of both immunogenic and tolerogenic responses however, demonstrates the likely complexity that underlies LC tolerance. However, successful identification of the distinct immunological programmes exhibited by LCs mediating tolerance, could lead to the identification of molecular targets for therapeutic intervention. Increased understanding of LC immune may therefore provide unprecedented opportunity to alleviate inflammatory diseases effectively and for long term, at the skin and beyond.

Chapter 2 Methods

2.1 Data analysis of DC microarray transcriptomic data

2.1.1 Processing of DC microarray datasets collected from GEO

Datasets were selected from the Gene Expression Omnibus (GEO), a public repository for high-throughput genomic and transcriptomic data (**Table 1**). Datasets selected for analysis included microarray data of: MoDCs under different stimulatory conditions (GSE52894 (Malinarich *et al.*, 2015), GSE117946 (Comi *et al.*, 2020)); trypsinised (GSE23618) (Széles *et al.*, 2010) and migrated (GSE49475 (Polak *et al.*, 2014), GSE66355 (Artyomov *et al.*, 2015) LC experiments with accompanying data for other DC types (DDCs, MoDCs, CD1c DCs); placental DCs (PlaDC) with accompanying MoDCs (GSE52850) (Gorvel *et al.*, 2014) and a dataset containing dermal DC (DDC) subpopulations (GSE35457) (Haniffa *et al.*, 2012). All datasets were exported from GEO as either normalised expression matrices (GSE117946, GSE23618, SE49475, GSE52850), or as raw files which were then processed within R (GSE52894, GSE66355, GSE35457)(**Table 1**)**.** For processing of raw Illumina HumanHT-12 V4.0 expression beadchip files (GSE52894, GSE66355, GSE35457) were background corrected with control probes and quantile normalised using the Linear models for microarray data package(Limma) (Ritchie *et al.*, 2015).

Normalised log2 transformed whole transcriptome data were analysed through multi-dimensional scaling (MDS) on two-dimensional scatterplots representing the first 1-3 principle component dimensions. Log2 normalised datasets were submitted for differentially expressed gene (DEGs) analysis using R (version 3.6.1) package Limma (Ritchie *et al.*, 2015). Unlogged expression data for Limma identified DEGs with a Benjamini Hochberg (BH) adjusted p-value <0.05 and logFC>1 were uploaded in Graphia Pro (Kajeka, Edinburgh UK) for transcript-to-transcript co-expression analysis (Theocharidis *et al.*, 2009). Pearson coefficient parameters were adjusted (r=0.93-0.95), setting a transcript-to-transcript correlation threshold defining the number of probesets (genes) included in the non-directional cluster graph. In the graph, nodes represent individual probesets (genes) and edges between nodes represent Pearson correlation coefficients above the set threshold value. The Markov clustering algorithm (MCL), within Graphia Pro, was utilised to identify probesets with similar expression profiles across the sample data. The MCL inflation parameter, which controls clustering granularity, was set to 1.7, defining the distance metric for probeset clustering. Gene clusters were exported and associated ontologies were identified through gene ontology web-based tools Toppgene (Chen *et al.*, 2007) and DAVID (Huang, Sherman and Lempicki, 2008). A BH adjusted p-value<0.05 threshold was selected for significance. Gene expression data and gene

ontology analyses was plotted using Prism 8 software (GraphPad, California US). Gene ontology data was summarized using -log10 BH adjusted p-values. T-test statistical analysis was performed within Prism 8 software when comparing gene expression values (p-value<0.05). DEG lists were compared using Venn diagrams in Venny 2.0 (Oliveros, 2007). Heatmaps were plotted within R, using the gplots package (Canberra, ward.D cluster metrics).

Dataset	**Dataset composition**	**Microarray**	**Processing**
GSE52894	3 x biological replicates: • Immature MoDC (iMoDC), • LPS stimulated MoDC (LPSMoDC) • Dexamethasone and VitaminD3 stimulated MoDC (TolMoDC) • LPS and Dexamethasone and VitaminD3 stimulated MoDC (LPS-TolMoDC)	Illumina HumanHT-12 V4.0 expression beadchip	Processed from raw files. Background corrected with control probes and quantile normalised using Limma(Ritchie *et al.*, 2015).
GSE117946	3 x biological replicates: • Immature MoDC (iMoDC) • LPS stimulated MoDC (LPSMoDC) • IL-10 stimulated MoDC (IL10MoDC) • LPS and IL-10 stimulated MoDC (LPS-IL10MoDC)	Affymetrix Human Gene 1.0 ST Array	Robust multichip average (RMA) algorithm normalised series matrix file was downloaded from GEO.
GSE23618	3 x biological replicates from healthy breast and abdominal skin and blood donors: • Trypsinised steady-state LC • Trypsinised steady-state CD1a+ DDC • MoDC • CD1c+ blood DC	Affymetrix Human Genome U133 Plus 2.0 Array	Robust multichip average (RMA) algorithm normalised series matrix file was downloaded from GEO.
GSE49475	3 x biological replicates, each with 2 x technical replicates from healthy breast and abdominal skin donors:	Affymetrix Human Genome U219 Array	Robust multichip average (RMA) algorithm normalised

	• migrated LC • migrated CD11c+ DDC		series matrix file was downloaded from GEO.
GSE66355	Biological replicates from healthy skin donors (body site not specified). All samples are extracted via migration: • 6 x LC • 4 x CD14+ DDC • 3 x CD141+ DDC • 4 x CD14-CD141- DDC (DN-DDC)	Illumina HumanHT-12 V4.0 expression beadchip	Processed from raw files. Background corrected with control probes and quantile normalised using Limma(Ritchie *et al.*, 2015).
GSE52850	Biological replicates from healthy at-term placentas and blood donors: • 5 x Placental DC (PlaDC) • 3 x MoDC	Agilent-014850 Whole Human Genome Microarray 4x44K	Agi4x44PreProcess normalised series matrix file was downloaded from GEO.
GSE35457	4 x biological replicates from healthy breast skin donors. All samples are collagenase digested steady-state: • CD14+ DDC • CD141+ DDC • CD1c+ DDC • CD1c+ CD141+ DDC	Illumina HumanHT-12 V4.0 expression beadchip	Processed from raw files. Background corrected with control probes and quantile normalised using Limma(Ritchie *et al.*, 2015).

Table 1. Microarray datasets of DCs used in transcriptomic analysis. Microarray GEO accession numbers are listed with dataset constituents annotated. Microarray method is listed along with file processing procedure.

2.1.2 Petri-net modelling

In silico gene regulatory network (GRN) modelling was performed using the framework of a signalling Petri-net model representing the LC IRF-GRN, originally used to predict LC immunological outcomes from gene expression data (Polak *et al.*, 2017). The signalling Petri-net network diagram has been assembled using mEPN network architecture (O'Hara *et al.*, 2016)(Ruths *et al.*, 2008). The

model was constructed and edited within yED (yFiles, Germany). Here, the nodes represent biological entities (genes, DNA sequences) and the edges represent biological interactions and progressions through the model. The abundance of individual nodes is represented by the number of 'tokens' passing through the node. The edges represent the direction in which 'tokens' 'flow' through the system. Black edges indicate positive edges, whilst red edges indicate inhibitory interactions. The network is composed of TF nodes, in which tokens for the network enter, as well as DNA binding region nodes and output gene nodes, which determine the prediction of immunological pathways of activation. The signalling Petri-net (SPN) algorithm is modelled within Graphia Pro. Here, the stochastic 'flow' of variable numbers of 'tokens' through the network is modelled, based on network architecture and the number of initial 'tokens' only. More detailed description of model construction can be found in original study (Polak *et al.*, 2017).

For simulations of MoDC microarray data, means of TF expression values from triplicate transcriptomic measurements for each MoDC condition were used as starting 'tokens' input into network. Model parameters were set to 100-time blocks and 500 runs during SPN simulation within Graphia Pro. Mean output 'token' values from triplicate simulations, in which the means of the final 10-time blocks were calculated, were used to display simulation outputs. For inclusion of *MYC* into the IRF-GRN, model architecture was edited within yED and before SPN simulation in Graphia Pro.

2.2 In vitro processing of primary human skin tissue and LC

2.2.1 Extraction of steady-state and migrated LC from primary human skin

Human mastectomy and abdominoplasty skin samples were collected with written consent from donor and ethical approval (study number: 16/LO/0999). Samples were washed in PBS before fat was cut away and discarded. The remaining skin tissue was cut into small strips (~½cm width by ~1cm length) and added to 25ml 2U ml^{-1} dispase (Gibco, ThermoFisher, UK) for ~20 hours at 4°C. The skin was washed in PBS, before the epidermis was mechanically separated from the dermis.

For the extraction of steady-state LC through digestion, the epidermis was finely chopped using a scalpel and added to 13 U ml^{-1} liberase in R10 media (RPMI, 10% FBS and 1% penicillin/streptomycin)(Roche, UK) for 2 hours at 37°C with agitation. Samples were suspended in MACS buffer (0.5% BSA-PBS, Sigma, UK, 0.4% 0.5M EDTA, Gibco, UK) and filtered through a 70µM filter. Cells were washed in R10 media (all centrifugations of LC performed at 300rcf, 10 minutes), stained with trypan blue and subsequently counted using a haemocytometer to assess cell number and viability. During extraction of migrated LC, epidermal sheets were cultured in R10 for 48 hours at 37°C. The culture media containing migratory LCs was then collected, washed using R10 media

and counted after trypan blue staining. Steady-state and Migratory LCs were then: processed and stained for flow cytometry; purified using fluorescence-activated cell sorting (FACS) or OptiPrep™(volumes 1:3, STEMCELL, UK and R10 media) for *in vitro* analyses or Drop-seq; or cryopreserved in 90% FBS (Gibco, UK), 10% DMSO (Sigma, UK).

2.2.2 In vitro modulation of primary LC

OptiPrep™ purified migratory LC were utilised in unstimulated and TNFα stimulated LC processed for Drop-seq. TNFα stimulated migrated LCs were incubated for 24 hours in R10 media with 25ng/ml TNFα. LCs were then collected, washed in R10 media and counted after trypan blue staining. TNFα stimulated migrated LCs were processed through the Drop-seq pipeline.

Dexamethasone stimulated migratory LCs were extracted during 48-hour culture of epidermal fragments in R10 media containing dexamethasone (1μM, Hameln, UK). Dexamethasone stimulated migrated LC were washed thoroughly with R10 media prior to use in flow cytometry or FACS purified for *in vitro* co-culture assays.

2.3 Human PBMC isolation

10ml aliquots of blood were isolated from healthy donors following informed written consent (study number: 16/LO/0999). Collection tubes were washed out with 10ml PBS and overlaid onto 20ml lymphoprep™(Stemcell, UK), density gradient separation. Tubes were spun (600rcf, 30 minutes, 4°C, no brake or acceleration). The PBMCs mobilised at the interphase were then aspirated and collected. PBMCs were washed with PBS and spun (300rcf, 10 minutes) to remove residual lymphoprep. Cells were counted in trypan blue using a haemocytometer to assess cell numbers and viability.

2.3.1 Naïve T cell purification

Naïve T cells were purified using the human naïve CD4+ T cell isolation kit II (Miltenyi, UK). Briefly, PBMCs were counted with subsequent solution volumes in the protocol adjusted according to cell numbers (10μl per 10^7 PBMCs). PBMCs were pelleted and resuspended in 4x volume MACS buffer (0.5% BSA-PBS, 0.4% 0.5M EDTA). 1x volume of cocktail 1 (biotinylated CD45RO, CD8, CD14, CD15, CD16, CD19, CD25, CD34, CD36, CD56, CD123, anti-TCRγ/δ, anti-HLA-DR, and CD235a (glycophorin A) antibodies) was added (5 minutes, 4°C). 3x volume of MACS buffer (0.5% BSA-PBS, 0.4% 0.5M EDTA), 2x volume of cocktail 2 (anti-biotin microbeads) and 1x volume human CD14 microbeads (Miltenyi, UK) were then added (10 minutes, 4°C). Magnetically labelled non-naïve CD4+ T cell populations were then depleted after running cell suspensions 2x through LS columns (Miltenyi,

UK), using MACS buffer. Double LS column filtering was performed to ensure sufficient removal of non-naïve T cell populations. The negative fraction of naïve CD4+ T cells was collected and washed in PBS prior to *in vitro* experiments.

2.4 Skin resident memory T cell isolation

Skin resident memory T cells (TRMs) were extracted from epidermal sheets isolated from whole skin after 2U ml^{-1} dispase (Gibco, ThermoFisher, UK) for ~20 hours at 4°C. Epidermal sheets were cultured in R10 media for 48 hours at 37°C. The culture media containing TRMs which had migrated from the epidermal tissues was collected and cells washed in R10 media (300rcf, 10 minutes). TRMs were purified using density gradient separation (volumes 1:3, Optiprep™, STEMCELL, UK and R10 media).

2.5 THP-1 monocyte cell line culture

The THP-1 monocyte cell line (gifted by Dr Tilman Sanchez-Elsner, University of Southampton, UK) was utilised in optimisation of Drop-seq encapsulation and library preparation experiments. THP-1 cells were cultured in R10 media, 37°C. Cultures were passaged every 3-4 days, through removing a fraction of culture volume and replacing with fresh warmed R10 media. Cells were washed in PBS (300rcf, 10 minutes) prior to Drop-seq experiments.

2.6 Flow cytometry and FACS

2.6.1 Purification of LC

To enrich and purify samples of LC extracted from human epidermis, FACS was used. After isolation from epidermis as describe above, LCs were pelleted (300rcf, 10 mins). For surface staining of live cells, PBS buffer containing 0.5% BSA (Sigma, UK) was used for all antibody staining. LCs were incubated with 10µl of FcR blocker (Miltenyi, UK) for 10 minutes at room temperature prior to staining with fluorescently labelled antibodies, to prevent non-specific antibody binding to FcR receptors on LC. Antibodies used for cell staining were pre-titrated and used at optimal concentrations. LCs were stained for LC markers CD207 (anti-CD207, PeCy7, Miltenyi, UK), CD1a (anti CD1a, VioBlue/V1, Miltenyi, UK) and HLA-DR (anti-HLA-DR, Viogreen/V2, Miltenyi, UK) and the activation marker CD86 (anti-CD86, PerCP-Cy5.5, Miltenyi, UK) for 15 minutes, room temperature and in darkness (**Table 2**). Cells were washed twice with 1 ml MACS buffer (0.5% BSA-PBS, Sigma, UK, 0.4% 0.5M EDTA, Gibco, UK) before resuspending cells in ~300µl 0.5% BSA-PBS for flow cytometry/FACS. FACS two-way sorting was performed on a FACS Aria flow cytometer (Becton

Dickinson, USA), isolating LCs positively expressing CD207, CD1a and HLA-DR, or additionally CD86high/low fractions in steady-state LC immunocompetency experiments. After cell sorting, cells were washed in R10 media or PBS and recounted in trypan blue. Flow cytometry FACSDiva files were analysed using FlowJo software (FlowJo, Oregon US).

Surface Marker	**Colour**
CD207	PeCy7
CD1a	VioBlue/V1
HLA-DR	VioGreen/V2
CD86	PerCP-Cy5.5
Intracellular marker	
IDO1	AlexaFluor647

Table 2. Surface and intracellular antibody staining panel used for FACS and flow cytometry analysis of LCs.

2.6.2 LC intracellular staining for IDO1

IDO1 intracellular staining of LCs was performed using Intracellular Fixation & Permeabilization Buffer Set (eBioscience, UK), following the kits protocol. Briefly, 300µl of Intracellular Fixation Buffer (1x) was added (30 minutes, room temperature). Cells were subsequently washed with 1ml Permeabilization Buffer (eBioscience, UK) and spun (350rcf, 10 minutes). Cell pellets were stained using anti-IDO1 (AlexaFluor647, Biolegend, UK, 30 minutes, room temperature, darkness, **Table 2**), washed with Permeabilisation Buffer and resuspended in 0.5% BSA PBS for flow cytometry.

2.6.3 T cell staining

For T cell flow cytometry analysis to identify Treg populations, pellets were surface stained for CD3 (anti-CD3, PerCP, Miltenyi, UK), CD4 (anti-CD4, Viogreen/V2, Miltenyi, UK) CD127 (anti-CD127, Pe,Miltenyi, UK) and CD25 (anti-CD25, PeCy7, Invitrogen, UK, **Table 3**) for 15 minutes, room temperature and in darkness, before washing in 0.5% BSA-PBS.

For intranuclear FOXP3 staining, T cells were permeabilised using the FOXP3/Transcription Factor Staining Buffer Set (eBiosciences, UK), following the manufacturers protocol. Briefly, 500µl of Fixation/Permeabilisation solution was added to the T cells (30 minutes, RT, darkness). 1ml of Permeabilisation Wash (1x) was added and spun (350rcf, 10 minutes). Cell pellets were stained using anti-FOXP3 (FITC, eBiosciences, UK) or a FITC isotype control (eBiosciences, UK), washed with Permeabilisation Wash (1x) and resuspended in 0.5% BSA PBS for flow cytometry.

For intracellular IL-10 staining, T cells were initially stained with LIVE/DEAD Fixable Violet Cell Stain Kit (VioBlue/V1, Invitrogen, UK) to distinguish live cells, followed by anti-CD3 and anti-CD4 surface staining as described above. Cells were then stimulated with Cell Stimulation Cocktail (eBioscience, UK) for 6 hours, followed by incubation with Golgi Plug (BD Biosciencies, UK) for 5 hours, to prevent intracellular protein transport (eBioscience, UK). Intracellular staining was performed in Permeabilizing Solution 2 (BD Biosciencies, UK) with anti-IL-10 (Pe, Miltenyi, UK). IC was used to distinguish true IL-10 positive staining.

Surface Marker	**Colour**
CD3	PerCP
CD4	VioGreen/V2
CD127	Pe
CD25	PeCy7
Intranuclear marker	
FOXP3	FITC
Intracellular marker	
IL-10	Pe

Table 3. Surface, intranuclear and intracellular antibody staining panel used for FACS and flow cytometry analysis of T cells to identify Treg populations.

2.7 Co-culture and inhibition assays

2.7.1 LC and T cell co-culture assays

Purified LC and either purified naïve CD4 T cells or TRMs were co-cultured in human serum supplemented R10 media (RPMI, Gibco, UK, 10% human serum, Sigma, UK, 100 IU/ml penicillin and 100 mg/ml streptomycin, Sigma, UK) at a 1:50 ratio for 5-days at 37°C, in wells of a 48 well plate. Plates were incubated at a tilt for the first 4 hours to ensure contact between LC and T cells. After 5-day co-culture cells were extracted, the wells washed out using PBS, before cells were washed in RPMI media. T cells were then stained for Treg markers for flow cytometry/FACS (**Table 3**).

For IDO1 inhibition experiments, co-cultures were performed as described above, except NLG-919 (10μM, Cambridge Bioscience UK), an immune checkpoint inhibitor and epacadostat (EPAC, 1μM, Cambridge Bioscience UK), a selective inhibitor of tryptophan catabolism were added to the media during migrated LC and naïve CD4+ T cell 5-day co-cultures.

2.7.2 PBMC suppression assays

Proliferation assays were set up through combining FACS-purified CD3+CD4+CD127-CD25+ Tregs, induced after 5-day co-culture of naïve CD4+ T cells with LC, with autologous CFSE labelled PBMCs. PBMCs were labelled with CFSE using the CellTrace™ CFSE Cell Proliferation Kit (Invitrogen, UK), following the kits protocol. Briefly, after cell counting, T cells were resuspended in ice-cold 0.5% BSA-PBS (1ml per 10^6 cells). Cells were then stained with CSFE (1μl per 10^6 cells, 10 minutes, room temperature). 25ml of ice cold R10 media was then added (10 minutes, on ice). Cells were washed with ice cold R10 media (3x, 15ml, 300rcf, 10 minutes). Cells were recounted after CFSE labelling to assess viability. Wells of a 96 well flat-bottomed plate were coated with 1μg/ml anti-CD3 monoclonal antibody (OKT3, eBioscience, UK) diluted PBS and incubated for 24 hours (4°C) and washed 3x with PBS prior prior to co-culture set up. CD3+CD4+CD127-CD25+ Tregs and CFSE labelled PBMCs were co-cultured for 3 days in human serum supplemented R10 media (RPMI, Gibco, UK, 10% human serum, Sigma, UK, 100 IU/ml penicillin and 100 mg/ml streptomycin, Sigma, UK), with 1μg/ml soluble anti-CD28, in wells of a 96 well flat-bottomed plate. Co-cultures were set up in ratios of 1:1 and 1:3 Treg:PBMC. Co-cultures were incubated at a tilt for the first 24 hours to ensure Treg/PBMC contact. After 3 days, cells were collected and washed in R10 media (300rcf, 10 minutes). T cells were stained for CD3 (anti-CD3, VioBlue/V1, Miltenyi, UK), CD4 (anti-CD4, APC, Miltenyi, UK) and CD8 (anti-CD8, APC-Cy7, Miltenyi, UK)(15 minutes, room temperature, darkness, **Table 4**) to assess proliferation rate (CFSE fluorescence diffusion) across CD4 and CD8 T cell populations. Cells were resuspended in 0.5% BSA PBS for flow cytometry.

Surface Marker	Colour
CD3	VioBlue/V1
CD4	APC
CD8	APC-Cy7

Table 4. Antibody staining panel used for flow cytometry analysis to measure CD4 and CD8 T cell proliferation in the CFSE-labelled PBMC proliferation assay.

2.8 Drop-seq

2.8.1 Producing microfluidic droplet devices

PDMS microfluidic devices were produced following the protocol developed by Dr Jonathan West and Dr Patrick Stumpf at the University of Southampton (**Figure 9**). For a single device containing 6 microfluidic channels, 12g of PDMS pre-polymer and 1.2g of curing agent were mixed and degassed in a vacuum desiccator before pouring into moulds. Devices were baked at 60°C for 90 minutes. Inlet and outlet holes were created using a 1-mm biopsy punch. Devices were positioned onto a glass microscope slide and the contact sealed using plasma activation in a Diener Femto SRS Plasma System (Diener, Germany). 1% trichloro(1H,1H,2H,2H-perfluoro-octyl)silane (Sigma-Aldrich, UK) was flushed through the device via inlet holes and left to incubate for 10 minutes. Contents of device were then ejected using a N_2 gun before storage at room temperature.

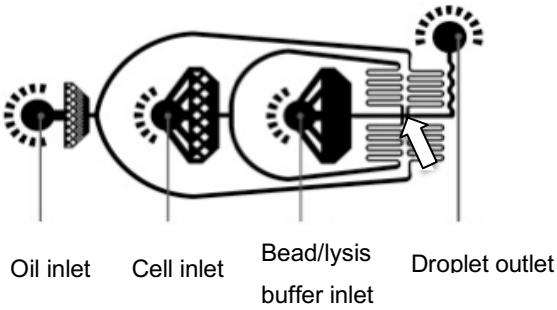

Figure 9. Microfluidic device used to create nanoliter sized droplets containing single cell and primer coated bead. Fluid runs through the 1mm diameter channels in the device from inlets. At the interphase in which aqueous cell and bead flow meet the oil, encapsulation events occur (arrow). Droplets exit the device at outlet for collection and subsequent processing. Image edited from Macosko et al. 2015(Macosko *et al.*, 2015).

2.8.2 Production of single cell and bead loaded droplets

Drop-seq was performed following the Drop-seq protocol designed by the McCarrol Lab(Macosko *et al.*, 2015). Devices were positioned onto an inverted 10x microscope (Olympus, UK) to observe droplet formation. Syringe contents for the 3 device inlets were prepared. A 5ml syringe (Henke-Sass Wolf, HSW, Germany) was loaded with droplet generation oil (Bio-Rad, UK) for insertion into the oil inlet. LCs suspensions were diluted to a concentration of 120 cells/µl in 0.02% BSA-PBS and loaded into a 1ml syringe (HSW, Germany) for the cell inlet. Uniquely barcoded primer coated beads produced through phosphoramidite synthesis (ChemGenes, USA) were suspended in 1ml lysis buffer, which contained 50µl 1M DTT (Sigma-Aldrich, UK), 40µl 0.5M EDTA (Fisher Scientific, UK), 100µl 2M Tris pH 7.5 (Sigma-Aldrich, UK), 10µl 20% Sarkosyl, 300µl (Sigma-Aldrich, UK) 20% Ficoll PM-400 (Sigma-Aldrich, UK) and 500µl nuclease free water (Fisher Scientific, UK). Beads were diluted at a concentration of 120 beads/µl and loaded into a 3ml syringe (HSW, Germany) for the bead inlet. A small stirrer magnet was added to cell and bead syringes and a magnetic plate placed in close proximity ensured homogenous suspensions were maintained. Syringes were attached to device inlets via 0.38mm diameter polyethylene tubing (Smiths Medical, Fisher Scientific). Tubing was attached to device outlet to allow collection of droplet emulsion into a 50ml Falcon tube. Syringes were placed onto the Drop-seq device in which rotating motors were primed at the top of syringe plungers. Motors were activated at a flow rate of 14,000 µl/hr for the oil and 4000 µl/hr for cell and bead suspensions, initiating droplet production. Outflow was collected and observed using a light microscope to check uniformity of droplet emulsion

2.8.3 Extraction and purification of beads from emulsion

The oil layer at the bottom of droplet collections was first discarded. 30 ml of room temperature 6X SSC (Fisher Scientific, UK) and 1ml of perfluorooctanol (PFO, Sigma-Aldrich, UK) were added before shaking (5 times). Tubes were spun at 1000rcf for 1 minute and the supernatant layer at the top of the tubes was discarded. 30ml 6x SSC was ejected into tubes and supernatant containing suspended beads was transferred into a new 50ml Falcon tube after allowing time (~3 seconds) for the oil to sink. Tubes were spun again at 1000rcf for 1 minute to pellet the beads. The pellet was then transferred into a 1.5ml DNA low bind tube (Eppendorf, UK) and washed twice with 1ml 6X SSC and once with 300µl 5X RT buffer.

2.8.4 Reverse transcription and endonuclease treatment

200µl reverse transcriptase mix (75µl water, 40µl Maxima 5x RT buffer, 40µl 20% Ficoll PM-400, 20µl 10mM dNTPs, 5µl RNase inhibitor, 10µl 50µM template switch oligo (TSO) and 10µl Maxima

H- RTase) was added to each sample of beads. Samples were incubated with rotation at room temperature for 30 minutes followed by 90 minutes at 42°C. Beads were washed with 1ml TE-SDS (10mM Tris pH 8.0 1mM EDTA, 5% SDS) and twice with 1ml TE-TW (10mM Tris pH 8.0 1mM EDTA, 0.01% Tween-20). Beads were washed with 1ml 10mM Tris pH 8.0. 200µl of exonuclease mix (20µl 10X Exo I Buffer, 10µl Exo I, 170µl water) was added before incubating with rotation at 37°C for 45 minutes. Beads were then washed with TE-SDS and twice with TE-TW.

2.8.5 PCR and cDNA library purification

2000 bead aliquots equivalent to 100 STAMPs were used in each PCR reaction. Beads were washed with 200µl endonuclease free water before 50µl PCR mix was added (25µl 2X Kapa HiFi Hotstart Readymix, 0.4µl 100µM SMART PCR Primer, 24.6µl water) and proceeding to PCR (**Table 5**). At the second denaturing, annealing and extension stage different cycling parameters were tested. cDNA libraries from 100 STAMPs were generated at a time, with different number of PCR cycles (12-16 cycles) initially tested to determine the lowest number of cycles required to produce sufficient quantities of cDNA (>100pg/µl). Lower cycling parameters reduces overamplification of high abundant transcripts, resulting in higher quality cDNA libraries. Once optimal cycling parameters were determined, the total required number of STAMPS were converted into cDNA libraries. cDNA libraries were purified using AMPure XP magnetic beads (Beckman Coulter, UK). 30µl of AMPure beads were added to PCR samples and vortexed for 5 minutes. Samples were incubated for 5 minutes at room temperature before being placed onto a 96 well magnetic plate. After 2 minutes of magnetic separation the supernatant was removed, leaving the magnetic AMPure beads bound with the cDNA. Tubes were washed twice with 200µl 70% ethanol. Tubes were dried before cDNA was eluted and collected in 10µl of endonuclease free water, before AMPure beads were discarded. Samples were run using a DNA hypersensitivity kit on an Agilent Bioanalyser (Agilent, UK) to test for successful cDNA library production.

Phase	Cycles	Temperature	Time
Denaturation	1	95°C	3 minutes
Denaturation	4	98°C	20 seconds
Annealing		65°C	45 seconds
Extension		72°C	3 minutes
Denaturation	12-16 cycles (Sample dependent)	98°C	20 seconds
Annealing		67°C	20 seconds
Extension		72°C	3 minutes
Extension	1	72°C	5 minutes

Table 5. PCR parameter used for cDNA library amplification

2.8.6 Tagmentation of cDNA

In preparation for next generation sequencing, cDNA libraries were labelled with a unique index sequence and molecular handle through tagmentation (Nextera XT DNA library preparation kit, Illumina), for compatibility with the Illumina Next-seq protocol. Volumes of purified cDNA libraries containing 600pg of DNA were diluted in nuclease free water a total volume of 5µl. 10µl of Nextera TD buffer and 5µl Amplicon Tagment Enzyme was added before incubating at 55°C for 5 minutes. 5µl of Neutralisation buffer was added and sample was incubated at room temperature for 5 minutes. In chronological order, 15µl Nextera PCR mix (Illumina), 8µl water, 1µl 10µM New-P5-SMART PCR hybrid oligo and 1µl 10µM Nextera N70X oligo (Illumina) was added before PCR tagmentation (**Table 6**). DNA was purified using AMPure XP magnetic beads (Beckman Coulter, UK) and eluted in 10µl water. DNA was quantified using a DNA hypersensitivity kit on an Agilent Bioanalyser.

Phase	**Cycles**	**Temperature**	**Time**
Denaturation	1	95°C	30 seconds
Denaturation	12	95°C	10 seconds
Annealing		55°C	30 seconds
Extension		72°C	30 seconds
Extension	1	72°C	5 minutes

Table 6. PCR parameters used for cDNA Nextera XT tagmentation

2.8.7 Sequencing

Custom read 1 primer was diluted to a working concentration of 0.3µM by adding 6µl 100µM Custom read 1 primer stock to 1994µl HT1 buffer (Next-Seq 500/550 v2.5 kit, Illumina). Tagmented libraries were pooled together at a total concentration of 2nM. 10µl of 2nM pooled library was added to 10µl 0.2N NaOH. Working on ice, 980µl ice-cold HT1 buffer was added. 130µl of the mix was transferred into 1170µl HT1 buffer, diluting the concentration of library to 2pM. 2pM libraries and 0.3µM custom read 1 primer were loaded onto a reagent cartridge from an Illumina Next-Seq 500/550 v2.5 kit (Illumina, California US). Flow cell, buffer cartridge reagent cartridges were loaded onto an Illumina NextSeq sequencer (Illumina, Californa US), on NextSeq on a paired end run

(1.5x10E5 read per cell for maximal coverage, read1=20bp, read2=50bp, index1=8bp) at the Wessex Investigational Sciences Hub laboratory, University of Southampton (Southampton, UK).

2.8.8 Read alignment

Sequencing output files were uploaded onto a user account in Iridis4 (University of Southampton). Sequencing data was de-multiplexed to separate sequencing date derived from each sample, followed by removal of UMIs from reads and captured transcripts inferred through using the bcl2fasq software from Illumina. The resulting read 1 and read 2 fastq files for each sample were aligned to the human_hg19 reference genome using STAR, creating a data matrix containing gene transcript counts detected within each single cell.

2.8.9 Drop-seq primers

Sequences of all primer utilised in the regular Drop-seq procedures were consistent to those used in Macosko et al. (Macosko *et al.*, 2015). All primers were ordered from IDT (Iowa, US) (**Table 7**).

Name	Sequence
Barcoded Bead SeqB	5'–Bead–Linker-TTTTTTTAAGCAGTGGTATCAAC GCAGAGTACJJJJJJJJJJJNNNNNNNN TTTTTTTTTTTTTTTTTTTTTTTTTTTT-3'
TSO	AAGCAGTGGTATCAACGCAGAGTGAATrGrGrG
SMART PCR primer	AAGCAGTGGTATCAACGCAGAGT
New-P5-SMART PCR hybrid oligo	AATGATACGGCGACCACCGAGATCTACACGCCT GTCCGCGGAAGCAGTGGTATCAACGCAGAGT* A*C
Custom Read 1 primer	GCCTGTCCGCGGAAGCAGTGGTATCAACGCAG AGTAC

Table 7. Barcoded primer bead and primer sequences utilised in Drop-seq protocol.

2.8.10 Drop-seq data analysis

Analyses was performed using the python-based Scanpy pipeline(version 1.5.0) (Wolf, Angerer and Theis, 2018) except where stated otherwise. High quality barcodes, discriminated from background RNA barcodes, were selected based on the overall UMI distribution using EmptyDrops (Lun *et al.*, 2019). The filtering criteria (min and max counts) was adjusted to match estimated the number of

true cells/STAMPs processed. Low quality cells, with a high fraction of counts from mitochondrial genes (20% or more) indicating stressed or dying cells were removed. In addition, genes with expression detected in less than 10 cells from an overall quantity of 680-972 cells, depending on the dataset (breast, foreskin, abdominal skin LC), were excluded. Datasets were normalised using Scran, using rpy2 within python (Lun, Bach and Marioni, 2016). Here, subclusters in the data are first identified (Counts per ten thousand (CPTT) normalised, n_pcs=15, Leiden r=0.5 (Traag, Waltman and van Eck, 2019)), before the Scran normalisation (computeSumFactors) is performed on subcluster annotated raw data. Briefly, sums of expression values in annotated subclusters in the raw data are identified. Pooled size factors are then calculated to deconvolute and produce individual cell-based factors for normalisation. Highly variable genes (top 2000) were selected using distribution criteria: min_mean=0, max_mean=4, min_disp=0.1. A single-cell neighbourhood graph was computed on the first principal components that sufficiently explain the variation in the data using 10 nearest neighbours. Uniform Manifold Approximation and Projection (UMAP) was performed for dimensionality reduction. Leiden algorithm (Traag, Waltman and van Eck, 2019) was used to identify clusters within cell populations (Leiden r = 0.5, n_pcs=25-50, n_neighbours=50). Marker genes for clusters were identified using logistic regression. Differentially expressed genes (DEGs) between cell clusters were identified using T-test or MAST (BH adj.p-value<0.05). Trajectory inference analysis was performed using partition based graph abstraction (PAGA) (Wolf *et al.*, 2019) initialisation within Scanpy. Here, the Fruchterman Reingold (FR) force directed graph layout was used to maintain data topology. Gene ontology analysis for marker genes and DEGS was performed in Toppgene (BH adj.p-value<0.05) and gene ontology results summarised using Revigo. Gene ontology data was summarized using -log10 BH adjusted P-Values with plotting performed using Prism 8 software.

Regulatory network inference analysis was performed using single-cell regulatory network inference and clustering (SCENIC) within python (Aibar *et al.*, 2017). Briefly, gene and TF co-expression networks are first calculated using the GENIE3 algorithm (Huynh-Thu *et al.*, 2010), before putative direct binding targets within co-expressed modules are discerned using RcisTarget (Aibar *et al.*, 2017) *cis*-regulatory motif analysis, to identify regulons. TF binding regions 500bp upstream of starting sequence were searched. The most highly enriched regulons could be identified between cell populations and regulon enrichment (Z-scores) in each single cell could be traced and plotted within the Scanpy pipeline.

2.8.11 Targeted Drop-seq

Drop-seq experiments were processed as normal from encapsulation through to extraction and purification of beads from droplet emulsion. During reverse transcription however, TSO was absent from the reaction. This resulted in cDNA fragments without SMART primer binding sites at the 3' end of the Macosko bead primers, which are produced in regular drop-seq (Vallejo *et al.*, 2019).

Primers targeting genes of interest were designed using Beacon Designer primer design software (PREMIER Biosoft, California US) (**Table 8**). The 55 gene panel was designed in order to identify LC, determine LC activation or tolerogenic status, identify melanocytes (MC), identify PBMC populations and detect general housekeeping genes to evaluate transcript detection. LC and MC detection panel included known markers from literature and the top consistently expressed genes detected from previously analysed single cell transcriptome data (ranked by expression, dropout rate<5%). Markers of LC activation/tolerance were chosen from literature on DC activation and tolerance and results from tolerogenic DC transcriptomic analysis. Using results from previously processed PBMC single cell RNA-seq dataset, the top two markers of each cluster, identified using k-means clustering were included for markers of PBMC populations. Housekeeping genes were selected from genes highly expressed across previously experimented LC and PBMC datasets (ranked by expression, dropout rate<5%). DNA sequences for genes were uploaded into the Beacon Designer software for identifying optimal primers specific to gene of interest. The last 14 bases from the SMART primer sequence (TATCAACGCAGAGT) were added to the 5' end of the designed primers. Desired features of primers included: a length between 32-38 base pairs, 40-60% GC content, a primer melting temperature between 52-58°C with minimal chance of secondary structures being produced. The panel of 55 primers were designed (IDT, Iowa US). Primers were pooled at 10µM. 50µl amplification mix was added (25µl 2X Kapa HiFi Hotstart Readymix, 0.4µl 10µM primer pool, 24.6µl water) to aliquots of 2000 beads (100 STAMPs). 20 rounds of linear amplification were first performed (**Table 9**) before continuing the regular Drop-seq protocol for library preparation with PCR amplification and tagmentation (**Table 5** & **Table 6**). cDNA libraries were purified using AMPure XP magnetic beads and libraries assessed using a bioanalyser before tagmentation and Next-seq sequencing.

Gene	Population targetted	Gene	Population targetted
BIRC2	LC	***IRF1***	LC activation/tolerance
CCL22	LC activation/tolerance	***IRF4***	LC activation/tolerance
CCL5	PBMC	***LDHB***	PBMC
CD1A	LC	***LST1***	PBMC
CD207	LC	***LYN***	LC
CD274	LC	***LYZ***	PBMC
CD40	LC activation/tolerance	***MALT1***	LC
CD70	LC activation/tolerance	***MLANA***	MC
CD74	LC	***MS4A1***	PBMC
CD79A	PBMC	***MYC***	LC activation/tolerance
CD80	LC activation/tolerance	***NFKB1***	LC activation/tolerance
CD86	LC	***NFKB2***	LC activation/tolerance
CFL1	Housekeeping	***NFKBIA***	LC activation/tolerance
CLEC10A	PBMC	***NFKBIZ***	LC
CLF1	PBMC	***PRF1***	PBMC
CYBB	LC activation/tolerance	***PSME1***	LC activation/tolerance
FCER1A	PBMC	***RPL10***	Housekeeping
FCGR3A	PBMC	***S100A9***	PBMC
GZMB	PBMC	***SOCS1***	LC activation/tolerance
GZMK	PBMC	***SOCS3***	LC activation/tolerance
HLA-DPA1	LC	***SOCS5***	LC activation/tolerance
HLA-DQA1	LC	***SOCS6***	LC activation/tolerance
HLA-DRB1	LC	***SQSTM1***	PBMC
HLA-E	Housekeeping	***STAT3***	LC activation/tolerance
IDO1	LC activation/tolerance	***TNFAIP3***	LC activation/tolerance
IGFBP7	MC	***TYRP1***	MC
IL10RA	LC activation/tolerance	***UBB***	Housekeeping
IL7R	PBMC		

Table 8. Primer panel for investigating cell populations in the human epidermis. Panel included 55 primers for genes that would identify LC, determine LC activation or tolerogenic status, identify melanocytes (MC), identify PBMC populations and general housekeeping genes to evaluate transcript detection. Primers were designed using Beacon Designer primer design software.

Phase	Cycles	Temperature	Time
Denaturation	1	98°C	3 minutes
Denaturation	20	98°C	20 seconds
Annealing		62°C	45 seconds
Extension		72°C	2 minutes
Extension	1	72°C	5 minutes

Table 9. Linear amplification parameters for Constellation Drop-seq

2.9 qPCR

FACS purified migrated LC were added to RLT buffer (Qiagen, UK), 1% β-mercaptoethanol. RNA was extracted and purified using a Qiagen RNeasy micro kit (Qiagen, UK), following manufacturers protocol. Using an Agilent RNA 600 pico kit, RNA concentrations and quality (RIN score >9 in all samples) were assessed. Reverse transcription was performed using a Maxima First Strand cDNA Synthesis Kit for RT-qPCR (ThermoFisher, UK) accordingly to the manufacturer's protocol. Briefly, volumes of RNA equivalent to 20ng were combine with 4µl 5x reaction mix and 2µl Maxima enzyme mix, up to a volume of 20µl with nuclease free water, prior to incubation (25°C 10 minutes, 50°C 15 minutes). Primers targeting genes of interest were designed using Beacon Designer primer design software (PREMIER Biosoft, California US). The SYBR green (iTaq™ Universal SYBR® Green Supermix, Bio-Rad, UK) quantitative PCR (qPCR) gene expression assay was utilised. Following the kit protocol, 5µl of iTaq Universal SYBR Green Supermix, 2.5µl nuclease free water, 0.5µl 10µM primer mix (Forward and Reverse) and 2µl cDNA was distributed into wells of a 364 well plate. Assays were run on a 7900HT Fast Real-Time PCR System (**Table 10**). Melting curve analysis was performed to ensure specificity of product amplification by SYBR Green.

Step	Phase	Temperature	Time
Step 1	Activation	95°C	10 minutes
Step 2 (x35 cycles)	Denaturation	95°C	15 seconds
	Extension	60°C	1 minute

Table 10. qPCR cycling parameters

2.10 Mathematical modelling

The 'toggle-switch' ODE model used was adapted from Huang et al. (Huang *et al.*, 2007), in which the observed functional interactions are depicted in an 'influence' network, rather than molecular mechanisms of interaction. The model is constructed from two first order ODEs which depict the rate of change of TFs ($x1$ and $x2$) which define two phenotypical states, i.e. in the model by Huang et al., *GATA1*=erythroid differentiation and *PU.1*=myeloid differentiation from progenitor populations. Each ODE is composed of 3 terms, with the regulatory influences modelled using Hill functions to describe sigmoidal associations. The first term represents the auto-amplification of TFs that define each phenotype. In the model, the parameters *a1* and *a2* represent the relative strength of the 'influences' promoting the auto-amplification of TFs which define the immunogenic and tolerogenic phenotype, respectively. In the deficiency of $x1$ and $x2$, auto-amplification is absent. The second term describes the cross inhibition between opposing TFs from each phenotype. Here, *b*1 and *b*2 explain the 'influence' of the cross-inhibition to each respective phenotype's activation. *k1, k2* represent the rate of the first order deactivation. The constant θ depicts the threshold or inflection point of the sigmoidal functions within the model, depicting the relative strength of regulatory interactions. The constant *n* depicts the Hill coefficient, which controls the steepness or 'step like' quality of the sigmoidal function.

The model was translated for LCs, with $x1$ defining immunogenic inducing TFs (*I*) and $x2$ defining tolerogenic inducing TFs (*T*) (**Equation 1**). In line with the original model, in which the described biochemistry captured by the parameters *a1, a2*, *b*1, *b*2, *k1, k2*, *n* and θ are unknown, *a, b, k, n* and θ were set to the same values across both equations (*a*,*b*,*k*=1, n=4 and θ=0.5) in accordance with these parameters creating a stable attractor landscape containing 3 states as described in the model by Huang et al.

Analysis and plotting of the ODE model was performed within MATLAB (Mathworks, Inc.). ODE solving was performed using the ode45 solver (time interval 0-8) for trajectory plotting, whilst phase portrait plotting was performed using quiver. TF expression values or Z-scores representing expression of multiple TFs in each single cell were exported from Scanpy scRNA-seq analysis, scaled within 0-2 to fit phase portrait boundaries and then utilised as time 0 starting points from which trajectories were calculated and plotted. The total number of cells trajectories ending at each of the 3 attractors after simulation was quantified and then plotted as pie charts in GraphPad Prism 8 software for comparison.

$$\frac{dI}{dt} = a_1 \frac{I^n}{\theta_{a_1}^n + I^n} + b_1 \frac{\theta_{b_1}^n}{\theta_{b_1}^n + T^n} - k_1 I$$

$$\frac{dT}{dt} = a_2 \frac{T^n}{\theta_{a_2}^n + T^n} + b_2 \frac{\theta_{b_2}^n}{\theta_{b_2}^n + I^n} - k_2 T$$

Equation 1. 'Toggle-switch' ODE model describing the activation of Immunogenic and tolerogenic LC states. First order ODEs representing the activation of immunogenic (*I*) and tolerogenic (*T)* states in LCs. The dotted box represents terms describing the auto-amplification of each respective states. The dashed box represents terms describing the cross-inhibition from opposing states, whilst the solid box depicts the first-order decay rate (*k*) for TFs defining each state. (*a*,*b*,*k*=1, n=4 and θ=0.5).

Chapter 3 Identifying a gene expression programme encoding tolerogenic immune responses in human DCs

3.1 Introduction

The ability to induce tolerance is a key characteristic of DC function, accompanying their potency to prime and induce immunogenic responses (Steinman, Hawiger and Nussenzweig, 2003)(Audiger *et al.*, 2017). Such tolerogenicity, as a fundamental property of DC, is likely to be encoded by a conservative set of genes (a "transcriptomic programme") universal across many different DC types and regulated by a dedicated set of TFs, within a GRN.

TFs are capable of initiating the expression of specific target genes through sequence specific binding to DNA promoter and enhancer regions, increasing the efficiency for RNA polymerase binding and therefore initiating gene transcription (Spitz and Furlong, 2012). The expression level of specific TFs can therefore indicate specific biological pathways or processes a cell is undertaking. We aimed to identify specific TFs fundamental for both DC tolerogenic and immunogenic immunity, to uncover transcriptomic programmes present and absent during tolerogenic activity.

Importantly, multiple TFs can act in concert, forming complex GRNs controlling gene expression (Singh, Khan and Dinner, 2014). The identification of GRNs offers unprecedented opportunity to comprehensively investigate transcriptomic regulation under different cellular conditions. For example, the assembly of the LC IRF-GRN, which comprises IRF family members, such as *IRF1*, *IRF4* and *IRF8*, as well as components of the ETS and AP-1 TF family (Polak *et al.*, 2017), into a Petri-net model has enabled *in silico* modelling to predict gene expression under different conditions. Model input of TF transcriptomic expression values has led to predictions of gene expression changes of genes associated with immunogenic LC immune pathways, including Th1 and Th2 T-cell differentiation and MHC I and II antigen processing and presentation.

To define a universal transcriptional programme encoding tolerance in DCs, we sought to explore the transcriptomes and elements of GRNs in DCs that are induced during diverse tolerogenic and immunogenic states. We utilised two publicly available datasets (GSE52894, GSE117946) comprising MoDCs that were unstimulated (iMoDC), conditioned with LPS (LPSMoDC), conditioned with tolerogenic stimulus: dexamethasone and VitD3 (TolMoDC) in GSE52894; or IL10 (IL10MoDC) in GSE117946, or a combination of both (LPS-TolMoDC (GSE52894), LPS-IL10MoDC (GSE117946)) (**Table 1, Table 11**). MoDC provide a valuable source to investigate basic DC biology and immune function *in vitro.* After isolation of monocytes from PBMCs, culture in the presence of IL-4 and GM-

CSF can produce sufficient MoDC numbers for downstream *in vitro* analysis. The potential of tolerogenic MoDC for inducing tolerogenic immunity has been demonstrated in numerous studies and trials(Giannoukakis *et al.*, 2011)(Phillips *et al.*, 2017)(Anderson *et al.*, 2017). Tolerogenic MoDCs generated using dexamethasone, NFκB inhibitors and anti CD40/80/86 oligonucleotides are currently being used in phase I clinical trials to treat autoimmune conditions such as type 1 diabetes, rheumatoid arthritis and Crohn's disease (Marín, Cuturi and Moreau, 2018). In some trials, vaccination with TolMoDC resulted in the induction of Tregs in the blood and a decrease in IFNγ concentrations, proving the potential for these cells to mediate tolerogenic responses. Whilst biologically different to LC, mostly due to the artificial origin of MoDCs through *in vitro* culture, the converging function of all DCs for antigen presentation and priming adaptive immunity suggests that homology between how DCs coordinate different immune responses, including tolerance, might exist. We therefore hypothesised that the transcriptomes of MoDCs would reveal common transcriptional programmes associated with different DC immune pathways, that were common in LCs. Within the MoDC datasets identified from GEO, we aimed to identify specific gene expression profiles associated with tolerogenic and immunogenic function and furthermore, specific TFs which could be regulating these specific profiles. The identification of immunogenic and tolerogenic pathway defining gene expression profiles and TFs within MoDCs could be then be assessed across different DC types, including LCs.

To delineate the transcriptomic programme of tolerogenic DC, we performed whole transcriptome analysis for MoDCs in tolerising vs immunogenic conditions, identifying sets of differentially expressed genes (DEGs), specific co-regulated networks and the key transcriptomic regulators of tolerance, such as TFs. Through identifying genes sets which co-express under unique biological conditions, we revealed insights into specific biological pathways that define DC immunological characteristics. We then investigated the accuracy of the LC IRF-GRN model for predicting MoDC immune responses during tolerising vs immunogenic conditions. While the power of the model to accurately predict LC immunogenic function after inflammatory TNFα and TSLP stimulation has been shown (Polak *et al.*, 2017), the behaviour of the IRF-GRN using transcriptomic data from other DC types, such as MoDCs, is currently unexplored, nor is it understood how the model would behave using transcriptomic data from tolerised DCs. Additionally, the model was adapted to include TF modules induced by MoDC during tolerogenic conditions, to evaluate the likelihood for their association with the IRF-GRN and DC transcriptomic regulation during immune responses.

3.1.1 Hypothesis

Tolerogenic DCs exhibit a unique transcriptomic expression profile coordinated by specific TFs, as compared to immature or immunogenic DCs.

3.1.2 Aims

- Identify unique tolerogenic associated DC transcriptomic profiles.
- Identify TFs which regulate the tolerogenic DC transcriptomic programme.
- Validate the similarity between gene regulation of MoDCs and LCs using the IRF-GRN.
- Modify the current IRF-GRN to include tolerogenic regulatory modules.

3.2 Results

3.2.1 Transcriptomes programmes of MoDCs induced to promote tolerance are defined by the suppression of inflammatory stimuli responsive genes, but lack universal tolerogenic gene signature

MoDCs provide a good model to explore the phenotypes and transcriptomes of immature DCs, whilst also being easily modulated by both immunogenic and tolerogenic stimuli to explore different immunological phenotypes. Using publicly available datasets from GEO, the transcription profiles associated with different states of MoDC activation were therefore investigated. Two microarray datasets (GSE52894, GSE117946) were identified that comprised MoDCs in various stimulatory conditions: (**Table 11**) unstimulated (iMoDC); conditioned with LPS (LPSMoDC); conditioned with tolerogenic stimulus: dexamethasone and VitD3 (TolMoDC) in GSE52894; or IL10 (IL10MoDC) in GSE117946; or both (LPS-TolMoDC (GSE52894), LPS-IL10MoDC (GSE117946)). All MoDC conditions in each dataset were in triplicate.

	GSE52894	**GSE117946**
Unstimulated	iMoDC	iMoDC
Immunogenic	LPSMoDC	LPSMoDC
Tolerogenic	TolMoDC (dexamethasone and VitD3)	IL10MoDC
Immunogenic/ Tolerogenic	LPS-TolMoDC	LPS-IL10MoDC

Table 11. Sample composition of MoDC datasets selected for analyses. Microarray datasets from GEO (GSE52894, GSE117946) were selected for transcriptomic analyses of tolerogenic DC immune responses. MoDCs were annotated according to experimental conditions, which could be summarised as unstimulated, immunogenic, tolerogenic or immunogenic/tolerogenic. All MoDC conditions in each dataset were in triplicate.

GSE52894, an Illumina HumanHT-12 V4.0 expression beadchip dataset, was first background corrected and quantile normalised and filtered, resulting in expression values for 22,216 gene probes utilised in downstream analyses. GSE117946, an Affymetrix Human Gene 1.0 ST Array, contained robust multichip average (RMA) algorithm normalised and filtered data, with 21,620 gene probes used for subsequent analyses. Due to the likelihood of batch effects between the data processing and microarray platforms, datasets were analysed separately and the resulting expression patterns identified between different stimulatory conditions were then compared.

An overall comparison of the differences between gene expression profiles within each dataset was assessed using multi-dimensional scaling (MDS) plotting. This reduced the whole transcriptome data into 2D format, for observing the first three principle components (PCs), which described the sample-to-sample variation (**Figure 10**). In each dataset, all 4 MoDC conditions displayed unique gene expression profiles with discreet isolated clusters being formed. The tight grouping of all replicates from each condition showed that the different stimulants were consistent in the unique expression profiles they induced. In GSE52894, PC1 clearly indicated the substantial effects of LPS treatment on the MoDC transcriptome, with LPSMoDCs and LPS-TolMoDCs positioned separately from the other MoDCs to the left of the MDS plot. PC2 however clearly displayed the distinct transcriptomic changes induced by tolerogenic stimuli (dexamethasone and VitD3). Similarly, in GSE117946, LPSMoDCs clearly separated from the other MoDC populations along PC1. However, unlike GSE52894, GSE117946 tolerogenic IL10MoDCs were less distinct to both iMoDCs and LPSMoDCs along PCs 1-3. This suggests that the use of diverse tolerogenic stimuli results in distinct transcriptomic programming.

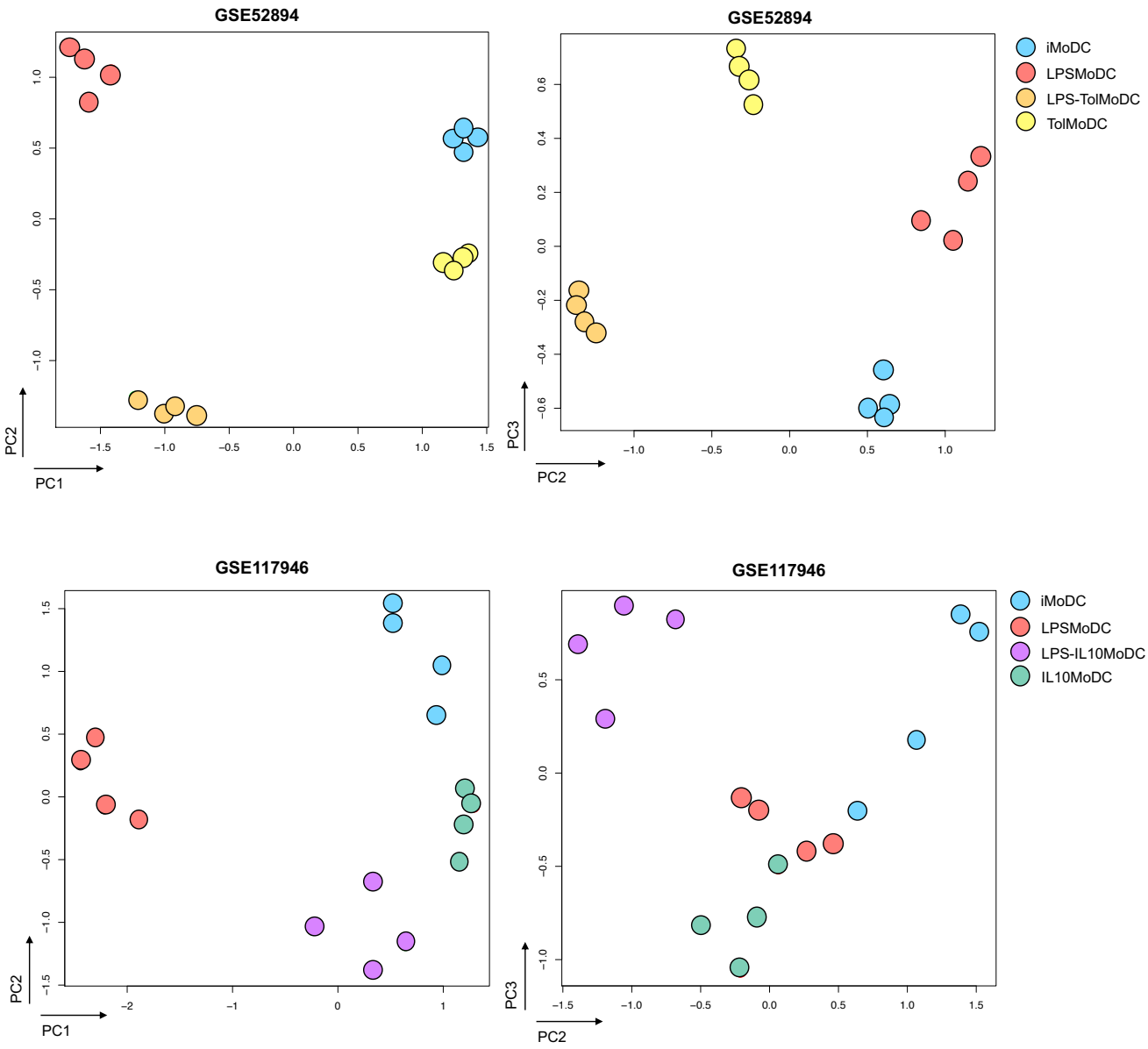

Figure 10. Dimensionality reduction of whole MoDC transcriptomes revealed each stimulation condition created distinct gene expression profiles. Visualisation of normalised, log transformed whole transcriptome data (top GSE52894, bottom GSE117946), reduced into two-dimensional format via multi-dimensional scaling (MDS) using Limma within R. The first 3 PCs are displayed, PC1 and PC2 (left) and PC2 and PC3 (right), with distances between samples representing level of similarity in each PC.

Firstly, we focussed our analysis on dataset GSE52894. To gain insight into the transcriptomic profile influencing tolerogenic function, differentially expressed gene (DEG) analysis comparing TolMoDC to all other MoDC conditions was performed using Limma (Ritchie *et al.*, 2015), version 3.40.6) within R. The model identified a list of 1171 probesets which were upregulated in TolMoDC

compared to at least one of the 3 other MoDC conditions (adj.p-value<0.05, logFC>1). To identify networks of co-expressed genes induced by different treatments, DEGs were uploaded into the gene co-expression network tool Graphia Pro (Theocharidis *et al.*, 2009). Transcript-to-transcript clustering using Pearson correlation (r = 0.93) and Markov clustering algorithm (MCL=1.7), identified 28 gene co-expression clusters (**Figure 11A**). Gene ontology analysis in Toppgene (Chen *et al.*, 2007) was performed to identify associated biological pathways for the gene lists and to recognise gene profiles potentially key for mediating tolerogenic function (**Table 12**). Systematic analysis of the cluster profiles, identified three profiles of interest for characterising specific gene regulation mechanisms promoting tolerance. These could be broadly split into clusters upregulated or downregulated by tolerogenic stimuli, with those upregulated by the latter being further split into clusters unaffected or downregulated after LPS addition. Analysis of the largest cluster exhibiting one of the profiles of interest was performed to identify the predominant transcriptomic programme associated with each profile. This revealed differences in specific immune related biological processes upregulated in profiles of interest (**Figure 11B&C)**. Cluster 6, containing 20 genes, was upregulated in both TolMoDC and LPS-TolMoDC and these genes were therefore induced by tolerogenic stimuli and resistant to immunogenic stimulus. Gene ontology for this cluster included immune-response activating signal transduction (adj.p-value=3.9E-2), activation of immune response (adj.p-value=3.9E-2), cellular carbohydrate metabolic process (adj.p-value=3.9E-2) and negative regulation of immune system process (adj.p-value=4.3E-2). Genes associated with negative regulation of immune system process, included *MYC, PIK3AP1, CD14* and *PRNP*. Gene ontology terms for cluster 7, which contained 23 genes upregulated in TolMoDCs, but down regulated in LPS-TolMoDCs included positive regulation of vasculature development (adj.p-value=2.3E-2), regulation of cellular localisation (adj.p-value=2.3E-2), and regulation of secretion by cell (adj.p-value=2.3E-2). Cluster 4, contained 69 genes and was upregulated in LPSMoDC only and not in LPS-TolMoDC. Tolerogenic stimuli was therefore suppressing their activation after the addition of LPS. Gene ontology for cluster 4 genes included response to cytokine (adj.p-value=3.9E-6), immune response (adj.p-value=1.0E-5), positive regulation of defence response (adj.p-value=3.9E-6) and positive regulation of innate immune response (adj.p-value=4.3E-5).

Clusters of interest were inspected for potential transcription factors (TFs) which could be orchestrating gene co-expression (**Figure 11D**). Cluster 6, associated with tolerogenic responses, included the TF *MYC,* which was highly upregulated in MoDCs exposed to tolerogenic stimuli. Cluster 4 included *IRF1* and *IRF4*, both known inducers of DC immune activation. These TFs followed the expression pattern of cluster 4 with upregulated expression in LPSMoDC only.

Cluster	No. of Genes	Cluster Profile	ID	Name	FDR B&H
1	292	i=High, T=High	GO:0006614	SRP-dependent cotranslational protein targeting to membrane	1.92E-19
			GO:0006613	cotranslational protein targeting to membrane	3.81E-19
			GO:0006413	translational initiation	3.81E-19
			GO:0045047	protein targeting to ER	3.81E-19
			GO:0000184	nuclear-transcribed mRNA catabolic process, nonsense-mediated decay	4.40E-19
2	196	L=High, LT=High	GO:0045087	innate immune response	4.20E-39
			GO:0060337	type I interferon signaling pathway	2.13E-38
			GO:0071357	cellular response to type I interferon	2.19E-38
			GO:0034340	response to type I interferon	8.60E-38
			GO:0006955	immune response	1.59E-37
3	167	LT=High	GO:0006955	immune response	7.77E-11
			GO:0006952	defense response	7.77E-11
			GO:0032101	regulation of response to external stimulus	1.81E-08
			GO:0080134	regulation of response to stress	1.81E-08
			GO:0045087	innate immune response	2.42E-08
4	69	L=High, LT=Low	GO:0034097	response to cytokine	3.85E-06
			GO:0031349	positive regulation of defense response	3.85E-06
			GO:0006955	immune response	1.00E-05
			GO:0050776	regulation of immune response	3.42E-05
			GO:0045088	regulation of innate immune response	3.42E-05
5	68	i=High, T=Low	GO:0048003	antigen processing and presentation of lipid antigen via MHC class Ib	1.04E-03
			GO:0048007	antigen processing and presentation, exogenous lipid antigen via MHC class Ib	1.04E-03
			GO:0001775	cell activation	1.39E-03
			GO:0002250	adaptive immune response	2.32E-03
			GO:0009611	response to wounding	2.97E-03
6	20	LT=High, T=High	GO:0002757	immune response-activating signal transduction	3.86E-02
			GO:0002253	activation of immune response	3.86E-02
			GO:2000106	regulation of leukocyte apoptotic process	3.86E-02
			GO:0044262	cellular carbohydrate metabolic process	3.86E-02
			GO:0002683	negative regulation of immune system process	4.32E-02
7	22	LT=Low, T=High	GO:1904018	positive regulation of vasculature development	2.26E-02
			GO:0060341	regulation of cellular localization	2.33E-02
			GO:0050708	regulation of protein secretion	2.33E-02
			GO:0051049	regulation of transport	2.33E-02
			GO:1903530	regulation of secretion by cell	2.33E-02
9	11	LT=Low, T=Moderate	GO:0010638	positive regulation of organelle organization	4.30E-02
			GO:2000573	positive regulation of DNA biosynthetic process	4.30E-02
			GO:0044711	single-organism biosynthetic process	4.30E-02
			GO:0033979	box H/ACA snoRNA metabolic process	4.30E-02
			GO:0090669	telomerase RNA stabilization	4.30E-02
10	9	LT=High	GO:0030593	neutrophil chemotaxis	2.31E-03
			GO:1990266	neutrophil migration	2.31E-03
			GO:0071621	granulocyte chemotaxis	2.31E-03
			GO:0097530	granulocyte migration	2.42E-03
			GO:0097529	myeloid leukocyte migration	5.49E-03
12	8	i=Moderate, L=High	GO:0051235	maintenance of location	4.62E-02
			GO:0034120	positive regulation of erythrocyte aggregation	4.62E-02
			GO:0060627	regulation of vesicle-mediated transport	4.62E-02
			GO:0045185	maintenance of protein location	4.62E-02
			GO:0051651	maintenance of location in cell	4.62E-02

13	**7**	**LT=Moderate, L=High**	GO:0032612	interleukin-1 production	1.12E-02
			GO:0072682	eosinophil extravasation	1.12E-02
			GO:1904458	regulation of substance P secretion	1.12E-02
			GO:1904496	positive regulation of substance P secretion, neurotransmission	1.12E-02
			GO:1904335	regulation of ductus arteriosus closure	1.12E-02
14	**7**	**LT=High, T=High**	GO:0090505	epiboly involved in wound healing	9.81E-03
			GO:0044319	wound healing, spreading of cells	9.81E-03
			GO:0090504	epiboly	9.81E-03
			GO:0002011	morphogenesis of an epithelial sheet	2.27E-02
			GO:0060356	leucine import	2.67E-02
15	**7**	**i=Moderate, T=Low**	GO:0071718	sodium-independent icosanoid transport	2.13E-02
17	**6**	**i=High, T=High**	GO:0001676	long-chain fatty acid metabolic process	1.75E-02
			GO:0036111	very long-chain fatty-acyl-CoA metabolic process	1.75E-02
			GO:0033559	unsaturated fatty acid metabolic process	1.75E-02
			GO:0072330	monocarboxylic acid biosynthetic process	3.36E-02
			GO:0036112	medium-chain fatty-acyl-CoA metabolic process	3.36E-02
18	**5**	**LT=Moderate**	GO:0006953	acute-phase response	2.24E-02
			GO:1904445	negative regulation of establishment of Sertoli cell barrier	3.05E-02
			GO:1904444	regulation of establishment of Sertoli cell barrier	3.05E-02
			GO:0002526	acute inflammatory response	4.53E-02
19	**5**	**i=High, L=High, T=Moderate**	GO:0001895	retina homeostasis	2.56E-02
20	**4**	**Equal in all**	GO:0001869	negative regulation of complement activation, lectin pathway	2.46E-02
			GO:0001868	regulation of complement activation, lectin pathway	2.46E-02
			GO:0032489	regulation of Cdc42 protein signal transduction	2.46E-02
			GO:0051056	regulation of small GTPase mediated signal transduction	2.46E-02
			GO:0038027	apolipoprotein A-I-mediated signaling pathway	2.46E-02
21	**4**	**i= Low, LT=Low, T=Moderate**	GO:0002687	positive regulation of leukocyte migration	2.20E-02
			GO:0014739	positive regulation of muscle hyperplasia	2.20E-02
			GO:0002685	regulation of leukocyte migration	2.20E-02
			GO:0002274	myeloid leukocyte activation	2.20E-02
			GO:0014738	regulation of muscle hyperplasia	2.20E-02
22	**4**	**LT=Low**	GO:0006744	ubiquinone biosynthetic process	4.25E-02
			GO:0006743	ubiquinone metabolic process	4.25E-02
			GO:1901663	quinone biosynthetic process	4.25E-02
			GO:0034453	microtubule anchoring	4.25E-02
			GO:0071294	cellular response to zinc ion	4.25E-02
25	**4**	**i=Low, L=High, T=Low**	GO:0006656	phosphatidylcholine biosynthetic process	2.41E-02
			GO:0019433	triglyceride catabolic process	2.41E-02
			GO:0046464	acylglycerol catabolic process	2.41E-02
			GO:0046461	neutral lipid catabolic process	2.41E-02
			GO:0046503	glycerolipid catabolic process	2.63E-02
27	**4**	**LT=High**	GO:0042986	positive regulation of amyloid precursor protein biosynthetic process	1.80E-02
			GO:0042983	amyloid precursor protein biosynthetic process	1.80E-02
			GO:0042984	regulation of amyloid precursor protein biosynthetic process	1.80E-02
			GO:0034379	very-low-density lipoprotein particle assembly	1.80E-02
			GO:0010878	cholesterol storage	1.80E-02

Table 12. GSE52894 co-expressed cluster profiles with associated gene ontologies. Transcript-to-transcript co-expression analysis of 1171 probesets differentially regulated in TolMoDCs compared to at least one other MoDC condition, using Graphia Pro (Pearson correlation r = 0.93, MCL = 1.7), identified 28 clusters. Table includes clusters which were associated with specific biological processes identified in Toppgene (adj.p-value=<0.05), with the top 5 displayed. Clusters were annotated with number of genes in each cluster and with their general expression profile across MoDC conditions (i=iMoDC, L=LPSMoDC, LT=LPS-TolMoDC, T=TolMoDC).

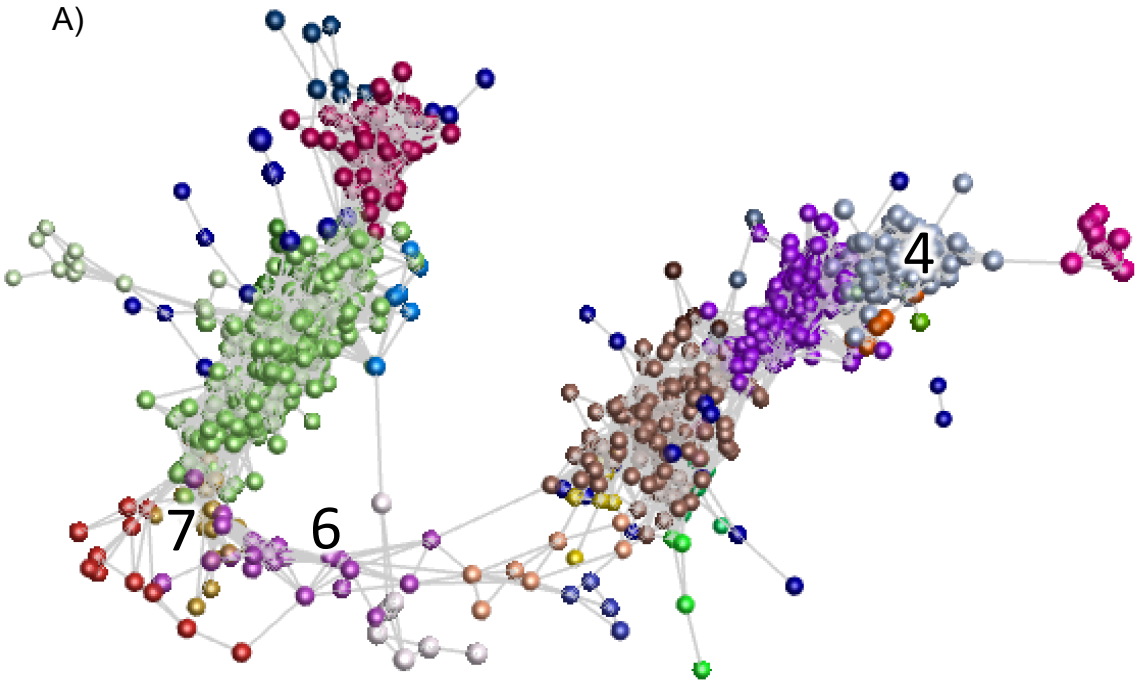
A)
4
7
6

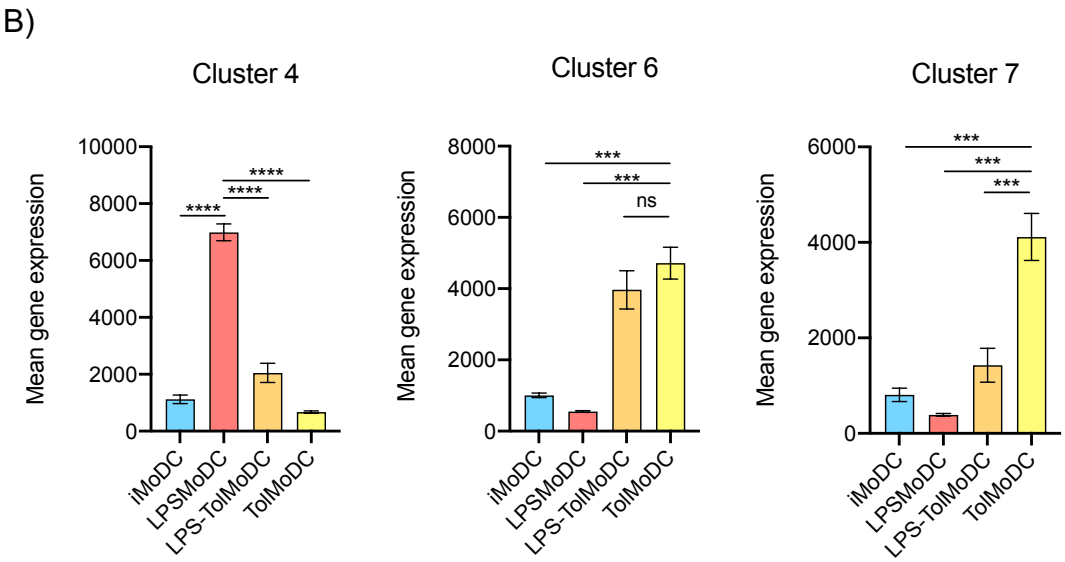
B)
Cluster 4
Cluster 6
Cluster 7
Mean gene expression
10000
8000
6000
4000
2000
0
****
****
****
***
***
ns
***
***
***
iMoDC
LPSMoDC
LPS-TolMoDC
TolMoDC

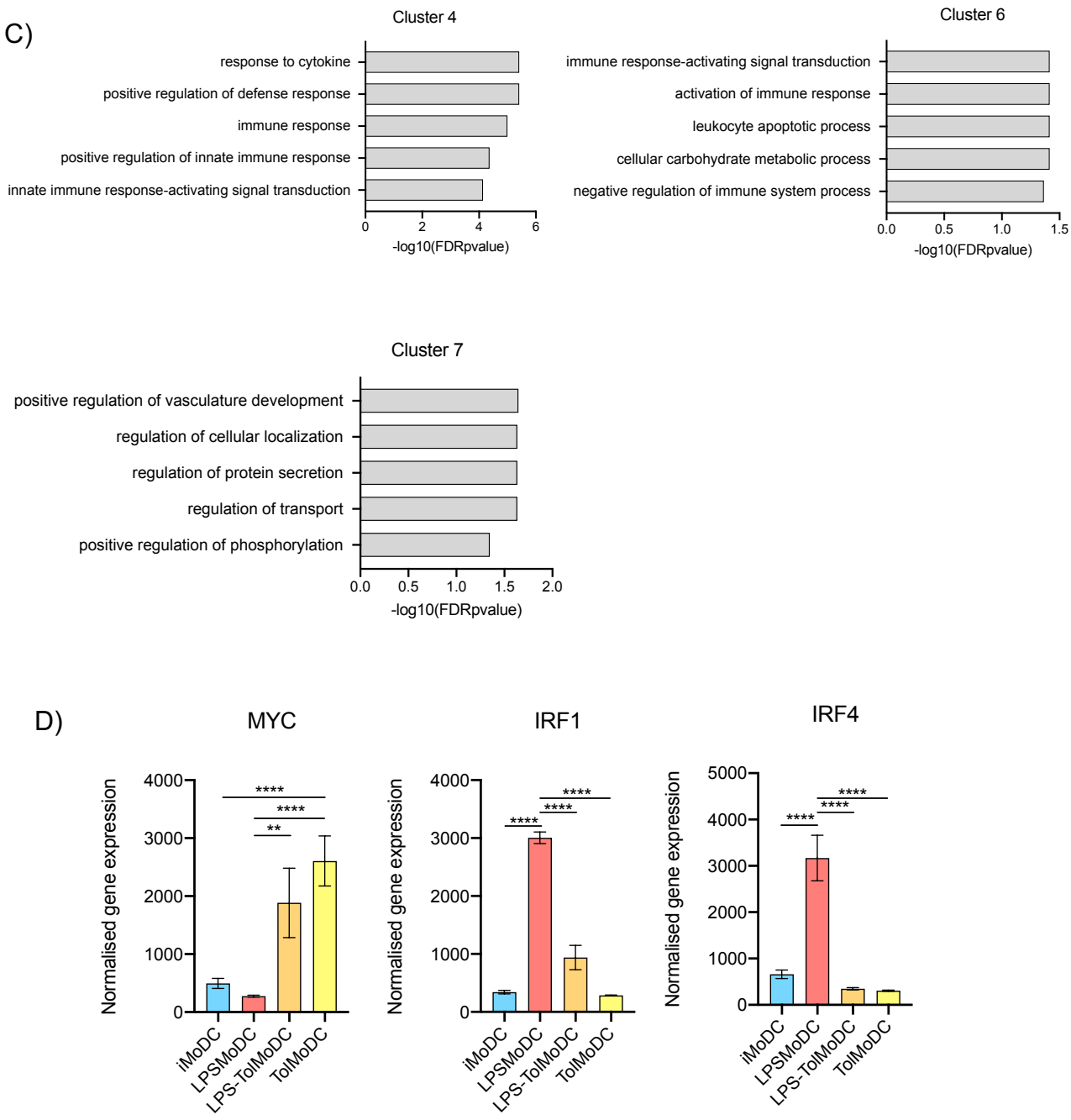

Figure 11. GSE52894 MoDC gene co-expression network analysis. A) Transcript-to-transcript co-expression analysis of 1171 probesets differentially regulated in TolMoDCs compared to atleast one other MoDC condition, using Graphia Pro (Pearson correlation r = 0.93, MCL = 1.7). 3 clusters were highlighted as having an expression profile linked to the regulation of tolerance (Clusters 4,6 and 7, labelled on plot). Lines (edges) represent the similarity between transcript expression; circles (nodes) represent genes. **B)** Mean (±SD) cluster expression values across the different MoDC conditions. **C)** Cluster Toppgene gene ontology analysis for the 69, 20 and 23 genes in clusters 4, 6 and 7, respectively (-log10FDRPvalues). **D)** Mean (±SD) expression of TFs MYC (Cluster 6), IRF1 and IRF4 (Cluster 4) across different MoDC conditions. p-values = *<0.05, **<0.01, ***<0.001, ****<0.0001, unpaired T-test.

Dataset GSE117946 was explored using the same analysis pipeline. After Limma DEG analysis comparing IL10MoDC to all other MoDC conditions, 8544 genes were subsequently submitted to co-expression analysis in Graphia Pro (Pearson correlation r=0.93, MCL=1.7) (**Figure 12A**). Over 100 clusters were identified, leading to us to focus on clusters containing at least 20 genes (**Table 13**). The largest clusters displaying one of the cluster profiles of interested identified during analysis of GSE52894, included clusters 1, 3 and 6 (**Figure 12B**). Cluster 6 which contained 82 genes, was upregulated in IL10MoDCs only. However, its only associated ontology after Toppgene gene ontology analysis, was G protein-coupled purinergic nucleotide receptor signalling pathway (adj.p-value=4.3E-2). Cluster 3, containing 395 genes was significantly upregulated in IL10MoDCs and LPS-IL10MoDCs compared to iMoDCs and LPSMoDCs. Gene ontology analysis found associations with myeloid leukocyte activation (adj.p-value=1.3E-12), neutrophil activation (adj.P-value=1.6E-12), vesicle organisation (adj.P-value=1.8E-12) and the immune effector process (adj.p-value=6.7E-8). Despite no specific associations with immune tolerance, this cluster which was specifically upregulated in all IL10 exposed MoDC, contained the TF *MYC* (**Figure 12C**). Similar to GSE52894, a large LPSMoDC upregulated cluster (cluster 1) was detected, which contained 1422 genes. This cluster was associated with response to virus (adj.p-value=1.1E-17), protein ubiquitination (adj.p-value=2.6E-16), response to cytokines (adj.p-value=7.5E-15) and innate immune response (adj.p-value=7.6E-11). Included in cluster 1, was the TFs *IRF1* and *IRF4*, again highlighting their association with the regulation of DC immunogenic responses (**Figure 12D**).

Cluster	No. of Genes	Cluster Profile	ID	Name	FDR B&H
1	1422	L=High	GO:0070647	protein modification by small protein conjugation or removal	1.07E-17
			GO:0009615	response to virus	1.07E-17
			GO:0016567	protein ubiquitination	2.62E-16
			GO:0032446	protein modification by small protein conjugation	8.19E-16
			GO:0045087	innate immune response	7.64E-11
2	426	i=High, IL10=High	GO:0048006	antigen processing and presentation, endogenous lipid antigen via MHC class Ib	3.69E-02
			GO:0048007	antigen processing and presentation, exogenous lipid antigen via MHC class Ib	8.34E-02
			GO:0048003	antigen processing and presentation of lipid antigen via MHC class Ib	8.34E-02
			GO:0006629	lipid metabolic process	1.46E-01
			GO:1903463	regulation of mitotic cell cycle DNA replication	2.90E-01
3	395	i=Moderate/High, L-IL10=High, IL10=High	GO:0002274	myeloid leukocyte activation	1.32E-12
			GO:0042119	neutrophil activation	1.64E-12
			GO:0036230	granulocyte activation	1.64E-12
			GO:0016050	vesicle organization	1.78E-12
			GO:0002252	immune effector process	6.71E-08
4	227	i=High, L-IL10=Moderate/High, IL10=High	GO:0016050	vesicle organization	1.83E-07
			GO:0002274	myeloid leukocyte activation	3.34E-05
			GO:0002446	neutrophil mediated immunity	3.34E-05
			GO:0090174	organelle membrane fusion	3.34E-05
			GO:0048284	organelle fusion	4.47E-05
5	68	L=High, L-IL10=High	GO:0009607	response to biotic stimulus	2.31E-06
			GO:0098542	defense response to other organism	2.31E-06
			GO:0051707	response to other organism	2.31E-06
			GO:0043207	response to external biotic stimulus	2.31E-06
			GO:0034097	response to cytokine	7.56E-06
6	82	IL10=High	GO:0002757	immune response-activating signal transduction	4.27E-02
7	56	L-IL10=High	GO:0071216	cellular response to biotic stimulus	7.44E-03
			GO:0071222	cellular response to lipopolysaccharide	1.53E-02
			GO:0071219	cellular response to molecule of bacterial origin	1.53E-02
			GO:0060907	positive regulation of macrophage cytokine production	1.53E-02
			GO:0002684	positive regulation of immune system process	1.77E-02
8	50	L-IL10=High	GO:0010273	detoxification of copper ion	3.01E-05
			GO:1990169	stress response to copper ion	3.01E-05
			GO:0061687	detoxification of inorganic compound	3.01E-05
			GO:0097501	stress response to metal ion	3.01E-05
			GO:0046688	response to copper ion	3.01E-05
9	46	L-IL10=Moderate, IL10=Moderate	GO:1904351	negative regulation of protein catabolic process in the vacuole	2.30E-02
			GO:1905166	negative regulation of lysosomal protein catabolic process	2.30E-02
			GO:0016050	vesicle organization	3.13E-02
			GO:0001775	cell activation	3.13E-02
			GO:0001816	cytokine production	3.13E-02
13	32	i=High, IL10=Moderate	GO:0120032	regulation of plasma membrane bounded cell projection assembly	9.07E-03
			GO:0060491	regulation of cell projection assembly	9.07E-03
21	22	LT=Moderate, L=High	GO:0019730	antimicrobial humoral response	4.08E-06
			GO:0042742	defense response to bacterium	3.30E-05
			GO:0002274	myeloid leukocyte activation	1.11E-04
			GO:0045321	leukocyte activation	1.11E-04
			GO:0042119	neutrophil activation	1.11E-04
22	21	LT=High, T=Moderate	GO:0007040	lysosome organization	1.82E-02
			GO:0080171	lytic vacuole organization	1.82E-02

Table 13. GSE117946 co-expressed cluster profiles with associated gene ontologies. Transcript-to-transcript co-expression analysis of 8544 probesets differentially regulated in IL10MoDCs compared to at least one other MoDC condition, using Graphia Pro (Pearson correlation r = 0.93, MCL = 1.7), identified over 100 clusters. Clusters with at least 20 genes and with specific associated ontologies identified using Toppgene (adj.p-value=<0.05, top 5 ontologies displayed) were included in the table. Clusters were annotated with number of genes in each cluster and with their general expression profile across MoDC conditions (i=iMoDC, L=LPSMoDC, L-IL10=LPS-IL10MoDC, IL10=IL10MoDC).

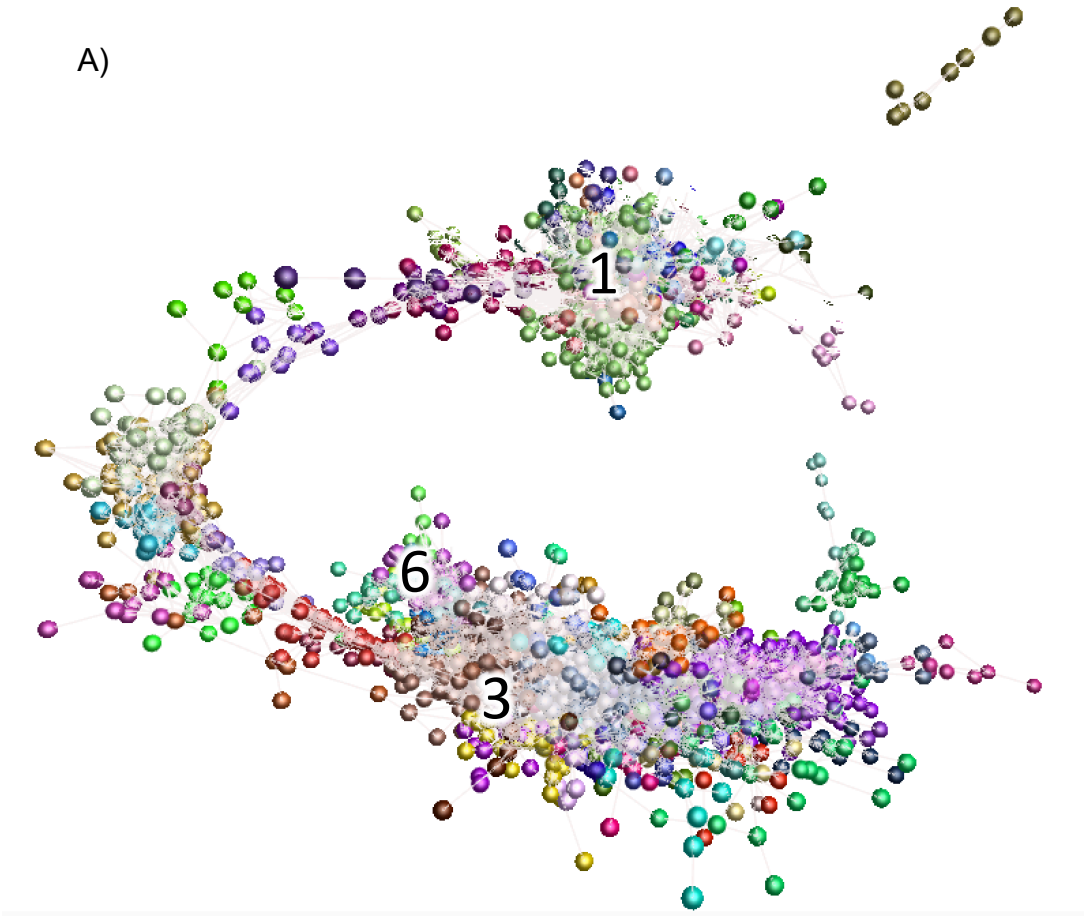
A)
1
6
3

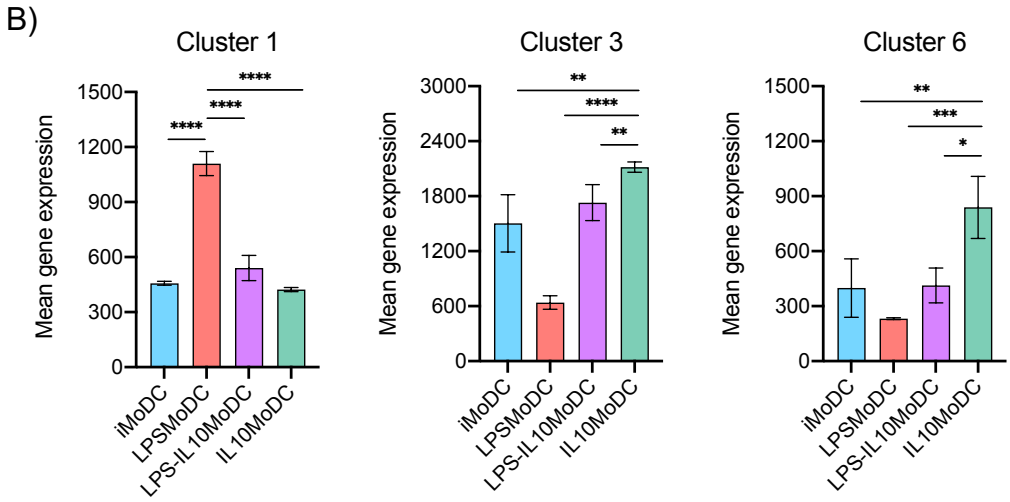
B)
Cluster 1
Cluster 3
Cluster 6
Mean gene expression
iMoDC
LPSMoDC
LPS-IL10MoDC
IL10MoDC

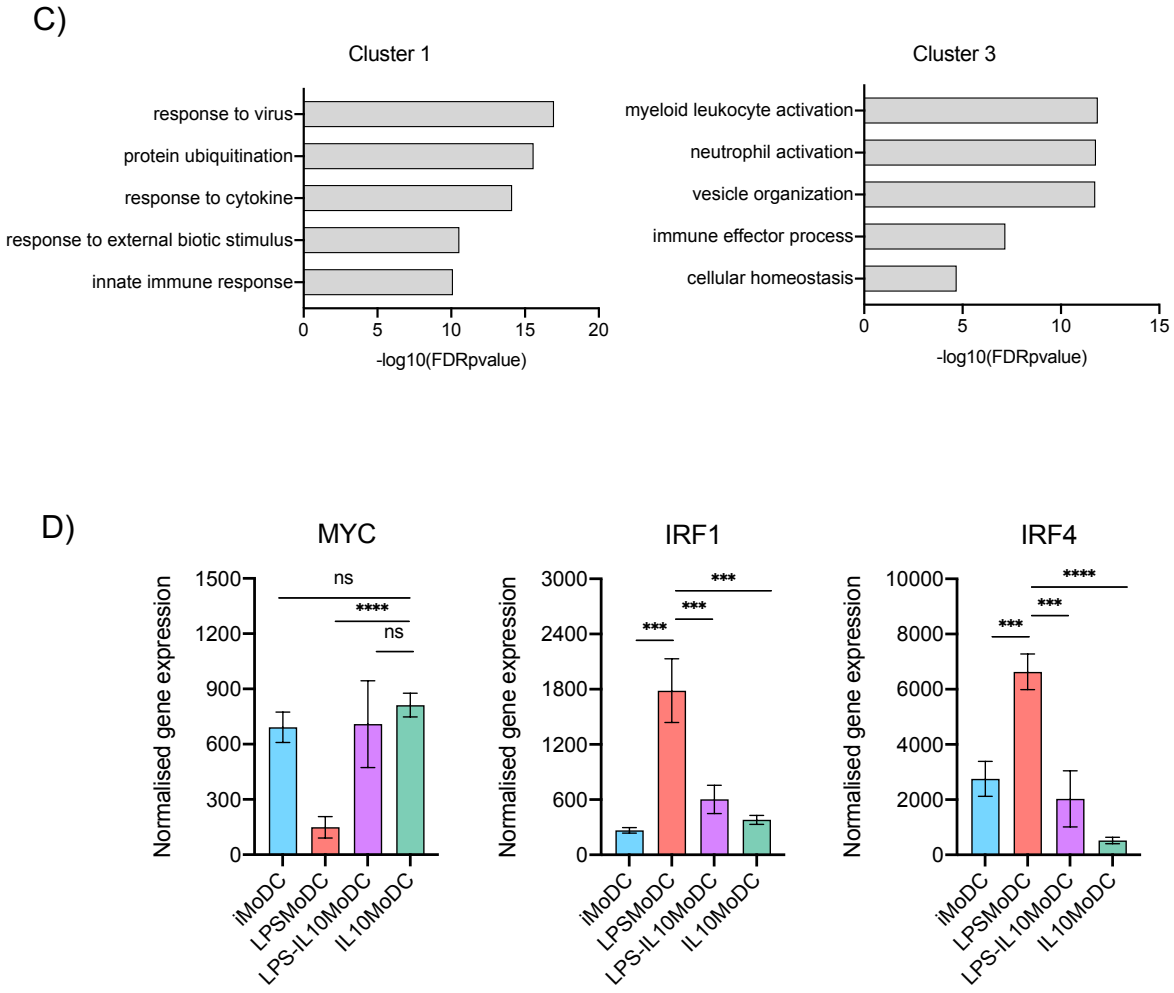

Figure 12. GSE117946 MoDC gene co-expression network analysis. A) Transcript-to-transcript co-expression analysis of 8544 probesets differentially regulated in IL10MoDCs compared to at least one other MoDC condition, using Graphia Pro (Pearson correlation r = 0.93, MCL = 1.7). Clusters 1-100 are displayed. 3 clusters were highlighted as having an expression profile linked to the regulation of tolerance (Clusters 1, 3 and 6, labelled on plot). Lines (edges) represent the similarity between transcript expression; circles (nodes) represent genes. **B)** Mean (±SD) cluster expression values for cluster 1, 3 and 6 across the different MoDC conditions. **C)** Cluster Toppgene gene ontology analysis for the 1422, 395 and 82 genes in clusters 1, 3 and 6, respectively (-log10FDRPvalues). **D)** Mean (±SD) expression of TFs MYC (Cluster 3), IRF1 and IRF4 (Cluster 1) across different MoDC conditions. p-values = *<0.05, **<0.01, ***<0.001, ****<0.0001, unpaired T-test.

Having identified corresponding immunogenic clusters, 4 (GSE52894) and 1 (GSE117946) and tolerogenic clusters, 6 (GSE52894) and 3 (GSE117946) from the two datasets, the cluster gene lists were compared using Venn diagrams (**Figure 13A**). Additionally, tolerogenic MoDC cluster genes were compared to 147 upregulated genes identified in published analyses (PMID:29109727) comparing tolerogenic monophosphoryl lipid A (MPLA) and dexamethasone (MPLA-Dex) stimulated MoDC to unstimulated MoDC. For immunogenic clusters, there was an overlap of 45 genes from the 69 genes (cluster 4) and 1422 (cluster 1) genes contributed by GSE52894 and GSE117946, respectively. As well as the TFs *IRF1* and *IRF4*, common genes included *NFKB1, CD80, CCR7, BIRC3, STAT3*, *STAT5A* and interestingly, the tolerogenic associated protein *IDO1*. Gene ontology analysis for the 45 common genes again resulted in associations with response to cytokine (adj.p-value=1.2E-6) and positive regulation of immune system process (adj.p-value=2.4E-6, **Figure 13B**). Intriguingly, negative regulation of immune system process (adj.p-value=1.7E-5) was also identified as an associated ontology, due to the presence of *IRF1, IRF4, IDO1, CD80, STAT5A, CASP3, ID2, TRAFD1, SAMSN1* and *DHX58*. Minimal overlap was identified in tolerogenic clusters with just 1 common gene, *MYC,* common between the 20 genes (cluster 6, TolMoDC) from GSE52894, the 395 genes (cluster 3, IL10MoDC) from GSE117946 and the 147 MPLA-Dex MoDC upregulated genes. *COQ2* and *PRNP* were common between TolMoDCs and IL10MoDCs only and *CD14* was common between TolMoDCs and MPLA-Dex MoDCs only. 18 genes were common between IL10MoDCs and MPLA-Dex MoDCs, including *C1QA, C1QB, FCGR2A, FCGR2B* and *CCL13.* Gene ontology analysis for these 18 genes revealed associations with monocyte chemotaxis (adj.p-value=7.3E-5), positive regulation of immune system process (adj.p-value=2.8E-4) and negative regulation of DC antigen processing and presentation (adj.p-value=2.6E-2). Overall, whilst a common TF was identified in both datasets, the overall transcriptomic programme of tolerance differed.

In summary, LPSMoDCs upregulate immunogenic and inflammatory associated genes, which correlates with increased expression of *IRF1* and *IRF4.* Interestingly, LPS also upregulated a tolerogenic gene module, identified in both datasets. However, the transcriptomic modulation by MoDCs exposed to tolerogenic factors appears to be largely specific to individual stimuli. Still, upregulated expression of *MYC* was identified in TolMoDCs, IL10MoDCs and MPLA-Dex MoDCs, leading us to hypothesise its importance for regulating the tolerogenic programmes in DCs.

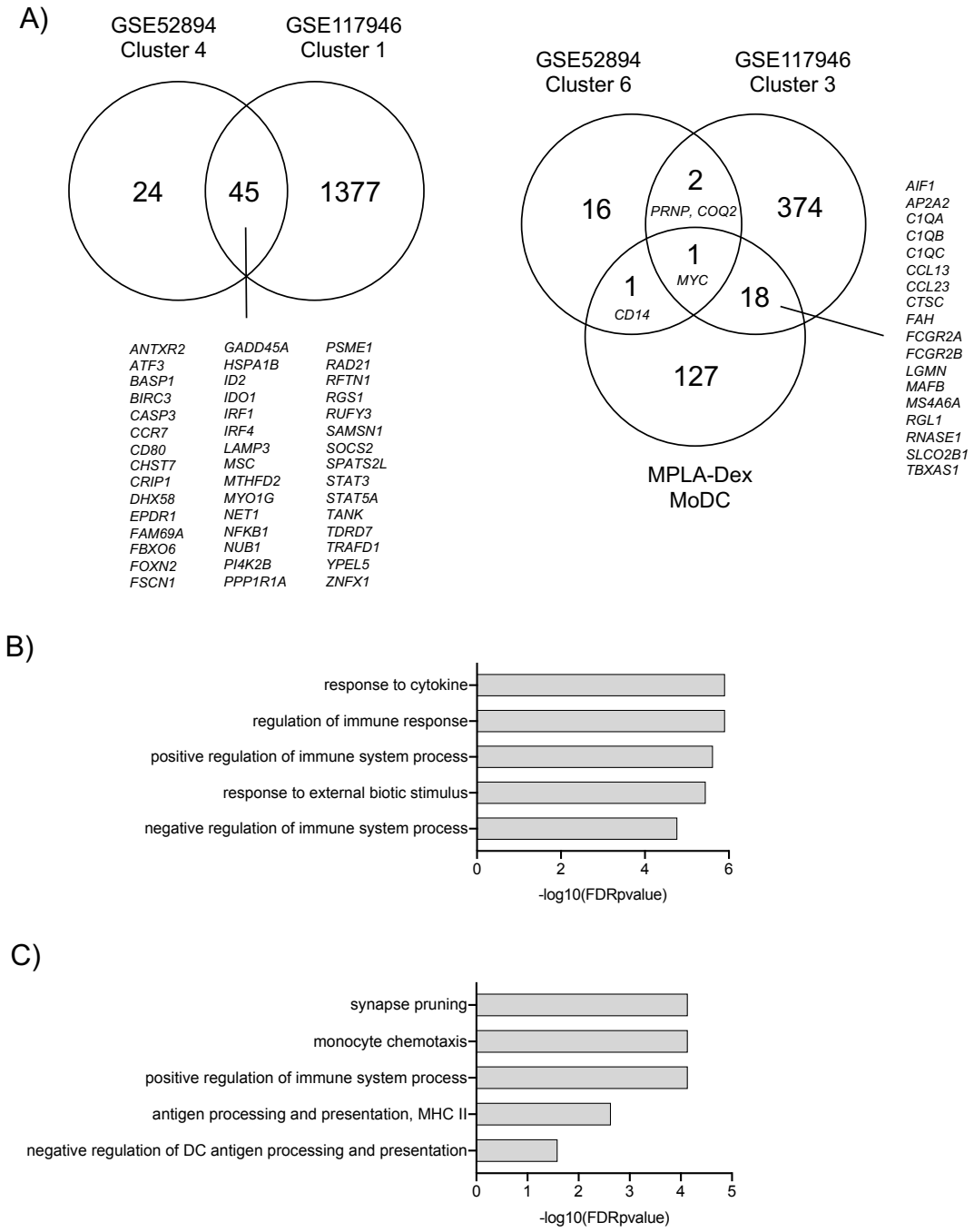

Figure 13. Comparisons between LPSMoDC upregulated and tolerogenic MoDC upregulated clusters in both MoDC datasets, reveals a tolerogenic gene module shared between LPS stimulated MoDCs. **A)** Venn diagrams cross comparing gene lists for LPSMoDC cluster 4 (GSE52894) and cluster 1 (GSE117946) and tolerogenic MoDC cluster 6 (TolMoDCs, GSE52894), cluster 3 (IL10MoDCs, GSE117946) and 147 MPLA-Dex stimulated MoDC upregulated genes compared to unstimulated MoDC (PMID:29109727). **B)** Toppgene gene ontology analysis for the 45 genes commonly expressed in LPSMoDC cluster 4 (GSE52894) and cluster 1 (GSE117946, -log10FDRPvalues). **C)** Toppgene gene ontology analysis for the 18 genes commonly expressed in TolMoDC cluster 3 (GSE117946) and MPLA-Dex MoDC (-log10FDRPvalues).

3.2.2 *In silico* modelling of IRF-GRN confirms importance of *IRF1* and *IRF4* for DC immunogenic function

Analysis of MoDC datasets identified *IRF1* and *IRF4* expression as a common feature for immunogenic DC expression profiles. *IRF1* and *IRF4* are both key components of an IRF-GRN mediating LC immune response, assembled by Polak et al. (Polak *et al.*, 2017). The LC IRF-GRN has been assembled as a Petri-net model amenable to dynamic *in silico* simulations which predicts immune response outcomes from TF gene expression data (**Figure 14A**). Tokens run along the network from TF inputs as expression data, through TF associated DNA binding motifs (ISRE, AICE, EICE), to output genes associated with specific immunological processes. Whilst this model was specifically developed for *in silico* modelling of LC immunological outcomes, the similar characteristics between LCs and other DC populations suggest the predicted biological outcomes could be similar. To test the uniformity between immunogenic transcriptional programmes of MoDCs and LCs, gene expression values for interferon regulatory factor family TFs *IRF1, IRF4, IRF8* and IRF binding partners; the AP-1 TF family (*cJUN, cFOS, BATF, BATF3*) and the ETS TF family (*ELF1, ELF2, ELF4, ELK1, ELK3, ETS1, ETS2, EHF, ETV3, ETV6*, *GABPα*) from the MoDC microarray datasets, was input into the model for *in silico* simulation.

For GSE52894, the model correctly predicted the gene expression profile displayed by the different MoDCs conditions, for some genes (*TAP1, TAP2, PSME1, PSME2, CD80, CD86, TAPBPL, PSMB10, IL15 and HLA-A, B, C, E, F, G* and *H*) included in the output from the ISRE and AICE network nodes, termed 'Programme A' (**Figure 14B**). 'Programme A' genes were elevated in MoDC stimulated with LPS and are associated with MHC I antigen processing and presentation and Th1 T-cell induction. *In silico* modelling therefore linked the increased expression of *IRF1* and *IRF4* induced by inflammatory LPS signalling to an increase in immunogenic DC biological processes. It also suggested that immunogenic programmes were similarly regulated by the IRF-GRN between MoDCs and LCs. The *in silico* model however, could not correctly predict gene expression for genes included in the output from EICE, termed 'Programme B', associated with MHC II antigen processing and presentation and Th2 T-cell induction (**Figure 14C**). The regulation of 'Programme B' therefore differed between MoDCs and LCs.

Unlike GSE52894, the GSE117946 MoDC dataset performed poorly at predicting gene expression values for all genes in both 'Programme A' (**Figure 14D**) and 'Programme B' (**Figure 14E**). The same genes that were correctly predicted in GSE52894 are displayed for comparison. *In silico* modelling predicted high expression of 'Programme A' genes in LPSMoDC, IL10MoDC and LPS-IL10MoDC, however expression followed a similar pattern to that seen in GSE52894, where expression was

only elevated in LPS stimulated MoDCs. Only *TAPBPL* displayed some similarity in the pattern of expression between model prediction and microarray data.

Overall our *in silico* simulations of MoDC gene expression data (GSE52894), could link high expression of *IRF1* and *IRF4* to the induction of some immunogenic DC output genes. It also highlighted that at least some immunogenic pathways are similarly regulated between MoDCs and LCs. However, the LC IRF-GRN model was unable to correctly predict MoDC gene expression after stimulation with IL10 (GSE117946), indicating that GRN regulation was stimuli specific.

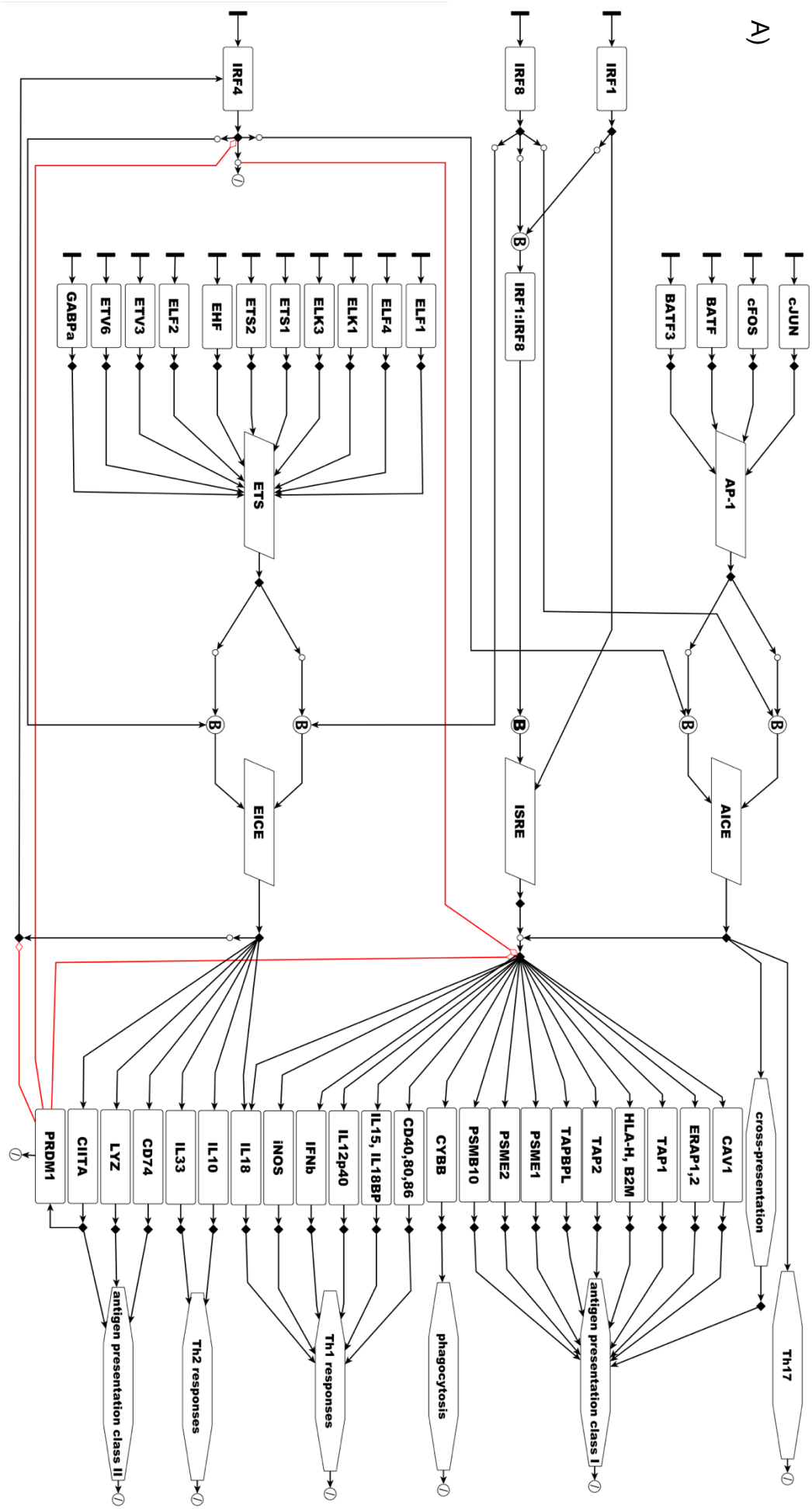
A)
IRF4
IRF8
IRF1
IRF1:IRF8
cJUN
cFOS
BATF
BATF3
AP-1
GABPa
ETV6
ETV3
ELF2
EHF
ETS2
ETS1
ELK3
ELK1
ELF4
ELF1
ETS
EICE
ISRE
AICE
PRDM1
CIITA
LYZ
CD74
IL33
IL10
IL18
iNOS
IFNb
IL12p40
IL15, IL18BP
CD40,80,86
CYBB
PSMB10
PSME2
PSME1
TAPBPL
TAP2
HLA-H, B2M
TAP1
ERAP1,2
CAV1
cross-presentation
antigen presentation class II
Th2 responses
Th1 responses
phagocytosis
antigen presentation class I
Th17

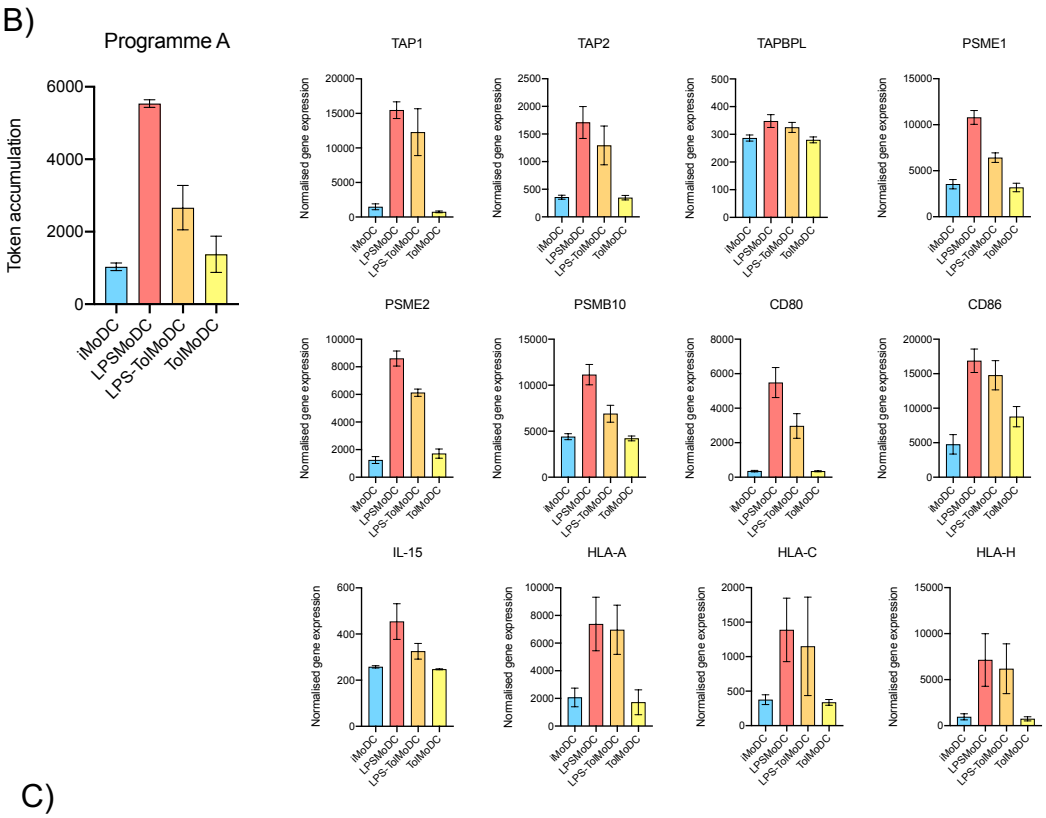
B)
Programme A
Token accumulation
6000
4000
2000
0
iMoDC
LPSMoDC
LPS-TolMoDC
TolMoDC
TAP1
TAP2
TAPBPL
PSME1
PSME2
PSMB10
CD80
CD86
IL-15
HLA-A
HLA-C
HLA-H
Normalised gene expression

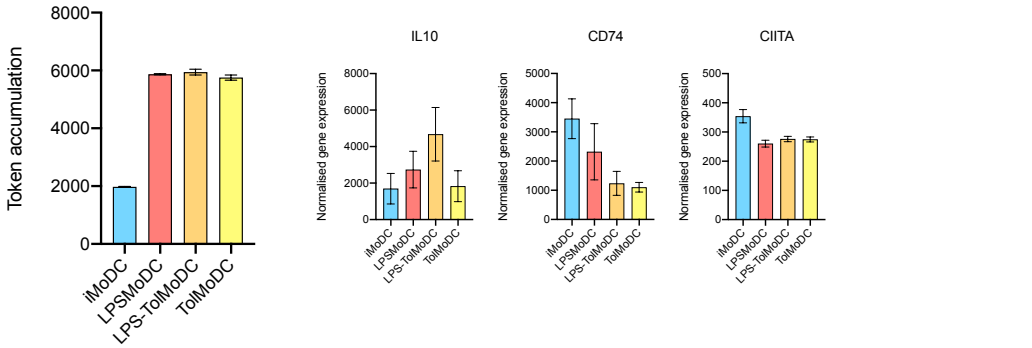
C)
Programme B
Token accumulation
8000
6000
4000
2000
0
iMoDC
LPSMoDC
LPS-TolMoDC
TolMoDC
IL10
CD74
CIITA
Normalised gene expression

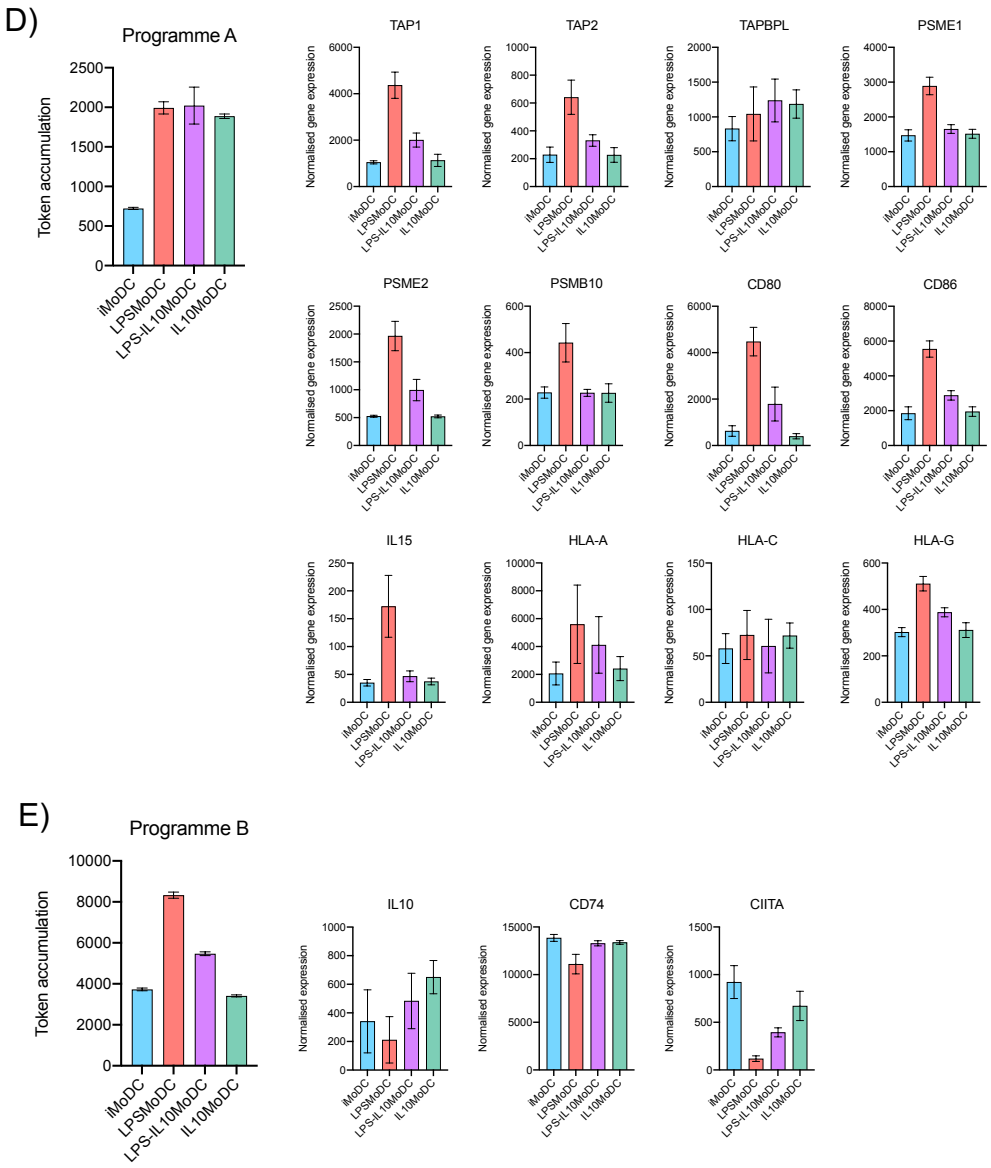

Figure 14. IRF-GRN in silico simulation identifies *IRF1* and *IRF4* as important regulators of MoDC immune activation. A) Structure of the LC IRF-GRN constructed by Polak et al.(Polak *et al.*, 2017) with the TF input nodes on the left. Means of TF expression values for triplicates of each MoDC condition were used as starting tokens for the network. Tokens run along IRF-GRN, through TF associated DNA binding motifs (ISRE, AICE, EICE), towards the resulting gene output and immune response nodes on the right. Black edges indicate positive edges, whilst red edges indicate inhibitory interactions. GSE52894 microarray data *in silico* predictions of 'Programme A' **B)** and 'Programme B' **C)** output genes, with actual gene expression data from microarray displayed alongside. GSE117946 microarray data *in silico* predictions of 'Programme A' **D)** and 'Programme B' **E)** output genes, with actual gene expression data from microarray displayed alongside. Model parameters=100 time blocks, 500 runs. Mean token values from triplicate simulations, in which the means of the final 10-time blocks were calculated, are displayed.

3.2.3 Inclusion of *MYC*-regulated module in IRF-GRN network allows simulation of tolerogenic regulation in MoDCs

Having established the power of the IRF-GRN model to predict immunogenic 'Programmed A' in GSE52894 MoDCs, the model was then edited to include input from *MYC*, to investigate potential mechanisms of tolerogenic regulation. Due to the complete switch in *IRF1* and *IRF4* expression compared to *MYC* between immunogenic and tolerogenic MoDCs, hypothetical mutually inhibitory edges between *MYC* and either *IRF1* and *IRF4,* or both, were modelled *in silico* **(Figure 15, Figure 16A)**. First, the plausibility of such regulatory interactions was tested. For the regulatory interaction to be deemed plausible, inclusion of *MYC*, into the already established GRNs of each MoDC condition, using transcriptomic expression data from each respective MoDC condition, would result in no change to the *in silico* predicted expression of 'Programme A' from **Figure 14B.** If *MYC* inclusion detrimentally effected the *in silico* prediction then this would suggest that an interaction with *IRF1* and *IRF4* was unlikely. For all 3 regulatory interactions tested (*MYC-IRF1, MYC-IRF1, MYC-IRF1/IRF4)*, the predicted expression profile of 'Programme A' remained relatively unchanged and *MYC* inclusion therefore did not negatively alter the accuracy of the model. Whilst all simulations were incredibly similar, the model with inhibitory edges between MYC and both IRF1 and IRF4 were utilised for downstream analysis. The decision to use this model was based on the higher token accumulation for LPS-TolMoDCs, which was more similar to the gene expression data of 'Programme A' genes. Also, *IRF1* and *IRF4* exhibit near identical profiles across MoDC conditions, which highly opposes changes in *MYC,* further supporting their association with a shared regulatory module.

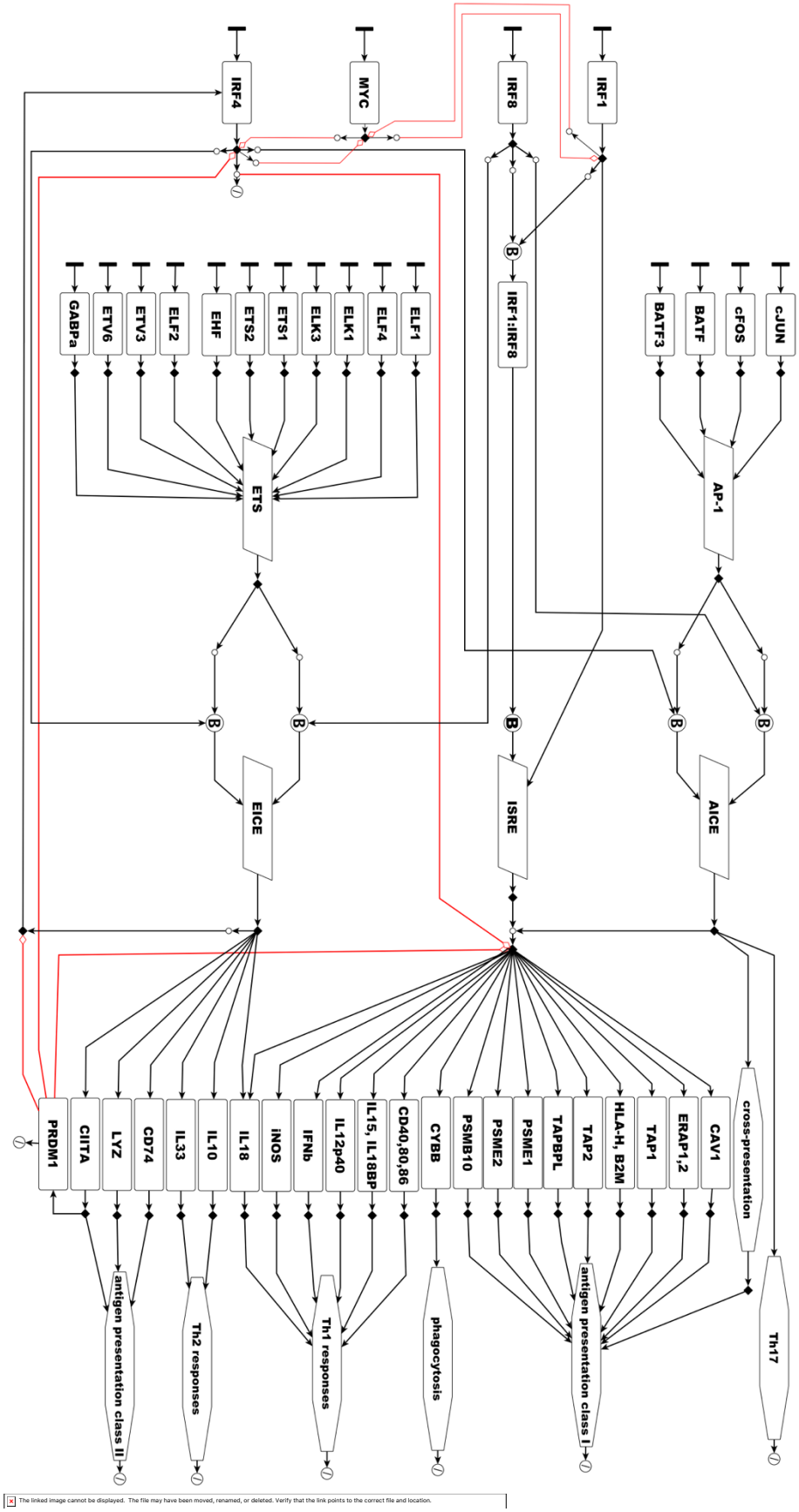

Figure 15. IRF-GRN Petri-net model with inclusion of *MYC*. Mutually inhibitory edges between *MYC* and both *IRF1* and *IRF4* were added to the model for in silico simulation of this hypothetical regulatory interaction. Petri-net graph was edited within yED software.

To test how fluctuations in *MYC* expression could alter MoDC expression profiles, *in silico* simulations were performed of the LPSMoDC IRF-GRN with *MYC* input values replaced with the high expression value from TolMoDCs. Correspondingly, *in silico* simulations of the TolMoDC IRF-GRN with *IRF1* and *IRF4* input values replaced with the high expression values from LPSMoDCs were performed **(Figure 16B)**. These perturbations allowed investigation into how immunogenic programmes could be switched to tolerogenic programmes and vice versa. *In silico* simulation of the LPSMoDC IRF-GRN with TolMoDC *MYC* expression values resulted in a decrease in the token accumulation at 'Programme A', resulting in a switch towards a more tolerogenic profile. Doubling of the TolMoDC *MYC* input was also modelled, to test how theoretical amplifications of inhibitory signalling, not accounted for with just the inclusion of MYC expression values, could affect model dynamics. As expected, doubling the input further enhanced the decrease in 'Programme A' token accumulation. Similarly, *in silico* simulation of the TolMoDC IRF-GRN with LPSMoDC *IRF1* and *IRF4* expression values resulted in an increase in token accumulations for 'Programme A', switching to a more immunogenic profile **(Figure 16C)**. Again, doubling of *IRF1* and *IRF4* expression values further enhanced these changes to a profile resembling the unmodified LPSMoDC *in silico* prediction. Overall, using IRF-GRN modelling a hypothetical inhibitory loop between *MYC* and *IRF1* and *IRF4* has been acknowledged that could describe how tolerogenic dexamethasone and VitD3 stimulated MoDCs switch to an immunogenic LPS stimulated MoDC profile and vice versa.

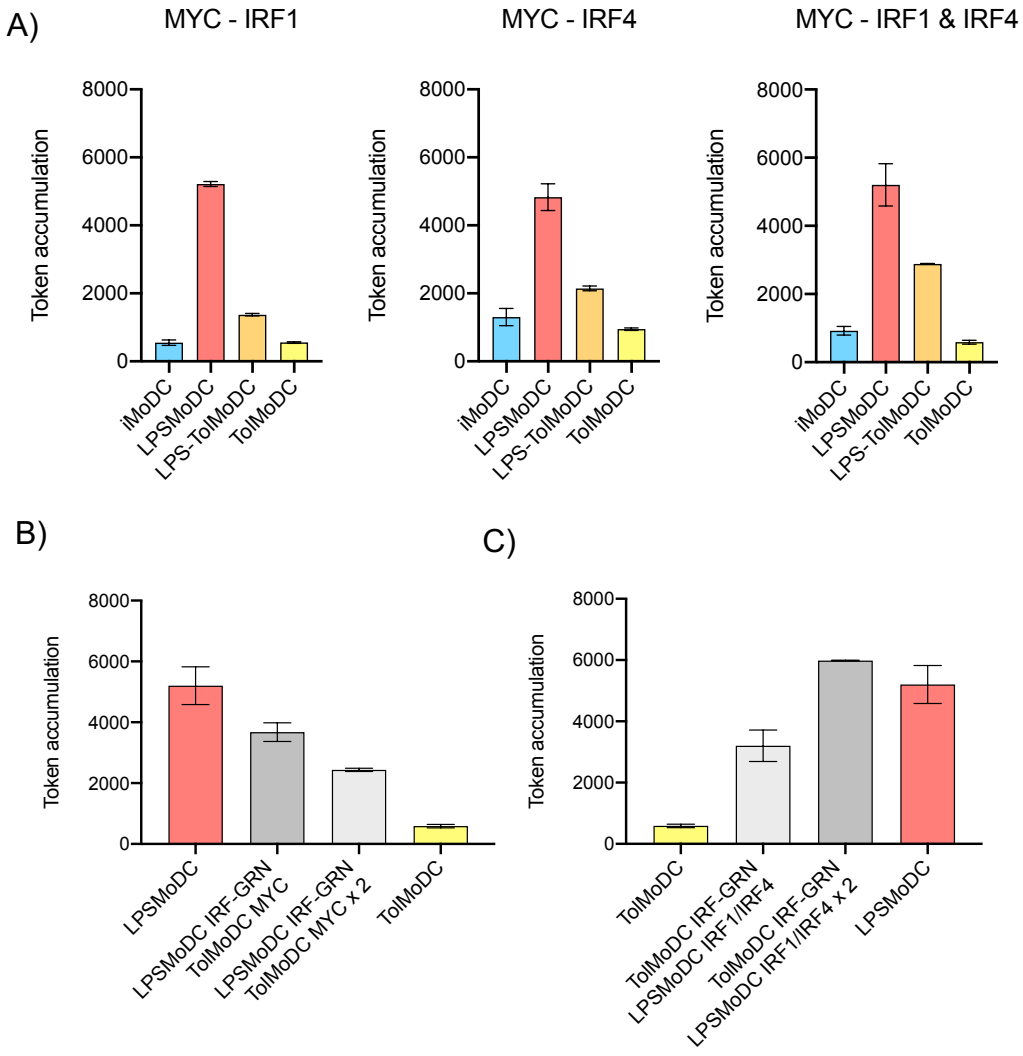

Figure 16. Integration of *MYC* into the IRF-GRN identifies a potential regulatory interaction with both *IRF1* and *IRF4*, which could explain the switch between tolerogenic and immunogenic states. **A)** Inhibitory interactions between *MYC-IRF1, MYC-IRF4* and *MYC-IRF1/IRF4* were modelled *in silico* and predicted expression profile of "Programme A" was assessed for comparison with unmodified network (Figure 8B). Mean *MYC* expression values from respective MoDCs were utilised as token input. Modification of **B)** the TolMoDC IRG-GRN to include LPSMoDC *IRF1* and *IRF4* expression values (1x and 2x) and **C)** the LPSMoDC IRF-GRN to included TolMoDC *MYC* expression values (1x and 2x). Model parameters=100 time blocks, 500 runs. Mean token values from triplicate simulations, in which the means of the final 10-time blocks were calculated, are displayed.

3.3 Discussion

3.3.1 Transcriptomic programmes of MoDCs induced to promote tolerance are defined by the suppression of inflammatory stimuli responsive genes, but lack universal tolerogenic gene signature

Suppressive alterations of T cell state mediated by DC encounter can be actively tolerogenic, whereby DC actively delete self-reactive T cell or mediate conversion into Tregs. This differs from anergic responses, in which lack of DC co-stimulatory molecule expression leads to absent activation of T cells, or exhaustion, in which chronic overactivation of T cells by DC leads to functional hypo-responsiveness (Schietinger and Greenberg, 2014). To begin our investigation into transcriptional programmes specifically encoding tolerance in LCs, we sought to identify a universal mechanism by exploring model systems of DC tolerance. This was to identify potential transcriptomic profiles key to DC tolerogenic immune function and understand how gene expression was regulated under different stimulatory conditions and in particular, tolerogenic stimuli. Also, if gene regulation between MoDC and LC was revealed to be similar, then the highly versatile MoDC *in vitro* model could be utilised in downstream analyses.

Analysis of a microarray datasets (GSE52894, GSE117946) containing MoDCs unstimulated or after treatment with LPS, tolerogenic stimuli (dexamethasone and VitD3, IL10) or a combination of both LPS and tolerogenic stimuli, identified DC gene expression profiles associated with immunotolerance. Through our initial MDS plot, it was seen that tolerogenic stimulated MoDC (TolMoDC and IL10MoDC) transcriptomes were unique, clustering away from all other MoDCs in their respective datasets. In both datasets the tolerogenic stimulated MoDCs were most similar to iMoDCs, which may be expected due to evidence for tolerogenic inducing properties of DC when immature and inactivated (Mahnke *et al.*, 2002). The isolated clustering of TolMoDCs and IL10MoDCs however, indicates that a specific gene expression profile is triggered by tolerogenic stimuli, which endows the cells with enhanced tolerogenic characteristics. Within this gene expression profile, we believed key molecular coordinators underpinning tolerogenic function could be identified.

Using gene co-expression clustering analysis of the GSE52894 MoDC dataset, we identified a cluster of 20 genes (cluster 6), which had increased expression in both TolMoDC and LPS-TolMoDCs and were associated with negative regulation of immune system process through gene ontology, due to the presence of *MYC, CEBPB, PIK3AP1, CD14* and *PRNP*. The upregulation of these genes in both TolMoDCs and LPS-TolMoDCs showed the resistance of these genes to changes in gene expression after stimulation by LPS and could therefore represent core tolerogenic genes. In the GSE117946

MoDC dataset, a gene cluster upregulated in both IL10MoDC and LPS-IL10MoDC was identified (cluster 3), which although was associated with regulation of immune responses, a specific association with tolerogenic immunity was not identified. However, cluster 3 did contain *MYC,* again linking the expression of *MYC* to the regulation of tolerance. Furthermore, *MYC* expression is also upregulated in tolerogenic MoDCs stimulated with MPLA and dexamethasone (MPLA-Dex MoDC). Interestingly *MYC* has been associated with the induction of immune suppression in the context of cancer. MYC has been found to induce inhibitors of immunity, such *PD-L1* (Casey, Baylot and Felsher, 2017). High *MYC* expression in Burkitt lymphoma leads to suppression of type 1 IFN, correlating with reduced expression of inflammatory NFκB targets (Schlee *et al.*, 2007). Whilst the importance for *MYC* in driving functionality of Tregs has been recognised, the association with *MYC* expression and DC tolerance is unexplored (Saravia *et al.*, 2020).

Tolerogenic clusters 7 (GSE52894) and cluster 6 (GSE117946) had a less obvious impact on MoDC tolerance. Cluster 7 genes expression was suppressed after the addition of LPS in LPS-TolMoDCs, as were cluster 6 genes after LPS addition in LPS-IL10MoDCs. Therapeutic targeting of these genes to induce tolerance would therefore be ineffective, as their activation is not maintained in the presence of immunogenic signalling. Gene ontology of cluster 7 genes was associated with immune responses, suggesting some contribution to DC immune regulation. It is doubtful that immunogenic DCs and tolerogenic DCs represent completely static states, which are unable to change function in response to different environmental cues. The addition of danger signals such as LPS would shift the requirement in favour of immunogenic DC responses in a bid to clear infection, therefore requiring the suppression of tolerogenic DCs responses. Maintenance of tolerogenic function in response to harmful stimuli, such as LPS, could have detrimental effects and therefore the ability to down regulate tolerogenic genes may grant some fluidity, allowing DCs to change immune responses to fit their current requirements.

Whilst it is understandable that certain genes are upregulated during tolerogenic immune responses, it is also expected that certain inflammatory genes and pathways must be downregulated and suppressed. Cluster 4 (GSE52894), a larger cluster of 68 genes associated with inflammatory immune activation was upregulated in LPSMoDCs only. Although LPS-TolMoDCs showed a slight increase in expression of this cluster compared to iMoDCs and TolMoDCs, the tolerogenic stimuli was preventing the expression levels seen with LPS stimuli alone. This same pattern in expression was identified in cluster 1 (GSE117946). The expression of these genes must therefore be suppressed to maintain tolerance. A recurrent trait of genes upregulated by LPS exposure included the upregulation of IRF and NFκB TF family members, known mediators of DC development and maturation. Cluster 4 (GSE52894) genes included *IRF1, IRF4* and *NFKB1*. Cluster 1 (GSE177946) genes included *IRF1, IRF4, NFKB1, NKFB2, RELB* and *REL*. The IRF and NFκB family

were therefore highly associated with immunogenic DC activation which has been highlighted in previous studies. *IRF1* deletion in murine DC results in DC inability to adopt fully mature phenotypes skewing responses in IL-10 production and Treg cell induction (Gabriele *et al.*, 2006). *IRF4* is required for DC development and also mediates DC migration out of the skin (Bajana *et al.*, 2012). *IRF4* expression also determines DC immune regulation. Murine CD11b+ and human CD1c+ DCs which express IRF4 facilitate Th17 polarisation through IL-23 production (Schlitzer *et al.*, 2013). NFκB has diverse roles in coordinating the immune system. It controls the activity of diverse proinflammatory cytokines and maintains the activation, differentiation and survival of immune cell types, including DCs (Liu *et al.*, 2017),(Rescigno *et al.*, 1998). The activity of the IRF and NFκB family is also interlinked, with NFκB known to regulate *IRF4* expression (Gabriele and Ozato, 2007). Down regulation of these immune regulators is therefore an understandable requirement for tolerance. The key role for *IRF1, IRF4* and NFκB TFs during inflammatory processes, could imply that their down regulation is an observation seen across a variety of different dendritic cell types or even other immune cell types during immunotolerance. However, when LPS-induced programmes of both datasets were compared, a common tolerogenic gene module was identified through gene ontology analysis. Contributing to the annotation was *IRF1* and *IRF4.* In T cells, IRF1 modulation of the chromatin landscape has been shown to enhance the induction of IL10-producing type I Tregs in mice (Karwacz *et al.*, 2017). Likewise *IRF4*-deficient murine bone marrow DCs are also compromised in their affinity to induce Tregs (Vander Lugt, Riddell, Aly A. Khan, *et al.*, 2017). Interestingly, this suggests that both *IRF1* and *IRF4* are involved in mediating both immunogenic and tolerogenic immune responses and it therefore may not be as clear-cut for upregulation to only occur during immunogenic and inflammatory conditions. It is therefore unclear how such distinguishable responses by *IRF1* and *IRF4* are differentially regulated in DCs.

3.3.2 *In silico* modelling of IRF-GRN confirms importance of *IRF1* and *IRF4* for DC immunogenic function

Having used MoDC datasets to establish how DC gene expression profiles are determined by their immunological states or stimulatory conditions, we were able to identify *IRF1* and *IRF4* expression as a common feature for immunogenic DC expression profiles. To determine the involvement on *IRF1* and *IRF4* in mediating immunogenic responses in MoDCs we used Petri-net *in silico* modelling of the IRF-GRN, which was constructed to predict LC mediated immune regulation (Polak *et al.*, 2017). Using the IRF-GRN model, we could also observe differences in the accuracy of IRF-GRN *in silico* modelling to predict immunogenic responses in MoDCs compared to LC. Simulations with the LPSMoDC gene expression data from GSE52894 predicted increased expression of genes involved in Th1 T cell induction and MHC I regulation, compared to simulations performed using gene

expression data from the other MoDC types, which matched actual transcriptomic data. This data therefore indicates that high *IRF1* and *IRF4* expression is pre-requisite for DC activation and the ability to regulate immune responses. Whilst the accuracy of the model in predicting some outcome genes was observed, the model was not able to correctly predict the pattern of expression of gene associated with Th2 T cell induction and MHC II regulation. This inaccuracy of the model was further noted during *in silico* simulation of the GSE117946 MoDC data, in which the pattern of expression across the different MoDC conditions for none of the output genes were correctly predicted.

Overall this indicates that the IRF-GRN model, constructed for modelling LC data, may be missing certain TF regulators pivotal to MoDC immune regulation. Thus, this highlights the diverse regulatory networks which underpin the regulation of immune responses between different subgroups of DC. Regulation of tolerogenic responses in MoDCs may therefore greatly differ to regulation in LCs, with *in vitro* DC models therefore of limited use to observe the true mechanisms of LC tolerogenic immune regulation.

3.3.3 Inclusion of a *MYC*-regulated module in the IRF-GRN identified a potential mechanism by which DCs regulate immunogenic vs tolerogenic responses

After identifying *MYC* as a potential candidate for regulating tolerogenic immune responses in MoDCs, it was included in the IRF-GRN model via a mutually inhibitory loop with both *IRF1* and *IRF4* due to opposing expression patterns across the MoDC conditions. *In silico* modelling of GSE52894 data showed that *MYC* could potentially modulate gene expression via such interaction as it could be integrated into the established models with no effect on the accurate *in silico* predictions of 'Programme A'. We could further model how upregulation of *MYC* expression could perturb an immunogenic IRF-GRN to become tolerogenic. The same modulation could be modelled for conversion of a tolerogenic IRF-GRN to an immunogenic one via upregulation of *IRF1* and *IRF4.* This overall supported our hypothesis that *MYC* and both *IRF1* and *IRF4* are constituents of a mutually inhibitory network that could control the switch between immunogenic and tolerogenic DC activation. However, the inability of the IRF-GRN to accurately predict IL10MoDC immunogenic gene expression and therefore explore and test for a *MYC-IRF1/IRF4* regulatory interaction in IL10MoDCs, hinders the credibility of this hypothetical switch. To be able to test this, the IRF-GRN would need to be specifically altered to more accurately reflect MoDC regulation, as compared to LCs.

Whilst an inhibitory mechanism of gene regulation was hypothesised for *MYC,* it is important to consider biological processes it can upregulate. Included in the annotation for the co-expressed genes in GSE52894 cluster 6 genes, which comprises *MYC,* was an association with metabolic

processes. There is growing evidence highly linking the regulation of metabolism and immune responses. In immature DCs, catabolic metabolic processes are favoured, such as oxidative phosphorylation (OXPHOS), whilst activated DCs utilise more anabolic processes and favour glycolysis over OXPHOS (Wculek *et al.*, 2019)(Kelly and O'Neill, 2015). Published analysis on the GSE52894 dataset by Malinarich et al. 2015 demonstrated that whilst TolMoDCs and LPSMoDCs displayed similarities in glycolytic rate, TolMoDCs displayed enhanced OXPHOS and a dependence on the fatty acid oxidation (FAO) pathway (Malinarich *et al.*, 2015). Similarly, VitD3 only stimulated MoDCs also display enhanced glycolytic metabolism and OXPHOS compared to unstimulated MoDCs, along with inhibition of T-cell IFNγ production, when co-cultured (Ferreira *et al.*, 2015). *MYC* is a known modulator of metabolism, particularly in the context of cancer, in which enhancement of metabolic pathways such as glycolysis, can enhance tumour growth (Stine *et al.*, 2015). The upregulation of *MYC* in TolMoDCs therefore indicates that enhancement of immune tolerance may be modulated via changes to cellular metabolism.

3.3.4 Evaluation of tolerised MoDCs as a model to investigate LC tolerogenic immune regulation

In summary, our analyses have shown that DC transcriptomes display distinct gene expression programmes, dependent on immunological conditions such as immunogenic and tolerogenic states. We have also identified key transcriptional regulators specifically expressed in each programme. However, the transferability of these findings to the immunological expression programmes within LC is unknown.

All DCs are hallmarked by the ability to process and present antigen and migrate to secondary lymphoid tissues to promote adaptive immunity. Nonetheless, there are many unique subtypes of DC, distinguishable by lineage pathway, location in the body and preference for different immune responses (Collin, McGovern and Haniffa, 2013). MoDCs are artificially generated *in vitro* from blood monocytes, whilst LC are unique to other DC through their unique developmental pathway, which is similar to tissue resident macrophages and they specifically reside within epidermal tissue (Hoeffel *et al.*, 2012). At the level of surface marker expression MoDCs and LCs differ. Markers of LCs include CD207, CD1a and E-cadherin, whilst MoDCs express high levels of CD1a, CD11c and CD1c (Collin, McGovern and Haniffa, 2013)(Collin and Bigley, 2018). Nevertheless, how significant such differences in development and surface marker expression are reflected at the level of the whole transcriptome is not completely understood. Our analyses identified some similarities between MoDCs and LCs, including the modulation of *IRF1* and *IRF4* during inflammatory conditions, which are key components of the LC IRF-GRN and orchestrate immunogenic responses (Polak *et al.*, 2017). However, the overall success of *in silico* modelling using MoDC expression data

to predict immunogenic programmes was limited, suggested that whilst common immune associated transcriptional regulators were identified between MoDCs and LCs, the composition or activity of the GRN differed between subtypes. Our analysis did confirm that in silico modelling of transcriptomic programmes using GRN models could be a useful tool for investigations of DC immune biology. However, the application of MoDCs to accurately explore the mechanisms of tolerance exhibited by LCs requires further investigation and evaluation.

Chapter 4 Transcriptomes of human primary LCs encode a unique tolerogenic programme

4.1 Introduction

The epidermis is continuously exposed to a broad variety of antigen stimuli, which are detected by immune sentinel LCs. The induction of tolerance by LCs is therefore believed to be critical for maintaining homeostasis at the skin (Clayton *et al.*, 2017)(West and Bennett, 2018) (Seneschal *et al.*, 2012)(Deckers, Hammad and Hoste, 2018). Current mechanisms identified by which LCs mediate tolerance include clearance of apoptotic KCs, epidermal barrier maintenance and the induction of epidermal Tregs (Hatakeyama *et al.*, 2017),(Kubo *et al.*, 2009),(Seneschal *et al.*, 2012). The expression of tolerogenic mediators such as IL-10, IDO1 and PD-L1 have been demonstrated to be important for LC tolerogenic function (Yoshiki *et al.*, 2010) (von Bubnoff *et al.*, 2004)(Pêa-Cruz *et al.*, 2010). The residence of LCs within the highly exposed epidermis likely modulates the immunological role of LCs and alters their function and transcriptomic networks. This microenvironment-specific biology could therefore highly contrast with other DC subtypes, which reside in other tissue compartments. Indeed, earlier work from our group and others demonstrated that transcriptional network of human LCs dramatically differs from other skin resident DCs (Polak *et al.*, 2014)(Artyomov *et al.*, 2015). However, the extent to which LCs differ to other DCs in immune regulation of tolerogenicity at the transcriptomic level, is not completely understood.

LCs mediate induction of tolerance both locally *in situ* (Seneschal *et al.*, 2012) and after trafficking self-antigen to the local lymph nodes through migration (King *et al.*, 2015)(Hemmi *et al.*, 2001)(Yoshino *et al.*, 2006)(Ghigo *et al.*, 2013). Both of these states need to be analysed carefully to determine the molecular networks regulating LC-dependent immune tolerance. Therefore, to comprehensively assess mechanisms of immunotolerance in LCs, datasets containing digested and migrated LCs, extracted from healthy donors undergoing corrective breast or abdominal surgeries, along with other DC subtypes, also extracted from healthy donors, were selected for analyses.

Whilst the tolerogenic potential of LCs is key for epidermal homeostasis, tolerogenic function of other DC subtypes critically orchestrate immunotolerance in other tissues. $CD11c^{Low}CD45RB^{HIgh}$ spleen DCs display enhanced ability to induce IL-10 producing Tregs, contrasting the superior ability of $CD11c^{High}CD45RB^{-}$ spleen DCs to induce IFNγ producing Th1 T cells (Wakkach *et al.*, 2003). In the gut, tolerance induced by DC is paramount to prevent unwarranted immune responses to microflora and food antigens (Steimle and Frick, 2016). $CD103^{+}$ expressing DCs are strongly

associated with tolerogenic regulation in the gut (Scott, Aumeunier and Mowat, 2011)(Coombes and Powrie, 2008). $CD103^{+}$ DCs express higher levels of IDO and TGFβ, resulting in reduced Th1 and Th17 differentiation, whilst enhancing the differentiation of Tregs (Matteoli *et al.*, 2010)(Coombes *et al.*, 2007). pDC antigen presentation of myelin to CD4+ T cells results in antigen specific Treg induction, with loss of pDC antigen presentation resulting in experimental autoimmune encephalitis (EAE) (Irla *et al.*, 2010). A CCR9+ subset of pDCs has been specifically associated with elevated tolerogenic function, inducing Tregs and thus preventing graft versus host disease (GVHD) in allogenic T cell transplanted mice (Hadeiba *et al.*, 2008). Interestingly, specific subpopulations of dermal DCs (DDCs) are attributed to tolerogenic mechanisms (Haniffa, Gunawan and Jardine, 2015). CD141+CD14+ DDCs can produce high levels of IL-10 and can induce the differentiation of Tregs which potently suppress pathology induced in mouse models of allogenic induce inflammation (Chu *et al.*, 2012). CD14+ DDCs also display decreased T cell stimulatory capacity compared to CD1a+ and CD14-CD1a- DDC populations (Nestle *et al.*, 1993). A further example of a DC subset highly attributed to tolerogenic function include DCs that reside at the foeto-maternal interface. Here, tolerance must be maintained to ensure the foetus is tolerated by the maternal immune system and DCs from the placenta (PlaDC) are key to mediating such tolerance via the secretion of IL-10 (Gorvel *et al.*, 2014). Whilst several mechanisms of tolerance regulation therefore do appear to be common across DC subpopulations, including LCs, the extent of commonality is unknown.

To identify a molecular signature encoding tolerance in tissue residing DC for comparison with LCs, we identified a GEO dataset containing primary PlaDCs, that were extracted from healthy at term birth placentas, as well as MoDCs, which allowed us to investigate tolerogenic responses mediated within the placenta. Whilst a potential gender bias could be induced by analysing female PlaDC and LC that could have been extracted from both male and female donors, the use of these datasets, along with datasets of artificially induced TolMoDCs and IL10MoDCs, allowed comprehensive investigations of the transcriptomic programmes expressed by DCs that are associated with tolerogenic immune function *in situ,* in order to identify commonalities. Furthermore, in depth comparison between LC and DDCs, from healthy donors, was performed to ascertain similarities in tolerance regulation between different skin DC subsets. Cross-comparisons between tolerogenic DC subtypes highlighted specific pathways commonly associated with tolerance regulation by DCs, whilst also emphasising the largely unique transcriptomes exhibited by each subtype.

Overall, our analyses could characterise the unique nature of LC transcriptomes to other DC populations, including tolerogenic programmes. Whilst our earlier analyses on MoDCs stimulated with tolerogenic stimuli provided a good model of tolerogenic DC transcriptomic programming, our analyses of transcriptomic programmes from tissue derived LC and DC, further expand our understanding of how DC tolerance is regulated *in vivo.*

4.1.1 Hypothesis

LCs transcriptional networks contain a unique module/programme specifically associated with the regulation of tolerogenic immune responses.

4.1.2 Aims

- Define the unique transcriptomic programme of LCs.
- Identify molecular signature encoding tolerance across tolerogenic DC.
- Explore the similarities in mechanisms of skin tolerance regulation between LCs and DDCs

4.2 Results

4.2.1 Transcriptomic analysis reveals gene expression programmes unique and characteristic to LCs

LC tolerogenic function *in situ* has been reported in human and murine studies and is believed to be their key cellular characteristic (Shklovskaya *et al.*, 2011)(Kitashima *et al.*, 2018)(Seneschal *et al.*, 2012). LCs therefore appear to be more regulatory in contrast to blood CD1c DCs, DDCs and MoDCs, i.e. reduced production of proinflammatory cytokines (TNFα, IL1β) (Collin, McGovern and Haniffa, 2013)(Haniffa *et al.*, 2012). To investigate was underlies heightened tolerogenic potential in LCs, LC and cross-DC type transcriptomic analysis was performed. The transcriptomes were obtained from GEO repository (dataset (GSE23618)).

Using an RMA normalised Affymetrix Human Genome U133 Plus 2.0 microarray reads, enzymatically digested steady-state LC, enzymatically digested dermal DC (DDC), MoDC and CD1c blood DC triplicate transcriptomic data was analysed. Steady-state LCs and DDCs were enzymatically digested from respective epidermal and dermal compartments, before purification using CD1a microbeads was performed. MDS plotting revealed each DC population had unique transcriptomes, suggesting preferences for unique biological pathways and processes (**Figure 17A**). The close grouping of LCs and CD1a+ DDCs, suggested some similarity between transcriptomes could originate due to residence at skin, in contrast to blood CD1c DCs and MoDCs. 10,446 DEGs identified through comparison of LCs to all the other DC types were identified using Limma, emphasising the uniqueness of LC transcriptomes. The DEG list was uploaded into gene co-expression analysis tool Graphia Pro (Pearson correlation r=0.93, MCL=1.7, **Figure 17B**). Over 250 clusters were identified leading us to focus on the 25 clusters containing 30 or more genes. Of these 25 clusters, 20 were associated with specific biological processes (**Table 14**),

Cluster	No. of Genes	Cluster Profile	ID	Biological Process	FDR P-Val
1	1672	MoDC=High	GO:0002274	myeloid leukocyte activation	7.00E-20
			GO:0016050	vesicle organization	1.92E-19
			GO:0048284	organelle fusion	9.97E-19
			GO:0006906	vesicle fusion	1.01E-18
			GO:0002252	immune effector process	2.03E-12
2	1047	CD1c=High	GO:0016071	mRNA metabolic process	1.12E-12
			GO:0042254	ribosome biogenesis	3.37E-10
			GO:0002479	antigen processing and presentation of exogenous peptide antigen via MHC class I	1.42E-05
			GO:0050852	T cell receptor signaling pathway	1.29E-03
			GO:0007049	cell cycle	1.52E-03
3	719	MoDC=High, CD1c=High	GO:0045333	cellular respiration	2.39E-14
			GO:0006091	generation of precursor metabolites and energy	1.59E-12
			GO:0015980	energy derivation by oxidation of organic compounds	3.52E-12
			GO:0042775	mitochondrial ATP synthesis coupled electron transport	3.89E-10
			GO:0006119	oxidative phosphorylation	3.89E-10
4	391	LC=High	GO:0140014	mitotic nuclear division	1.95E-09
			GO:0000278	mitotic cell cycle	1.95E-09
			GO:0000819	sister chromatid segregation	1.32E-08
			GO:0022402	cell cycle process	2.13E-07
			GO:0070925	organelle assembly	3.01E-07
5	377	DDC=High	GO:0006954	inflammatory response	3.14E-16
			GO:0034097	response to cytokine	4.16E-15
			GO:0019221	cytokine-mediated signaling pathway	4.16E-15
			GO:0032101	regulation of response to external stimulus	5.75E-15
			GO:0006952	defense response	2.14E-14
6	198	DDC=Moderate, LC=Moderate	GO:0060429	epithelium development	6.77E-13
			GO:0008544	epidermis development	2.28E-12
			GO:0043588	skin development	2.69E-11
			GO:0050673	epithelial cell proliferation	3.17E-11
			GO:0030855	epithelial cell differentiation	5.60E-11
7	168	CD1c=High	GO:0002682	regulation of immune system process	6.34E-06
			GO:0071674	mononuclear cell migration	6.34E-06
			GO:0071621	granulocyte chemotaxis	7.92E-06
			GO:0006952	defense response	7.92E-06
			GO:0048245	eosinophil chemotaxis	7.92E-06
8	149	DDC=Moderate	GO:0030198	extracellular matrix organization	5.03E-07
			GO:0043062	extracellular structure organization	1.27E-05
			GO:0001501	skeletal system development	4.78E-05
			GO:0070848	response to growth factor	4.78E-05
			GO:0072359	circulatory system development	8.36E-05
9	120	DDC=Moderate, LC=Moderate, CD1c=High	GO:0006397	mRNA processing	2.05E-11
			GO:0016071	mRNA metabolic process	2.05E-11
			GO:0000398	mRNA splicing, via spliceosome	1.16E-06
			GO:0000377	RNA splicing, via transesterification reactions with bulged adenosine as nucleophile	1.16E-06
			GO:0000375	RNA splicing, via transesterification reactions	1.16E-06
10	104	DDC=Moderate, LC=High, CD1c=Moderate	GO:2000113	negative regulation of cellular macromolecule biosynthetic process	3.06E-03
			GO:0010558	negative regulation of macromolecule biosynthetic process	4.09E-03
			GO:0031327	negative regulation of cellular biosynthetic process	4.27E-03
			GO:0009890	negative regulation of biosynthetic process	4.27E-03
			GO:0006997	nucleus organization	4.27E-03

11	96	DDC=High, LC=High	GO:0060816	random inactivation of X chromosome	4.41E-02
			GO:0000079	regulation of cyclin-dependent protein serine/threonine kinase activity	4.41E-02
			GO:0030951	establishment or maintenance of microtubule cytoskeleton polarity	4.41E-02
			GO:0061470	T follicular helper cell differentiation	4.41E-02
			GO:1904029	regulation of cyclin-dependent protein kinase activity	4.41E-02
12	77	LC=High, CD1c=High	GO:1902494	catalytic complex	8.67E-05
			GO:0071013	catalytic step 2 spliceosome	3.54E-02
			GO:0000974	Prp19 complex	3.54E-02
13	65	DDC=High, LC=High	GO:0051250	negative regulation of lymphocyte activation	1.15E-03
			GO:0050868	negative regulation of T cell activation	1.15E-03
			GO:0032088	negative regulation of NF-kappaB transcription factor activity	2.03E-03
			GO:0010648	negative regulation of cell communication	2.52E-03
			GO:0023057	negative regulation of signaling	2.52E-03
14	54	DDC=Moderate	GO:0062023	collagen-containing extracellular matrix	1.49E-02
			GO:0005604	basement membrane	1.49E-02
			GO:0031012	extracellular matrix	3.63E-02
15	51	DDC=Moderate, LC=Moderate	GO:0008544	epidermis development	2.77E-05
			GO:0043588	skin development	5.52E-04
			GO:0009913	epidermal cell differentiation	1.22E-03
			GO:0070268	cornification	1.70E-03
			GO:1903575	cornified envelope assembly	1.70E-03
16	38	DDC=Moderate, LC=Moderate	GO:0009887	animal organ morphogenesis	9.33E-03
			GO:0006941	striated muscle contraction	1.42E-02
			GO:0006942	regulation of striated muscle contraction	1.42E-02
			GO:0043010	camera-type eye development	1.42E-02
			GO:0001654	eye development	1.74E-02
17	37	CD1c=Moderate	GO:0070488	neutrophil aggregation	2.41E-03
			GO:0050729	positive regulation of inflammatory response	3.62E-03
			GO:0030593	neutrophil chemotaxis	6.70E-03
			GO:0050832	defense response to fungus	6.70E-03
			GO:0050727	regulation of inflammatory response	6.70E-03
19	34	DDC=Moderate, CD1c=High	GO:0035455	response to interferon-alpha	3.98E-03
			GO:0071345	cellular response to cytokine stimulus	3.98E-03
			GO:0035456	response to interferon-beta	4.02E-03
			GO:0019221	cytokine-mediated signaling pathway	5.42E-03
			GO:1903265	positive regulation of tumor necrosis factor-mediated signaling pathway	1.92E-02
20	33	LC=Moderate, CD1c=High	GO:0006260	DNA replication	1.28E-05
			GO:0071897	DNA biosynthetic process	1.41E-05
			GO:0033260	nuclear DNA replication	9.19E-04
			GO:0006259	DNA metabolic process	1.03E-03
			GO:0044786	cell cycle DNA replication	1.06E-03
23	31	DDC=Moderate, LC=Moderate, CD1c=High	GO:0006614	SRP-dependent cotranslational protein targeting to membrane	1.61E-09
			GO:0006613	cotranslational protein targeting to membrane	1.61E-09
			GO:0045047	protein targeting to ER	1.76E-09
			GO:0000184	nuclear-transcribed mRNA catabolic process, nonsense-mediated decay	1.76E-09
			GO:0072599	establishment of protein localization to endoplasmic reticulum	1.84E-09

Table 14. GSE23618 co-expressed cluster profiles with associated gene ontologies. Transcript-transcript co-expression analysis of 10,446 probesets differentially regulated in steady-state LC (LC) compared to steady-state CD1a+ DDCs (DDC) , MoDC and blood CD1c DC (CD1c), using Graphia Pro (Pearson correlation r = 0.93, MCL = 1.7), identified 25 clusters (>30 genes). Clusters with associated ontologies identified using Toppgene (adj.p-value=<0.05, top 5 ontologies displayed) were included in the table. Clusters were annotated with number of genes in each cluster and with their general expression profile across the DCs.

4 gene clusters that had elevated expression in LCs compared to immunogenic DC types were identified (Clusters 4, 10, 18 and 22). The largest of these clusters, cluster 4, which contained 391 genes, was highly enriched in genes encoding cell cycle and cell division processes (gene ontology analysis, ToppGene, adj.p-value=2.7E-7). Cluster 10 was associated with negative regulation of cellular macromolecule biosynthetic process (adj.p-value=3.1-3). Gene ontology analysis for other gene clusters however did not expose specific associated biological processes or pathways. Consistent with their reported immunogenic function, the 3 largest gene clusters upregulated in each of the other DC types were found to be strongly enriched in genes involved in immune and inflammatory processes. Cluster 2 which contained 1047 genes highly expressed in CD1c blood DCs comprised genes associated with mRNA metabolism (adj.p-value=3.8E-11), MHC I antigen processing and presentation (adj.p-value=1.2E-4), as well as the T cell receptor signalling pathway (adj.p-value=1.3E-3). Cluster 5, which contained 377 genes upregulated in CD1a+ DDCs were associated with the inflammatory response (adj.p-value=3.1E-16) and response to cytokine (adj.p-value=4.1E-15), whilst cluster 1 containing 1672 genes highly expressed in MoDCs were associated with myeloid leukocyte activation (adj.p-value=7.0E-20) and the immune effector process (adj.p-value= 2.0E-12)(**Figure 17C**). Interestingly, cluster 13 which included 65 genes, was highly expressed in both CD1a+ DDC and LC and appeared associated with mechanisms of immune tolerance (**Figure 17D**). Gene ontology found associations with negative regulation of T cell activation (adj.p-value= 1.2E-3), due to the expression of *RUNX3, TNFAIP3, NFKBID, CD74, PELI1, SDC* and *ZC3H12A.* An association with negative regulation of NFκB transcription factor activity (adj.p-value= 2.0E-3) was also identified due to the expression of *NFKBIA, NFKBIB, TNFAIP3, PELI1* and *ZC3H12A.* The common expression of these genes amongst LC and CD1a+ DDC signified the importance of these tolerogenic processes at the skin.

As our MoDC analysis identified *MYC* as a potential regulator of tolerogenic function, we interrogated its expression in the steady state LC population. Whilst a large and significant increase in *MYC* expression was identified in LCs compared to CD1c DCs, only a non-significant trend for increased *MYC* expression was seen in LCs compared to MoDCs and CD1a+ DDCs (**Figure 17E**). Intriguingly, despite the low inflammatory profile of LC, *IRF1* expression in LCs was comparable with DDCs and CD1c+ DCs and *IRF4* expression was only significantly decreased compared to DDCs, yet still displayed relatively high expression (**Figure 17E**).

A)

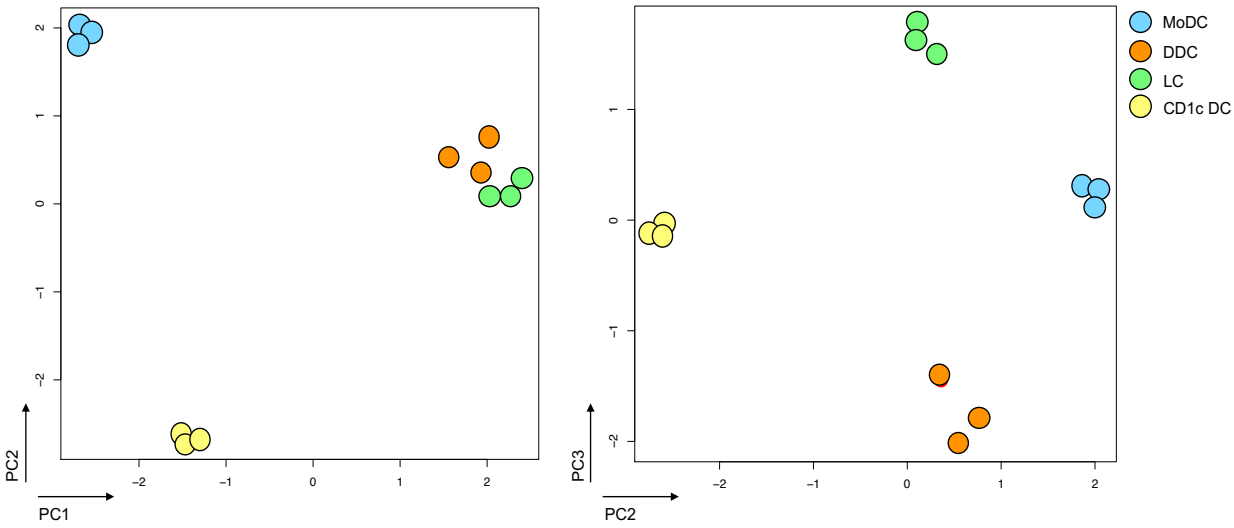

B)

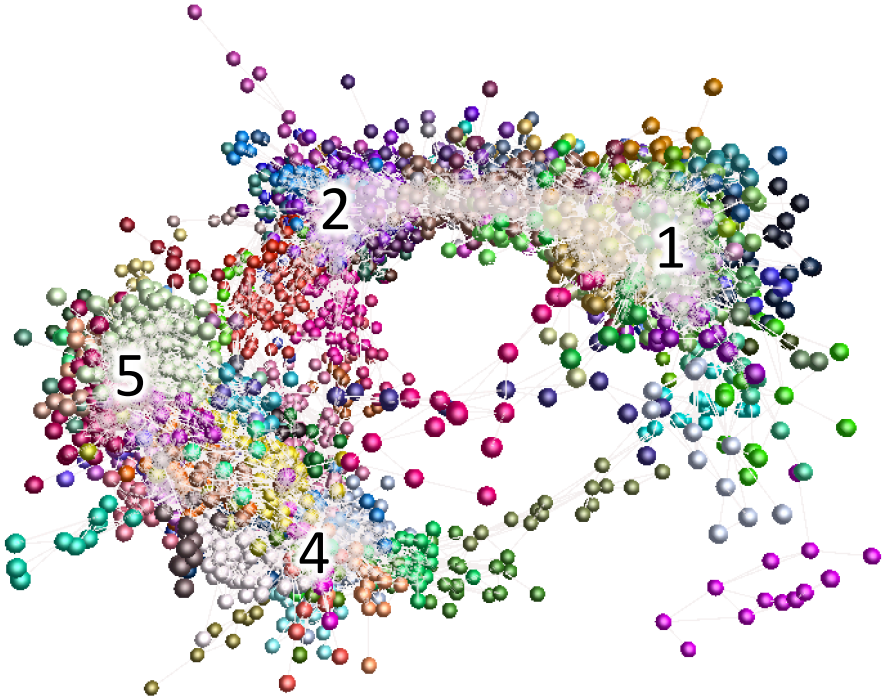

C)

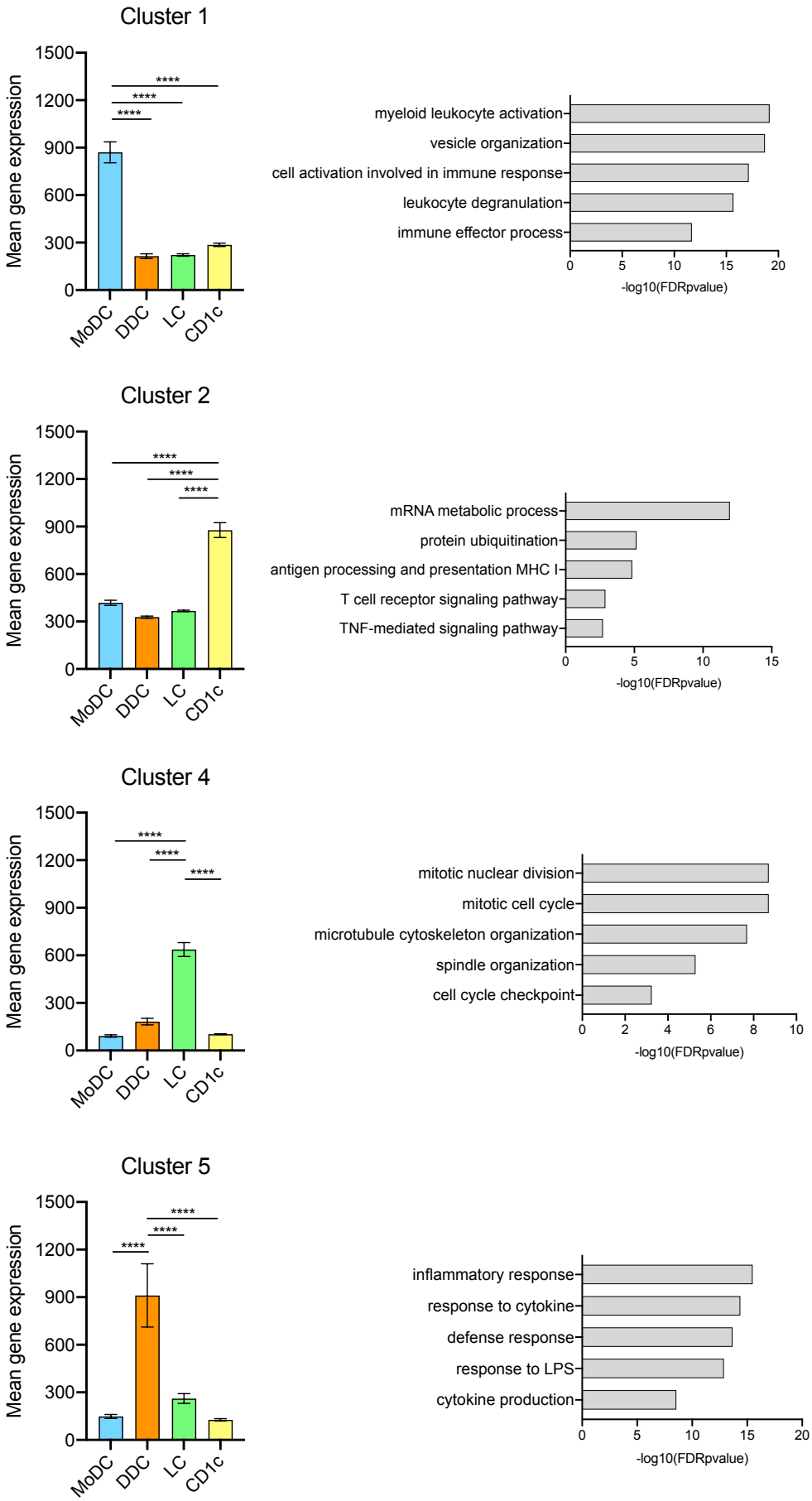
Cluster 1
Mean gene expression
1500
1200
900
600
300
0
****
****
****
MoDC
DDC
LC
CD1c
myeloid leukocyte activation
vesicle organization
cell activation involved in immune response
leukocyte degranulation
immune effector process
0
5
10
15
20
-log10(FDRpvalue)
Cluster 2
Mean gene expression
1500
1200
900
600
300
0
****
****
****
MoDC
DDC
LC
CD1c
mRNA metabolic process
protein ubiquitination
antigen processing and presentation MHC I
T cell receptor signaling pathway
TNF-mediated signaling pathway
0
5
10
15
-log10(FDRpvalue)
Cluster 4
Mean gene expression
1500
1200
900
600
300
0
****
****
****
MoDC
DDC
LC
CD1c
mitotic nuclear division
mitotic cell cycle
microtubule cytoskeleton organization
spindle organization
cell cycle checkpoint
0
2
4
6
8
10
-log10(FDRpvalue)
Cluster 5
Mean gene expression
1500
1200
900
600
300
0
****
****
****
MoDC
DDC
LC
CD1c
inflammatory response
response to cytokine
defense response
response to LPS
cytokine production
0
5
10
15
20
-log10(FDRpvalue)

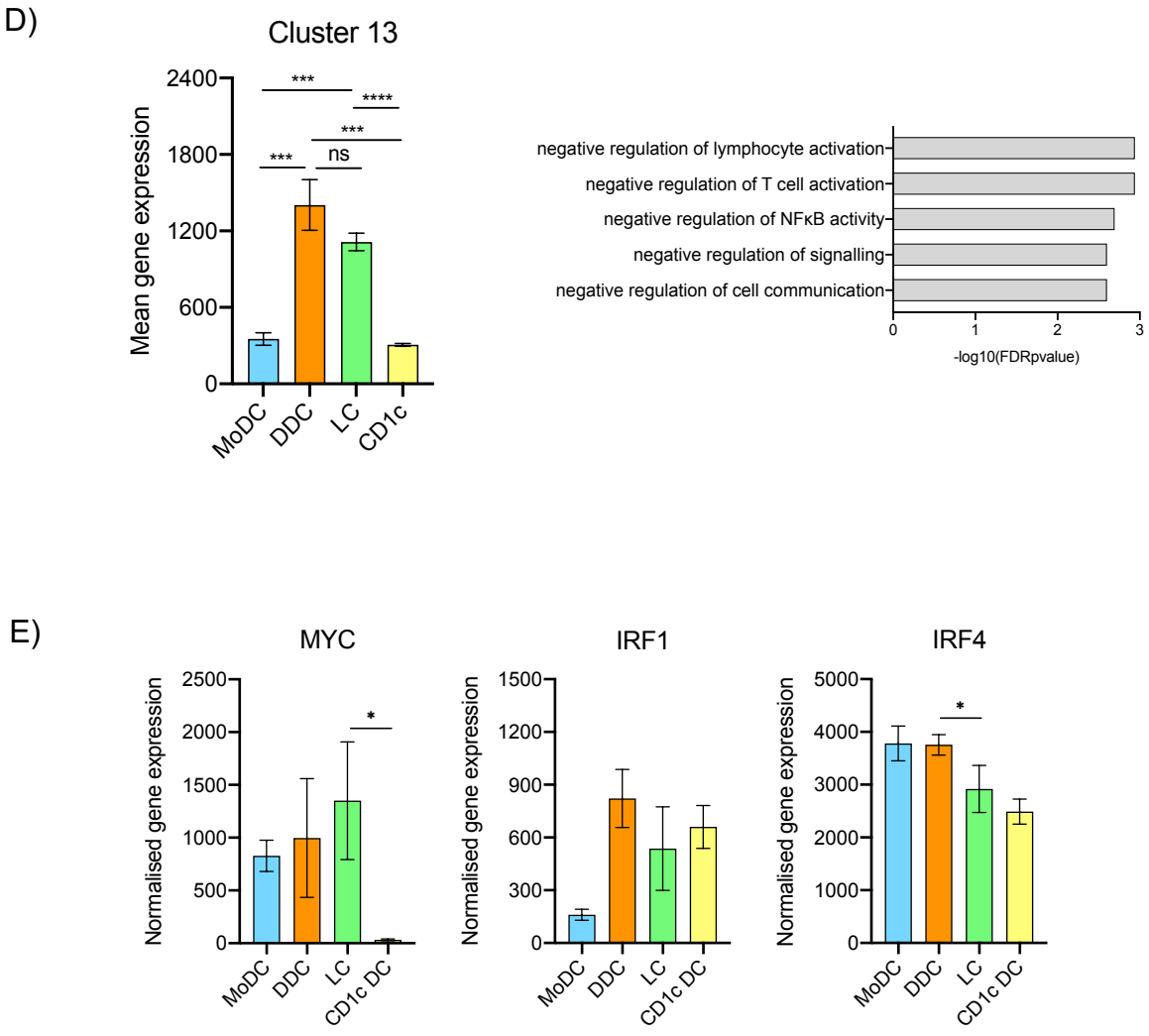

Figure 17. Transcriptomes of steady state LCs are distinct from other DC types and are distinguished by low expression of immunogenic genes. A) MDS plot of normalised, log transformed whole transcriptome data of MoDCs, steady-state CD1a+ DDCs, steady-state LCs and CD1c DCs (GSE23618). The first 3 PCs are displayed, PC1 and PC2 (left) and PC2 and PC3 (right). **B)** Transcript-transcript co-expression analysis of 10,446 probesets differentially regulated in LC compared to DDCs, MoDCs and CD1c DCs (Graphia Pro, Pearson=0.93, MCL=1.7). Cluster 1-100 are displayed. The largest clusters with a predominant upregulation in each of the 4 DCs are highlighted (clusters 1, 2, 4 and 5). **C)** Mean (±SD) cluster expression profiles for the largest clusters with a predominant upregulation in each of the 4 DCs (clusters 1, 2, 4 and 5). Toppgene gene ontology analyses is displayed alongside each cluster (-log10FDRp-values). **D)** Mean (±SD) cluster 13 expression profile with Toppgene gene ontology analysis (-log10FDRp-values). **E)** Mean (±SD) normalised expression of TFs MYC *IRF1* and *IRF4* across the four DC subtypes. Unpaired T-test p-values = *<0.05, **<0.01, ***<0.001, ****<0.0001, unpaired T-test.

To expand the analysis of differences and similarities between LCs and DDCs, suggested as the closest LC counterparts, we analysed an RMA normalised Affymetrix Human Genome U219 microarray dataset containing migrated LCs (mLCs) and CD11c+ migrated DDCs (mDDCs, GSE49475). Migratory LCs were purified using CD1a microbeads, whilst migratory DDC were purified using CD11c microbeads, to extract whole epidermal and dermal populations, respectively. Each subtype was isolated from three biological donors (paired samples for LCs and DDCs from each donor), and the microarray experiment was performed with technical duplicates. MDS plotting revealed the unique gene expression displayed by both mLCs and CD11c+ mDDCs along PC1 (**Figure 18A**). 5,687 DEGs were identified with 8 gene clusters containing 30 or more genes, produced using Graphia Pro (Pearson= 0.94, MCL=1.7, **Figure 18B**). Five clusters (clusters 1, 4, 6, 7 and 8) had increased expression in LCs, whilst three clusters (clusters 2, 3 and 5) had increased expression in DDCs. Clusters with associated ontologies were summarised (**Table 15**).

Cluster	No. of Genes	Cluster Profile	ID	Biological Process	FDR P-Val
1	1693	mLC=High	GO:0140053	mitochondrial gene expression	7.94E-31
			GO:0006091	generation of precursor metabolites and energy	2.35E-25
			GO:0009117	nucleotide metabolic process	3.19E-20
			GO:0006119	oxidative phosphorylation	1.18E-18
			GO:0010389	regulation of G2/M transition of mitotic cell cycle	2.20E-11
2	928	mDDC=High	GO:0002274	myeloid leukocyte activation	2.44E-40
			GO:0045321	leukocyte activation	6.25E-34
			GO:0001775	cell activation	2.86E-32
			GO:0042119	neutrophil activation	8.41E-31
			GO:0002444	myeloid leukocyte mediated immunity	1.06E-30
3	228	mDDC=High	GO:0001775	cell activation	1.13E-16
			GO:0002252	immune effector process	9.61E-15
			GO:0006952	defense response	9.61E-15
			GO:0045321	leukocyte activation	3.71E-14
			GO:0002682	regulation of immune system process	9.92E-13
4	98	mLC=High	GO:0003712	transcription coregulator activity	6.75E-03
			GO:0003713	transcription coactivator activity	6.75E-03
5	91	mDDC=Moderate	GO:0016791	phosphatase activity	1.91E-02

Table 15. GSE49475 co-expressed cluster profiles with associated gene ontologies. Transcript-transcript co-expression analysis of 5,687 probesets differentially regulated in migrated LC (mLC) compared to CD11c+ migrated DDCs (mDDC) using Graphia Pro (Pearson correlation r = 0.94, MCL = 1.7), identified 8 clusters (>30 genes). Clusters with associated ontologies identified using Toppgene (adj.p-value=<0.05, top 5 ontologies displayed) were included in the table. Clusters were annotated with number of genes in each cluster and with their general expression profile across the DCs.

Cluster 1, upregulated in mLCs, contained 1693 genes and was associated with the generation of precursor metabolites and energy (adj. p-value=2.4E-25) and regulation of G2/M transition of mitotic cell cycle (adj. p-value=2.2E-11). Cluster 4 containing 98 genes, was also upregulated in mLCs and was associated with transcription coregulator activity (adj. p-value= 6.8-3). No associated ontologies were identified for clusters 6, 7 and 8 when analysed alone. Due to the overall similarity between the cluster expression profiles and to further summarise the general upregulated pathways in mLCs compared to CD11c+ mDDCs, the combined total of 1926 genes in clusters 1, 4, 6, 7 and 8 were submitted into Toppgene together. Overall this summarised mLC upregulated pathways as being associated with mitochondrial processes, oxidative phosphorylation and the cell cycle (**Figure 18C)**. In contrast gene clusters upregulated in DDCs (clusters 2, 3 and 5) were involved with immune and inflammatory responses when the combined 1247 genes were submitted to Toppgene together. Individually, cluster 2, containing 928 genes, was associated with myeloid leukocyte activation (adj. p-value=2.4E-40) and cluster 3, containing 228 genes, was associated with the immune effector process(adj. p-value=9.6E-15). Cluster 5 containing 91 genes was associated with phosphatase activity (adj. p-value=1.9E-2) (**Figure 18C**).

Genes within the tolerogenic module, which was shared between steady-state LCs and DDCs and associated with negative regulation of T cell activation and NFκB activation (*RUNX3, TNFAIP3, NFKBIA, NFKBIB, NFKBID, CD74, PELI1, SDC* and *ZC3H12A,* **Figure 17D**), was inspected amongst migrated mLCs and mDDCs (**Figure 18D**). Some of these genes were differentially regulated (*RUNX3, NFKBIA, NFKBID* and *ZC3H12A*) or lowly expressed in both LC and DDC (*NFKBIB* and *SDC*). The shared tolerogenic module was therefore lost in LC and DDC upon migration.

We next inspected the expression of *MYC, IRF1* and *IRF4* in the mLC and mDDC gene expression data (**Figure 18E**). Interestingly, *MYC* expression was significantly increased in mDDCs compared to mLCs. Furthermore, whilst the expression of *IRF1* was similar between mLC and mDDC, the expression of *IRF4* was significantly increased in mLCs. This contrasted the expression of IRF4 in MoDCs, in which increased *IRF4* expression correlated with increased inflammatory gene expression.

A)

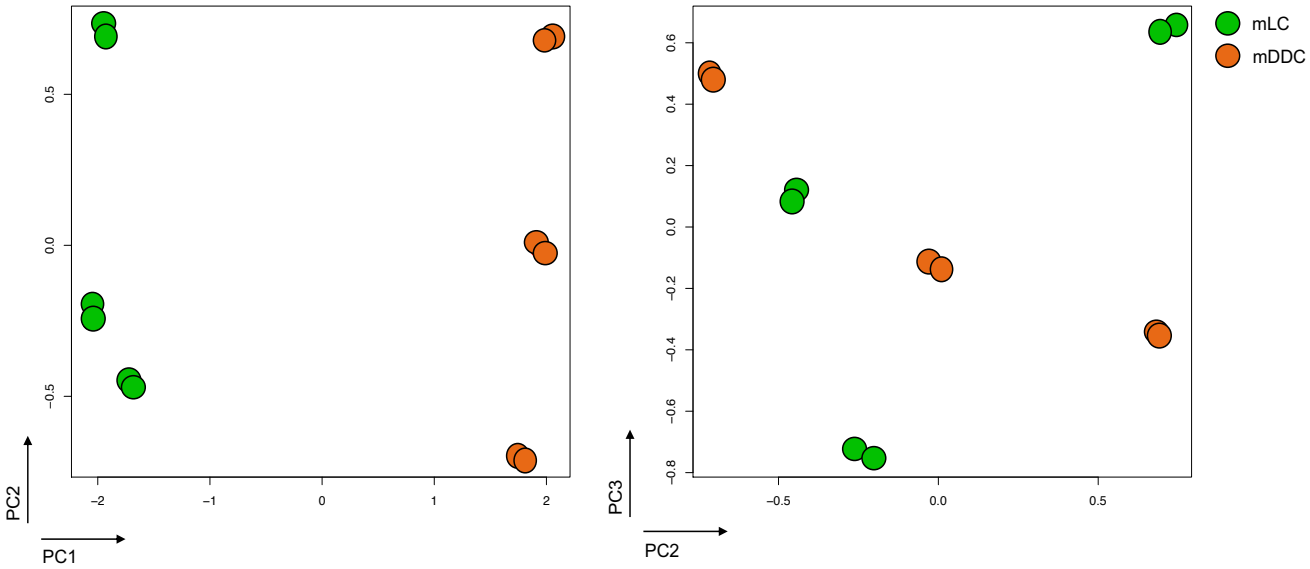

B)

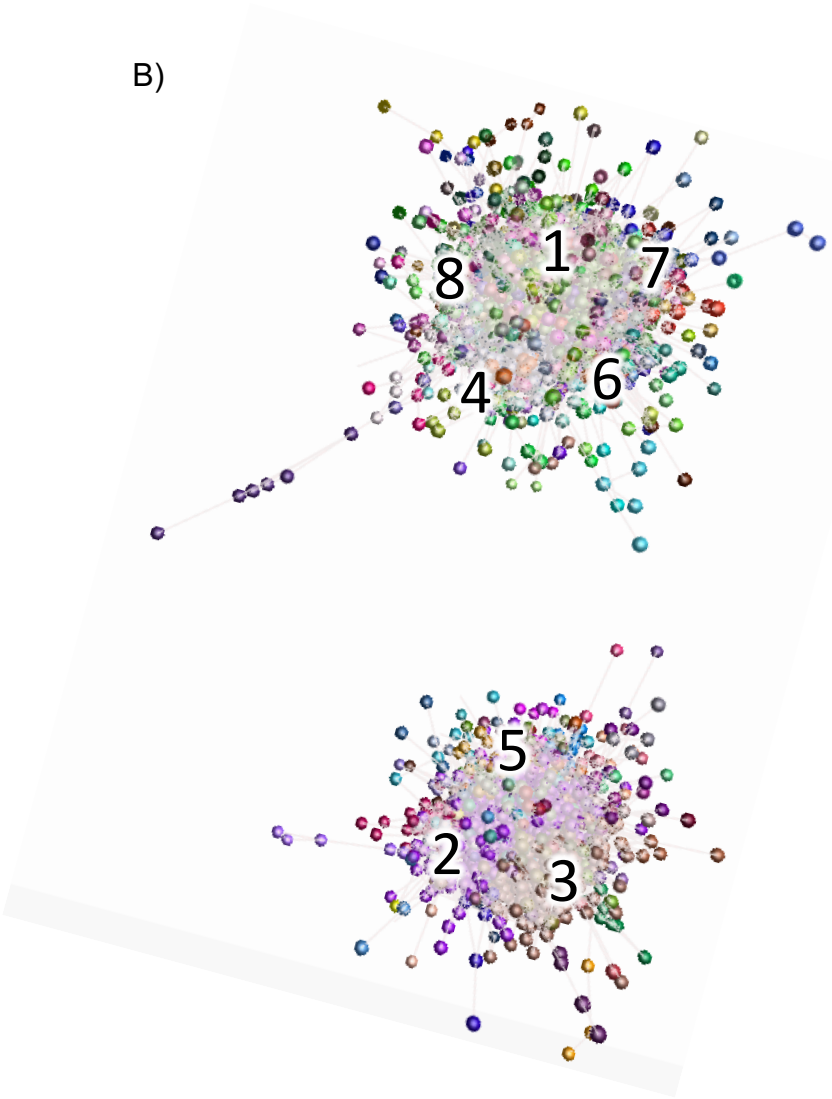

C)

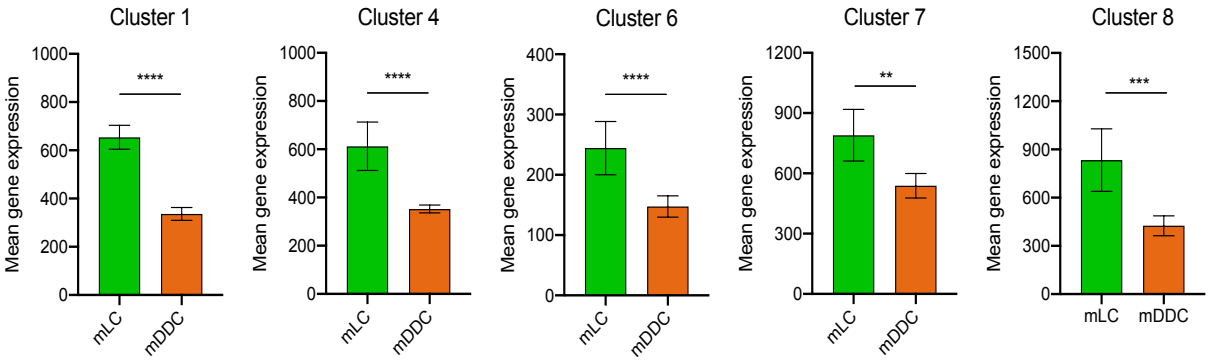
Cluster 1
Cluster 4
Cluster 6
Cluster 7
Cluster 8
Mean gene expression
****
**
***
mLC
mDDC

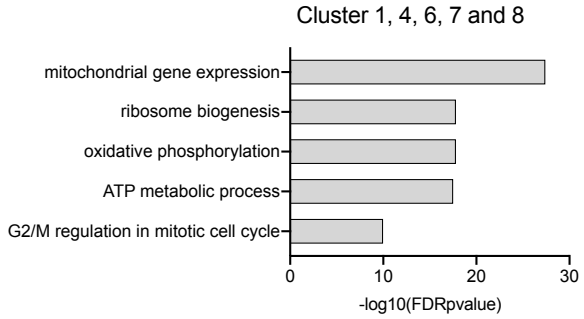
Cluster 1, 4, 6, 7 and 8
mitochondrial gene expression
ribosome biogenesis
oxidative phosphorylation
ATP metabolic process
G2/M regulation in mitotic cell cycle
-log10(FDRpvalue)

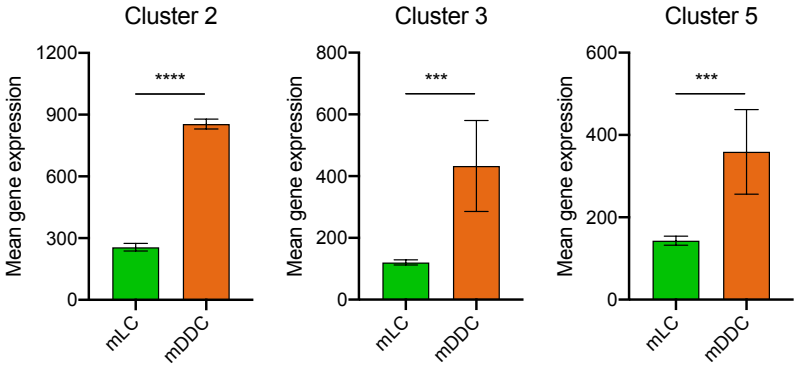
Cluster 2
Cluster 3
Cluster 5
Mean gene expression
****
***
mLC
mDDC

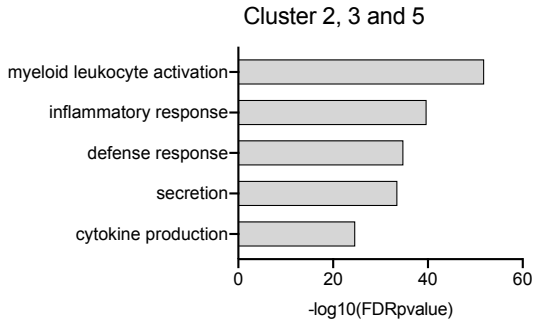
Cluster 2, 3 and 5
myeloid leukocyte activation
inflammatory response
defense response
secretion
cytokine production
-log10(FDRpvalue)

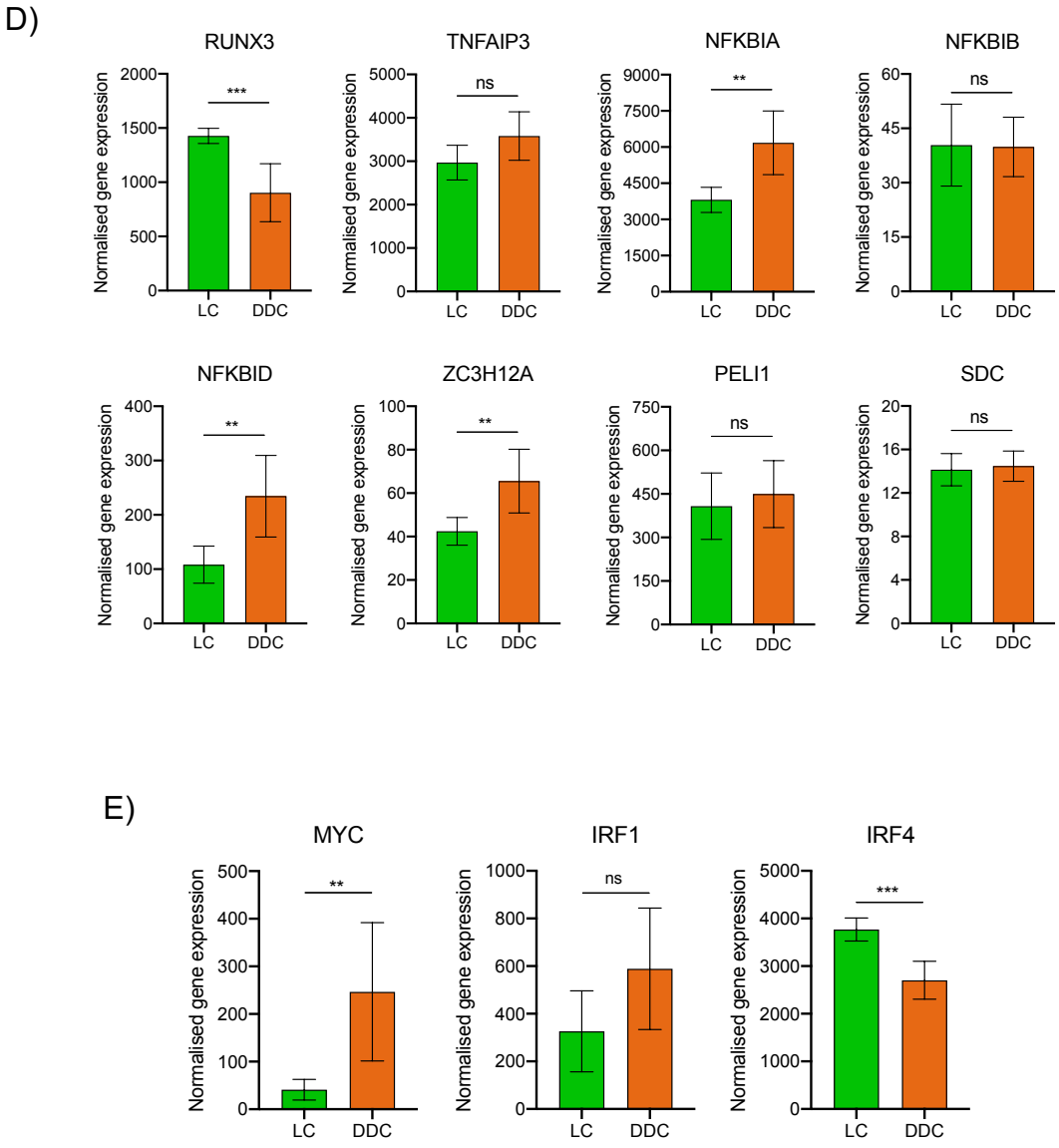

Figure 18. Transcriptomes of LCs isolated through migration are distinct from migrated DDCs. A) MDS plot of normalised, log transformed whole transcriptome data migrated LC (mLC) and CD11c+ migrated DDC (mDDC, GSE49475). The first 3 PCs are displayed, PC1 and PC2 (left) and PC2 and PC3 (right). **B)** Transcript-transcript co-expression analysis of 5,687 probesets differentially regulated between migrated LCs and DDCs (Graphia Pro, Pearson=0.94, MCL=1.7). Clusters with greater than 30 genes (Clusters 1-8) are highlighted. **C)** Mean (±SD) expression profiles of clusters upregulated in migrated LC (Clusters 1, 4 and 6, 7 and 8, containing) and migrated DDC (Clusters 2, 3 and 5) with associated gene ontology analysis (Toppgene, p-value<0.05). **D)** Mean (±SD) normalised expression of genes associated with negative regulation of T cell activation and NFκB activation identified as a shared tolerogenic module in steady-state LC and DDC (**Figure 11D**) **E)** Mean (±SD) normalised expression of TFs MYC IRF1 and IRF4. Unpaired T-test p-values = *<0.05, **<0.01, ***<0.001, ****<0.0001, unpaired T-test.

Overall, DEG gene co-expression cluster analysis revealed that LCs displayed reduced expression of inflammatory immune pathways as compared to other DC subtypes, regardless of LC activation state. This overall suggests less involvement of LCs in immunogenic immune pathways and therefore a potential preferential association with immunoregulatory processes. In the steady-state LCs, an immunosuppressive gene module was identified, which was common with steady-state DDCs (Cluster 13) and marked by upregulation of genes mediating inhibition of NFκB and T cell activation. In contrast, migratory LCs were discernible by high expression of genes encoding metabolic processes.

To identify a specific molecular signature of tissue-derived DC types associated with predominantly tolerogenic responses, we chose to analyse transcriptomes of placental derived DCs (plaDC), available in GEO (GSE52850). The dataset comprised of plaDCs with MoDCs, which were used as a suitable molecular reference for our analyses. MDS plotting revealed PlaDCs and MoDCs to be to greatly different (**Figure 19A**). 3,040 genes were identified after DEG analysis and filtering. Gene co-expression analysis was performed, identifying 7 gene clusters in total (Pearson=0.95, MCL=1.7) (**Figure 19B**). Of these 7 clusters, cluster 1 and 6 was elevated in MoDCs and clusters 2-5 and 7 were upregulated in PlaDCs. 5 clusters (clusters 1, 2, 3, 4 and 5) were associated with specific biological processes and pathways after gene ontology analysis (**Table 16**).

Cluster 1 was upregulated in MoDCs and included 1467 genes. Genes were associated with metabolic pathways (adj.p-value=2.9E-16), leukocyte activation (adj.p-value=1.8E-11) and T-cell activation (adj.p-value=2.1E-7). High expression of MHC II molecules also resulted with an association with antigen processing and presentation (adj.p-value=3.3E-5). The remaining 3 clusters were all upregulated in plaDCs. Cluster 2 included 387 genes and was associated with response to endogenous stimulus (adj.p-value=2.1E-6) and the reproduction process (adj.p-value=1.0E-7). Cluster 3 included 279 genes and was associated with the defence response (adj.p-value=5.9E-6) and positive regulation of signal transduction (adj.p-value=5.9E-6). Genes were also associated with the murine phenotype, decreased inflammatory response (adj.p-value=7.3E-5), annotated due to the expression of NFκB inhbitors, such as *TNFAIP3, NFKBIA, NFKBIB* and *PELI1*. Cluster 4 with 258 genes was associated with negative regulation of gene expression (adj.p-value=2.4E-4) and biosynthetic processes (adj.p-value=2.4E-4). Cluster 5 with 242 genes was associated with the nuclear chromatin (adj.p-value=4.4E-3) The combined gene list from all PlaDC upregulated clusters (2-5 and 7) and all MoDC upregulated clusters (1 and 6) were subjected to gene ontology analysis together to capture overall profiles of both PlaDC and MoDC upregulated gene expression (**Figure 19C**).

Consistent with our analysis in MoDCs and LCs we inspected the expression of *MYC, IRF1* and *IRF4.* No difference in *MYC* or *IRF1* expression was identified between PlaDCs and MoDCs (**Figure 19D**). However, *IRF4* was significantly decreased in PlaDCs compared to MoDCs.

Cluster	No. of Genes	Cluster Profile	ID	Biological Process	FDR P-Val
1	1467	MoDC=High	GO:0019637	organophosphate metabolic process	2.92E-16
			GO:1901135	carbohydrate derivative metabolic process	2.92E-16
			GO:0009260	ribonucleotide biosynthetic process	7.84E-14
			GO:0045321	leukocyte activation	1.75E-11
			GO:0042110	T cell activation	2.03E-07
2	387	PlaDC=High	GO:0040007	growth	7.94E-08
			GO:0022414	reproductive process	1.02E-07
			GO:0007565	female pregnancy	1.25E-07
			GO:0009719	response to endogenous stimulus	2.12E-06
			GO:0016477	cell migration	6.14E-06
3	279	PlaDC=High	GO:0080134	regulation of response to stress	1.29E-07
			GO:0006952	defense response	5.92E-06
			GO:0010942	positive regulation of cell death	5.92E-06
			GO:0009967	positive regulation of signal transduction	5.92E-06
			GO:0006954	inflammatory response	3.17E-05
4	258	PlaDC=High	GO:1903507	negative regulation of nucleic acid-templated transcription	2.41E-04
			GO:1902679	negative regulation of RNA biosynthetic process	2.41E-04
			GO:0051253	negative regulation of RNA metabolic process	2.54E-04
			GO:0045892	negative regulation of transcription, DNA-templated	4.62E-04
			GO:0010558	negative regulation of macromolecule biosynthetic process	6.16E-04
5	242	PlaDC=High	GO:0000790	nuclear chromatin	4.35E-03
			GO:0017146	NMDA selective glutamate receptor complex	6.09E-03
			GO:0045211	postsynaptic membrane	9.46E-03
			GO:0097060	synaptic membrane	1.61E-02
			GO:0008328	ionotropic glutamate receptor complex	1.61E-02

Table 16. GSE52850 co-expressed cluster profiles with associated gene ontologies. Transcript-transcript co-expression analysis of 3,040 probesets differentially regulated in placental derived DCs (PlaDCs) compared to MoDCs using Graphia Pro (Pearson correlation r = 0.95, MCL = 1.7), identified 7 clusters in total. Clusters with associated ontologies identified using Toppgene (adj.p-value=<0.05, top 5 ontologies displayed) were included in the table. Clusters were annotated with number of genes in each cluster and with their general expression profile across the DCs.

A)

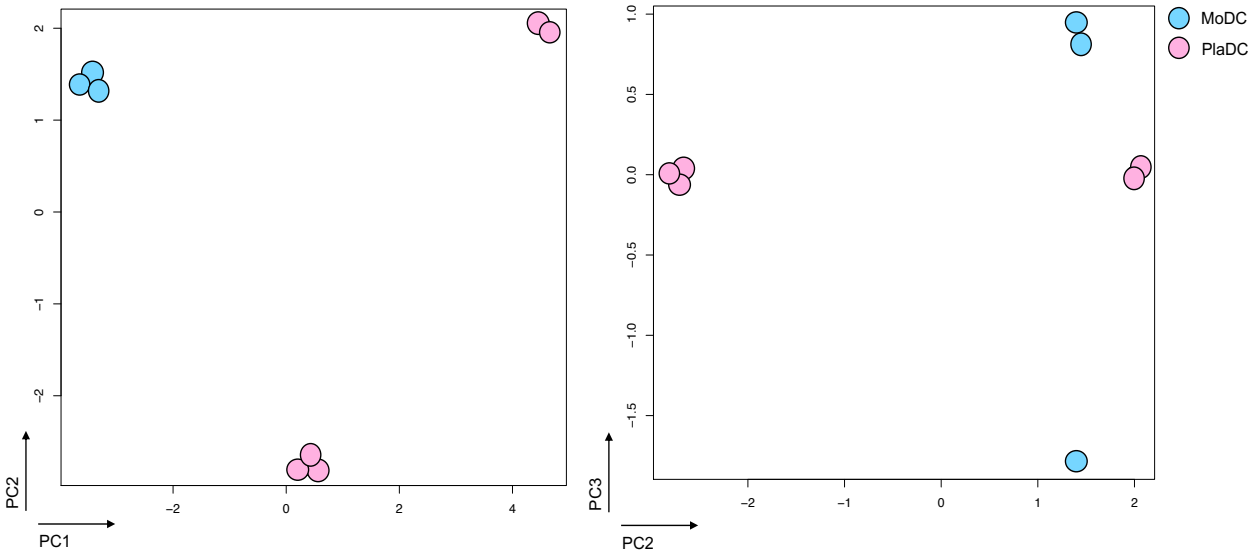

B)

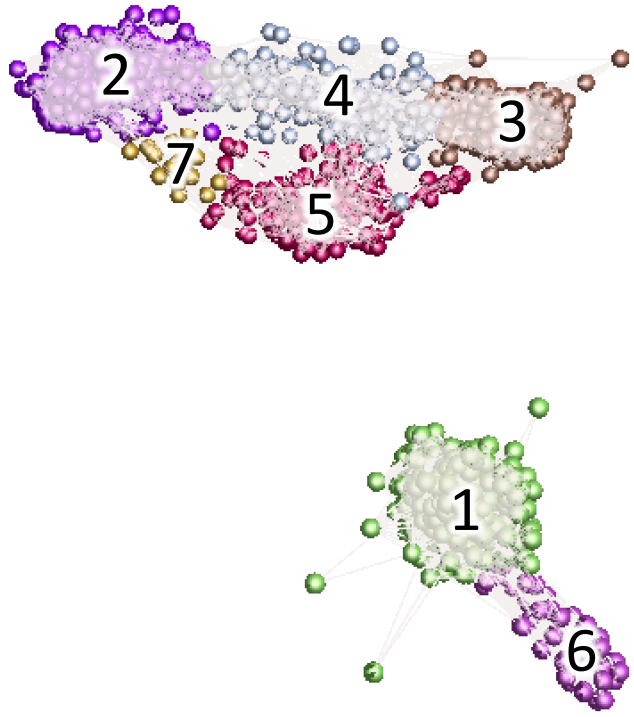

C)

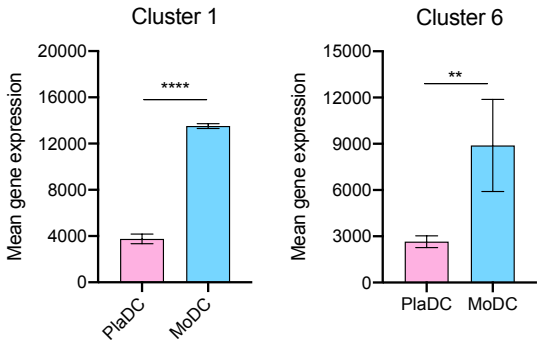
Cluster 1
Mean gene expression
20000
16000
12000
8000
4000
0
****
PlaDC
MoDC
Cluster 6
Mean gene expression
15000
12000
9000
6000
3000
0
**
PlaDC
MoDC

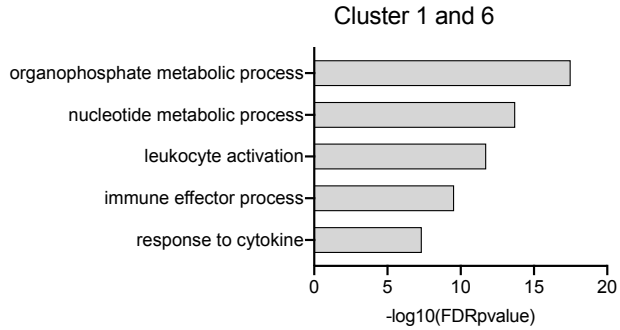
Cluster 1 and 6
organophosphate metabolic process
nucleotide metabolic process
leukocyte activation
immune effector process
response to cytokine
0
5
10
15
20
-log10(FDRpvalue)

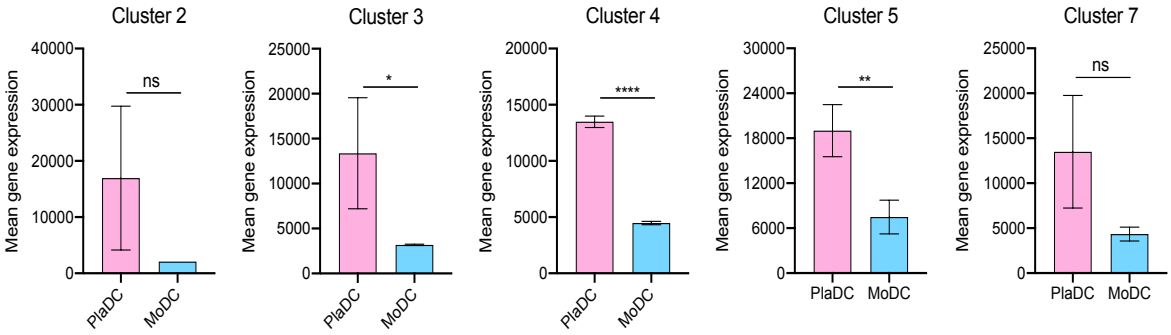
Cluster 2
Mean gene expression
40000
30000
20000
10000
0
ns
PlaDC
MoDC
Cluster 3
Mean gene expression
25000
20000
15000
10000
5000
0
*
PlaDC
MoDC
Cluster 4
Mean gene expression
20000
15000
10000
5000
0
****
PlaDC
MoDC
Cluster 5
Mean gene expression
30000
24000
18000
12000
6000
0
**
PlaDC
MoDC
Cluster 7
Mean gene expression
25000
20000
15000
10000
5000
0
ns
PlaDC
MoDC

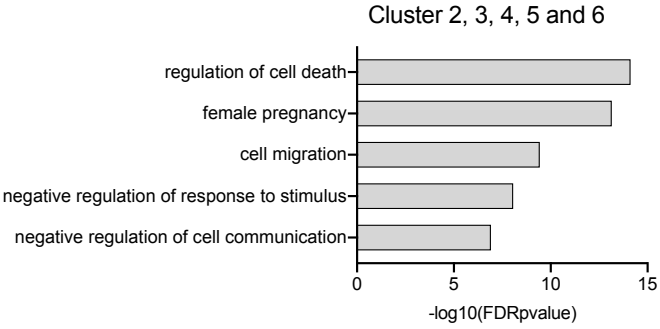
Cluster 2, 3, 4, 5 and 6
regulation of cell death
female pregnancy
cell migration
negative regulation of response to stimulus
negative regulation of cell communication
0
5
10
15
-log10(FDRpvalue)

D)

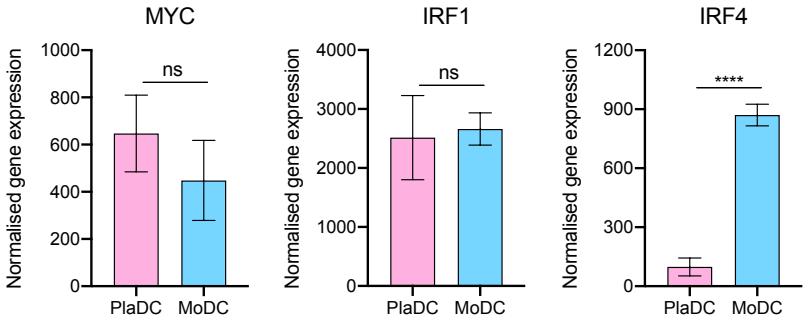

Figure 19. PlaDCs and MoDCs display unique transcriptomic profiles. A) MDS plot of normalised, log transformed whole transcriptome PlaDC and MoDC data (GSE52850). The first 3 PCs are displayed, PC1 and PC2 (left) and PC2 and PC3 (right). B) Transcript-to-transcript co-expression analysis of 3,040 differentially regulated probesets between PlaDCs and MoDCs, identified 7 co-expressed clusters (Graphia Pro, Pearson correlation r=0.95, MCL=1.7). C) Mean (±SD) expression profiles of clusters upregulated in PlaDC (Clusters 2, 3, 4, 5 and 7) and MoDC (Cluster 1 and 6), with associated gene ontology analysis for combined gene lists for PlaDC and MoDC upregulated clusters (Toppgene, p-value<0.05). D) Mean (±SD) normalised gene expression of the TF MYC IRF1 and IRF4. Unpaired T-test p-values = *<0.05, **<0.01, ***<0.001, ****<0.0001, unpaired T-test.

4.2.2 Comparative analysis between tolerogenic DC transcriptomes indicates some overlapping tolerogenic programmes, whilst highlighting the overall unique transcriptomic programmes expressed by LCs

LCs, PlaDCs, TolMoDCs and IL10MoDCs have all been reported to exert tolerogenic function. Therefore, we sought to delineate common and unique transcriptomic programmes underpinning their biology. To perform cross comparison between tolerogenic DC transcriptomes, immature MoDCs from respective datasets were used as a common reference to identify genes consistently associated with tolerogenic function across the four DC populations, through using DEG analysis. The results of DEGs analysis were compared and visualised using a Venn diagram (**Figure 20A**). 1622 genes, 1012 genes, 160 genes and 306 genes were identified from steady-state LC-MoDC analysis, PlaDC-MoDC analysis, TolMoDC-MoDC analysis and IL10MoDC-MoDC analysis, respectively. Interestingly, there was little convergence of the DEG lists, suggesting the tolerogenic programmes are cell subset specific, rather than a common immunotolerant DC programme. 0 genes were commonly upregulated in all four comparisons. It is however of note, that significantly bigger overlap was observed between tissue derived tolerogenic DCs than their counterparts differentiated *in vitro* (120 common genes between LCs and PlaDCs), suggesting that the artificial nature of TolMoDC and IL10MoDC induction may cause a significant difference in tolerogenic

function, or state of immunosuppression to that seen *in vivo*. Gene ontology analysis for the 120 genes common between LCs and PlaDCs were associated with response to lipopolysaccharide (adj.p-value=5.9E-7), regulation of the response to stress (adj.p-value=5.9E-7), negative regulation of response to stimulus (adj.p-value=3.4E-6) (**Figure 20B**). Interestingly, an association with response to steroid hormone (adj.p-value=4.6E-5) and therefore immunosuppressive stimuli was also identified, due to the expression of *CLDN1, DNAJA1, DUSP1, ERRFI1, FHL2, HMGB2, KRAS, LBH, PGRMC2, PLPP1. PMEPA1, PTGS2, SIRT1* and *ZFP36.* Similarly, gene ontology analysis was performed for the 217 genes (**Appendix 1 A.2**) which were commonly upregulated in two or more of the four DC conditions to assess common upregulated pathways (**Figure 20C**), revealing associations with response to lipopolysaccharide (adj.p-value= 2.9E-11), cell migration (adj.p-value= 2.3E-8), negative regulation of response to stimulus (adj.p-value=4.6E-8) and negative regulation of signal transduction (adj.p-value=6.4E-7) (**Figure 20C**). An association with the NFκB signalling pathway (adj.p-value=3.1E-2) was also identified, partly due to the upregulated expression of *NFKBIA* and *TNFAIP3*, both inhibitors of NFκB activation. Similarly, the 154 genes upregulated in LCs and at least one other DC condition were subjected to gene ontology analysis, in order to specifically investigate the DC tolerogenic genes mutual expressed with LCs (**Figure 20D**). Again, the gene list was associated with response to lipopolysaccharide (adj.p-value=3.0E-6), negative regulation of response to stimulus (adj.p-value=7.4E-6) and negative regulation of cell communication (adj.p-value=2.1E-4). Consistent with previous analysis of the DEGs uniquely upregulated in steady-state LCs compared to DDCs, CD1c DCs and MoDCs, the 1468 genes upregulated in LCs compared to MoDCs only, were associated with the cell cycle (adj.p-value=2.1E-14) (**Figure 20E**). Overall, despite a small overlap in tolerogenic gene expression between different tolerogenic DC types, a common downregulation in pathways responsive to stimulus and signalling, including NFκB signalling, was observed. The upregulated pathways therefore suggest a connection with a state of immunosuppression and non-responsiveness.

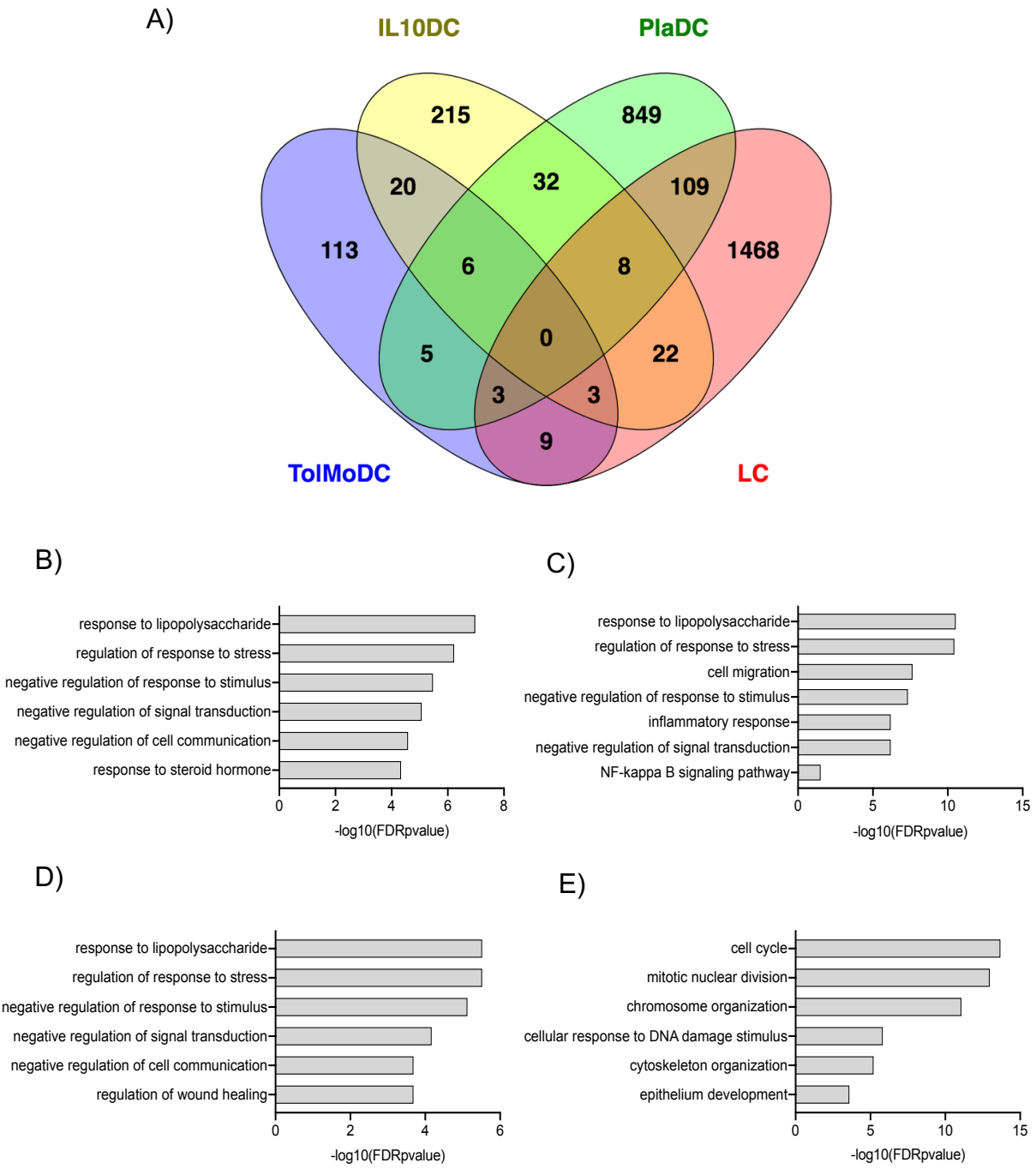

Figure 20. Cross comparison of LCs, PlaDCs, TolMoDCs and IL10MoDCs upregulated DEGs compared to immature MoDCs A) Venn Diagram displaying the overlap in upregulated DEGs, identified during comparison between steady-state LC-MoDC (1622 genes), PlaDC-MoDC (1012 genes), TolMoDC-MoDC (160 genes) and IL10MoDC-MoDC (306 genes). B) Gene ontology analysis (Toppgene) for the 120 genes which were co-upregulated in LC and PlaDC (-log10adj.p-values). C) Gene ontology analysis (Toppgene) for the 217 genes which were co-upregulated in two or more of the tolerogenic DC conditions (-log10adj.p-values). D) Gene ontology analysis (Toppgene) for the 154 genes upregulated in LC and at least one other DC condition (-log10adj.p-values). E) Gene ontology analysis (Toppgene) for the 1468 genes upregulated in LC only (-log10adj.p-values).

The expression of the common tolerogenic DC associated gene signatures was then tracked across the different LC and DC datasets analysed above to assess variation in signature expression across DC subtypes. A heatmap displaying the expression of 217 genes commonly upregulated in two or more of the tolerogenic DC conditions (**Figure 20C, Appendix 1 A.2**) was displayed for LCs and DCs in the GSE23618 and GSE49475 datasets (**Figure 21**). In GSE23618, containing steady-state LC, steady-state DDC, blood CD1c+ DC and MoDC, the elevated expression of the tolerogenic signature appeared to be shared between both LC and DDC. The immunosuppressive associated pathways therefore appear to be active in DC populations of both the epidermis and dermis at the steady-state. In GSE49475, containing migrated mLC and mDDC, the expression of the tolerogenic signature became more divergent. Here, a large proportion of the genes appeared to be lowly expressed in mLC, but highly expressed in mDDC.

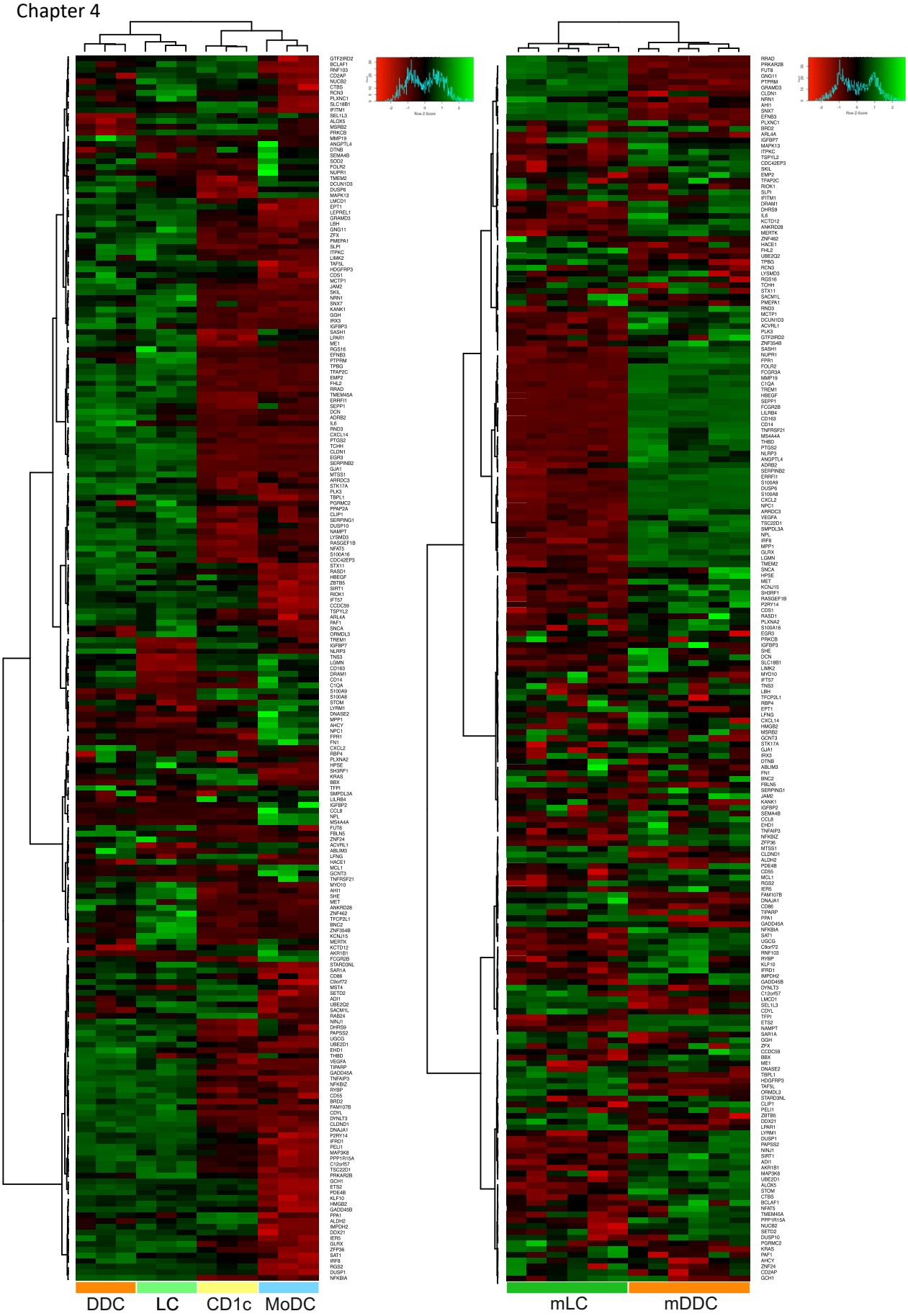

Figure 21. Tracking the tolerogenic DC signature across LC and DC subpopulations. The 217 genes commonly upregulated in at least 2 of the DC conditions (**Figure 20A&C**) were tracked in heatmaps (canberra, ward.D) of log2 normalised expression data for GSE23618 (steady-state LC and DDC, CD1c+ blood DC and MoDC) and GSE49475 (migrated mLC and mDDC) datasets.

4.2.3 LC regulation of tolerogenic transcriptomic programmes differs to DDCs

Investigations into the expression of the 217 genes upregulated in tolerance associated DC and LC across GSE23618 and GSE49475 datasets revealed elevated expression of this module in both steady-state and migrated DDCs. As DDC populations have been linked to tolerance regulation in the dermis (Haniffa, Gunawan and Jardine, 2015)(Chu *et al.*, 2012)(Chu, Di Meglio and Nestle, 2011) we sought to further inspect the presence of the tolerance associated expression profile amongst DDC subpopulations. While a comprehensive study including all tolerogenic skin DC types isolated in consistent manner yet need to be done, datasets from individual populations are available. DDCs in GSE23618 (steady-state CD1a DDCs) and GSE49475 (migrated CD11c DDCs) account for all known DC subpopulations present in the dermis. To explore whether heterogeneity in the tolerogenic gene module could be identify amongst DDC subpopulations, a background corrected and quantile normalised Illumina HumanHT-12 V4.0 expression beadchip microarray dataset (GSE35457) containing collagenase digested steady-state CD14+, CD141^{high}, CD1c+ and CD1c+CD141^{high} DDC populations was analysed. The heterogeneity amongst the DDC subpopulations was confirmed by MDS plotting of whole transcriptome data (**Figure 22**). Here, separation of CD14+ and CD141^{high} DDCs along PC1 was observed, whilst CD1c+ and CD1c+CD141^{high} DDCs clustered together. Interestingly, along PC2 CD14+ and CD141^{high} DDCs clustered together and again, CD1c+ and CD1c+CD141^{high} DDCs were localised.

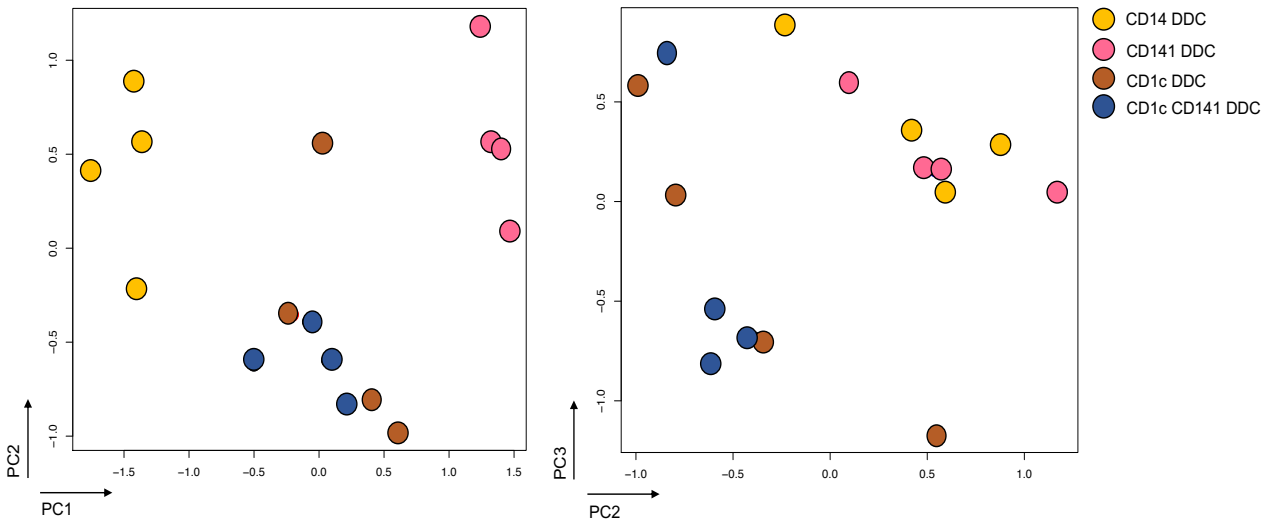

Figure 22. Dimensionality reduction analysis of whole transcriptome data reveals variation amongst DDC subpopulations. A) MDS plot of normalised, log transformed whole transcriptome data of collagenase digested steady-state CD14+, CD141^{high}, CD1c+ and CD1c+CD141^{high} DDC populations (GSE35457). The first 3 PCs are displayed, PC1 and PC2 (left) and PC2 and PC3 (right).

The expression of the 217 genes in the tolerance associated module (**Figure 20C, Appendix 1 A.2)** was then explored in the DDC populations through heatmap plotting (**Figure 23A**). Sample hierarchical clustering of the heatmap displayed the same population similarities as displayed in PC1 from MDS plots. Overall, the appearance of large distinct gene clusters amongst the DDC populations was more infrequent than observed in **Figure 21**. However, some small gene clusters, as defined by the hierarchical clustering parameters, could be identified in both CD14+ DDCs and CD141^{high} DDCs, which were polarised between the two populations. CD14+ and CD141^{high} DDC subpopulations therefore expressed some pathways of the tolerogenic gene module, although the pathways that DDCs did express were specific to either CD14+ or CD141^{high} DDC subpopulations (highlighted on heatmap, 57 genes in CD141^{high} DDCs and 41 genes in CD14+ DDCs). Genes clusters from the tolerogenic gene module which were more preferentially expressed in either CD141^{high} (57 genes) or CD14+ (41 genes) DDCs were submitted to gene ontology analysis in Toppgene (**Figure 23B**). Results for CD141^{high} DDCs revealed associations with response to LPS (adj.p-value=4.6E-4), response to cytokine (adj.p-value=7.4E-3) and response to steroid hormone (adj.p-value=1.6E-2). Negative regulation of immune effector process (adj.p-value=3.4E-2) was also associated due to the expression of *CD55, DUSP1, NFKBIA, PAF1, PELI1, TNFAIP3* and *ZFP36*. Results for CD14+ DDCs revealed associations with regulation of response to external stimulus (adj.p-value=1.4E-7), cell chemotaxis (adj.p-value=7.2E-2), negative regulation of response to stimulus (adj.p-value=4.3E-5) and negative regulation of response to cell communication (adj.p-value=5.5E-3). An association with regulation of homeostasis (adj.p-value=6.8E-6) was found due to the expression of *ADRB2, S100A9, SERPINB2, SERPING1, TFPI* and *THBD.* Furthermore, an association with negative regulation of humoral immune response (adj.p-value=6.7E-3) was also identified due to the expression of *FCGR2B* and *SERPING1*. Therefore, despite few distinct clusters being expressed in CD14+ and CD141^{high} DDCs, the clusters that were highly expressed revealed associations with tolerogenic processes.

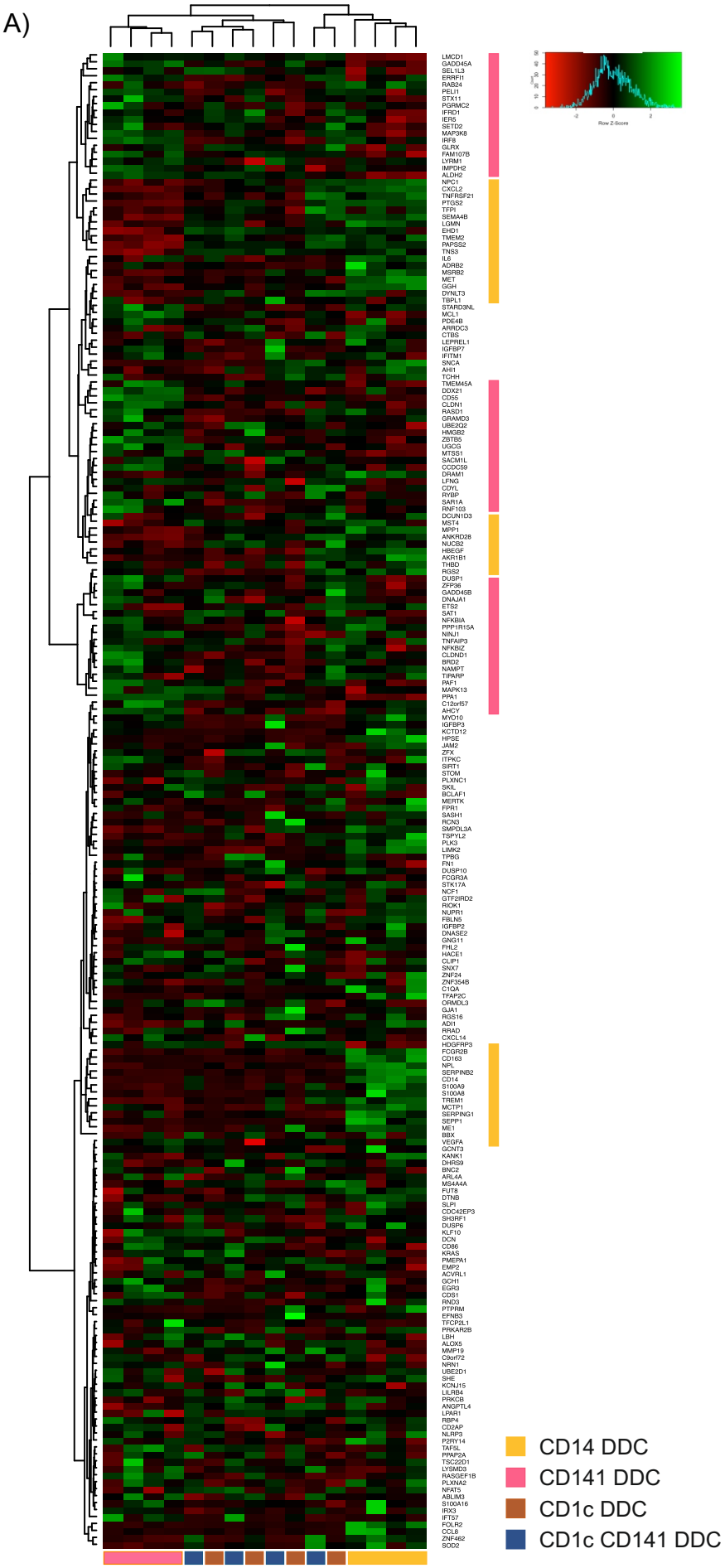
A)
CD14 DDC
CD141 DDC
CD1c DDC
CD1c CD141 DDC

B)

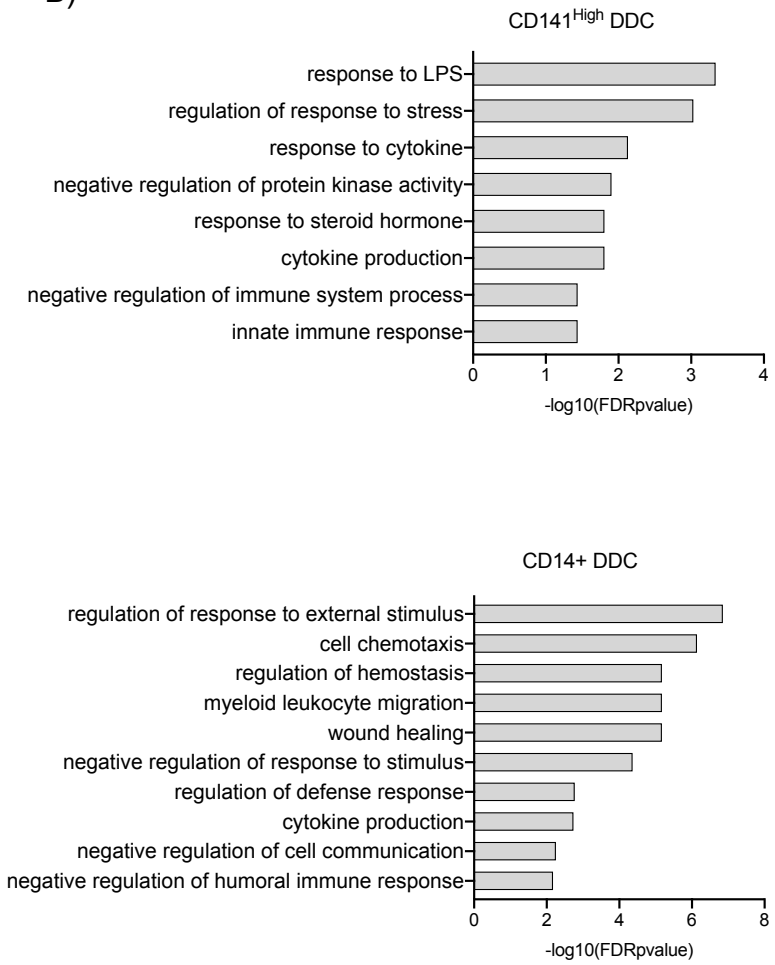

Figure 23. Tracking the tolerogenic DC signature across DDC subpopulations. A) The 217 genes commonly upregulated in at least 2 of the DC conditions (**Figure 20A&C**) were tracked in heatmaps (complete, ward.D) of log2 normalised expression data for GSE35457 containing steady-state CD14+, CD141^{high}, CD1c+ and CD1c+CD141^{high} DDC subpopulations. CD14+ and CD141^{high} DDC associated gene module clusters are highlighted. **B)** Gene ontology analysis (Toppgene) for the 57 genes upregulated in CD141^{high} DDCs (Top) and 41 genes upregulated in CD14+ DDCs (Bottom) as highlighted on heatmap in **A)** (-log10adj.p-values).

Having identified specific modules of tolerogenic signature in different DDC subpopulations, we sought to compare and contrast it with LCs. A background corrected and quantile normalised Illumina HumanHT-12 V4.0 expression beadchip dataset (GSE66355) containing migrated mLC, migrated CD14+ mDDC, migrated CD141+ mDDC, and CD14 and CD141 double negative migrated DDC (DN-mDDC) was used to track the modules across all tolerogenic skin DC populations. MDS plotting revealed the heterogeneity amongst the skin DC populations across PC1 and PC2, with mLCs and DN-mDDCs clustering on the right and CD14+ and CD141+ mDDCs clustering on the left (**Figure 24**). 6218 DEGs were identified through Limma DEG analysis comparing LCs to each of the DDC subpopulations and submitted to gene co-expression analysis tool Graphia Pro (**Figure 25)**, Pearson correlation r=0.93, MCL=1.7). Over 250 clusters were identified leading us to focus on the 20 clusters containing 25 or more genes. Of these 20 clusters, 9 were associated with specific biological processes (**Table 17)**, containing the top 5 biological processes associated with each cluster).

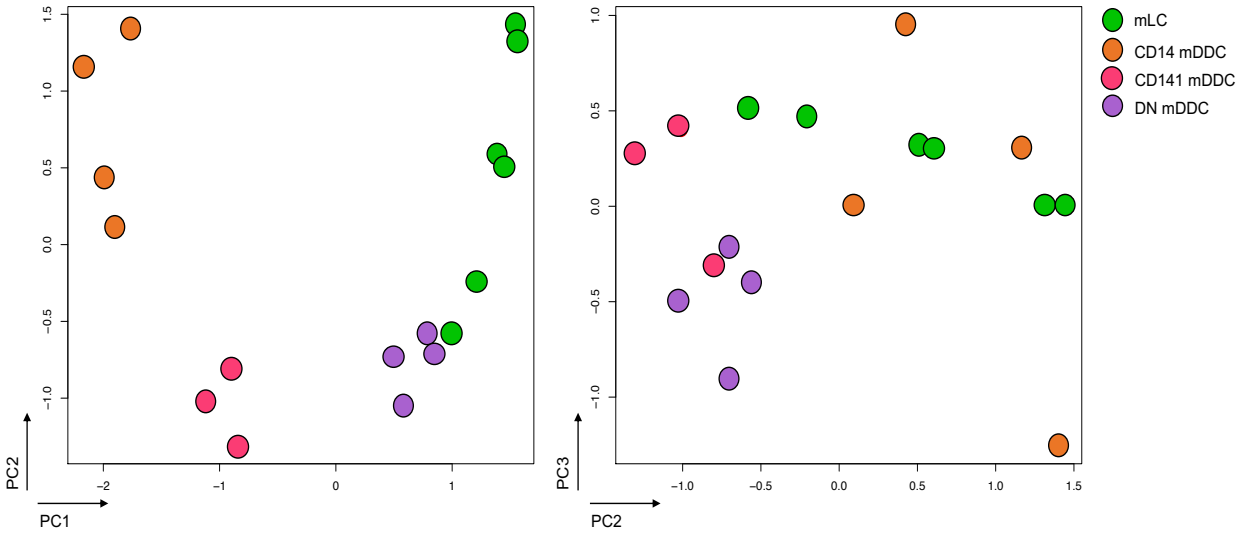

Figure 24. Dimensionality reduction analysis of whole transcriptome data reveals variation amongst migrated LC and DDC subpopulations. A) MDS plot of normalised, log transformed whole transcriptome data of migrated mLC, CD14+ mDDC, CD141+ mDDC and double negative CD14-CD141- mDDC (DN mDDC) populations (GSE66355). The first 3 PCs are displayed, PC1 and PC2 (left) and PC2 and PC3 (right).

Cluster	No. of Genes	Cluster Profile	ID	Biological Process	FDR P-Val
2	481	CD14+DDC = High	GO:0002274	myeloid leukocyte activation	2.49E-49
			GO:0042119	neutrophil activation	7.19E-40
			GO:0002252	immune effector process	2.11E-36
			GO:0045055	regulated exocytosis	2.66E-36
			GO:0002682	regulation of immune system process	1.02E-24
3	163	LC = High	GO:0006695	cholesterol biosynthetic process	2.48E-05
			GO:1902653	secondary alcohol biosynthetic process	2.48E-05
			GO:0030043	actin filament fragmentation	1.58E-03
			GO:0071470	cellular response to osmotic stress	6.45E-03
			GO:0007049	cell cycle	3.54E-02
6	79	CD14+DDC = High	GO:0045321	leukocyte activation	1.36E-06
			GO:0002446	neutrophil mediated immunity	1.36E-06
			GO:0006952	defense response	5.85E-06
			GO:0002252	immune effector process	6.99E-06
			GO:0006954	inflammatory response	5.38E-05
7	54	DN-DDC = High, LC = High	GO:0006614	SRP-dependent cotranslational protein targeting to membrane	1.15E-60
			GO:0006613	cotranslational protein targeting to membrane	2.48E-60
			GO:0000184	nuclear-transcribed mRNA catabolic process, nonsense-mediated decay	5.09E-59
			GO:0045047	protein targeting to ER	5.09E-59
			GO:0072599	establishment of protein localization to endoplasmic reticulum	1.42E-58
8	52	DN-DDC = High, LC = High	GO:0045859	regulation of protein kinase activity	5.21E-04
			GO:0051338	regulation of transferase activity	1.59E-03
			GO:0071850	mitotic cell cycle arrest	3.07E-03
			GO:0071900	regulation of protein serine/threonine kinase activity	3.07E-03
			GO:1902533	positive regulation of intracellular signal transduction	1.57E-02
9	41	CD14+DDC = Moderate	GO:0030097	hemopoiesis	2.40E-03
			GO:0006000	fructose metabolic process	2.40E-03
			GO:0002682	regulation of immune system process	2.40E-03
			GO:0048534	hematopoietic or lymphoid organ development	2.40E-03
			GO:0046903	secretion	2.40E-03
12	28	CD141+DDC = High, CD14+DDC = High	GO:0046903	secretion	2.21E-07
			GO:1901700	response to oxygen-containing compound	9.95E-07
			GO:0002274	myeloid leukocyte activation	5.40E-06
			GO:0071222	cellular response to lipopolysaccharide	5.40E-06
			GO:0006954	inflammatory response	1.18E-05
14	26	DN-DDC = High, LC = High	GO:0001731	formation of translation preinitiation complex	5.74E-04
			GO:0002183	cytoplasmic translational initiation	7.02E-03
			GO:0022618	ribonucleoprotein complex assembly	8.28E-03
			GO:0045047	protein targeting to ER	3.67E-02
			GO:0016032	viral process	4.17E-02
18	26	DN-DDC = High, LC = High	GO:0019441	tryptophan catabolic process to kynurenine	1.17E-02
			GO:0034627	'de novo' NAD biosynthetic process	1.17E-02
			GO:0034354	'de novo' NAD biosynthetic process from tryptophan	1.17E-02
			GO:0046218	indolalkylamine catabolic process	1.25E-02
			GO:0006569	tryptophan catabolic process	1.25E-02

Table 17. GSE66355 co-expressed cluster profiles with associated gene ontologies. Transcript-transcript co-expression analysis of 6,218 probesets differentially regulated in migrated mLCs compared to migrated CD14+ mDDCs, CD141+ mDDCs and double negative CD14- CD141- mDDCs (DN-DDC) using Graphia Pro (Pearson correlation r = 0.93, MCL = 1.7), identified 20 clusters (>25 genes). Clusters with associated ontologies identified using Toppgene (adj.p-value=<0.05, top 5 ontologies displayed) were included in the table. Clusters were annotated with number of genes in each cluster and with their general expression profile across the DC subpopulations.

Annotatable clusters that were upregulated in LCs, revealed predominant associations with metabolic processes, including nuclear transcribed mRNA catabolic process (Cluster 7, adj.p-value=5.1E-59), cholesterol biosynthetic process (Cluster 3, adj.p-value=2.5E-5), the cell cycle (Cluster 3, adj.p-value=2.5E-2) and protein targeting to the ER (Cluster 7, adj.p-value=5.1E-59). In contrast, DDCs upregulated clusters were heavily associated with immunogenic and inflammatory immune pathways. For CD14+ DDCs this included the immune effector process (Clusters 2 and 6, adj.p-value=2.1E-36 and 7.0E-6) and the inflammatory response (Clusters 6 and 12, adj.p-value=5.4E-12 and 1.2E-12). For CD141+ DDCs this included myeloid leukocyte activation (Cluster 12, adj.p-value=5.4E-6) and the inflammatory response (Cluster 12, adj.p-value=1.2E-12). Clusters upregulated in DN-DDC were parallel with LC upregulated clusters, consistent with their localisation together along PC1 and PC2 in MDS plotting (**Figure 24**), suggesting this population could be *in situ* migrating LCs from the dermis.

Specific interrogation of clusters with annotations linked to immune tolerance, identified tolerogenic pathways upregulated in CD14+ DDC and LC (Highlighted in **Figure 25**). Interestingly, whilst CD14+ DDC upregulated clusters were highly associated with immunogenic and inflammatory mechanisms, upregulated programmes also included genes associated with

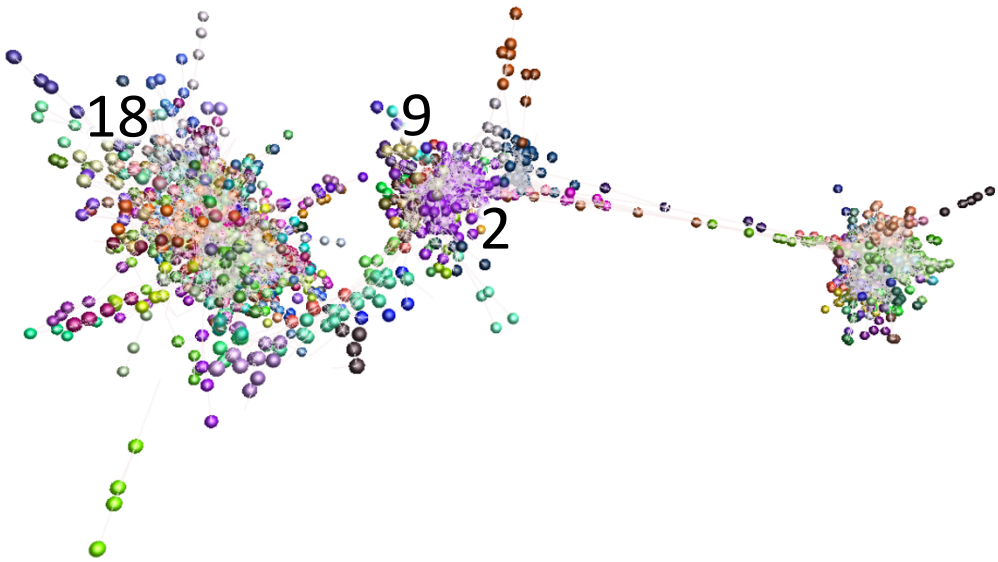

Figure 25. Gene coexpression analysis identifies gene cluster linked to tolerogenic processes in CD14+ DDCs and LCs. Transcript-to-transcript co-expression analysis of 6,218 probesets differentially regulated in migrated mLCs compared to migrated CD14+ mDDCs, CD141+ mDDC and double negative CD14- CD141- mDDC (DN DDC) using Graphia Pro (Pearson correlation r = 0.93, MCL = 1.7). Gene clusters 2 and 9 linked the negative regulation of immune system process (adj.p-value=1.1E-9 and 4.2E-2) in CD14+ DDC s are highlighted, as well as LC upregulated cluster 18, which was associated with the tolerogenic tryptophan catabolism to kynurenine process (adj.p-value=1.2E-2).

tolerogenic immune pathways. CD14+ DDC cluster 2 was associated with negative regulation of the immune system process (adj.p-value=1.1E-9), due the elevated expression of *ATM, BST2, C1QC, CCL2, CD14, CD200R1, CD37, CD68, CEBPB, CR1, FCER1G, FCGR2B, GPNMB, GPX1, GRAMD4, GRN, HAVCR2, IL4R, IL7R, INPP5D, IRAK3, LMO2, LPXN, LST1, LY96, MAFB, MILR1, NOTCH1, PAG1, PIK3AP1, PRNP, PTPN6, SAMHD1, SLAMF8, SPN, THBS1, TLR4, TLR6, TYROBP, VSIG4* and *VSIR.* CD14+ DDC cluster 9 was also associated with negative regulation of immune systems process (adj.p-value=4.2E-2) due to elevated expression of *CD300LF, LILRB4, MMP12, MNDA* and *MYC*. For LC, an association with tolerogenic mechanisms was identified for cluster 18, which due to elevated expression of *IDO1* and *IDO2,* was linked to tryptophan catabolism to kynurenine (adj.p-value=1.2E-2). Interestingly, cluster 18 also included the TF *IRF4.*

The expression of the common tolerogenic DC associated gene signature (**Figure 20A&C**) was tracked across the migrated LC and DDC subpopulations through heatmap plotting (**Figure 26**). Interestingly, distinct gene clusters, predominantly expressed in either CD14+ and CD141+ DDC or LC and DN-DDC, could be identified. The similarities in expression observed between each pair reflected the overall similarities in transcriptomes seen in MDS plotting and gene co-expression analysis (**Figure 24, Table 17**). Importantly, tolerogenic networks detected in CD14+ and CD141+ mDDC differed from those expressed by mLC. Heterogeneity however could be identified between CD14+ and CD141+ mDDCs, with CD14+ mDDCs displaying elevated expression of a greater number of gene clusters amongst the tolerogenic programme.

In summary, we have revealed the heterogeneity amongst DDC subpopulations and highlighted mechanisms by which they regulate tolerance at the dermis. CD14+ mDDC appear more heavily associated with the expression of tolerogenic pathways than other DDC subpopulations. Interestingly, CD14+ mDDCs and mLCs appear distinct in the tolerogenic mechanisms they express.

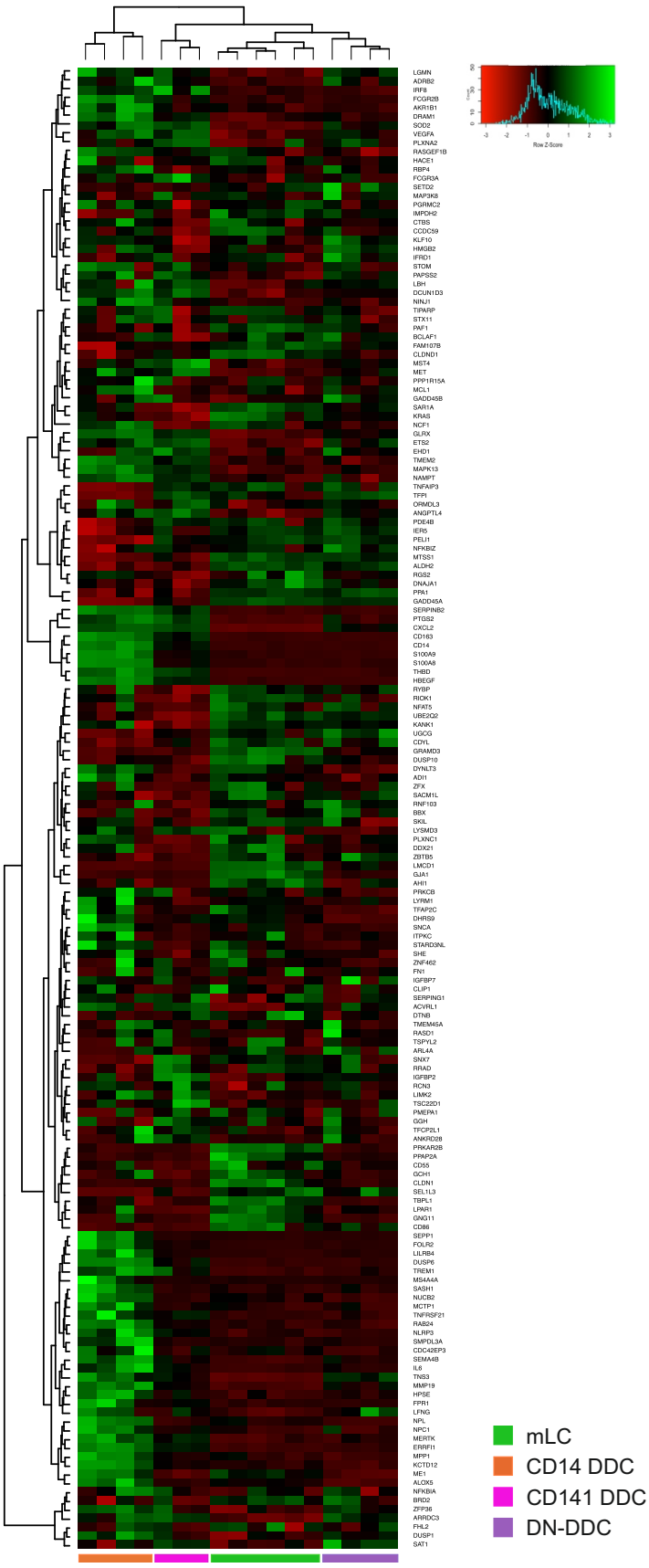

Figure 26. Tracking the tolerogenic DC signature across migrated LC and DDC subpopulations. The 217 genes commonly upregulated in at least 2 of the DC conditions (**Figure 20A&C**) were tracked in heatmaps (complete, ward.D) of log2 normalised expression data (GSE66355) of mLC, CD14+ mDDC, CD141+ mDDC, and CD14 and CD141 double negative mDDC (DN-DDC).

4.3 Discussion

4.3.1 LC transcriptomes are highly unique to other DCs

Comparative analysis of LCs to other DC types was performed to identify the unique features of the LC transcriptome and find evidence for how they mediate tolerance at the epidermis. Transcriptomic analysis inferred that steady-state LCs expressed a highly unique transcriptomic profile compared to other DCs (MoDC, DDC, CD1c DC). Similarly, migrated LC transcriptomes highly differed from migrated DDCs. The high level of dissimilarity between the transcriptomes of DCs subtypes analysed indicated profound differences in their biology and function. Factors we consider that likely contribute to the differences in LC transcriptomes, include their unique developmental pathway, originating from yolk sac and foetal liver monocytes and their localisation in the epidermis, in which LC are in close contact with the external environment and signalling from other epidermal cells (Hoeffel *et al.*, 2012)(Ginhoux and Merad, 2010). Indeed, when LCs and DDCs were contrasted with other DC types, steady-state LC and DDC transcriptomes were most similar and this could in part be due to their residence in similar tissue compartments, as compared to blood derived CD1c DC and artificially developed *in vitro* MoDC (Santegoets *et al.*, 2008)(Széles *et al.*, 2010). The profound differences in the transcriptomes of LCs and MoDC indicated that MoDCs are likely not a good model for studying the biology of primary tissue residing LC.

Intriguingly, our analyses revealed that cell cycle processes were common upregulated pathways in LCs. Maintenance of the LC network within the epidermis is dependent on self-amplification within the tissue, rather than depending on bone marrow derived precursors like conventional DC (Collin and Milne, 2016)(Doebel, Voisin and Nagao, 2017). It may therefore be unsurprising that cell cycle processes are significantly upregulated in epidermal residing steady-state LCs compared to conventional DCs. Through our comparisons between migrated LCs and migrated CD11c+ DDCs (GSE49475), a specific association with metabolic processes was observed during ontology analysis of migrated LC upregulated genes. This pulled similarities from our analysis on TolMoDCs, in which upregulation of metabolic processes was observed, therefore further implicating the importance of metabolic programming for immune regulation (Wculek *et al.*, 2019)(Kelly and O'Neill, 2015). Additionally, during comparison between migrated LC and CD14+, CD141+ and DN-DDC (GSE66355), high *IDO1* and *IDO2* expression in LC was associated with tryptophan catabolism, which is a potent mechanism for T cell tolerance induction by DC (Mellor and Munn, 2004)(Li *et al.*, 2016).

Whilst digested steady-state LC displayed no uniquely upregulated immune-related biological pathways, a common association with negative regulation of immune system processes was shared with steady-state DDCs. Interestingly this suggests that in the steady-state, the prevention of

immune activation is an important process within both the epidermal and dermal skin compartments. Like LCs, DDCs also display tolerogenic function. CD141+ DDCs have been shown to produce IL-10 and expand functional Treg populations, whilst murine migratory RELB+ DDCs have been shown to induce skin antigen specific Treg induction in the lymph nodes (Chu *et al.*, 2012)(Azukizawa *et al.*, 2011). Furthermore, genes upregulated in both digested steady-state LC and DDC were involved in negative regulation of NFκB activity. This coincided with our observations in MoDCs, in which immunogenic LPSMoDCs displayed elevated expression of NFκB family members, which were however downregulated in tolerogenic TolMoDCs and IL10MoDCs. Interestingly, this shared tolerogenic module was absent between migrated LC and migrated CD11c+ DDC (GSE49475), in which heterogeneous gene expression, or low expression of module constituents was identified. Therefore, it appears that the migration process further diverges the transcriptomic differences displayed between LCs and DDCs. Direct comparison in the transcriptomic programmes induced in steady-state and migrated LCs could therefore be important for comprehensive understanding of LC tolerogenic regulation.

Analysis of TolMoDCs and IL10MoDCs identified an association between *MYC* upregulation and the induction of tolerogenic DC transcriptomes. We therefore inspected *MYC* expression amongst LC and the other DC subtypes. Interestingly, a highly significant increase in *MYC* expression was observed in steady-state LC compared to CD1c DC and an increasing trend was observed compared to both MoDC and DDC. The expression of *MYC* in LC and DDC was most similar, linking with the identification of a mutual tolerogenic cluster 13 module in both subtypes, albeit the programme of expression of *MYC* compared to cluster 13 differed. In migrated LC, *MYC* was significantly downregulated compared to migrated CD11c+ DDCs and the expression of *MYC* visually correlated with inflammatory associated DDC clusters 2, 3 and 5. Furthermore, no significant difference in *MYC* expression was identified between tolerogenic PlaDCs and MoDCs. Overall, contradicting evidence for *MYC* involvement in DC tolerogenic transcriptomes limits the universality of an association of *MYC* regulation with DC tolerance induction. *MYC* interaction with *mTOR1* in the *mTORC1-MYC* pathway is critical for DC development and differentiation, including LC (He *et al.*, 2019). *MYC* also heavily interlinks with cell cycle regulation, the predominant programme exhibited by steady-state LC (Gnanaprakasam and Wang, 2017). Its high expression in steady-state LCs may therefore be involved in the population maintenance of LCs, linking with the high level of cell cycles associated processes, rather than specific mediation of tolerogenic programmes.

Highlighted as being critical for LC immune regulation (Polak *et al.*, 2017)(Sirvent *et al.*, 2020) and having been linked with both immunogenic and tolerogenic immune regulation in LPSMoDCs, the expression of *IRF1* and *IRF4* was investigated in each dataset. At the steady-state, no significant difference in *IRF1* expression was identified and a small significant decrease in *IRF4* expression was

identified through comparison to DDCs. Interestingly however, whilst comparisons between migrated LC and DDC revealed a slight trend for *IRF1* decrease, *IRF4* was significantly upregulated. *IRF4* induction during LC migration is well documented, with its critical role in genomic programming of LC to enhance their ability to coordinate T cell response explored (Sirvent *et al.*, 2020)(Polak *et al.*, 2017)(Bajana *et al.*, 2012). However as revealed from analysis of migrated LC and DDC, increased *IRF4* expression does not necessarily correlate with increase in inflammatory transcriptomic modules. In murine studies, *IRF4*-deficient DCs are impaired for the induction of Tregs *in vivo* (Vander Lugt, Riddell, Aly A. Khan, *et al.*, 2017). Furthermore, CRISPR-Cas9 knockout of IRF4 in migratory LC leads upregulated expression of genes associated with inflammatory cytokine and oxidative stress signalling, indicating a role of *IRF4* in immune homeostasis (Sirvent *et al.*, 2020). Thus, a dual role of IRF4 in priming both immunogenic and tolerogenic DC activation requires consideration.

4.3.2 Tolerogenic DC transcriptomes largely differ, although common features of gene include inhibition of NFκB activation and responsiveness to stimuli

To assess how common or unique transcriptomic networks underpinning DC immunotolerance are, we further analysed PlaDC, a DC subset which mediates tolerance at the foetal-maternal interface. The PlaDC population was selected for investigation due their critical tolerogenic role during the prevention of immune responses to foetal alloantigen during the long term growth and residence of the 'allograft' foetus (Tagliani and Erlebacher, 2011)(Blois *et al.*, 2007). Results from PlaDCs analysis highly correlated with those seen in the tolerogenic MoDC datasets, with *IRF4* being lowly expressed in PlaDCs, thus again highlighting *IRF4* as a key regulator of immunogenic responses. Similar to trypsisnised steady-state LCs, associations with NFκB inhibition were identified. To more thoroughly cross compare the tolerogenic profiles of tolerance associated DC sub populations (LC, PlaDC, TolMoDC and IL10MoDC), their transcriptomes were compared to immature MoDCs, which acted as a consistent reference within each dataset. Whilst minimal convergence was overall identified, common modules were revealed. This included the upregulation NFκB inhibitors, such as *NFKBIA* and *TNFAIP3* and the association with negative regulation of signal and stimuli responsiveness. Inhibition of NFκB is therefore highlighted as an important aspect for the induction of DC tolerance. During the steady-state, DCs remain unchanged in response to low levels of inflammatory stimuli (Audiger *et al.*, 2017)(Hasegawa and Matsumoto, 2018). Suppression of signalling may therefore be a mechanism by which DC prevent uncontrolled and unwarranted immune activation at the steady-state and could reflect a state of immunosuppression.

Also, of note in our analyses was the discovery that tissue derived DCs (LC and PlaDC) displayed more homologous gene expression as compared to tolerogenic DCs induced *in vitro* (TolMoDC,

IL10MoDC), suggesting innate tolerance found in specific tissue microenvironments differs from artificial states of tolerance induced *in vitro*. Again, these results question the applicability of *in vitro* DC models to specifically investigate LC tolerance. Overall the cross comparison suggested that different subtypes of DC regulate tolerance via distinct mechanisms. Consistent with this idea was our analysis on *IRF1, IRF4* and *MYC* expression in each of the datasets, in which the expression of each TF highly differed within each dataset, therefore concluding that gene regulation pathways involving these TFs differed across different DC subtypes.

4.3.3 DDCs and LCs are distinct in the tolerogenic mechanisms they exhibit, highlighting the unique nature of LC tolerance regulation at the epidermis

Tracking the common tolerogenic DC signature across the datasets of LC and other DC again revealed similarities in the expression of tolerance associated genes between steady-state LC and DDC. Interestingly, tracking the expression of the tolerogenic module in migrated LC and the whole CD11c+ migrated DDC population revealed a divergence in module expression. This observation was similar to the dissolution of the tolerogenic gene cluster which was identified in gene co-expression analysis of steady-state LC and DDC. LCs and DDCs are both implicated in immune tolerance regulation and we therefore wanted to compare and contrast how these DC regulate tolerance in the closely located, yet unique, epidermal and dermal skin compartments. The DDC population is comprised of different subpopulations characterised by different immune functions and associations with tolerance (Haniffa, Gunawan and Jardine, 2015)(Nestle *et al.*, 1993). To therefore fully comprehend the differences between tolerance regulation between LCs and DDCs, analysis comprising all DDC subpopulations was required. Our analysis using a dataset (GSE35457), containing different DDC subpopulations, revealed that CD14+ and CD141^{High} DDCs specifically, expressed some genes within our identified tolerogenic gene module that were associated with specific tolerogenic ontologies. This was consistent with *in vivo* and *vitro* studies, which identified potent tolerogenic mechanisms for CD14+ and CD141+ DDCs in mice and reduced immunogenic capacity of the CD14+ DDC subpopulation (Chu *et al.*, 2012)(Nestle *et al.*, 1993). Furthermore, when migrated CD141+ and CD14+ DDCs and migrated LCs were directly compared, further differences in overall gene expression were identified, including differential expression of gene programmes linked to tolerance, as identified in gene co-expression analyses and through inspecting the expression of our identified tolerogenic DC gene panel. Overall, our comparisons between LC and DDC populations has revealed that at the steady-state, LCs and DDCs appear to share some gene expression programmes linked with tolerance regulation. However, LCs and DDCs extracted via migration acquire unique tolerogenic programmes. This emphasises the difference in immune regulation orchestrated by the closely located, yet biologically dissimilar epidermal LC and DDC and

further highlights the biological differences driven by the migration extraction process on LC genomic programming.

4.3.4 Further investigations are required into the differences between steady-state and migrated LC transcriptomic programming and tolerogenic capacity

In summary, we have confirmed the unique properties of LC transcriptomes compared to other DC subtypes, which display reduced expression of inflammatory immune genes. The largescale differences observed between LCs and other DC subtypes supported out conclusion that further transcriptomic and *in vitro* experiments on LC tolerance required primary tissue extracted human LC and not *in vitro* DC models. Our analyses suggest that inhibition of the *NFκB* pathway is prerequisite during DC tolerance regulation, but TFs of the IRF family (*IRF4, IRF1)* may be required for regulation of both immunogenic and tolerogenic responses.

Importantly, different transcriptomic programming could be identified in steady-state LC and migrated LC when compared to other DCs, which supports current understanding that the two states are phenotypically different (Sirvent *et al.*, 2020). However, complete comprehension of how these phenotypic differences impact capacity to induce tolerogenic responses is unknown. Further analyses comparing the role of differentially activated steady-state and migrated LC in mediating tolerogenic immunity is therefore required.

Chapter 5 Analysing heterogeneity of LC populations

5.1 Introduction

Transcriptomic analysis of bulk DC populations highlighted the unique qualities of LC transcriptomics, but the precise mechanisms by which LCs mediate tolerogenic immune responses remained unclear. Factors likely influencing the uniqueness of LC immunology is their specific developmental origin from the yolk-sac and foetal monocyte precursors, as well as their life-long residency in the epidermal compartment (Hoeffel *et al.*, 2012)(Merad *et al.*, 2013). The latter in particular appears critical for determining LC immune responses. Skin, and especially its outermost layer, the epidermis, is constantly exposed to numerous varying stimuli from the external environment (Clayton *et al.*, 2017). As immune sentinels resident in the epidermis, LCs react to environmental stimuli, whilst also responding to changes in the tissue microenvironment. Considering the possible non-uniform distribution of immune stimuli throughout the epidermis and with LCs known to express both immunogenic and tolerogenic capabilities, it is conceivable that the LC population at the epidermis is heterogeneous. The differences between LCs exposed to different stimuli/performing different biological functions would likely be reflected within the transcriptomic expression profiles, or programmes, they exhibit. However, analysis of bulk transcriptome data, using either bulk RNA-seq or microarray methods, does not allow investigating of heterogeneity in cell populations, as gene expression data is averaged across all cells within the sample. We hypothesised that this was the reason why molecular signals encoding tolerance was not clearly discernible in LC populations. We therefore optimised a scRNA-seq protocol called Drop-seq (Macosko *et al.*, 2015), in order to produce single cell transcriptomic data of LCs to analyse cell heterogeneity.

Two methodologies, enzymatic digestion and migration of LCs from epidermal sheets are widely used for isolation of human LCs to examine their function *in vitro* (Sirvent *et al.*, 2020)(Polak *et al.*, 2012)(Polak *et al.*, 2014)(Klechevsky *et al.*, 2008)(Seneschal *et al.*, 2012). These two methods yield LCs in two contrasting functional states. Due to the rapid process of enzymatically extracting LCs from epidermal tissue, LCs isolated in this method are considered to be at the steady-state and display an immature phenotype. At the steady-state murine LCs *in situ* display tolerogenic functions, mediating removal of apoptotic cells and the induction of Tregs to promote tolerance and homeostasis (West and Bennett, 2018)(Seneschal *et al.*, 2012)(Hatakeyama *et al.*, 2017). Analysis of the gene expression profile of digested LC would therefore provide insights into how

homeostasis and tolerance is regulated at the steady-state. In contrast, migrated LCs are extracted though culture of epidermal sheets in media, allowing LCs to crawl out of the tissue, mimicking to some degree, the initial stages of LC migration out of the epidermis as they begin their journey from the epidermis to the local lymph nodes. The migration process entails reduction of cell-to-cell contact with keratinocytes and induces LCs to upregulate T cell costimulatory molecules and antigen processing molecules. They therefore display a more immune activated phenotype compared to steady-state LCs (Sirvent *et al.*, 2020)(Clayton *et al.*, 2017). This is further translated into increased ability to induce adaptive immune responses, including efficient antigen processing and presentation, resulting in augmented CD4 and CD8 T cell stimulation (Sirvent *et al.*, 2020)(Polak *et al.*, 2014),(Polak *et al.*, 2012),(Klechevsky *et al.*, 2008). Therefore, in comparison to steady-state LCs, migration induces significant maturation of LCs. Classically, the immature state of a DC is associated with induction of tolerance and the mature, activated state with immunogenicity (Steinman 2003, Lutz and Schuler 2002). In LCs, the state of LC activation has been shown to have a profound effect on immune response mediation, with murine steady-state LC facilitating cytotoxic T cell tolerance, whilst mature LCs induce effector cytotoxic T cell response (Strandt *et al.*, 2017). Thus, we hypothesised that single cell analysis of the steady-state LC population, isolated through enzymatic digestion, would reveal specific LC populations undergoing biological processes associated with tolerance, in comparison to more immunogenic migrated LCs.

Using scRNA-seq we sought to investigate if steady-state and migrated LC populations contain unique subpopulations driving distinct immunological pathways, such as tolerogenic and immunogenic responses and reveal how differences in activation may affect immunological outcomes. Furthermore, taking into account that specific cellular phenotypes are underpinned by unique transcriptional programmes controlled by networks of TFs, proteins that control and modulate gene expression (Spitz and Furlong, 2012)(Xue *et al.*, 2014), we aimed to elucidate the TF networks controlling human LC biology.

Skin is the largest organ of the human body (1.5-2 m^2 surface area). It is therefore unsurprising that areas of skin can differ in their morphology and function. Transcriptomic analysis of skin tissue fibroblasts taken from multiple different anatomical sites (arm, leg, hand, foot, chest), from the same donor, for comparison across different donors, revealed sample clustering was determined by anatomical site in cross-donor analysis (Rinn *et al.*, 2006). In foreskin tissues, increased keratinisation of the inner foreskin is characterised by increasing age and history of tissue infection (Qin *et al.*, 2009). Heterogeneity in LCs from different skin tissues is also observed. For example, LCs from the inner foreskin display augmented antigen sampling and environmental sensing compared to outer foreskin LCs, which has implications in HIV infection or immunity (Fahrbach *et al.*, 2010). Heterogeneity in CD4 expression, the main receptor for HIV entry, is also observed in

LCs from the foreskin, oral and vaginal epithelium (Hussain, Lehner and Thomas, 1995). Using scRNA-seq the heterogeneity in the expression of immune programmes has been identified in structural and immune cell components of foreskin, scalp, trunk and psoriatic skin (Cheng *et al.*, 2018). Diversity in the skin is also mediated by the microbes which colonise it and also its exposure to chemicals and cosmetics/toiletries (Bouslimani *et al.*, 2015). The inner foreskin for example, display increased colonisation by anaerobic bacteria which is believed to effect the inflammatory environment (Esra *et al.*, 2016)(Price *et al.*, 2010). To investigate location specific diversity and the effects of tissue microenvironment conditioning, LCs isolated from human foreskin epidermis at the steady-state and through migration were processed through Drop-seq and compared with LCs isolated from breast skin tissue.

One of LCs key functions is to respond to signals from the microenvironment and external environment *in situ*. Therefore, to investigate LC transcriptomes in situ, protocols allowing the least experimental manipulation are preferable. However, investigations of the "in situ" state pose a significant experimental challenge at two levels; low frequency of LCs in the epidermis, and their responsiveness to manipulation. Purification protocols are likely to affect LC biology, which as a type of DC, are very sensitive to manipulation. Common methods required for purification such as FACS or bead-based purification may activate LCs and thus alter cell transcriptomes, obscuring true biology. However, the relatively low frequency of LCs within the epidermal population means large numbers of epidermal cells would need to be sequenced to acquire sufficient numbers of LCs, without further purification, to ascertain any meaningful biology. Sequencing large numbers of cells comes at great financial cost, therefore restricting the size of single cell datasets that can feasibly be produced. To counter these problems, an extension to the Drop-seq protocol was developed (Constellation Drop-seq). Constellation Drop-Seq includes a step of linear amplification using gene specific primers, prior to PCR amplification, which allows targeted amplification of genes of interest (Vallejo *et al.*, 2019). This allows the focussing of the sequencing depth onto specific cell types of interest. LC heterogeneity could therefore be investigated in large numbers at the steady-state, in the context of other cell types from the epidermis, thus demonstrating the power of the Constellation Drop-seq protocol.

5.1.1 Hypothesis

Steady-state LC and migrated LC transcriptomes are distinct, with steady-state LCs containing subpopulations of cells with elevated genes linked to tolerogenic pathways.

5.1.2 Aims

- Optimise the scRNA-seq method Drop-seq for creation of LC single cell transcriptomic data
- Compare and contrast the heterogeneity and gene expression of steady-state and migrated LC transcriptomes.
- Identify tolerance encoding programmes differentially regulated between LC states.
- Elucidate TF networks controlling differences in genes expression between LC states.
- Investigate the effect of tissue microenvironments at different body sites on LC programming (breast skin vs foreskin).
- Utilise Constellation Drop-seq to investigate unperturbed LC in the context of whole epidermal tissue.

5.2 Results

5.2.1 Optimisation of the Drop-seq encapsulation protocol and the creation of primary human LC single cell transcriptomic data

To enable the production of single cell LC transcriptomic data, in house Drop-seq set-up was optimised for LC encapsulation and analysis. Single LCs were co-encapsulated into nanolitre-sized droplets with a single barcoded primer coated bead (barcodeseqB, ChemGenes), using Drop-seq microfluidic devices (**Figure 27A**). Efficient Drop-seq runs occurred when encapsulation at interphase remained constant, with minimum disturbance at the point of droplet formation. Speeds of aqueous bead and cell inlets (4000μl/hr) and oil inlets (14000μl/hr) created a co-encapsulation efficiency of 5%, consistent with efficiency of the published Drop-seq protocol. Droplets were visually inspected to assess consistency in size and shape and the occurrence of single bead occupancy within them (**Figure 27B**). Homogeneity of droplet sizes reduced the occurrence of bead and cell doublets, whilst also creating the optimal sized special environment to maximise mRNA capture to the barcoded bead primers. After post-encapsulation processing, aliquots of 100 STAMPs (single transcriptomes attached to microparticles) were initially processed for cDNA library amplification using PCR at an array of different cycling parameters. The quality and quantity of the cDNA libraries was assessed using a DNA high sensitivity kit run on an Agilent Bioanalyser. The minimum cycling parameters that created sufficient concentrations of cDNA (>100pg/μl) required for tagmentation were used to amplify the overall desired number of STAMPs for each sample.

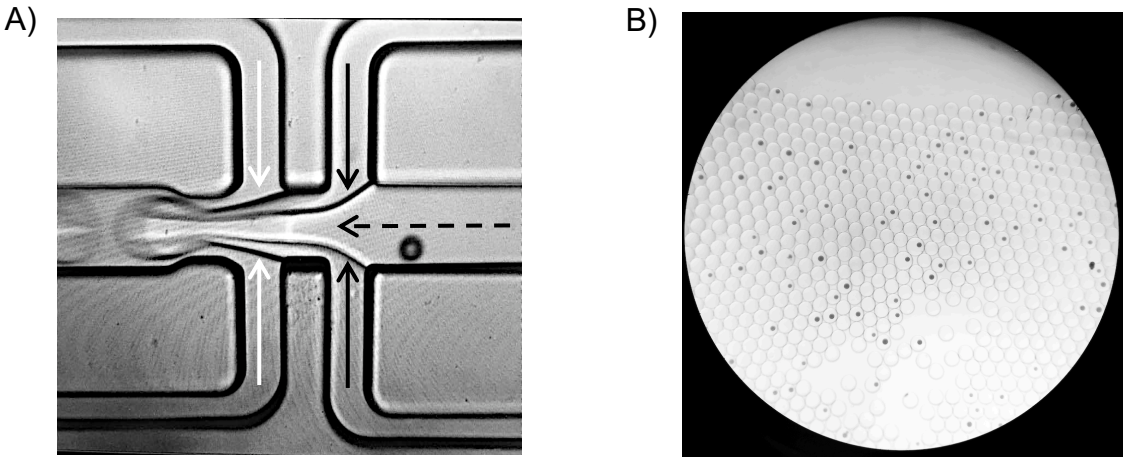

Figure 27. Optimisation of Drop-seq encapsulation. A) Magnification of microfluidic drop-seq device at encapsulation site. nl sized droplets containing single cell and bead flow out of device for collection. Aqueous cell (solid black arrows) and aqueous bead (dashed black arrow) and oil (white arrows) flow is highlighted. **B)** Droplet emulsions produced by Drop-seq encapsulation visualised under a light microscope (10x) were analysed to assess the uniformity of droplet sizes and the occurrence of single bead occupancy.

The Drop-seq pipeline was first optimised using the THP-1 monocyte cell line before proceeding to processing of primary LC samples. Single cell suspensions were created in both 0.02% BSA-PBS solution, as used in the Drop-seq protocol, and also in 10% OptiPrep™ 0.02% BSA-PBS solution. The inclusion of OptiPrep™ was investigated to assess whether it improved the buoyancy of cells whilst loaded on the Drop-seq pumps, reducing the adverse effects of cell sedimentation and therefore increasing the frequency of encapsulation events including the cells. After encapsulation, 100 STAMPs from each sample were processed into cDNA libraries and quantified using a DNA high sensitivity kit on an Agilent Bioanalyser (**Figure 28**). Overall libraries prepared without OptiPrep™ had higher concentration of cDNA. The concentration of cDNA library prepared without OptiPrep™ was 212 pg/µl, whilst the concentration of the OptiPrep™ prepared sample was 59 pg/µl. Whilst OptiPrep™ may be countering the effects of cell sedimentation it appeared to be disrupting the efficiency of mRNA capture or reverse transcription. OptiPrep™ was therefore not included in subsequent Drop-seq experiments.

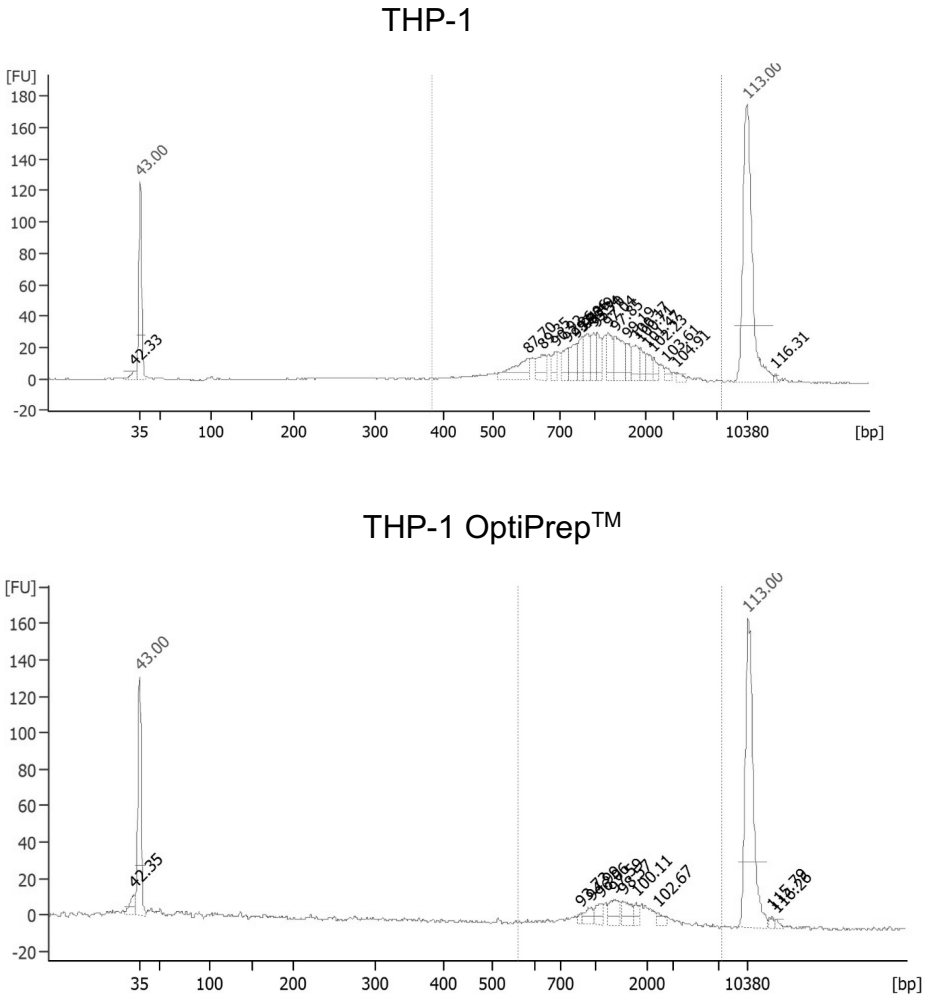

Figure 28. Optimisation of cDNA library preparation using THP-1 cells. DNA high sensitivity kit Agilent Bioanalyser analysis of THP-1 monocyte cell line cDNA libraries after processing through Drop-seq with and without OptiPrep™ solution. Upper (10380bp) and lower (35bp) marker DNA was included for reference. Vertical dotted lines depict area in which cDNA library concentrations were quantified. cDNA libraries without OptiPrep™ = 212 pg/μl and with OptiPrep™ = 59 pg/μl.

To produce our own LC Drop-seq datasets to investigate heterogeneity, LCs were first extracted from primary human skin tissue using enzymatic digestion and migration methods. In the digestion protocol, steady-state LC are dissociated from healthy skin using the dispase/liberase protocol (Sirvent *et al.*, 2020). In migration, 48 hour culture of epidermal fragments, allows LC to migrate out of the tissue for collection, a process resulting in LC maturation (Polak *et al.*, 2014)[,](Klechevsky *et al.*, 2008)[,](Sirvent *et al.*, 2020). Isolated cells were subsequently purified using fluorescence-activated cell sorting (FACS) of cells positively stained for CD207, CD1a and HLA-DR (**Figure 29**). High quality and pure LC population was isolated through gating on singlets, removing debris and strictly selecting the LC population (CD207+, CD1a+ and HLA-DR+). Purified cells were next processed through the Drop-seq encapsulation protocol producing STAMPs (**Figure 30**). From these STAMPS, cDNA libraries were prepared using Kapa HiFi Hotstart enzyme mix, as described in the Drop-seq protocol(Macosko *et al.*, 2015), before being quantified using an Agilent Bioanlayser (**Figure 31**). Using optimised cycling parameters for each sample, the total number of STAMP cDNA libraries required were produced. cDNA libraries were then tagmented in preparation for sequencing, with the quality and quantity of tagmented cDNA libraries assessed on an Agilent Bioanlayser, before sequencing on an Illumina NextSeq sequencer (**Figure 32**). In total, roughly 800 steady-state and 400 migrated breast skin (both extracted from same donor) derived LC STAMPs were processed, as well 500 steady-state (pool of 2 donors) and 500 migrated (pool of 3 donors) foreskin derived LC STAMPs.

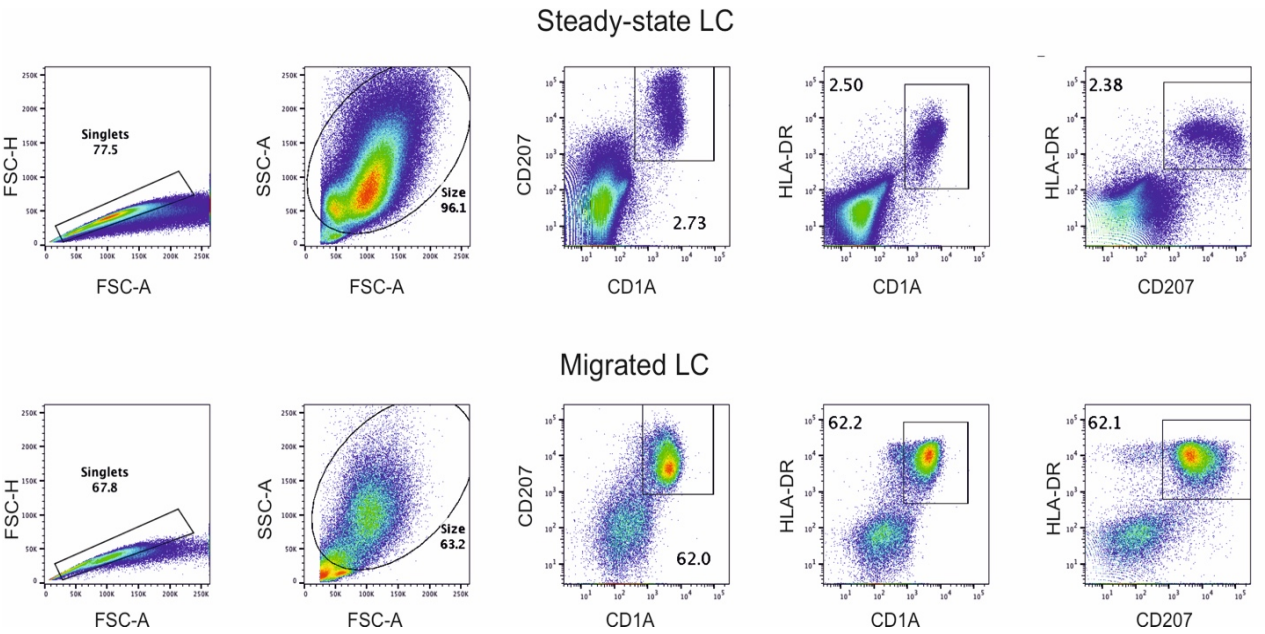

Figure 29. FACS gating strategy for purifying steady-state and migrated LCs. High quality and pure LC populations were isolated using FACS. Cells were gated for singlets (FSC-A, FSC-H) and removing small particulate debris (SSC-A, FSC-A) through forward scatter and side scatter gating. Pure LCs were selected for through strict gating of CD207+, CD1a+ and HLA-DR+ populations. Steady-state and migrated LCs were isolated through sorting and subsequently processed for Drop-seq.

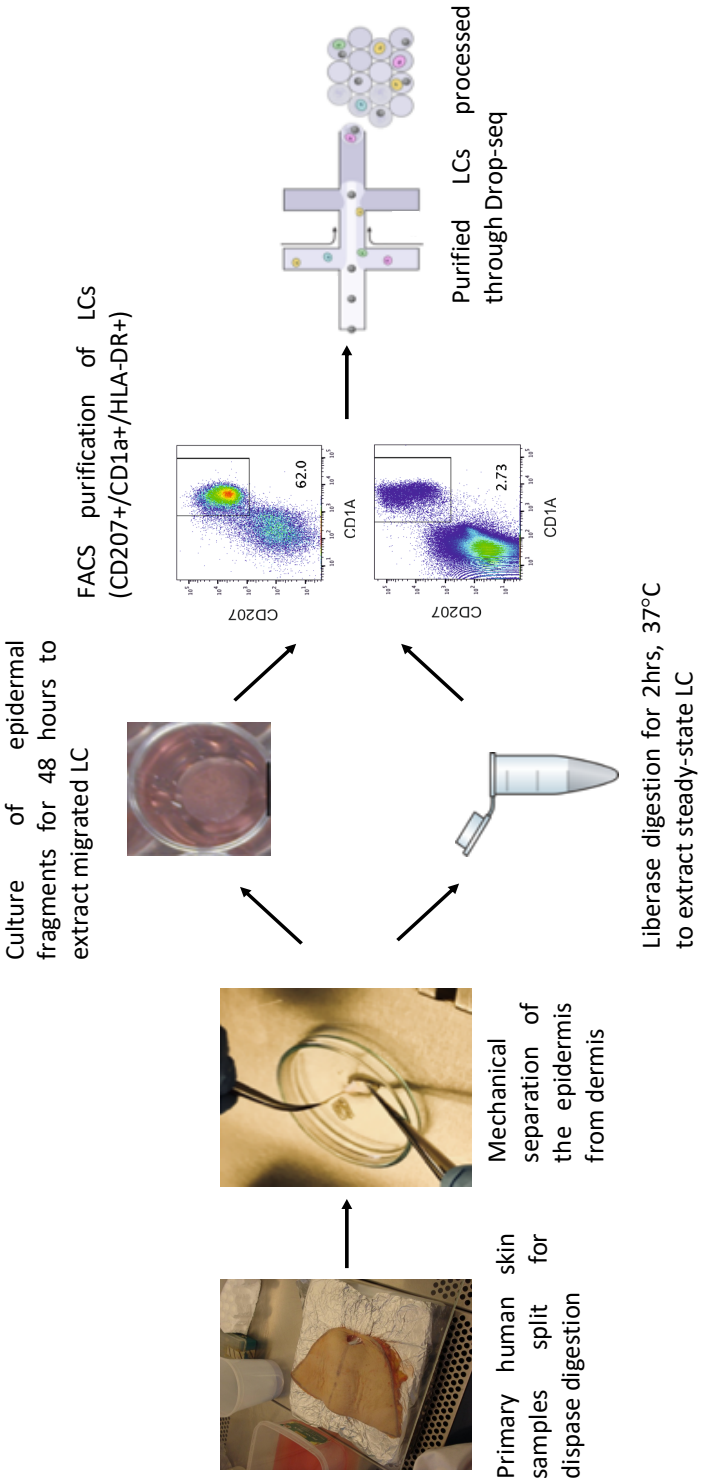

Figure 30. Protocol for extraction of human LCs from primary skin tissue for processing through Drop-seq. Primary human skin samples were digested in dispase (1U/ml, 24 hours, 4°C). Epidermal fragments were then mechanically separated from the dermis. To extract steady-state LCs, epidermal fragments were chopped and digested in Liberase Tm for 2 hours, 37°C. Migrated LCs were extracted from epidermal sheets cultures in media for 48hours, allowing LCs to crawl out of epidermal tissue. FACS purification of steady-state and migrated LC populations was performed through staining for CD207, CD1a and HLA-DR. Single cell suspensions of purified cells were processing through Drop-seq scRNA-sequencing.

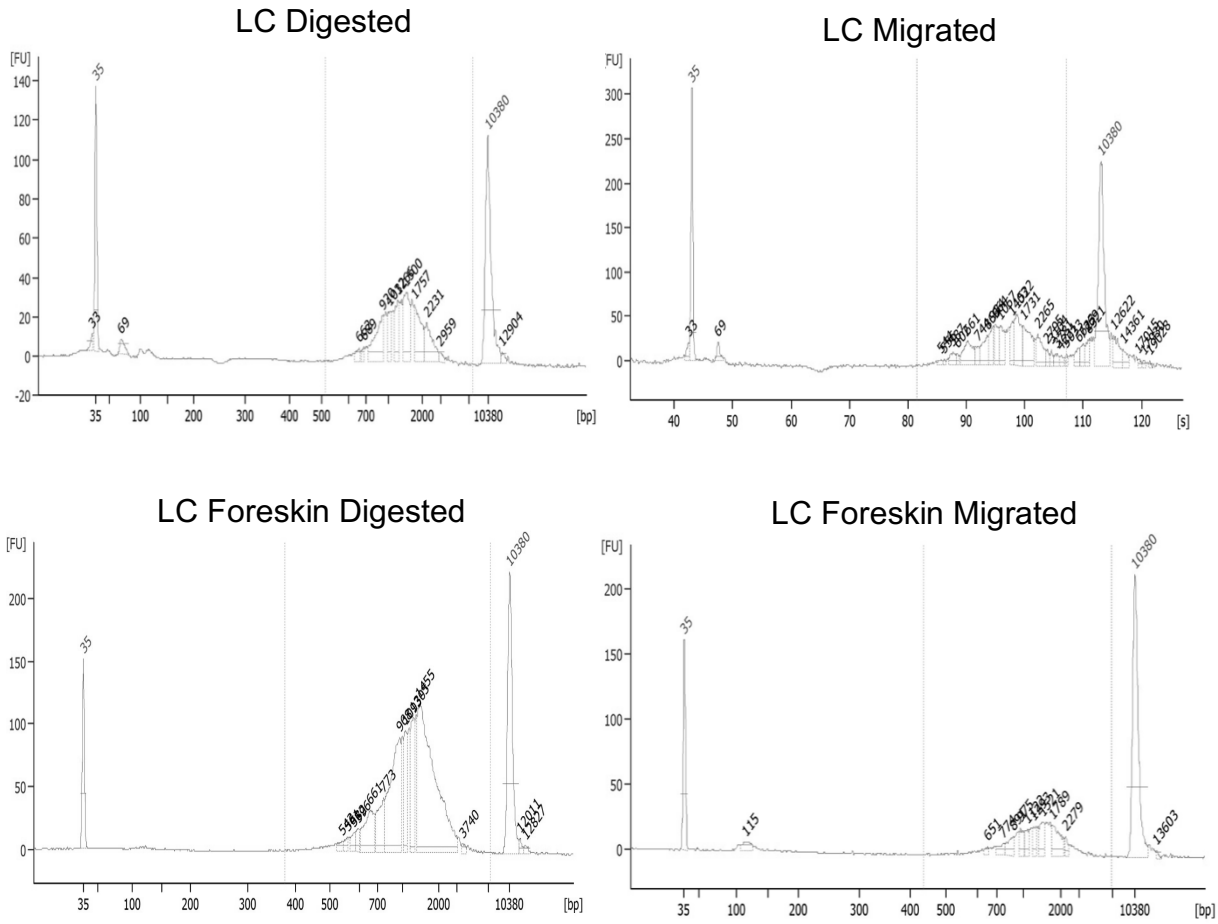

Figure 31. LC cDNA was amplified from STAMPs through PCR, with optimised cycling parameters utilised that produced sufficient concentrations. Prepared cDNA libraries were quantified using a DNA high sensitivity kit run on an Agilent Bioanalyser. Concentrations were required to be >100 pg/μl to proceed to tagmentation. All prepared libraries exceeded this threshold when measured. LC digested = 226 pg/μl, LC Migrated = 234 pg/μl, LC Foreskin Digested = 526 pg/μl, LC Foreskin Migrated = 110 pg/μl. Upper (10380bp) and lower (35bp) marker DNA was included for reference. Vertical dotted lines depict area in which cDNA library concentrations were quantified.

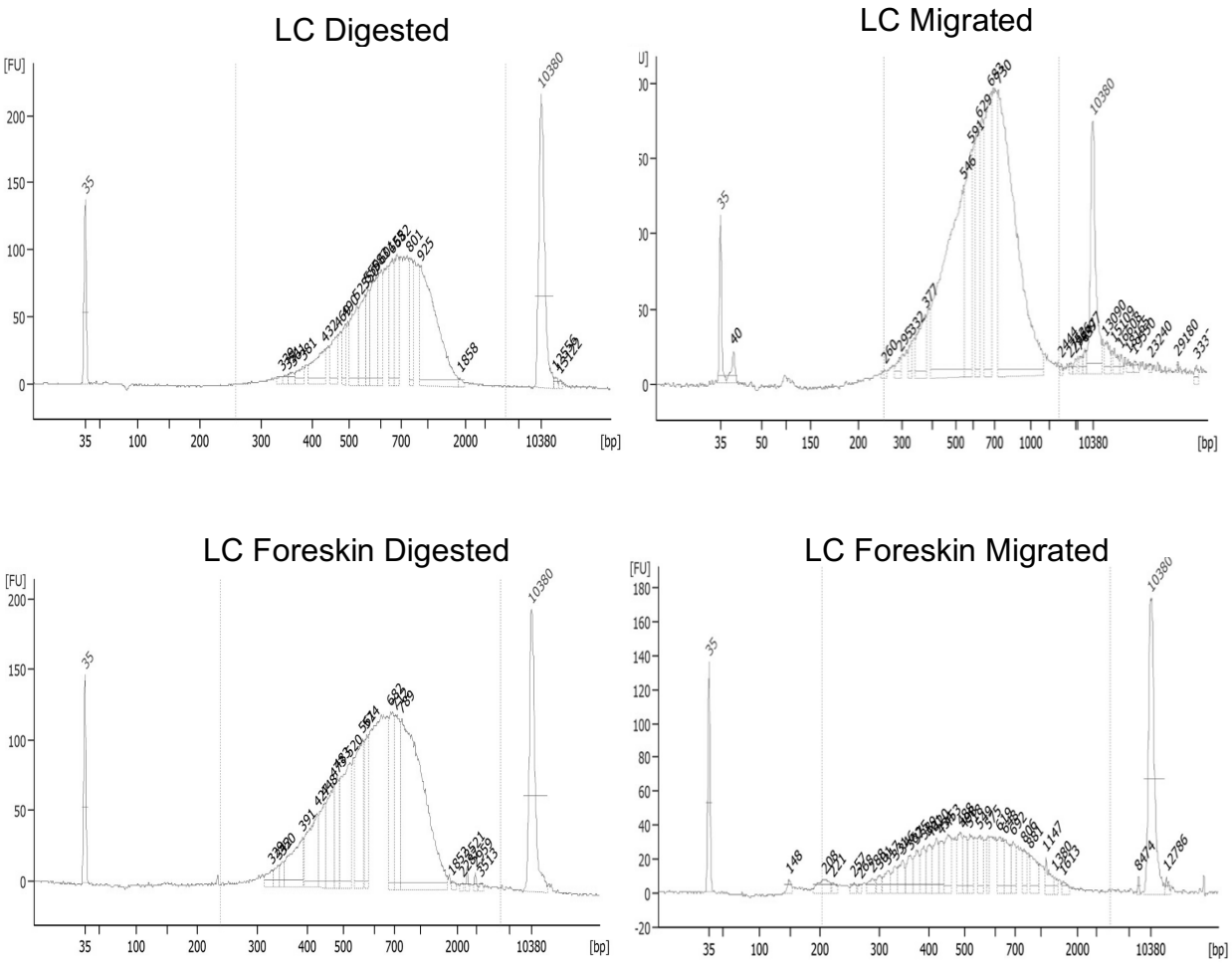

Figure 32. LC cDNA was tagmented in preparation for sequencing. The quality and concentration of tagmented libraries was assessed using a DNA hypersensitivity kit run on an Agilent Bioanlayser. 600 pg/μl of cDNA libraries was used in the tagmentation reaction. LC Digested = 2 nM, LC Migrated = 4.2 nM, LC Foreskin Digested = 2.1 nM, LC Foreskin Migrated = 2.1 nM. Libraries were pooled at 2 nM for sequencing. Upper (10380bp) and lower (35bp) marker DNA was included for reference. Vertical dotted lines depict area in which cDNA library concentrations were quantified.

5.2.2 Migrated LCs display a more immune activated and immunocompetent expression profile compared to steady-state LC.

To explore the gene expression profiles underlying healthy LC tolerogenic function and to evaluate population heterogeneity *in situ* we performed single cell RNAseq on "steady-state LC" dissociated from healthy skin using the dispase/liberase digestion protocol and on "migrated LC", in which LCs are extracted through self-extraction from epidermal sheets during 48 hour culture, as published previously (Sirvent *et al.*, 2020).

After gene (expression detected in <10 cells) and cell filtering (EmptyDrops (Lun *et al.*, 2019), count threshold filtering), expression data for 5864 genes from 585 steady-state LCs and 387 migrated LCs remained. UMAP dimensionality reduction analysis (Scanpy, Version=1.5.0) revealed steady-state and migratory LCs to exhibit distinct transcriptomes with separate localisation of either state (**Figure 33A**). The vast difference in gene expression was further observed during heatmap plotting of the top 100 DEGs (T-test, adj.p-value<0.05) defining each state (**Figure 33B**). Gene ontology analysis for the top 100 DEGs (**Figure 33C)** of each state revealed that steady-state upregulated genes were associated with protein targeting to the ER (adj.p-value=5.8E-47), nuclear transcribed mRNA catabolic process (adj.p-value=2.6E-46), cellular amide metabolic process (adj.p-value=2.2E-21) and response to cytokine (adj.p-value=1.0E-10). In contrast, migrated LC upregulated genes were associated with the immune effector process (adj.p-value=4.2E-8), response to cytokine (adj.p-value=1.5E-7), myeloid leukocyte activation (adj.p-value=1.1E-6) and the innate immune response (adj.p-value=1.4E-5). Migrated LC gene expression therefore appeared to present an enhanced state of immune activation compared to steady-state LC **(Figure 33D)**. Included in this expression programme were antigen presenting genes (*B2M, CD74, HLA-B*) and genes from both the IRF (*IRF4)* and NFκB (*RELB, MAP3K14)* TF pathways. To further investigate the changes in gene expression linked with immune regulation, the expression of antigen presentation, co-stimulatory molecules and activation markers were inspected across the two populations (**Figure 33E)**. This revealed that whilst many MHC II genes were relatively homogenous across both states (*HLA-DRA, HLA-DRB1, HLA-DMA, HLA-DPA1, HLA-DPB1*), steady-state preferentially expressed some genes involved in this pathway (*HLA-DQA1, HLA-DQA2, HLA-DQB1, HLA-DQB2*). However migrated LC clearly displayed increase expression of MHC I (*HLA-A, HLA-B, HLA-C, HLA-E, HLA-F*) and activation markers (*CD83, CCR7*).

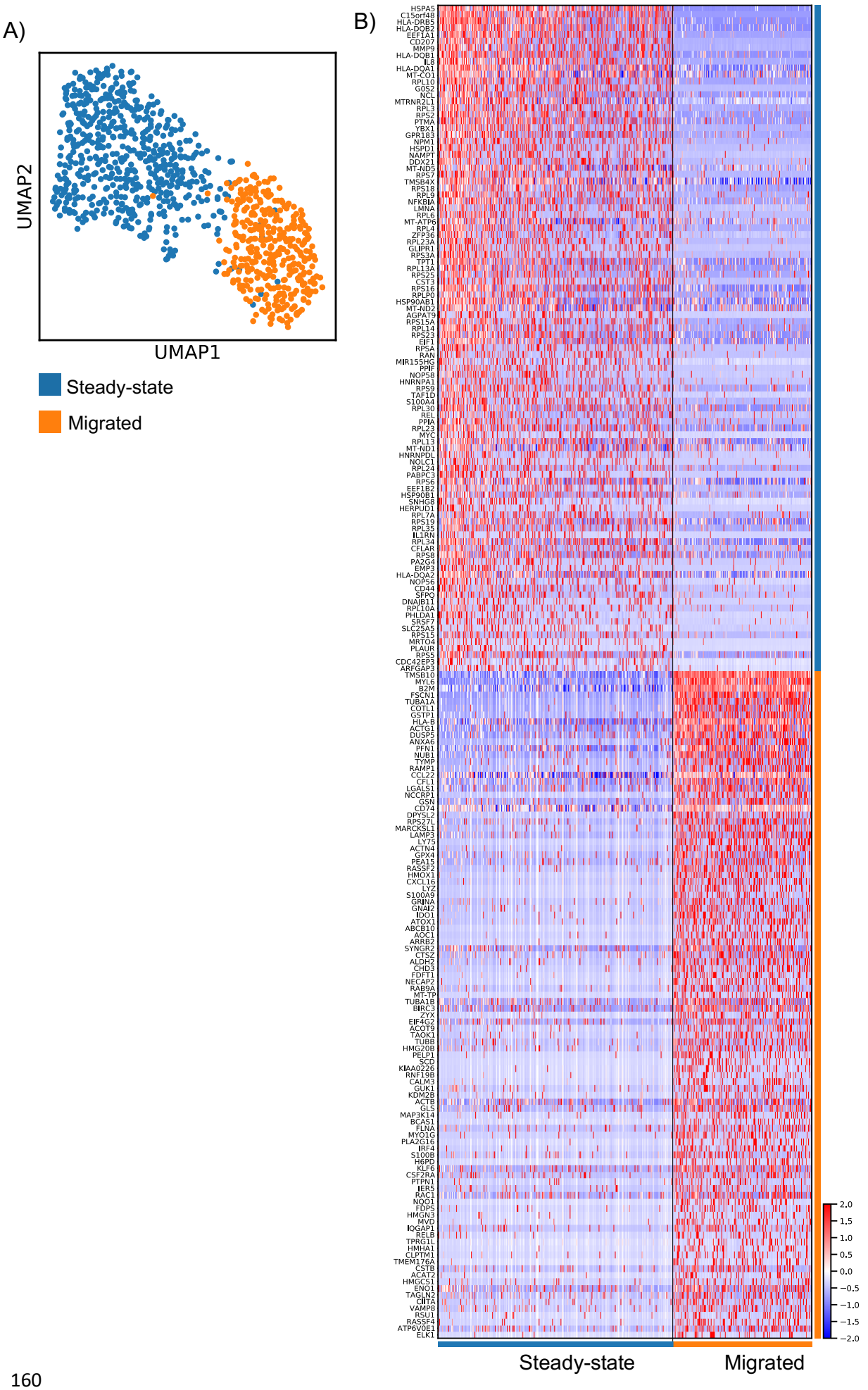
A)
UMAP2
UMAP1
Steady-state
Migrated
B)
HSPA5
C15orf48
HLA-DRB5
HLA-DQB2
EEF1A1
CD207
MMP9
HLA-DQB1
IL8
HLA-DQA1
MT-CO1
RPL10
G0S2
NCL
MTRNR2L1
RPL3
RPS2
PTMA
YBX1
GPR183
NPM1
HSPD1
NAMPT
DDX21
MT-ND5
RPS7
TMSB4X
RPS18
RPL9
NFKBIA
LMNA
RPL6
MT-ATP6
RPL4
ZFP36
RPL23A
GLIPR1
RPS3A
TPT1
RPL13A
RPS25
CST3
RPS16
RPLP0
HSP90AB1
MT-ND2
AGPAT9
RPS15A
RPL14
RPS23
EIF1
RPSA
RAN
MIR155HG
PPIF
NOP58
HNRNPA1
RPS9
TAF1D
S100A4
RPL30
REL
PPIA
RPL23
MYC
RPL13
MT-ND1
HNRNPDL
NOLC1
RPL24
PABPC1
RPS6
EEF1B2
HSP90B1
SNHG8
HERPUD1
RPL7A
RPS19
RPL35
IL1RN
RPL34
CFLAR
RPS8
PA2G4
EMP3
HLA-DQA2
NOP56
CD44
SFPQ
DNAJB11
RPL10A
PHLDA1
SRSF7
SLC25A5
RPS15
MRTO4
PLAUR
RPS5
CDC42EP3
ARFGAP3
TMSB10
MYL6
B2M
FSCN1
TUBA1A
COTL1
GSTP1
HLA-B
ACTG1
DUSP5
ANXA6
PFN1
NUB1
TYMP
RAMP1
CCL22
CFL1
LGALS1
NCCRP1
GSN
CD74
DPYSL2
RPS27L
MARCKSL1
LAMP3
LY75
ACTN4
GPX4
PEA15
RASSF2
HMOX1
CXCL16
LYZ
S100A9
GRINA
GNAI2
IDO1
ATOX1
ABCB10
AOC1
ARRB2
SYNGR2
CTSZ
ALDH2
CHD3
FDFT1
NECAP2
RAB9A
MT-TP
TUBA1B
BIRC3
ZYX
EIF4G2
ACOT9
TAOK1
TUBB
HMG20B
PELP1
SCD
KIAA0226
RNF19B
CALM3
GUK1
KDM2B
ACTB
GLS
MAP3K14
BCAS1
FLNA
MYO1G
PLA2G16
IRF4
S100B
H6PD
KLF6
CSF2RA
PTPN1
IER5
RAC1
NQO1
FDPS
HMGN3
MVD
IQGAP1
RELB
TPRG1L
HMHA1
CLPTM1
TMEM176A
CSTB
ACAT2
HMGCS1
ENO1
TAGLN2
CIITA
VAMP8
RSU1
RASSF4
ATP6V0E1
ELK1
2.0
1.5
1.0
0.5
0.0
−0.5
−1.0
−1.5
−2.0
Steady-state
Migrated

C)

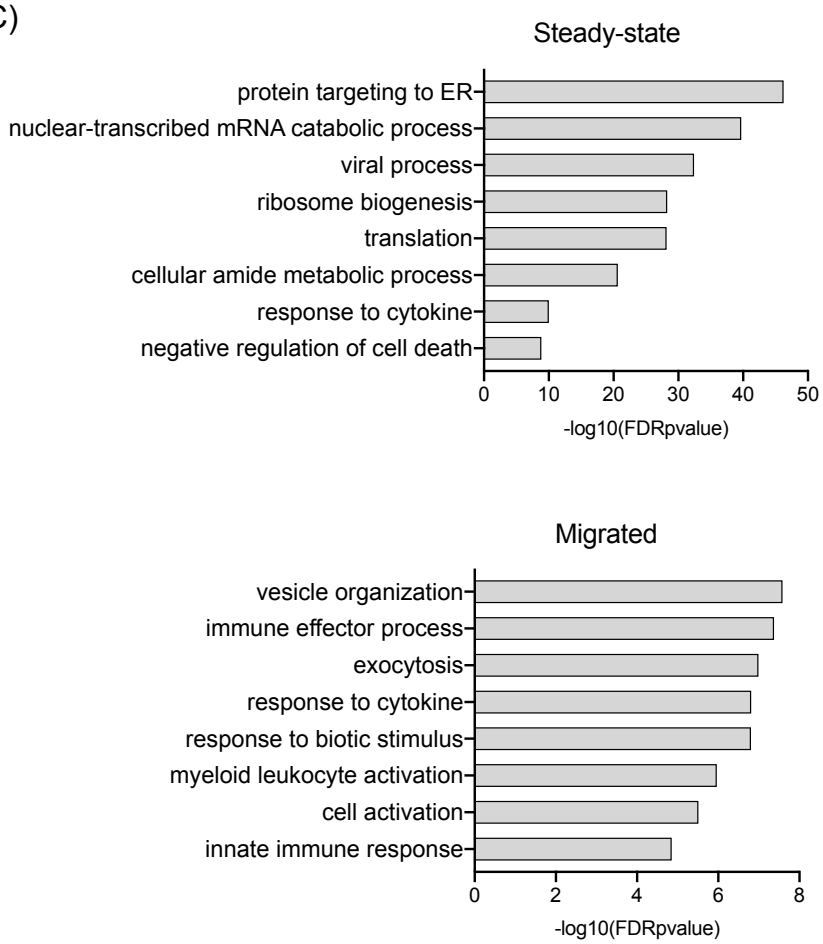
Steady-state
protein targeting to ER
nuclear-transcribed mRNA catabolic process
viral process
ribosome biogenesis
translation
cellular amide metabolic process
response to cytokine
negative regulation of cell death
0
10
20
30
40
50
-log10(FDRpvalue)
Migrated
vesicle organization
immune effector process
exocytosis
response to cytokine
response to biotic stimulus
myeloid leukocyte activation
cell activation
innate immune response
0
2
4
6
8
-log10(FDRpvalue)

D)

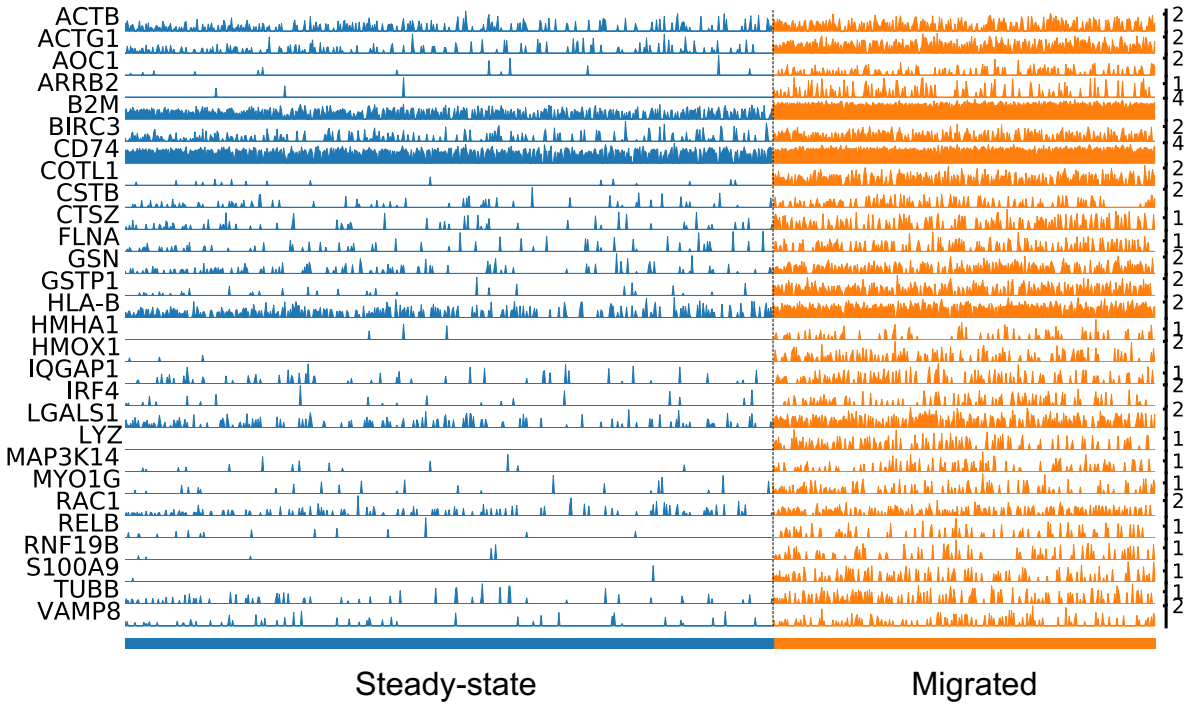
ACTB
ACTG1
AOC1
ARRB2
B2M
BIRC3
CD74
COTL1
CSTB
CTSZ
FLNA
GSN
GSTP1
HLA-B
HMHA1
HMOX1
IQGAP1
IRF4
LGALS1
LYZ
MAP3K14
MYO1G
RAC1
RELB
RNF19B
S100A9
TUBB
VAMP8
Steady-state
Migrated

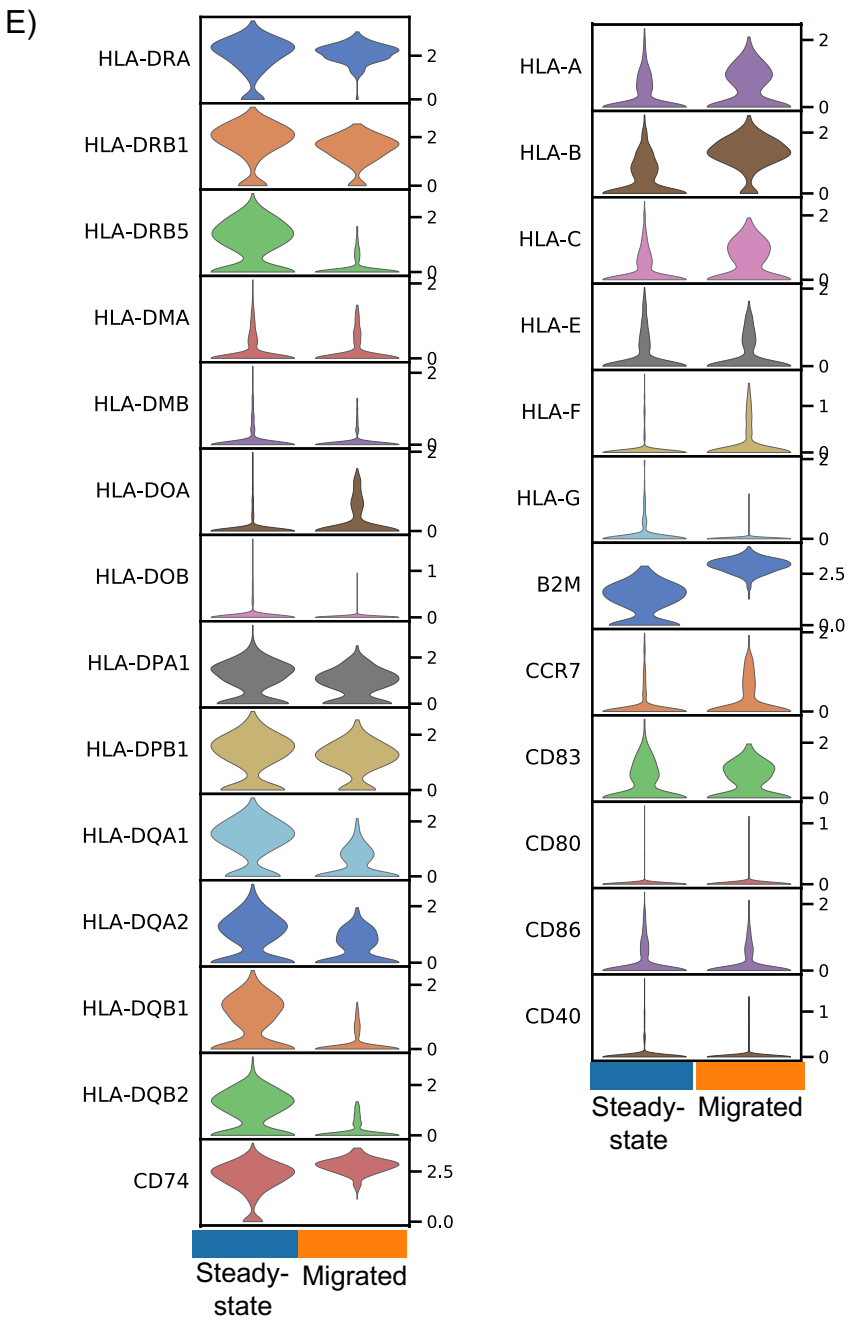

Figure 33. Migrated LCs display a more immune activated and immunocompetent expression profile compared to steady-state LC. A) UMAP dimensionality reduction analysis of Scran normalised single cell data from steady-state and migrated breast derived skin LCs. **B)** Heatmap displaying the top 100 DEGs upregulated in both steady-state and migrated LCs. **C)** Gene ontology analysis (Toppgene) for the 100 DEGs (T-Test, BH adj.p-value<0.05) upregulated in both steady-state and migrated LCs, as shown in **B)**. -log10adj.p-values are displayed. **D)** Trackplot of the genes included in the ontology 'immune effector process, highlighted as one of the top enriched ontologies in migrated LC. Each line represents the level of gene expression from a single cell. **E)** Violin plots displaying the expression of classic DC activation markers (MHC I, MHC II, co-stimulatory molecules) in steady-state and migrated LCs.

5.2.3 Migrated LCs have upregulated expression of genes associated with DC tolerance.

To investigate the presence of genes associated with tolerogenic function across the two LC states, the expression of the tolerogenic DC genes signature containing 40 genes, curated from literature which explore genes associated with DC tolerogenic function were investigated (Tolerogenic DC signature 1, **Appendix A.1**). Furthermore, the tolerogenic DC gene signature, identified in **Chapter 4, Figure 20A&C** which contained 217 genes commonly upregulated in steady-state LC, PlaDC, TolMoDC and IL10MoDC (Tolerogenic DC signature 2, **Appendix A.2**), was assessed amongst the scRNAseq steady-state and migrated LC data. The presence of genes within these two signatures was first assessed in the single cell LC transcriptomes (**Figure 34A**). From the 40 genes from signature 1, 19 genes were identified and from the 217 genes in signature 1, 112 genes were identified. 2 genes were common to both signatures 1 and 2 (*VEGFA, CD86*). To compare the enrichment of the two signatures across steady-state and migrated LCs, Gene Set Variation Analysis (GSVA) was performed **(Figure 34B)**. GSVA analysis identified a moderate enrichment of both tolerogenic DC signatures in migrated LCs, with genes from signature 1 (logFC=0.21, adj.p-value=9.7E-22) being more enriched than signature 2 (logFC=0.12, adj.p-value=2.8E-9). Tolerogenic gene regulation therefore appears to be enhanced during the migration process. The expression of each signature was plotted using trackplots across the steady-state and migrated LCs to assess the overall expression of the DC tolerance associated genes **(Figure 34C&D)**. The presence of genes from the top 100 migrated LC DEGs was then assessed amongst the two tolerogenic signatures to identify the most highly expressed tolerogenic genes. 4 genes (*HMOX1, IDO1, LGALS1,* RELB) from signature 1 and 3 genes from signature 2 (*ALDH2, IER5, S100A9*) were in the top 100 migrated LC DEG list. The detection of these genes was observed amongst the LC populations, with *IDO1, LGALS1* and *RELB* expression by migrated LC also validated by qPCR (**Figure 34E&F**).

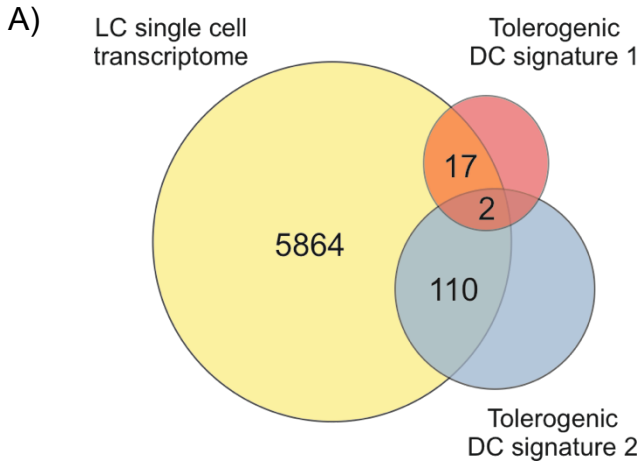
A)
LC single cell transcriptome
Tolerogenic DC signature 1
Tolerogenic DC signature 2
5864
17
2
110

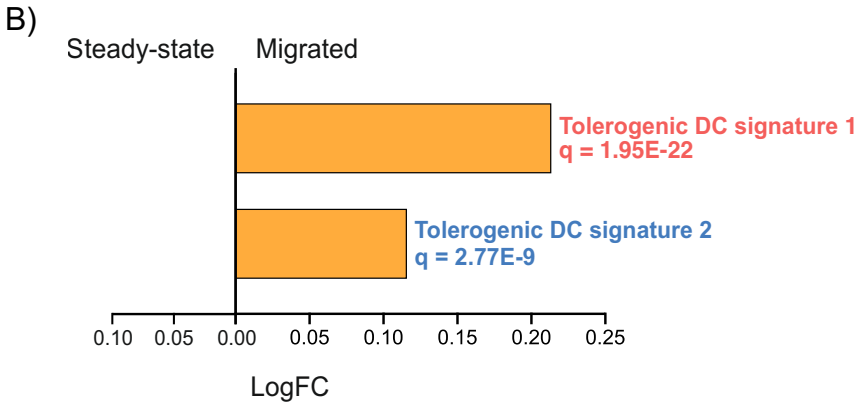
B)
Steady-state
Migrated
Tolerogenic DC signature 1
q = 1.95E-22
Tolerogenic DC signature 2
q = 2.77E-9
0.10
0.05
0.00
0.05
0.10
0.15
0.20
0.25
LogFC

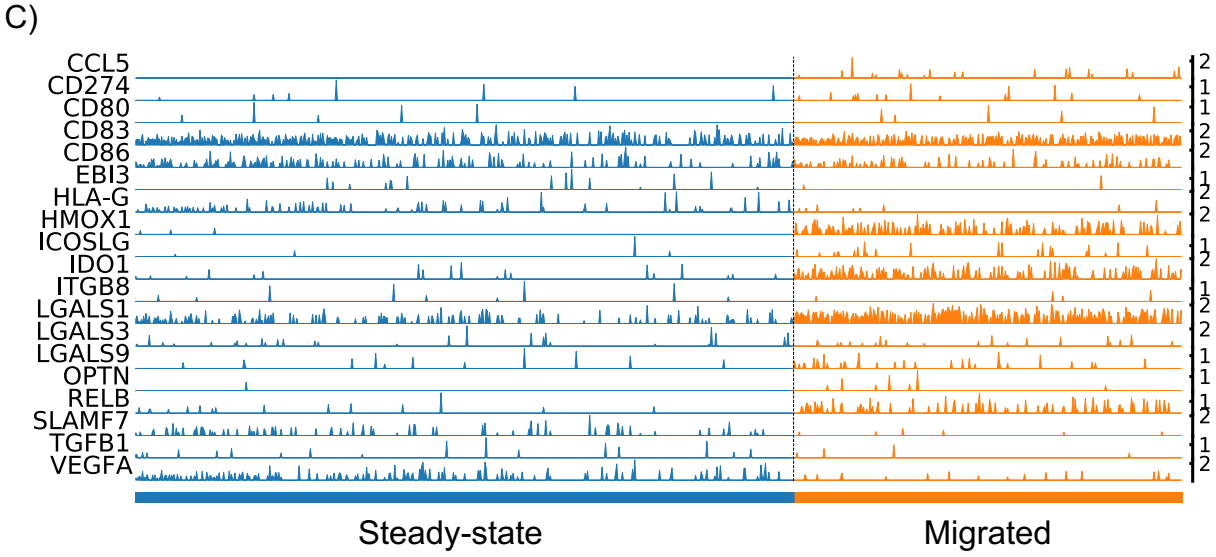
C)
CCL5
CD274
CD80
CD83
CD86
EBI3
HLA-G
HMOX1
ICOSLG
IDO1
ITGB8
LGALS1
LGALS3
LGALS9
OPTN
RELB
SLAMF7
TGFB1
VEGFA
Steady-state
Migrated

D)

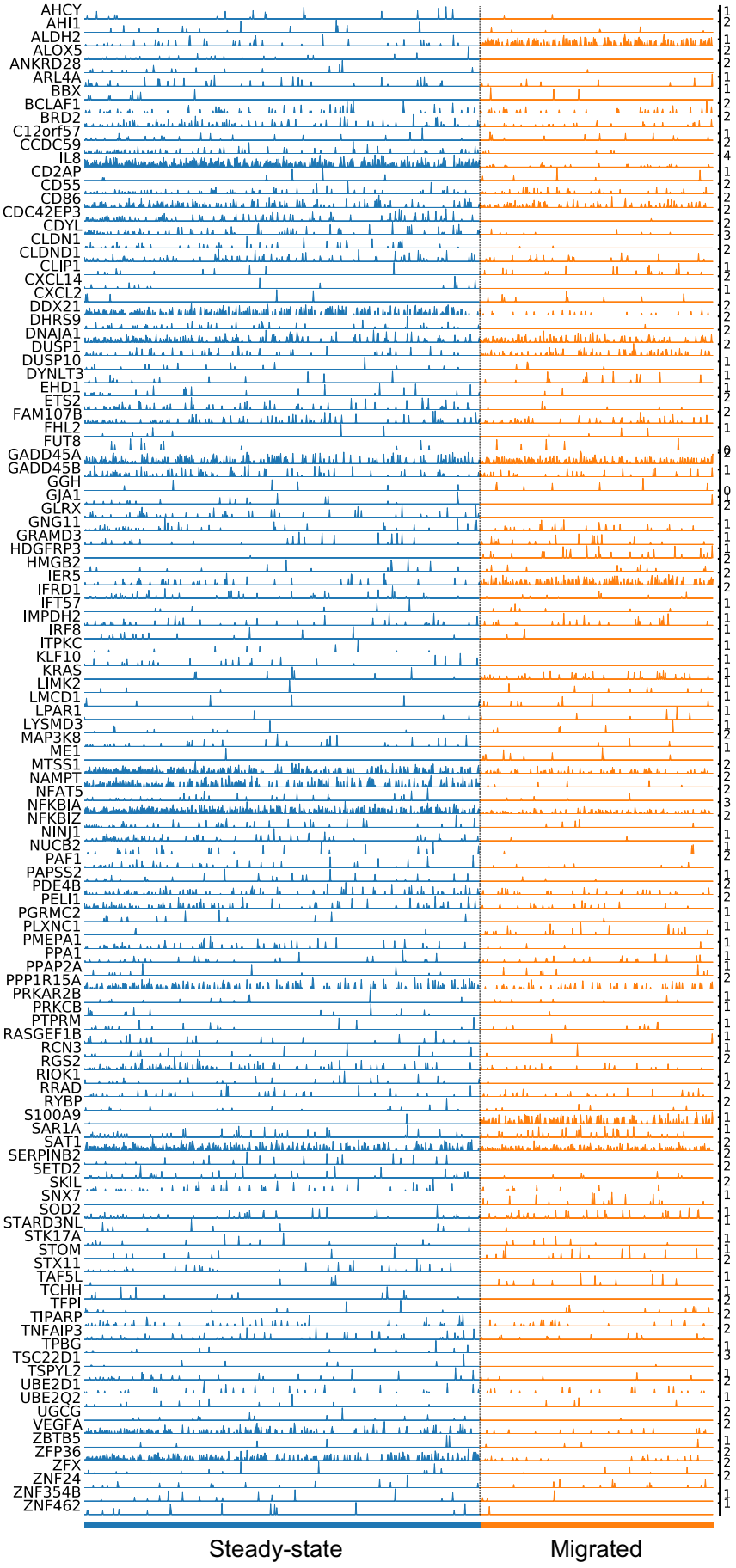
AHCY
AHI1
ALDH2
ALOX5
ANKRD28
ARL4A
BBX
BCLAF1
BRD2
C12orf57
CCDC59
IL8
CD2AP
CD55
CD86
CDC42EP3
CDYL
CLDN1
CLDND1
CLIP1
CXCL14
CXCL2
DDX21
DHRS9
DNAJA1
DUSP1
DUSP10
DYNLT3
EHD1
ETS2
FAM107B
FHL2
FUT8
GADD45A
GADD45B
GGH
GJA1
GLRX
GNG11
GRAMD3
HDGFRP3
HMGB2
IER5
IFRD1
IFT57
IMPDH2
IRF8
ITPKC
KLF10
KRAS
LIMK2
LMCD1
LPAR1
LYSMD3
MAP3K8
ME1
MTSS1
NAMPT
NFAT5
NFKBIA
NFKBIZ
NINJ1
NUCB2
PAF1
PAPSS2
PDE4B
PELI1
PGRMC2
PLXNC1
PMEPA1
PPA1
PPAP2A
PPP1R15A
PRKAR2B
PRKCB
PTPRM
RASGEF1B
RCN3
RGS2
RIOK1
RRAD
RYBP
S100A9
SAR1A
SAT1
SERPINB2
SETD2
SKIL
SNX7
SOD2
STARD3NL
STK17A
STOM
STX11
TAF5L
TCHH
TFPI
TIPARP
TNFAIP3
TPBG
TSC22D1
TSPYL2
UBE2D1
UBE2Q2
UGCG
VEGFA
ZBTB5
ZFP36
ZFX
ZNF24
ZNF354B
ZNF462
Steady-state
Migrated

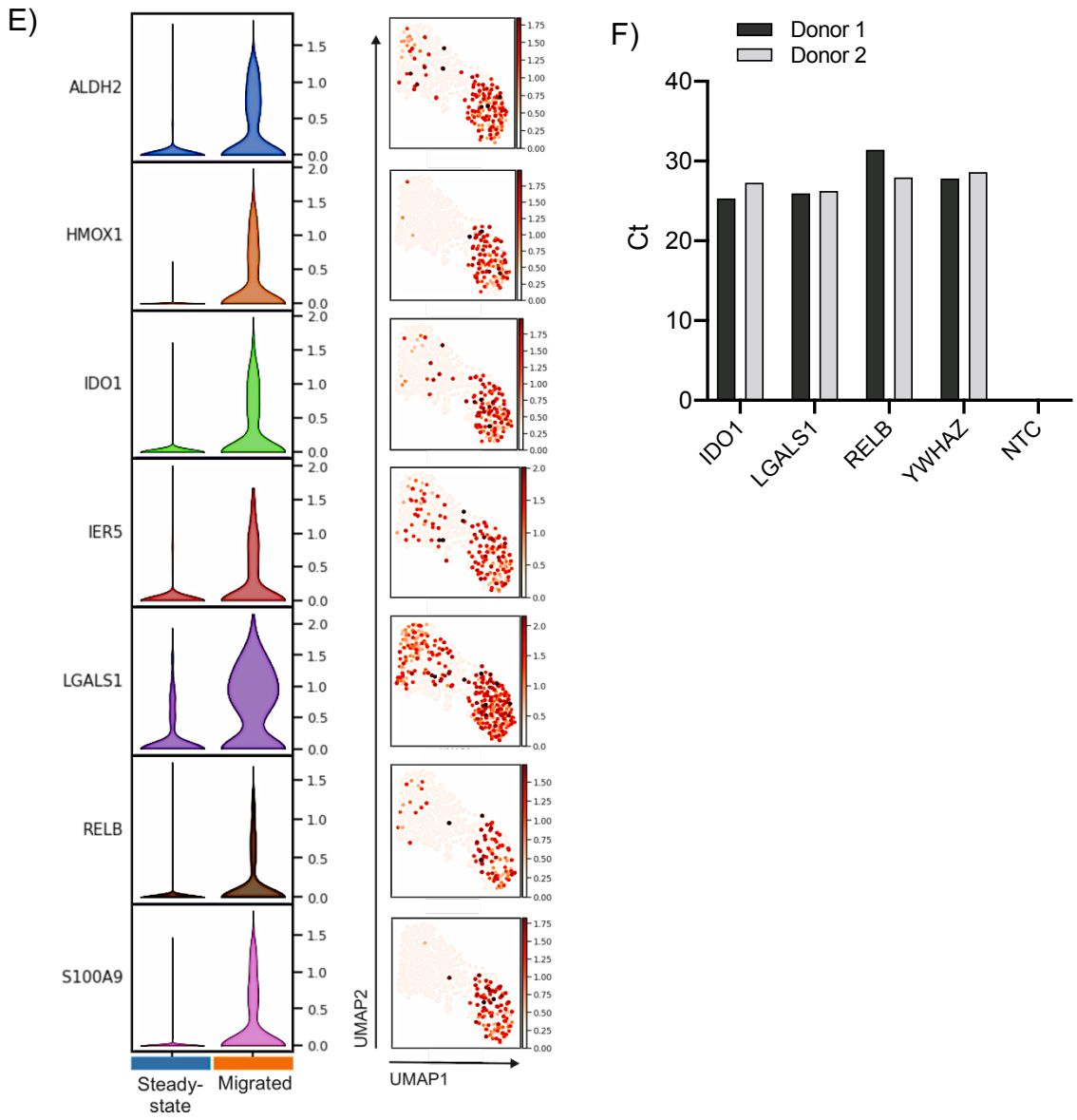

Figure 34. Migrated LCs display elevated expression of tolerance associated genes. A) Venn diagram displaying the number of genes from tolerogenic gene signature 1 (curated from papers reviewing molecular mechanism of DC tolerance induction, **Appendix A.1**) and tolerogenic genes signature 2 (identified in **Chapter 4, Figure 20A&C, Appendix A.2**) that were identified in the whole single cell transcriptomes of breast skin derived LCs. **B)** Gene Set Variation Analysis (GSVA) displaying enrichment of the two tolerogenic signatures in LC populations. BH adjusted p-values and logFC are displayed. **C)** Trackplot displaying the expression of genes from tolerogenic gene signature 1 across steady-state and migrated LCs. **D)** Trackplot displaying the expression of genes from tolerogenic gene signature 2 across steady-state and migrated LCs. **E)** Violin plots and UMAP marker plots displaying the expression of the 7 genes from tolerogenic genes signatures 1 and 2 which were in the top 100 DEGs upregulated in migrated LCs. **F)** qPCR validation of *IDO1, LAGLS1* and *RELB* expression in migrated LC (Ct). Housekeeping gene (*YWHAZ*) and no template control (NTC) Ct values are displayed.

5.2.4 The tolerogenic genomic programme of migrated LCs is underlined by unique TF networks

After identifying the unique expression profile exhibited by steady-state and migrated LC, the underlying TFs responsible for genomic programming were investigated using single cell regulatory network and inference clustering (SCENIC)(Aibar *et al.*, 2017). Using a reference database of TF binding sites, co-expressed genes were inspected for TF binding regions 500bp upstream of starting sequence. SCENIC therefore identified genes within regulons of TFs expressed within the dataset and therefore under their control.

SCENIC analysis revealed that the regulons identified in steady-state and migrated LC highly differed (**Figure 35A**). For steady-state LC, the *MYC, ETS2* and *ETV3* regulons were the most highly enriched. In contrast, migrated LC exhibited a greater number of enriched regulons, including *ELK1, RELA, KLF6, MXI1*, *JUND, RELB* and *IRF4.* The diverse transcriptomes observed between steady-state and migrated LC were therefore underlined by unique TF networks.

To ascertain the key programme promoting TFs, the expression level of TFs themselves and their regulon enrichment score was interrogated (**Figure 35B)**. TFs with both highly differential expression levels in migrated LC, and with high regulon enrichment scores included *IRF4, JUND, RELA, RELB, ELK1, HMGN3, KLF6* and *KLF13*. To further inspect the importance of each regulon for migrated LC gene regulation, the TFs with regulons enriched in migrated were investigated amongst the top 100 DEGs. *IRF4, RELB, ELK1, HMGN3* and *KLF6* were identified.

In order to trace whether the 7 tolerogenic associated genes within the top 100 upregulated DEGs in migrated LCs (*ALDH2, HMOX1, IDO1, IER5, LGALS1, RELB* and *S100A9*) could be under the control of the upregulated TFs, their presence within the TF regulons was inspected (**Figure 35C**). Here, tolerogenic genes were found to be in the regulons of *RELA, RELB, HMGN3, ELK1, JUND, KLF6* and KLF13. Additionally, the co-expression scores of tolerogenic genes with each TF were analysed to apprehend the level of co-regulation (**Figure 35D**). Highly co-expressed TFs and genes included *IRF4-LGALS1, RELB-IDO1, JUND-IER5, ELK1-IDO1/LGALS1, HMGN3-LGALS1/S100A9* and *KLF6-IER5.*

Overall, the enhanced tolerogenic programming of migrated LCs has been recognised, with tolerogenic genes *ALDH2, HMOX1, IDO1, IER5, LGALS1, RELB* and *S100A9* identified as being differentially expressed. Furthermore, the unique programming of migrated LCs is underlined by the differential induction of specific TF regulons, which we can link to the regulation of some tolerogenic genes.

A)

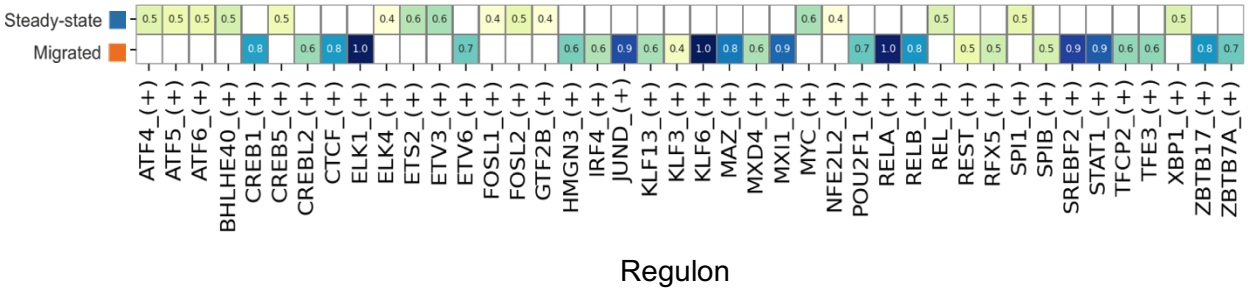
Steady-state
Migrated
ATF4_(+)
ATF5_(+)
ATF6_(+)
BHLHE40_(+)
CREB1_(+)
CREB5_(+)
CREBL2_(+)
CTCF_(+)
ELK1_(+)
ELK4_(+)
ETS2_(+)
ETV3_(+)
ETV6_(+)
FOSL1_(+)
FOSL2_(+)
GTF2B_(+)
HMGN3_(+)
IRF4_(+)
JUND_(+)
KLF13_(+)
KLF3_(+)
KLF6_(+)
MAZ_(+)
MXD4_(+)
MXI1_(+)
MYC_(+)
NFE2L2_(+)
POU2F1_(+)
RELA_(+)
RELB_(+)
REL_(+)
REST_(+)
RFX5_(+)
SPI1_(+)
SPIB_(+)
SREBF2_(+)
STAT1_(+)
TFCP2_(+)
TFE3_(+)
XBP1_(+)
ZBTB17_(+)
ZBTB7A_(+)
Regulon

B)

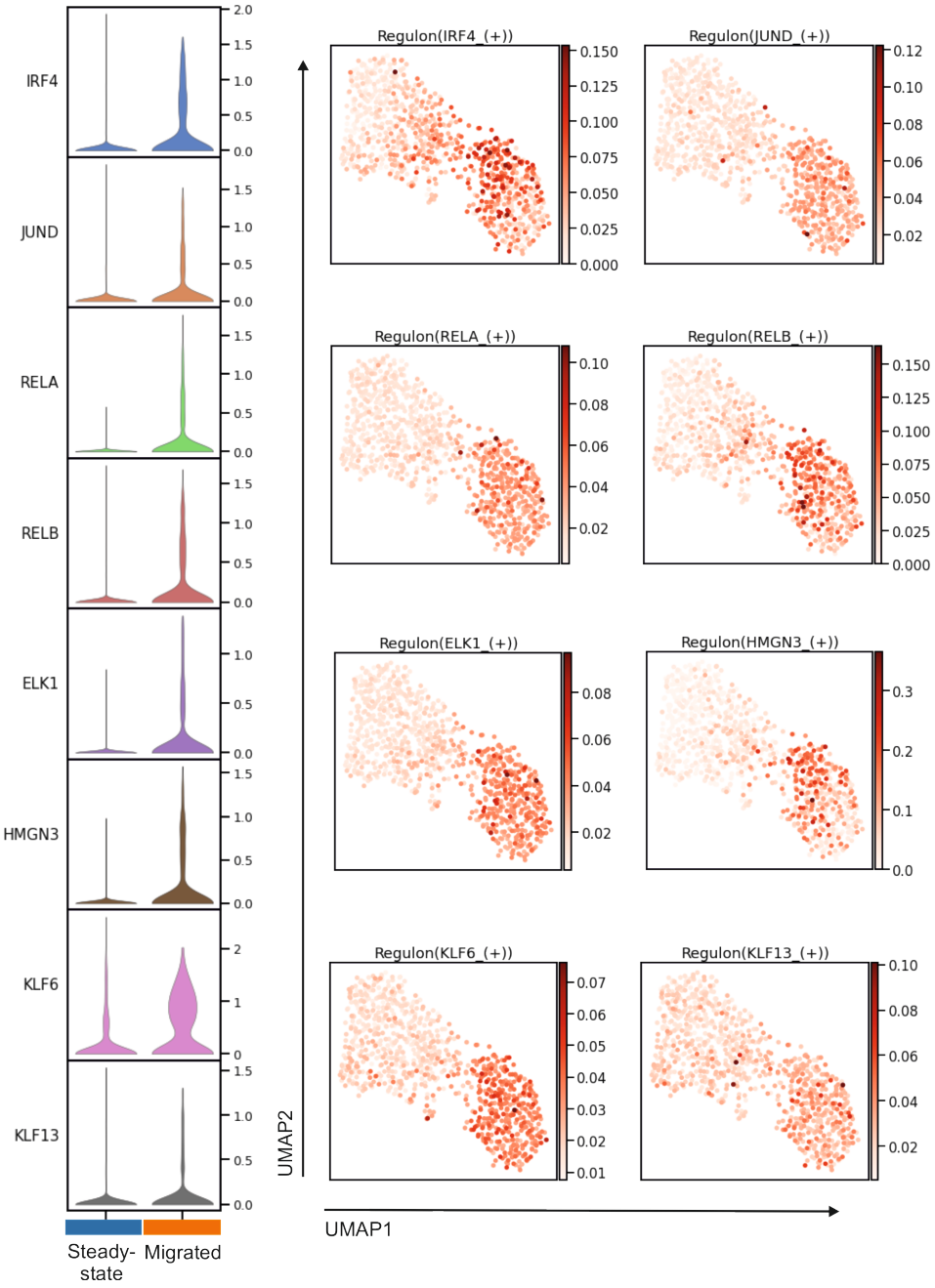
IRF4
JUND
RELA
RELB
ELK1
HMGN3
KLF6
KLF13
Steady-state
Migrated
Regulon(IRF4_(+))
Regulon(JUND_(+))
Regulon(RELA_(+))
Regulon(RELB_(+))
Regulon(ELK1_(+))
Regulon(HMGN3_(+))
Regulon(KLF6_(+))
Regulon(KLF13_(+))
UMAP1
UMAP2

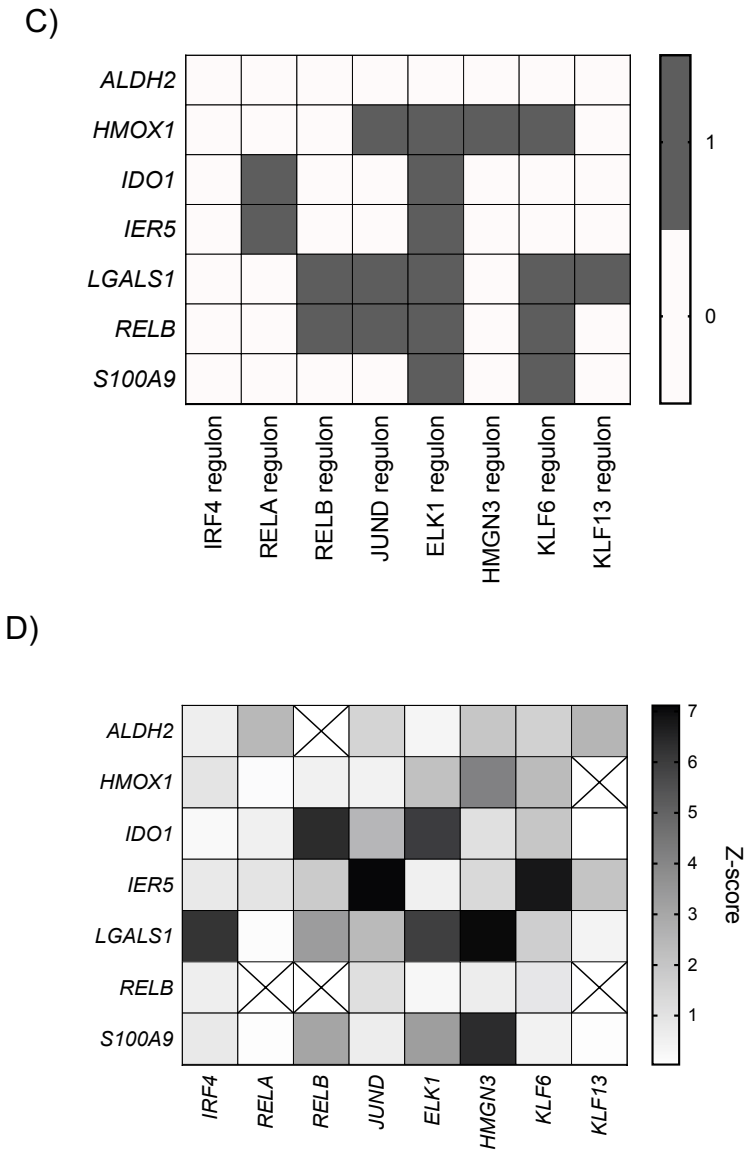

Figure 35. The tolerogenic gene expression programme in migrated LCs is underlined by a unique TF network. A) SCENIC regulatory network and inference clustering analysis revealed TF regulons which were enriched in steady-state and migrated LCs. Z-score heatmap of enriched regulons are displayed. **B)** Violin plots displaying the TFs enriched in migrated LCs with UMAP marker plots displaying TF regulon enrichment Z-scores in each cell, across the two LC populations. **C)** Binary heatmap displaying the presence/absence of the 7 tolerogenic associated genes, identified in the top 100 DEGs upregulated in migrated LCs, within the regulons enriched in migrated LCs. **D)** Heatmap displaying the SCENIC correlation Z-scores for each of the 7 tolerogenic associated genes with the TFs from the migrated LC enriched regulons. Crosses indicate absent correlation scores.

5.2.5 Steady-state LCs are divided into two populations distinguished by state of immunocompetency

Leiden clustering (r=0.5) of the steady-state and migrated LC populations could distinguish two separate clusters within the steady-state LC population, labelled steady-state 1 (S1) and 2 (S2)(**Figure 36A**). To identify the unique qualities of each population, DEG analysis was performed (T-test, BH adj.p-value<0.05) and the top 100 DEGs for each cluster analysed. Interestingly for S1, only 2 significantly upregulated genes compared to S2 were identified (*SERPINB2, MT-ND2*). Gene ontology analysis was performed for the 100 most DEGs for S2, revealing associations with protein targeting to the ER (adj.p-value=1.4E-66), response to cytokine (adj.p-value=5.5E-13), antigen processing and presentation (adj.p-value=3.1E-9), the T cell receptor signalling pathway (adj.p-value=2.9E-8) and positive regulation of the immune response (adj.p-value=2.1E-7)**(Figure 36B)**. S2 therefore represented LCs in an increased state of immunocompetency, which could further be shown through comparing the expression of DC immunocompetency markers across the two populations(**Figure 36C**).

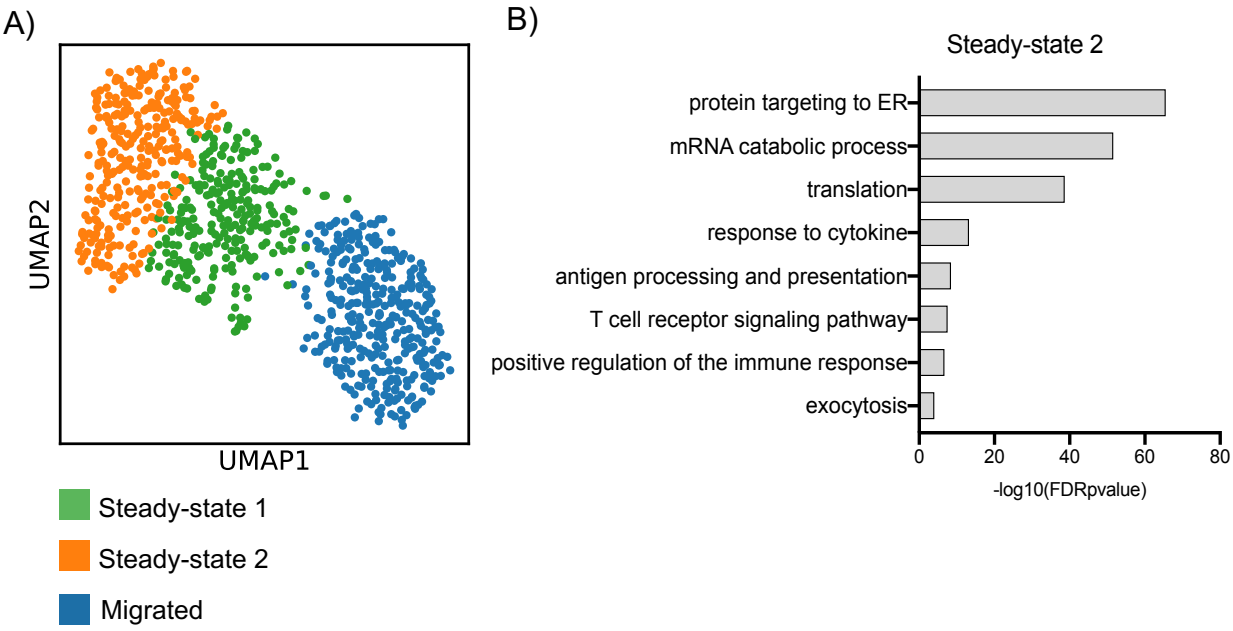

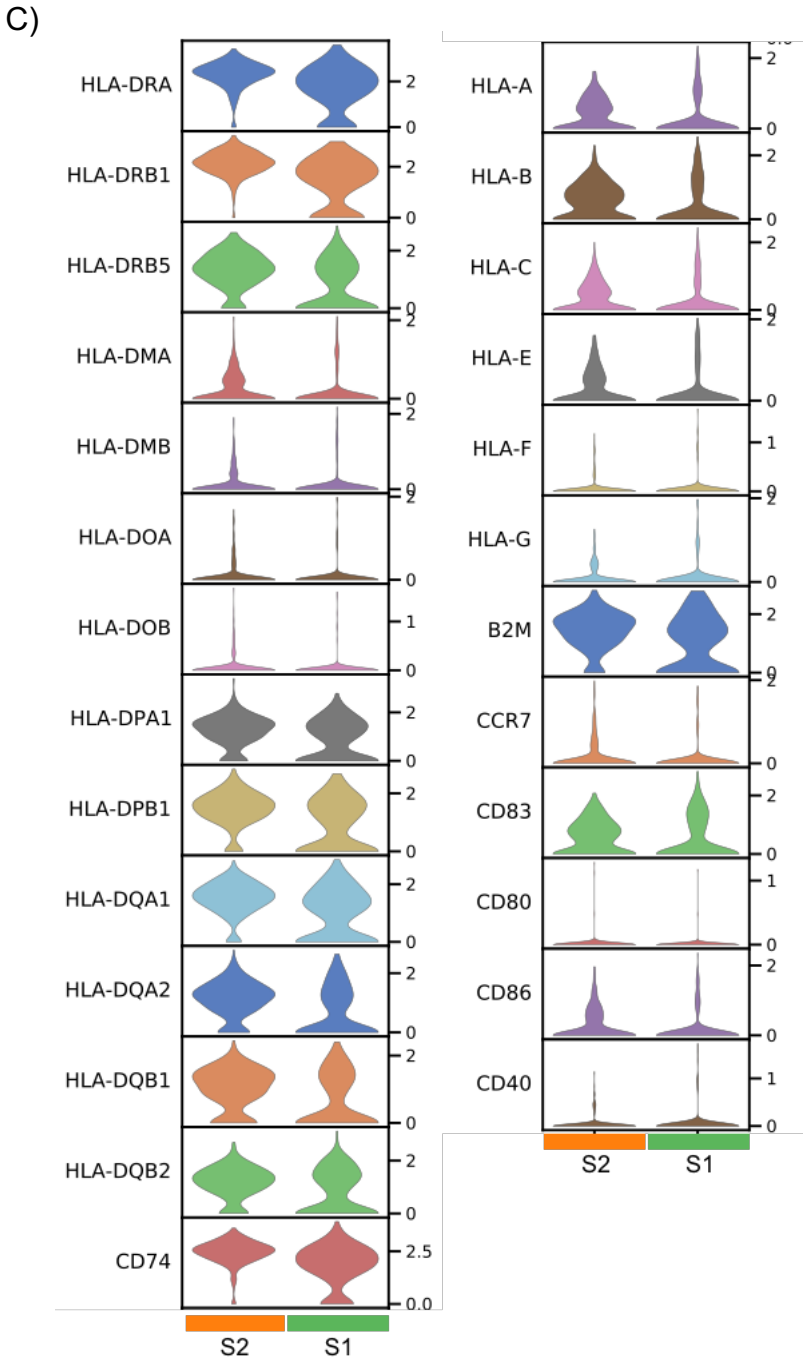

Figure 36. Steady-state LCs can be divided into two subpopulations, distinct through level of immunocompetency. A) Leiden (r=0.5) clustering analysis revealed 3 clusters amongst the steady-state and migrated LCs populations – labelled steady-state 1 (S1), steady-state 2 (S2) and migrated. **B)** Gene ontology analysis for the 100 DEGs (T-test) upregulated in steady-state 2 compared to steady-state 1 LCs. -log10adj.p-values are displayed. **C)** Violin plots displaying the expression of classic DC activation markers (MHC I, MHC II, co-stimulatory molecules) in S1 and S2 populations.

5.2.6 The foreskin microenvironment alters transcriptional networks in human LCs

To assess the divergences in the biology of LCs extracted from skin at different body sites, digested steady-state and migrated LCs obtained from foreskins were processed through Drop-seq for single cell transcriptomic analysis. After cell (EmptyDrop, count threshold filtering) filtering a total of 680 foreskin LCs (424 steady-state, 256 migrated) were used for comparison to the breast skin LCs. To directly compare the steady-state and migrated LC populations from breast and foreskin tissue, data was integrated using BBKNN and embedded together using UMAP dimensionality reduction (**Figure 37A**). Interestingly, steady-state LC from each tissue localised together on the left of the UMAP whilst migrated LC tissue localised together on the right. However, each state from respective tissues still clustered separately, showing the heterogeneity between LCs extracted from different body sites. Trackplots of the top 10 markers genes (Logistic regression) of each state from each tissue also revealed the level of heterogeneity present**(Figure 37B**).

To understand the differences in gene expression between each tissue, steady-state LCs from breast and foreskin and migrated LCs from breast and foreskin were compared via DEG analysis (T-test, BH adj.p-value<0.05). Gene ontology analysis for the top 100 DEGs upregulated in steady-state LC from each tissue compared to the other, revealed differences in genomic programming **(Figure 37C**). Breast steady-state LCs upregulated DEGs were associated with ribosome biogenesis (adj.p-value=1.7E-16), rRNA metabolic process (adj.p-value=1.4E-11), response to cytokine stimulus (adj.p-value=3.6E-5) and oxidative phosphorylation (adj.p-value=7.6E-5). Foreskin steady-state upregulated DEGs were associated with neutrophil activation (adj.p-value=2.4E-7), cell activation involved in the immune response (adj.p-value=4.7E-7), the immune effector process (adj.p-value=3.1E-5) and cytokine production (adj.p-value=2.3E-4). Foreskin steady-state LC gene expression therefore reflected an increase state of immune activation and inflammation.

Gene ontology analysis for the top 100 DEGs upregulated in migrated LCs from breast compared to foreskin migrated LCs revealed associations with response to biotic stimulus (adj.p-value=1.3E-5), defence response to other organism (adj.p-value=8.4E-4), response to cytokine (adj.p-value=9.3E-5) and the immune effector process (adj.p-value=1.1E-3)**(Figure 37D**). Similar annotations of response to cytokine (adj.p-value=1.3E-6), defense response (adj.p-value=2.2E-5) and immune effector process (adj.p-value=1.2E-4) were identified in the analysis of the top 100 DEGs upregulated in foreskin LCs compared to breast. However, interestingly an additional ontology of an association with the inflammatory response (adj.p-value=1.5E-4) was revealed in foreskin upregulated DEGs.

Full top 100 DEG lists for each LC state in each tissue were plotted for comparison, further revealing the extent of differentially expressed programmes**(Figure 37E&F**).

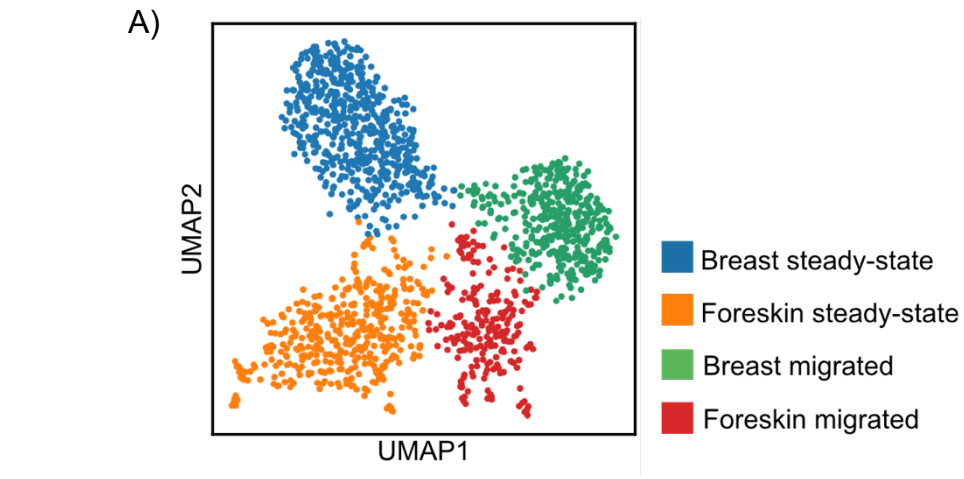
A)
UMAP2
UMAP1
Breast steady-state
Foreskin steady-state
Breast migrated
Foreskin migrated

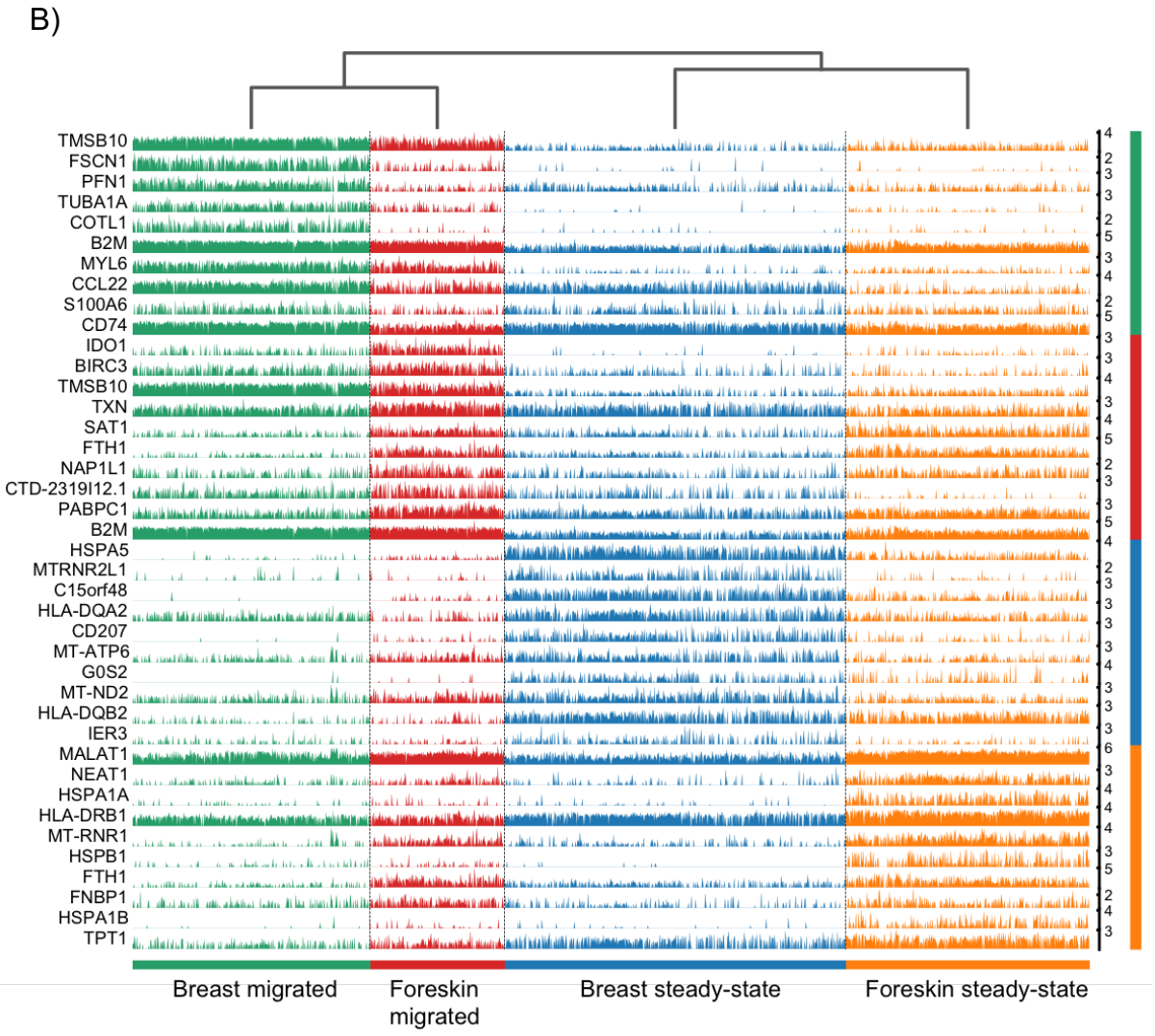
B)
TMSB10
FSCN1
PFN1
TUBA1A
COTL1
B2M
MYL6
CCL22
S100A6
CD74
IDO1
BIRC3
TMSB10
TXN
SAT1
FTH1
NAP1L1
CTD-2319I12.1
PABPC1
B2M
HSPA5
MTRNR2L1
C15orf48
HLA-DQA2
CD207
MT-ATP6
G0S2
MT-ND2
HLA-DQB2
IER3
MALAT1
NEAT1
HSPA1A
HLA-DRB1
MT-RNR1
HSPB1
FTH1
FNBP1
HSPA1B
TPT1
Breast migrated
Foreskin migrated
Breast steady-state
Foreskin steady-state

C)

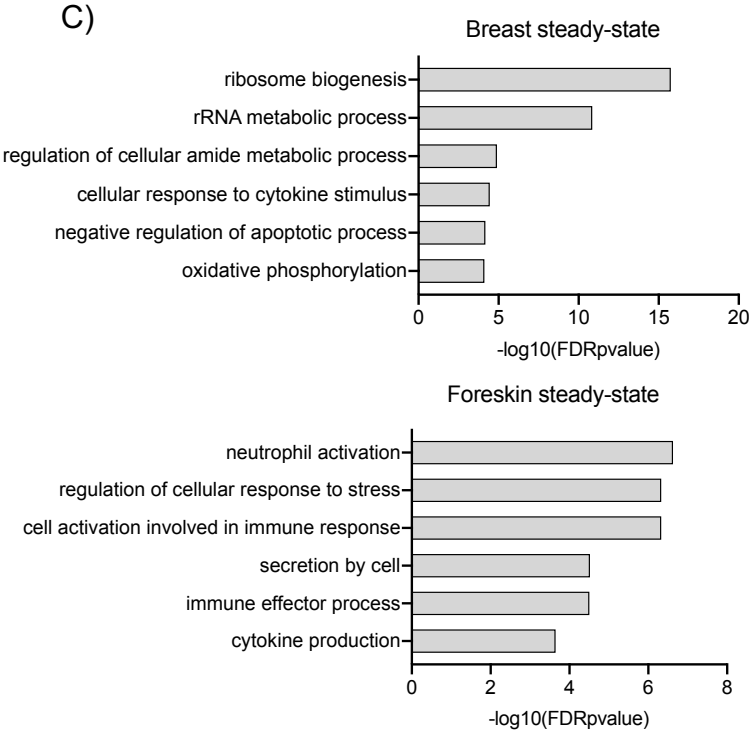
Breast steady-state
ribosome biogenesis
rRNA metabolic process
regulation of cellular amide metabolic process
cellular response to cytokine stimulus
negative regulation of apoptotic process
oxidative phosphorylation
0
5
10
15
20
-log10(FDRpvalue)
Foreskin steady-state
neutrophil activation
regulation of cellular response to stress
cell activation involved in immune response
secretion by cell
immune effector process
cytokine production
0
2
4
6
8
-log10(FDRpvalue)

D)

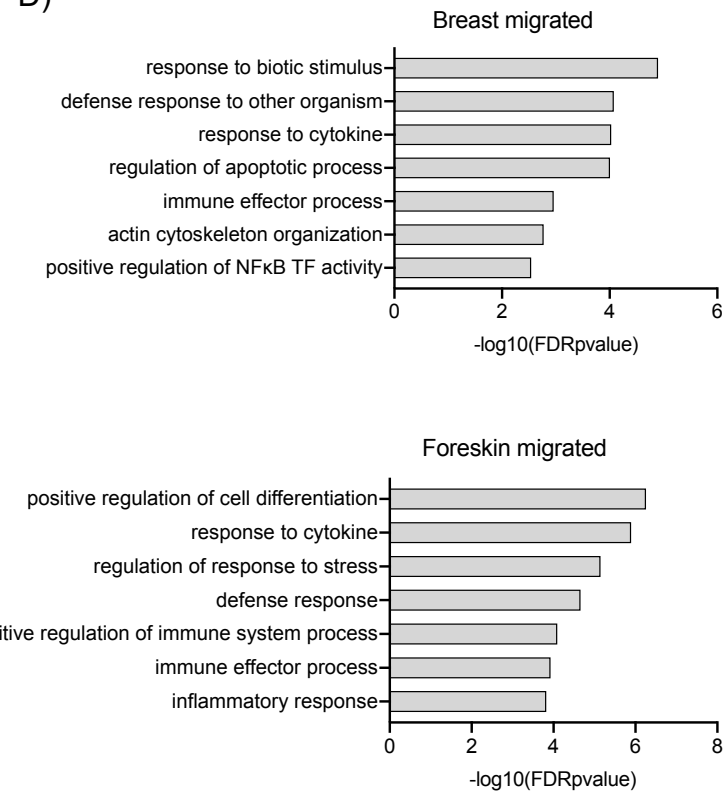
Breast migrated
response to biotic stimulus
defense response to other organism
response to cytokine
regulation of apoptotic process
immune effector process
actin cytoskeleton organization
positive regulation of NFκB TF activity
0
2
4
6
-log10(FDRpvalue)
Foreskin migrated
positive regulation of cell differentiation
response to cytokine
regulation of response to stress
defense response
positive regulation of immune system process
immune effector process
inflammatory response
0
2
4
6
8
-log10(FDRpvalue)

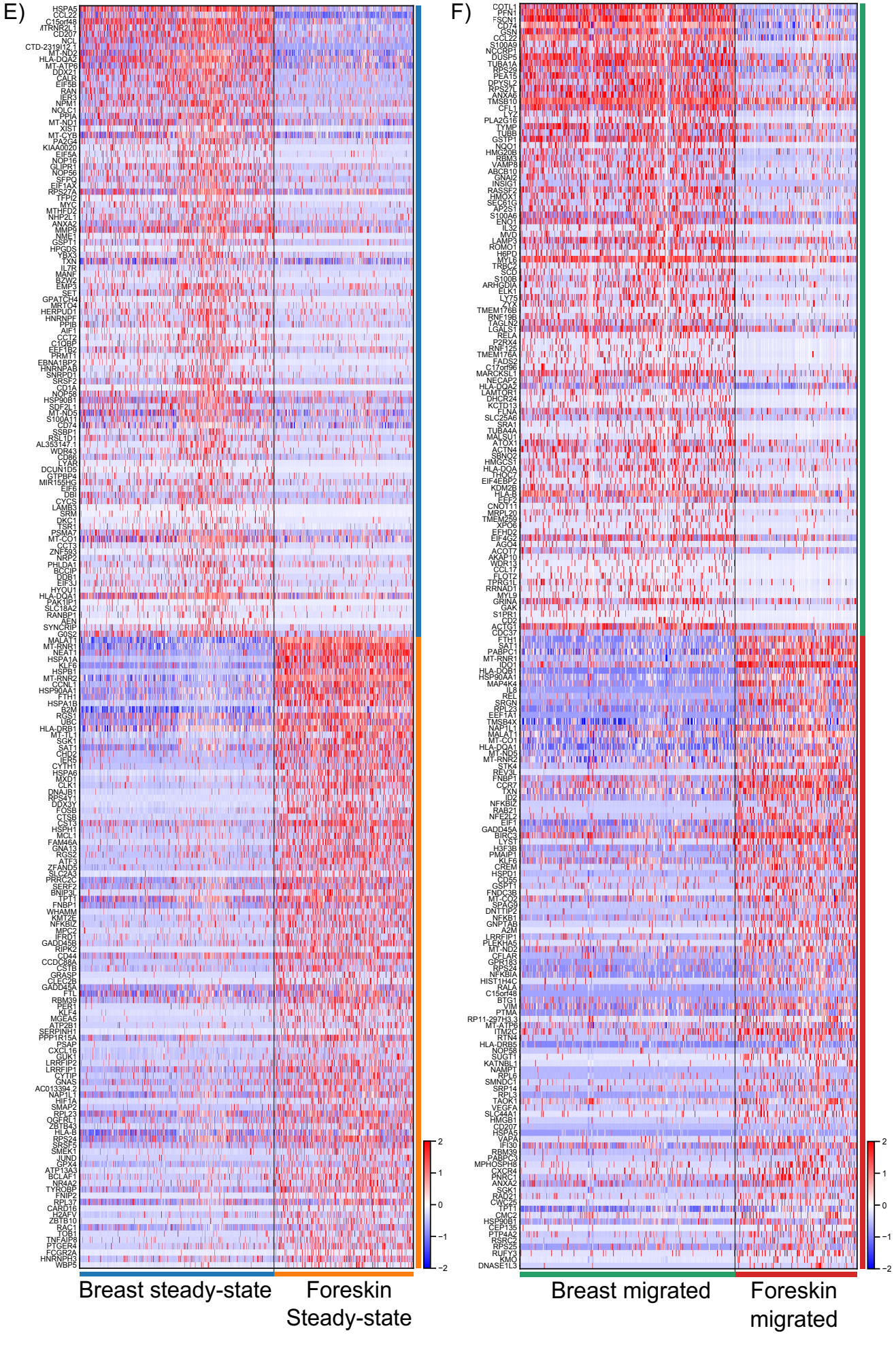
E)
F)
Breast steady-state
Foreskin
Steady-state
Breast migrated
Foreskin
migrated

Figure 37. Steady-state and migrated LCs derived from breast skin and foreskin display differences in gene expression. *figure finishes on previous page **A)** UMAP dimensionality reduction analysis of Scran normalised, BBKNN integrated, single cell data from steady-state and migrated foreskin LCs extracted from breast skin and foreskin. **B)** Trackplots displaying the top 10 markers genes (Logistic regression) for each of the LC populations. **C)** Gene ontology analysis (Toppgene) for the 100 DEGs (T-Test, BH adj.p-value<0.05) upregulated in steady-state breast vs foreskin LC (top) and foreskin vs breast LC (bottom). -log10adj.p-values are displayed. **D)** Gene ontology analysis (Toppgene) for the 100 DEGs (T-Test, BH adj.p-value<0.05) upregulated in migrated breast vs foreskin LC (top) and foreskin vs breast LC(bottom). -log10adj.p-values are displayed. **E)** Heatmap displaying the top 100 DEGs upregulated in comparisons of steady-state breast vs foreskin LC. **F)** Heatmap displaying the top 100 DEGs upregulated in comparisons of migrated breast vs foreskin LCs.

For further investigation into the transcriptomic differences between steady-state and migrated foreskin LCs, separate analysis was performed. UMAP dimensionality reduction analysis identified a similar population structure as observed in breast skin extracted LCs and from combined analyses, with steady-state and migrated LCs separating away from each other (**Figure 38A**). Gene ontology analysis and heatmap plotting of the top 100 DEGs (T-test) defining steady-state and migrated foreskin LCs was performed **(Figure 38B&C)**. Steady-state DEGs were associated with protein targeting to the ER (adj.p-value=8.2E-49), mRNA catabolic process (adj.p-value=1.6E-37), response to cytokine (adj.p-value=1.5E-7), the innate immune response (adj.p-value=1.3E-4) and antigen processing and presentation (adj.p-value=2.3E-2). Migrated LC DEGs were associated with oxidative phosphorylation (adj.p-value=5.5E-5), immune effector process (adj.p-value=1.7E-4), response to cytokine (adj.p-value=8.8E-4), T cell mediated immunity (adj.p-value=2.1E-3) and a defence response (adj.p-value=2.3E-3). Interestingly, an association with negative regulation of the immune system process (adj.p-value=1.5E-2) was also identified, due to the expression of *IDO1, CD86*, *IL74*, *A2M, ARRB2, CST7, GCSAM, SAMSN1* and *VIMP.* The expression of classical DC activation markers was also investigated(**Figure 38D)**. Interestingly, steady-state LCs displayed elevated expression the maturation marker *CD83*. However, foreskin migrated LCs displayed increase expression of MHC I (*HLA-A, HLA-B, HLA-C, HLA-E, HLA-F*) and *CCR7,* with the addition of substantial *CD86* upregulation. Overall, the immunocompetent profile of migrated foreskins LCs, similarly reflected the profile of migrated breast LCs. However steady-state foreskin LCs appeared more mature then their counterparts from the breast.

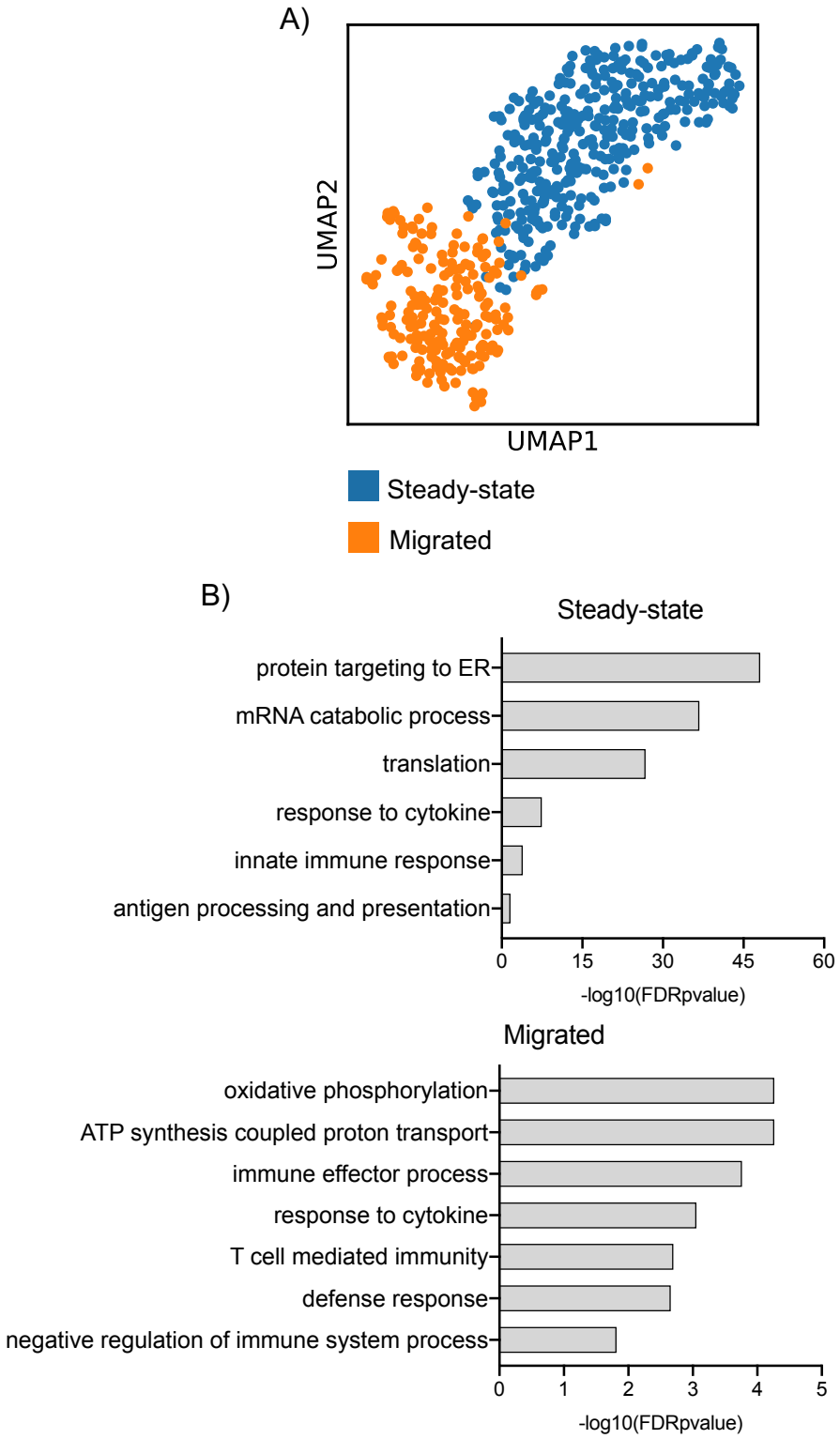

Figure 38. Steady-state and migrated foreskin derived LCs differ in state of immunocompetency. A) UMAP dimensionality reduction analysis of Scran normalised single cell data from steady-state and migrated foreskin derived skin LCs. **B)** Gene ontology analysis (Toppgene) for the 100 DEGs (T-Test, BH adj.p-value<0.05) upregulated in both steady-state and migrated LCs. -log10adj.p-values are displayed. **C)** *On next page. Heatmap displaying the top 100 DEGs upregulated in both steady-state and migrated foreskin LCs. **D)** On next page. Violin plots displaying the expression of classic DC activation markers (MHC I, MHC II, co-stimulatory molecules) in steady-state and migrated foreskin LCs.

C)

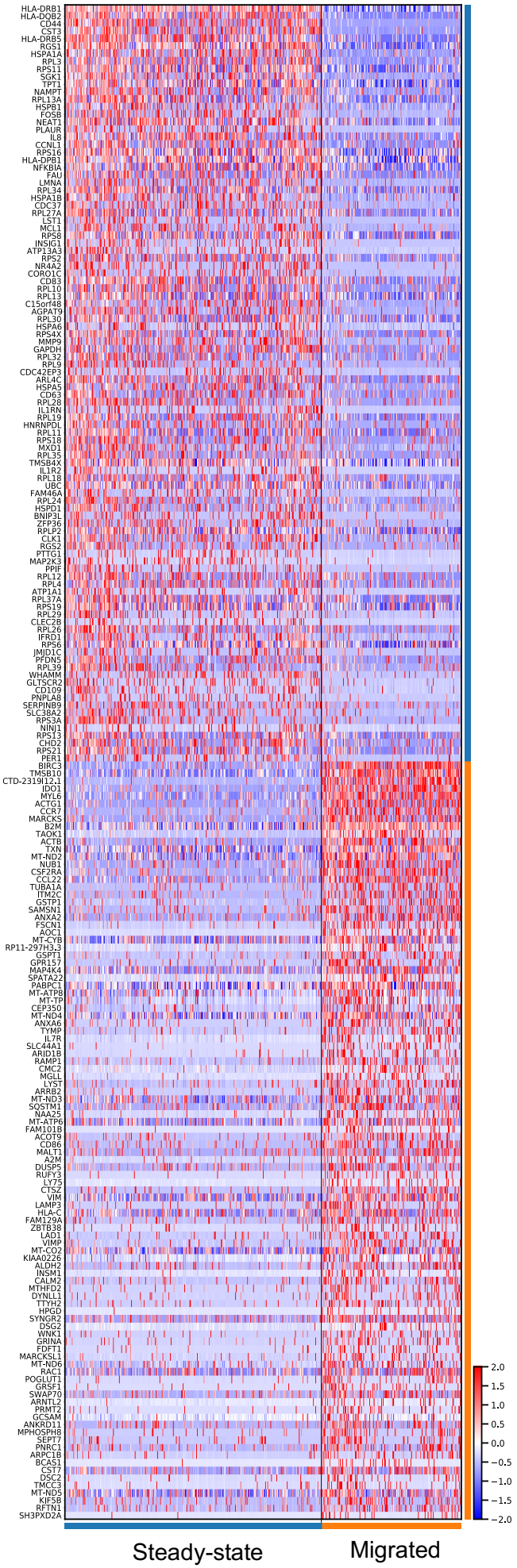
HLA-DRB1
HLA-DQB2
CD44
CST3
HLA-DRB5
RGS1
HSPA1A
RPL3
RPS11
SGK1
TPT1
NAMPT
RPL13A
HSPB1
FOSB
NEAT1
PLAUR
IL8
CCNL1
RPS16
HLA-DPB1
NFKBIA
FAU
LMNA
RPL34
HSPA1B
CDC37
RPL27A
LST1
MCL1
RPS8
INSIG1
ATP13A3
RPS2
NR4A2
CORO1C
CD83
RPL10
RPL13
C15orf48
AGPAT9
RPL30
HSPA6
RPS4X
MMP9
GAPDH
RPL32
RPL9
CDC42EP3
ARL4C
HSPA5
CD63
RPL28
IL1RN
RPL19
HNRNPDL
RPL11
RPS18
MXD1
RPL35
TMSB4X
IL1R2
RPL18
UBC
FAM46A
RPL24
HSPD1
BNIP3L
ZFP36
RPLP2
CLK1
RGS2
PTTG1
MAP2K3
PPIF
RPL12
RPL4
ATP1A1
RPL37A
RPS19
RPL29
CLEC2B
RPL26
IFRD1
RPS6
JMJD1C
PFDN5
RPL39
WHAMM
GLTSCR2
CD109
PNPLA8
SERPINB9
SLC38A2
RPS3A
NINJ1
RPS13
CHD2
RPS21
PER1
BIRC3
TMSB10
CTD-2319I2.1
IDO1
MYL6
ACTG1
CCR7
MARCKS
B2M
TAOK1
ACTB
TXN
MT-ND2
NUB1
CSF2RA
CCL22
TUBA1A
ITM2C
GSTP1
SAMSN1
ANXA2
FSCN1
AOC1
MT-CYB
RP11-297H3.3
GSPT1
GPR157
MAP4K4
SPATA22
PABPC1
MT-ATP8
MT-TP
CEP350
MT-ND4
ANXA6
TYMP
IL7R
SLC44A1
ARID1B
RAMP1
CMC2
MGLL
LYST
ARRB2
MT-ND3
SQSTM1
NAA25
MT-ATP6
FAM101B
ACOT9
CD86
MALT1
A2M
DUSP5
RUFY3
LY75
CTSZ
VIM
LAMP3
HLA-C
FAM129A
ZBTB38
LAD1
VIMP
MT-CO2
KIAA0226
ALDH2
INSM1
CALM2
MTHFD2
DYNLL1
TTYH2
HPGD
SYNGR2
DSG2
WNK1
GRINA
FDFT1
MARCKSL1
MT-ND6
RAC1
POGLUT1
GRSF1
SWAP70
ARNTL2
PRMT2
GCSAM
ANKRD11
MPHOSPH8
SEPT7
PNRC1
ARPC1B
BCAS1
CST7
DSC2
TMCC3
MT-ND5
KIF5B
RFTN1
SH3PXD2A
2.0
1.5
1.0
0.5
0.0
−0.5
−1.0
−1.5
−2.0
Steady-state
Migrated

D)

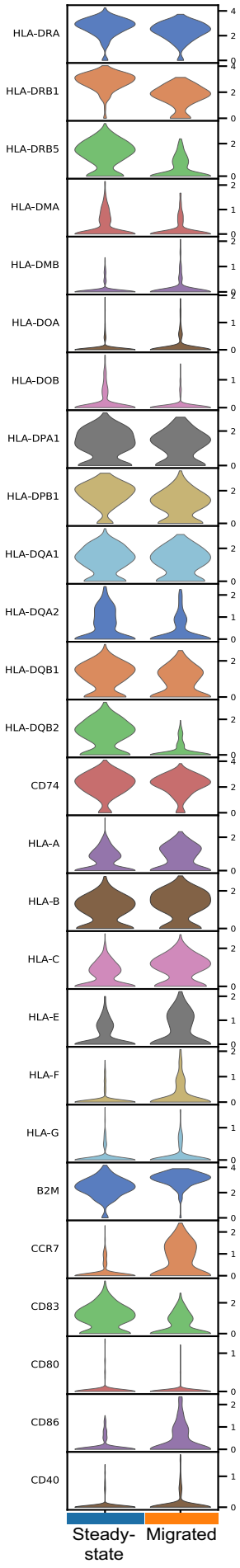
HLA-DRA
HLA-DRB1
HLA-DRB5
HLA-DMA
HLA-DMB
HLA-DOA
HLA-DOB
HLA-DPA1
HLA-DPB1
HLA-DQA1
HLA-DQA2
HLA-DQB1
HLA-DQB2
CD74
HLA-A
HLA-B
HLA-C
HLA-E
HLA-F
HLA-G
B2M
CCR7
CD83
CD80
CD86
CD40
Steady-state
Migrated

UMAP dimensionality reduction and Leiden (r=0.5) clustering of steady state foreskin LCs alone identified a similar population structure to breast LCs, with steady-state LCs forming 2 clusters (S1 and S2) and migrated LCs forming 1 (**Figure 39A**). To identify the unique qualities of each population, DEG analysis was performed (T-test, BH adj.p-value<0.05) and the top 100 DEGs for each cluster analysed. Gene ontology analysis for the top 100 DEGs in S1 LCs revealed associations with antigen processing and presentation (adj.p-value=1.9E-5), response to cytokine (adj.p-value=2.4E-5), appositive regulation of the ATP metabolic process (adj.p-value=2.1E-3) and the innate immune response (adj.p-value=6.1E-3)(**Figure 39B)**. Gene ontology analysis for the top 100 DEGs in S2 LCs revealed associations with protein folding (adj.p-value=3.5E-15), response to temperature stimulus (adj.p-value=7.0E-11), leukocyte activation involved in the immune response (adj.p-value=3.6E-6) and response to cytokine (adj.p-value=2.2E-4)**(Figure 39C)**. Unlike breast skin derived steady-state LCs, steady-state foreskin populations were much more defined by distinct biological pathways rather than a spectrum of immunocompetency. However, the expression of classical DC activation markers was also investigated, revealing foreskin S1 LCs to have increased expression of most genes within the panel, reflecting increased immunocompetency **(Figure 39D)**.

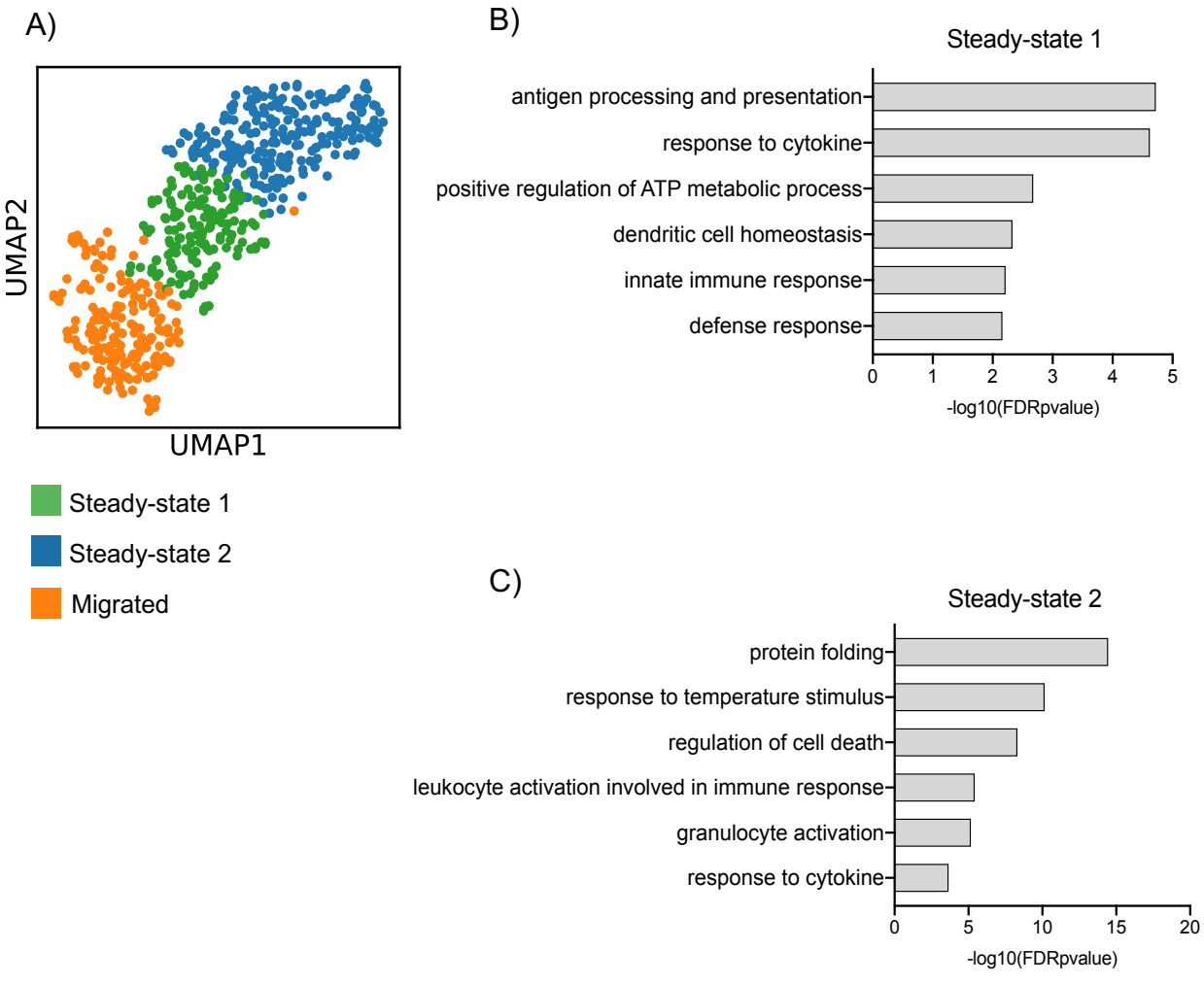

D)

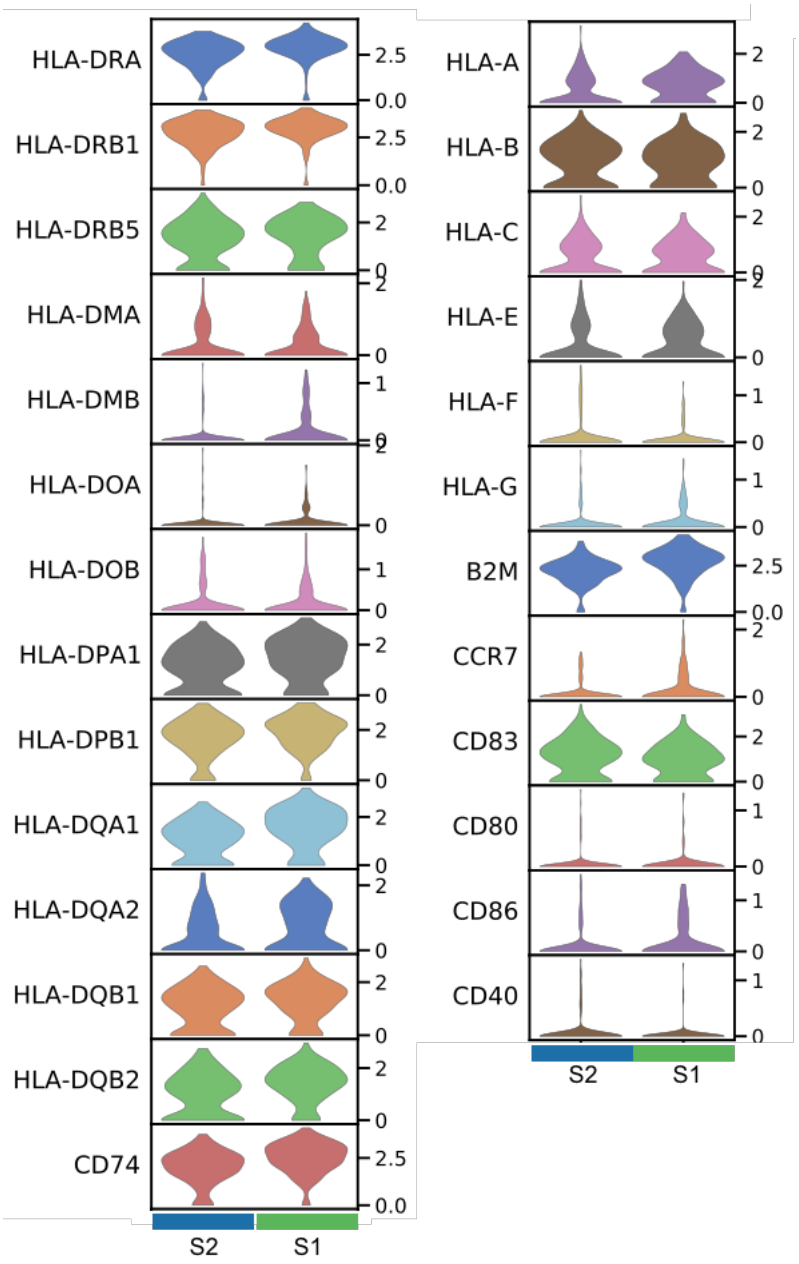

Figure 39. Steady-state LCs can be divided into two subpopulations, distinct through expression of unique biological pathways and level of immunocompetency. A) Leiden (r=0.5) clustering analysis revealed 3 clusters amongst the steady-state and migrated LCs populations – labelled steady-state 1 (S1), steady-state 2 (S2) and migrated. **B)** Gene ontology analysis for the 100 DEGs (T-test) upregulated in S1 LC compared to S2 LCs. -log10adj.p-values are displayed. **C)** Gene ontology analysis for the 100 DEGs (T-test) upregulated in steady-state 2 compared to steady-state 1 LCs. -log10adj.p-values are displayed. **D)** Violin plots displaying the expression of classic DC activation markers (MHC I, MHC II, co-stimulatory molecules) in S1 and S2 populations.

5.2.7 The foreskin microenvironment increases the expression of tolerogenic gene signature 1 in LCs

For comparison with breast LCs, the two tolerogenic signatures were inspected amongst the steady-state and migrated foreskin LC populations(**Figure 40A**). 19 genes from signature 1 and 110 genes from signature 2, were identified amongst the whole single cell transcriptome. 2 genes were common to both signatures 1 and 2 (*VEGFA, CD86*). Similar to breast LCs, GSVA analysis revealed that signature 1 was enriched in migrated LCs (logFC=0.19, adj.p-value=3.9E-12). However, signature 2 was more enriched in steady-state foreskin LC. (logFC=0.1, adj.p-value=2.3E-10) **(Figure 40B)**. The genes within each signature were observed in both populations using trackplots **(Figure 40C&D)**. The presence of signature 1 genes amongst the top 100 migrated LC DEGs was investigated, revealing *CD86* and *IDO1* to be amongst the list. *ALDH2* from signature 2 was also present in the top 100 migrated LC DEGs**.** In steady-state LCs signature 2 genes, *CD83, CDC42EP3, IFRD1, MCL1, NAMPT, NFKBIA, NINJ1, RGS2* and *ZFP36* were found amongst the steady-state LC top 100 DEG list (**Figure 40E&F)**.

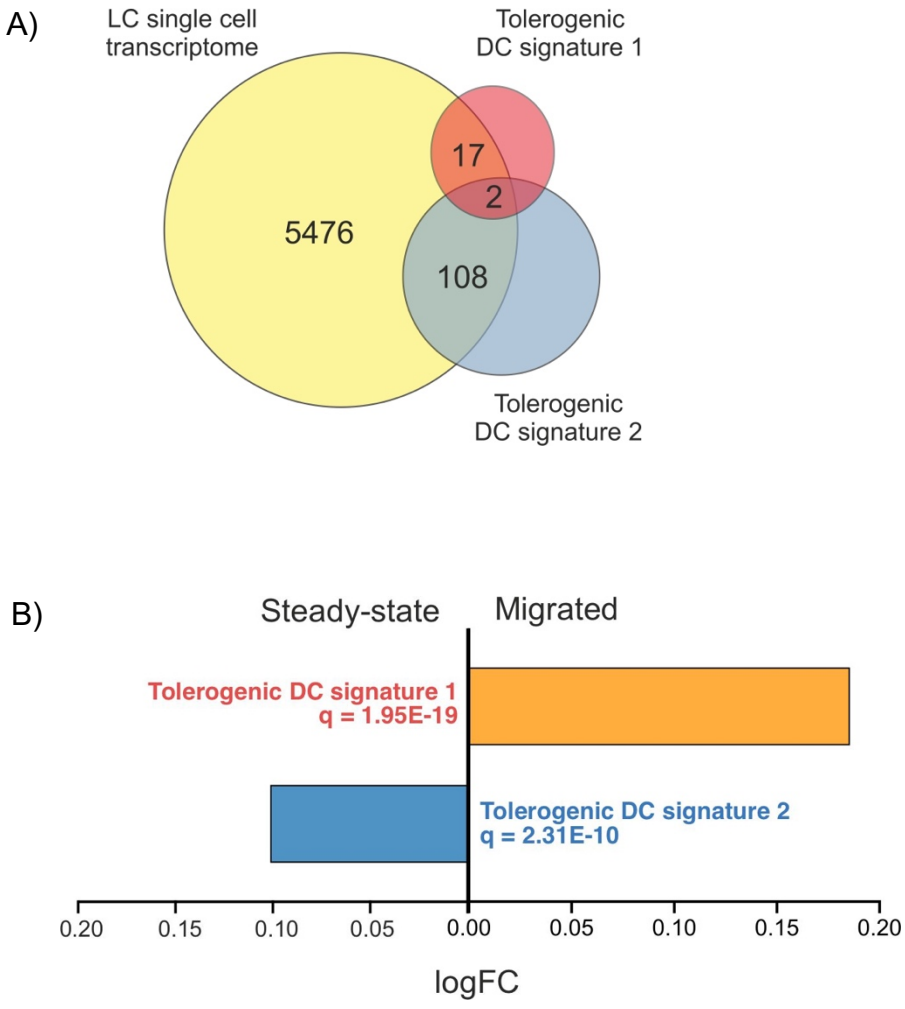

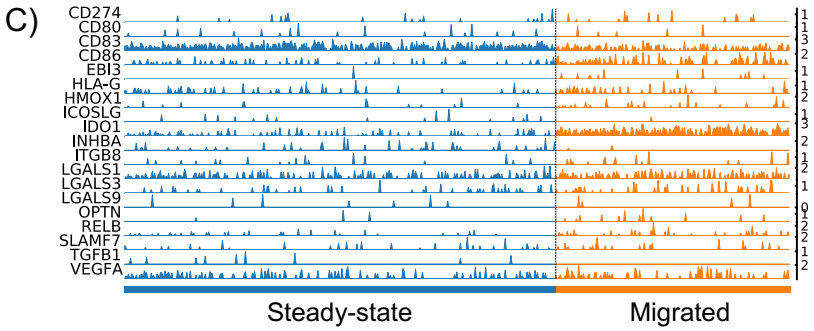
C)
CD274
CD80
CD83
CD86
EBI3
HLA-G
HMOX1
ICOSLG
IDO1
INHBA
ITGB8
LGALS1
LGALS3
LGALS9
OPTN
RELB
SLAMF7
TGFB1
VEGFA
Steady-state
Migrated

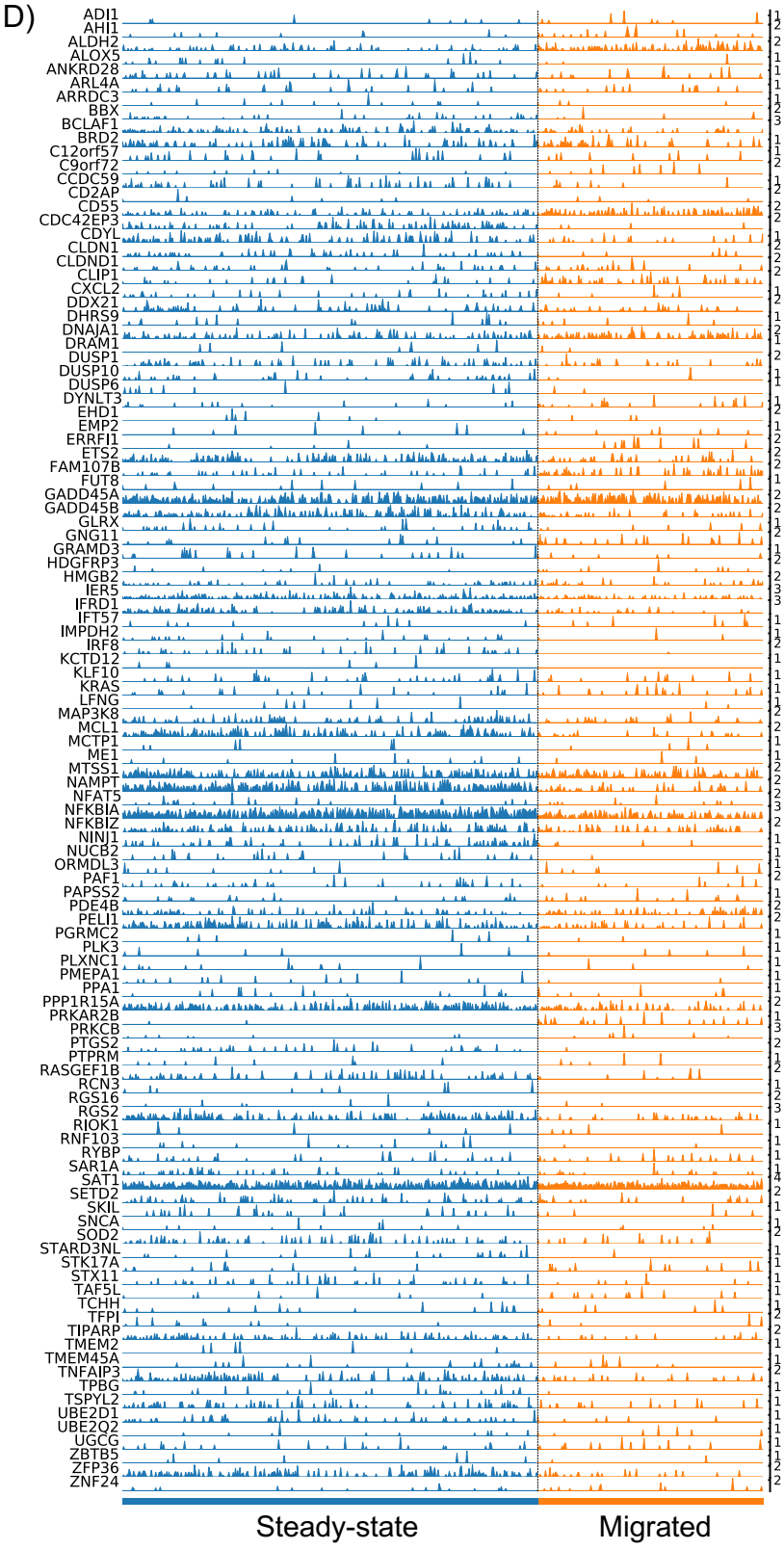
D)
ADI1
AHI1
ALDH2
ALOX5
ANKRD28
ARL4A
ARRDC3
BBX
BCLAF1
BRD2
C12orf57
C9orf72
CCDC59
CD2AP
CD55
CDC42EP3
CDYL
CLDN1
CLDND1
CLIP1
CXCL2
DDX21
DHRS9
DNAJA1
DRAM1
DUSP1
DUSP10
DUSP6
DYNLT3
EHD1
EMP2
ERRFI1
ETS2
FAM107B
FUT8
GADD45A
GADD45B
GLRX
GNG11
GRAMD3
HDGFRP3
HMGB2
IER5
IFRD1
IFT57
IMPDH2
IRF8
KCTD12
KLF10
KRAS
LFNG
MAP3K8
MCL1
MCTP1
ME1
MTSS1
NAMPT
NFAT5
NFKBIA
NFKBIZ
NINJ1
NUCB2
ORMDL3
PAF1
PAPSS2
PDE4B
PELI1
PGRMC2
PLK3
PLXNC1
PMEPA1
PPA1
PPP1R15A
PRKAR2B
PRKCB
PTGS2
PTPRM
RASGEF1B
RCN3
RGS16
RGS2
RIOK1
RNF103
RYBP
SAR1A
SAT1
SETD2
SKIL
SNCA
SOD2
STARD3NL
STK17A
STX11
TAF5L
TCHH
TFPI
TIPARP
TMEM2
TMEM45A
TNFAIP3
TPBG
TSPYL2
UBE2D1
UBE2Q2
UGCG
ZBTB5
ZFP36
ZNF24
Steady-state
Migrated

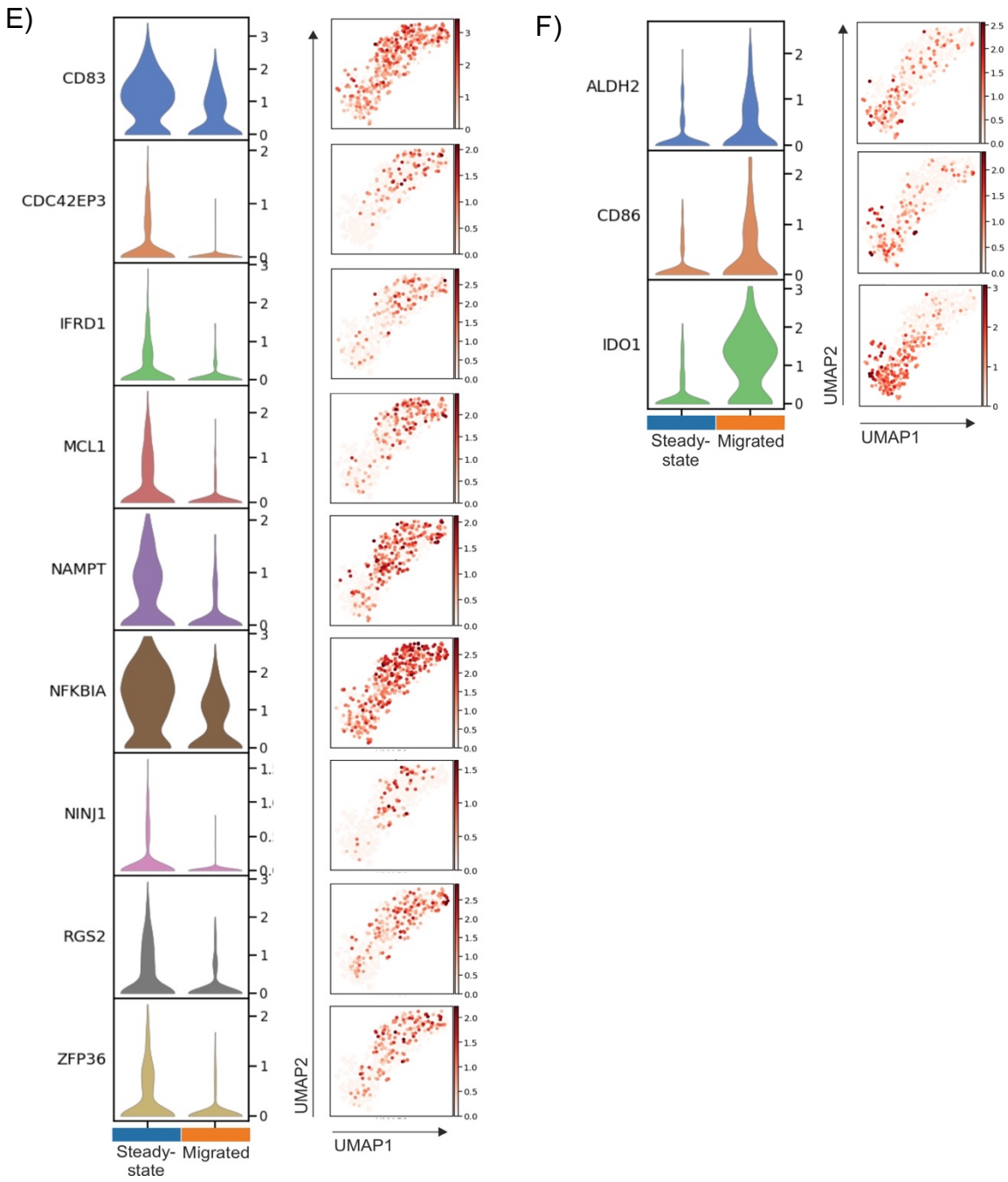

Figure 40. Steady-state and Migrated foreskin LCs display differential expression of tolerance associated genes. A) Venn diagram displaying the number of genes from tolerogenic gene signature 1 (curated from papers reviewing molecular mechanism of DC tolerance induction, **Appendix 1 A.1**) and tolerogenic genes signature 2 (identified in **Chapter 4**, (**Figure 20A&C, Appendix 1 A.2**) that were identified in the whole single cell transcriptomes of foreskin skin derived LCs. **B)** GSVA displaying enrichment of the two tolerogenic signatures in foreskin LC populations. BH adjusted p-values and logFC are displayed. **C)** Trackplot displaying the expression of genes from tolerogenic gene signature 1. **D)** Trackplots displaying the expression of genes from tolerogenic gene signature 2. **E)** Violin plots and UMAP marker plots displaying the expression of the 9 genes from tolerogenic genes signatures 1 which were in the top 100 DEGs upregulated in steady-state foreskin LCs. **F)** Violin plots and UMAP marker plots displaying the expression of the 3 genes from tolerogenic genes signatures 1 and 2 which were in the top 100 DEGs upregulated in migrated foreskin LCs.

5.2.8 Foreskin LCs display differential regulon enhancement compares to breast skin LCs

SCENIC regulatory network and inference was performed and revealed that the regulons enriched highly differed between the two foreskin LC populations (**Figure 41A**). Common TF regulons identified in both steady-state breast skin and foreskin LCs included *MYC, ETS2, FOSL2* and *SPI1*. Common TFs identified in both migrated breast skin and foreskin LCs included *IRF4, ETS1, KLF13, SREBF2, CTCF* and *REST.* However, unique regulons in foreskin steady-state LCs (*FOSB, JUN, HIF1A)* and migrated foreskin LCs (*IRF2, RUNX3*) could be identified. Overall, the diverse transcriptomes observed between steady-state and migrated foreskin LC were therefore underlined by unique TF networks - similar to what was observed in breast skin LCs.

To ascertain the most highly influential TFs that could be inducing tolerogenic genomic programming, the expression level of TFs themselves and their regulon enrichment score was interrogated. TFs with both highly differential expression levels and with high regulon enrichment scores in each population were identified. For steady-state LC, this included *BHLHE40, ETS2, FOSB, JUN* and *MYC* TFs **(Figure 41B)**. For migrated LC, this included *CREM, IRF2, IRF4, KLF13, REST* and *SREBF2* **(Figure 41C)**.

In order to trace whether the tolerogenic upregulated in steady-state (*CD83, CDC42EP3, IFRD1, MCL1, NAMPT, NFKBIA, NINJ1, RGS2* and *ZFP36*) and migratory (*ALDH2, CD86* and *IDO1*) foreskin LC could be under the control of the upregulated TFs in each state, their presence within the regulons of the TFs was inspected **(Figure 41D&E)**. Here, tolerogenic genes could be found in all the enriched regulons of steady-state LCs and in the regulons of *IRF2* and *IRF4* in migrated LC. The SCENIC co-expression scores from the tolerogenic genes within each TF regulon were analysed to apprehend the level of co-regulation **(Figure 41F&G)**. Highly co-expressed TFs and genes for steady-state LCs included *BHL3HE40-CD83/NFKBIA/ZFP36*, *FOSB-IFRD1/MCL1/NFKBIA* and *JUN-MCL1/NAMPT*. Highly co-expressed TFs and genes for migrated LCs included *CREM-ALDH2/IDO1, IRF2-IDO1* and *IRF4-IDO.*

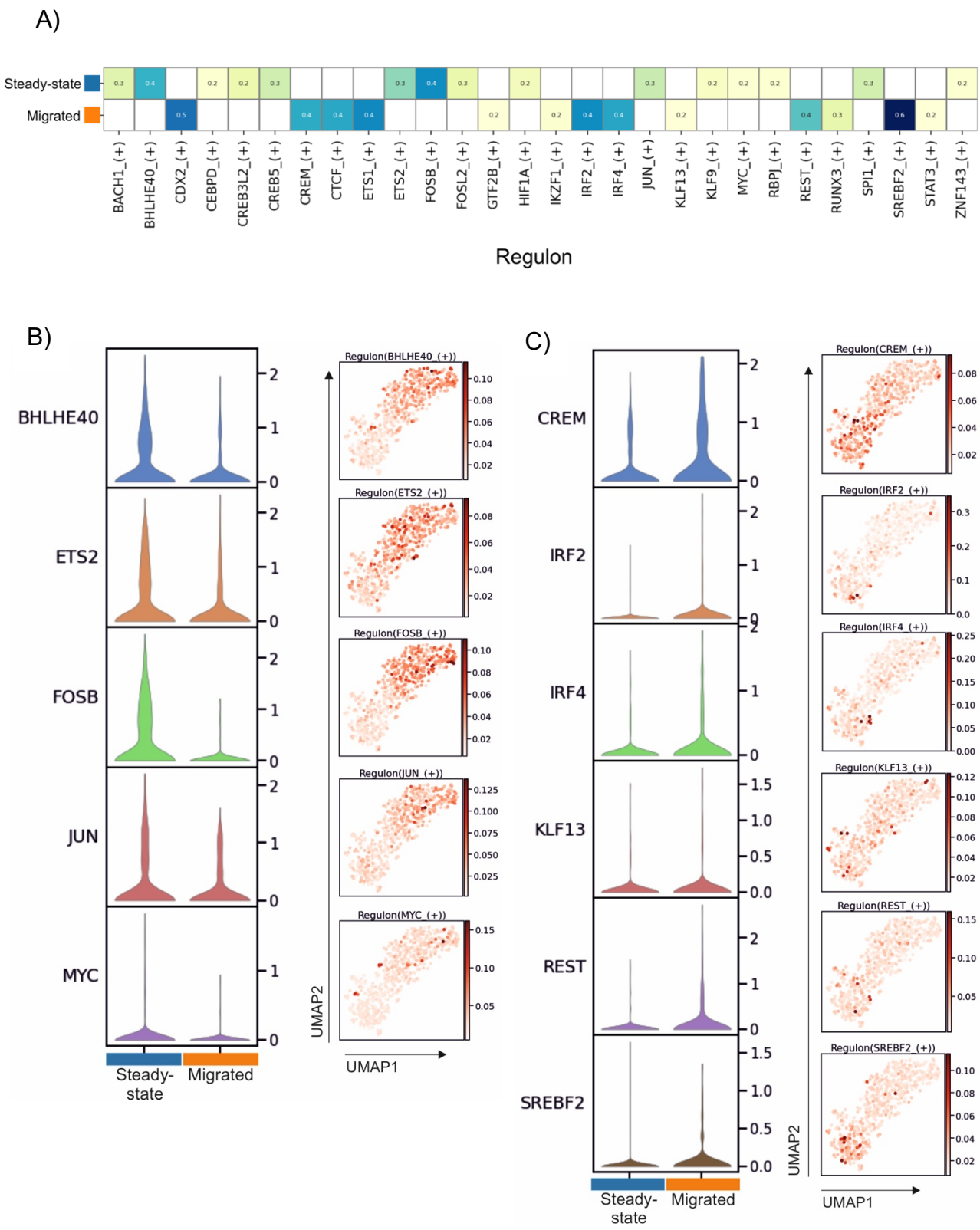
A)
Steady-state
Migrated
BACH1_(+)
BHLHE40_(+)
CDX2_(+)
CEBPD_(+)
CREB3L2_(+)
CREB5_(+)
CREM_(+)
CTCF_(+)
ETS1_(+)
ETS2_(+)
FOSB_(+)
FOSL2_(+)
GTF2B_(+)
HIF1A_(+)
IKZF1_(+)
IRF2_(+)
IRF4_(+)
JUN_(+)
KLF13_(+)
KLF9_(+)
MYC_(+)
RBPJ_(+)
REST_(+)
RUNX3_(+)
SPI1_(+)
SREBF2_(+)
STAT3_(+)
ZNF143_(+)
Regulon
B)
BHLHE40
ETS2
FOSB
JUN
MYC
Steady-state
Migrated
Regulon(BHLHE40_(+))
Regulon(ETS2_(+))
Regulon(FOSB_(+))
Regulon(JUN_(+))
Regulon(MYC_(+))
UMAP2
UMAP1
C)
CREM
IRF2
IRF4
KLF13
REST
SREBF2
Steady-state
Migrated
Regulon(CREM_(+))
Regulon(IRF2_(+))
Regulon(IRF4_(+))
Regulon(KLF13_(+))
Regulon(REST_(+))
Regulon(SREBF2_(+))
UMAP2
UMAP1

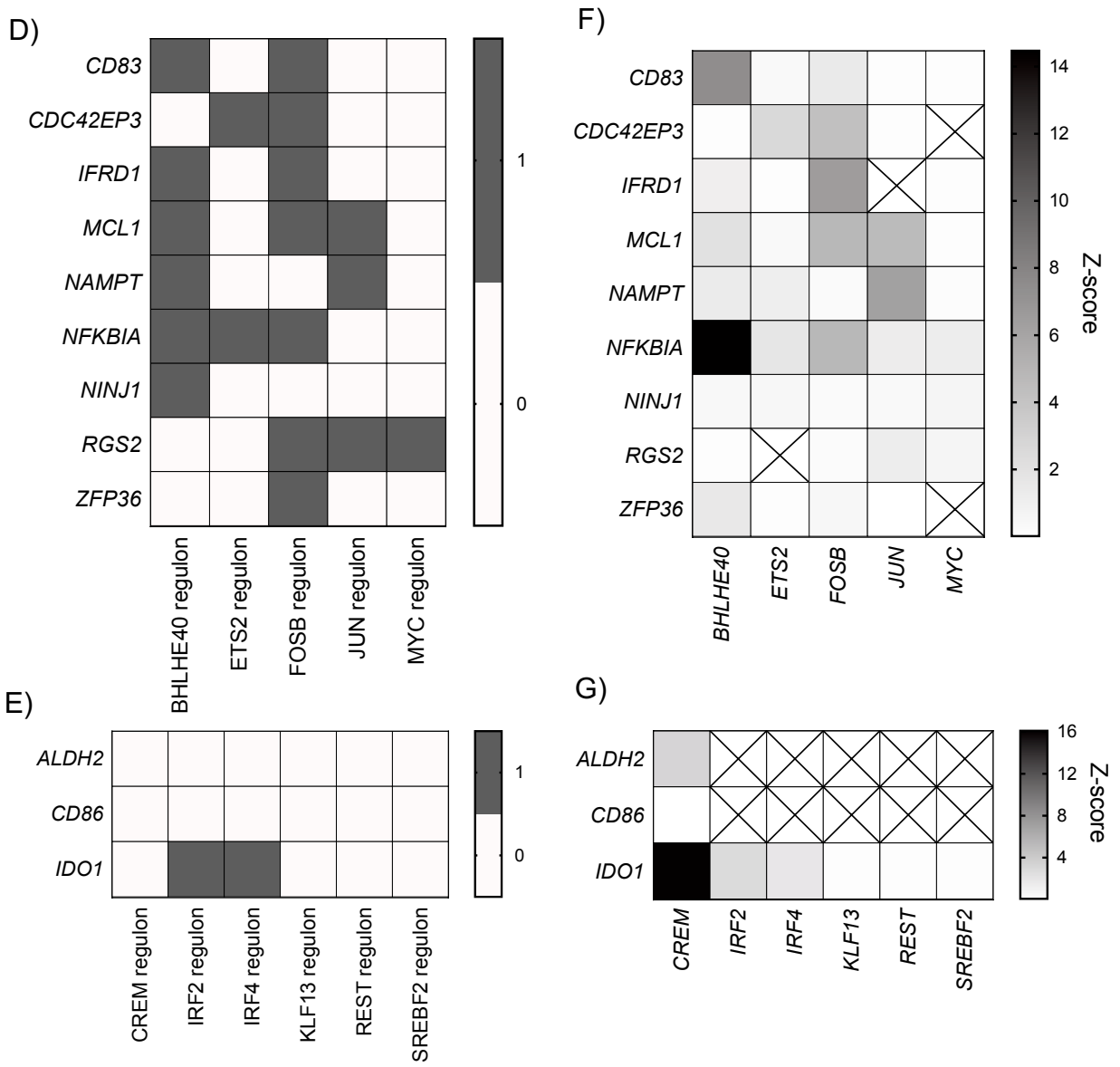

Figure 41. The tolerogenic gene expression programme in migrated LCs is underlined by a unique TF network. A) SCENIC regulatory network and inference clustering analysis revealed TF regulons which were enriched in steady-state and migrated foreskin LCs. Z-scores for enriched regulons are displayed. **B)** Violin plots displaying gene expression of foreskin steady-state LC enriched TFs with accompanying UMAP marker plots displaying TF regulon enrichment Z-scores across the two LC populations. **C)** Violin plots displaying gene expression of foreskin migrated LC enriched TFs with accompanying UMAP marker plots displaying TF regulon enrichment Z-scores, across the two LC populations. **D)** Binary heatmap displaying the presence of the 9 tolerogenic associated genes, identified in the top 100 steady-state LC DEGs, in the regulons enriched in steady-state LCs. **E)** Binary heatmap displaying the presence of the 3 tolerogenic associated genes, identified in the top 100 migrated LC DEGS, in the regulons enriched in migrated LCs. **F)** Heatmap displaying the SCENIC correlation Z-scores for each of the 9 tolerogenic associated genes in foreskin steady-state LCs, with the TFs from the steady-state LC enriched regulons. **G)** Heatmap displaying the SCENIC correlation Z-scores for each of the 3 tolerogenic associated genes in foreskin migrated LCs, with the TFs from the migrated LC enriched regulons. Crosses indicate absent correlation scores.

5.2.9 Constellation Drop-seq validates LC transcriptomic programmes and enhances investigations into LCs in the context of whole epidermis

Drop-seq scRNA-seq analysis of LC is limited to the acquisition of sufficient skin tissue for LC extraction and for effective purification of LC from whole epidermal tissue. Alternatively, without purification, LCs could be sequenced and analysed in the context of whole epidermal tissue. However, low frequency of LCs in the epidermis limits the level of meaningful data which could be analysed without the need to process hundreds of thousands of cells. To counter this problem and to investigate LCs *in situ* in the epidermis and without any manipulation that occurs during normal extraction procedures via FACS, whole epidermis samples were processed using our own developed targeted Drop-seq protocol (Constellation Drop-seq) (Vallejo *et al.*, 2019). Using Constellation Drop-seq, genes of interest are specifically targeted for using a panel of designed primers, allowing investigation into transcripts of interest amongst cell populations. The regular Drop-seq protocol was also performed on whole epidermis tissue for direct comparison. After encapsulation and post-processing, cDNA library concentrations for both the regular Drop-seq and Constellation Drop-seq experiments were analysed to ensure sufficient cDNA concentrations and quality **(Figure 42A)**. Clearly observable was the more 'spiked' quality of the cDNA library in Constellation Drop-seq, showing the preferentially expansion of transcripts from targets of interest. Libraries were subsequently processed through tagmentation before sequencing (**Figure 42B**).

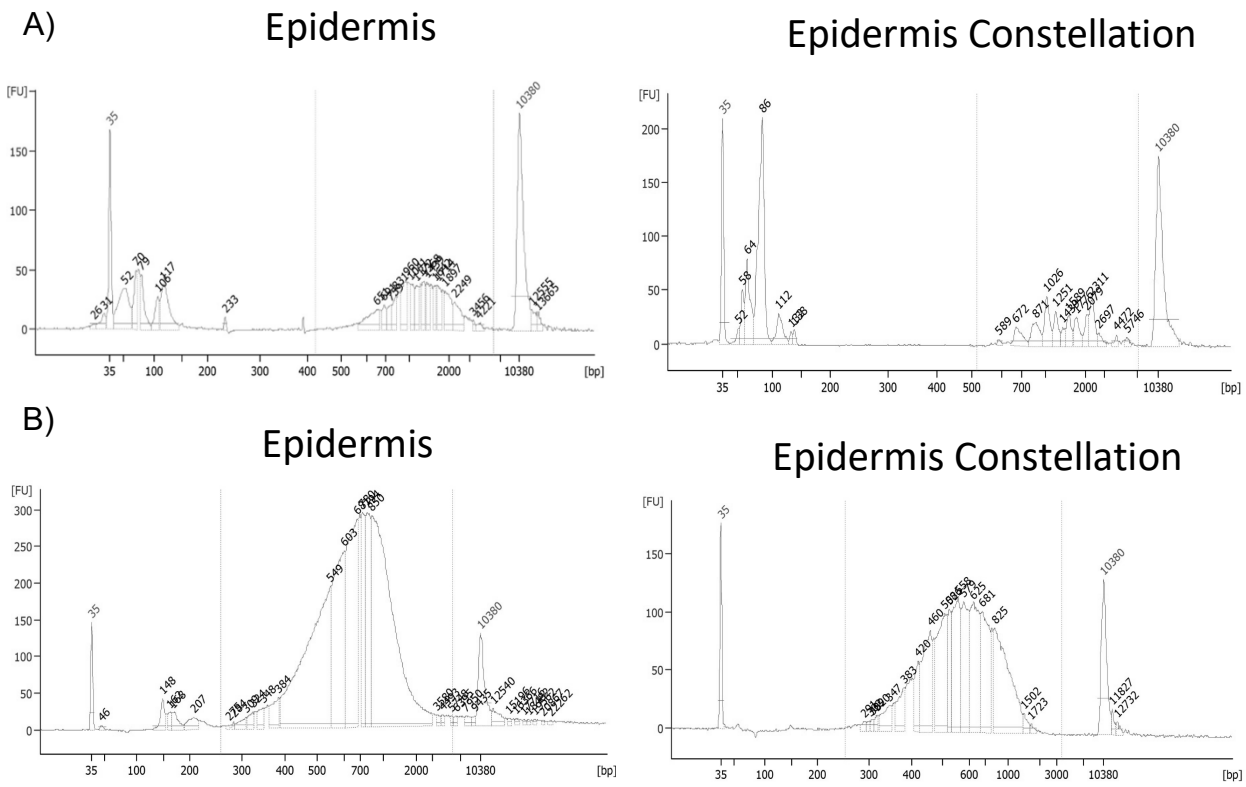

Figure 42. cDNA libraries of whole epidermis were prepared for sequencing. A) cDNA libraries for whole epidermis processed using regular Drop-seq and Constellation drop-seq were quantified using a DNA high sensitivity kit, run on an Agilent Bioanalyser. Epidermis = 234 pg/µl and Epidermis Constellation = 165 pg/µl. **B)** 600 pg of cDNA library was tagmented with libraries quantified using a DNA high sensitivity kit, run on an Agilent Bioanalyser. Libraries were pooled at 2 nM ready for sequencing. Epidermis = 7.7 nM and Epidermis Constellation = 4.8 nM. Upper (10380bp) and lower (35bp) marker DNA was included for reference. Vertical dotted lines depict area in which cDNA library concentrations were quantified.

Using the regular Drop-seq protocol, 100 STAMPs from steady-state digested primary human epidermis were processed through to sequencing. The cellular composition was analysed to investigate whether LCs could be detected in the context of the whole epidermal population. Prior to analysis the data frame was filtered, resulting in expression data for 2212 genes and 80 cells. UMAP dimensionality reduction analysis on the scran normalised data revealed one overall cluster (**Figure 43**). Inspecting the population for *CD207* expression revealed just 5 cells (6.25%) expressed some level of expression, although expression level was variable. *MLANA,* a marker of melanocytes was observed in 7 cells (8.75%). Keratinocyte markers *KRT10* (74 cells, 92.5%), *KRT1* (65 cells, 81.25%), *KRT5* (17 cells, 21.25%) and KRT14 (12 cells, 15%) were detected in the majority of cells. Using standard Drop-seq on whole epidermal different cell types of the epidermis could be distinguished. However, as expected LCs were observed at low frequencies amongst the whole population.

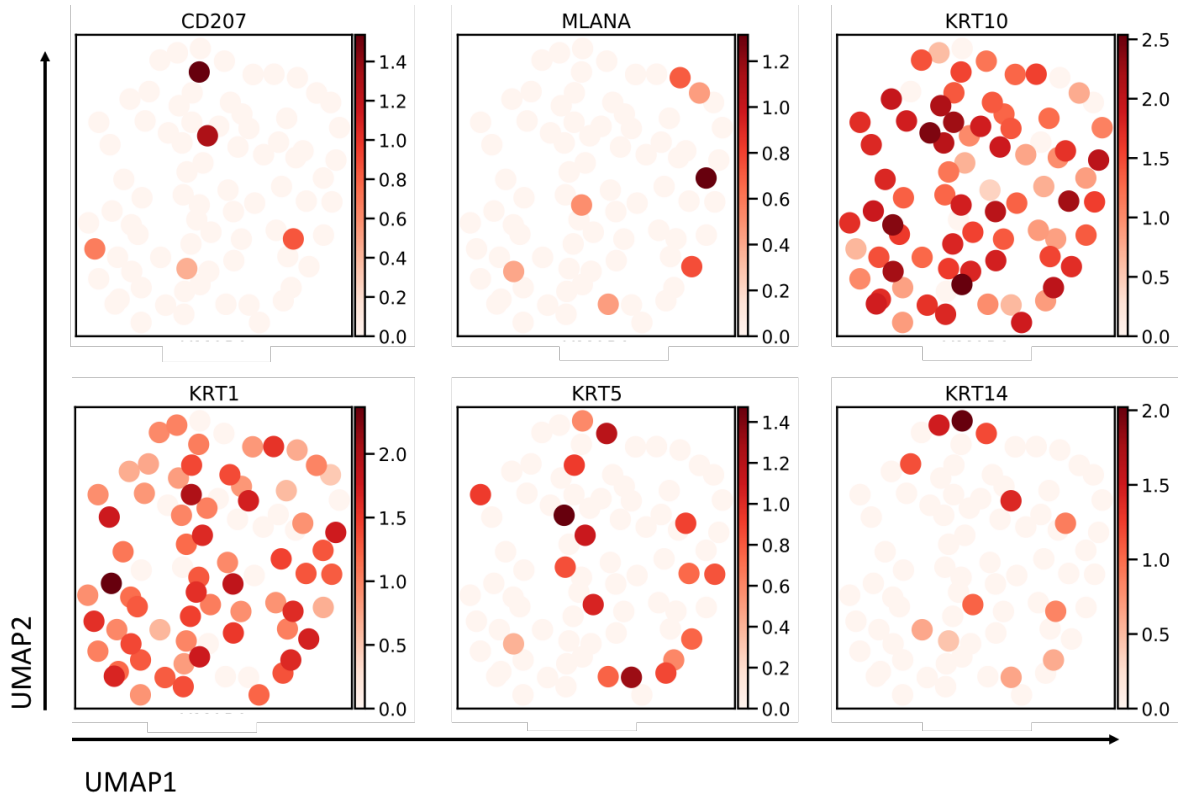

Figure 43. Drop-seq of whole epidermal tissue with limited cell numbers cannot distinguish clear subpopulations of LC. UMAP dimensionality reduction analysis displaying marker genes for LC (*CD207*), melanocytes (*MLANA*) and keratinocytes (*KRT10, KRT1, KRT5* and *KRT14*).

In order to investigate the LC population in greater numbers, whilst still in the context of whole epidermis, our targeted Constellation Drop-seq approach was implemented. In this approach gene expression of LC markers and genes corresponding to their state of activation (inflammatory and tolerogenic), as well as PBMC population markers, were amplified using 55 gene specific primers (**Table 8**) incorporated into the cDNA library preparation protocol. Using this method, sequencing data from 1000 STAMPS were sequenced whilst still using the same capacity and space on an Illumina Next-seq run as 100 STAMPs processed in the regular Drop-seq protocol, due to the restriction of sequencing depth to a limited number of transcripts. After filtering 286 cells with expression for 376 genes remained for analysis. The 714 cells removed after filtering from the initial 1000 STAMPs processed likely included KCs. No KC marker genes were included in the primer panel and so whilst they will have been encapsulated during the Drop-seq procedure, KC specific transcripts will not have been detected and therefore will have been removed after filtering.

From initial UMAP dimensionality reduction analysis and clustering (leiden r=0.5), 4 populations (labelled 1-4) could be identified (**Figure 44A**). Investigating the marker genes for each population revealed that cluster 1 (140 cells) and 2 (108 cells) contained high to low expression of *CD207, CD1A*

and *HLA-DRB5.* Interestingly cluster 3 (21 cells) was marked by high expression of *LYZ*, a marker of monocytes and cluster 4 (17 cells) displayed high expression of *GZMB* and *CCL5,* markers of CD8+ T cells(**Figure 44B**). Through a targeted Constellation Drop-seq approach, using the same sequencing space as 100 standard Drop-seq STAMPs, populations of LCs in greater numbers could be identified, as well as monocytes and CD8+ T cells populations which were not detected at all in regular Drop-seq.

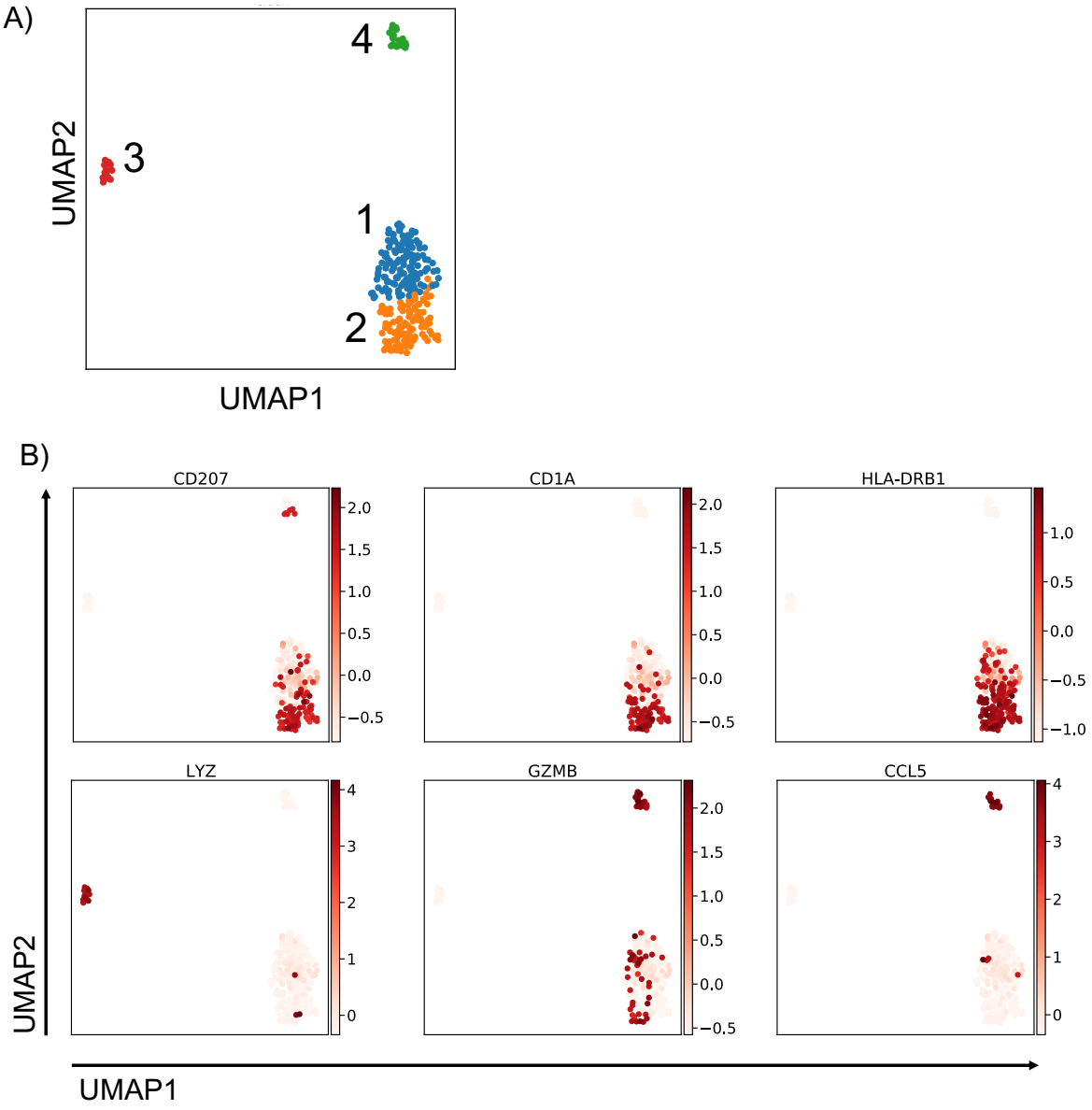

Figure 44. Constellation Drop-seq allows identification of large populations of LCs amongst whole epidermal tissue. A) UMAP dimensionality reduction analysis and leiden clustering (r=0.5) identified 4 distinct populations (labelled 1-4). **B)** Populations could be identified as LCs (1,2) displaying low-high expression of LC markers (*CD207, CD1A, HLA-DRB1*), as well as monocytes (3, *LYZ*) and T cells (4, *GZMB, CCL5*).

Having identified LCs were present in the dataset, analysis was performed on the LC population only, through sub-setting the data to cells filtered by *CD207* expression (Scran normalised *CD207*>0). Clustering (leiden=0.4) of the LC population identified 3 distinct clusters (labelled 1-3) which displayed unique genes expression (**Figure 45A**). Marker genes for each population were investigated, but cluster 3 displayed no unique markers genes compared to the other two populations. Cluster 2 marker genes included *CD1A, LIMS1, HLA-DRB1, FCER1A* and *NFKB1* and cluster 1 markers genes included *NFKBIA, NFBKIZ, TNFAIP3, HLA-DQA2* and *UBB.* Interestingly, the expression of NFκB (*NFKB1*) and its inhibitors (*NFKBIA, NFKBIZ* and *TNFAIP*) therefore appeared to be differentially regulated **(Figure 45B)**. Constellation Drop-seq therefore confirmed heterogeneity in the steady-state LC populations, especially in the context of NFκB regulation.

To assess the comparability between unsorted steady-state LCs in Constellation Drop-seq to FACS sorted steady-state LCs in regular Drop-seq, the expression level of genes within the Constellation Drop-seq primer panel were compared across both datasets. Heatmap plots showed comparable levels of expression of most panel genes, including high expression of *CD74, NFKBIA, CCL22, HLA-DBRB1* and *HLA-DQA1*, as well as absent/low expression of *IRF4, IDO1* (not detected in Constellation Drop-seq), *IRF1, CD40* and *CCL5* **(Figure 45C)**. Overall, this suggests that changes induced during the FACS purification process of LCs in regular Drop-seq are minimal and that Constellation Drop-seq results were in line with previous observations of steady-state LCs.

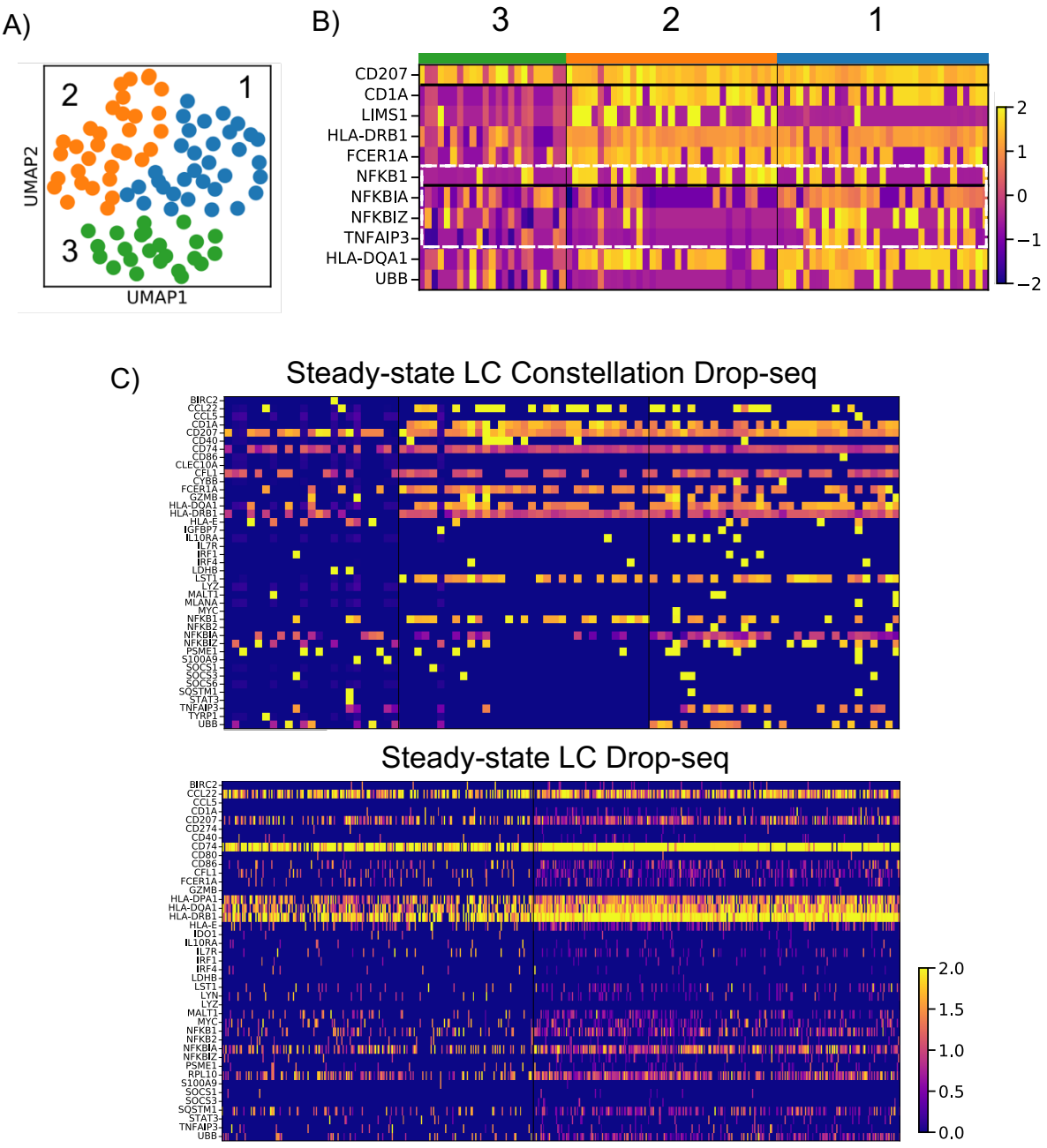

Figure 45. Constellation Drop-seq reveals heterogeneity in the regulation of NFκB activation in LCs and reveals comparability in gene expression to steady-state LCs processed through regular Drop-seq. A) UMAP dimensionality reduction analysis and leiden clustering (r=0.5) of the LCs (*CD207*+) identified through constellation Drop-seq revealed 3 distinct populations. **B)** Heatmap displaying marker genes (Logistic regression) for clusters 1 and 2. White dashed box highlights the heterogeneity between *NFKB1*, which was highly expressed in cluster 2 LC and NFκB inhibitors (*NFKBIA, NFKBIZ, TNFAIP3*), which were upregulated in cluster 1 LC. **C)** Heatmaps displaying the comparable levels of expression between steady-state LCs identified using the Constellation Drop-seq protocol on digested whole epidermis (Top), compared to steady-state LCs processed through regular Drop-seq after FACS purification (Bottom). Values in both datasets were both scaled between 0-2 for direct comparison.

5.3 Discussion

Utilising the scRNA-seq method Drop-seq has allowed in depth analysis into LC heterogeneity in both steady-state and migrated LC populations. Steady-state LCs and migrated LCs have been shown to be phenotypically distinct and to display differences in capacity to induce immune responses (Sirvent *et al.*, 2020). However, until now, the level of transcriptomic heterogeneity in LC populations extracted in the steady-state or through migration at the single cell level was unexplored. Thus, we have revealed the unique gene expression exhibited by steady-state and migrated LCs and highlighted the distinct expression of tolerogenic associated genes across the two states.

5.3.1 Optimisation of Drop-seq allowed effective investigations into LC heterogeneity

In order to investigate high quality single cell transcriptomic data using Drop-seq, we first ensured that the protocol was fully optimised and that tissue of high quality was used. Successful single cell and bead encapsulation events are heavily reliant on ensuring that cell and microparticle bead suspensions are at the correct concentrations and run through the Drop-seq device at a constant flow rate. Utilising THP-1 cell lines, optimal pump speeds, buffer (+/- optiprep) and cell concentrations were optimised prior to the use of cells derived from primary tissue. Post-encapsulation, the amplification of cDNA libraries during sample preparation for sequencing was also optimised. Multiple PCR cycling parameters were first utilised, to identify a minimum number of PCR cycles required to produce sufficient cDNA, whilst reducing the overamplification of high abundance transcripts. PCR cycling parameters have been shown to be highly variable between cell types, therefore highlighting the importance of initial cycling parameter testing (Macosko *et al.*, 2015).

Similar to the experimental Drop-seq procedure, the bioinformatic analysis pipeline of single cell data also required optimisation. An important first step during bioinformatic analysis of the single cell transcriptomic data is the filtering of low-quality cells and lowly expressed genes, to increase the likelihood for identifying meaningful biological discoveries amongst the cell populations (Luecken and Theis, 2019). One of the challenges with Drop-seq is the presence of contaminating mRNA which can become encapsulated into droplets and occlude true cell information. To counter this, the EmptyDrop bioinformatic analysis package was included in the analysis pipeline to filter out empty droplets and identify ‘ambient’ genes, which represent contamination across the single cells captured (Lun *et al.*, 2019). Furthermore, the process of extracting single cell suspensions and processing them through Drop-seq can put the cells processed under stress and lead to the induction of apoptosis, in which mitochondrial genes are upregulated (AlJanahi, Danielsen and

Dunbar, 2018). Cells displaying an elevated abundance (>20% mitochondrial fraction of whole transcriptome) of mitochondrial genes were therefore removed.

5.3.2 Steady-state and Migrated LCs are distinct with migrated LCs displaying upregulated expression of immunocompetency genes and tolerogenic programmes

We first analysed the transcriptomic profiles of steady-state and migrated LCs extracted from human breast skin tissue. Strikingly, UMAP plotting of steady-state and migrated LC transcriptomes revealed significant differences between the different states. Investigations into the genes differentially regulated between each state revealed migrated LC transcriptomes contained elevated expression of genes associated with immunocompetency and immune activation. This observation is consistent with *in vitro* studies demonstrating migrated LCs increased activation status and an enhanced ability to mediate immunogenic CD4 and CD8 T cell responses, as well as the low level of co-stimulatory protein expression on steady-state LCs (Sirvent *et al.*, 2020)(Polak *et al.*, 2012),(Polak *et al.*, 2014),(Klechevsky *et al.*, 2008). Additionally, consistent with previous analysis of migrated LCs, we observed that the increase in immunocompetency markers correlated with increased expression of *IRF4,* which orchestrates genomic programming of LC activation (Sirvent *et al.*, 2020)(Polak *et al.*, 2017).

Using single cell transcriptomic analysis, we aimed to explore unique subpopulations of LCs which could be responsible for the induction of immune tolerance. However, our analysis revealed that few subpopulations promoting unique biological pathways were identified, with steady-state LCs consisting of just two subpopulations defined by immunocompetency and migrated LCs consisting of just one population. Comparative analysis of steady-state and migrated LC single cell transcriptomes was therefore performed to identify whether changes in state reflected different tolerogenic gene programming. To investigate this, two panels of tolerogenic associated genes were utilised. One compiled from literature reviews of DC tolerogenic function and the other from our tolerogenic profile identified as common between LCs and tolerogenic associated DCs explored in transcriptomic analysis from **Chapter 4**. Our analysis therefore combined 'known' and 'novel' signatures of DC tolerance for robust analysis into tolerogenic genes expression. Our previous transcriptomic analysis of microarray data investigating LC tolerogenic signatures revealed that in comparison to other DC types, both steady-state and migrated LCs were similarly defined by low expression of inflammatory immune associated genes. Interestingly, despite evidence of steady-state LC coordinating the activation of epidermal Tregs to mediate immune tolerance and homeostasis (Seneschal *et al.*, 2012), GSVA analysis of our two defined tolerogenic signatures were both revealed to be enriched in migrated LC. The most highly expressed tolerogenic genes identified in migrated LC included *IDO1, HMOX1*, *LGALS1, RELB, ALDH2* and *S100A9.*

IDO1 is a classical tolerogenic mediator, which catabolises tryptophan resulting in skewing of T cell differentiation towards Tregs (Curti *et al.*, 2009). Identified as an interferon stimulated gene (ISG), *IDO1* has been previously associated with DC activation by IFNs and TNF-α and has been implicated in a number of regulatory feedback loops in cross-talk with other cell types – e.g. activation of CTLA4 receptors on T cells in turn induces IDO1 expression in DCs (Obregon *et al.*, 2017)(Mellor, Lemos and Huang, 2017)(Braun, Longman and Albert, 2005). Two studies involving human LCs previously demonstrated induction of *IDO1* in steady-state LCs and demonstrated its importance for inhibition of effector T cell proliferation (von Bubnoff *et al.*, 2004)(Koch *et al.*, 2017). The identification of *IDO1* augmentation in migrated LCs, similarly reflected our observations during comparison to CD14+ and CD141+ DDCs explored in **Chapter 4** using microarray data. Galectin-1 encoded by the *LGALS1* gene has been shown to promote the generation of tolerogenic DCs and to enable Tr1 type Tregs to supress Th1- and Th17-mediated inflammation (Sundblad *et al.*, 2017)(Martínez Allo *et al.*, 2020). *HMOX1* encodes an enzyme which degrades haem to produce carbon monoxide and is implicated in the suppression of immune activation through Treg induction and the inhibition of T cell proliferation (Riquelme *et al.*, 2016)(Domogalla *et al.*, 2017). *ALDH2* activity induces tolerance through induction of retinoic acid, which promotes Treg induction (Bazewicz *et al.*, 2019). Intriguingly, whilst *S100A9* was included in the list of tolerogenic genes and can be implicated in the induction of self-tolerance, it is more commonly associated with pro-inflammatory conditions, promoting the recruitment of immune cells and cytokine production and as such, is widely used as a biomarker for inflammatory disorders, such as inflammatory bowel disease (Wang *et al.*, 2018). Interestingly, *RELB,* the main TF subunit of the non-canonical NFκB pathway was in the curated tolerogenic signature and highly upregulated in migrated LC. Importantly, our observation of absent *RELB* expression in steady-state is consistent with previous studies (Clark *et al.*, 1999). IDO upregulation in DCs, as a results of CD40 ligation, is dependent of the activation of the non-canonical NFκB pathway (Tas *et al.*, 2007). Additionally, the non-canonical NFκB pathway in pDCs is fundamental for IDO1 induction and the induction of Tregs (Manches *et al.*, 2012). Further supporting the importance of non-canonical NFκB pathway activation was the presence of *MAP3K14* (NIK), which is a critical inducer of *RELB* activation and is restricted specifically to the non-canonical NFκB pathway (Sun, 2017), within the top upregulated DEGs in migrated LCs.

The population structure of steady-state LCs revealed the presence of two distinct populations within unstimulated epidermis, differentiated by state of immunocompetency. Here, we revealed the heterogeneity to be driven by the overall frequency of transcript expression, with S1 LCs displaying just 2 upregulated genes in comparison to S2. The strikingly different gene expression observed in the S2 cluster reflected an increased state of immunocompetency, with upregulated genes enriched for antigen processing and presentation, T cell receptor signalling, and induction of

immune response pathways. Consistent with these observations, all classic DC activation markers such as MHC I, MHC II and co-stimulatory molecules, as well as CD207, were upregulated in S2 LCs. In the steady-state, LCs therefore appeared to be present in a spectrum of activation from immaturity (steady-state 1) to immunocompetency (steady-state2). With consideration to current paradigms, which suggest state of DC immune activation and maturation reflect ability to promote tolerogenic immune response (Steinman, Hawiger and Nussenzweig, 2003), it would be interesting to investigate how the two steady-state populations differ in their ability to mediate tolerogenic responses.

In summary, scRNA-seq analysis has revealed the diverse genes expression exhibited by LCs at the steady-state and after migration. Critically, this included heterogeneous expression of immunocompetency markers in breast skin steady-state LCs and a marked induction of gene associated with immune effector process in migrated LCs. Differences in genes expression between steady-state and migrated LC were revealed to be governed by the regulation of unique TF networks that could be linked to the induction of tolerogenic genes. In our search to reveal genes linked with tolerance regulation by LCs, we consistently observed a dramatic increase of *IDO1* expression in migrated LC from both breast skin and foreskin. *IDO1* induction therefore appears to be a hallmark of migrated LC gene expression and could be a critical mechanism by which LCs regulate tolerogenic immunity. Our results highlight features of LC gene expression that would be interesting to investigate phenotypically *in vitro.* Foremost, how the state of immunocompetency and activation of LCs influences ability to induce tolerogenic responses. Secondly, to discern the influence of tolerance associated genes, such as *IDO1*, for functional LC tolerogenic responses.

5.3.3 Steady-state and migrated LC display remarkable differences in TF programming

Regulatory network and inference analysis using SCENIC revealed the vast differences in TF regulation in steady-state and migrated LCs. We expected the different regulons may reveal how the gene expression of tolerogenic associated genes is orchestrated. Migrated LC from both breast skin and foreskin were marked by the upregulation of the *IRF4* regulon*,* which was expected due to the association with *IRF4* and genomic programming of LC immune activation (Polak *et al.*, 2017)(Sirvent *et al.*, 2020). *IRF4* has also been linked with the restriction of inflammatory cytokine responsive genes and consistent with our finding that *IRF4* highly correlated with *LGALS1* expression in SCENIC analysis, is the observation that CRISPR knockouts of *IRF4* in human LC, leads to *LGALS1* downregulation (Sirvent *et al.*, 2020). *IRF4* expression by bone marrow derived DCs in the context of the steady-state is also fundamental for the regulation of tolerance, with bone marrow derived DCs from IRF4 knockout mice displaying diminished ability to induce Tregs and display increased expression of inflammatory cytokines (TNFα, IL-12) (Vander Lugt, Riddell, Aly A.

Khan, *et al.*, 2017). *IRF4* may therefore have a dual role in both LC maturation/immunocompetency and tolerance regulation. Regulons upregulated in migrated LCs also included NFκB TFs, *RELA* and *RELB.* In the steady-state, canonical NFκB activation involving *RELA,* governs the regulation of tolerance and the prevention of spontaneous autoimmunity (Baratin *et al.*, 2015) and as discussed above, *RELB* and the non-canonical NFκB pathway in DCs is implicated in the induction of IDO and T cell tolerance induction (Tas *et al.*, 2007)(Manches *et al.*, 2012). However, whilst the correlation of *RELB* and *IDO1* was identified, *IDO1* was not identified in the regulon of *RELB.* Positive regulation of *IDO1* expression by *RELB* may therefore be through an intermediate TF. Interestingly, in T cells, a positive regulatory interaction between *RELB* and *IRF4* has been identified (Boddicker *et al.*, 2015). Furthermore, binding of *RELB* to *IRF4* promoters has been identified in DC, suggesting a regulatory interaction (Lehtonen *et al.*, 2005). *KLF6,* which correlated with all of the tolerogenic genes has previously been shown to be upregulated in migratory DCs, correlating with the increased expression of tolerance associated genes (Vander Lugt, Riddell, Aly A. Khan, *et al.*, 2017). Additionally, regulons for components of the ETS TF family (*ELK1*) and AP-1 TF family (*JUND*), which have also been implicated in LC genomic programming during activation, were also upregulated in migrated LC (Polak *et al.*, 2017). Potential interactions with IRF4 at AP-1-IRF composite elements (AICE) and Ets-IRF composite elements (EICE), may have implications on the induction of tolerogenic genes (Vander Lugt, Riddell, Aly A. Khan, *et al.*, 2017).

5.3.4 The foreskin microenvironment leads to significant changes in LC transcriptomic programming

It has previously been shown that cells of the same type, isolated from skin at different body sites, display significant heterogeneity. Single cell RNA-seq for example, has revealed heterogeneity between human trunk, scalp and neonatal foreskin epidermal keratinocyte populations, with neonatal KCs containing a unique subpopulation expressing ligands for epidermal growth factor receptor (EGFR), which induce KC proliferation (Cheng *et al.*, 2018). Transcriptomic differences between fibroblast from different body sites has also been identified (Rinn *et al.*, 2006). LCs from the oral mucosa are also known to display lower levels of CD4 expression as compared to LCs from the vaginal epithelium and foreskin, influencing their capacity for HIV infection (Hussain, Lehner and Thomas, 1995). LCs from the oral mucosa also display more spherical morphologies as compared to LCs from the penis and conjunctiva epithelium, which may reflect more inactive status (Omine *et al.*, 2015). Furthermore, heterogeneity in skin due to ethnicity has also been explored, with reconstructed epidermal models from Caucasian and African keratinocytes and fibroblasts, displaying unique histology and transcriptomes (Girardeau-Hubert *et al.*, 2019). In depth single cell transcriptomic analysis comparing LCs derived from breast/trunk skin tissue and foreskin LCs has

until now been unexplored. Interestingly, despite differences in sex, ethnicity, and body site, adult foreskin and breast skin epidermal steady-state and migrated LCs appeared largely analogous. Here, steady-state LCs from both sites could be divided into two populations, whilst migrated LC consisted of one distinct cluster.

In comparison to steady-state LC from each respective tissue, both breast derived and foreskin migrated LCs displayed elevated expression of gene associated with immune effector processes and activation in comparison to LCs at the steady-state. Also, consistent between migrated LCs from both sites was the upregulation of tolerogenic associated *IDO1* and *ALDH2* expression, suggesting overlapping mechanisms of tolerance regulation. Common upregulated TFs and regulons were also identified, including *IRF4* and *ELK1.* However, DEG analysis directly comparing migrated LCs from each tissue compartment revealed diverse gene expression. Whilst common associated pathways such as response to cytokine and the immune effector process could be identified, a unique association of foreskin migrated LCs with the inflammatory response was identified.

The comparison between steady-state LCs from each site identified heterogeneity in gene expression. We also observed enrichment for tolerogenic gene signature 2 in steady state foreskin LCs, revealing differences in tolerogenic programming between steady-state LC from the two sites. In our regulatory network and inference analysis common steady-state LC TFs were identified including *MYC, ETS2, FOSL2* and *SPI1.* The expression pattern of *MYC* was consistent with microarray analysis of steady-state and migrated LC (**Chapter 4**) in which high *MYC* expression was observed in steady-state LC, with low expression in migrated LC. Similar to observations in migrated LCs, comparison between steady-state LCs from each site revealed marked differences in gene expression. Whilst breast derived steady-state LC were enriched for genes associated with metabolism, steady-state foreskin LC were enriched for genes associated with immune activation and effector processes, as well as cytokine production. Thus, foreskin LCs were consistently associated with increased expression of inflammatory pathway. Studies comparing blood T cells and foreskin T cells have revealed the elevated cytokine production in foreskin CD4+ (IL-17 and IL-22) and CD8+ (TNFα and IFNγ) populations, with foreskin CD4+ T cells displaying a predominant effector memory phenotype (Prodger *et al.*, 2012). The inner foreskin has also been shown to display a pro-inflammatory environment marked by increased expression of IFNγ, RANTES, GM-CSF and IP-10 (Lemos *et al.*, 2014). The foreskin has also been shown to accommodate greater microbiota diversity compared to post-circumcision, especially species of anaerobic bacteria, which likely have implications on the inflammatory environment (Price *et al.*, 2010)(Esra *et al.*, 2016). The foreskin therefore appears to be a pro-inflammatory site, which may explain the differences in inflammatory programming observed between breast skin and foreskin LC. Consistent with the idea that the foreskin may represent a more inflamed tissue were the differences in gene expression

profiles exhibited by steady-state subpopulations from each skin tissue. Whilst two distinct populations could be observed in steady-state LCs from both sites, foreskin LC populations appeared more distinct, instead of simply being differentiated by immunocompetency like breast skin steady-state LC. Foreskin S1 and S2 LCs DEGs were associated with common pathways of response to cytokine and immune activation, suggesting core enhancement of immune activation which could be programmed by the more inflammatory foreskin microenvironment.

Whilst differences in inflammatory signalling environments in foreskin tissue could explain some of the observations, it is also important to consider that differences in sex, ethnicity and age could also be influencing the results. Here, in our analyses we compared breast skin derived LC from a Caucasian female to foreskin derived LCs from black males. Interestingly, in murine studies, gender biasis have been observed in the expression of *IRF5* in total splenic cells and pDC from females (Shen *et al.*, 2010)(Griesbeck *et al.*, 2015). Phenotypic differences have also identified during comparison of fibroblast cultures from African and Caucasian skin (Girardeau *et al.*, 2009). Here, increased keratinocyte growth factor (KGF) and matrix metalloprotease 1 (MMP1) expression is observed in the former. The exact contribution of sex and ethnicity on LC biology are currently unexplored and we therefore cannot discard their potential influence on our observations. Also unadjusted for in our analysis was the age of the donors. Defective immunity in DCs from aged-patients is explored, with aged DCs displaying overall increased activation status and increased pro-inflammatory cytokine production, which leads to increased susceptibility of autoimmunity (Agrawal *et al.*, 2012). Interestingly, bullous pemphigoid, an autoimmune skin condition in which tolerance to Dsg1 and Dsg3 is lost, increases in prevalence with age, suggesting that LC tolerogenic responses may decline over time (Hammers and Stanley, 2016).

5.3.5 Constellation Drop-seq validates LC transcriptomic programmes and enhances investigations into LCs in the context of whole epidermis

The low frequency of LCs amongst the epidermal population limits large scale investigation into LC transcriptomics. The purification of LCs from the epidermis through FACS before Drop-seq could also induce changes to LC transcriptomes, impeding our ability to investigate true LC biology. To bypass this problem and in order to analyse large numbers of LCs in the context of the whole epidermis, we developed a targeted Drop-seq approach, called Constellation Drop-seq. We designed a panel of primers targeting genes of interest, including markers of PBMC populations, markers of LC activation and transcription factors important for LC immune function. Using Constellation Drop-seq we restricted the sequencing potential to a small selection of genes, therefore maximising the number of cells we could sequence by 10-fold for the same read-depth utilisation. Using Constellation Drop-seq we were able to produce single cell sequencing data for a

significantly large number of LCs, in the context of the whole epidermal tissue. This revealed that observations in steady-state LC purified by FACS and processed through normal Drop-seq, such as absent *IRF4* and *IDO1* expression, were true to the steady-state LC epidermal population and not an artefact of the purification process. However, this still does not negate the potential for the enzymatic digestion process to alter steady-state LC gene expression. As we demonstrated ability to identify additional cell populations within the epidermis, such as CD8 T cells (*GZMB*) and monocytes (*LYZ*), also provided additional information as to the state of inflammation in the tissue, whilst also highlighting the increased power for cell subset specific investigations using Constellation Drop-seq instead of regular Drop-seq.

Using Constellation Drop-seq we were also able to identify heterogeneity in gene expression not previously identified using regular Drop-seq, such as divergent expression of canonical NFκB (*NFKB1*) and NFκB inhibitors (*NFKBIA, NFKBIZ* and *TNFAIP3*). *NFκB* is a widespread mediator indispensable for immune cell function, survival and differentiation (Grumont and Gerondakis, 2000). Its activity has also been associated with augmented DC inflammatory responses (Hayden, West and Ghosh, 2006)(Hayden and Ghosh, 2011) as well as tolerance (Baratin *et al.*, 2015). As discussed above, elevated *RELA*, a C-terminal transactivation domain component of the canonical *NFκB* TF family, was upregulated in migrated LCs derived from breast skin compared to steady-state LCs. However, during SCENIC regulatory network inference analysis its expression lowly correlated with genes within the tolerogenic programme. In migrated LCs, canonical *NFκB* may therefore have a predominant role in general immunocompetency programming or additionally, could even influence LCs immunogenic capacity. Therefore, steady-state LCs with elevated canonical NFκB expression and decreased NFκB inhibitor expression may be in a state conditioned for immunocompetent programming, whilst those with the opposite expression may favour immunosuppression. To mediate its extensive regulation of the immune system NFκB can induce the activation of other TFs. Interestingly, *NFκB* heterodimer binding to the *IRF4* promoter has been demonstrated (Shaffer *et al.*, 2009)(Boddicker *et al.*, 2015). Upstream activation of *NFκB* to induce *IRF4* expression therefore appears a plausible pathway to induce LC activation and migration. Interestingly, *IRF4* has been demonstrated to inhibit *NFκB* expression in CRISP-Cas9 *IRF4* knockouts in human LCs, suggesting feedback interactions are important for LC regulation, with both TFs tightly interlinked (Sirvent *et al.*, 2020).

Chapter 6 *In* vitro investigations into the determinants of LC mediated tolerogenic responses

6.1 Introduction

Our single cell transcriptomic analysis of steady-state and migrated LCs identified profound differences in the state of activation, consistent with phenotypic analysis of cell surface markers (**Chapter 5**)(Davies *et al.*, 2019)(Sirvent *et al.*, 2020) and identified 3 distinct populations of LCs: steady-state S1, steady-state S2 and migratory LCs. The analyses revealed that steady-state LCs exist in a spectrum of immune activation from immaturity to immunocompetency, placing cells in a trajectory from inactive/immature cells to full maturity. Interestingly, the increase in immunocompetent programming of migrated LC was coupled with the expression of a tolerogenic gene module, suggesting programming of tolerogenic function in migrated mature LCs. We therefore sought to understand whether the expression of tolerogenic genes exhibited by steady-state and migrated LC, translates into their functional capacity to induce tolerogenic T cell responses.

The relation between maturation and tolerance has been previously discussed in the context of other DC populations, with many studies implying DC maturation as regulatory for tolerance. Maturation of DCs is a central process in DC immunity that switches the antigen capturing phenotype of immature DC into a highly mature phenotype, in which DC are primed for T interaction, through elevated expression of MHC and costimulatory molecules (Mellman and Steinman, 2001)(Audiger *et al.*, 2017). In contrast, immature DCs, marked by low expression of maturation markers, have been shown to induce T cell anergy or Treg differentiation (Steinman *et al.*, 2000)(Banchereau and Steinman, 1998)(Steinman, Hawiger and Nussenzweig, 2003)(Lutz and Schuler, 2002)(Audiger *et al.*, 2017)(Fucikova *et al.*, 2019). Steady-state immature DC processing and presenting self-antigens in the context of low level costimulatory molecules and cytokines can tolerise the immune system, through defining self from non-self (Mellman and Steinman, 2001)(Steinman *et al.*, 2003). This tolerising process induced by steady-state DC suppresses the induction of autoimmunity to self-antigen, even when inflammation and infection disrupt homeostasis. Therefore, the immature S1 steady-state population of LCs, identified by single cell transcriptomics, are likely key to tolerance induction during uninflamed conditions, with tolerance

diminishing and immunogenic responses becoming dominant during increased immunocompetency in S2 steady-state LCs and migratory LCs.

However, mature DCs have also been shown to display plasticity in immune responses, with the potential to induce tolerogenic T cell responses. Phenotypically mature CD83^{high}CCR7+HLA-DR^{high} IL-10DC induced Tregs are much more potent than Tregs that are induced by phenotypically immature CD83^{low}CCR7-HLA-DR^{low} IL-10DC (Kryczanowsky *et al.*, 2016). Furthermore, mature human CD123+ MoDCs expressing IDO, potently inhibit T cell proliferation *in vitro* (Munn *et al.*, 2002). Coupled with DC maturation is migration, which we observed in our LC single cell RNA-sequencing. Interestingly, DCs in non-inflamed conditions migrate to the lymph nodes and can promote tolerance through cross-presentation tolerization of CD8 T cells (Albert, Jegathesan and Darnell, 2001). Overall this implies that DC maturation may not be limited to the induction of immunogenic responses and could suggest a tolerogenic role for immunocompetent migratory LC.

In addition to maturation status, tolerogenic DC potential is mediated by expression and secretion of specific tolerogenic signals. Functionally tolerogenic DCs have been associated with high levels of immune inhibitory molecules such as IDO1, galectins, PD-L1 and HLA-G (Obregon *et al.*, 2017)(Munn *et al.*, 1998)(Pëa-Cruz *et al.*, 2010)(Martínez Allo *et al.*, 2020). Furthermore, IDO1+ DCs preferentially promote FOXP3+ Treg induction over immunogenic CD8+ T cells (Harden *et al.*, 2011)(Fallarino *et al.*, 2006). Indeed, our Drop-seq analysis revealed marked upregulation of *IDO1* expression in migratory LCs, amongst other genes implicated in tolerance. Therefore, we sought to investigated the importance of *IDO1* expression for LC ability to induce Tregs in an *in vitro* experimental system.

While steady-state tolerance is key to immune homeostasis, therapeutic interventions often rely on modulation of inflammation through induction of tolerogenic responses. The immunomodulatory drug dexamethasone is widely utilised in medicine for its immunosuppressive capacity. The effects of dexamethasone can be observed at the molecular level. As explored in **Chapter 3**, dexamethasone stimulation of MoDC, in conjunction with VitD3, induced the expression of tolerogenic gene modules. The specific tolerogenic capacity of dexamethasone for modulating DC function is shown in clinical trials utilising dexamethasone stimulated MoDCs to treat rheumatoid arthritis and furthermore, the inhibition of anti-tumour CD4+ and CD8+ T cell responses to melanoma by dexamethasone stimulated MoDCs (Nikolic and Roep, 2013)(Falcón-Beas *et al.*, 2019). Additionally, dexamethasone stimulation in MoDCs is associated with upregulated *IDO1* expression (García-González *et al.*, 2019). We therefore explored how dexamethasone stimulation modulated LC ability to induce Tregs and investigated whether any changes could be the result of modulation of tolerance associated genes.

6.1.1 Hypothesis

LC tolerogenic capacity is determined by the state of immunocompetency and dependent on the expression of mediators encoded in tolerogenic transcriptional programme.

6.1.2 Aims

- Determine the capacity of immature and immunocompetent steady-state LC populations for inducing Tregs.
- Compare the capacity of steady-state LCs and migratory LCs to induce Tregs.
- Investigate the functionality of LCs induced Tregs.
- Explore how dependent LC tolerogenic responses are on *IDO1* expression.
- Investigate how LC tolerogenic immune responses can be modulated by tolerogenic dexamethasone stimuli.

6.2 Results

6.2.1 Immunocompetency of steady-state LCs is critical for their ability to induce Tregs

As activation status defined LC subpopulations in the steady-state, the expression of classical DC activation markers and LC markers including *CD86, CD83, CD40* and MHC II (*HLA-DRA*) was assessed across LC populations to identify markers which could distinguish immature and immunocompetent steady-state LC populations (**Figure 46**). CD40 was lowly detected in all steady-state LCs, whilst high HLA-DRA expression was detected in LCs from both clusters. CD83 displayed elevated expression in S2, however its expression spilled over highly into the S1 population. The most distinguishable marker, CD86 was more frequently expressed in the S2 immunocompetent population only.

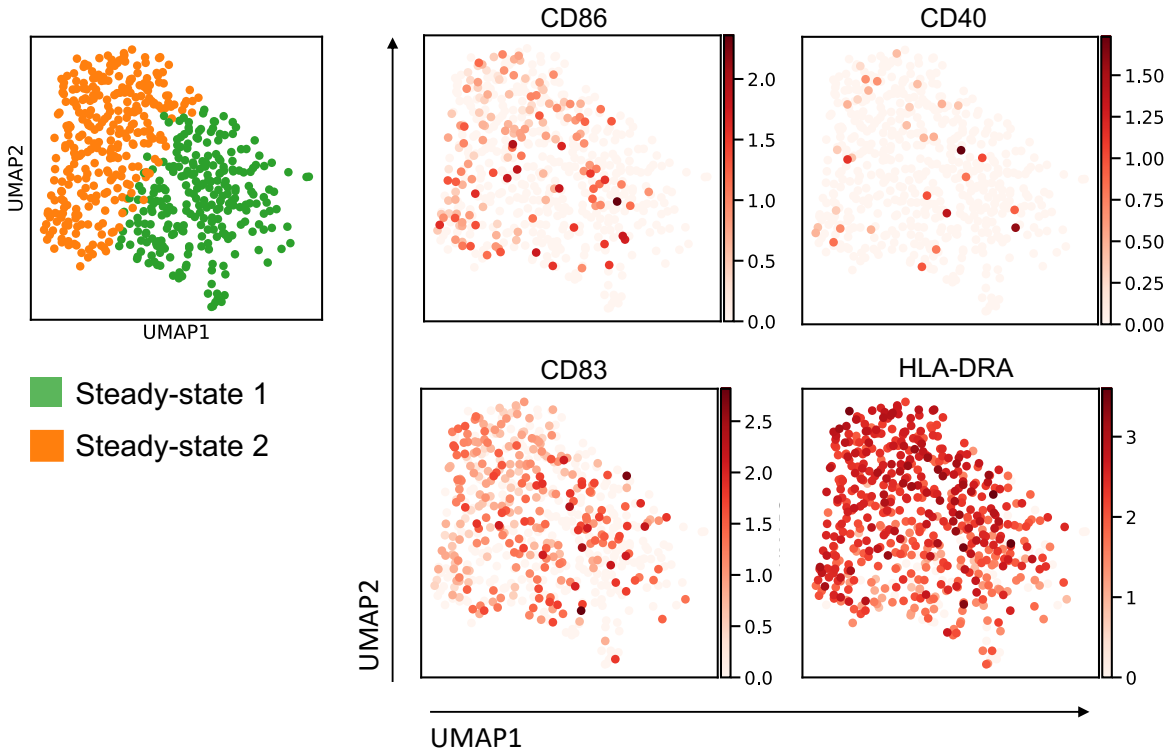

Figure 46. Steady state immunocompetent LC can be distinguished through increased CD86 expression. UMAP visualisation of the 2 breast skin steady-state LC populations, with accompanying UMAP marker plots displaying the expression of DC activation markers *CD86, CD40, CD83* and *HLA-DRA.*

Single cell RNA-seq analysis revealed CD86 to be an effective marker to distinguish immunocompetent and immature LCs. Thus, CD86 expression at the protein level was analysed using flow cytometry, using the same gating strategies as shown in **Figure 29** to identify steady state LC populations (**Figure 47A**). Consistent to RNA expression levels, a spectrum from low to high CD86 expression could be observed in steady-state LC at the protein level. Whilst donor to donor variation in the spectrum of CD86 expression could be seen, LCs falling into either CD86High or CD86Low expression could be distinguished in all 3 donors studied. To explore the tolerogenic potential of both immunocompetent and immature LCs, CD86High and CD86Low steady-state LC populations were FACS sorted for *in vitro* analyses. The boundary for gating CD86High and CD86Low, was based around the central density of cells in the FACS plot in each of the 3 donors.

After FACS isolation of steady-state LC CD86High and CD86Low populations, LCs were co-cultured with CD4+ naïve T cells for 5-days, after which the expansion of CD25+FOXP3+ Tregs was quantified. High purity of CD4+ naïve T cells was ensured using double column filtering during magnetic column isolation, ensuring sufficient depletion of memory T cell populations. Treg differentiation from pure naïve CD4+ T cells therefore tests the potential of LCs to prime Treg differentiation rather than expanding existing Tregs. Percentages of Tregs induced after co-culture were identified through gating of CD3+CD4+CD127-CD25+FOXP3+ T cells (**Figure 47B**). Interestingly, CD86Low immature LCs did not increase the number of CD25+FOXP3+ Tregs compared to control (CD4+ naïve T cells cultured alone). In contrast, CD86High immunocompetent LC significantly expanded the number of CD25+FOXP3+ Tregs compared to both control ($p=0.0143$) and CD86Low LC ($p=0.0129$, $n=3$ independent skin donors), revealing that the state of immunocompetency associates with LC ability to promote T cell-mediated immune tolerance (**Figure 47C**).

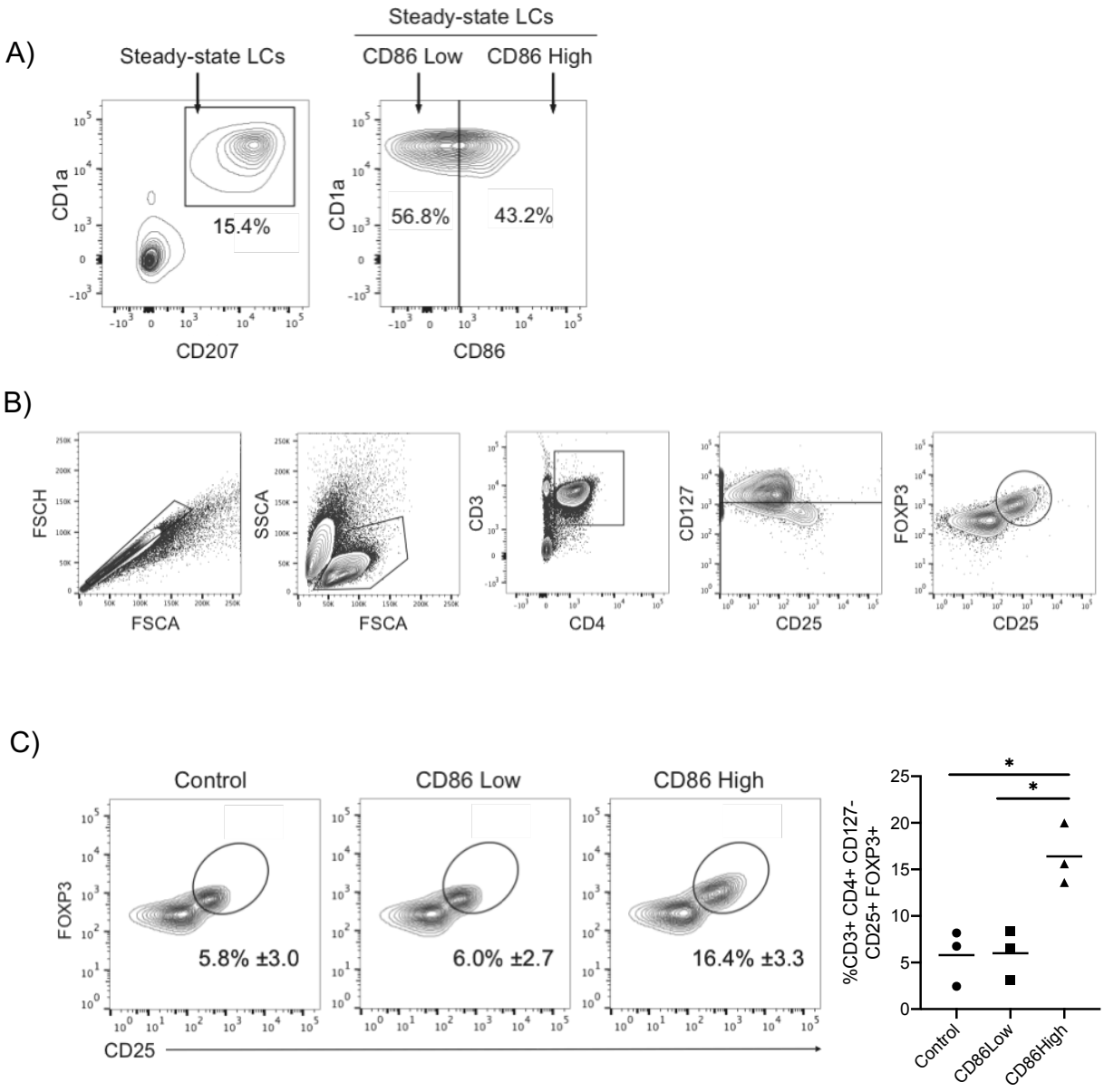

Figure 47. Steady state immunocompetent LCs are superior at inducing FOXP3+ Tregs. A) Flow cytometry analysis of steady-state LCs identified as CD207/CD1a high cells (Left panel). LC populations were separated into CD1a+ CD86Low and CD86High by FACS (Right panel). Representative example from n=3 independent LC donors. **B)** Gating strategy for investigating the quantity of CD3+CD4+CD127-CD25+FOXP3+ Tregs after co-culture of CD4 naïve T cells with LC for 5-days. Representative example from n=3 independent LC donors **C)** Co-culture of CD4+ naive T cells with either CD86Low or CD86High steady-state LCs. Control cultures involved CD4+ naïve T cells in the absence of LCs. After 5 days of co-culture Tregs were quantified by FACS as CD3+CD4+CD127-CD25+FOXP3+ cells. n=3 independent LC donor paired experiments. *p<0.05.

6.2.2 Highly immunocompetent migrated LCs are more effective at inducing Tregs than steady-state LCs

To test the observation that LC immunocompetency enhances tolerance induction, we sought to investigate the effect of *in vitro* migration from epidermal sheets on LCs tolerogenic potential. Following 5 days co-culture with naive CD4+ T cells, both steady-state and migrated LC significantly expanded the population of CD3+CD4+CD127-CD25+FOXP3+ Tregs compared to control (n=6 independent skin donors, steady-state LCs p=0.0101, migrated LCs p=<0.0001). However, LCs ability to amplify Tregs was significantly augmented by migration, with increased percentages of CD25+FOXP3+ Tregs induced compared to steady-state LCs (p=<0.0001, MeanFC=3, **Figure 48A**). The increased immunocompetency of migrated LC therefore correlated with increased potential to prime Tregs from naïve CD4+ T cells. Additionally, the efficiency of migrated LC to induce Tregs from autologous resident memory T cells TRMs isolated from healthy epidermal tissue was assessed in our lab by Dr Sofia Sirvent (**Figure 48B**). Co-culture of migrated LCs with TRMs significantly increased the number of CD25+FOXP3+ Tregs compared to control TRMs cultured alone (n=5 independent skin donors, p=0.0025, **Figure 48C**). Furthermore, co-culture of migrated LCs with autologous TRMs also drove expansion of IL-10 producing CD4+ T cells (n=8 independent skin donors, p=0.0451, **Figure 48D**). In the context of autologous cells from skin tissue, immunocompetent migratory LCs demonstrated their highly tolerogenic potential. Overall these results further demonstrate the link between increasing LC immunocompetency and increased ability to induce tolerogenic T cell responses.

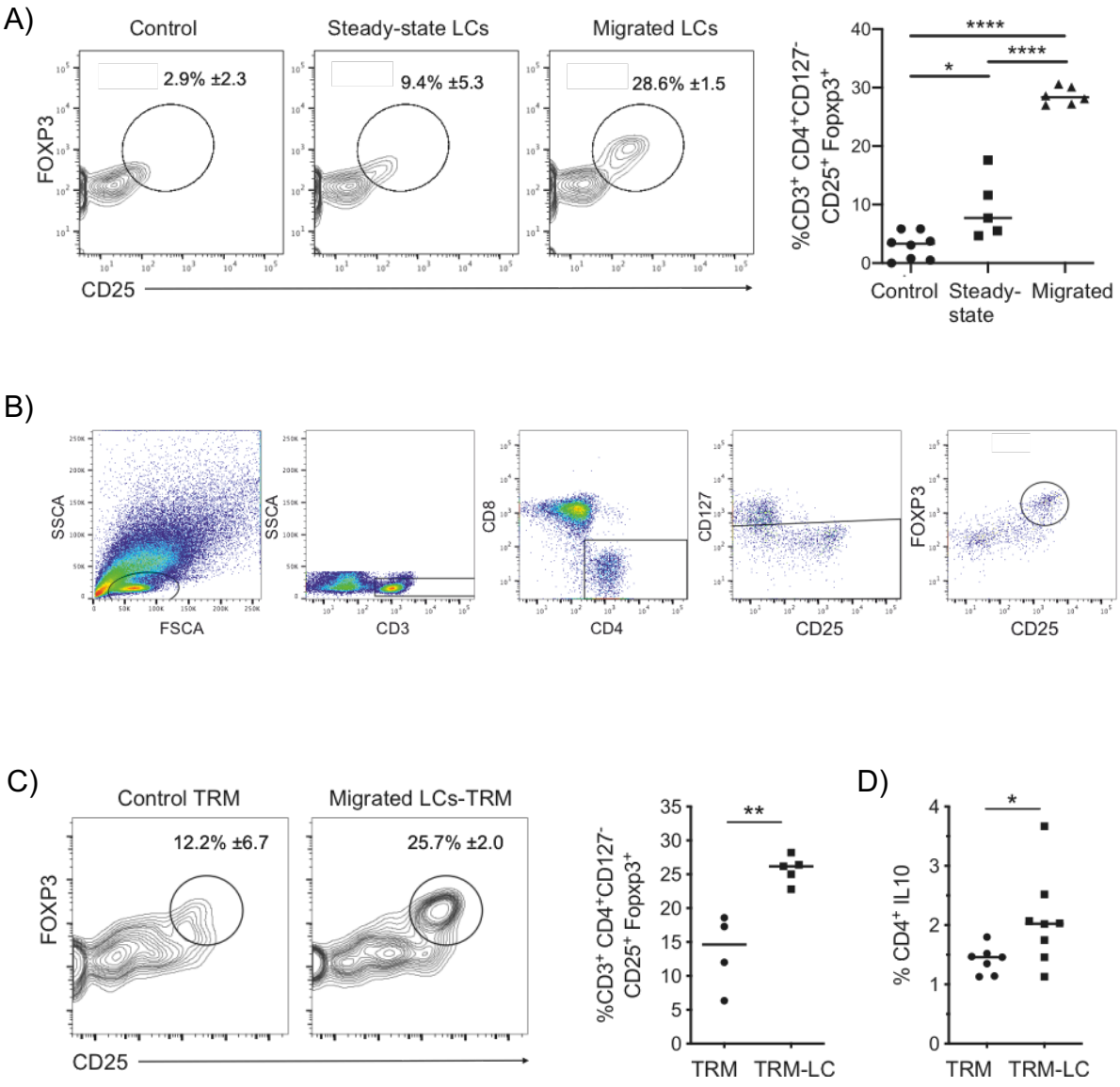

Figure 48. Migration enhances the tolerogenic potential of LCs. A) Flow cytometry analysis of Tregs induced after co-culture of steady-state and migrated LC with CD4+ naïve T cells as in **Figure 47C,** n=8 control, n=5 steady-state LCs, n=6 migrated LCs from independent donors. **B)** Gating strategy for investigating the quantitiy of Tregs induced during 5-day co-culture of autologous TRMs with migrated LC. Representative figure from **C)** Flow cytometry assessment of the percentage of Tregs induced after 5-day co-culture of migrated LC with autologous TRMs extracted from human epidermis. 5-day cultures of TRMs alone were used as control. Tregs were identified as CD3+CD4+CD127-CD25+FOXP3+ cells. n=5 independent LC donors. **p<0.01. **D)** Percentage of IL-10 producing CD4+ cells after co-culture of TRMs in the presence or absence of migrated LC. n=8. *p<0.05. Figure 48C&D experiments were performed by Dr Sofia Sirvent.

6.2.3 Migrated LCs induce functionally suppressive Tregs

Having established the enhanced capacity of LC to induce Tregs upon migration, driven by increasing immunocompetency, we next sought to test the functionality of LC induced Tregs and determine if they are functionally suppressive. After 5-day co-culture of CD4+ naïve T cells with migrated LC, populations of CD3+CD4+CD127-CD25+ expressing Tregs were FACS purified (**Figure 49A**). Purified Tregs were co-cultured with antiCD3/CD28-stimulated PBMCs at 1:1 and 1:3 ratios (Treg:PBMC), to test Treg immunosuppressive capacity in the context of proliferative signalling. Different ratios were tested to assess the potencies of suppression of the purified Tregs. Cultures of PBMCs unstimulated or with antiCD3/CD28 were used as negative and positive controls. Tregs expanded with migratory LCs potently inhibited both activated CD4+ and CD8+ T cell proliferation at both 1:1 and 1:3 ratios Treg:PBMC, with increased quantities of Treg in 1:1 ratio amplifying the suppressive effect (CD4 1:1 $p=0.0088$, CD4 1:3 $p=0.0277$, CD8 1:1 $p=0.0007$, CD8 1:3 $p=0.0111$, $n=5$ from Tregs differentiated by 3 independent LC donors, **Figure 49B&C**). Overall this highlighted the highly immunosuppressive capabilities of Tregs that are induced by LCs.

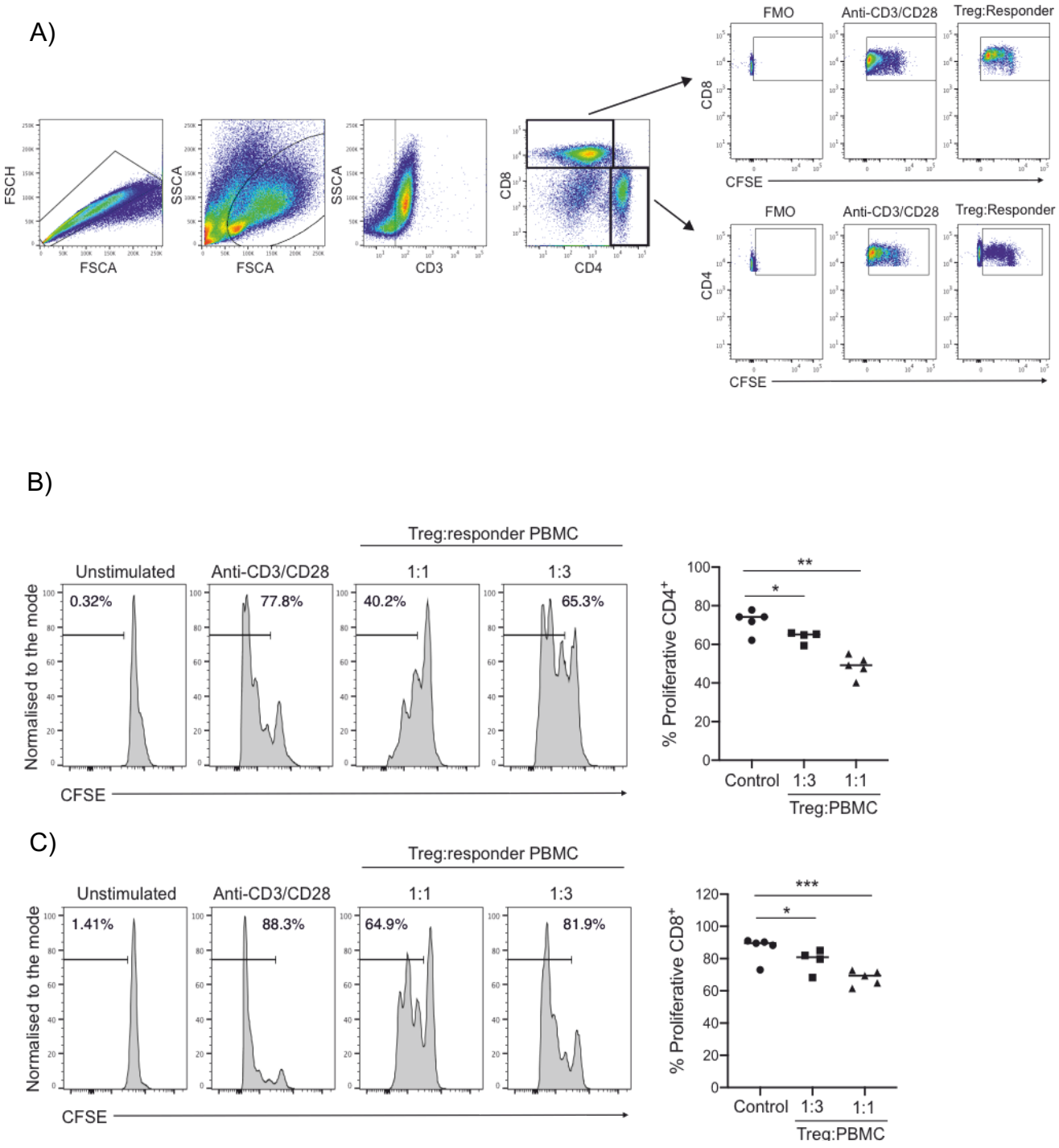

Figure 49. LC induced Tregs are functionally immunosuppressive. A) Gating strategy for investigating the inhibition of CD4+ and CD8+ Teff proliferation by Tregs induced in co-culture with migrated LC for 5 days. Proliferation analysis of CD4+ and CD8+ T cells using CFSE labelled PBMCs after 3-day co-culture with purified CD3+CD4+CD127- CD25+ Tregs. Proliferation analysis of **B)** CD4+ T cells and **C)** CD8+ T cells using CFSE labelled PBMCs after 3-day co-culture with autologous purified CD3+CD4+CD127-CD25+ Tregs. The percentages of proliferating CD4+ cells stimulated with plate bound anti-CD3 and soluble anti-CD28 are displayed at ratios of 1:1 and 1:3 Treg:PBMC (n=5 from 3 independent LC donors). *p<0.05, **p<0.01, , ***p<0.001. Normalised to mode expression is displayed, which adjusts for heterogeneous sample sizes across samples, allowing direct comparison of CFSE diffusion.

6.2.4 IDO1 expression is required to exhibit full tolerogenic potential of migrated LCs and can be modulated through tolerogenic dexamethasone stimuli.

Single cell RNA-seq analysis highlighted IDO1 amongst the potential mediators of immunotolerance in immunocompetent LCs, as being uniquely induced after migration. The homogenous upregulated expression of IDO1 in migratory LC compared to steady-state LC indicated the importance of this molecule for enhanced LC potential to induce Tregs. To test whether the IDO1 transcript was translated into a protein, IDO1 levels were measured intracellularly in steady-state and migratory LCs using flow cytometry (**Figure 50A&B**). Additionally, to assess whether the IDO1 expression level could be altered by therapeutic interventions, protein levels were measured when LCs were migrated from epidermal sheets in the media supplemented with Dexamethasone (1μM). Consistent with the single cell RNA-seq data, the level of IDO1 protein expression was considerably and significantly higher in migrated LCs compared to steady-state LC (n=5 independent skin donors, p=0.0002, **Figure 50B**). Furthermore, IDO1 concentration was significantly higher when LCs were migrated in the presence of dexamethasone, enhancing the tolerogenic phenotype (**Figure 50B**, p=0.0142, n=5 independent skin donors)

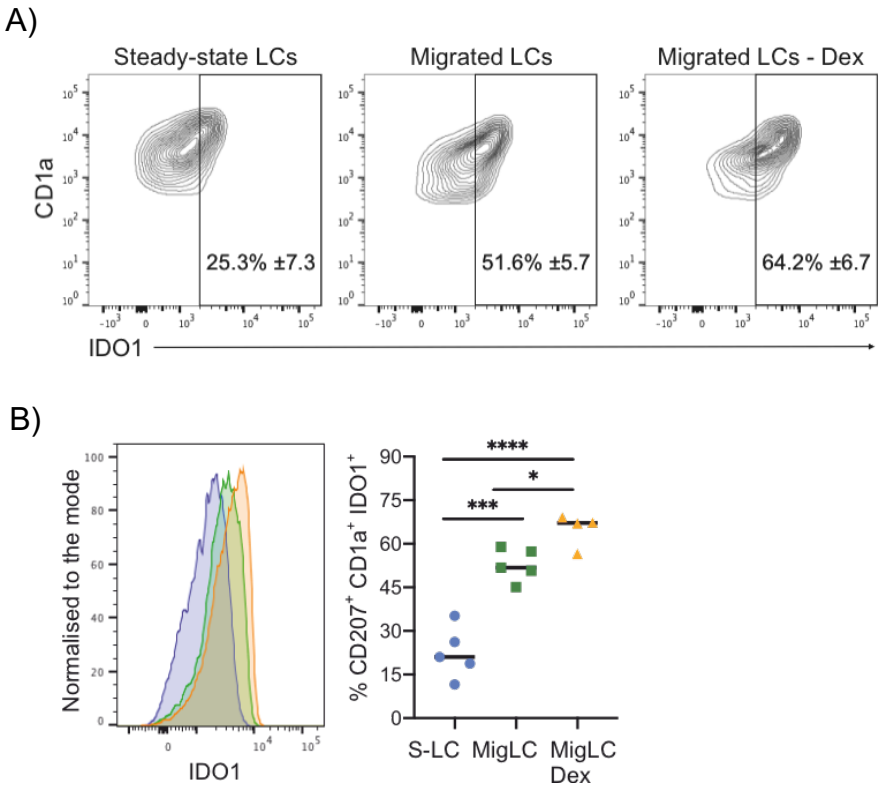

Figure 50. LC expression of IDO1 is enhanced by migration and immunotherapeutic intervention. A) Gating strategy to define the percentage of IDO1 expression in steady-state LC, migrated, and dexamethasone migrated LC. n=5 steady-state and migrated LC experiments, n=4 migrated dexamethasone experiments. **B)** Flow cytometry assessment of the percentage of IDO1 expression in steady-state LC and migrated LCs extracted by 48-hour culture of epidermal sheets with and without 1M dexamethasone. n=5 steady-state and migrated independent LCs, n=4 migrated dexamethasone independent LCs. *p<0.05, ***p<0.001, ****p<0.0001.

With the increase in IDO1 expression migratory LC validated at the protein level we next explored the importance of IDO1 signalling for LC tolerogenic function. IDO1 signalling was blocked during co-culture of migrated LC and naïve CD4+ T cells (n=4 paired experiments), using two molecular compounds NLG-919 and epacadostat (EPAC). NLG-919, an immune checkpoint inhibitor, significantly impaired LCs ability to expand Tregs (p=0.0354, **Figure 51**). Interestingly, interference with IDO1 using EPAC, a selective inhibitor of tryptophan catabolism was less potent and although a trend for reduced Treg induction could be observed, this was not statistically significant (p=0.0583, **Figure 51**). IDO1 expression by LCs therefore appears important for full tolerogenic potential of LC to prime Tregs.

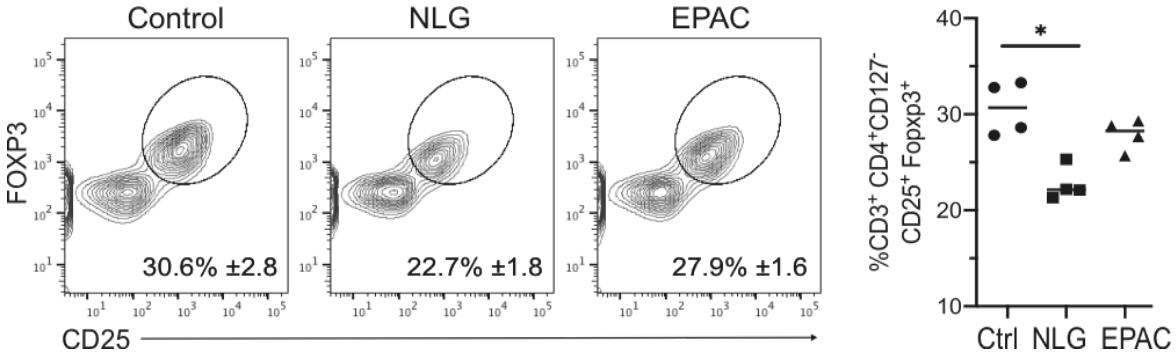

Figure 51. Inhibition of IDO1 downregulates LC tolerogenic function. Flow cytometry analysis of the percentage of Tregs induced after 5-day co-culture of migrated LC with CD4+ naïve T cells in the presence of IDO1 inhibitors NLG-919 (NLG) and epacadostat (EPAC). 5-day cultures of CD4+ naïve T cells alone were used as control. Tregs were identified as CD3+CD4+CD127-CD25+FOXP3+ cells. n=4 independent LC donors. *p<0.05.

LCs ability to prime and expand tolerogenic T cells creates an exciting opportunity for therapeutic interventions. Since steady-state LCs exist in a spectrum of immunocompetence, with a subpopulation of LCs already poised for tolerance induction, we hypothesised that in situ treatment can further potentiate their tolerogenic behaviour upon migration. To test this, we treated LCs with the immunosuppressive drug dexamethasone, during migration from epidermal fragments in cell culture. Indeed, dexamethasone migrated LCs were significantly more potent in expanding CD25+FOXP3+ Tregs (n=4 independent skin donors, p=0.0271, **Figure 52A**) in comparison to their untreated migrated LC counterparts. Additionally, CD4+ T cells expanded by migratory LCs stimulated with dexamethasone (n=5 independent skin donors, p=0.0061) produced more IL10 than untreated migrated LC (p=0.028, **Figure 52B**), consistent with their tolerogenic phenotype. As shown above, importantly, the presence of dexamethasone during LC migration further increased the expression of IDO1 protein (n=4 independent skin donors, p=0.0142, **Figure 50B**), supporting the importance of IDO1 for LC tolerogenic function. Overall these results demonstrate that the potential of migratory LC to induce tolerogenic T cell responses could be enhanced by immunosuppressive dexamethasone signalling and correlated with increased expression of IDO1. Furthermore, our analyses suggest that LC exposure to immunomodulatory stimuli during LC migration and prior to the huge shift genomic programming it induces, could be key for predisposing LC immune responses towards tolerance.

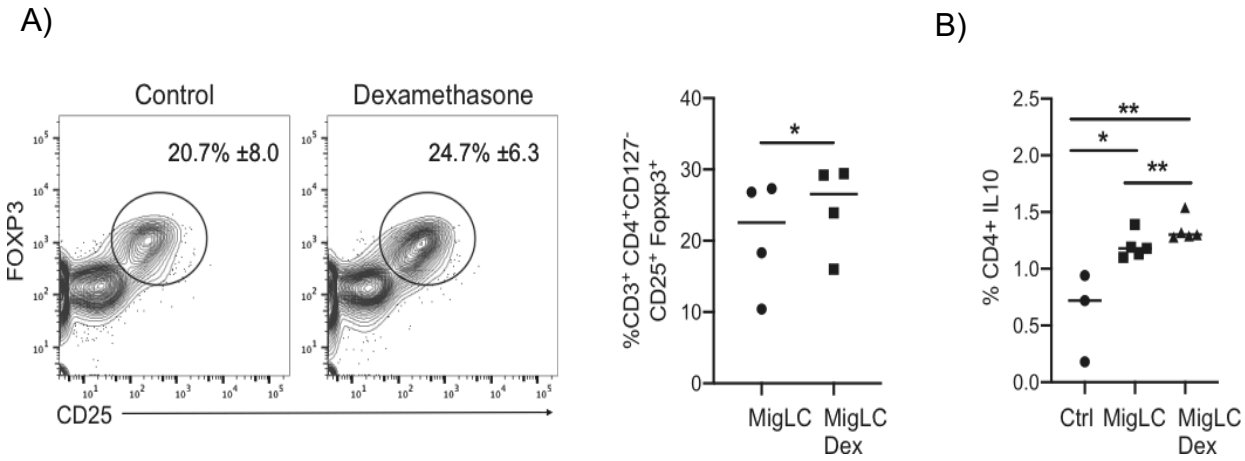

Figure 52. Inhibition of IDO1 downregulates LC tolerogenic function. A) Flow cytometry assessment of the percentage of Tregs induced after 5-day co-culture of migrated LC with and without dexamethasone stimulation, with CD4+ naive T cells. Tregs were identified as CD3+CD4+CD127-CD25+FOXP3+ cells. n=4 independent LC donors. *p<0.05. **B)** Flow cytometry analysis of the percentage of CD4+IL10+ T cells after 5-day co-culture of migrated LC with and without dexamethasone stimulation, with CD4+ naïve T cells. 5-day cultures of CD4+ naïve T cells alone were used as control. n=5 independent LC donors. *p<0.05, **p<0.01.

6.3 Discussion

6.3.1 The state of LC immunocompetency, which increases from steady-state to migrated LCs, is critical for tolerance regulation

Investigations into the genomic programs and molecular pathways that allow human LC to promote tolerogenic immune responses has been hindered by the lack of available technologies and suitable experimental systems. Drop-seq single-cell RNA sequencing analysis of steady-state and migrated LC populations revealed differences between states of immunocompetency and the expression of tolerogenic markers (**Chapter 5**). We therefore performed functional *in vitro* analyses to assess how our transcriptomic observations translated into LC tolerogenic capacity. Our analysis revealed that LC tolerogenic potential is indeed coupled with immunocompetency, with increasing tolerogenic capacity exhibited from immature to immunocompetent steady-state LCs, which is further enhanced upon migration.

Tolerance induction by DCs can be coordinated by the induction of central and peripheral tolerance. In central tolerance, the majority of self-reactive T cells are depleted, whilst peripheral tolerance ensures any remaining/emergent self-reactive T cells are controlled (Banchereau and Steinman, 1998)(Ardouin *et al.*, 2016)(Audiger *et al.*, 2017)(Oh and Shin, 2015). Typically, DC ability to induce tolerogenic immune responses in the periphery has been associated with an immature or semi-mature state (Steinman *et al.*, 2003)(Steinman, Hawiger and Nussenzweig, 2003)(Hasegawa and Matsumoto, 2018). Indeed, DCs expressing low levels of co-stimulatory and antigen presenting molecules can promote T cell anergy or Treg differentiation (Hasegawa and Matsumoto, 2018) (Mahnke *et al.*, 2002). In contrast, our *in vitro* analyses demonstrate that immature steady-state LCs do not induce Tregs, while a subpopulation of immunocompetent CD86 expressing steady-state LCs are able to do so. Furthermore, LC migration, which enhances LC immunocompetency, promotes increased ability to induce Tregs, as compared to immunocompetent steady-state LC. Tregs that were induced by migratory LCs were shown to be functionally tolerogenic, suppressing both CD4 and CD8 T cell proliferation in co-culture.

Co-stimulatory molecules expressed by DCs are critical for modulating T cell signalling pathways during engagement of the TCR and MHC within the immune synapse. Here, engagement of DC CD80/86 with CD28 on T cells, results in the activation of signalling kinases which highly amplify T cell modulation (Lanzavecchia and Sallusto, 2001). The increased expression of T cell co-stimulatory genes, such as CD86, in immunocompetent steady-state and migrated LCs, are suggestive of their importance for Treg induction. Indeed, increased CD86 expression is not always linked to immunogenic immunity. Increased expression of CD80 and CD86 is observed in migratory LC as a

result of epicutaneous immunisation, but does not result in efficient generation of effector memory CD4 T cells (Shklovskaya *et al.*, 2011). CD86 is also implicated in DC-mediated tolerance induction through interaction with CTLA4 on T cells (Mellor *et al.*, 2004)(Obregon *et al.*, 2017). Also, consistent with our findings, a study by Yamazaki et al. demonstrated that mature CD86High DCs were able to expand CD4+CD25+ T cells more effectively than CD86Low immature DCs (Yamazaki *et al.*, 2003). The importance for high levels of co-stimulatory molecules for tolerance induction could also be seen in our observation that LCs can prime naïve CD4+ T cells into functional Tregs. Here, this demonstrates a high level of signalling occurring at the LC/T cell immune synapse, as enhanced signalling is required to re-programme naïve T cell intracellular signalling pathways and promote differentiation (Lanzavecchia and Sallusto, 2001). Induction of tolerance by LCs therefore requires delivering of efficient signal 2 through co-stimulation. However, since LC ability to induce tolerogenic responses is substantially enhanced upon their migration out of the epidermis, and as Drop-seq showed CD86 expression is relatively high in both steady-state immunocompetent and migratory LC at the mRNA level, tolerance is likely governed by additional factors beyond the capacity to antigen present and co-stimulate. As both steady-state LCs and migratory LCs were extracted from unstimulated/non-diseased tissue, the antigen presentation exhibited between LCs and T cells would likely involve mostly self-antigen rather than strongly agonistic foreign antigens. Factors that may differentiate the induction of immunogenic or tolerogenic responses could therefore be dependent on the specific interactions between DC MHC complexes and T cell TCRs, in which weakly agonistic self-antigen may prime tolerogenic T cell responses over immunogenic ones(Lewis and Reizis, 2012). Additionally, DCs that spontaneously mature in the steady-state may have a shorter lifespan to DC that mature in the context of immunogenic signalling, failing to induce sufficient T cell proliferation and differentiation(Lanzavecchia and Sallusto, 2001). However, prolonged 5-day co-culture of LCs and T cells promoted considerable proliferation over the whole time period.

6.3.2 IDO1 is important for LC tolerogenic function, but is likely part of a wider tolerogenic programme

The signalling context in which engagement of the immune synapse occurs also modulates T cell immunological outcomes. In our Drop-seq analysis, a tolerogenic gene module consisting of *IDO1, HMOX1, ALDH2, IER5, S100A9, RELB* and *LGALS1* was observed in migratory LCs. Due the marked upregulation in *IDO1* expression between steady-state LCs and migratory LCs and the vast evidence linking *IDO1* with DC immune tolerance, we focussed our attention on validating its role in LC tolerance regulation, hypothesising that it was critical for tolerance induction. Our investigations of IDO1 protein expression confirmed that upregulated expression did indeed occur after LC

migration. Furthermore, the importance of *IDO1* for full LC tolerogenic was displayed in IDO1 inhibition experiments, in which the ability of LC to prime Tregs was diminished. *In vitro* models of human LCs, such as CD34+ LCs, have demonstrated LC *IDO1* expression and speculated its importance for tolerogenic function (Koch *et al.*, 2017). Furthermore, in human LCs, functional IDO1 expression can be detected in response to IFNγ stimulation, as well as the observation that the inhibition of T cell proliferation by supernatants from stimulated LCs, is dependent on functional IDO1 (von Bubnoff *et al.*, 2004). However, to our knowledge this is the first-time functional importance of IDO1 has been demonstrated for the induction of Treg differentiation during co-culture between primary human LCs and T cells. From our single cell analysis and previous studies, migration appears to be a critical step in which dramatic genomic programming occurs (Sirvent *et al.*, 2020). We therefore hypothesised that immunomodulatory dexamethasone stimulation during migration could enhance the tolerogenic phenotype of LCs. Dexamethasone stimulated migratory LCs displayed enhanced IDO1 expression, and furthermore confirmed that these LCs displayed enhanced ability to induce Tregs as compared to unstimulated migratory LCs.

Despite the reduction in Tregs after IDO1 inhibition, LCs still retained the ability to induce some Tregs. This is consistent with our observations that immunocompetent steady-state LC can prime Tregs despite low IDO1 expression. It is therefore likely, that IDO1 is an important part of a wider transcriptional programme and that additional molecular factors govern LC tolerogenic capacity. To explore the importance of each of the constituents of the tolerogenic module identified in **Chapter 5**, similar functional inhibition experiments could therefore be performed. Induction of T cell anergy and apoptosis are also mechanisms by which tolerance is induced/maintained by DC and it is therefore important to consider other mechanisms by which tolerance associated genes mediate tolerance induction. For example, whilst IDO1 activity is associated with induction T cell apoptosis and Tregs, functional studies of galectins reveal a principal involvement in T cell anergy and apoptosis induction, as well as inhibition of DC cytokine production (Hasegawa and Matsumoto, 2018)(Obregon *et al.*, 2017). Further *in vitro* studies that measure T cell anergy (proliferation assays) and apoptosis (annexin V staining) could therefore be explored to investigate all arms of T cell tolerance. Overall, a large quantity of different genes have been associated with immune tolerance induction by DCs, in accordance with the extensive tolerogenic DC associated gene panels explored in our analyses, thus highlighting that it is unlikely for one gene to be the sole mediator of tolerance in LCs. Interestingly some well characterised DC tolerance associated genes, including the cytokines TGF-β and IL-10, as well as the stimulatory molecules PD-L1 and PD-L2, were either not detected, or detected a low levels through Drop-seq transcriptomic analysis (Hasegawa and Matsumoto, 2018)(Obregon *et al.*, 2017). The absent/low expression of these genes could therefore be confirmed at the protein level *in vitro* using flow cytometry.

Our analyses have shown that LC tolerogenic function is paralleled by increasing immunocompetency, which differs between steady-state and migrated LC populations. It is therefore interesting to consider whether the state of immunocompetency is an indication of the underlying biology and specific role each subpopulation plays in immune regulation. For instance, previous analyses of steady-state LCs has revealed their importance for amplifying Tregs within the epidermis (Seneschal *et al.*, 2012). In non-inflamed conditions, immunocompetency of steady-state LC in the absence of tolerogenic factors that are induced during migration, may be sufficient to effectively expand resident epidermal Tregs, but with moderate ability to prime. In contrast, migratory LCs may further amplify tolerogenic potential to enhance efficiency for priming naïve T cells into Tregs, as well as maintaining the ability to efficiently expand Tregs. The same predominance of each LC population to either expand or prime may also be seen in regards to immunogenic T cell activation. It is also interesting to consider the composition of the LC population in the steady state. LCs have the ability to self-replicate in the epidermis to maintain the epidermal population (Ginhoux and Merad, 2010). Immature steady-state LCs could therefore be LCs that have recently replicated in the epidermis, before going on to progress to an immunocompetent state later in their life cycle. However, as only 1-2% of LCs replicate at any one time and we observe a spectrum of activation in steady-state LCs, this would suggest the transition to maturity at the steady-state is slow (Ginhoux and Merad, 2010).

Chapter 7 Utilising mathematical modelling to determine gene regulatory networks underlying LC tolerogenic responses

7.1 Introduction

Single cell RNA-seq analysis comparing steady-state LCs to migrated LCs revealed dramatic changes in LC genomic programming. Migratory LC were marked with enhanced expression of immunocompetency genes and we identified several transcription factors (TFs), which significantly induced expression levels upon migration, including *IRF4* and *RELB.* Furthermore, we identified rearrangement of TF regulons upon migration, further demonstrating their activity underlined the transformation of transcriptomic expression. However, whilst the association of migrated LC TFs with enhancement of maturation programmes was identified from gene ontology analysis, the specific role of these TFs in regulating immunogenic vs tolerogenic programmes was unknown.

Our *in vitro* analysis demonstrated the efficiency of migratory LCs to induce Tregs and tolerogenic T cell responses. However, previous *in vitro* experimentation documented that migration enhances the ability of LC to promote immunogenic CD8+ and CD4+ T cell activation (Sirvent *et al.*, 2020)(Klechevsky *et al.*, 2008). Therefore, while seemingly mature LCs can both tolerise and activate immune responses, the decision-making process within LCs which determines the outcome of T cell immunity remains unclear. Here we sought to delineate the underlying regulatory networks orchestrating activation of human LCs.

We hypothesised that while spontaneous migration in the absence of pro-inflammatory signalling reflects the scenario in which LCs mediate peripheral immune homeostasis and tolerance, LC driven immunity is determined by the context of the signalling environment. TNFα is an epidermal proinflammatory cytokine, which is produced by neighbouring keratinocytes in response to immunogenic stimuli and which enhances LC immunity (Barker *et al.*, 1991). TNFα stimulation of migratory LC heightens their ability to drive CD8 T cell activity through antigen cross-presentation (Sirvent *et al.*, 2020)(Polak *et al.*, 2014)(Polak *et al.*, 2012). Consistent with enhanced T cell activation, TNFα stimulation promotes the upregulation of costimulatory molecules and maturation markers in LC, as well as promoting migration (Berthier-Vergnes *et al.*, 2005)(Cumberbatch *et al.*, 1999)(Epaulard *et al.*, 2014). Furthermore, TNFα signalling augments LC mediated anti-viral immunity to HIV and Influenza antigen (Epaulard *et al.*, 2014). However, in the steady-state, DC migration and maturation is associated with immune tolerance and the differentiation of Tregs

(Baratin *et al.*, 2015). Importantly, a unique programme of genes is observed in DCs migrating in the steady-state, compared to those which migrate in the context of immunogenic signalling (Baratin *et al.*, 2015). Additionally, mature DC also tolerise CD8+ T cells during processing and presentation of self-antigen from apoptotic cells in the steady-state(Albert, Jegathesan and Darnell, 2001).

Based on these considerations, we assumed that in the context of immunogenic TNFα signalling, LCs favour immunogenic responses, whilst in the steady-state, LCs favour tolerogenic ones. Thus, in order to identify key molecular changes in genomic programming during transition from tolerogenic LCs to immunogenic LCs, we generated and contrasted single cell transcriptome data of human migratory LCs unstimulated and exposed to TNFα post-migration.

Immune cell function and behaviour are encoded by unique transcriptomic expression profiles – transcriptional programmes (Xue *et al.*, 2014). Changes in the transcriptional programmes, which reflect status of health or disease or environmental signalling, are coordinated by GRNs in which TFs play an essential role (Singh, Khan and Dinner, 2014)(Lin *et al.*, 2015). However, large scale investigations into the activity of individual GRN components and interactions between specific modules which underlie different transcriptomic programmes, and in particular the kinetics in which those programmes are executed, are difficult to investigate using functional *in vitro* methods (Ay and Arnosti, 2011). Therefore, mathematical modelling techniques are increasingly being utilised to counter this problem and include methods such as ordinary differential equation (ODE) modelling and Petri net modelling (Loriaux and Hoffmann, 2012)(Livigni *et al.*, 2018). Mathematical modelling can permit investigations of dynamic biological systems *in silico* to assess how different molecular signals can alter regulatory network behaviour. For example, Petri net modelling has revealed the LC IRF-GRN underlying immunogenic immune activation in response to different stimuli (**Chapter 3**)(Polak *et al.*, 2017). However, Signalling Petri Net (SPN) and similar methods allow only qualitative assessment of network behaviour, and limit the strength of predictions. In contrast, ODE modelling has allowed exploration into small TF networks and specific network elements, such as feedback loops and 'toggle switch' behaviours, which can define cell lineage determination and operon activation (Huang *et al.*, 2007)(Gardner, Cantor and Collins, 2000).

In GRNs, TFs act in concert with each other to coordinate different expression programmes. However, specific cellular phenotypes are determined by the increased expression of specific phenotype defining TFs. For example, in macrophages, whilst *NFKB1, JUNB* and *CREB1* define core programmes of activation, *STAT4* is specifically upregulated in the context of chronic inflammation, which correlates with increased expression of a specific gene programme containing *IL1α, CXCL5, CD25* and *CD14* (Xue *et al.*, 2014). We sought to identify specific TFs defining immunogenic and

tolerogenic states of LCs and to determine the regulatory interactions between the phenotype defining TFs. Combining single cell transcriptome analyses with a published 'toggle switch' ODE model defining self-amplification and mutual inhibition between two programmes of TF expression (Huang *et al.*, 2007), we identified regulatory modules defining immunogenic (*IRF1 +/-IRF4*) and tolerogenic (*IRF4, RELB, MAP3K14*) LC phenotypes. The model was used to predict LC phenotypes across steady-state and migrated LC from breast skin and foreskin datasets.

7.1.1 Hypothesis

In silico modelling of GRNs can predict phenotypic state and transcriptional programmes expressed by human LCs.

7.1.2 Aims

- Investigate the effects of inflammatory signalling (TNFα) on migrated LC gene expression.
- Identify the key TFs which define tolerogenic and immunogenic LC activation.
- Utilise mathematical modelling to understand the regulatory interactions between phenotype defining TFs.
- Evaluate the performance of the GRN to predict LC phenotypes across different datasets.

7.2 Results

7.2.1 TNFα stimulation of migratory LCs enhances transcriptomic programmes related to T cell immunogenic activation

To investigate the effect of TNFα signalling on LCs, STAMPs for 400 migrated and 400 migrated TNFα stimulated abdominal skin derived LCs were encapsulated using Drop-seq followed by cDNA library preparation, tagmentation and then sequencing (**Figure 53A&B**).

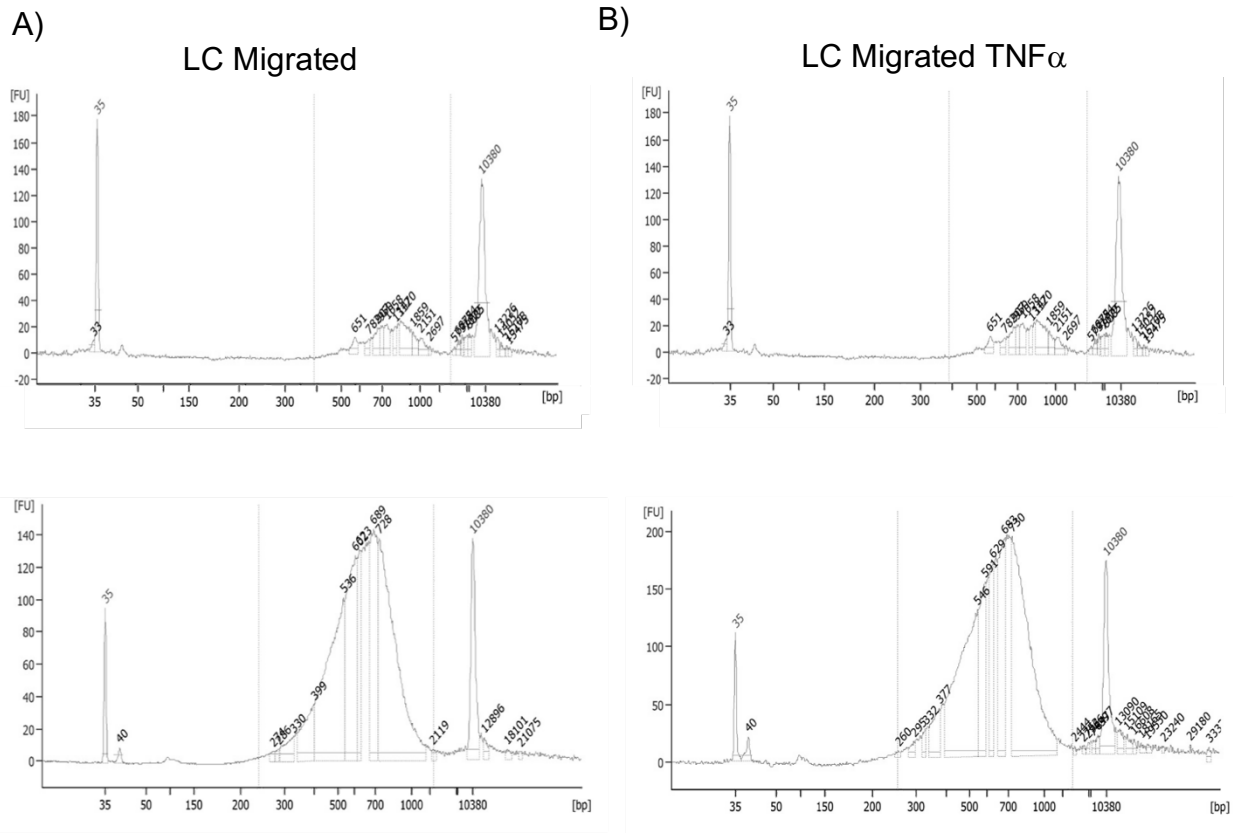

Figure 53. cDNA library amplification and tagmentation of unstimulated and TNFα stimulated migrated LCs. A) Unstimulated abdominal skin migrated LCs were processed through Drop-seq with cDNA libraries (Top, 163 pg/μl) amplified, prior to tagmentation (Bottom, 4.2nM) and sequencing. **B)** TNFα stimulated abdominal skin migrated LCs were processed through Drop-seq with cDNA libraries (Top, 141 pg/μl) amplified, prior to tagmentation (Bottom, 4.1nM) and sequencing. Concentrations were measured using a DNA high sensitivity kit run on an Agilent Bioanalyser. cDNA library concentrations were required to be >100 pg/μl with 600 pg/μl of cDNA librariy required for tagmentation. Libraries were pooled at 2 nM for sequencing. Upper (10380bp) and lower (35bp) marker DNA was included for reference. Vertical dotted lines depict area in which cDNA library concentrations were quantified.

After cell (EmptyDrops (Lun *et al.*, 2019), count threshold filtering) and gene (expression detected in <10 cells) filtering, a matrix of 775 cells and 7319 genes remained for analysis. UMAP dimensionality reduction analysis (ScanPy, version=1.5.0) revealed that both abdominal skin derived migrated LC and migrated TNF-α stimulated LC contained a predominant large cluster (1), confirmed to be LCs through high expression of MHC II genes which were in the top 10 cluster markers genes (e.g. *HLA-DRB1, HLA-DRB5*)(Logistic regression, ScanPy pipeline, version=1.5.0, **Figure 54A**,**B**&**C**). Additionally, two small populations of cells (2 and 3), contributed by cells from both conditions, clustered away from the LC population (**Figure 54A**). Included in the top 10 marker genes for cluster 2 was *TYRP1,* a gene which characterises melanocytes (**Figure 54B**&**C**). In the top 10 marker genes for cluster 3 was *CD3D,* a marker of T cells (**Figure 54B**&**C**). To focus our analysis on the transcriptomes of LC, the melanocyte and T cell populations were removed.

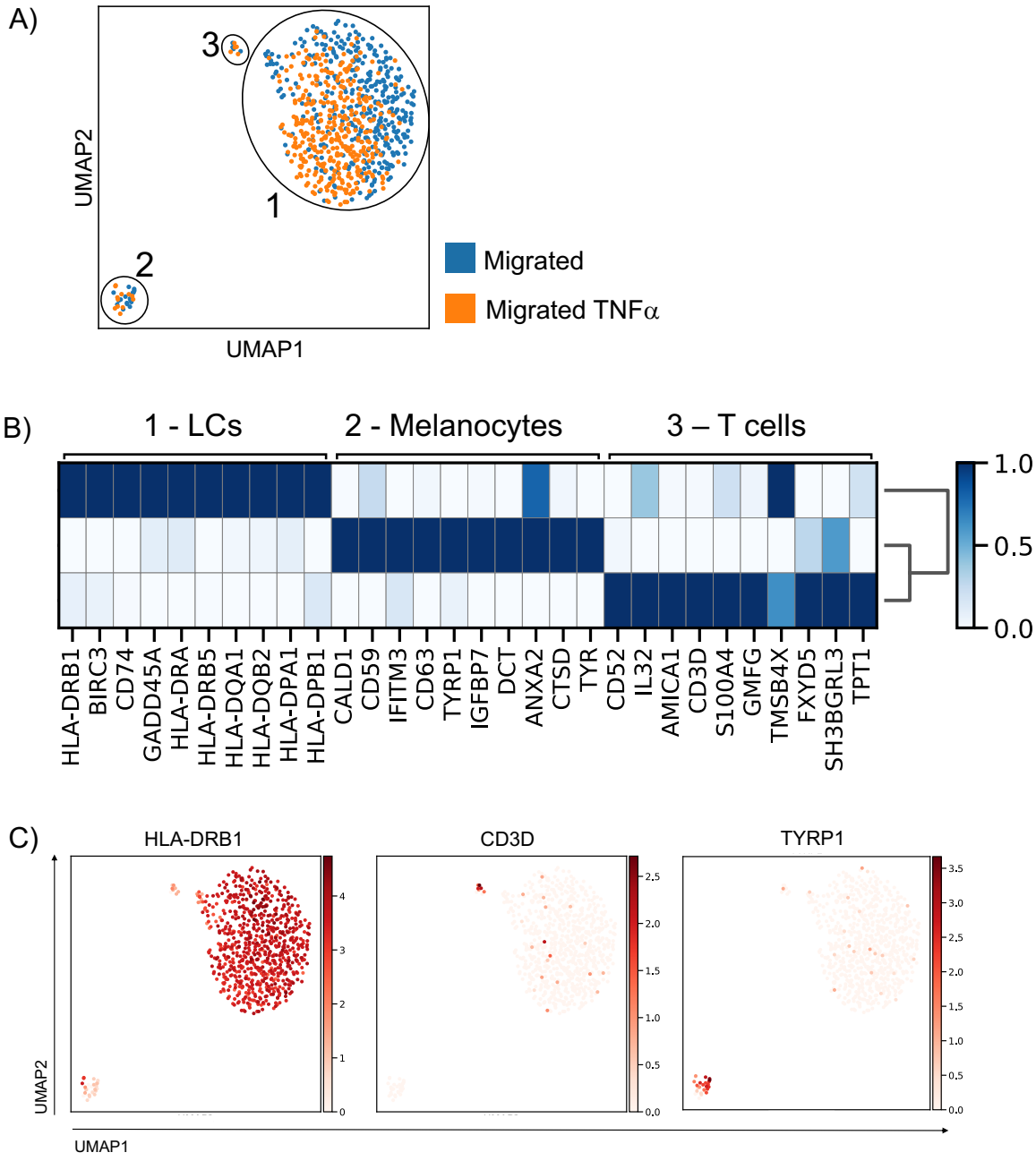

Figure 54. T cells and melanocytes could be identified amongst unstimulated and TNFα stimulated migrated LCs. ***On previous page **A) UMAP dimensionality reduction analysis of 775 unstimulated and TNFα stimulated abdominal skin derived migrated LCs. **B)** Top 10 markers genes for clusters 1-3 (t-test, ScanPy pipeline, version=1.5.0), revealed populations to be LCs (cluster 1), melanocytes (cluster 2) and T cells (cluster 3) **C)** UMAP marker plots displaying the expression of the LC marker *HLA-DRB1,* the T cell marker *CD3D* and the melanocyte marker *TYRP1.*

The heterogeneity of the 737 migrated LCs stimulated with or without TNFα (unstimulated = 375, TNFα stimulated = 362) were then analysed in UMAP space. Overall the cells appeared relatively homogenous consisting of one overall large population of LCs, consisting of separating sub clusters of unstimulated and TNFα stimulated LCs (**Figure 55A**). DEG analysis comparing migrated and migrated TNFα LCs identified 87 genes upregulated in migrated TNFα LCs and 61 genes upregulated in migrated LCs (MAST, adj.p-value<0.05). Gene ontology analysis for the 87 genes upregulated in migrated TNFα LCs was associated with cytokine mediated signalling pathways (adj. P-Value=2.2E-7) and positive regulation of alpha-beta T cell activation (adj. P-Value=1.5E-4, **Figure 55B**). TNFα stimulation therefore enhanced transcriptomic programmes associated with T cell immunogenic activation. Gene ontology analysis for the 61 genes upregulated in migrated LCs were associated with secretion by cell (adj. P-Value=5.3E-3) and regulation of the immune response (adj. P-Value=5.3E-3, (**Figure 55B**). Interestingly, an association with negative regulation of immune system process was identified from both sets of DEGs. Contributing to this ontology in migrated TNFα LCs was *CD86, DUSP1, IRF1, NFKBIA, PTK2B, SAMSN1* and *SOCS1* (adj. P-Value=2.3E-2). In unstimulated migrated LC *A2M, CST7, EZR, LGALS3, LY96, PTPRC* and *VIMP* (*SELENOS*) contributed to the ontology (adj. P-Value=2.5E-2).

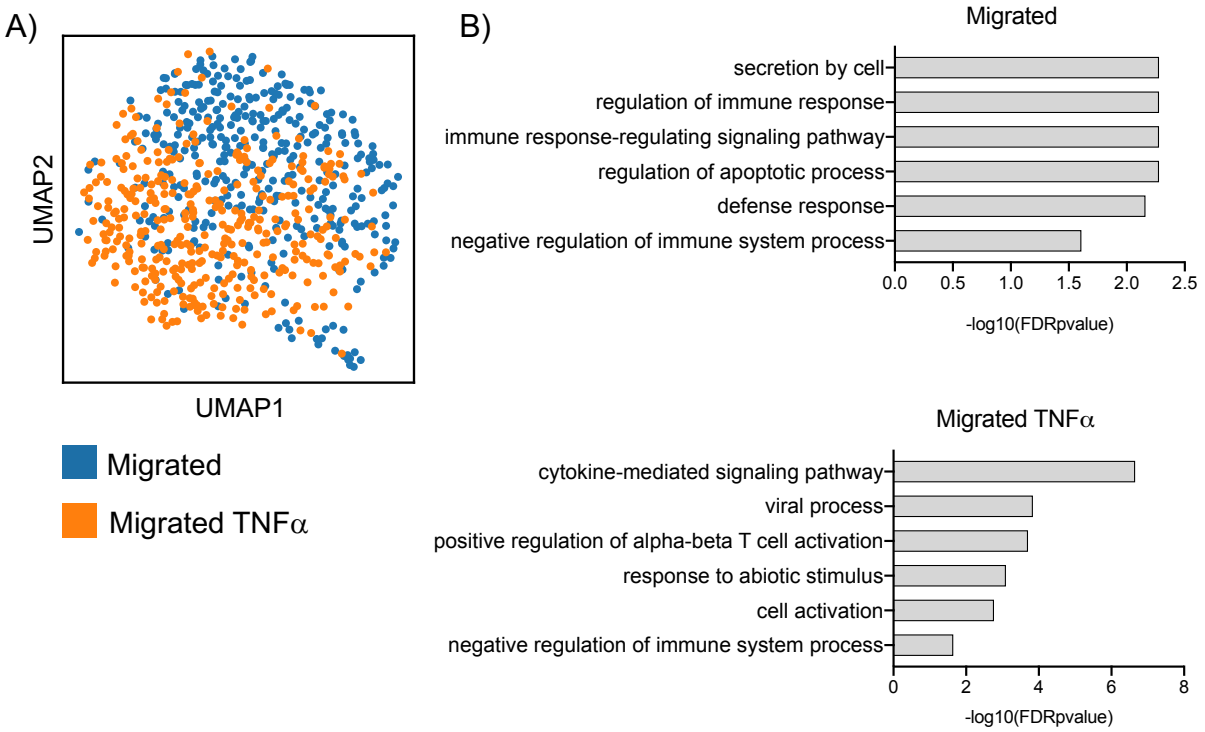

Figure 55. Unstimulated and TNFα stimulated migrated LCs display differential gene expression. A) UMAP dimensionality reduction analysis of 737 unstimulated and TNFα stimulated LCs. (unstimulated = 375, TNFα stimulated = 362). **B)** Gene ontology analysis (Toppgene) for the 61 DEGs identified in unstimulated migrated LC vs TNFα stimulated migrated LC and for the 87 DEGs identified in TNFα stimulated migrated LC vs unstimulated migrated LC using MAST DEG analysis (BH adj.p-value<0.05). -log10adj.p-values are displayed.

7.2.2 Subpopulations of migrated LCs appear primed for tolerogenic immune function, whilst TNFα stimulated migrated LCs appear predominantly immunogenic

The population of LC was then investigated to identify sub-clusters defined by unique biological pathways. Leiden clustering (ScanPy, r=0.5) identified 4 subpopulations (**Figure 56A**), defined by distinctive transcriptome expression in gene ontology analysis of marker genes (ScanPy, Logistic regression, 50 marker genes, **Figure 56B**). Cluster 1 was associated with positive regulation of alpha-beta T cell activation (adj. P-Value=4.4E-3) and cytokine mediated signalling pathway (adj. P-Value=2.6E-2). The association with alpha-beta T cell activation arose from elevated expression of *CCR7, CD83, EBI3, HLA-E* and *IRF1.* Cluster 2 was associated with cytokine production (adj. P-Value=7.0E-6) and negative regulation of immune system process (adj. P-Value=2.6E-3). Negative regulation of immune system process was contributed by the expression of *ARRB2, CD74, CIB1,*

CST7, HMOX1, IDO1, IL7R, IRF4, RUNX3. Cluster 3 was associated with ATP biosynthetic process (adj. P-Value=1.4E-7) and antigen processing and presentation of peptide antigen (adj. P-Value=4.4E-7), due to elevated expression of MHC II genes (*HLA-DRB1*, *HLA-DRB5, HLA-DQA1, HLA-DQA2* and *HLA-DMA*). Cluster 4 was associated with I-kappaB kinase/NF-kappaB signalling (adj. P-Value=1.2E-5) and response to external biotic stimulus. (adj. P-Value=2.2E-5).

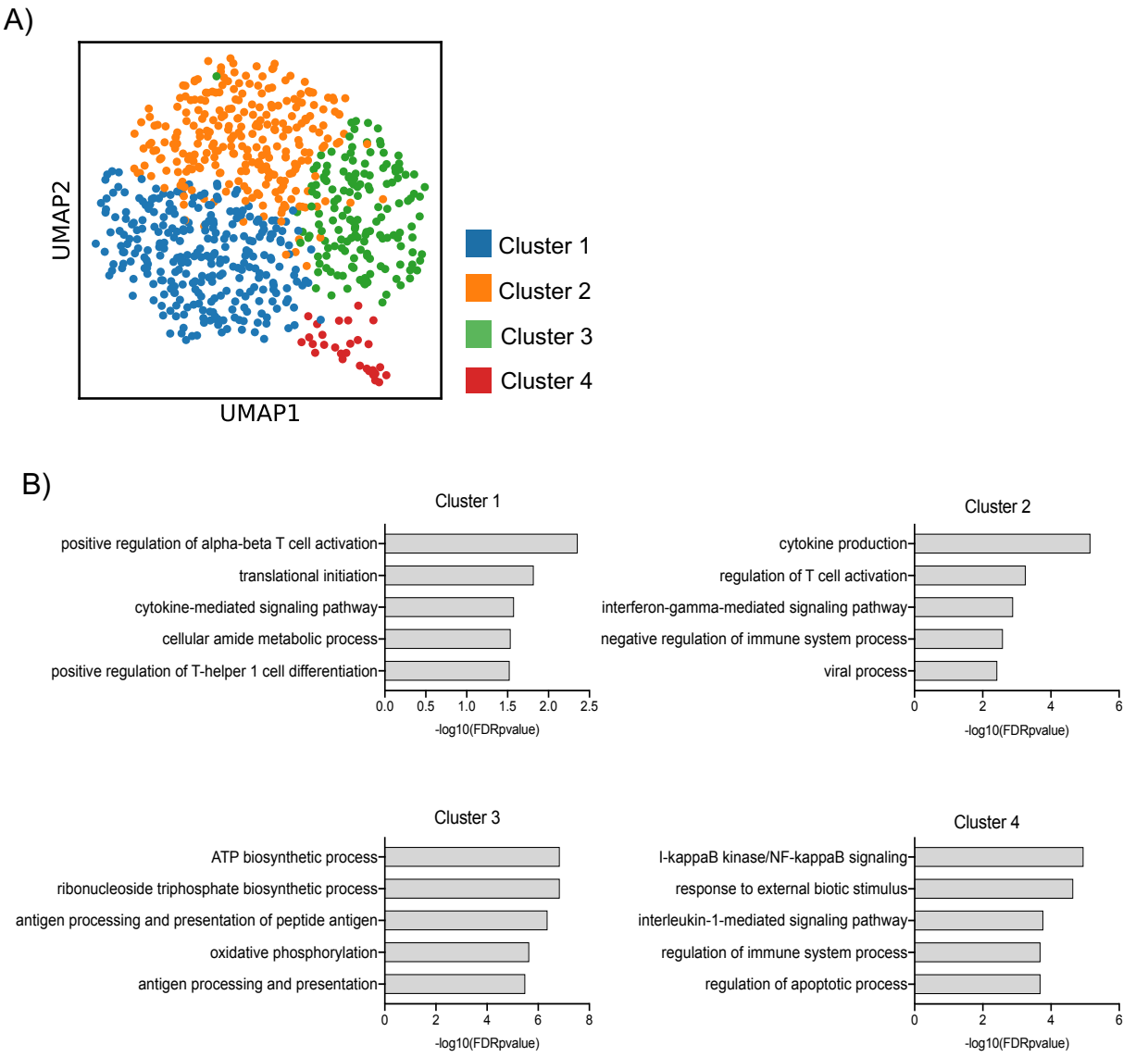

Figure 56. The population of unstimulated and TNFα stimulated LCs could be divided into 4 distinct clusters. A) Leiden clustering (r=0.5) identified 4 clusters amongst the population of unstimulated and TNFα stimulated migrated LC**. B)** Gene ontology analysis (Toppgene) for the top 50 marker genes (ScanPy, logistic regression) for each cluster identified during Scanpy analysis -log10adj.p-values are displayed.

Overall the mixed population of migratory unstimulated or TNFα stimulated LCs appeared to constitute of 3 main subpopulations (clusters 1-3). The proportion of unstimulated or TNFα stimulated LCs in each subpopulation also varied with the majority of cells in cluster 2 being unstimulated LCs, the majority of cells in cluster 1 being TNFα stimulated LCs and cells in cluster 3 being an equal proportion of both. Based on gene ontology for the top 50 markers genes, which displayed predominant cluster phenotypes, we labelled cluster 1 and 2 as immunogenic and tolerogenic LC, respectively. Labelling of cluster 3 was less obvious due to general association with antigen processing and presentation and ATP metabolism, signature features of mature LC (Romani *et al.*, 2003). To further explore the relationships between the 3 clusters, pseudotime trajectory analysis (PAGA, Partition based graph abstraction, within Scanpy) was performed to discern significant routes of connectivity which could represent pathways of differentiation(**Figure 57A**). Pseudotime pathways (DPT, Diffusion pseuodotime) originating from the centre of cluster 3 reached endpoints in both clusters 1 and 2, suggesting cluster 3 LCs could readily follow pathways to cluster 1 and 2 LC states. Alternative pseudotime pathway analysis originating at the centre of cluster 2 did not reach cluster 1 and similarly, pseudotrajectories originating at the centre of cluster 1 and ending at cluster 2 were relatively weak (**Figure 57B).** Analysis suggested cluster 3 were a transient population of mature LCs, which would differentiate into immunogenic or tolerogenic LCs depending on signalling. Cluster 3 LCs were therefore labelled as being 'primed' LCs.

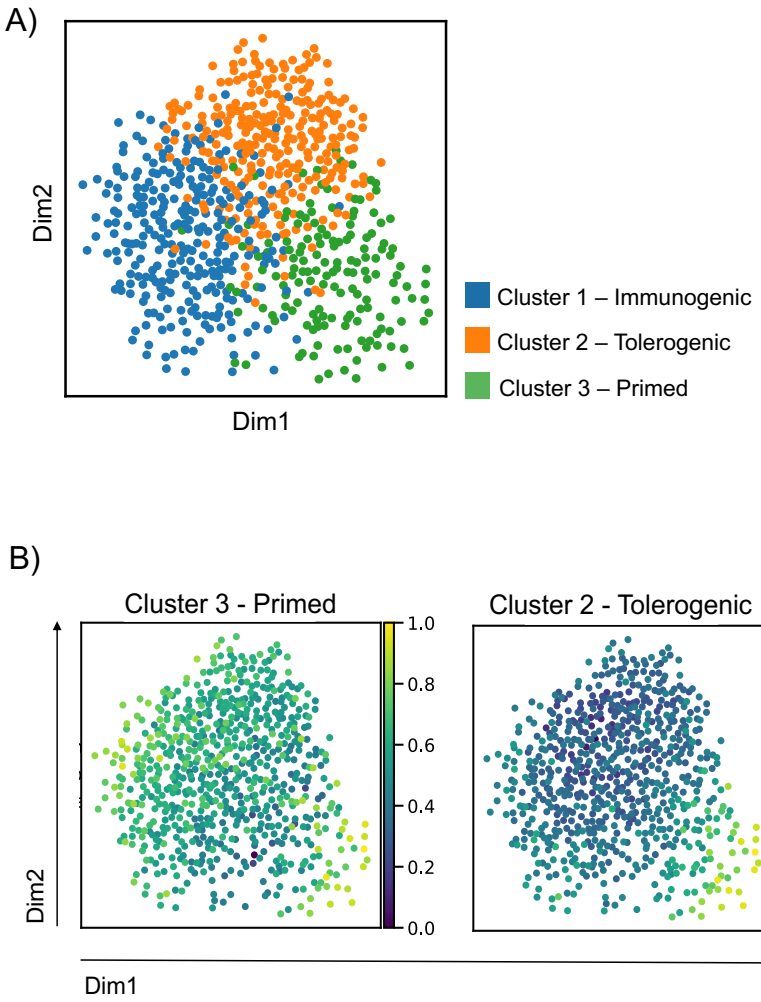

Figure 57. Pseudotime trajectory analysis reveals a transitional pathway from primed LCs to both tolerogenic and immunogenic LCs. A) Clusters 1-3 (Immunogenic, tolerogenic and primed LCs) were processed through PAGA analysis to assess cluster connectivity and embedded in geodesic space to maintain data topology (FR, Fruchterman Reingold force directed graph). **B)** Estimated pseudotime trajectories calculated using DPT (diffusion pseudotime) were plotted with starting points originating at the centre of cluster 3 (primed), cluster 2 (tolerogenic) and cluster 1 (immunogenic).

To gain a greater understanding of the differentiating pathways between immunogenic cluster 1 and tolerogenic cluster 2, MAST DEG analysis was performed (adj. P-Value<0.05). Gene ontologies identified from Toppgene were summarised using Revigo to display a greater overview of the general pathways upregulated in each cluster. The 65 DEGs upregulated in immunogenic cluster 1 were strongly associated with positive regulation of alpha-beta T cell activation and response to cytokine (**Figure 58A)**. 51 DEGs upregulated in tolerogenic cluster 2, were summarised into antigen processing and presentation via MHC II, response to cytokine, cell-cell adhesion and cell activation (**Figure 58B**). Interestingly associations with negative regulation of immune system processes could be identified in upregulated DEGs for each cluster. This was contributed by *A2M, HLA-DQA1, CD74, CST7, HMOX1, IL7R* in tolerogenic cluster 2 (adj. P-Value=3.0E-2) and *CD80, CD86, IRF1, DUSP1, NFKBIA, HLA-E, SOCS1, SAMSN1* and *PTK2B* in immunogenic cluster 2 (adj. P-Value=1.0E-3). However, the majority of immune associated annotations for cluster 1 were associated with activation of T cell effector processes.

A)

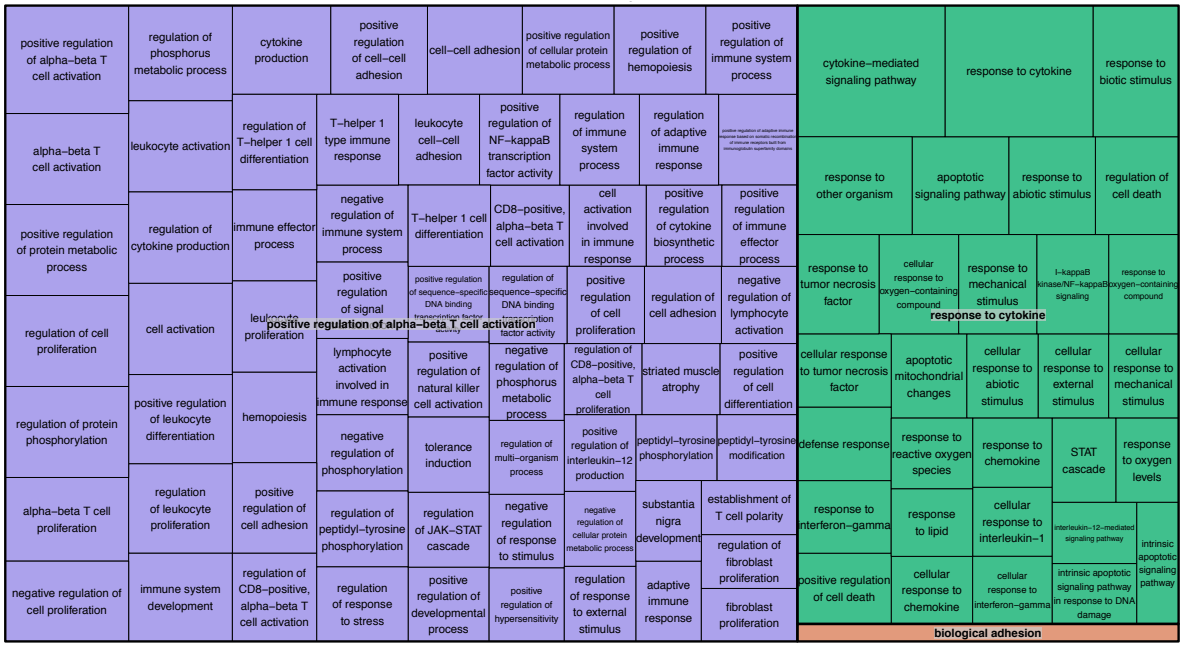

B)

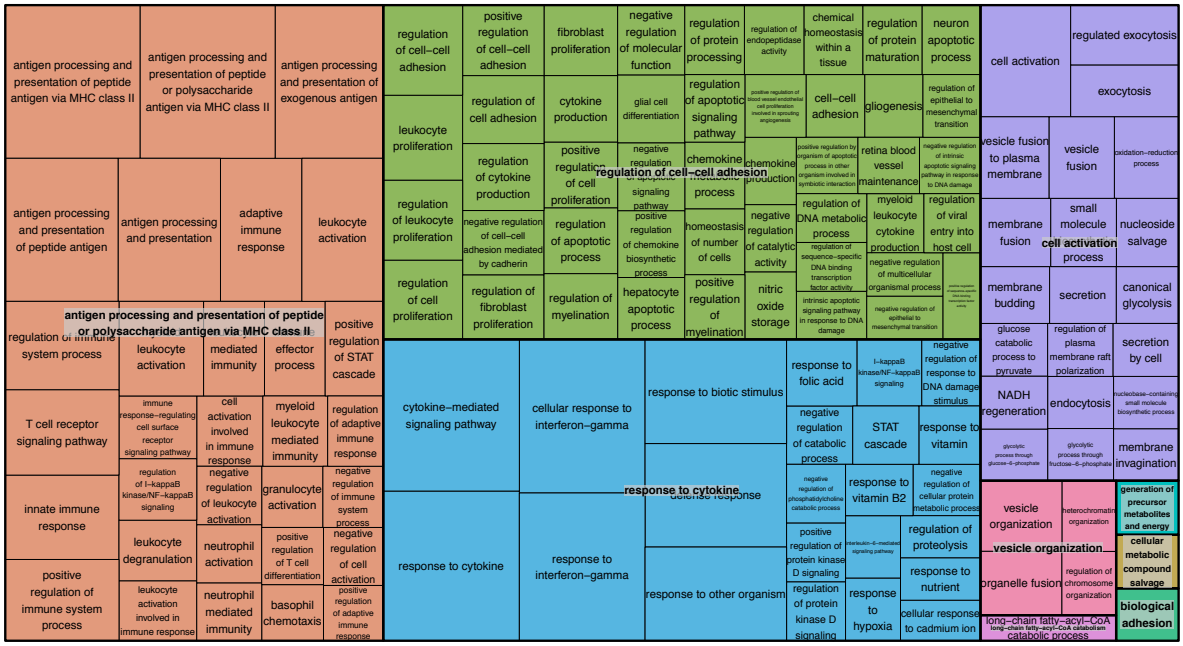

Figure 58. Immunogenic LCs upregulate gene expression programmes associated with T cell activation. MAST DEG analysis was performed comparing cluster 1 immunogenic LCs to cluster 2 tolerogenic LCs. **A)** Revigo Treemap summarising the top 200 biological pathways identified in Toppgene gene ontology analysis (BH adj.p-value<0.05) using the 65 genes upregulated in cluster 1 immunogenic LCs. **B)** Revigo Treemap summarising the top 200 biological pathways identified in Toppgene gene ontology analysis using the 51 genes upregulated in cluster 2 tolerogenic LCs.

With cluster 3 LCs labelled as baseline mature primed LC, gene expression was compared to clusters 1 and 2 through MAST DEG analysis to identity immunogenic and tolerogenic pathway defining genes. DEG analysis between cluster 2 and 3 identified 105 upregulated genes in cluster 2 and 86 upregulated genes in cluster 3. Cluster 2 genes were generally associated with regulation of the immune system process and response to cytokine (**Figure 59A**). Again, an association with negative regulation of immune system process was identified due to the upregulated expression of *IDO1, IRF4, IL7R, HLA-E, HLA-F, ID2, GRN, SAMSN1, ARRB2, TRAFD1, ZFP36L1, FER,* TMEM176A and TMEM176B (adj. P-Value=4.2E-4). Cluster 3 ontologies were grouped into leukocyte activation and response to ER stress (**Figure 59B**). Interestingly, an association with negative regulation of immune effector process was identified due to the expression of *ANXA1, CD59, LGALS3, NDFIP1* and *SERPINB9* (adj. P-Value=6.1E-3). DEG analysis between cluster 1 and 3 identified 178 genes upregulated in cluster 1 and 145 genes upregulated in cluster 3. Cluster 1 DEGs were generally associated with regulation of the immune system, response to cytokine, nuclear transcribed mRNA catabolism and SRP dependent co-translational targeting to membrane and therefore the overall profiles appeared similar to those identified in cluster 2 LCs (**Figure 59C**). However, genes upregulated in cluster 1 could again be associated with alpha-beta T cell activation (adj. P-Value=1.5E-5), as well as negative regulation of immune system process due to upregulated expression of *IDO1, IRF1, CD86, ID2, HLA-E, HLA-F, GBP1, SOCS1, NFKBIA, TRAFD1, ZFP36L1, PTK2B, CD84, GCSAM, SAMSN1, GPX1, DUSP1* and *TMEM176B* (adj. P-Value=3.2E-5). In contrast cluster 3 upregulated genes were associated with ATP metabolism, antigen processing and presentation, energy coupled protein transport down electrochemical gradient, response to ER stress and organelle fusion (**Figure 59D**). No association with tolerogenic immune regulation were identified.

A)

Cluster 2 (Tolerogenic) vs Cluster 3 (Primed)

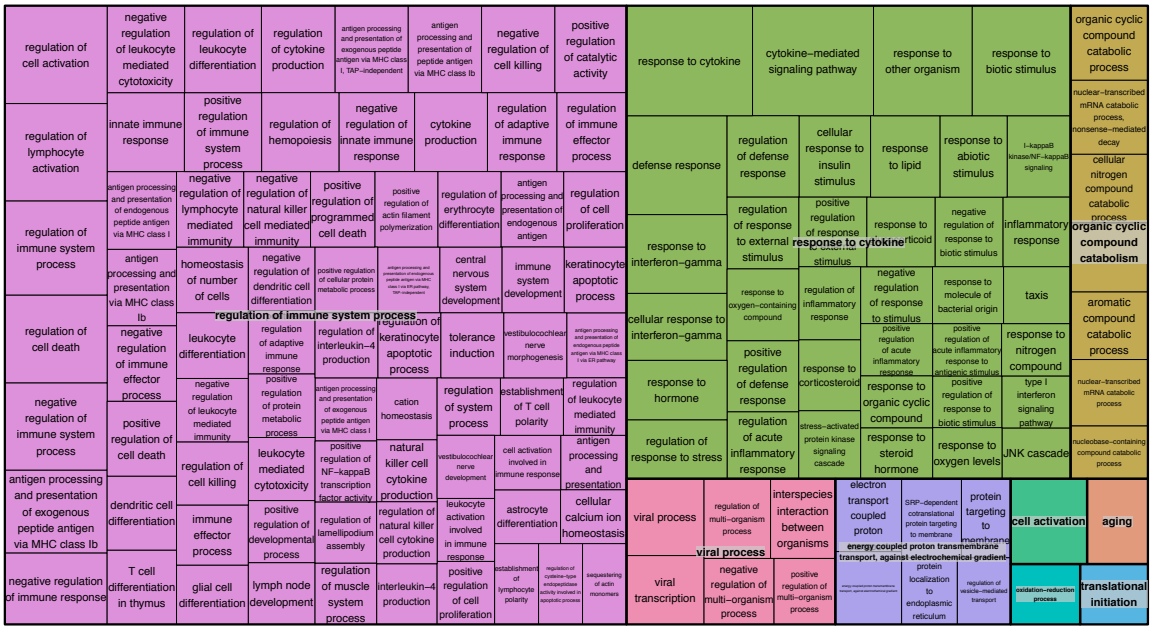

B)

Cluster 3 (Primed) vs Cluster 2 (Tolerogenic)

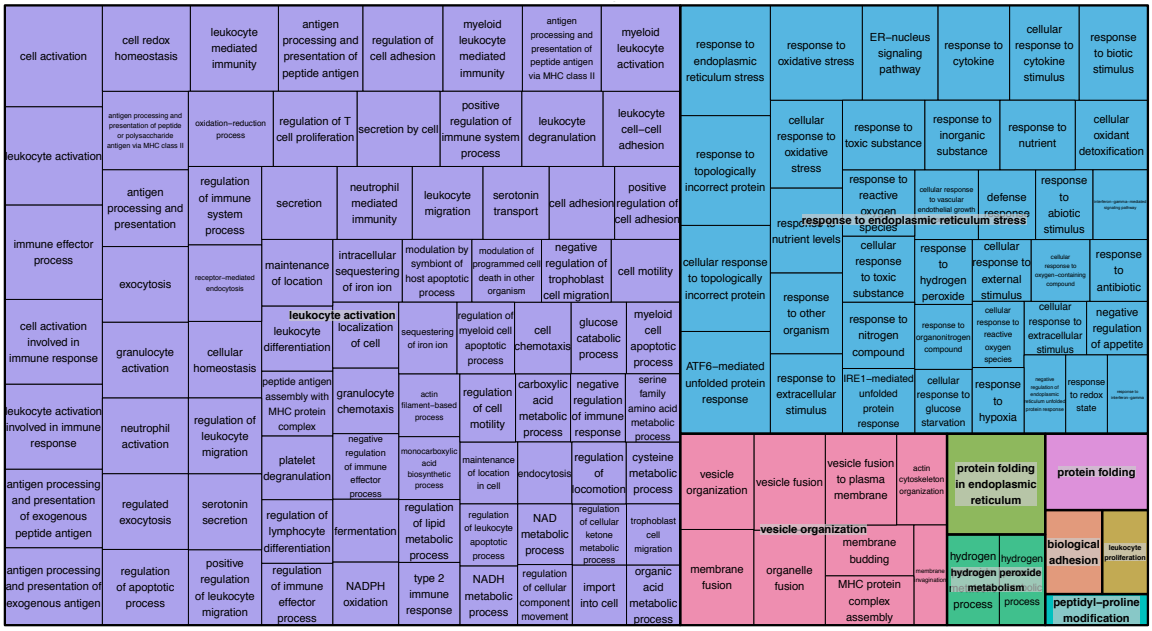

C)

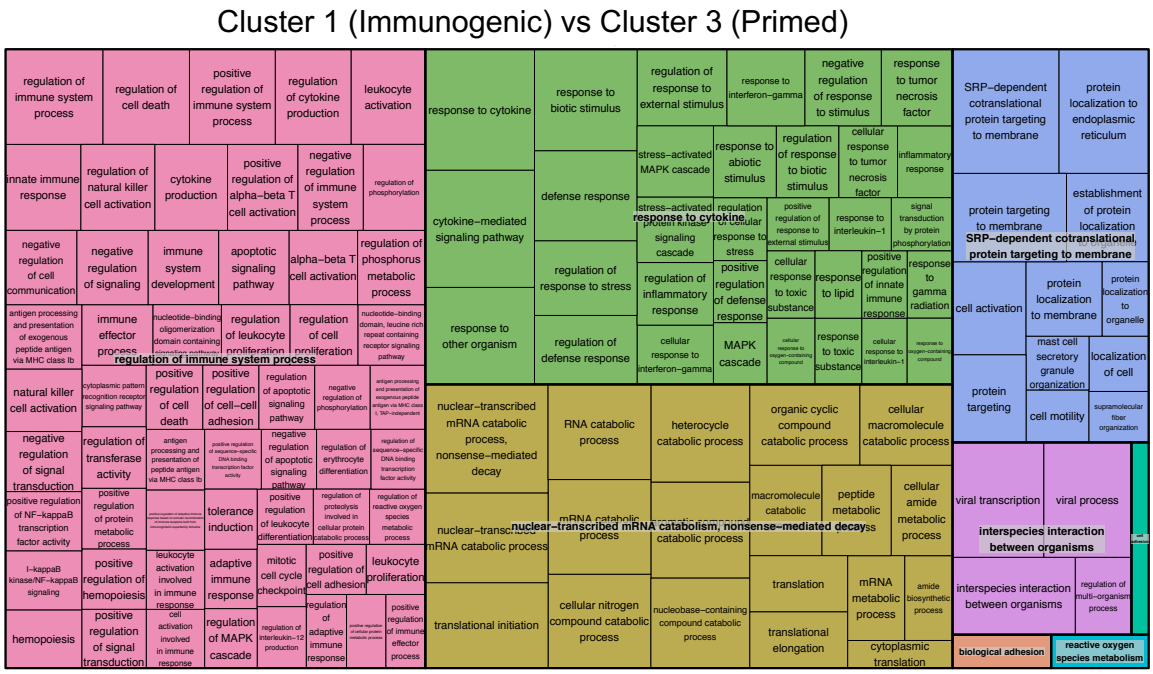

D)

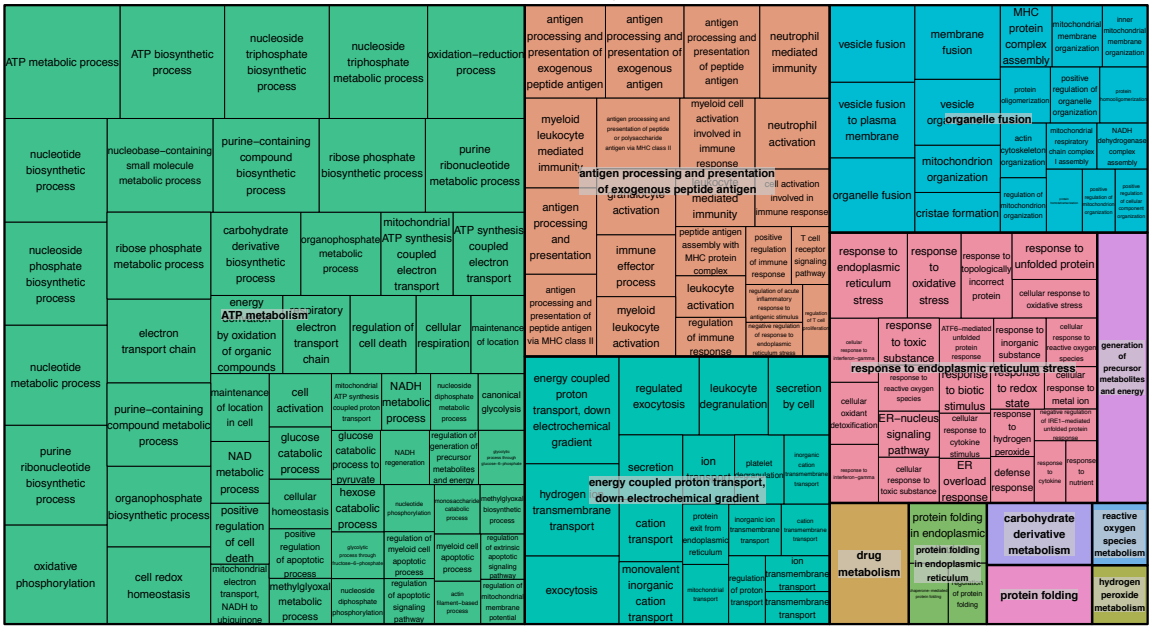

Figure 59. Tolerogenic and Immunogenic LCs upregulate genes associate with similar biological processes compared to mature primed LCs. MAST DEG analysis was performed comparing cluster 2 tolerogenic LCs to cluster 3 primed LCs and cluster 1 immunogenic LCs to cluster 3 primed LCs. Revigo Treemaps were used to summarise the top 200 biological pathways identified in Toppgene gene ontology analysis (BH adj.p-value<0.05) using the **A)** 105 genes upregulated in cluster 2 tolerogenic LCs vs cluster 3 primed LCs, **B)** 86 genes upregulated in cluster 3 mature LCs vs cluster 2 tolerogenic LCs, **C)** 178 genes upregulated in cluster 1 immunogenic LCs vs cluster 3 primed LCs and **D)** 145 genes upregulated in cluster 3 primed LCs vs cluster 1 immunogenic LCs.

The upregulated genes in comparisons of clusters 1 and 2 with cluster 3 were contrasted to identify how programs differed during differentiation from primed (cluster 3) to immunogenic (cluster 1) or tolerogenic (cluster 2) LCs. Of the 178 genes upregulated in cluster 1 and the 105 genes upregulated in cluster 2, 64 were common (**Figure 60A**). Gene ontology analysis and summarisation using Revigo of the 64 commonly upregulated genes revealed associations with antigen processing and presentation, response to cytokine, regulations of cell death and nuclear transcribed mRNA catabolism (**Figure 60B**). These pathways therefore appeared core to both tolerogenic and immunogenic LC differentiation from primed LCs. Interestingly this core programme included an association with negative regulation of immune system process (adj. P-Value=1.2E-2) due to elevated expression of *IDO1, SAMSN1, HLA-E, HLA-F, ZFP36L1, TMEM176B* and *TRAFD1*. The 114 uniquely upregulated genes in immunogenic cluster 1 LCs were associated with negative regulation of cell communication, nuclear transcribed mRNA catabolism, response to cytokine and SRP-dependent cotranslational targeting to membrane (**Figure 60C**). Again, many associations with alpha-beta T cell activation (adj. P-Value=1.9E-2) were identified, as well as negative regulation of immune system process (adj. P-Value=1.2E-2), due to the presence of *IRF1, CD86, CD84, SOCS1, NFKBIA, PTK2B, GCSAM, GBP1, GOX1* and *DUSP1*. Minimal associated gene ontologies were identified for the 41 uniquely upregulated genes in tolerogenic cluster 2, although importantly an association with negative regulation of immune effector process was observed (adj. P-Value=4.5E-2), due to the expression of *IL7R, ARRB2, GRN* and *FER* (**Figure 60D**).

Overall, the expression of tolerogenic gene modules appears to be core to mature LC in each cluster. However, in immunogenic LCs, tolerogenic gene modules are expressed in association with genes regulating immunogenic pathways. We sought to investigate how the balance of tolerogenic and immunogenic pathway defining genes may alter the balance of immune regulation leading to the predominant activity and expression of either phenotype.

A)

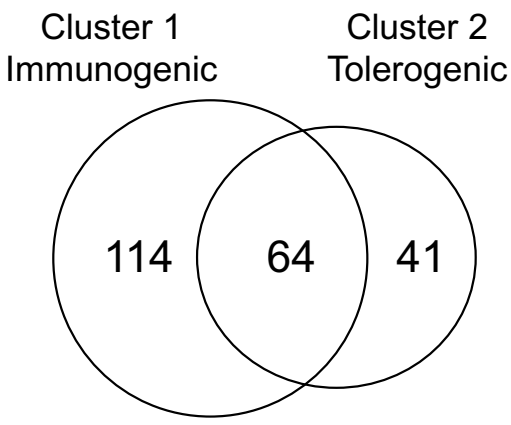

B)

Mutually upregulated (Cluster 1 and 2)

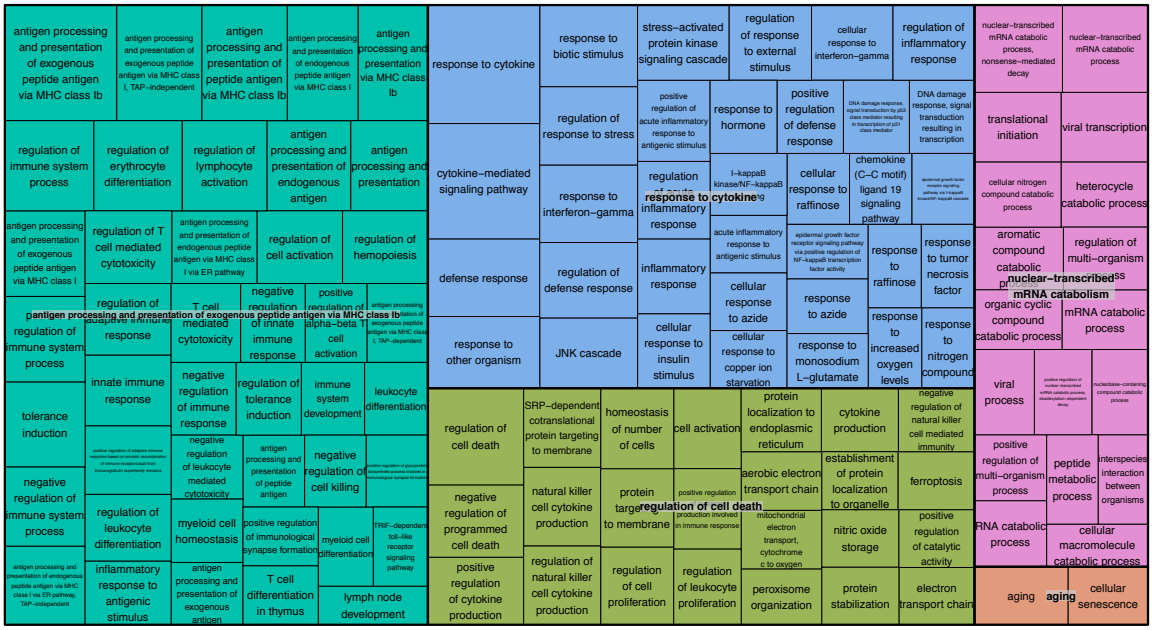

C)

Uniquely upregulated Cluster 1 (Immunogenic)

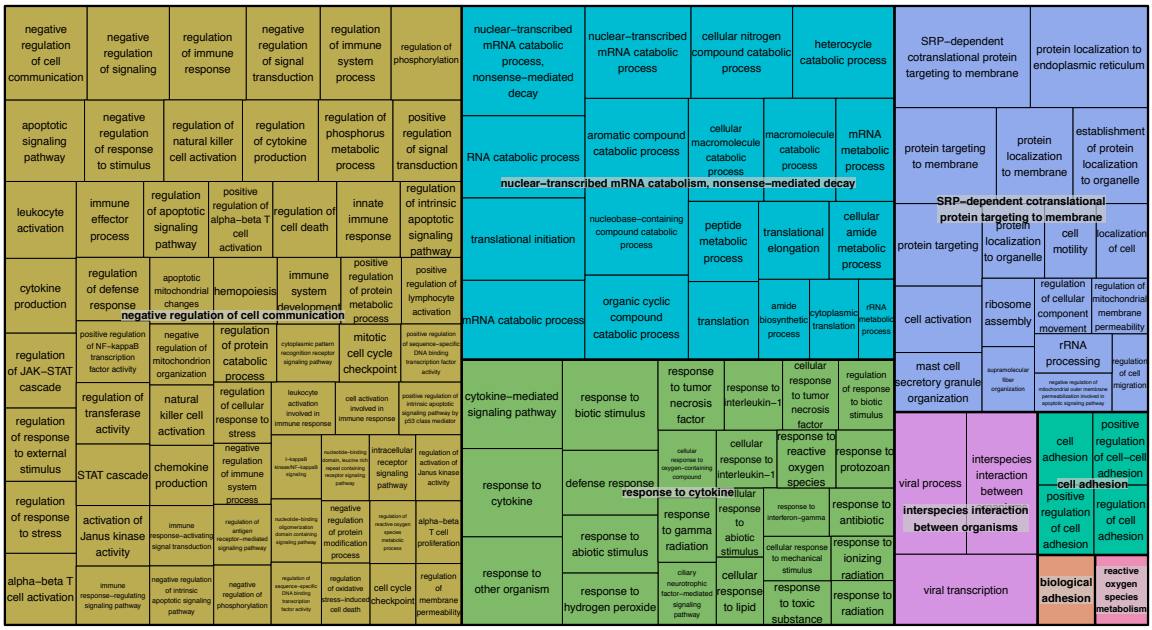

D)

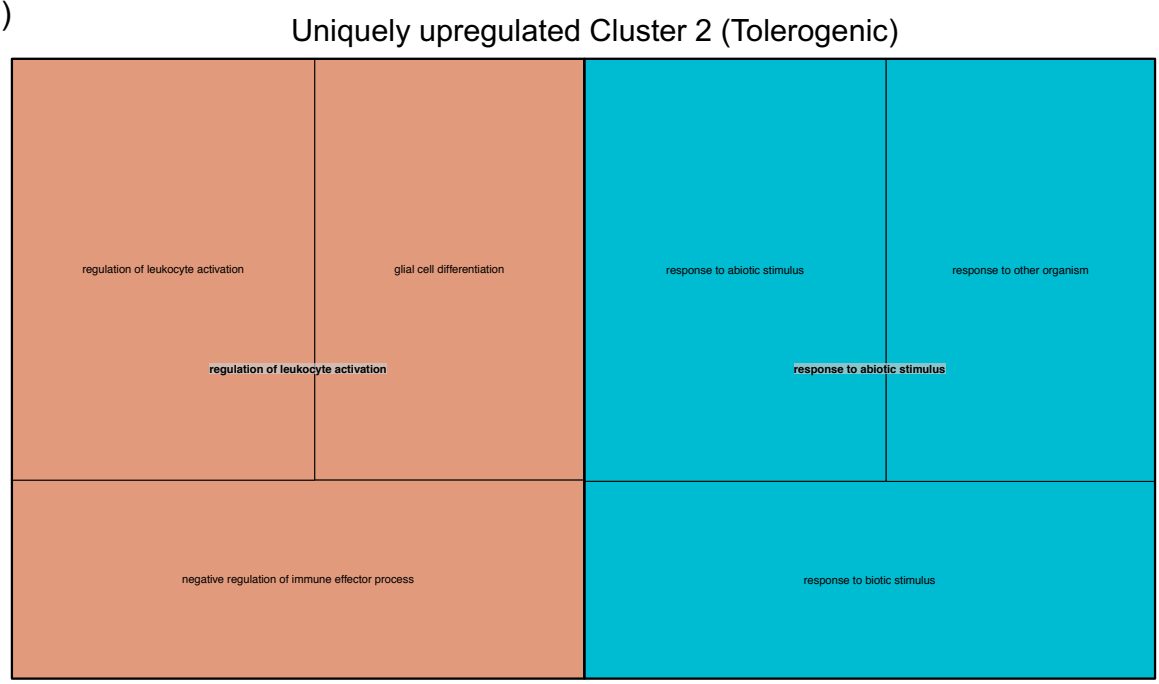

Figure 60. Common upregulated pathways can be identified in tolerogenic and immunogenic LCs. **A)** Venn Diagram displaying the overlap between cluster 1 immunogenic LCs upregulated genes compared to cluster 3 primed LCs and the genes upregulated in cluster 2 tolerogenic LCs compared to cluster 3 primed LCs. Revigo summarisation of the top 200 (if identified) biological pathways identified during Toppgene gene ontology analysis (BH adj.p-value<0.05), associated with the **B)** 64 genes commonly upregulated in cluster 1 immunogenic and cluster 2 tolerogenic LCs, **C)** 114 genes uniquely upregulated in cluster 1 immunogenic LCs and **D)** the 41 genes uniquely upregulated in cluster 2 tolerogenic LCs.

7.2.3 IRF1 and IRF4 regulons distinguish gene regulation in immunogenic and tolerogenic LCs

To identify the key TF regulators of the migrated LC programme, SCENIC (Aibar *et al.*, 2017) single cell regulatory network inference analysis was performed. Analysis identified IRF1 and IRF4 regulons as the most distinct upregulated regulons in immunogenic and tolerogenic LCs, respectively (cluster 1 immunogenic LC *IRF1* z-score = 0.4, cluster 2 tolerogenic LC, *IRF4* z-score = 0.2)(**Figure 61**). *IRF1* and *IRF4* were therefore identified as being core modulators of the gene regulatory changes necessary for either phenotype.

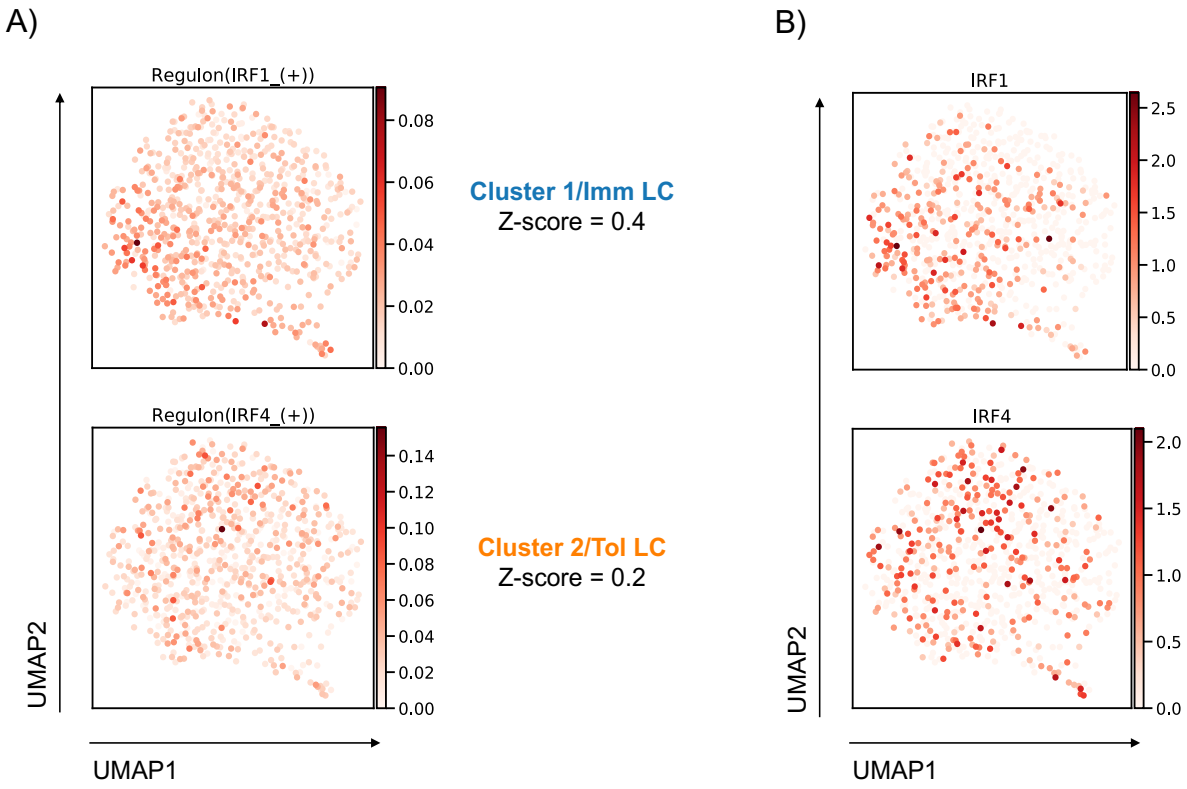

Figure 61. Immunogenic LCs are enriched for *IRF1* regulon activity, whilst tolerogenic LC are enriched for the *IRF4* regulon. A) UMAP plots displaying SCENIC regulatory network and inference clustering analysis enrichment scores for *IRF1* and *IRF4* regulons, identified as being the most enriched TF regulons in immunogenic and tolerogenic LCs, respectively. Z-scores for enriched regulons are displayed. **B)** UMAP marker plot displaying normalised *IRF1* and *IRF4* expression.

7.2.4 Utilising an ODE 'toggle switch' model to construct a decision-making circuit for LC immunogenic or tolerogenic responses

Based on published *in vitro* investigations displaying both immunogenic and tolerogenic T cell activation by migrated LCs (Sirvent *et al.*, 2020)(Polak *et al.*, 2012)(Klechevsky *et al.*, 2008)(Seneschal *et al.*, 2012) and the discoveries from our *in vitro* data exploring migrated LC tolerogenic potential, we postulated that migrated LCs represent an activation state under non-inflammatory conditions capable of priming both immunogenic and tolerogenic responses. However, in line with the importance of self-antigen transport by LCs migrating in steady-state contexts for mediating self-tolerance (Hemmi *et al.*, 2001)(Yoshino *et al.*, 2006), we also assumed that tolerogenic responses are preferential in unstimulated migrated LCs. From single cell RNA-seq observations we further assumed that the transcriptional programme of LCs can be altered in the context of inflammatory signalling, such as TNFα, to be more predominantly immunogenic. This proposal is consistent with discoveries from bulk RNA-seq and functional *in vitro* studies of TNFα stimulated LCs, which enhances immunogenic T cell activation (Sirvent *et al.*, 2020)(Polak *et al.*, 2014)(Polak *et al.*, 2012). From UMAP analysis, LCs appeared part of a single overall large population, in which subpopulations of phenotype specific (immunogenic, tolerogenic, primed) LCs could be identified. The subpopulations of immunogenic cluster 1 and tolerogenic cluster 2 LCs, which appeared to be end states compared to transient cluster 3 primed LCs, were in close proximity to each other in UMAP space. This suggested that some LCs were not in a distinct immunogenic and tolerogenic states, but were on the border between both, in which activation of immunogenic and tolerogenic pathways was equal. Overall, we therefore hypothesised that unstimulated and TNFα stimulated migrated LCs could follow pathways to 3 general states of activation - immunogenic, tolerogenic or a dual "mature" state (equal immunogenic and tolerogenic pathways)(**Figure 62**).

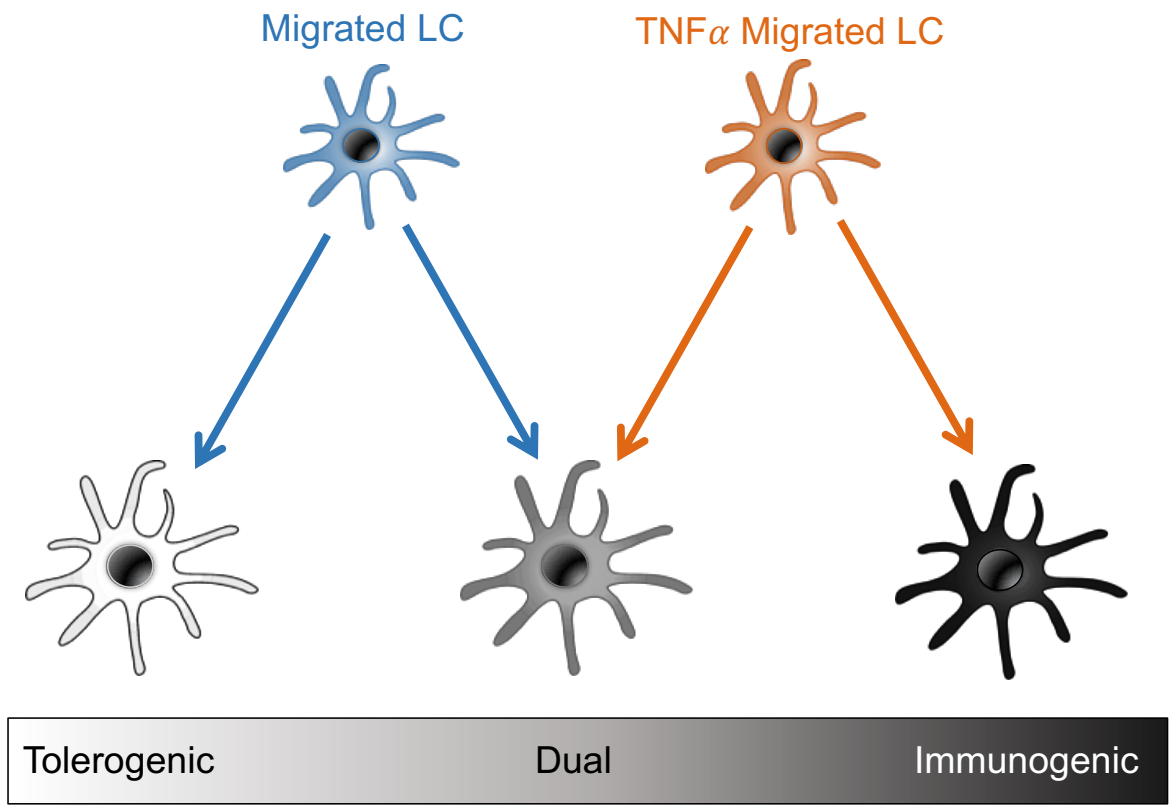

Figure 62. Migrated LCs are hypothesised to be capable of displaying 3 states of activation depending on the signalling context. Unstimulated migrated LC are hypothesised to predominantly represent states of tolerogenic and dual potential, in line with *in vitro* observations demonstrating both immunogenic and tolerogenic T cell induction. TNFα stimulated LC are hypothesised to display favouring of dual and immunogenic states, in accordance with *in vitro* observations of enhanced immunogenic function.

To explore how the balance in LC state is controlled, we utilised a tristable 'toggle switch' ODE model in which different activation states can be described based on the expression of a selected number of state/phenotype (immunogenic vs tolerogenic) defining TFs (Huang *et al.*, 2007). The ODE model contains 2 equations which each represent the activation of immunogenic (*I)* and tolerogenic (*T*) states, respectively. Each equation contains 3 terms, which represent auto-amplification (dotted box), cross-inhibition of opposing state TFs (dashed box) and first order decay of TF activity (solid box)(**Figure 63A, Equation 1**). The model therefore assumes that TFs that define each state auto-amplify their own expression, whilst inhibiting the expression of the opposite pathway/state. The tristable model describes a phenotypic 'attractor landscape' in which LCs can fall into an immunogenic (A), a tolerogenic (B) or a dual (C, equal ability to stimulate tolerogenic and immunogenic responses) state/phenotype (**Figure 63B**). In the phase portrait, A and B therefore represent states in which the expression of TFs from either pathway is dominant over the

other, whilst C represents a state in which there is equal expression of both immunogenic and tolerogenic pathways. The model can therefore be utilised on single cell data to predict the phenotypic state of individual LCs by plotting LC trajectories in state space using single cell expression data.

A)

$$\frac{dI}{dt} = a_1 \frac{I^n}{\theta_{a_1}^n + I^n} + b_1 \frac{\theta_{b_1}^n}{\theta_{b_1}^n + T^n} - k_1 I$$

$$\frac{dT}{dt} = a_2 \frac{T^n}{\theta_{a_2}^n + T^n} + b_2 \frac{\theta_{b_2}^n}{\theta_{b_2}^n + I^n} - k_2 T$$

B)

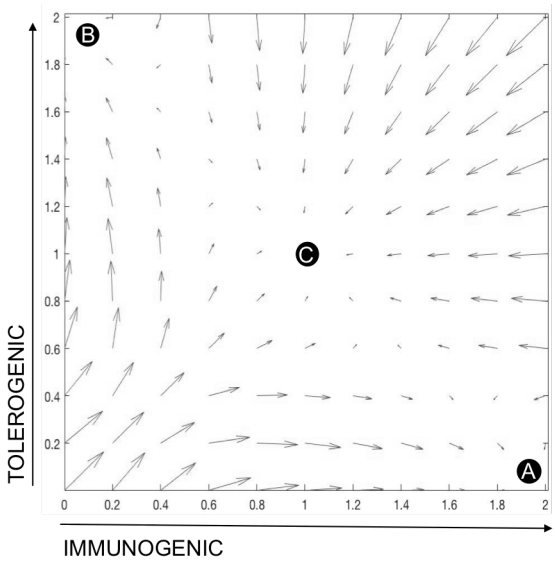

Figure 63. Application of a toggle-switch ODE model to predict LC phenotypes from single cell transcriptomic data. A) First order ODEs representing the activation of immunogenic (*I*) and tolerogenic (*T)* states in LCs. The dotted box represents terms describing the auto-amplification of each respective states. The dashed box represents terms describing the cross-inhibition from opposing states, whilst the solid box depicts the first-order decay rate (*k*) for TFs defining each state. **B)** Phase portrait of the toggle switch model in which two phenotype defining TFs/TF modules (immunogenic and tolerogenic) auto-amplify their own expression and are mutually repressive. Phase plane plots for toggle-switch model ODEs were plotted using quiver within Matlab. Black circles (A, B and C) represent end points for trajectories at stable attractors representing an immunogenic state (A), tolerogenic state (B) or a dual state (C).

The selection of TFs definitive for either immunogenic or tolerogenic responses was next required to construct the model. Based on our single cell transcriptomic analysis of migrated LC and migrated TNFα stimulated LCs, *IRF1* was a clear candidate for driving the immunogenic pathway, due its association as a marker gene for cluster 1 immunogenic LCs and enrichment of the *IRF1* regulon in SCENIC analysis. *IRF1* was also present within its own regulon, suggesting *IRF1* can self-amplify its expression, in line with the toggle-switch model assumptions. Similarly, *IRF4,* a top marker for cluster 2 tolerogenic LC, which also displayed enrichment for the *IRF4* regulon, was the most defining candidate for the tolerogenic pathway. Furthermore, *IRF4* is also present within its own regulon, satisfying the self-amplification requirements of the model.

To be consistent with observations of LC regulation of T cell responses, the model would be deemed to be correctly predictive, based on satisfying 3 criteria:

1. Unstimulated migrated LCs are predominantly in a tolerogenic or dual state.
2. TNFα stimulated migrated LCs display an attractor landscape more preferentially sided for immunogenic responses.
3. The number of LCs at the immunogenic attractor is increased in the cluster 1 immunogenic LC population and the number of LCs at the tolerogenic attractor is increased in cluster 2 tolerogenic population.

Normalised single cell RNA-seq TF expression values (scaled to 2) in each LC were utilised as starting points in the phaseplane. Trajectories of each LC in the phaseplane were plotted accordingly to the equation in **Equation 1**/**Figure 63A.** Here, depending on where trajectories started and on the phase plane landscape, LCs could be categorised as being in an immunogenic (A), tolerogenic (B) or dual (C) state, depending on what attractor the trajectories ended at. After *in silico* simulation, the number of trajectories finishing at each attractor were quantified and compared. Trajectories for all stimulated and unstimulated migrated LCs as a whole and the clusters defined from Scanpy leiden clustering (Clusters 1-4) were compared.

Plotting the trajectories for model 1, in which *IRF1* defined immunogenic states and *IRF4* defined tolerogenic states, revealed that the majority of both migrated (66.67%) and migrated TNFα (61.88%) LCs, regardless of cluster (Cluster 1-4), followed trajectories towards immunogenic phenotypes, going against our criteria that the majority of unstimulated migrated LCs would be in a tolerogenic or dual state (**Figure 64A**). However, a moderate reduction in the frequency of tolerogenic state LCs was observed in migrated TNFα LCs (18.51%) compared to migrated LCs (24%). There was also as a moderate increase in dual state LCs in migrated TNFα LC (19.61%) compared to unstimulated (9.33%). Observations were overall similar during comparison between cluster 1 (immunogenic) and cluster 2 (tolerogenic) LCs and in line with model criteria, the number of

tolerogenic LCs in cluster 2 increased (28.94%) compared to cluster 1 (15.25%)(**Figure 64B**). Overall whilst some criteria were met (change in frequency of immunogenic and tolerogenic LCs in stimulated and unstimulated LCs) the over prediction of LCs to be in an immunogenic state suggested the model needed further optimisation.

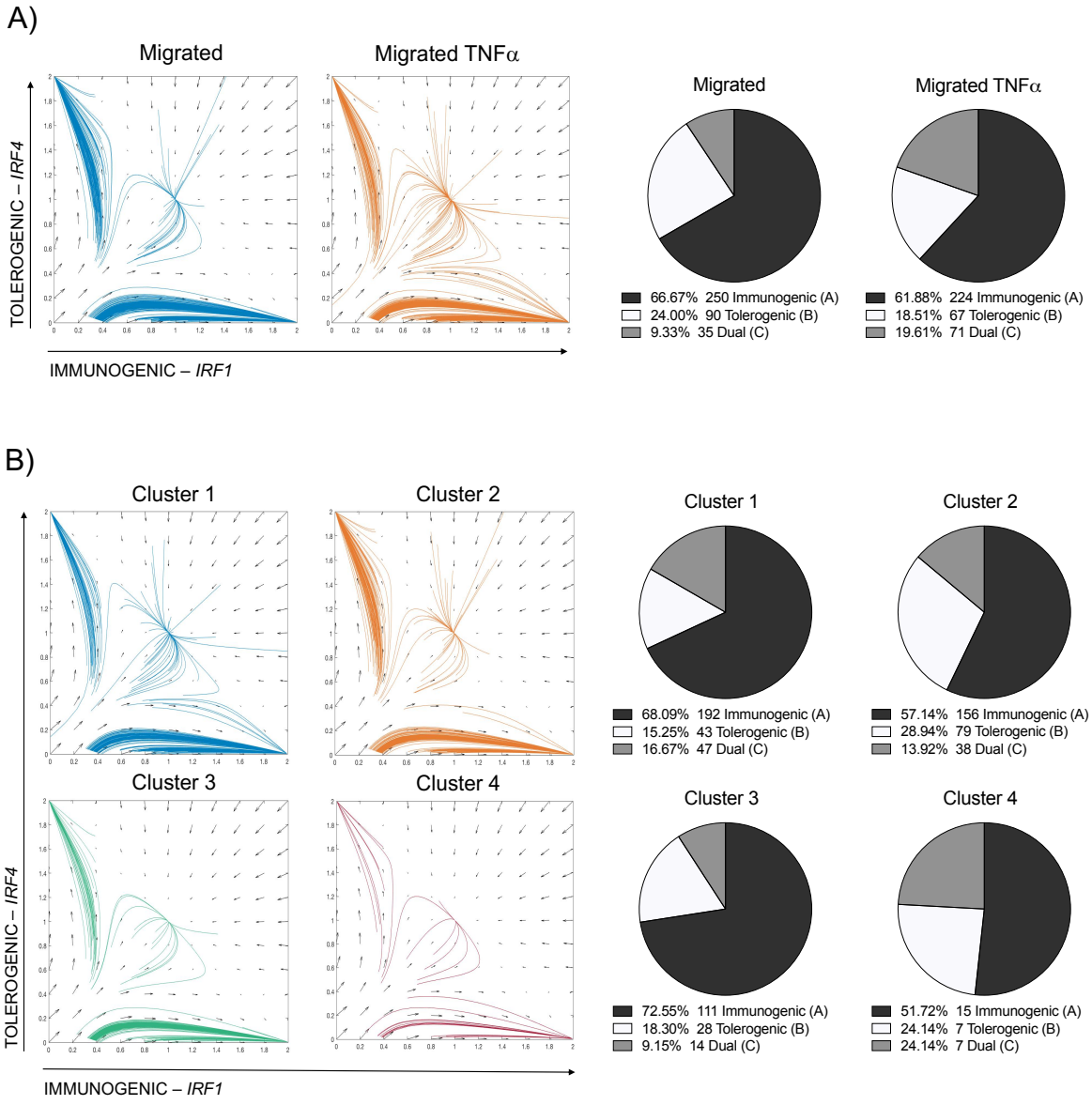

Figure 64. Model 1: *In silico* predictions of the toggle-switch model using *IRF1* and *IRF4* alone does not accurately represent the phenotypes observed in LCs. A) Phase portrait plot with single LC trajectories plotted from unstimulated and TNFα stimulated migrated LC. **B)** State space phase plane plot with single LC trajectories plotted as labelled from Scanpy leiden clustering. For each cell (starting point for line in the phaseplane) X-axis = normalised *IRF1* expression values scaled between 0-2, Y-axis – normalised *IRF4* expression values scaled between 0-2. Pie charts alongside display numbers and percentages of cells ending at each attractor and therefore assigned to each phenotype.

Inclusion of just *IRF1* and *IRF4* in the model was therefore insufficient for model predictions to match LC phenotypic observations. To finetune the model, so that its output could reflect *in vitro* and transcriptomic observations, we further queried what additional TF regulators could be determining LC phenotypes. We reviewed the expression of all TFs which were enriched in migrated LC compared to steady-state LC, from both breast skin and foreskin (**Chapter 5**). However, in unstimulated and TNFα stimulated migrated LC, none of these TFs (besides *IRF4*) were differentially regulated and therefore their importance for immunogenic vs tolerogenic responses seemed unlikely. However, inspection of genes within the top 50 marker genes for cluster 2 tolerogenic LCs revealed the presence of *MAP3K14* (*NIK*), the critical inducer of the non-canonical NFκB pathway involving *RELB*. Therefore, whilst *RELB* expression was homogenous across all populations, *RELB* activation was dependent on *MAP3K14* activity and increased non-canonical NFκB activation would only occur in cells that co-express high *MAP3K14* and *RELB* (**Figure 65A**).

IRF4 along with *MAP3K14* and *RELB* expression (Z-scores scaled to 2) were therefore used together to define the tolerogenic phenotype in model 2. The optimised model increased the number of unstimulated migrated LCs in a dual state (21.33%) and tolerogenic state (59.73%)(**Figure 65B**). The model also predicted that the majority of LCs in the tolerogenic cluster 2 (62.64%) were of a tolerogenic phenotype, whilst an increased proportion of immunogenic cluster 1 LCs were in an immunogenic (23.05%) and dual state (42.91%) in comparison (**Figure 65C**). However, the number of LCs predicted to be in an immunogenic state was near identical between unstimulated (18.93%) and TNFα stimulated (18.23%) LCs, although a reduction in tolerogenic state LCs (38.12%) and an increase in dual state LCs (43.65%) was observed in stimulated LCs. Overall, the model therefore improved the predictions in line with the model criteria. However, the lack of increased immunogenic state LCs in TNFα stimulated LC suggested a potential underestimation of TFs defining the immunogenic phenotype.

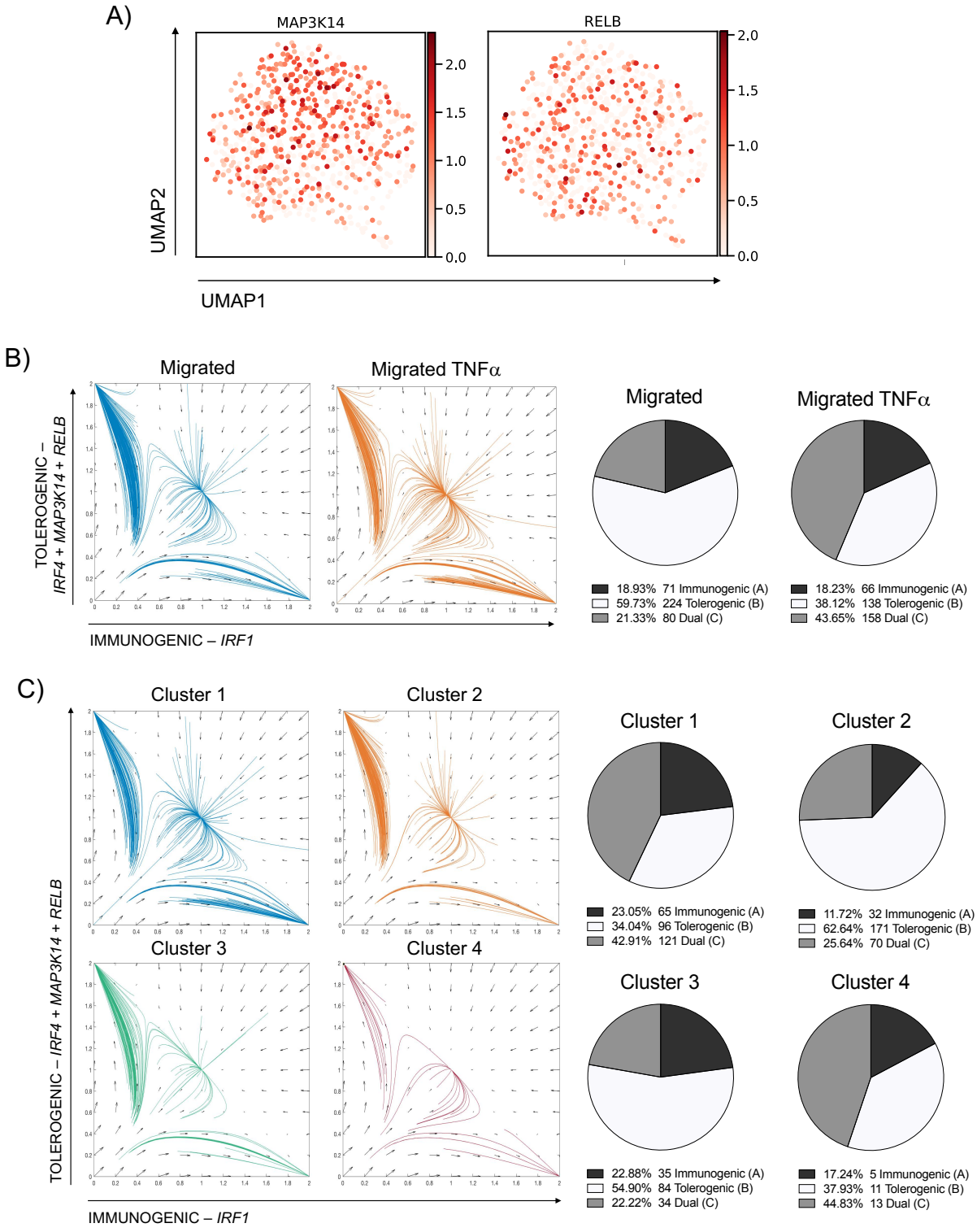

Figure 65. Model 2: The inclusion of non-canonical NFκB pathway components *RELB* and *MAP3K14* improved the toggle switch model. A) UMAP marker plots displaying *MAP3K14* and *RELB* expression. **B)** State space phase plane plot with single LC trajectories plotted from unstimulated and TNFα stimulated migrated LC. **C)** State space phase plane plot with single LC trajectories plotted as labelled from Scanpy leiden clustering. For each cell (starting point for line in the phaseplane) X-axis = normalised *IRF1* expression values scaled between 0-2, Y-axis – Z-scores combining *IRF4*, *RELB* and *MAP3K14* expression values scaled between 0-2. Pie charts alongside display numbers and percentages of cells assigned to each state/phenotype.

Previous studies investigating *IRF4* in DCs have revealed its importance in regulating both immunogenic and tolerogenic T cell responses, as well as LC activation and immune homeostasis (Vander Lugt, Riddell, Aly A. Khan, *et al.*, 2017)(Williams *et al.*, 2013)(Ainsua-Enrich *et al.*, 2019)(Sirvent *et al.*, 2020). Consistent with this idea was the observation that whilst *IRF4* was included as a marker gene for tolerogenic cluster 2 LCs, its expression was still relatively high in all unstimulated and TNFα stimulated LCs (**Figure 61B**). We therefore postulated that *IRF4* influenced both immunogenic and tolerogenic LC responses and its expression level (moderate/high) and interaction with co-regulators, influenced immunogenic vs tolerogenic output. In model 3, *IRF1* and *IRF4* (Z-scores scaled to 2) were used to define the immunogenic pathway and *IRF4, MAP3K14* and *RELB* (Z-scores scaled to 2) were used to define the tolerogenic pathway. Assessment of model predictions revealed that a large proportion of migrated LC now appeared in either a dual state (58.93%) or tolerogenic state (38.4%)(**Figure 66A**). This was therefore aligned with observations that unstimulated migrated LC can induce both immunogenic and tolerogenic immunity. Additionally, the minimal numbers of immunogenic state LCs (2.67%) revealed preference for tolerogenic activation in unstimulated migrated LC. In TNFα stimulated migrated LCs, there was an increased proportion of immunogenic state LCs (9.67%). Furthermore, TNFα stimulated migrated LCs had reduced frequency of tolerogenic state LCs (24.31%) and an increase in dual state LCs (66.02%). The proportion of tolerogenic LCs is therefore reduced in TNFα stimulated migrated LCs to accommodate an increase in dual and immunogenic state LCs. Similar observations were seen in cluster 1 and cluster 2 LC, with LCs exhibiting preferential immunogenic and tolerogenic states, respectively(**Figure 66B**). Overall, the optimised model 3 led to the satisfaction of increased immunogenic state LCs in the TNFα stimulated population, which was absent in model 2.

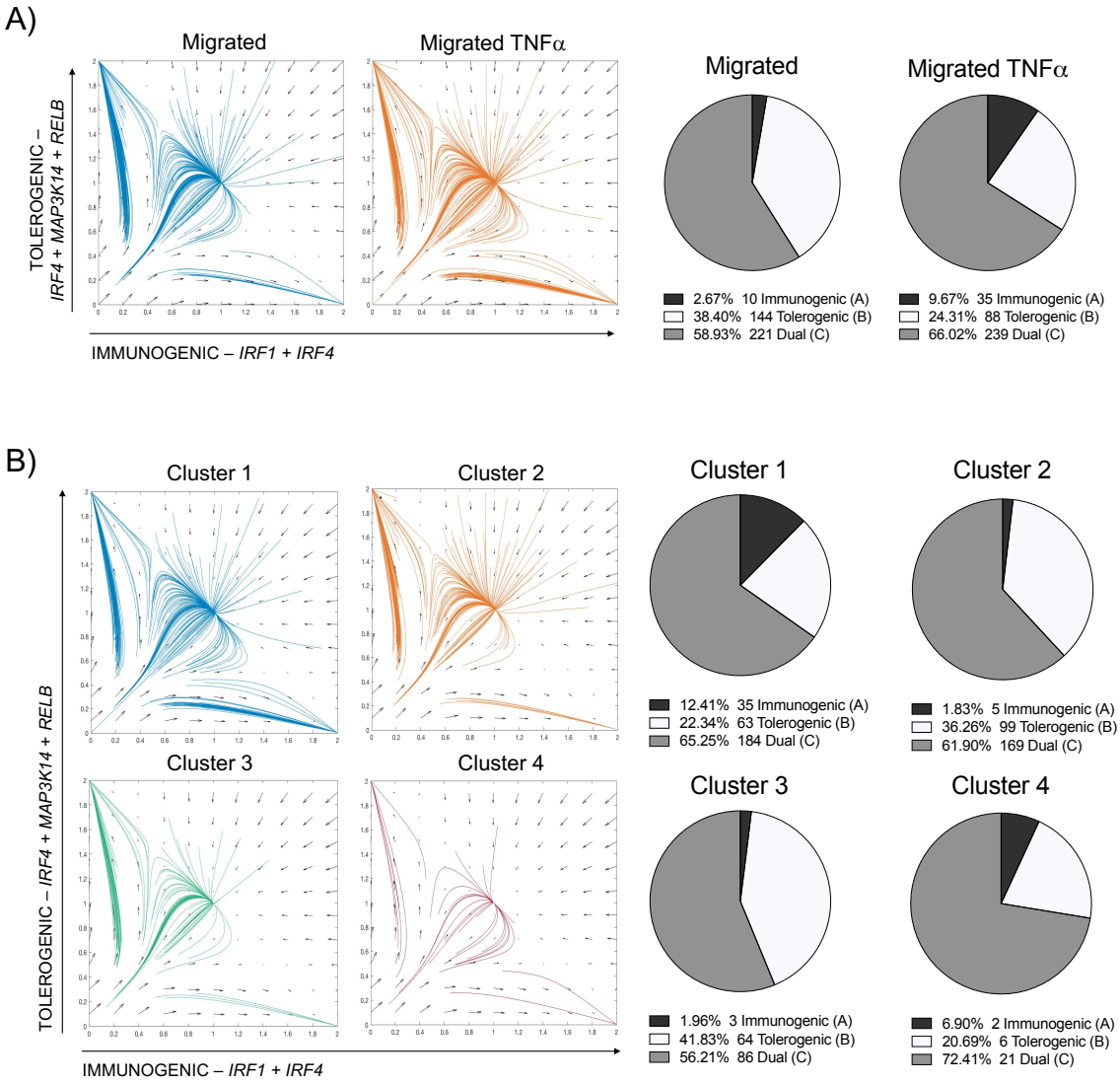

Figure 66. Model 3: Inclusion of *IRF4* as a regulator of both immunogenic and tolerogenic pathways further improves the *in silico* model predictions to match phenotypic data of LCs. A) State space phase plane plot with single LC trajectories plotted from unstimulated and TNFα stimulated migrated LC. **B)** State space phase plane plot with single LC trajectories plotted as labelled from Scanpy leiden clustering. For each cell (starting point for line in the phaseplane) X-axis = Z-scores combining *IRF1* and *IRF4* expression scaled between 0-2, Y-axis – Z-scores combining *IRF4*, *RELB* and *MAP3K14* expression scaled between 0-2. Pie charts alongside display numbers and percentages of cells assigned to each state/phenotype.

To assess how appropriate the TFs selected for models 2 and 3 were in correctly predicting LC phenotypes, we created a control model, choosing TFs not differentially expressed across the LC states. Here, the immunogenic pathway was defined by canonical NFκB components *RELA, REL* and *NFKB1*, whilst the tolerogenic pathway was defined by the expression of *ELK1, KLF6* and *JUND*. Canonical NFκB components were used as immunogenic components of the test model due to their association with enhancing DC immunogenic and inflammatory responses (Hayden, West and Ghosh, 2006)(Hayden and Ghosh, 2011). *ELK1, KLF6,* and *JUND* were selected for the tolerogenic pathway due to their association with the regulation of the migrated LC tolerogenic programme explored in **Chapter 5**. However, unlike models 2 and 3, none of the model criteria were met in the control model. Here the proportions of immunogenic, tolerogenic and dual state LCs was overall homogenous across both unstimulated and TNFα stimulated migrated LCs and clusters 1-4 (**Figure 67A**, **Figure 67B**). Overall, this highlighted that the TFs selected in models 2 and 3 were appropriate in distinguishing the divergent LC states and satisfying at least some, if not all of the criteria specified for creating a successful immunogenic vs tolerogenic LC model.

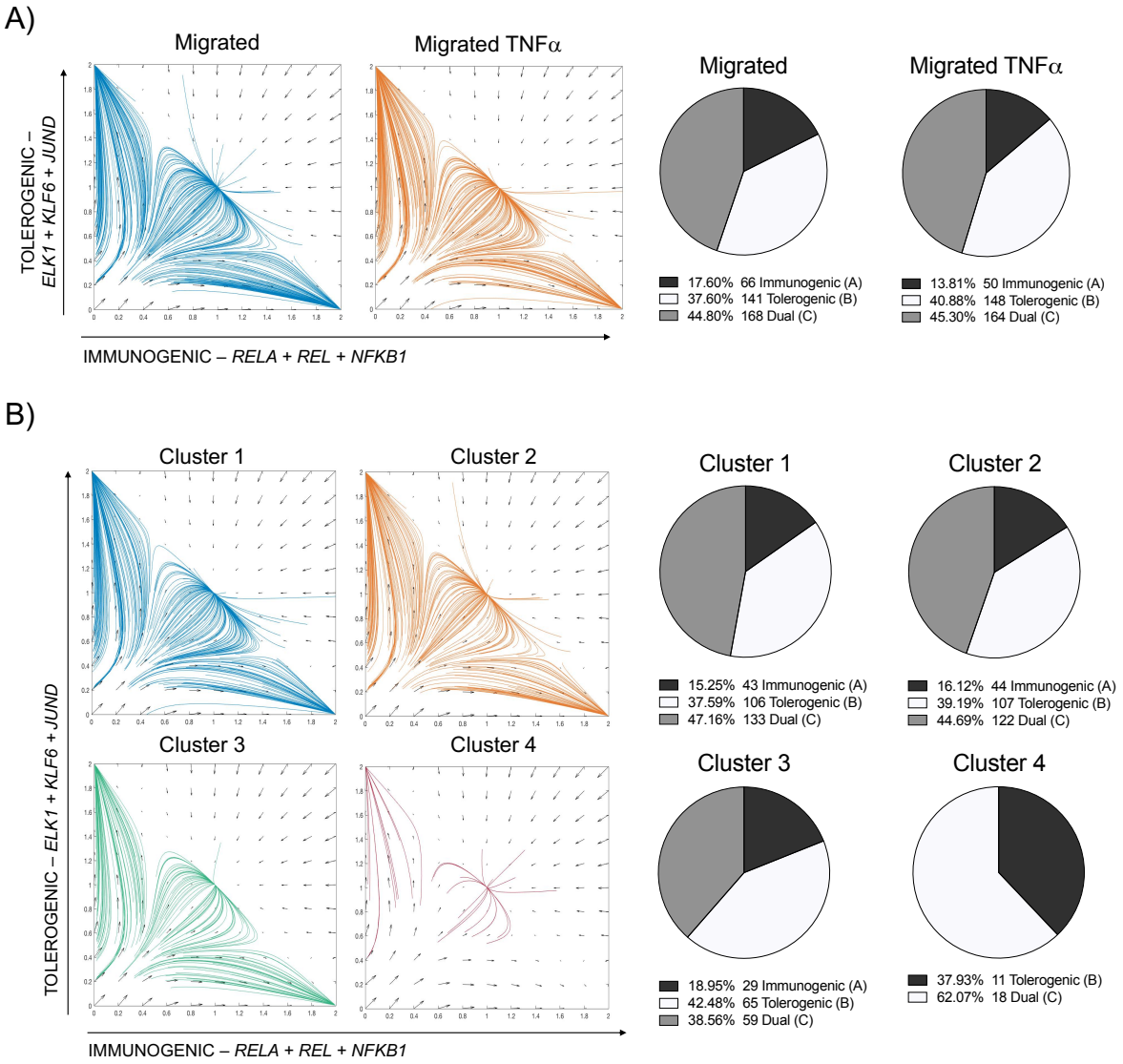

Figure 67. Control model: Using other TFs associated with immunogenic vs tolerogenic responses does not satisfy model criteria. A) State space phase plane plot with single LC trajectories plotted from unstimulated and TNFα stimulated migrated LC. **B)** State space phase plane plot with single LC trajectories plotted as labelled from Scanpy leiden clustering. For each cell (starting point for line in the phaseplane) X-axis = Z-scores combining canonical NFκB pathway *RELA, REL* and *NFKB1* expression scaled between 0-2, Y-axis – Z-scores combining *ELK1, KLF6* and *JUND* expression scaled between 0-2. Pie charts alongside display numbers and percentages of cells assigned to each state/phenotype.

7.2.5 The LC toggle-switch model can be used to predict LC phenotypes from transcriptomic data, in concordance with gene expression data.

Optimisation of the immunogenic vs tolerogenic toggle switch ODE model using data from abdominal skin derived unstimulated and TNFα stimulated migrated LC led to the generation of model predictions that were concordant with *in vitro* and transcriptomic observations of LC immunity. We therefore hypothesised that the model could be used to predict cell states across other LC transcriptomic datasets. The single cell transcriptomic data of steady-state and migrated breast skin and foreskin derived LCs explored in **Chapter 5** was utilised to validate the toggle-switch model's ability to predict LC phenotypes. Whilst model 3 appeared to perform best at satisfying our model criteria we tested both models 2 and 3 for a more comprehensive analysis of model performance. Here, we investigated the correspondence of the model *in silico* predictions to match observations from scRNA-seq data, in which DEG analysis comparing steady-state breast skin and foreskin LC revealed foreskin LC to be an increased state of immunogenic and inflammatory response activation (**Figure 68A&B**).

Using model 3, the majority of steady-state breast skin LCs, were identified to be in the dual state (68.95%), as well as the tolerogenic state (28.64%)(**Figure 68B**). Steady-state LCs therefore appear primed ready for both immunogenic and tolerogenic responses, with a favouring for the tolerogenic state. In contrast to breast skin, foreskin steady-state LC followed trajectories to all 3 states, with a great increase in the number of tolerogenic state (57.87%) and immunogenic state LCs (15.2%). This observation of increased immunogenic state LCs was consistent with the increased immunocompetent and activated transcriptomic profile of foreskin steady-state LCs compared to their parallels from the breast observed during DEG analysis in **Chapter 5**. Breast skin migrated LCs displayed similar state profiles to abdominal skin migrated LCs in the unstimulated/TNFα stimulated dataset, with the majority of LCs in a dual (59.71%) and tolerogenic (39.42%) state. This therefore validates the consistency of model predictions across datasets with similar constituents. DEG analysis from **Chapter 5** revealed that increased immunocompetency and an association with immune effector processes were central to migrated LCs from both skin tissues. However, similar to observations in foreskin steady-state LCs, foreskin migrated LCs were specifically associated with inflammatory responses. Consistent with these findings were our observations that migrated foreskin LCs followed trajectories to all 3 states, with an increased proportion of LCs in an immunogenic state (11.76%), similar to what was observed in steady-state foreskin LC. Comparable between breast skin and foreskin LCs was the observation that steady-state LC state profiles reflect those observed in migrated LC, suggesting that the phenotypes LC exhibit maybe predisposed prior to migration.

Using model 2, despite the expression of *IRF1, IRF4, RELB* and *MAP3K14* being relatively low in steady-state breast skin LCs, the majority of trajectories in model 2 ended in the dual state (52.32%) and tolerogenic state attractors (45.28%)(**Figure 68C**). Predominant tolerogenic (59.13%) and dual (40.0%) state were also exhibited by migrated breast skin LCs, similarly suggesting the pre-disposition of cell states prior to migration like in model 3. However, in comparisons to model predictions for unstimulated abdominal skin migrated LCs in which a significant proportion of LCs were labelled as being immunogenic, there was absence of a significant population of immunogenic state LC in migrated breast skin LCs. Therefore, unlike model 3, the predictions for unstimulated migrated LC from breast skin and abdominal skin were not comparable despite the relative similarities between tissues and processing. Still, trajectories for foreskin steady-state (14.13%) and migrated (9.8%) LC could be observed in the immunogenic state, in line with transcriptomic observations that foreskin LC are more immunogenic and inflammatory.

Overall, application of the toggle-switch model 3, to other LC datasets revealed consistencies in model predictions and produced model predictions that were concordant to observations from DEG and gene ontology analysis. The toggle-switch model therefore appears to be an effective tool for predicting the proportion of LCs displaying immunogenic, tolerogenic or dual phenotypes from transcriptomic data.

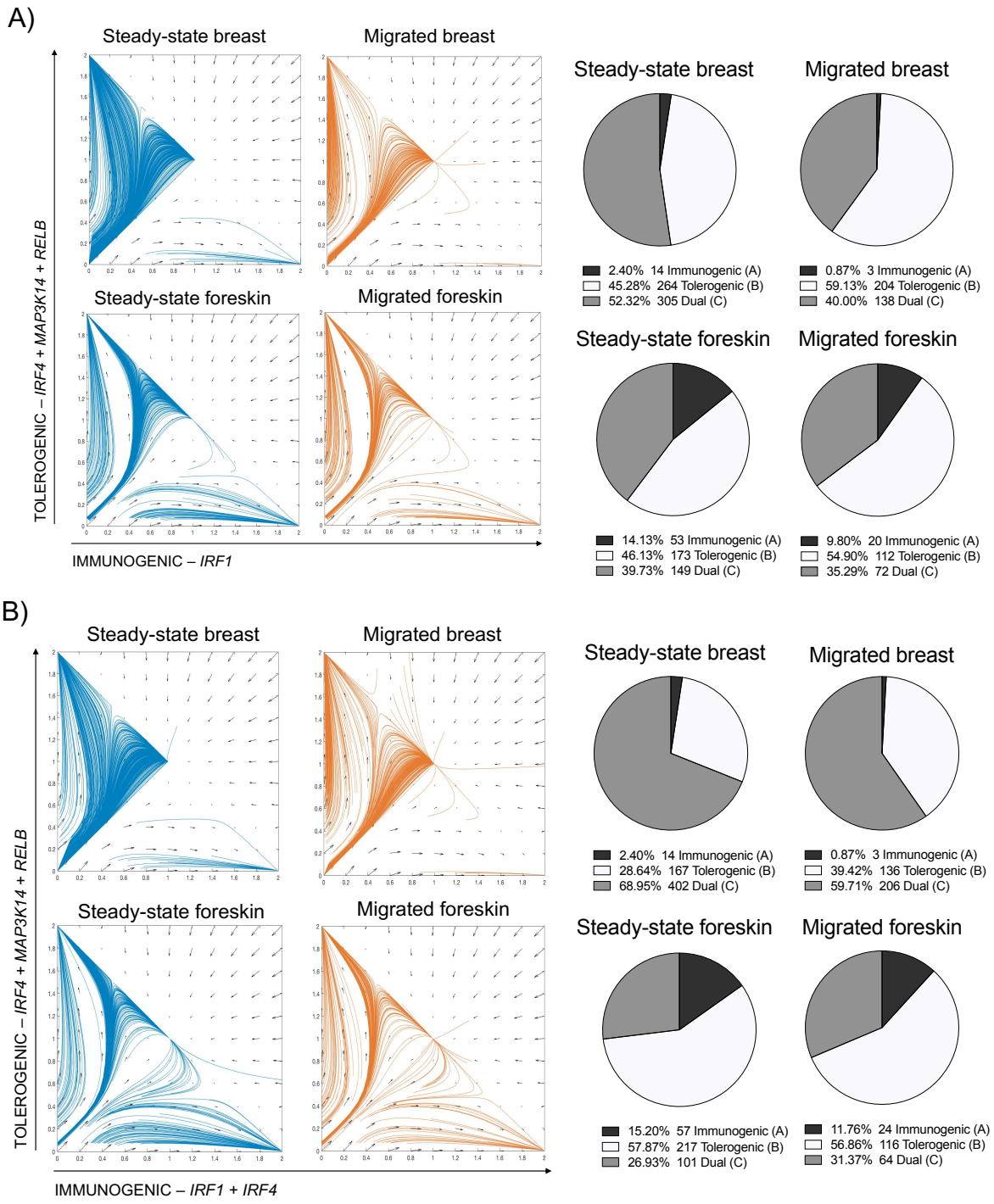

Figure 68. The optimised LC toggle-switch model can be applied to other single cell datasets of LCs to predict LC phenotypes. State space phase plane plot with single LC trajectories plotted from steady-state and migrated breast skin and foreskin derived LCs using models 2 (**A**) and 3 (**B**). For each LC (line in the phaseplane) X-axis = Z-scores combining *IRF1* (and *IRF4* in model 3) expression scaled between 0-2, Y-axis – Z-scores combining *IRF4*, *RELB* and *MAP3K14* expression scaled between 0-2. Pie charts alongside display numbers and percentages of cells assigned to each state/phenotype.

7.3 Discussion

Single cell transcriptomic analysis and the results from *in vitro* experimentation, measuring LC ability to induce tolerogenic T cell immunity, revealed that LCs extracted through migration were better primed for tolerance induction than steady-state LC. However from other studies measuring LC immunity, migrated LCs have also been shown to potently induce immunogenic T cell responses (Sirvent *et al.*, 2020)(Polak *et al.*, 2014)(Polak *et al.*, 2012)(Klechevsky *et al.*, 2008), indicating plasticity of LC function. Such plasticity can potentially be affected by signals from pathogens, dangers, and microenvironment. E.g. cytokines within the epidermal compartment are key regulators of LC immunological function and determine immune response outcomes. TNFα is a powerful proinflammatory cytokine produced by KCs, the structural cells of the epidermis, which enhances LC activation and cellular migration (Stoitzner *et al.*, 1999)(Théry and Amigorena, 2001). TNF-α also enhances LC capacity to cross-present antigen and prime immunogenic CD8 T cells (Sirvent *et al.*, 2020). The conflicting observations using migrated LC *in vitro* have therefore revealed the complexity in discerning the decision-making process of LCs to drive either immunogenic or tolerogenic responses. Overall, from published data and our own observations, unstimulated migrated LC appear to be primed for the induction of both immunogenic and tolerogenic T cell responses. The association of LC migration, during homeostatic conditions, in driving immune tolerance to self-antigen, suggests tolerance induction may even be favoured(Hemmi *et al.*, 2001)(Yoshino *et al.*, 2006). However, under different conditions, such as inflammatory cytokine signalling (TNFα), it would be expected that the propensity of LCs to drive either response will change. Here, we applied mathematical modelling using a 'toggle-switch' system, to a GRN depicting the immunogenic vs tolerogenic decision making process in LCs.

7.3.1 The unstimulated and TNFα stimulated migrated LC population is predominantly composed of 3 clusters, defined as being mature, immunogenic and tolerogenic

Drop-seq analysis of migratory LC compared to steady-state LC in Chapter 3, revealed the migrated LC population to be homogenous. Whilst migrated LC have enhanced immunogenic and tolerogenic capacity it was therefore unlikely that highly distinct populations promote either immunogenic or tolerogenic immune responses. The decision-making process of LC to direct either tolerogenic or immunogenic immune response was therefore unclear. Using scRNA-seq we explored whether immunogenic stimuli (TNFα) would induce changes in transcriptome expression that would reveal divergent programming of tolerogenic and immunogenic states. UMAP dimensionality reduction analysis revealed the TNFα stimulated population to be differential to unstimulated migrated LC. However, whilst a subpopulation of TNFα stimulated LC could be identified, both unstimulated and

TNFα stimulated LC were part of one overall cluster. The genomic programming induced by migration was therefore predominant over any changes induced by stimuli. This is consistent with our observations that the dramatic changes in genomic programming of LCs that occur during migration are fundamental for an enhanced activation state and LC immune potential (Sirvent *et al.*, 2020). In this instance, LCs were stimulated post migration and therefore after the migration induced genomic programming. Whilst TNFα did modulate LC transcriptomes post-migration, it would also be interesting to observe the transcriptomic changes induce when LCs are stimulated during the migration process.

Unsupervised clustering analysis identified 4 subpopulations amongst the combined unstimulated and TNFα stimulated population, with the majority of cells categorised into 3 of these clusters. Based on marker gene analysis these 3 clusters were categorised as immunogenic, tolerogenic and primed LCs. Here, immunogenic LCs were composed of predominantly TNFα stimulated LCs, tolerogenic LC were composed of predominantly unstimulated LCs and primed LCs contained a relatively equal proportion of both. Consistent with functional studies of TNFα stimulated migrated LCs, in which enhanced antigen cross presentation is observed (Sirvent *et al.*, 2020), DEGs upregulated in LCs stimulated with TNFα were associated with alpha-beta T cell activation (CD8+) and Th1 differentiation, highlighting their increased immunocompetency. Interestingly, a consistent observation in TNFα stimulated LCs and immunogenic cluster 1 was the identification of genes associated with tolerogenic regulation alongside immunogenic pathways. The simultaneous upregulation of both tolerogenic and immunogenic pathways, overall appears counterproductive if during the context of inflammatory signalling, immunogenic responses are required. However, some tolerogenic associated genes upregulated in TNFα stimulated/immunogenic LC are implicated in feedback mechanisms in response to inflammatory pathway activation. *SOCS1* for example, is implicated in the restriction of TLR signalling, as well as TNFα and IL-1 cytokine signalling in immune activated DCs (Gilboa, 2004), whilst *DUSP1* functional studies in murine macrophages have demonstrated its importance for preventing endotoxin induced shock in response to LPS (Hammer *et al.*, 2006). Furthermore, *NFKBIA,* a component of the IκB complex, is induced by NFκB activation and sequesters NFκB induced cytokine production and immune activation (Dorrington and Fraser, 2019). During inflammatory signalling the tolerance associated genes upregulated could therefore be required for finetuning immunogenicity and preventing overactivation, rather than inducing functional tolerance. Furthermore, whilst *CD80* and *CD86*, were included in the tolerance associated gene list, equally there association with immunogenic activation in DC is well recognised (Lenschow, Walunas and Bluestone, 1996).

Tolerogenic cluster 2 LC marker genes were specifically associated with negative regulation of immune system process, contributed by elevated *IDO1* expression, which we have validated as

being an important inducer of LC tolerogenic function *in vitro*. Furthermore cluster 2 LC and all unstimulated migrated LCs were absent for the induction of immunogenic (CD8+ and Th1) programmes. This overall may lead to dominating tolerogenic responses.

Immunogenic and tolerogenic LCs appeared to represent LC states primed for opposing immune regulation. Cluster 3 primed LCs however were marked by the expression of fundamental LC programmes such antigen presentation and ATP metabolism (Romani *et al.*, 2003), which during pseudotime analysis, appeared to be capable of following trajectories to both immunogenic and tolerogenic LC states. Interestingly, when comparing both cluster 1 immunogenic and cluster 2 tolerogenic LCs to baseline cluster 3 primed LCs, the predominant upregulated biological pathways appeared very similar (regulation of immune system process and response to cytokine). This suggested that similar biological pathways are activated during the transition from a primed state to an activated immunogenic/tolerogenic state. The overall differences driving the uniqueness of immunogenic and tolerogenic clusters may therefore be fairly subtle in the context of the whole transcriptome. Of note however were the pathways upregulated in cluster 3 primed LCs in comparison to cluster 1 immunogenic and cluster 2 tolerogenic clusters. In comparison to tolerogenic cluster 2 LCs, cluster 3 LC DEGs were associated with leukocyte activation processes. This difference however was not associated with the DEGs upregulated in primed cluster 3 LCs compared to immunogenic cluster 1 LCs. These biological processes were therefore specifically downregulated in the transition from primed LCs to the tolerogenic LCs, suggesting finetuning of the tolerogenic LC transcriptome for activation of immune pathways that specifically promote tolerance. In contrast the biological pathways upregulated in primed cluster 3 LC and downregulated in immunogenic cluster 1 LC included ATP metabolism. This again highlights the association of metabolic processes with immunological programming of DCs towards tolerogenic responses (He *et al.*, 2019)(Wculek *et al.*, 2019).

During analysis of the genes upregulated in cluster 1 immunogenic and cluster 2 tolerogenic, when compared to cluster 3 primed LCs, a significant proportion of genes mutually upregulated were identified. This again indicates the presence of a core upregulated programme during the transition from a primed state towards tolerogenic and immunogenic LCs. Intriguingly, included in the core programme was *IDO1.* However, similar to the tolerogenic associated genes upregulated in TNFα stimulated LC, even *IDO1* is induced by inflammatory signalling such as IFNγ and LPS, suggesting that it is also implicated in feedback mechanism to sequester overactivation (Harden and Egilmez, 2012)(Curti *et al.*, 2009). Interestingly however, fewer upregulated DEGs were identified during comparison of cluster 2 tolerogenic LCs with cluster 3 primed LCs, suggesting that primed LCs are more similar and therefore more predisposed to becoming tolerogenic. We therefore postulate that without inflammatory stimuli in the steady-state, primed LCs favour trajectories towards

tolerogenic states, whilst during inflammatory conditions primed LCs must induce more dramatic changes in genomic programming to follow trajectories to a more immunogenic state.

7.3.2 Utilising a toggle-switch ODE model permitted *in silico* exploration of the key regulators of tolerogenic and immunogenic LC programming

We utilised an ODE toggle-switch model, in which two TF mediated pathways display auto amplification of their own activity and cross inhibition of the other (Huang *et al.*, 2007). Huang et al. previously used this model to investigate the lineage potential of a stable population of bipotent cells towards either erythroid and myeloid differentiation pathways, with an intermediate stable state. We hypothesised that the model reflected the landscape of LC immune responses, in which cells could be categorised into distinct immunogenic and tolerogenic pathway phenotypes/states, as well as an intermediate dual phenotype/state, in which both pathways were equally active. We set criteria in order to test the model's accuracy. Firstly, that unstimulated migrated LCs were mostly classified to be in a tolerogenic or dual state of activation. This would therefore reflect: our observations of tolerogenic T cell responses induced by migrated LC; observations from other *in vitro* studies displaying the induction of both immunogenic (CD8+ and Th2 CD4+) and tolerogenic (Treg) T cell responses, and the potential preference for inducing self-tolerance through self-antigen trafficking in non-inflammatory conditions (Sirvent *et al.*, 2020)(Polak *et al.*, 2014)(Polak *et al.*, 2012)(Klechevsky *et al.*, 2008)(Seneschal *et al.*, 2012)(Hemmi *et al.*, 2001)(Yoshino *et al.*, 2006). Secondly, an observed increase in immunogenic state LCs after TNFα stimulation, to reflect the enhanced transcriptomic profile associated with alpha-beta CD8+ T cell activation identified in single cell analysis and observations *in vitro,* in which improved antigen cross-presentation and antiviral immunity is seen (Sirvent *et al.*, 2020)(Polak *et al.*, 2014)(Polak *et al.*, 2012). Finally, the proportions of the 3 states in cluster 1 immunogenic and cluster 2 tolerogenic LC, would reflect their transcriptomic profiles from gene ontology analysis, which identified preferences for immunogenic and tolerogenic responses, respectively.

Our investigations into the unstimulated and TNFα stimulated migrated LC populations revealed that the transcriptomic changes induced by inflammatory signalling were subtle in the context of the whole transcriptome. However, unique mechanisms of gene regulation in immunogenic and tolerogenic LC clusters could be identified and were therefore underlined by unique TF regulators. Exploration of key pathway defining TFs through assessing cluster marker genes, DEG analysis and SCENIC regulatory network inference analysis, highlighted *IRF1* and *IRF4* as being preferentially activated in immunogenic and tolerogenic LCs, respectively. In DCs, TLR-9 induced *IRF1* induction leads to the induction of IFNβ and interferon stimulated genes, driving efficient anti-viral immune responses (Schmitz *et al.*, 2007). *IRF1* activation in macrophages is associated with the polarisation

of macrophages towards the pro-inflammatory M1 phenotype (Chistiakov *et al.*, 2018). In fibroblast like synoviocytes (FLS), which are implicated in the inflammation in rheumatoid arthritis, TNFα mediated induction of *IRF1* leads to induction of inflammatory mediators, such as IFNβ (Bonelli *et al.*, 2019). *IRF1* upregulation in TNFα stimulated LCs is therefore in accordance with its association with pro-inflammatory and immunogenic activation. In contrast, *IRF4* was associated with the expression of tolerogenic genes during analysis of migrated breast derived and foreskin LCs, including *IDO1*. Moreover, *IRF4* activity has been associated with tolerance and homeostasis regulation in LCs, DCs and macrophages. CRISPR-Cas9 knockout of *IRF4* in human LCs has associated its expression with the suppression of cytokine response and oxidative stress signalling pathways (Sirvent *et al.*, 2020). Furthermore, in murine bone marrow DCs from *IRF4* knockouts, impaired Treg induction, reduced expression of RALDH2 and PD-L2 and increased expression of pro-inflammatory cytokines (TNFα and IL-12) are observed *in vitro*, as well as *in vivo* observations of impaired priming of peripheral tissue Tregs (Vander Lugt, Riddell, Aly A. Khan, *et al.*, 2017). In murine macrophages, *IRF4* is responsible for downregulating hyperresponsiveness to TLR signalling, with *IRF4* knockout mice displaying increased IL-12 and TNFα expression, resulting in death by uncontrolled inflammation (Honma *et al.*, 2005). In the context of *Leishmania major* infection, murine *IRF4* knockout DCs displayed increased induction of Th1 cells and the proinflammatory cytokine IL-12 (Akbari *et al.*, 2014). *In silico* modelling of the toggle-switch model using just *IRF1* and *IRF4* to define immunogenic and tolerogenic LC however, was insufficient to recapture the immunological landscape of LCs that reflects observed phenotypic migrated LC data, as it overproduced the number of LCs defined be in an immunogenic state.

The results from model 1 suggested an imbalance in the model, implying that factors critical for the induction of tolerogenic responses were missing. During the optimisation process we considered other TFs which could influence immunogenic vs tolerogenic regulation. Interestingly, the majority of TFs identified as potential regulators of tolerogenic programming in migrated LCs from **Chapter 5** were not differentially regulated between unstimulated and TNFα stimulated LC, suggesting they were core to migrated LC genomic programming and immunocompetency, rather than immunotolerance specifically. This assumption was further supported in our control model, in which homogenous output of model predictions was observed. However, *MAP3K14,* otherwise known as *NIK,* the critical inducer of the non-canonical NFκB pathway, was identified as being upregulated in cluster 2 tolerogenic LCs. Additionally, in **Chapter 5**, the functional TF component of the non-canonical NFκB pathway *RELB*, was identified as one of the upregulated TFs associated with the tolerogenic programming of migrated LCs, correlating with the expression of several tolerogenic genes, especially *IDO1. RELB* and the non-canonical NFκB pathway are implicated in DC tolerance. In steady-state migratory murine langerin+ DDCs, *RELB* expression is required for self-

antigen transport and Treg induction(Azukizawa *et al.*, 2011) and in human MoDCs and pDCs, RELB is implicated in the induction of IDO1 expression and Tregs (Tas *et al.*, 2007)(Manches *et al.*, 2012). Transfer of RELB+ DCs into RELB knockout mice, which have spontaneous allergic airway inflammation, also leads to a reduction in chemokines and Th2 cytokines, to prevent lung tissue inflammation and damage (Nair *et al.*, 2018). Furthermore, RELB+ DCs, can alleviate systemic inflammation in *RELB* knockout mice, through augmenting Tregs, in an IDO-dependent manner (O'Sullivan *et al.*, 2011). Interestingly, the relatively homogenous expression of *RELB* across both unstimulated and TNFα stimulated LC suggest all LC may be primed ready for activation of tolerogenic pathways dependent upon increased *MAP3K14* expression. In the context of resolving of inflammation, rapid induction of *MAP3K14* to activate pre-existing *RELB,* may swiftly redirect LC responses towards tolerance. Inclusion of *MAP3K14* and *RELB* in model 2 reduced the overestimation of immunogenic state LCs to be more in line with the model criteria. However, the predicted quantities of immunogenic LCs were equal between unstimulated and TNFα stimulated LC, with stimulated LCs just displaying an increase of LCs in a dual state and therefore reduction of tolerogenic state LCs. Whilst this could imply that the model is unbalanced in immunogenic defining TFs, it could also suggest that the determining of increased immunogenic responses is not simply mediated by increasing the quantity of LCs in a uniquely immunogenic state, but is induced by decreased activity of potently immunosuppressive tolerogenic state LCs.

When we reviewed the current understanding of LC genomic programming during immune regulation, we questioned the exclusivity of *IRF4* activation for tolerogenic responses only. Observations from human LC single cell RNA-sequencing implicate *IRF4* expression with immunogenic regulation. Here, *IRF4* expression coincides with the programming of antigen presentation and cross-presentation pathway genes, as well as the observation that LC maturation and immune activation genes are downregulated in *IRF4* CRISPR-Cas9 knockouts (Sirvent *et al.*, 2020). *IRF4* expressing DCs, in the context of influenza infection, are required for effective CD8+ T cell activation and the alleviation of disease pathology (Ainsua-Enrich *et al.*, 2019). Murine studies have also revealed a dependence for DC *IRF4* expression in mediating Th2 differentiation (Williams *et al.*, 2013). *IRF4* therefore appears core to both immunogenic and tolerogenic LC states, which is supported by the observation that IRF4 knockout mice are diminished in ability to induce both effector T cells and Tregs (Vander Lugt, Riddell, Aly A. Khan, *et al.*, 2017). Additionally, whilst *IRF4* expression was increased in tolerogenic cluster 2 LCs, its expression was well distributed across both unstimulated and TNFα stimulated LCs. This could infer that modulation of *IRF4* expression levels is important in regulating immunogenic vs tolerogenic LC responses. Here, moderate *IRF4* expression in the context of high *IRF1* expression would favour immunogenic responses, whilst high expression of *IRF4* in the context of high non-canonical NFκB activation would favour tolerogenic

responses. The inclusion of *IRF4* in both immunogenic and tolerogenic arms of the model in model 3, led to the satisfaction of the model criteria, with a predominance for unstimulated migrated LCs to be in a tolerogenic or dual state and an increase in immunogenic state LCs after TNFα stimulation. Interestingly, model 3 predicted the majority of both unstimulated and TNFα stimulated LCs to be in a dual state. However, in accordance with the close localisation of cluster 2 tolerogenic LCs and cluster 1 immunogenic LCs in UMAP space, we believe model 3 predictions may reflect the overall spectrum of immunogenic to tolerogenic states, in which only the very few cells at the extreme ends of the spectrum are classified as uniquely immunogenic or tolerogenic LC. Here, the majority of cells are somewhere in the middle, perhaps as stable intermediate states, or as LCs at earlier timepoints in their transition to specifically tolerogenic or immunogenic LCs. The near absent proportion of LCs in an immunogenic state in migrated LC, was also in line with UMAP plotting, in which the immunogenic cluster 1 population was mostly composed of migrated TNFα stimulated LCs, especially at the periphery of the cluster, which may reflect LCs in the most potent immunogenic states. Furthermore, in line with the more similar expression profiles of cluster 3 primed and cluster 2 tolerogenic LCs was the observation of comparable predicted trajectories. Whilst primed cluster 3 were phenotypically not defined as immunogenic or tolerogenic and may be expected to be in a dual state, the model predictions may reflect the end points for the pathways primed LCs are undertaking.

Overall, utilisation of scRNA-seq data for mathematical modelling permitted analyses of the immunogenic vs tolerogenic governing GRNs, allowing detailed investigations into LC population dynamics, which to our knowledge is previously unexplored. Whilst scRNA-seq allowed single cell resolution into exploration of LC phenotypes, it also important to consider how limitations in scRNA-seq technologies may affect results. Thus, random drop-outs of transcript detection may hinder the accurate identification of LC phenotypes, through absent detection of TFs included in the models which define the different states, as well as the detection of other key phenotype defining TFs, which were not identified in our analysis. To further validate the accuracy of model predictions, the identification of specific markers distinguishing immunogenic, tolerogenic and dual state LCs in unstimulated and TNFα stimulated populations could allow each state to analysed *in vitro*. Here, the expression of the immunogenic vs tolerogenic state defining TFs, could be confirmed at the protein level.

7.3.3 Application of the toggle switch model to steady-state and migrated LC datasets. captured the same observations from single cell transcriptomic analysis

To test and validate models 2 and 3, we applied them to the breast skin and foreskin steady-state and migrated LC datasets to see if the model predictions matched observations from single cell

transcriptomic analysis. In model 3 we found that the unstimulated migrated LCs from both abdominal and breast skin datasets displayed the same profile of the 3 states, demonstrating the consistency of the model's predictions. However, comparison between abdominal and breast skin migrated LCs for model 2 predictions however revealed differences in output. Whilst, this suggests lack of translatability of model 2 to other datasets, we must also consider that this may be a result of heterogeneity between samples and tissues. Interestingly, in both models, steady-state LCs were observed to have very similar profiles to migrated LC, which suggested that the preference of LCs to be in each state may be predetermined prior to migration. However, we acknowledge that the low expression of the model's TFs in steady-state LCs, may influence the accuracy of these predictions. Consistent with our observations during comparison between steady-state and migrated breast skin and foreskin LC transcriptomes (**Chapter 5**), in which foreskin LCs display enhanced inflammatory profiles, was the fact that both models revealed an increase in the number of immunogenic state LCs in foreskin data simulations. This increased number of LCs assigned to an immunogenic state in foreskin LC simulations similarly reflected the increase observed in TNFα stimulated LCs, thus supporting the reporting of the foreskin to be a pro-inflammatory tissue marked by elevated pro-inflammatory cytokines (Prodger *et al.*, 2012). Interestingly, in both foreskin LC populations, both models predicted that a larger proportion of LCs were in a tolerogenic state compared to breast skin LCs. This difference may reflect the finding that *IDO1* expression was increased in foreskin populations compared to breast skin populations, respectively (**Chapter 5**). Foreskin LCs therefore represent a population more defined by uniquely immunogenic and tolerogenic states compared to breast and abdominal skin, which may reflect a distinct immunological role at the foreskin not required in other skin tissues.

Overall, we have highlighted the complex transcriptomic regulation that underlines the LC decision making process to initiate either immunogenic or tolerogenic immunity. Through single cell transcriptomic analysis and mathematical modelling, we have revealed that subtle changes in genomic programming may be sufficient to alter LC immunological responses. Here, we have shown that external signalling, such as pro-inflammatory TNFα, can modulate the proportion of LCs in different immunological states. This may therefore reflect how LCs balance the need for different immunological responses to diverse biological stimuli. Furthermore, we have highlighted specific TF regulators critical for the modulation of both immunogenic and tolerogenic LCs states, which when translated into a mathematical model, we have demonstrated has the potential to predict LC phenotypes across different LC transcriptomic datasets.

Chapter 8 Final discussion/future work

8.1 The requirements for systems immunology methods to understand LC tolerance regulation

Despite LCs being the most studied antigen presenting cell populations, since their discovery by Paul Langerhans in 1868, their biological role in the immune system is still obscure (Valladeau and Saeland, 2005). LCs can be classified somewhere in-between classical DCs and macrophages, due to powerful antigen presenting capacity and distinct ontology, respectively (Doebel, Voisin and Nagao, 2017). Their specific residence at the epidermis, in the context of the skin, suggests a fundamental role for LCs here, which cannot be replaced by conventional DCs or macrophages. Increasingly, LCs have been critically associated with homeostatic regulation and tolerance (West and Bennett, 2018)(Clayton *et al.*, 2017) (Berger *et al.*, 2006)(Mutyambizi, Berger and Edelson, 2009)(Seneschal *et al.*, 2012)(Hemmi *et al.*, 2001)(Yoshino *et al.*, 2006). However, like tolerance regulation in conventional DCs, the precise molecular mechanisms central for tolerance regulation in LCs are overall elusive. In this project we therefore sought to expand understanding of LC tolerance regulation.

The challenges that have opposed the unveiling of LCs fundamental role in immunity, are the paucity of *in vitro* models, difficulties in obtaining sufficient cell numbers from tissues for functional studies and the discrepancies between human and murine immunology (Mestas and Hughes, 2004). These same scientific boundaries have therefore also hampered investigations into DC/LC tolerance regulation, specifically. The current theories for how the regulation of DC tolerance is determined include the concepts that immaturity equips tolerogenic function, as well as the idea that tolerance is promoted by unique subpopulations of DCs within tissues (Banchereau and Steinman, 1998)(Steinman *et al.*, 2000)(Mellman and Steinman, 2001)(Steinman, Hawiger and Nussenzweig, 2003). The transcriptomes of cells contain information regarding cell state and function. However, classical bulk RNA sequencing methods are unable to evaluate population heterogeneity and therefore incapable of assess whether such subpopulations of LCs exist *in situ* which promote diverse immune response outcomes. Furthermore, methods such as flow cytometry in which the phenotypes of individual cells can be assessed, are restricted to the investigation of only a select number of molecules. In recent years however, the rapidly advancing field of scRNA-seq has given unprecedented opportunity for scientists to broadly investigate whole transcriptome expression in individual cells across cell populations (Shapiro, Biezuner and Linnarsson, 2013)(Hwang, Lee and Bang, 2018). We therefore utilised the open-source system Drop-seq, a highly utilised scRNA-seq

protocol due to its speed, reliability and cost effectiveness ($0.10 per cell), with the additional advantage of being open to adaption, such as targeted approaches(Constellation Drop-seq, BD Rhapsody)(Macosko *et al.*, 2015)(Zhang *et al.*, 2019)(Vallejo *et al.*, 2019)(Shum *et al.*, 2019). Alongside the development of scRNA-seq methods, is the expansion of impressive bioinformatic methods, including optimised normalisation, dimensionality reduction and clustering pipelines, which greatly improve molecular and cellular biological discoveries (Chen, Ning and Shi, 2019). In our analyses, we adopted optimised procedures and cutting-edge bioinformatic methodologies to comprehensively investigate our research questions. Studies investigating cell states and population heterogeneity using scRNA-seq are now widely documented across broad immunological fields, including the skin (Villani *et al.*, 2017)(Cheng *et al.*, 2018)(Joost *et al.*, 2018). However, to our knowledge this study is the first time detailed scRNA-seq exploration into the determinants of LC tolerogenicity have been performed and until now the heterogeneity present within human LC populations at both the steady-state and after migration was unknown.

One of the key advancements transcriptomic analyses has permitted, is the investigations of complex GRNs which govern the regulation of specific cellular responses and phenotypes. Transcriptomic studies by Ido Amit et al. have demonstrated how dynamic interplay between TFs in DC GRNs direct diverse immunological outcomes in the context of pathogen specific responses (Amit *et al.*, 2009). Furthermore, from exploring GRN regulation during haematopoiesis, Olsson et al. have revealed the hierarchical transition from haematopoietic progenitor cells to monocytic and granulocytic lineages (Olsson *et al.*, 2016). Discerning such discoveries on GRN dynamics using classic functional *in vitro* methods would be incredibly challenging, if not impossible, due to the sheer number of molecules that would need to be experimentally measured and validated. GRN discoveries are therefore critical for informing on transitional cell states and pathways of cellular differentiation, at the steady state and under different biological conditions. Additionally, the utilisation of single cell transcriptomic data allows investigations into how GRNs are differentially regulated amongst cell populations. Hence, in our analysis the exploration of GRNs governing LC tolerance appeared fundamental to not only comprehend the distinct feature of LC tolerogenic transcriptomes, but also understand how they are regulated amongst the whole population.

Significant for scientific developments into the interpretation of transcriptomic data, especially single cell, are the applications of computational *in silico* modelling methods. The use of mathematical modelling techniques with transcriptomic data has undoubtedly expanded the capacity to understand previously obscure biological phenomenon in diverse research fields (Eftimie, Gillard and Cantrell, 2016). For example, in studies of GRNs in stem cell biology, the capacity to test multiple scenarios/versions of ODE models *in silico* has informed on the transitional pathway dynamics which underpin differentiation of embryonic stem cells to neuroprogenitor

cells(Stumpf *et al.*, 2017). In murine bone marrow derived macrophages and fibroblasts, the use of ODE modelling and model iteration has also revealed how the regulation of diverse pathogen response programmes by TFs (NFκB, IRFs, AP-1) is coordinated, as well as stimulus specific durational responses during NFκB activation (Cheng *et al.*, 2017)(Sen *et al.*, 2019). Mathematical modelling therefore allows unprecedented opportunity to test diverse hypotheses and unrestricted reiterative analyses. In LCs, the power of Petri-net modelling of GRNs for investigating immunogenic responses in response to divergent stimuli (TNFα and TSLP) has been shown (Polak *et al.*, 2017). ODE modelling has also been used to predict the pathway of LC repopulation from progenitor cells in murine models of GVHD (Ferrer *et al.*, 2019). However, until now the utilisation of ODE mathematical modelling, to investigate the GRNs mediating the decision-making process between immunogenic vs tolerogenic LC regulation, was unexplored.

Overall, in this project the application of broad cutting-edge scientific methods, such as bulk and single cell transcriptomic analysis, functional *in vitro* experimentation using primary tissues and mathematical modelling, allowed wide-spectrum, comprehensive analyses. This allowed us to discern the unique transcriptomic programmes underlying DC/LC tolerance; the immunological differences between LCs and other DC subtypes; identify critical mediators of human LC tolerance and determine the underlying TF regulatory networks which govern the propensity for the activation of different LC immune activation pathways.

8.2 Key findings and main conclusions:

1. **LC tolerogenic transcriptomic programmes are largely distinct compared to other DC subtypes**

- MoDC model systems of DC tolerance revealed a lack of a uniform tolerogenic signature is induced in the context of tolerogenic stimuli/conditions, other than downregulation of inflammatory signalling.
- LC transcriptomes are largely unique to other tolerogenic associated MoDC and tissue derived DC (DDC, PlaDC), with few common tolerogenic associated pathways identified.

2. **Migration and immunocompetency enhance LC tolerogenic function**

- Steady-state LC and migrated LC transcriptomes are distinct, with enhanced tolerogenic programming observed in migrated LCs.
- The heterogeneity exhibited between steady-state and migrated LC populations from breast skin derived LCs and foreskin LCs revealed the importance of the tissue microenvironment in regulating LC phenotypes.
- Immunocompetency of LC is critical for the capacity to induce Tregs.

- LC induction of Tregs is enhanced in migrated LCs compared to steady-state LCs.

3. A GRN underpins immunogenic vs tolerogenic LC activation

- *IRF4, RELB* (non-canonical NFκB) and *IRF1* seem to be the key TF regulating LC tolerogenicity vs immunogenicity
- Subtle changes in genomic programming, determined by an immunogenic (*IRF1±IRF4*) vs tolerogenic (*IRF4/MAP3K14/RELB*) TF regulatory axis, may alter LC phenotypes to favour immunogenic vs tolerogenic responses.

8.3 The distinct transcriptomics underlying LC immune regulation were revealed

Analysis of MoDC transcriptomes revealed that distinct tolerogenic gene regulation are induced under tolerogenic conditions, which we initially postulated could be common across different DC subtypes. Whilst tolerogenic MoDC signatures were overall unique, we discovered *MYC* to be consistently upregulated across different tolerogenic conditions (Dex/VitD3, IL-10, MPLA-Dex), highlighting it as potential key regulator of DC tolerogenic function. Using the LC IRF-GRN we identified a hypothetical co-repressive interaction between *MYC* and *IRF1/IRF4,* which when incorporated into the model could be shown to control a switch between immunogenic and tolerogenic MoDC profiles. Interestingly, in both breast skin and foreskin steady-state LCs, we observed an increase in *MYC* expression and enhancement of the *MYC* regulon, which contrasted migrated LCs that showed increased *IRF4* expression and enhancement of the *IRF4* regulon. Furthermore, *MYC* and *IRF4* were differentially regulated between steady-state and migrated LC, respectively. This could therefore suggest that the co-repressive interaction between these TFs is present in LCs. However, in CRISPR-Cas9 *IRF4* knockout in human LC, changes in *MYC* expression were not detected (Sirvent *et al.*, 2020). Furthermore, our analysis has highlighted a possible role of *IRF4* in tolerogenic regulation, which has also been demonstrated by others (Vander Lugt, Riddell, Aly A Khan, *et al.*, 2017)(Honma *et al.*, 2005)(Akbari *et al.*, 2014)(Sirvent *et al.*, 2020), therefore disputing *MYC* repression of *IRF4* expression as a mechanism for tolerance induction in LC. Investigations into the presence of this possible co-repression mechanism in MoDCs, through CRISPR-Ca9 knockouts, siRNAs or small molecular inhibitors of *MYC* and *IRF4*, could reveal if this is a mechanism utilised in other DC subtypes. With consideration of our transcriptomic and mathematical modelling results, displaying the vast differences between LCs and MoDC programming and our understanding of their differing ontologies and *in vitro* generation, we must appreciate that mechanisms of immune regulation in different DC subsets could greatly differ. Our analysis overall allowed us to conclude that MoDCs would not be the most applicable model for understanding true LC biology, leading us to focus our analysis in the project and in future studies

on using primary human LCs. Due to the distinctness of MoDC transcriptomes compared to tissue derived DCs, and the distinctness between tissue derived DCs themselves, we would furthermore advise caution when universally reflecting MoDC tolerogenic function to conventional DCs.

Tolerogenic programming of DC is elusive and despite our extensive explorations comparing different DC subtype transcriptomic programmes, a consistent tolerogenic signature was not identified, thus highlighting the overall complexity of DC tolerance regulation. Strikingly revealed from comparative analysis between LCs to other DC subtypes however, were their unique transcriptomic profiles, in which LCs displayed preferentially decreased expression of inflammatory associated genes. This overall highlighted that the regulation of LC tolerance was likely distinct to other DCs. The specific requirements for LC tolerogenic regulation has been speculated to be due to their residence in the epidermal skin compartment, which is highly exposed to diverse antigenic stimuli and must be responded to appropriately to prevent harmful inflammation (Nestle *et al.*, 2009)(Clayton *et al.*, 2017). LCs are not the only APCs found within skin however, with DDCs situated in the underlying dermis. Confusingly, in substantial studies, LCs seem dispensable for immunity to antigen and infectious agents, suggesting that the presence of DDCs in skin is sufficient for protecting immune responses (Shklovskaya *et al.*, 2011)(Ritter *et al.*, 2004)(Allan *et al.*, 2003). Whilst this may suggest a predominant role for LC tolerogenic responses, skin residing DDCs are also linked with tolerogenic function (Haniffa, Gunawan and Jardine, 2015)(Chu *et al.*, 2012). However, we revealed that alongside the diverse regulation of the whole transcriptome, the expression of tolerogenic programmes varied between LCs and DDC populations, including the regulation of *IDO1* expression. This therefore implies that whilst tolerance regulation is associated with populations from both epidermal and dermal skin compartments, the mechanisms and pathways differ, reflecting the divergent homeostatic requirements of each respective tissue. We propose that the reasons for different programmes induced in LCs and DDCs from epidermal and dermal tissues, respectively, could be due to the extent that they are exposed to external stimuli. In the steady-state and when skin barriers are only partially obstructed at the epidermis, the threat of pathogenic invasion is minimal and a more regulatory approach coordinated by LCs may be required (Doebel, Voisin and Nagao, 2017). Furthermore, the epidermal tissue is more highly exposed to abundant and ubiquitous stimuli, highlighting the importance for precise regulatory instructions. When both the epidermal and dermal barriers are breached and the threat of pathogen invasion is increased, DDCs may need to more extensively switch from a tolerogenic steady-state programme to an effective inflammatory programme to prevent establishment of infection (van der Aar *et al.*, 2013). This difference in programming is likely influenced by the lifelong residence of LCs within the epidermal microenvironment and distinct ontogeny, which conditions LCs for certain immunological pathways. Thus, LC tolerance is likely unique and specifically required

at epidermal tissues, whilst the mechanisms of DDC tolerance regulation may be more consistently observed across conventional DC subtypes. However, similar comparative analysis between DDCs and other conventional DC types would need to be performed to validate this. To more comprehensively confer the difference between skin DCs at different states to discern key biological functions, single transcriptomic datasets containing all known DDC populations and LCs could be analysed together, at the steady-state and post-migration.

8.4 Understanding the roles of steady-state and migrated LC in tolerance regulation

We had originally hypothesised that LCs in the steady-state would be more associated with tolerance and would therefore exhibit tolerogenic associated genes within their transcriptomes. Reduced inflammatory cytokine expression was consistently observed in LC compared to conventional DC subpopulations. Common pathways identified across tolerogenic *in vitro* DCs, tissue derived DCs and steady-state LCs, included negative regulation of response to stimulus, signal transduction and cell communication. These pathways therefore reflect a state of active immunosuppression to inflammatory or immune activating stimuli in steady-state LC, that could be a mechanism for restricting inflammatory signalling pathways at the highly exposed epidermis. Current concepts in DC biology include the theory that immaturity and inertia to activation are key to DC tolerance (Banchereau and Steinman, 1998)(Steinman *et al.*, 2000)(Mellman and Steinman, 2001). However, from our *in vitro* experiments on steady-state LCs, we strikingly revealed that immunocompetency is fundamental for LCs ability to induce Tregs. This revelation was more in line with several studies of DC tolerance, which highlight the importance of DC maturity (Yamazaki *et al.*, 2003)(Kryczanowsky *et al.*, 2016)(Munn *et al.*, 2002). Thus, this implies that for Treg induction to occur, LCs must be immunologically active and equipped to physically interact with T cells, whilst mediating immunosuppressive processes to downregulate inflammatory signalling. Whilst we cannot disagree that in some contexts, DC immaturity is important for T cell tolerance induction, the assumption that this is the most defined mechanism for tolerance induction could be opposed from our understanding of circumstances in which inflammatory T cells are activated when not regulated appropriately by DC. For example, in contexts where DCs are dysregulated and T cells response are inappropriately initiated, inflammatory autoimmune conditions, such as psoriasis, can occur (Cruz *et al.*, 2018). Furthermore, ablation of LC in mice exacerbates Th2 cytokine production in house dust mice allergen (HDM) stimulated T cells, in models of epicutaneous sensitisation (Deckers *et al.*, 2017). In the skin, CD103+ resident memory T cells also reside within epidermis tissue, primed for responsiveness to reencountered pathogens (Cruz *et al.*, 2018). As epidermal T cells are positioned to quickly and actively respond to antigen and mediate inflammation, the ability

for LCs to actively modulate T cell activity at the steady-state through immunosuppressive influences, suggests the vitalness of this function to prevent unwarranted inflammatory T cell activation and thus maintain homeostasis in non-inflammatory conditions. Skin T cells have also been shown to support keratinocyte growth and development through insulin like growth factor 1 (IGF1) production and IL-22 production (Toulon *et al.*, 2009)(Wolk and Sabat, 2006). Active cross talk with LC to suppress unwarranted T cell activation may therefore also be critical for upholding the epidermal barrier.

The enrichment of our defined tolerogenic gene programmes was minimal in steady-state LCs and as discussed, immunocompetency appeared to be the critical influencer for tolerance induction. To further validate the criticalness of immunocompetency and even specific molecules for Treg induction, we could perform co-cultures in the presence of co-stimulatory molecule inhibitors. Interestingly, inhibition of CD86 or CD80 in human MoDC, can enhance or inhibit Treg activity, respectively (Zheng *et al.*, 2004)(Perez *et al.*, 2008). Therefore, inhibition of CD86 expression in LCs would determine if it is utilised in a more tolerogenic mechanism, or similarly dispensable for tolerogenic function. In comparison to steady-state LCs, migrated LC from breast, abdominal and foreskin tissues were consistently observed to be enriched for tolerogenic gene modules, which included *IDO1*, coupled with immunocompetency. We further validated the importance of *IDO1* expression for Treg induction *in vitro,* in which inhibition of *IDO1* decreased tolerogenic potential. Performing costimulatory molecule inhibition experiments on migrated LC would therefore reveal the dependence of immunocompetency in the context of tolerogenic gene activation (*IDO1*) for effective tolerogenic function. Like the 3-step induction process (MHC, co-stimulation, cytokines) (Banchereau and Steinman, 1998)(Cruz *et al.*, 2018) which determines the potency of immunogenic activation, we suspect a similar induction process may orchestrate tolerance. Here, co-stimulatory molecules CD80 and CD86 may preferentially bind to suppressive CTLA4, instead of CD28, whilst the plethora of other tolerogenic ligands and enzymes (e.g. *IDO1, HMOX1,* LGALS1) may induce a dominantly tolerogenic context during interaction between LCs and T cells. Whilst *IDO1* was the most obvious candidate for tolerogenic regulation from our analysis, we identified several other genes upregulated in migrated LC that would be interesting to validate. This included *LGALS1, HMOX1, ALDH2* and *S100A9.* Our finding that *IDO1* inhibition does not completely aberrate LC tolerogenic function suggest these factors are also influential and the identification of similar molecular inhibitors or silencers of these molecules would therefore validate this. Overall, a resistance to overstimulation alongside an ability to communicate with T cells and promote Tregs through immunocompetency appears key for LCs to coordinate tolerance at the steady-state. However, whilst tolerogenic function of immunocompetent steady-state LCs was revealed, this was

modest compared to the tolerogenic potential of migrated LC which highly upregulated tolerogenic gene programmes, going against our initial hypothesis.

Our analysis suggests different immunological roles for steady-state LC residing in epidermal tissue and LC that have migrated from the epidermis. In line with our observations, we speculate that steady-state LCs may be responsible for the maintenance of local tissue homeostasis by inducing moderate turnover of Tregs, whilst resisting over activation and the generation of a hyperinflammatory state within epidermal tissue. Other key homeostatic functions identified to be coordinated by steady-state LC in the epidermis, include clearance of apoptotic cells and maintaining barrier integrity during antigen sampling, similar to the functions of tissue resident macrophages (West and Bennett, 2018). Hence, this may explain the reduced activity of immune effector programmes compared to migrated LC, whose main immunological role is to prime T cell responses at the lymph nodes, like classical DCs. Here, migrated LC phenotypical maturity and elevated immunocompetency, coupled with the induction of tolerogenic gene modules, may be required for priming more powerful tolerogenic T cell responses from naivety in the lymph nodes that are sufficient to induce systemic antigen tolerance. To address and validate some of these theories, we could perform comparative analysis into the functional tolerance of the LC induced Tregs to suppress T cell activation in co-culture. This would therefore reveal if Tregs induced in the context of high immunocompetency and tolerogenic stimuli (*IDO1*) by migrated LC are more potent than Tregs induced by immunocompetency alone in steady-state LC. Furthermore, whilst the ability of steady-state LC to prime Treg differentiation has been demonstrated, the ability to expand epidermal resident memory Tregs was only explored in migrated LC. Resident memory T cells are already differentiated towards Tregs and it would therefore be interesting to investigate how immunocompetency and tolerogenic factors influence expansion. If the former is the most influential on expansion, then steady-state and migrated LC expansion of resident memory Tregs could be comparable. This could therefore expose whether Treg expansion by steady-state LCs is one of their key roles in maintaining homeostasis at the epidermis. Whilst we have critically evaluated the regulation of Treg induction, other divisions of T cell tolerance induction include the promotion of T cell apoptosis and anergy (Obregon *et al.*, 2017)(Hasegawa and Matsumoto, 2018). T cell anergy and apoptosis of effector populations could therefore be measured after co-culture with LCs, through proliferation assays and annexin V staining, respectively.

Whilst immunocompetency of steady-state LC is critical for Treg induction, how responses are deviated away from immunogenic T cell activation without the tolerogenic programming seen in migrated LC is unclear. A plausible explanation could be that T cells resident in the epidermis are already primed for either regulatory or immunogenic programming. T cells have been observed to lose plasticity for polarisation into different phenotypes after a threshold of division, which is

believed to be regulated by epigenetic modifications (Grogan *et al.*, 2001)(Kaiko *et al.*, 2008). Thus, resident memory T cells in the skin would be expected to be already committed to a specific phenotype. Therefore, immunocompetent LCs could simply permit the expansion of T cells already primed to a particular state. Instead, the promotion of different T cell response could be overall conditioned by the tissue microenvironment, in which most cellular components of skin are capable of inducing cytokines and chemokines to modulate immune responses (Ho and Kupper, 2019). Here in steady-state contexts, Tregs could be preferentially active and expanded, whilst in inflammatory settings, resident immunogenic helper T cell and cytotoxic T cell populations are expanded. In this model, steady-state LCs therefore have a role for licensing and propagating already primed T cell immunological pathway, rather than actively determining them.

Our analysis of LC states incorporated investigations at opposite ends of a transitional spectrum – steady-state and migration. However, in future studies it would be informative to observe the phenotypes of LCs which remain resident within epidermal tissues after the 48-hour tissue culture, in which migrated LCs are harvested. Here, we could investigate whether LCs that do not migrate and are permanently resident in the epidermis have a distinct transcriptome with unique regulatory features. This would also allow us to discern the possibility that the two steady-state epidermal populations reflect LCs either primed for residency or migration. From UMAP plotting, steady-state 1/ immature LCs were spatially situated closer to migrated LCs. It could therefore be speculated that in an immature state, some steady-state LCs are primed for migration, whilst others follow separate trajectories to immunocompetent resident steady-state populations.

Additionally, we revealed that the tolerogenic stimuli dexamethasone augmented LC tolerogenic function to induce Tregs, which included enhanced *IDO1* expression. Our analysis could therefore highlight a specific mechanism by which corticosteroid treatment of skin disease leads to alleviation of inflammation. The characterisation of tolerogenic function from human LCs extracted from patients with inflammatory skin disease, such as atopic dermatitis, could highlight whether such LCs have dysregulated tolerance. The level of *IDO1* expression in these cells could furthermore highlight the importance of this molecule for tolerance regulation in diseased tissues.

8.5 The discovery of phenotype specific TFs that coordinate LC immunogenic vs tolerogenic responses is critical to understanding how LCs regulate immunity

A key ambition for the project was to discern the logic behind the LC immunogenic vs tolerogenic decision making process at the TF GRN level. *In vivo* analysis of human LC behaviour is unfeasible

and as discussed, *in vitro* methods are constrained. The utilisation of mathematical modelling is therefore fundamental to providing the ability to comprehend phenotypic states of LC *in situ*.

During unbiased and extensive analyses, we explored the expression of TFs across multiple datasets (LC vs other DCs) and utilised scRNA-seq in conjunction with innovative bioinformatic pipelines (ScanPy, SCENIC) to uncover phenotype specific TFs. From our scRNA-seq analysis we discovered that immunogenic gene regulation correlated with *IRF1* induction, whilst tolerogenic gene regulation correlated with upregulated *IRF4,* as well as *MAP3K14,* the activator of *RELB* and the non-canonical NFκB pathway. *IRF1* upregulation by inflammatory TNFα signalling in LC was parallel with LPS stimulated MoDCs, clearly associating its expression with immunogenic programming. It would therefore be interesting to see if *IRF1* expression is upregulated by other inflammatory mediators in LCs, to assess its universality of expression during inflammatory activation. Similar to CRISPR-Cas9 *IRF4* knockout studies in human LC (Sirvent *et al.*, 2020), knockout of *IRF1* expression in TNFα stimulated LC could therefore reveal which genes are specifically under its control, to reveal a core inflammatory LC genomic programme. Inhibition of *IRF1* and the inflammatory programme it regulates could potentially be a mechanism by which LCs could be reprogrammed for tolerance within inflamed skin tissues.

The interpretation of how *IRF4* regulates immunogenic vs tolerogenic phenotypes expression across our analyses was less defined, with it clearly being expressed across migrated LC which have immunogenic and tolerogenic properties, yet we identified a tolerogenic subcluster which had increased *IRF4* expression. Our analysis pulled similarities to the results of others who have identified immunogenic and tolerogenic response orchestration by *IRF4* in DC (Vander Lugt, Riddell, Aly A Khan, *et al.*, 2017)(Honma *et al.*, 2005)(Akbari *et al.*, 2014)(Ainsua-Enrich *et al.*, 2019)(Williams *et al.*, 2013). Mathematical modelling using the 'toggle switch' system model supported a potential dual role for *IRF4* in both immunogenic vs tolerogenic regulation and we suggest that its expression level and context with other TFs is responsible for the switch between the two phenotypes. In analysis of MoDCs, both *IRF1* and *IRF4* were included in the same upregulated programme post LPS stimulation. Thus, we propose that when *IRF4* is expressed in conjunction with *IRF1,* immunogenicity is favoured. However, other studies have revealed that *IRF4* can repress the activation of interferon-inducible genes at promoter interferon stimulated response element (ISRE) sequences through competitive binding with *IRF1* (Shaffer *et al.*, 2009). Therefore, in the steady-state, with absence of inflammatory stimuli which drive *IRF1* upregulation, elevated *IRF4* may suppress *IRF1* activity to promote tolerance. In tolerogenic LC, *IRF4* expression correlated with *MAP3K14* expression and therefore *RELB* and non-canonical NFκB activation. *RELB* has been observed to bind to *IRF4* promoter sequences in DCs (Lehtonen *et al.*, 2005), with evidence for a *IRF4*-non-canonical NFκB positive feedback loop in T cells (Boddicker *et al.*, 2015). Whilst *RELB* may

therefore simply enhance *IRF4* mediated tolerogenic programme, the non-canonical NFκB pathway is also implicated in DC tolerogenic programming (Tas *et al.*, 2007)(Manches *et al.*, 2012). CRISPR-Cas9 *RELB/MAP3K14* KO in human LC could therefore be performed for comparison with CRISPR-Cas9 *IRF4* Kos (Sirvent *et al.*, 2020) to discern the influence of each factor for LC tolerogenic programming.

With evidence of the critical role for *IRF4* in LC genomic programming during migration and maturation (Sirvent *et al.*, 2020), the increased expression of *IRF4* in tolerogenic LC further supports that maturation/immunocompetency is critical for tolerance. However, in steady-state LC the expression of *IRF4, MAP3K14* and *RELB* is sufficiently lower, yet immunocompetent LCs exist in the population. Whilst in immunocompetent steady-state LCs the expression of *IRF4* may be below a threshold of detection, it could suggest that there are differing programmes coordinating steady-state and migrated LC phenotypes, which again would reflect their differing potencies in tolerance activation. Whilst conclusions from the 'toggle switch' model propose similarities between the trajectories of steady-state and migrated LCs, independent steady-state and migrated models could be considered and tested in the future.

Mathematical modelling has been utilised extensively in the study of dynamical systems in immunology, including DCs, with variations in model complexity (Eftimie, Gillard and Cantrell, 2016). A system of 8 differential equations has been used in DCs to explore hypothetical scenarios of tumour treatments (e.g. dose timing, site of injections) in a multicompartment system (e.g. spleen, blood and tumour), with simulation matching observations from experimental data (DePillis, Gallegos and Radunskaya, 2013). Furthermore, the balance between DC regulation of immunogenic vs tolerogenic responses has also previously been explored using intricate stochastic modelling. However, unlike our 'toggle switch' ODE model, this stochastic model does not consider different phenotypes of DC, but instead postulates that the balance of effector and regulatory T cells in the system, which are homogenously activated by DC, determines immunological outcomes. In this model, the initial state of T cells within the system is therefore proposed to be more important than the phenotype of DC. Our analysis however identified the versatile nature of LC phenotypes which appear undeniably important for immunogenic vs tolerogenic regulation of T cell activation. Therefore, whilst the toggle switch ODE model is relatively simple in comparison, we believe that consideration of LC states is critically important for determining outcomes of immune activation. Future optimisations and expansions of the model to include hypothetical scenarios of LC immunogenic vs tolerogenic regulation in the context of T cells in different states could be explored.

Appendix A Tolerogenic DC gene signatures

A.1 Tolerogenic DC gene signature 1

PubMed ID	29541071	29375543	29520275	29250057	29535726	28521905	29158348
Author	Vendelova et al. 2018	Domogalla et al. 2017	Marin et al. 2018	Obregon et al. 2017	Hasegawa et al. 2018	Horton et al. 2017	Sundblad et al. 2017
Gene list	ADORA2A	CD80	FASL (FASLG)	FASL (FASLG)	BTLA	CD80	LGALS1
	ALDH1A2	CD86	HLA-G	HLA-G	CD80	CD86	LGALS3
	CCL5	FASL (FASLG)	HMOX-1	HMOX1	CD86	FASL (FASLG)	LGALS9
	CD200	HMOX-1	ICOSLG	IDO1	FASL (FASLG)	IDO1	
	PD-L1 (CD274)	IDO1	IDO1	ILT2 (LILRB1)	ICOSL	IL-10	
	CD83	IL-12	IL-10	ILT4 (LILRB2)	IDO1	PD-L1 (CD274)	
	HLA-G	IL-6	IL-27	LGALS1	IL-27	TGFB1/TGFB2	
	IDO1	ILT3 (LILRB4)	IL-35	PD-L1 (CD274)	ILT3	TRAIL (TNFSF10)	
	IL2B	ILT4 (LILRB2)	ILT2 (LILRB1)	PD-L2 (PDCD1LG2)	ILT4		
	INHBA	PD-L1 (CD274)	ILT3 (LILRB4)		LGALS9		
	ITGB8	PD-L2 (PDCD1LG2)	ILT4 (LILRB2)		PD-L1 (CD274)		
	OPTN	TRAIL (TNFSF10)	NOS2 (iNOS)		PD-L2 (PDCD1LG2)		
	RELB		PD-L1 (CD274)		THBS1		
	SLAMF1		TGF-beta		TRAIL (TNFSF10)		
	SLAMF7						
	SOCS2						
	TGFB2						
	THBS1						
	VEGFA						

Table 18. Tolerogenic DC signature 1 compilation from literature reviews.

Tolerogenic DC signature 1			
1	ADORA2A	21	INHBA
2	ALDH1A2	22	ITGB8
3	BTLA	23	LGALS1
4	CCL5	24	LGALS3
5	CD200	25	LGALS9
6	CD274	26	LILRB1
7	CD80	27	LILRB2
8	CD83	28	LILRB4
9	CD86	29	NOS2
10	EBI3	30	OPTN
11	FASLG	31	PDCD1LG2
12	HLA-G	32	RELB
13	HMOX1	33	SLAMF1
14	ICOSLG	34	SLAMF7
15	IDO1	35	SOCS2
16	IL10	36	TGFB1
17	IL12A	37	TGFB2
18	IL27p28	38	THBS1
19	IL2B	39	TNFSF10
20	IL6	40	VEGFA

Table 19. Tolerogenic DC gene signature 1 gene list.

A.2 Tolerogenic DC gene signature 2

Tolerogenic DC signature 2									
1	ABLIM3	51	EHD1	101	LGMN	151	PTPRM	201	TNFAIP3
2	ACVRL1	52	EMP2	102	LILRB4	152	RAB24	202	TNFRSF21
3	ADI1	53	EPT1	103	LIMK2	153	RASD1	203	TNS3
4	ADRB2	54	ERRFI1	104	LMCD1	154	RASGEF1B	204	TPBG
5	AHCY	55	ETS2	105	LPAR1	155	RBP4	205	TREM1
6	AHI1	56	FAM107B	106	LYRM1	156	RCN3	206	TSC22D1
7	AKR1B1	57	FBLN5	107	LYSMD3	157	RGS16	207	TSPYL2
8	ALDH2	58	FCGR2B	108	MAP3K8	158	RGS2	208	UBE2D1
9	ALOX5	59	FCGR3A	109	MAPK13	159	RIOK1	209	UBE2Q2
10	ANGPTL4	60	FHL2	110	MCL1	160	RND3	210	UGCG
11	ANKRD28	61	FN1	111	MCTP1	161	RNF103	211	VEGFA
12	ARL4A	62	FOLR2	112	ME1	162	RRAD	212	ZBTB5
13	ARRDC3	63	FPR1	113	MERTK	163	RYBP	213	ZFP36
14	BBX	64	FUT8	114	MET	164	S100A16	214	ZFX
15	BCLAF1	65	GADD45A	115	MMP19	165	S100A8	215	ZNF24
16	BNC2	66	GADD45B	116	MPP1	166	S100A9	216	ZNF354B
17	BRD2	67	GCH1	117	MS4A4A	167	SACM1L	217	ZNF462
18	C12orf57	68	GCNT3	118	MSRB2	168	SAR1A		
19	C1QA	69	GGH	119	MST4	169	SASH1		
20	C9orf72	70	GJA1	120	MTSS1	170	SAT1		
21	CCDC59	71	GLRX	121	MYO10	171	SEL1L3		
22	CCL8	72	GNG11	122	NAMPT	172	SEMA4B		
23	CD14	73	GRAMD3	123	NCF1	173	SEPP1		
24	CD163	74	GTF2IRD2	124	NFAT5	174	SERPINB2		
25	CD2AP	75	HACE1	125	NFKBIA	175	SERPING1		
26	CD55	76	HBEGF	126	NFKBIZ	176	SETD2		
27	CD86	77	HDGFRP3	127	NINJ1	177	SH3RF1		
28	CDC42EP3	78	HMGB2	128	NLRP3	178	SHE		
29	CDS1	79	HPSE	129	NPC1	179	SIRT1		
30	CDYL	80	IER5	130	NPL	180	SKIL		
31	CLDN1	81	IFITM1	131	NRN1	181	SLC18B1		
32	CLDND1	82	IFRD1	132	NUCB2	182	SLPI		
33	CLIP1	83	IFT57	133	NUPR1	183	SMPDL3A		
34	CTBS	84	IGFBP2	134	ORMDL3	184	SNCA		
35	CXCL14	85	IGFBP3	135	P2RY14	185	SNX7		
36	CXCL2	86	IGFBP7	136	PAF1	186	SOD2		
37	DCN	87	IL6	137	PAPSS2	187	STARD3NL		
38	DCUN1D3	88	IMPDH2	138	PDE4B	188	STK17A		
39	DDX21	89	IRF8	139	PELI1	189	STOM		
40	DHRS9	90	IRX3	140	PGRMC2	190	STX11		
41	DNAJA1	91	ITPKC	141	PLK3	191	TAF5L		
42	DNASE2	92	JAM2	142	PLXNA2	192	TBPL1		
43	DRAM1	93	KANK1	143	PLXNC1	193	TCHH		
44	DTNB	94	KCNJ15	144	PMEPA1	194	TFAP2C		
45	DUSP1	95	KCTD12	145	PPA1	195	TFCP2L1		
46	DUSP10	96	KLF10	146	PPAP2A	196	TFPI		
47	DUSP6	97	KRAS	147	PPP1R15A	197	THBD		
48	DYNLT3	98	LBH	148	PRKAR2B	198	TIPARP		
49	EFNB3	99	LEPREL1	149	PRKCB	199	TMEM2		
50	EGR3	100	LFNG	150	PTGS2	200	TMEM45A		

Table 20. Tolerogenic DC signature 2 gene list. Gene list was composed of the 217 genes which were co-upregulated in two or more of the tolerogenic DC conditions (Steady-state LC, PlaDC, TolMoDC, IL10MoDC) when each compared to unstimulated MoDC, as explored in **Figure 20C, Chapter 4.**

List of References

van der Aar, A. M. G. *et al.* (2013) 'Langerhans Cells Favor Skin Flora Tolerance through Limited Presentation of Bacterial Antigens and Induction of Regulatory T Cells', *Journal of Investigative Dermatology*, 133(5), pp. 1240–1249. doi: 10.1038/jid.2012.500.

Agrawal, A. *et al.* (2012) 'Dendritic cells and aging: Consequences for autoimmunity', *Expert Review of Clinical Immunology*. NIH Public Access, pp. 73–80. doi: 10.1586/eci.11.77.

Aibar, S. *et al.* (2017) 'SCENIC: Single-cell regulatory network inference and clustering', *Nature Methods*. Nature Publishing Group, 14(11), pp. 1083–1086. doi: 10.1038/nmeth.4463.

Ainsua-Enrich, E. *et al.* (2019) 'IRF4-dependent dendritic cells regulate CD8+ T-cell differentiation and memory responses in influenza infection', *Mucosal Immunology*. Nature Publishing Group, 12(4), pp. 1025–1037. doi: 10.1038/s41385-019-0173-1.

Akbari, M. *et al.* (2014) ' IRF4 in Dendritic Cells Inhibits IL-12 Production and Controls Th1 Immune Responses against Leishmania major ', *The Journal of Immunology*. The American Association of Immunologists, 192(5), pp. 2271–2279. doi: 10.4049/jimmunol.1301914.

Akira, S. (2003) 'Mammalian Toll-like receptors', *Current Opinion in Immunology*. Elsevier Current Trends, 15(1), pp. 5–11. doi: 10.1016/S0952-7915(02)00013-4.

Albert, M. L., Jegathesan, M. and Darnell, R. B. (2001) 'Dendritic cell maturation is required for the cross-tolerization of CD8+ T cells', *Nature Immunology*. Nat Immunol, 2(11), pp. 1010–1017. doi: 10.1038/ni722.

Alberts, B. *et al.* (2002a) 'B Cells and Antibodies'. Garland Science. Available at: https://www.ncbi.nlm.nih.gov/books/NBK26884/ (Accessed: 7 November 2018).

Alberts, B. *et al.* (2002b) 'The Adaptive Immune System'. Garland Science. Available at: https://www.ncbi.nlm.nih.gov/books/NBK21070/ (Accessed: 7 November 2018).

AlJanahi, A. A., Danielsen, M. and Dunbar, C. E. (2018) 'An Introduction to the Analysis of Single-Cell RNA-Sequencing Data', *Molecular Therapy - Methods and Clinical Development*. Cell Press, pp. 189–196. doi: 10.1016/j.omtm.2018.07.003.

Allan, R. S. *et al.* (2003) 'Epidermal viral immunity induced by CD8alpha+ dendritic cells but not by Langerhans cells.', *Science (New York, N.Y.)*. American Association for the Advancement of Science, 301(5641), pp. 1925–8. doi: 10.1126/science.1087576.

Altschuler, S. J. *et al.* (2010) 'Cellular Heterogeneity: Do Differences Make a Difference?', *Cell*. Wiley-Interscience, New York, 141(4), pp. 559–563. doi: 10.1016/j.cell.2010.04.033.

Alvarez, D., Vollmann, E. H. and von Andrian, U. H. (2008) 'Mechanisms and Consequences of Dendritic Cell Migration', *Immunity*. NIH Public Access, pp. 325–342. doi: 10.1016/j.immuni.2008.08.006.

Amagai, M. (2016) 'Cracking the code of skin inflammation with CD1a', *Nature Immunology*. Nature Publishing Group, 17(10), pp. 1133–1134. doi: 10.1038/ni.3557.

Amit, I. *et al.* (2009) 'Unbiased reconstruction of a mammalian transcriptional network mediating pathogen responses.', *Science (New York, N.Y.)*. NIH Public Access, 326(5950), pp. 257–63. doi:

10.1126/science.1179050.

Anderson, A. E. *et al.* (2017) 'Tolerogenic dendritic cells generated with dexamethasone and vitamin D3 regulate rheumatoid arthritis CD4 $^{+}$ T cells partly via transforming growth factor- **β** 1', *Clinical & Experimental Immunology*. Blackwell Publishing Ltd, 187(1), pp. 113–123. doi: 10.1111/cei.12870.

Ardouin, L. *et al.* (2016) 'Broad and Largely Concordant Molecular Changes Characterize Tolerogenic and Immunogenic Dendritic Cell Maturation in Thymus and Periphery', *Immunity*. Cell Press, 45(2), pp. 305–318. doi: 10.1016/J.IMMUNI.2016.07.019.

Artyomov, M. N. *et al.* (2015) 'Modular expression analysis reveals functional conservation between human Langerhans cells and mouse cross-priming dendritic cells.', *The Journal of experimental medicine*. Rockefeller University Press, 212(5), pp. 743–57. doi: 10.1084/jem.20131675.

Audiger, C. *et al.* (2017) 'The Importance of Dendritic Cells in Maintaining Immune Tolerance', *The Journal of Immunology*, 198(6), pp. 2223–2231. doi: 10.4049/jimmunol.1601629.

Ay, A. and Arnosti, D. N. (2011) 'Mathematical modeling of gene expression: A guide for the perplexed biologist', *Critical Reviews in Biochemistry and Molecular Biology*. NIH Public Access, pp. 137–151. doi: 10.3109/10409238.2011.556597.

Azukizawa, H. *et al.* (2011) 'Steady state migratory RelB+ langerin+ dermal dendritic cells mediate peripheral induction of antigen-specific CD4+CD25+Foxp3+ regulatory T cells', *European Journal of Immunology*. John Wiley & Sons, Ltd, 41(5), pp. 1420–1434. doi: 10.1002/eji.201040930.

Bainbridge, M. N. *et al.* (2006) 'Analysis of the prostate cancer cell line LNCaP transcriptome using a sequencing-by-synthesis approach.', *BMC genomics*. BioMed Central, 7, p. 246. doi: 10.1186/1471-2164-7-246.

Bajana, S. *et al.* (2012) 'IRF4 Promotes Cutaneous Dendritic Cell Migration to Lymph Nodes during Homeostasis and Inflammation', *The Journal of Immunology*, 189(7), pp. 3368–3377. doi: 10.4049/jimmunol.1102613.

Banchereau, J. and Steinman, R. M. (1998) 'Dendritic cells and the control of immunity', *Nature*. Nature Publishing Group, 392(6673), pp. 245–252. doi: 10.1038/32588.

Baratin, M. *et al.* (2015) 'Homeostatic NF-κB Signaling in Steady-State Migratory Dendritic Cells Regulates Immune Homeostasis and Tolerance', *Immunity*, 42, pp. 627–639. doi: 10.1016/j.immuni.2015.03.003.

Barbaroux, J.-B. O. *et al.* (2008) 'Epidermal receptor activator of NF-kappaB ligand controls Langerhans cells numbers and proliferation.', *Journal of immunology (Baltimore, Md. : 1950)*, 181(2), pp. 1103–8. Available at: http://www.ncbi.nlm.nih.gov/pubmed/18606662 (Accessed: 15 November 2018).

Barker, J. N. W. N. *et al.* (1991) 'Keratinocytes as initiators of inflammation', *The Lancet*. Elsevier, 337(8735), pp. 211–214. doi: 10.1016/0140-6736(91)92168-2.

Baroni, A. *et al.* (2012) 'Structure and function of the epidermis related to barrier properties', *Clinics in Dermatology*. Elsevier, 30(3), pp. 257–262. doi: 10.1016/J.CLINDERMATOL.2011.08.007.

Bazewicz, C. G. *et al.* (2019) 'Aldehyde dehydrogenase in regulatory T-cell development, immunity and cancer', *Immunology*. Blackwell Publishing Ltd, pp. 47–55. doi: 10.1111/imm.13016.

Beissert, S. *et al.* (1995) 'Supernatants from UVB radiation-exposed keratinocytes inhibit Langerhans cell presentation of tumor-associated antigens via IL-10 content', *Journal of Leukocyte Biology*. John Wiley & Sons, Ltd, 58(2), pp. 234–240. doi: 10.1002/jlb.58.2.234.

Bell, G. M. *et al.* (2017) 'Autologous tolerogenic dendritic cells for rheumatoid and inflammatory arthritis.', *Annals of the rheumatic diseases*. BMJ Publishing Group Ltd, 76(1), pp. 227–234. doi: 10.1136/annrheumdis-2015-208456.

Bentley, D. R. *et al.* (2008) 'Accurate whole human genome sequencing using reversible terminator chemistry', *Nature*. Nature Publishing Group, 456(7218), pp. 53–59. doi: 10.1038/nature07517.

Berger, C. L. *et al.* (2006) 'Langerhans cells: Mediators of immunity and tolerance', *The International Journal of Biochemistry & Cell Biology*. Pergamon, 38(10), pp. 1632–1636. doi: 10.1016/J.BIOCEL.2006.03.006.

Bernard, F.-X. *et al.* (2012) 'Keratinocytes under Fire of Proinflammatory Cytokines: Bona Fide Innate Immune Cells Involved in the Physiopathology of Chronic Atopic Dermatitis and Psoriasis', *Journal of Allergy*. Hindawi, 2012, pp. 1–10. doi: 10.1155/2012/718725.

Berthier-Vergnes, O. *et al.* (2005) 'TNF-α enhances phenotypic and functional maturation of human epidermal Langerhans cells and induces IL-12 p40 and IP-10/CXCL-10 production', *FEBS Letters*. No longer published by Elsevier, 579(17), pp. 3660–3668. doi: 10.1016/j.febslet.2005.04.087.

Bertolini, M. *et al.* (2020) 'Hair follicle immune privilege and its collapse in alopecia areata', *Experimental Dermatology*. Blackwell Publishing Ltd, pp. 703–725. doi: 10.1111/exd.14155.

Bigley, V. *et al.* (2011) 'The human syndrome of dendritic cell, monocyte, B and NK lymphoid deficiency.', *The Journal of experimental medicine*. The Rockefeller University Press, 208(2), pp. 227–34. doi: 10.1084/jem.20101459.

Bittner-Eddy, P. D. *et al.* (2016) 'Mucosal Langerhans Cells Promote Differentiation of Th17 Cells in a Murine Model of Periodontitis but Are Not Required for *Porphyromonas gingivalis* –Driven Alveolar Bone Destruction', *The Journal of Immunology*, 197(4), pp. 1435–1446. doi: 10.4049/jimmunol.1502693.

Blois, S. M. *et al.* (2007) 'Dendritic Cells: Key to Fetal Tolerance?1', *Biology of Reproduction*, 77(4), pp. 590–598. doi: 10.1095/biolreprod.107.060632.

Bobr, A. *et al.* (2012) 'Autocrine/paracrine TGF-β1 inhibits Langerhans cell migration.', *Proceedings of the National Academy of Sciences of the United States of America*. National Academy of Sciences, 109(26), pp. 10492–7. doi: 10.1073/pnas.1119178109.

Boddicker, R. L. *et al.* (2015) 'The oncogenic transcription factor IRF4 is regulated by a novel CD30/NF- B positive feedback loop in peripheral T-cell lymphoma', *Blood*, 125(20), pp. 3118–3127. doi: 10.1182/blood-2014-05-578575.

Bonelli, M. *et al.* (2019) 'IRF1 is critical for the TNF-driven interferon response in rheumatoid fibroblast-like synoviocytes: JAKinibs suppress the interferon response in RA-FLSs', *Experimental and Molecular Medicine*. Nature Publishing Group, 51(7), pp. 1–11. doi: 10.1038/s12276-019-0267-6.

Bourke, C. D. *et al.* (2015) 'Epidermal keratinocytes initiate wound healing and pro-inflammatory immune responses following percutaneous schistosome infection'. doi:

10.1016/j.ijpara.2014.11.002.

Bouslimani, A. *et al.* (2015) 'Molecular cartography of the human skin surface in 3D.', *Proceedings of the National Academy of Sciences of the United States of America*. National Academy of Sciences, 112(17), pp. E2120-9. doi: 10.1073/pnas.1424409112.

Braun, D., Longman, R. S. and Albert, M. L. (2005) 'A two-step induction of indoleamine 2,3 dioxygenase (IDO) activity during dendritic-cell maturation', *Blood*. American Society of Hematology, 106(7), pp. 2375–2381. doi: 10.1182/BLOOD-2005-03-0979.

ten Broeke, T., Wubbolts, R. and Stoorvogel, W. (2013) 'MHC class II antigen presentation by dendritic cells regulated through endosomal sorting.', *Cold Spring Harbor perspectives in biology*. Cold Spring Harbor Laboratory Press, 5(12), p. a016873. doi: 10.1101/cshperspect.a016873.

Broere, F. *et al.* (2011) 'A2 T cell subsets and T cell-mediated immunity', in *Principles of Immunopharmacology*. Basel: Birkhäuser Basel, pp. 15–27. doi: 10.1007/978-3-0346-0136-8_2.

von Bubnoff, D. *et al.* (2004) 'Human Epidermal Langerhans Cells Express the Immunoregulatory Enzyme Indoleamine 2,3-Dioxygenase', *Journal of Investigative Dermatology*. Elsevier, 123(2), pp. 298–304. doi: 10.1111/J.0022-202X.2004.23217.X.

Buermans, H. P. J. and den Dunnen, J. T. (2014) 'Next generation sequencing technology: Advances and applications', *Biochimica et Biophysica Acta (BBA) - Molecular Basis of Disease*. Elsevier, 1842(10), pp. 1932–1941. doi: 10.1016/J.BBADIS.2014.06.015.

Casey, S. C., Baylot, V. and Felsher, D. W. (2017) 'MYC: Master Regulator of Immune Privilege', *Trends in Immunology*. Elsevier Ltd, pp. 298–305. doi: 10.1016/j.it.2017.01.002.

Caux, C. *et al.* (1999) 'Respective involvement of TGF-β and IL-4 in the development of Langerhans cells and non-Langerhans dendritic cells from CD34 $^{+}$ progenitors', *Journal of Leukocyte Biology*. Wiley-Blackwell, 66(5), pp. 781–791. doi: 10.1002/jlb.66.5.781.

Chakravarti, A. *et al.* (2009) 'Surface RANKL of Toll-like receptor 4-stimulated human neutrophils activates osteoclastic bone resorption Activation of neutrophil membrane-bound RANKL was linked to tyrosine phosphorylation of Src-homology domain-containing cytosolic phospha-tase 1 with ', *Blood*, 114, pp. 1633–1644. doi: 10.1182/blood-2008.

Chaplin, D. D. (2010) 'Overview of the immune response', *Journal of Allergy and Clinical Immunology*, 125(2 SUPPL. 2), pp. 35294–2170. doi: 10.1016/j.jaci.2009.12.980.

Charles A Janeway, J. *et al.* (2001) 'T Cell-Mediated Immunity'. Garland Science. Available at: https://www.ncbi.nlm.nih.gov/books/NBK10762/ (Accessed: 27 July 2020).

Chen, G., Ning, B. and Shi, T. (2019) 'Single-cell RNA-seq technologies and related computational data analysis', *Frontiers in Genetics*. Frontiers Media S.A., p. 317. doi: 10.3389/fgene.2019.00317.

Chen, J. *et al.* (2007) 'Improved human disease candidate gene prioritization using mouse phenotype', *BMC Bioinformatics*. BioMed Central, 8(1), p. 392. doi: 10.1186/1471-2105-8-392.

Cheng, C. S. *et al.* (2017) 'Iterative Modeling Reveals Evidence of Sequential Transcriptional Control Mechanisms', *Cell Systems*, 4, pp. 330-343.e5. doi: 10.1016/j.cels.2017.01.012.

Cheng, J. B. *et al.* (2018) 'Transcriptional Programming of Normal and Inflamed Human Epidermis at Single-Cell Resolution', *Cell Reports*. Cell Press, 25(4), pp. 871–883. doi: 10.1016/J.CELREP.2018.09.006.

Chistiakov, D. A. *et al.* (2018) 'The impact of interferon-regulatory factors to macrophage differentiation and polarization into M1 and M2', *Immunobiology*. Elsevier GmbH, pp. 101–111. doi: 10.1016/j.imbio.2017.10.005.

Chopin, M. *et al.* (2013) 'Langerhans cells are generated by two distinct PU.1-dependent transcriptional networks.', *The Journal of experimental medicine*. Rockefeller University Press, 210(13), pp. 2967–80. doi: 10.1084/jem.20130930.

Chopin, M. and Nutt, S. L. (2015) 'Establishing and maintaining the Langerhans cell network', *Seminars in Cell and Developmental Biology*. Elsevier Ltd, pp. 23–29. doi: 10.1016/j.semcdb.2014.02.001.

Chorro, L. *et al.* (2009) 'Langerhans cell (LC) proliferation mediates neonatal development, homeostasis, and inflammation-associated expansion of the epidermal LC network.', *The Journal of experimental medicine*. The Rockefeller University Press, 206(13), pp. 3089–100. doi: 10.1084/jem.20091586.

Chu, C. C. *et al.* (2012) 'Resident CD141 (BDCA3) + dendritic cells in human skin produce IL-10 and induce regulatory T cells that suppress skin inflammation', *Journal of Experimental Medicine*. The Rockefeller University Press, 209(5), pp. 935–945. doi: 10.1084/jem.20112583.

Chu, C. C., Di Meglio, P. and Nestle, F. O. (2011) 'Harnessing dendritic cells in inflammatory skin diseases', *Seminars in Immunology*. Elsevier, pp. 28–41. doi: 10.1016/j.smim.2011.01.006.

Cieślik, M. and Chinnaiyan, A. M. (2017) 'Cancer transcriptome profiling at the juncture of clinical translation', *Nature Reviews Genetics*. Nature Publishing Group, 19(2), pp. 93–109. doi: 10.1038/nrg.2017.96.

Clambey, E. T. *et al.* (2014) 'Molecules in medicine mini review: the αβ T cell receptor NIH Public Access', *J Mol Med (Berl)*, 92(7), pp. 735–741. doi: 10.1007/s00109-014-1145-2.

Clark, G. J. *et al.* (1999) 'Expression of the RelB transcription factor correlates with the activation of human dendritic cells', *Immunology*. Wiley-Blackwell, 98(2), pp. 189–196. doi: 10.1046/j.1365-2567.1999.00829.x.

Clausen, B. E. and Stoitzner, P. (2015) 'Functional specialization of skin dendritic cell subsets in regulating T cell responses', *Frontiers in Immunology*. Frontiers Media S.A., 6(OCT), p. 534. doi: 10.3389/fimmu.2015.00534.

Clayton, K. *et al.* (2017) 'Langerhans Cells—Programmed by the Epidermis', *Frontiers in Immunology*. Frontiers, 8, p. 1676. doi: 10.3389/fimmu.2017.01676.

Collin, M. and Bigley, V. (2018) 'Human dendritic cell subsets: an update', *Immunology*. Blackwell Publishing Ltd, pp. 3–20. doi: 10.1111/imm.12888.

Collin, M., McGovern, N. and Haniffa, M. (2013) 'Human dendritic cell subsets.', *Immunology*. Wiley-Blackwell, 140(1), pp. 22–30. doi: 10.1111/imm.12117.

Collin, M. and Milne, P. (2016) 'Langerhans cell origin and regulation.', *Current opinion in hematology*, 23(1), pp. 28–35. doi: 10.1097/MOH.0000000000000202.

Comi, M. *et al.* (2020) 'Coexpression of CD163 and CD141 identifies human circulating IL-10-producing dendritic cells (DC-10)', *Cellular and Molecular Immunology*. Springer Nature, 17(1), pp. 95–107. doi: 10.1038/s41423-019-0218-0.

Coombes, J. L. *et al.* (2007) 'A functionally specialized population of mucosal CD103+ DCs induces Foxp3+ regulatory T cells via a TGF-β -and retinoic acid-dependent mechanism', *Journal of Experimental Medicine*. J Exp Med, 204(8), pp. 1757–1764. doi: 10.1084/jem.20070590.

Coombes, J. L. and Powrie, F. (2008) 'Dendritic cells in intestinal immune regulation.', *Nature reviews. Immunology*. Europe PMC Funders, 8(6), pp. 435–46. doi: 10.1038/nri2335.

Cruz, M. S. *et al.* (2018) 'Human αβ and γδ T cells in skin immunity and disease', *Frontiers in Immunology*. Frontiers Media S.A., p. 1. doi: 10.3389/fimmu.2018.01304.

Cumberbatch, M. *et al.* (1999) 'Tumour necrosis factor-α induces Langerhans cell migration in humans', *British Journal of Dermatology*. Br J Dermatol, 141(2), pp. 192–200. doi: 10.1046/j.1365-2133.1999.02964.x.

Cumberbatch, M., Dearman, R. J., Griffiths, C. E. M., *et al.* (2000) 'Langerhans cell migration. Experimental dermatology . Review article', *Clinical and Experimental Dermatology*. John Wiley & Sons, Ltd (10.1111), 25(5), pp. 413–418. doi: 10.1046/j.1365-2230.2000.00678.x.

Cumberbatch, M., Dearman, R. J., Uribe-Luna, S., *et al.* (2000) 'Regulation of epidermal Langerhans cell migration by lactoferrin', *Immunology*, 100(1), pp. 21–28. doi: 10.1046/j.1365-2567.2000.00014.x.

Cumberbatch, M. *et al.* (2005) 'Impact of cutaneous IL-10 on resident epidermal Langerhans' cells and the development of polarized immune responses.', *Journal of immunology (Baltimore, Md. : 1950)*, 175(1), pp. 43–50. Available at: http://www.ncbi.nlm.nih.gov/pubmed/15972630 (Accessed: 14 November 2018).

Cumberbatch, M. *et al.* (2006) 'Impaired Langerhans cell migration in psoriasis.', *The Journal of experimental medicine*. The Rockefeller University Press, 203(4), pp. 953–60. doi: 10.1084/jem.20052367.

Cumberbatch, M., Dearman, R. J. and Kimber, I. (1999) 'Inhibition by dexamethasone of Langerhans cell migration: influence of epidermal cytokine signals.', *Immunopharmacology*, 41(3), pp. 235–43. Available at: http://www.ncbi.nlm.nih.gov/pubmed/10428652 (Accessed: 18 April 2018).

Cumberbatch, M. and Kimber, I. (1992) 'Dermal tumour necrosis factor-alpha induces dendritic cell migration to draining lymph nodes, and possibly provides one stimulus for Langerhans' cell migration.', *Immunology*, 75(2), pp. 257–63. Available at: http://www.ncbi.nlm.nih.gov/pubmed/1551688 (Accessed: 17 April 2018).

Curti, A. *et al.* (2009) 'The role of indoleamine 2,3-dioxygenase in the induction of immune tolerance: focus on hematology', *Blood*. American Society of Hematology, 113(11), pp. 2394–2401. doi: 10.1182/BLOOD-2008-07-144485.

Czernielewski, J. M. and Demarchez, M. (1987) 'Further Evidence for the Self-Reproducing Capacity of Langerhans Cells in Human Skin', *Journal of Investigative Dermatology*. Elsevier, 88(1), pp. 17–20. doi: 10.1111/1523-1747.EP12464659.

van Dalen, R. *et al.* (2017) 'Staphylococcus aureus wall teichoic acid is a pathogen-associated molecular pattern that is recognized by langerin (CD207) on skin Langerhans cells', *bioRxiv*, p. 238469. doi: 10.1101/238469.

Dam, T. N. *et al.* (1996) 'The vitamin D3 analog calcipotriol suppresses the number and antigen-presenting function of Langerhans cells in normal human skin.', *The journal of investigative*

dermatology. Symposium proceedings, 1(1), pp. 72–7. Available at: http://www.ncbi.nlm.nih.gov/pubmed/9627697 (Accessed: 18 April 2018).

Davies, J. *et al.* (2019) 'Single cell transcriptomic analysis indentifies Langerhans cells immunocompetency is critical for IDO1- dependent ability to induce tolerogenic T cells', *bioRxiv*. Cold Spring Harbor Laboratory, p. 2019.12.20.884130. doi: 10.1101/2019.12.20.884130.

Deckers, J. *et al.* (2017) 'Epicutaneous sensitization to house dust mite allergen requires interferon regulatory factor 4–dependent dermal dendritic cells', *Journal of Allergy and Clinical Immunology*. Mosby Inc., 140(5), pp. 1364-1377.e2. doi: 10.1016/j.jaci.2016.12.970.

Deckers, J., Hammad, H. and Hoste, E. (2018) 'Langerhans Cells: Sensing the Environment in Health and Disease', *Frontiers in Immunology*, 9, p. 93. doi: 10.3389/fimmu.2018.00093.

Deng, Q. *et al.* (2014) 'Single-Cell RNA-Seq Reveals Dynamic, Random Monoallelic Gene Expression in Mammalian Cells', *Science*. American Association for the Advancement of Science, 343(6167), pp. 193–196. doi: 10.1126/science.1245316.

DePillis, L., Gallegos, A. and Radunskaya, A. (2013) 'A model of dendritic cell therapy for melanoma', *Frontiers in Oncology*. Frontiers Media SA, 3 MAR. doi: 10.3389/fonc.2013.00056.

Der, E. *et al.* (2019) 'Tubular cell and keratinocyte single-cell transcriptomics applied to lupus nephritis reveal type I IFN and fibrosis relevant pathways', *Nature Immunology*. Nature Publishing Group, 20(7), pp. 915–927. doi: 10.1038/s41590-019-0386-1.

Dioszeghy, V. *et al.* (2011) 'Epicutaneous Immunotherapy Results in Rapid Allergen Uptake by Dendritic Cells through Intact Skin and Downregulates the Allergen-Specific Response in Sensitized Mice', *The Journal of Immunology*, 186(10), pp. 5629–5637. doi: 10.4049/jimmunol.1003134.

Dioszeghy, V. *et al.* (2018) 'Antigen Uptake by Langerhans Cells Is Required for the Induction of Regulatory T Cells and the Acquisition of Tolerance During Epicutaneous Immunotherapy in OVA-Sensitized Mice', *Frontiers in Immunology*. Frontiers Media S.A., 9(SEP), p. 1951. doi: 10.3389/fimmu.2018.01951.

Doebel, T., Voisin, B. and Nagao, K. (2017) 'Langerhans Cells – The Macrophage in Dendritic Cell Clothing', *Trends in Immunology*. Elsevier, 540(0), pp. 448–452. doi: 10.1016/j.it.2017.06.008.

Dommett, R. *et al.* (2005) 'Innate immune defence in the human gastrointestinal tract', *Molecular Immunology*. Pergamon, 42(8), pp. 903–912. doi: 10.1016/J.MOLIMM.2004.12.004.

Domogalla, M. P. *et al.* (2017) 'Tolerance through education: How tolerogenic dendritic cells shape immunity', *Frontiers in Immunology*. Frontiers Media S.A., p. 1764. doi: 10.3389/fimmu.2017.01764.

Dorrington, M. G. and Fraser, I. D. C. (2019) 'NF-κB signaling in macrophages: Dynamics, crosstalk, and signal integration', *Frontiers in Immunology*. Frontiers Media S.A., p. 705. doi: 10.3389/fimmu.2019.00705.

Dubrac, S., Schmuth, M. and Ebner, S. (2010) 'Atopic dermatitis: the role of Langerhans cells in disease pathogenesis', *Immunology and Cell Biology*. Nature Publishing Group, 88(4), pp. 400–409. doi: 10.1038/icb.2010.33.

Duluc, D. *et al.* (2014) *Transcriptional fingerprints of antigen-presenting cell subsets in the human vaginal mucosa and skin reflect tissue-specific immune microenvironments*. doi: 10.1186/s13073-014-0098-y.

Dupuy, P. *et al.* (1991) 'Cyclosporin A Inhibits the Antigen-Presenting Functions of Freshly Isolated Human Langerhans Cells In Vitro', *Journal of Investigative Dermatology*. Elsevier, 96(4), pp. 408–413. doi: 10.1111/1523-1747.EP12469772.

Ebner, S. *et al.* (2007) 'Thymic stromal lymphopoietin converts human epidermal Langerhans cells into antigen-presenting cells that induce proallergic T cells', *Journal of Allergy and Clinical Immunology*. Mosby, 119(4), pp. 982–990. doi: 10.1016/j.jaci.2007.01.003.

Eftimie, R., Gillard, J. J. and Cantrell, D. A. (2016) *Mathematical Models for Immunology: Current State of the Art and Future Research Directions*, *Bulletin of Mathematical Biology*. doi: 10.1007/s11538-016-0214-9.

Eidsmo, L. and Martini, E. (2018) 'Human Langerhans Cells with Pro-inflammatory Features Relocate within Psoriasis Lesions', *Frontiers in Immunology*. Frontiers, 9, p. 300. doi: 10.3389/FIMMU.2018.00300.

Elias, P. M. (2007) 'The skin barrier as an innate immune element.', *Seminars in immunopathology*, 29(1), pp. 3–14. Available at: http://www.ncbi.nlm.nih.gov/pubmed/17621950 (Accessed: 7 November 2018).

Enk, A. H. and Katz, S. I. (1992) 'Identification and induction of keratinocyte-derived IL-10.', *Journal of immunology (Baltimore, Md. : 1950)*, 149(1), pp. 92–5. Available at: http://www.ncbi.nlm.nih.gov/pubmed/1607665 (Accessed: 14 November 2018).

Epaulard, O. *et al.* (2014) 'Macrophage- and Neutrophil-Derived TNF-α Instructs Skin Langerhans Cells To Prime Antiviral Immune Responses', *The Journal of Immunology*. The American Association of Immunologists, 193(5), pp. 2416–2426. doi: 10.4049/jimmunol.1303339.

Esra, R. T. *et al.* (2016) 'Does HIV exploit the inflammatory milieu of the male genital tract for successful infection?', *Frontiers in Immunology*. Frontiers Research Foundation, p. 1. doi: 10.3389/fimmu.2016.00245.

Fahrbach, K. M. *et al.* (2010) 'Enhanced cellular responses and environmental sampling within inner foreskin explants: Implications for the foreskin's role in HIV transmission', *Mucosal Immunology*. Nature Publishing Group, 3(4), pp. 410–418. doi: 10.1038/mi.2010.18.

Falcón-Beas, C. *et al.* (2019) 'Dexamethasone turns tumor antigen-presenting cells into tolerogenic dendritic cells with T cell inhibitory functions', *Immunobiology*. Elsevier GmbH, 224(5), pp. 697–705. doi: 10.1016/j.imbio.2019.05.011.

Fallarino, F. *et al.* (2006) 'The Combined Effects of Tryptophan Starvation and Tryptophan Catabolites Down-Regulate T Cell Receptor ζ-Chain and Induce a Regulatory Phenotype in Naive T Cells', *The Journal of Immunology*. The American Association of Immunologists, 176(11), pp. 6752–6761. doi: 10.4049/jimmunol.176.11.6752.

Ferreira, G. B. *et al.* (2015) 'Vitamin D3 Induces Tolerance in Human Dendritic Cells by Activation of Intracellular Metabolic Pathways', *Cell Reports*, 10(5), pp. 711–725. doi: 10.1016/j.celrep.2015.01.013.

Ferrer, I. R. *et al.* (2019) 'A wave of monocytes is recruited to replenish the long-term Langerhans cell network after immune injury', *Science Immunology*. American Association for the Advancement of Science, 4(38). doi: 10.1126/sciimmunol.aax8704.

Fricke, I. and Gabrilovich, D. I. (2006) 'Dendritic cells and tumor microenvironment: A dangerous liaison', *Immunological Investigations*. NIH Public Access, pp. 459–483. doi:

10.1080/08820130600803429.

Fucikova, J. *et al.* (2019) 'Induction of tolerance and immunity by dendritic cells: Mechanisms and clinical applications', *Frontiers in Immunology*. Frontiers Media S.A. doi: 10.3389/fimmu.2019.02393.

Gabriele, L. *et al.* (2006) 'IRF-1 deficiency skews the differentiation of dendritic cells toward plasmacytoid and tolerogenic features', *Journal of Leukocyte Biology*, 80(6), pp. 1500–1511. doi: 10.1189/jlb.0406246.

Gabriele, L. and Ozato, K. (2007) 'The role of the interferon regulatory factor (IRF) family in dendritic cell development and function', *Cytokine & Growth Factor Reviews*, 18(5), pp. 503–510. doi: 10.1016/j.cytogfr.2007.06.008.

García-González, P. A. *et al.* (2019) 'Regulation of Tolerogenic Features on Dexamethasone-Modulated MPLA-Activated Dendritic Cells by MYC', *Frontiers in Immunology*. Frontiers Media S.A., 10(MAY), p. 1171. doi: 10.3389/fimmu.2019.01171.

Gardner, T. S., Cantor, C. R. and Collins, J. J. (2000) 'Construction of a genetic toggle switch in Escherichia coli', *Nature*. Nature Publishing Group, 403(6767), pp. 339–342. doi: 10.1038/35002131.

Ghigo, C. *et al.* (2013) 'Multicolor fate mapping of Langerhans cell homeostasis.', *The Journal of experimental medicine*. Rockefeller University Press, 210(9), pp. 1657–64. doi: 10.1084/jem.20130403.

Giannoukakis, N. *et al.* (2011) 'Phase I (safety) study of autologous tolerogenic dendritic cells in type 1 diabetic patients', *Diabetes Care*, 34(9), pp. 2026–2032. doi: 10.2337/dc11-0472.

Gierahn, T. M. *et al.* (2017) 'Seq-Well: portable, low-cost RNA sequencing of single cells at high throughput', *Nature Methods*. Nature Publishing Group, 14(4), pp. 395–398. doi: 10.1038/nmeth.4179.

Gilboa, E. (2004) 'Knocking the SOCS1 off dendritic cells', *Nature Biotechnology*. Nature Publishing Group, pp. 1521–1522. doi: 10.1038/nbt1204-1521.

Ginhoux, F. and Merad, M. (2010) 'Ontogeny and homeostasis of Langerhans cells', *Immunology & Cell Biology*. John Wiley & Sons, Ltd, 88(4), pp. 387–392. doi: 10.1038/icb.2010.38.

Girardeau-Hubert, S. *et al.* (2019) 'Reconstructed Skin Models Revealed Unexpected Differences in Epidermal African and Caucasian Skin', *Scientific Reports*. Nature Publishing Group, 9(1). doi: 10.1038/s41598-019-43128-3.

Girardeau, S. *et al.* (2009) 'The Caucasian and African skin types differ morphologically and functionally in their dermal component', *Experimental Dermatology*. Blackwell Publishing Ltd, 18(8), pp. 704–711. doi: 10.1111/j.1600-0625.2009.00843.x.

Gnanaprakasam, J. N. R. and Wang, R. (2017) 'MYC in regulating immunity: Metabolism and beyond', *Genes*. MDPI AG. doi: 10.3390/genes8030088.

Gorvel, L. *et al.* (2014) 'Myeloid decidual dendritic cells and immunoregulation of pregnancy: defective responsiveness to Coxiella burnetii and Brucella abortus.', *Frontiers in cellular and infection microbiology*. Frontiers Media SA, 4, p. 179. doi: 10.3389/fcimb.2014.00179.

Grabbe, S. *et al.* (1995) 'Removal of the majority of epidermal Langerhans cells by topical or

systemic steroid application enhances the effector phase of murine contact hypersensitivity.', *The Journal of Immunology*, 155(9).

Griesbeck, M. *et al.* (2015) 'Sex Differences in Plasmacytoid Dendritic Cell Levels of IRF5 Drive Higher IFN- Production in Women', *The Journal of Immunology*. The American Association of Immunologists, 195(11), pp. 5327–5336. doi: 10.4049/jimmunol.1501684.

Grogan, J. L. *et al.* (2001) 'Early transcription and silencing of cytokine genes underlie polarization of T helper cell subsets', *Immunity*. Cell Press, 14(3), pp. 205–215. doi: 10.1016/S1074-7613(01)00103-0.

Grumont, R. J. and Gerondakis, S. (2000) 'Rel induces interferon regulatory factor 4 (IRF-4) expression in lymphocytes: modulation of interferon-regulated gene expression by rel/nuclear factor kappaB.', *The Journal of experimental medicine*. The Rockefeller University Press, 191(8), pp. 1281–92. Available at: http://www.ncbi.nlm.nih.gov/pubmed/10770796 (Accessed: 25 January 2019).

Habib, M. *et al.* (2007) 'Cutting edge: small molecule CD40 ligand mimetics promote control of parasitemia and enhance T cells producing IFN-gamma during experimental Trypanosoma cruzi infection.', *Journal of immunology (Baltimore, Md. : 1950)*, 178(11), pp. 6700–4. Available at: http://www.ncbi.nlm.nih.gov/pubmed/17513713 (Accessed: 7 November 2018).

Hadeiba, H. *et al.* (2008) 'CCR9 expression defines tolerogenic plasmacytoid dendritic cells able to suppress acute graft-versus-host disease', *Nature Immunology*. Nat Immunol, 9(11), pp. 1253–1260. doi: 10.1038/ni.1658.

Hammer, M. *et al.* (2006) 'Dual specificity phosphatase 1 (DUSP1) regulates a subset of LPS-induced genes and protects mice from lethal endotoxin shock', *Journal of Experimental Medicine*. The Rockefeller University Press, 203(1), pp. 15–20. doi: 10.1084/jem.20051753.

Hammers, C. M. and Stanley, J. R. (2016) 'Mechanisms of Disease: Pemphigus and Bullous Pemphigoid', *Annual Review of Pathology: Mechanisms of Disease*. Annual Reviews Inc., 11, pp. 175–197. doi: 10.1146/annurev-pathol-012615-044313.

Hampton, H. R. and Chtanova, T. (2019) 'Lymphatic migration of immune cells', *Frontiers in Immunology*. Frontiers Media S.A., p. 1168. doi: 10.3389/fimmu.2019.01168.

Haniffa, M. *et al.* (2012) 'Human Tissues Contain CD141 hi Cross-Presenting Dendritic Cells with Functional Homology to Mouse CD103 + Nonlymphoid Dendritic Cells', *Immunity*. Immunity, 37(1), pp. 60–73. doi: 10.1016/j.immuni.2012.04.012.

Haniffa, M., Gunawan, M. and Jardine, L. (2015) 'Human skin dendritic cells in health and disease.', *Journal of dermatological science*. Elsevier, 77(2), pp. 85–92. doi: 10.1016/j.jdermsci.2014.08.012.

Harden, J. L. *et al.* (2011) 'Dichotomous Effects of IFN-γ on Dendritic Cell Function Determine the Extent of IL-12–Driven Antitumor T Cell Immunity', *The Journal of Immunology*. The American Association of Immunologists, 187(1), pp. 126–132. doi: 10.4049/jimmunol.1100168.

Harden, J. L. and Egilmez, N. K. (2012) 'Indoleamine 2,3-dioxygenase and dendritic cell tolerogenicity', *Immunological Investigations*. NIH Public Access, 41(6–7), pp. 738–764. doi: 10.3109/08820139.2012.676122.

Harman, A. N. *et al.* (2013) 'Identification of Lineage Relationships and Novel Markers of Blood and Skin Human Dendritic Cells', *The Journal of Immunology*, 190(1), pp. 66–79. doi:

10.4049/jimmunol.1200779.

Hasegawa, H. and Matsumoto, T. (2018) 'Mechanisms of Tolerance Induction by Dendritic Cells In Vivo.', *Frontiers in immunology*. Frontiers Media SA, 9, p. 350. doi: 10.3389/fimmu.2018.00350.

Hashimshony, T. *et al.* (2012) 'CEL-Seq: single-cell RNA-Seq by multiplexed linear amplification.', *Cell reports*. Elsevier, 2(3), pp. 666–73. doi: 10.1016/j.celrep.2012.08.003.

Hatakeyama, M. *et al.* (2017) 'Anti-Inflammatory Role of Langerhans Cells and Apoptotic Keratinocytes in Ultraviolet-B–Induced Cutaneous Inflammation', *The Journal of Immunology*, 199(8), pp. 2937–2947. doi: 10.4049/jimmunol.1601681.

Hayden, M. S. and Ghosh, S. (2011) 'NF-κB in immunobiology', *Cell Research*. Nature Publishing Group, pp. 223–244. doi: 10.1038/cr.2011.13.

Hayden, M. S., West, A. P. and Ghosh, S. (2006) 'NF-κB and the immune response', *Oncogene*. Nature Publishing Group, pp. 6758–6780. doi: 10.1038/sj.onc.1209943.

He, Z. *et al.* (2019) 'Metabolic regulation of dendritic cell differentiation', *Frontiers in Immunology*. Frontiers Media S.A., p. 410. doi: 10.3389/fimmu.2019.00410.

Heath, W. R. and Carbone, F. R. (2013) 'The skin-resident and migratory immune system in steady state and memory: innate lymphocytes, dendritic cells and T cells', *Nature Immunology*. Nature Publishing Group, 14(10), pp. 978–985. doi: 10.1038/ni.2680.

Heesters, B. A., Myers, R. C. and Carroll, M. C. (2014) 'Follicular dendritic cells: Dynamic antigen libraries', *Nature Reviews Immunology*. Nature Publishing Group, pp. 495–504. doi: 10.1038/nri3689.

Hemmi, H. *et al.* (2001) 'Skin antigens in the steady state are trafficked to regional lymph nodes by transforming growth factor-β1-dependent cells', *International Immunology*. Oxford University Press, 13(5), pp. 695–704. doi: 10.1093/intimm/13.5.695.

Henry, C. J. *et al.* (2008) 'IL-12 produced by dendritic cells augments CD8+ T cell activation through the production of the chemokines CCL1 and CCL17.', *Journal of immunology (Baltimore, Md. : 1950)*. NIH Public Access, 181(12), pp. 8576–84. Available at: http://www.ncbi.nlm.nih.gov/pubmed/19050277 (Accessed: 7 November 2018).

Ho, A. W. and Kupper, T. S. (2019) 'T cells and the skin: from protective immunity to inflammatory skin disorders', *Nature Reviews Immunology*. Nature Publishing Group, pp. 490–502. doi: 10.1038/s41577-019-0162-3.

Hoeffel, G. *et al.* (2012) 'Adult Langerhans cells derive predominantly from embryonic fetal liver monocytes with a minor contribution of yolk sac-derived macrophages', *Journal of Experimental Medicine*, 209(6), pp. 1167–1181. doi: 10.1084/jem.20120340.

Hoffmann, A. (2016) 'Immune Response Signaling: Combinatorial and Dynamic Control', *Trends in Immunology*. Elsevier Ltd, pp. 570–572. doi: 10.1016/j.it.2016.07.003.

Honma, K. *et al.* (2005) 'Interferon regulatory factor 4 negatively regulates the production of proinflammatory cytokines by macropages in response to LPS', *Proceedings of the National Academy of Sciences of the United States of America*. National Academy of Sciences, 102(44), pp. 16001–16006. doi: 10.1073/pnas.0504226102.

Horton, C., Shanmugarajah, K. and Fairchild, P. J. (2017) 'Harnessing the properties of dendritic

cells in the pursuit of immunological tolerance', *Biomedical Journal*. Elsevier B.V., 40(2), pp. 80–93. doi: 10.1016/j.bj.2017.01.002.

Huang, D. W., Sherman, B. T. and Lempicki, R. A. (2008) 'Systematic and integrative analysis of large gene lists using DAVID bioinformatics resources', *Nature Protocols*, 4(1), pp. 44–57. doi: 10.1038/nprot.2008.211.

Huang, Q. *et al.* (2001) 'The Plasticity of Dendritic Cell Responses to Pathogens and Their Components', *Science*, 294(5543).

Huang, S. *et al.* (2007) 'Bifurcation dynamics in lineage-commitment in bipotent progenitor cells', *Developmental Biology*. Academic Press Inc., 305(2), pp. 695–713. doi: 10.1016/j.ydbio.2007.02.036.

Hubo, M. *et al.* (2013) 'Costimulatory molecules on immunogenic versus tolerogenic human dendritic cells.', *Frontiers in immunology*. Frontiers Media SA, 4, p. 82. doi: 10.3389/fimmu.2013.00082.

Hunger, R. E. *et al.* (2004) 'Langerhans cells utilize CD1a and langerin to efficiently present nonpeptide antigens to T cells.', *The Journal of clinical investigation*. American Society for Clinical Investigation, 113(5), pp. 701–8. doi: 10.1172/JCI19655.

Hussain, L. A., Lehner, T. and Thomas, S. (1995) *Comparative investigation of Langerhans' cells and potential receptors for HIV in oral, genitourinary and rectal epithelia*, *Immunology*. Available at: https://www.ncbi.nlm.nih.gov/pmc/articles/PMC1383923/pdf/immunology00069-0131.pdf (Accessed: 9 November 2018).

Huynh-Thu, V. A. *et al.* (2010) 'Inferring Regulatory Networks from Expression Data Using Tree-Based Methods', *PLoS ONE*. Edited by M. Isalan. Public Library of Science, 5(9), p. e12776. doi: 10.1371/journal.pone.0012776.

Hwang, B., Lee, J. H. and Bang, D. (2018) 'Single-cell RNA sequencing technologies and bioinformatics pipelines', *Experimental and Molecular Medicine*. Nature Publishing Group, p. 96. doi: 10.1038/s12276-018-0071-8.

Igyártó, B. Z. *et al.* (2011) 'Skin-Resident Murine Dendritic Cell Subsets Promote Distinct and Opposing Antigen-Specific T Helper Cell Responses', *Immunity*, 35(2), pp. 260–272. doi: 10.1016/j.immuni.2011.06.005.

Imai, Y. *et al.* (2008) 'Freshly isolated Langerhans cells negatively regulate naïve T cell activation in response to peptide antigen through cell-to-cell contact', *Journal of Dermatological Science*. Elsevier, 51(1), pp. 19–29. doi: 10.1016/J.JDERMSCI.2008.01.005.

Irla, M. *et al.* (2010) 'MHC class II-restricted antigen presentation by plasmacytoid dendritic cells inhibits T cell-mediated autoimmunity', *Journal of Experimental Medicine*. The Rockefeller University Press, 207(9), pp. 1891–1905. doi: 10.1084/jem.20092627.

Iweala, O. I. and Nagler, C. R. (2006) 'Immune privilege in the gut: the establishment and maintenance of non-responsiveness to dietary antigens and commensal flora', *Immunological Reviews*. John Wiley & Sons, Ltd, 213(1), pp. 82–100. doi: 10.1111/j.1600-065X.2006.00431.x.

Joost, S. *et al.* (2016) 'Single-Cell Transcriptomics Reveals that Differentiation and Spatial Signatures Shape Epidermal and Hair Follicle Heterogeneity', *Cell Systems*. Cell Press, 3(3), pp. 221-237.e9. doi: 10.1016/j.cels.2016.08.010.

Joost, S. *et al.* (2018) 'Single-Cell Transcriptomics of Traced Epidermal and Hair Follicle Stem Cells Reveals Rapid Adaptations during Wound Healing', *CellReports*, 25, pp. 585-597.e7. doi: 10.1016/j.celrep.2018.09.059.

Kaiko, G. E. *et al.* (2008) 'Immunological decision-making: how does the immune system decide to mount a helper T-cell response?', *Immunology*. Wiley-Blackwell, 123(3), pp. 326–38. doi: 10.1111/j.1365-2567.2007.02719.x.

Kaisho, T. and Akira, S. (2001) 'Dendritic-cell function in Toll-like receptor- and MyD88-knockout mice', *Trends in Immunology*. Elsevier Current Trends, 22(2), pp. 78–83. doi: 10.1016/S1471-4906(00)01811-1.

Kanitakis, J., Petruzzo, P. and Dubernard, J.-M. (2004) 'Turnover of Epidermal Langerhans' Cells', *New England Journal of Medicine*. Massachusetts Medical Society , 351(25), pp. 2661–2662. doi: 10.1056/NEJM200412163512523.

Kaplan, D. H. *et al.* (2005) 'Epidermal Langerhans cell-deficient mice develop enhanced contact hypersensitivity', *Immunity*. Immunity, 23(6), pp. 611–620. doi: 10.1016/j.immuni.2005.10.008.

Kaplan, D. H. (2017) 'Ontogeny and function of murine epidermal Langerhans cells', *Nature Immunology*. Nature Publishing Group, pp. 1068–1075. doi: 10.1038/ni.3815.

Karwacz, K. *et al.* (2017) 'Critical role of IRF1 and BATF in forming chromatin landscape during type 1 regulatory cell differentiation', *Nature Immunology*. Nature Publishing Group, 18(4), pp. 412–421. doi: 10.1038/ni.3683.

Kashem, S. W., Haniffa, M. and Kaplan, D. H. (2017) 'Antigen-Presenting Cells in the Skin', *Annual Review of Immunology*. Annual Reviews , 35(1), pp. 469–499. doi: 10.1146/annurev-immunol-051116-052215.

Katz, S. I., Tamaki, K. and Sachs, D. H. (1979) 'Epidermal Langerhans cells are derived from cells originating in bone marrow', *Nature*. Nature Publishing Group, 282(5736), pp. 324–326. doi: 10.1038/282324a0.

Kautz-Neu, K. *et al.* (2011) 'Langerhans cells are negative regulators of the anti-Leishmania response.', *The Journal of experimental medicine*. The Rockefeller University Press, 208(5), pp. 885–91. doi: 10.1084/jem.20102318.

Keir, M. E. *et al.* (2008) 'PD-1 and its ligands in tolerance and immunity', *Annual Review of Immunology*. Annual Reviews , pp. 677–704. doi: 10.1146/annurev.immunol.26.021607.090331.

Kel, J. M. *et al.* (2010) 'TGF- Is Required To Maintain the Pool of Immature Langerhans Cells in the Epidermis', *The Journal of Immunology*, 185(6), pp. 3248–3255. doi: 10.4049/jimmunol.1000981.

Kelly, B. and O'Neill, L. A. J. (2015) 'Metabolic reprogramming in macrophages and dendritic cells in innate immunity', *Cell Research*. Nature Publishing Group, pp. 771–784. doi: 10.1038/cr.2015.68.

Kim, J. H. *et al.* (2016) 'CD1a on Langerhans cells controls inflammatory skin disease', *Nature Immunology*, 17(10), pp. 1159–1166. doi: 10.1038/ni.3523.

King, J. K. *et al.* (2015) 'Langerhans Cells Maintain Local Tissue Tolerance in a Model of Systemic Autoimmune Disease.', *Journal of immunology (Baltimore, Md. : 1950)*. NIH Public Access, 195(2), pp. 464–76. doi: 10.4049/jimmunol.1402735.

Kissenpfennig, A. *et al.* (2005) 'Disruption of the langerin/CD207 gene abolishes Birbeck granules without a marked loss of Langerhans cell function.', *Molecular and cellular biology*. American Society for Microbiology Journals, 25(1), pp. 88–99. doi: 10.1128/MCB.25.1.88-99.2005.

Kitashima, D. Y. *et al.* (2018) 'Langerhans Cells Prevent Autoimmunity via Expansion of Keratinocyte Antigen-Specific Regulatory T Cells', *EBioMedicine*, 27, pp. 293–303. doi: 10.1016/j.ebiom.2017.12.022.

Klechevsky, E. *et al.* (2008) 'Functional specializations of human epidermal Langerhans cells and CD14+ dermal dendritic cells.', *Immunity*. NIH Public Access, 29(3), pp. 497–510. doi: 10.1016/j.immuni.2008.07.013.

Koch, S. *et al.* (2017) 'AhR mediates an anti-inflammatory feedback mechanism in human Langerhans cells involving FcεRI and IDO', *Allergy*, 72(11), pp. 1686–1693. doi: 10.1111/all.13170.

Kraft, S. *et al.* (2002) 'Aggregation of the high-affinity IgE receptor FcεRI on human monocytes and dendritic cells induces NF-κB activation', *Journal of Investigative Dermatology*. Elsevier, 118(5), pp. 830–837. doi: 10.1046/j.1523-1747.2002.01757.x.

Kryczanowsky, F. *et al.* (2016) 'IL-10–Modulated Human Dendritic Cells for Clinical Use: Identification of a Stable and Migratory Subset with Improved Tolerogenic Activity', *The Journal of Immunology*. The American Association of Immunologists, 197(9), pp. 3607–3617. doi: 10.4049/jimmunol.1501769.

Kubo, A. *et al.* (2009) 'External antigen uptake by Langerhans cells with reorganization of epidermal tight junction barriers', *Journal of Experimental Medicine*, 206(13), pp. 2937–2946. doi: 10.1084/jem.20091527.

Kucuksezer, U. C. *et al.* (2013) 'Mechanisms of immune tolerance to allergens in children', *Korean Journal of Pediatrics*. Korean Pediatric Society, pp. 505–513. doi: 10.3345/kjp.2013.56.12.505.

Kukurba, K. R. and Montgomery, S. B. (2015) 'RNA Sequencing and Analysis.', *Cold Spring Harbor protocols*. NIH Public Access, 2015(11), pp. 951–69. doi: 10.1101/pdb.top084970.

Lacy, P. and Stow, J. L. (2011) 'Cytokine release from innate immune cells: Association with diverse membrane trafficking pathways', *Blood*. American Society of Hematology, pp. 9–18. doi: 10.1182/blood-2010-08-265892.

Lanzavecchia, A. and Sallusto, F. (2001) 'Regulation of T cell immunity by dendritic cells', *Cell*. Cell Press, pp. 263–266. doi: 10.1016/S0092-8674(01)00455-X.

Lapteva, N. *et al.* (2007) 'Enhanced Activation of Human Dendritic Cells by Inducible CD40 and Toll-like Receptor-4 Ligation', *Cancer Research*, 67(21), pp. 10528–10537. doi: 10.1158/0008-5472.CAN-07-0833.

Larregina, A. T. and Falo, L. D. (2005) 'Changing paradigms in cutaneous immunology: adapting with dendritic cells.', *The Journal of investigative dermatology*. Elsevier, 124(1), pp. 1–12. doi: 10.1111/j.1523-1747.2004.23554.x.

Lavin, Y. *et al.* (2014) 'Tissue-Resident Macrophage Enhancer Landscapes Are Shaped by the Local Microenvironment', *Cell*, 159(6), pp. 1312–1326. doi: 10.1016/j.cell.2014.11.018.

Lehtonen, A. *et al.* (2005) 'Differential Expression of IFN Regulatory Factor 4 Gene in Human Monocyte-Derived Dendritic Cells and Macrophages', *The Journal of Immunology*, 175(10).

Lemos, M. P. *et al.* (2014) 'The Inner Foreskin of Healthy Males at Risk of HIV Infection Harbors Epithelial CD4+ CCR5+ Cells and Has Features of an Inflamed Epidermal Barrier', *PLoS ONE*. Edited by K. Broliden. Public Library of Science, 9(9), p. e108954. doi: 10.1371/journal.pone.0108954.

Lenschow, D. J., Walunas, T. L. and Bluestone, J. A. (1996) *CD28/B7 SYSTEM OF T CELL COSTIMULATION*, *Annu. Rev. Immunol*. Available at: www.annualreviews.org (Accessed: 4 August 2020).

Lewis, K. L. and Reizis, B. (2012) 'Dendritic cells: arbiters of immunity and immunological tolerance.', *Cold Spring Harbor perspectives in biology*, 4(8), p. a007401. doi: 10.1101/cshperspect.a007401.

Li, Q. *et al.* (2016) 'Tolerogenic Phenotype of IFN-γ-Induced IDO+ Dendritic Cells Is Maintained via an Autocrine IDO-Kynurenine/AhR-IDO Loop.', *Journal of immunology (Baltimore, Md. : 1950)*. American Association of Immunologists, 197(3), pp. 962–70. doi: 10.4049/jimmunol.1502615.

Lin, Q. *et al.* (2015) 'Epigenetic program and transcription factor circuitry of dendritic cell development', *Nucleic Acids Research*. Oxford University Press, 43(20), p. gkv1056. doi: 10.1093/nar/gkv1056.

Liu, T. *et al.* (2017) 'NF-κB signaling in inflammation', *Signal Transduction and Targeted Therapy*. Springer Nature, 2. doi: 10.1038/sigtrans.2017.23.

Livigni, A. *et al.* (2018) 'A graphical and computational modeling platform for biological pathways', *Nature Protocols*. Nature Publishing Group, 13(4), pp. 705–722. doi: 10.1038/nprot.2017.144.

Lombardi, T., Hauser, C. and Budtz-Jorgensen, E. (1993) 'Langerhans cells: structure, function and role in oral pathological conditions', *Journal of Oral Pathology and Medicine*. John Wiley & Sons, Ltd (10.1111), 22(5), pp. 193–202. doi: 10.1111/j.1600-0714.1993.tb01056.x.

López, C. B., Yount, J. S. and Moran, T. M. (2006) 'Toll-like receptor-independent triggering of dendritic cell maturation by viruses.', *Journal of virology*. American Society for Microbiology (ASM), 80(7), pp. 3128–34. doi: 10.1128/JVI.80.7.3128-3134.2006.

Loriaux, P. M. and Hoffmann, A. (2012) 'A framework for modeling the relationship between cellular steady-state and stimulus-responsiveness.', *Methods in cell biology*. NIH Public Access, 110, pp. 81–109. doi: 10.1016/B978-0-12-388403-9.00004-7.

Luecken, M. D. and Theis, F. J. (2019) 'Current best practices in single-cell RNA-seq analysis: a tutorial', *Molecular Systems Biology*. EMBO, 15(6). doi: 10.15252/msb.20188746.

Vander Lugt, B. *et al.* (2014) 'Transcriptional programming of dendritic cells for enhanced MHC class II antigen presentation', *Nature Immunology*. Nature Publishing Group, 15(2), pp. 161–167. doi: 10.1038/ni.2795.

Vander Lugt, B., Riddell, J., Khan, Aly A, *et al.* (2017) 'Transcriptional determinants of tolerogenic and immunogenic states during dendritic cell maturation.', *The Journal of cell biology*. Rockefeller University Press, 216(3), pp. 779–792. doi: 10.1083/jcb.201512012.

Vander Lugt, B., Riddell, J., Khan, Aly A., *et al.* (2017) 'Transcriptional determinants of tolerogenic and immunogenic states during dendritic cell maturation', *The Journal of cell biology*, 216(3), pp. 779–792. doi: 10.1083/jcb.201512012.

Lun, A. T. L. *et al.* (2019) 'EmptyDrops: Distinguishing cells from empty droplets in droplet-based single-cell RNA sequencing data', *Genome Biology*. BioMed Central Ltd., 20(1), p. 63. doi:

10.1186/s13059-019-1662-y.

Lun, A. T. L., Bach, K. and Marioni, J. C. (2016) 'Pooling across cells to normalize single-cell RNA sequencing data with many zero counts', *Genome Biology*. BioMed Central Ltd., 17(1), p. 75. doi: 10.1186/s13059-016-0947-7.

Lutz, M. B., Döhler, A. and Azukizawa, H. (2010) 'Revisiting the tolerogenicity of epidermal Langerhans cells', *Immunology and Cell Biology*. Nature Publishing Group, 88(4), pp. 381–386. doi: 10.1038/icb.2010.17.

Lutz, M. B. and Schuler, G. (2002) 'Immature, semi-mature and fully mature dendritic cells: Which signals induce tolerance or immunity?', *Trends in Immunology*. Trends Immunol, pp. 445–449. doi: 10.1016/S1471-4906(02)02281-0.

Mabbott, N. A. *et al.* (2013) 'An expression atlas of human primary cells: Inference of gene function from coexpression networks', *BMC Genomics*. BioMed Central, 14(1), p. 632. doi: 10.1186/1471-2164-14-632.

Mackay, I. R. (2000) 'Science, medicine, and the future: Tolerance and autoimmunity.', *BMJ (Clinical research ed.)*. British Medical Journal Publishing Group, 321(7253), pp. 93–6. doi: 10.1136/BMJ.321.7253.93.

Macneil, L. T. and Walhout, A. J. M. (2011) 'Gene regulatory networks and the role of robustness and stochasticity in the control of gene expression.', *Genome research*. Cold Spring Harbor Laboratory Press, 21(5), pp. 645–57. doi: 10.1101/gr.097378.109.

Macosko, E. Z. *et al.* (2015) 'Highly Parallel Genome-wide Expression Profiling of Individual Cells Using Nanoliter Droplets', *Cell*. AAAI Press, Menlo Park, Calif, 161(5), pp. 1202–1214. doi: 10.1016/j.cell.2015.05.002.

Madigan, M. *et al.* (2012) *Brocks Biology of Microorganisms*. 13th Editi. Pearson.

Mahnke, K. *et al.* (2002) 'Immature, but not inactive: the tolerogenic function of immature dendritic cells', *Immunology and Cell Biology*. John Wiley & Sons, Ltd, 80(5), pp. 477–483. doi: 10.1046/j.1440-1711.2002.01115.x.

Malinarich, F. *et al.* (2015) 'High Mitochondrial Respiration and Glycolytic Capacity Represent a Metabolic Phenotype of Human Tolerogenic Dendritic Cells', *The Journal of Immunology*, 194(11), pp. 5174–5186. doi: 10.4049/jimmunol.1303316.

Manches, O. *et al.* (2012) 'Activation of the noncanonical NF-κB pathway by HIV controls a dendritic cell immunoregulatory phenotype.', *Proceedings of the National Academy of Sciences of the United States of America*. National Academy of Sciences, 109(35), pp. 14122–7. doi: 10.1073/pnas.1204032109.

Marín, E., Cuturi, M. C. and Moreau, A. (2018) 'Tolerogenic Dendritic Cells in Solid Organ Transplantation: Where Do We Stand?', *Frontiers in Immunology*. Frontiers, 9, p. 274. doi: 10.3389/fimmu.2018.00274.

Martínez Allo, V. C. *et al.* (2020) 'Suppression of age-related salivary gland autoimmunity by glycosylation-dependent galectin-1driven immune inhibitory circuits', *Proceedings of the National Academy of Sciences of the United States of America*. National Academy of Sciences, 117(12), pp. 6630–6639. doi: 10.1073/pnas.1922778117.

Matteoli, G. *et al.* (2010) 'Gut CD103+ dendritic cells express indoleamine 2,3-dioxygenase which

influences T regulatory/T effector cell balance and oral tolerance induction', *Gut*. Gut, 59(5), pp. 595–604. doi: 10.1136/gut.2009.185108.

Mbongue, J. *et al.* (2014) 'The role of dendritic cells in tissue-specific autoimmunity', *Journal of Immunology Research*. Hindawi Publishing Corporation. doi: 10.1155/2014/857143.

Mc Dermott, R. *et al.* (2002) 'Birbeck granules are subdomains of endosomal recycling compartment in human epidermal Langerhans cells, which form where Langerin accumulates.', *Molecular biology of the cell*. American Society for Cell Biology, 13(1), pp. 317–35. doi: 10.1091/mbc.01-06-0300.

Di Meglio, P., Perera, G. K. and Nestle, F. O. (2011) 'The multitasking organ: recent insights into skin immune function.', *Immunity*. Elsevier, 35(6), pp. 857–69. doi: 10.1016/j.immuni.2011.12.003.

Mellman, I. and Steinman, R. M. (2001) 'Dendritic cells: Specialized and regulated antigen processing machines', *Cell*. Cell Press, pp. 255–258. doi: 10.1016/S0092-8674(01)00449-4.

Mellor, A. L. *et al.* (2004) 'Specific subsets of murine dendritic cells acquire potent T cell regulatory functions following CTLA4-mediated induction of indoleamine 2,3 dioxygenase', *International Immunology*, 16(10), pp. 1391–1401. doi: 10.1093/intimm/dxh140.

Mellor, A. L., Lemos, H. and Huang, L. (2017) 'Indoleamine 2,3-Dioxygenase and Tolerance: Where Are We Now?', *Frontiers in Immunology*. Frontiers, 8, p. 1360. doi: 10.3389/fimmu.2017.01360.

Mellor, A. L. and Munn, D. H. (2004) 'IDO expression by dendritic cells: Tolerance and tryptophan catabolism', *Nature Reviews Immunology*, pp. 762–774. doi: 10.1038/nri1457.

Merad, M. *et al.* (2013) 'The dendritic cell lineage: ontogeny and function of dendritic cells and their subsets in the steady state and the inflamed setting.', *Annual review of immunology*. NIH Public Access, 31, pp. 563–604. doi: 10.1146/annurev-immunol-020711-074950.

Mestas, J. and Hughes, C. C. W. (2004) 'Of Mice and Not Men: Differences between Mouse and Human Immunology', *The Journal of Immunology*. The American Association of Immunologists, 172(5), pp. 2731–2738. doi: 10.4049/jimmunol.172.5.2731.

Mohammed, J. *et al.* (2016) 'Stromal cells control the epithelial residence of DCs and memory T cells by regulated activation of TGF-β.', *Nature immunology*. NIH Public Access, 17(4), pp. 414–21. doi: 10.1038/ni.3396.

Mü Nz, C. *et al.* (2005) 'Mature myeloid dendritic cell subsets have distinct roles for activation and viability of circulating human natural killer cells'. doi: 10.1182/blood-2004-06-2492.

Munn, D. H. *et al.* (1998) 'Prevention of allogeneic fetal rejection by tryptophan catabolism', *Science*. American Association for the Advancement of Science, 281(5380), pp. 1191–1193. doi: 10.1126/science.281.5380.1191.

Munn, D. H. *et al.* (2002) 'Potential regulatory function of human dendritic cells expressing indoleamine 2,3-dioxygenase', *Science*. American Association for the Advancement of Science, 297(5588), pp. 1867–1870. doi: 10.1126/science.1073514.

Munn, D. H. and Mellor, A. L. (2013) 'Indoleamine 2,3 dioxygenase and metabolic control of immune responses.', *Trends in immunology*. NIH Public Access, 34(3), pp. 137–43. doi: 10.1016/j.it.2012.10.001.

Mutyambizi, K., Berger, C. L. and Edelson, R. L. (2009) 'The balance between immunity and tolerance: the role of Langerhans cells.', *Cellular and molecular life sciences : CMLS*. NIH Public Access, 66(5), pp. 831–40. doi: 10.1007/s00018-008-8470-y.

Nagl, M. *et al.* (2002) 'Phagocytosis and killing of bacteria by professional phagocytes and dendritic cells.', *Clinical and diagnostic laboratory immunology*. American Society for Microbiology (ASM), 9(6), pp. 1165–8. doi: 10.1128/CDLI.9.6.1165-1168.2002.

Nair, P. M. *et al.* (2018) 'RelB-Deficient Dendritic Cells Promote the Development of Spontaneous Allergic Airway Inflammation', *American Journal of Respiratory Cell and Molecular Biology*. American Thoracic Society, 58(3), pp. 352–365. doi: 10.1165/rcmb.2017-0242OC.

Nestle, F. O. *et al.* (1993) 'Characterization of dermal dendritic cells obtained from normal human skin reveals phenotypic and functionally distinctive subsets.', *The Journal of Immunology*, 151(11).

Nestle, F. O. *et al.* (2009) 'Skin immune sentinels in health and disease.', *Nature reviews. Immunology*. NIH Public Access, 9(10), pp. 679–91. doi: 10.1038/nri2622.

Nickoloff, B. J. *et al.* (1995) 'Direct and Indirect Control of T-Cell Activation by Keratinocytes', *Journal of Investigative Dermatology*. Elsevier, 105(1), pp. S25–S29. doi: 10.1038/JID.1995.6.

Nikolic, T. and Roep, B. O. (2013) 'Regulatory Multitasking of Tolerogenic Dendritic Cells – Lessons Taken from Vitamin D3-Treated Tolerogenic Dendritic Cells', *Frontiers in Immunology*, 4, p. 113. doi: 10.3389/fimmu.2013.00113.

Nikolich-Žugich, J., Slifka, M. K. and Messaoudi, I. (2004) 'The many important facets of T-cell repertoire diversity', *Nature Reviews Immunology*. Nature Publishing Group, pp. 123–132. doi: 10.1038/nri1292.

O'Hara, L. *et al.* (2016) 'Modelling the Structure and Dynamics of Biological Pathways', *PLOS Biology*. Public Library of Science, 14(8), p. e1002530. doi: 10.1371/journal.pbio.1002530.

O'Sullivan, B. J. *et al.* (2011) 'Immunotherapy with Costimulatory Dendritic Cells To Control Autoimmune Inflammation', *The Journal of Immunology*. The American Association of Immunologists, 187(8), pp. 4018–4030. doi: 10.4049/jimmunol.1101727.

Obregon, C. *et al.* (2017) 'Update on Dendritic Cell-Induced Immunological and Clinical Tolerance', *Frontiers in Immunology*. Frontiers, 8, p. 1514. doi: 10.3389/fimmu.2017.01514.

Oeckinghaus, A. and Ghosh, S. (2009) 'The NF-kappaB family of transcription factors and its regulation.', *Cold Spring Harbor perspectives in biology*, 1(4). doi: 10.1101/cshperspect.a000034.

Oh, J. and Shin, J.-S. (2015) 'The Role of Dendritic Cells in Central Tolerance.', *Immune network*. The Korean Association of Immunologists, 15(3), pp. 111–20. doi: 10.4110/in.2015.15.3.111.

Ohkura, N., Kitagawa, Y. and Sakaguchi, S. (2013) 'Development and maintenance of regulatory T cells.', *Immunity*. Elsevier, 38(3), pp. 414–23. doi: 10.1016/j.immuni.2013.03.002.

Oliveros, J. C. (2007) *VENNY. An interactive tool for comparing lists with Venn Diagrams. http://bioinfogp.cnb.csic.es/tools/venny/index.html*, *Bioinfogp.Cnb.Csic.Es/Tools/Venny/Index.Html*. Available at: http://bioinfogp.cnnb.csic.es/tools/venny/index.html (Accessed: 1 July 2020).

Olsson, A. *et al.* (2016) 'Single-cell analysis of mixed-lineage states leading to a binary cell fate choice', *Nature*. Nature Publishing Group, 537(7622), pp. 698–702. doi: 10.1038/nature19348.

Omine, Y. *et al.* (2015) 'Regional differences in the density of langerhans cells, CD8-positive T lymphocytes and CD68-positive macrophages: A preliminary study using elderly donated cadavers', *Anatomy and Cell Biology*. Korean Association of Anatomists, 48(3), pp. 177–187. doi: 10.5115/acb.2015.48.3.177.

Paust, S. and Cantor, H. (2005) 'Regulatory T cells and autoimmune disease', *Immunological Reviews*. John Wiley & Sons, Ltd, pp. 195–207. doi: 10.1111/j.0105-2896.2005.00247.x.

Pẽa-Cruz, V. *et al.* (2010) 'PD-1 on immature and PD-1 ligands on migratory human langerhans cells regulate antigen-presenting cell activity', *Journal of Investigative Dermatology*. NIH Public Access, 130(9), pp. 2222–2230. doi: 10.1038/jid.2010.127.

Peiser, M. *et al.* (2008) 'Human Langerhans cells selectively activated via Toll-like receptor 2 agonists acquire migratory and CD4 $^{+}$ T cell stimulatory capacity', *Journal of Leukocyte Biology*. Wiley, 83(5), pp. 1118–1127. doi: 10.1189/jlb.0807567.

Pennock, N. D. *et al.* (2013) 'T cell responses: Naïve to memory and everything in between', *American Journal of Physiology - Advances in Physiology Education*. American Physiological Society, 37(4), pp. 273–283. doi: 10.1152/advan.00066.2013.

Perez, N. *et al.* (2008) ' Preferential Costimulation by CD80 Results in IL-10-Dependent TGF-β1 + -Adaptive Regulatory T Cell Generation ', *The Journal of Immunology*. The American Association of Immunologists, 180(10), pp. 6566–6576. doi: 10.4049/jimmunol.180.10.6566.

Peterson, V. M. *et al.* (2017) 'Multiplexed quantification of proteins and transcripts in single cells', *Nature Biotechnology*. Nature Publishing Group, 35(10), pp. 936–939. doi: 10.1038/nbt.3973.

Phillips, B. E. *et al.* (2017) 'Clinical Tolerogenic Dendritic Cells: Exploring Therapeutic Impact on Human Autoimmune Disease.', *Frontiers in immunology*. Frontiers Media SA, 8, p. 1279. doi: 10.3389/fimmu.2017.01279.

Picelli, S. *et al.* (2014) 'Full-length RNA-seq from single cells using Smart-seq2', *Nature Protocols*. Nature Publishing Group, 9(1), pp. 171–181. doi: 10.1038/nprot.2014.006.

Polak, M. E. *et al.* (2012) 'CD70-CD27 interaction augments CD8+ T-cell activation by human epidermal Langerhans cells.', *The Journal of investigative dermatology*. Elsevier, 132(6), pp. 1636–44. doi: 10.1038/jid.2012.26.

Polak, M. E. *et al.* (2014) 'Distinct Molecular Signature of Human Skin Langerhans Cells Denotes Critical Differences in Cutaneous Dendritic Cell Immune Regulation', *Journal of Investigative Dermatology*, 134(3), pp. 695–703. doi: 10.1038/jid.2013.375.

Polak, M. E. *et al.* (2017) 'Petri Net computational modelling of Langerhans cell Interferon Regulatory Factor Network predicts their role in T cell activation', *Scientific Reports*, 7(1), p. 668. doi: 10.1038/s41598-017-00651-5.

Price, J. G. *et al.* (2015) 'CDKN1A regulates Langerhans cell survival and promotes treg cell generation upon exposure to ionizing irradiation', *Nature Immunology*. Nature Publishing Group, 16(10), pp. 1060–1068. doi: 10.1038/ni.3270.

Price, L. B. *et al.* (2010) 'The effects of circumcision on the penis microbiome', *PLoS ONE*. Public Library of Science, 5(1). doi: 10.1371/journal.pone.0008422.

Prodger, J. L. *et al.* (2012) 'Foreskin T-cell subsets differ substantially from blood with respect to HIV co-receptor expression, inflammatory profile, and memory status', *Mucosal Immunology*. NIH

Public Access, 5(2), pp. 121–128. doi: 10.1038/mi.2011.56.

Pulendran, B. *et al.* (1997) 'Developmental pathways of dendritic cells in vivo: distinct function, phenotype, and localization of dendritic cell subsets in FLT3 ligand-treated mice.', *Journal of immunology (Baltimore, Md. : 1950)*, 159(5), pp. 2222–31. Available at: http://www.ncbi.nlm.nih.gov/pubmed/9278310 (Accessed: 10 November 2018).

Qin, Q. *et al.* (2009) 'Langerhans' cell density and degree of keratinization in foreskins of Chinese preschool boys and adults', *International Urology and Nephrology*, 41(4), pp. 747–753. doi: 10.1007/s11255-008-9521-x.

Reis e Sousa, C., Stahl, P. D. and Austyn, J. M. (1993) *Phagocytosis of antigens by langerhans cells in vitro*, *Journal of Experimental Medicine*. doi: 10.1084/jem.178.2.509.

Rescigno, M. *et al.* (1998) 'Dendritic cell survival and maturation are regulated by different signaling pathways', *Journal of Experimental Medicine*. The Rockefeller University Press, 188(11), pp. 2175–2180. doi: 10.1084/jem.188.11.2175.

Ribeiro, C. M. S. *et al.* (2016) 'Receptor usage dictates HIV-1 restriction by human TRIM5α in dendritic cell subsets', *Nature*. Nature Publishing Group, 540(7633), pp. 448–452. doi: 10.1038/nature20567.

Rinn, J. L. *et al.* (2006) 'Anatomic Demarcation by Positional Variation in Fibroblast Gene Expression Programs', *PLoS Genetics*. Edited by V. van Heyningen. Public Library of Science, 2(7), p. e119. doi: 10.1371/journal.pgen.0020119.

Riquelme, S. A. *et al.* (2016) 'Modulation of antigen processing by haem-oxygenase 1. Implications on inflammation and tolerance', *Immunology*. Blackwell Publishing Ltd, 149(1), pp. 1–12. doi: 10.1111/imm.12605.

Ritchie, M. *et al.* (2015) 'limma powers di erential expression analyses for RNA-sequencing and microarray studies.', *Nucleic Acids Research*, 43(7), p. e47.

Ritter, U. *et al.* (2004) 'CD8α- and Langerin-negative dendritic cells, but not Langerhans cells, act as principal antigen-presenting cells in leishmaniasis', *European Journal of Immunology*, 34(6), pp. 1542–1550. doi: 10.1002/eji.200324586.

Romani, N. *et al.* (2003) 'Langerhans cells - Dendritic cells of the epidermis', *APMIS*. John Wiley & Sons, Ltd, pp. 725–740. doi: 10.1034/j.1600-0463.2003.11107805.x.

Romani, N., Clausen, B. E. and Stoitzner, P. (2010) 'Langerhans cells and more: langerin-expressing dendritic cell subsets in the skin'. doi: 10.1111/j.0105-2896.2009.00886.x.

Rowden, G., Lewis, M. G. and Sullivan, A. K. (1977) 'Ia antigen expression on human epidermal Langerhans cells', *Nature*. Nature Publishing Group, 268(5617), pp. 247–248. doi: 10.1038/268247a0.

Ruths, D. *et al.* (2008) 'The Signaling Petri Net-Based Simulator: A Non-Parametric Strategy for Characterizing the Dynamics of Cell-Specific Signaling Networks', *PLoS Computational Biology*. Edited by S. Miyano. Public Library of Science, 4(2), p. e1000005. doi: 10.1371/journal.pcbi.1000005.

Saikia, M. *et al.* (2019) 'Simultaneous multiplexed amplicon sequencing and transcriptome profiling in single cells', *Nature Methods*. Nature Publishing Group, 16(1), pp. 59–62. doi: 10.1038/s41592-018-0259-9.

Santegoets, S. J. A. M. *et al.* (2008) 'Transcriptional profiling of human skin-resident Langerhans cells and CD1a $^{+}$ dermal dendritic cells: differential activation states suggest distinct functions', *Journal of Leukocyte Biology*, 84(1), pp. 143–151. doi: 10.1189/jlb.1107750.

Saravia, J. *et al.* (2020) 'Homeostasis and transitional activation of regulatory T cells require c-Myc', *Science Advances*. American Association for the Advancement of Science, 6(1), p. eaaw6443. doi: 10.1126/sciadv.aaw6443.

Savina, A. and Amigorena, S. (2007) 'Phagocytosis and antigen presentation in dendritic cells', *Immunological Reviews*. Blackwell Publishing Ltd, 219(1), pp. 143–156. doi: 10.1111/j.1600-065X.2007.00552.x.

Schietinger, A. and Greenberg, P. D. (2014) 'Tolerance and exhaustion: Defining mechanisms of T cell dysfunction', *Trends in Immunology*. NIH Public Access, pp. 51–60. doi: 10.1016/j.it.2013.10.001.

Schlee, M. *et al.* (2007) 'c-MYC activation impairs the NF-κB and the interferon response: Implications for the pathogenesis of Burkitt's lymphoma', *International Journal of Cancer*. John Wiley & Sons, Ltd, 120(7), pp. 1387–1395. doi: 10.1002/ijc.22372.

Schlitzer, A. *et al.* (2013) 'IRF4 Transcription Factor-Dependent CD11b+ Dendritic Cells in Human and Mouse Control Mucosal IL-17 Cytokine Responses', *Immunity*. Elsevier, 38(5), pp. 970–983. doi: 10.1016/j.immuni.2013.04.011.

Schmidt, S. V., Nino-Castro, A. C. and Schultze, J. L. (2012) 'Regulatory dendritic cells: there is more than just immune activation', *Frontiers in Immunology*. Frontiers, 3, p. 274. doi: 10.3389/fimmu.2012.00274.

Schmitz, F. *et al.* (2007) 'Interferon-regulatory-factor 1 controls Toll-like receptor 9-mediated IFN-β production in myeloid dendritic cells', *European Journal of Immunology*. John Wiley & Sons, Ltd, 37(2), pp. 315–327. doi: 10.1002/eji.200636767.

Schöppl, A. *et al.* (2015) 'Langerhans cell precursors acquire RANK/CD265 in prenatal human skin.', *Acta histochemica*. Elsevier, 117(4–5), pp. 425–30. doi: 10.1016/j.acthis.2015.01.003.

Scott, C. L., Aumeunier, A. M. and Mowat, A. M. I. (2011) 'Intestinal CD103 + dendritic cells: Master regulators of tolerance?', *Trends in Immunology*. Elsevier Current Trends, pp. 412–419. doi: 10.1016/j.it.2011.06.003.

Sen, S. *et al.* (2019) 'Gene Regulatory Strategies that Decode the Duration of NFκB Dynamics Contribute to LPS- versus TNF-Specific Gene Expression', *Cell Systems*. doi: 10.1016/j.cels.2019.12.004.

Seneschal, J. *et al.* (2012) 'Human epidermal Langerhans cells maintain immune homeostasis in skin by activating skin resident regulatory T cells.', *Immunity*. NIH Public Access, 36(5), pp. 873–84. doi: 10.1016/j.immuni.2012.03.018.

Seré, K. *et al.* (2012) 'Two Distinct Types of Langerhans Cells Populate the Skin during Steady State and Inflammation', *Immunity*, 37(5), pp. 905–916. doi: 10.1016/j.immuni.2012.07.019.

Shaffer, A. L. *et al.* (2009) 'IRF4: Immunity. Malignancy! Therapy?', *Clinical Cancer Research*, 15(9), pp. 2954–2961. doi: 10.1158/1078-0432.CCR-08-1845.

Shapiro, E., Biezuner, T. and Linnarsson, S. (2013) 'Single-cell sequencing-based technologies will revolutionize whole-organism science', *Nature Reviews Genetics*. Nature Publishing Group, pp.

618–630. doi: 10.1038/nrg3542.

Shen, H. *et al.* (2010) 'Gender-dependent Expression of Murine Irf5 Gene: Implications for Sex Bias in Autoimmunity', *Journal of Molecular Cell Biology*. Oxford University Press, 2(5), p. 284. doi: 10.1093/jmcb/mjq023.

Shklovskaya, E. *et al.* (2011) 'Langerhans cells are precommitted to immune tolerance induction.', *Proceedings of the National Academy of Sciences of the United States of America*. National Academy of Sciences, 108(44), pp. 18049–54. doi: 10.1073/pnas.1110076108.

Shum, E. Y. *et al.* (2019) 'Quantitation of mRNA Transcripts and Proteins Using the BD Rhapsody™ Single-Cell Analysis System', in *Advances in Experimental Medicine and Biology*. Springer New York LLC, pp. 63–79. doi: 10.1007/978-981-13-6037-4_5.

Simon, J. C. *et al.* (1991) 'Ultraviolet B radiation converts Langerhans cells from immunogenic to tolerogenic antigen-presenting cells. Induction of specific clonal anergy in CD4+ T helper 1 cells.', *Journal of immunology (Baltimore, Md. : 1950)*, 146(2), pp. 485–91. Available at: http://www.ncbi.nlm.nih.gov/pubmed/1670944 (Accessed: 14 November 2018).

Singh, H., Khan, A. A. and Dinner, A. R. (2014) 'Gene regulatory networks in the immune system', *Trends in Immunology*. Elsevier Current Trends, 35(5), pp. 211–218. doi: 10.1016/J.IT.2014.03.006.

Sirvent, S. *et al.* (2020) 'Genomic programming of IRF4-expressing human Langerhans cells', *Nature Communications*. Nature Research, 11(1), pp. 1–12. doi: 10.1038/s41467-019-14125-x.

Smith-Garvin, J. E., Koretzky, G. A. and Jordan, M. S. (2009) 'T Cell Activation', *Annual Review of Immunology*, 27(1), pp. 591–619. doi: 10.1146/annurev.immunol.021908.132706.

Spitz, F. and Furlong, E. E. M. (2012) 'Transcription factors: From enhancer binding to developmental control', *Nature Reviews Genetics*. Nature Publishing Group, pp. 613–626. doi: 10.1038/nrg3207.

Steimle, A. and Frick, J.-S. (2016) 'Molecular Mechanisms of Induction of Tolerant and Tolerogenic Intestinal Dendritic Cells in Mice', *Journal of Immunology Research*. Hindawi Limited, 2016. doi: 10.1155/2016/1958650.

Steinman, R. M. (1991) 'The Dendritic Cell System and its Role in Immunogenicity', *Annual Review of Immunology*. Annual Reviews, 9(1), pp. 271–296. doi: 10.1146/annurev.iy.09.040191.001415.

Steinman, R. M. *et al.* (2000) *The Induction of Tolerance by Dendritic Cells That Have Captured Apoptotic Cells*, *J. Exp. Med*. Available at: http://www.jem.org (Accessed: 14 November 2018).

Steinman, R. M. *et al.* (2003) 'Dendritic cell function in Vivo during the steady state: A role in peripheral tolerance', in *Annals of the New York Academy of Sciences*. New York Academy of Sciences, pp. 15–25. doi: 10.1111/j.1749-6632.2003.tb06029.x.

Steinman, R. M. (2007) 'Dendritic cells: Understanding immunogenicity', *European Journal of Immunology*. John Wiley & Sons, Ltd, 37(SUPPL. 1), pp. S53–S60. doi: 10.1002/eji.200737400.

Steinman, R. M., Hawiger, D. and Nussenzweig, M. C. (2003) 'T OLEROGENIC D ENDRITIC C ELLS', *Annual Review of Immunology*. Annual Reviews 4139 El Camino Way, P.O. Box 10139, Palo Alto, CA 94303-0139, USA , 21(1), pp. 685–711. doi: 10.1146/annurev.immunol.21.120601.141040.

Stine, Z. E. *et al.* (2015) 'MYC, metabolism, and cancer', *Cancer Discovery*. American Association for Cancer Research Inc., pp. 1024–1039. doi: 10.1158/2159-8290.CD-15-0507.

Stockwin, L. H. *et al.* (2000) 'Dendritic cells: immunological sentinels with a central role in health and disease.', *Immunology and cell biology*, 78(2), pp. 91–102. doi: 10.1046/j.1440-1711.2000.00888.x.

Stoitzner, P. *et al.* (1999) 'Migration of langerhans cells and dermal dendritic cells in skin organ cultures: augmentation by TNF-alpha and IL-1beta.', *Journal of leukocyte biology*, 66(3), pp. 462–70. Available at: http://www.ncbi.nlm.nih.gov/pubmed/10496317 (Accessed: 17 January 2019).

Strandt, H. *et al.* (2017) 'Neoantigen Expression in Steady-State Langerhans Cells Induces CTL Tolerance.', *Journal of immunology (Baltimore, Md. : 1950)*. The American Association of Immunologists, Inc., 199(5), pp. 1626–1634. doi: 10.4049/jimmunol.1602098.

Stumpf, P. S. *et al.* (2017) 'Stem Cell Differentiation as a Non-Markov Stochastic Process', *Cell Systems*, 5, pp. 268-282.e7. doi: 10.1016/j.cels.2017.08.009.

Sugita, K. *et al.* (2007) 'Innate immunity mediated by epidermal keratinocytes promotes acquired immunity involving Langerhans cells and T cells in the skin', *Clinical and Experimental Immunology*. Wiley-Blackwell, 147(1), pp. 176–183. doi: 10.1111/j.1365-2249.2006.03258.x.

Sun, S.-C. (2017) 'The non-canonical NF-κB pathway in immunity and inflammation.', *Nature reviews. Immunology*. NIH Public Access, 17(9), pp. 545–558. doi: 10.1038/nri.2017.52.

Sundblad, V. *et al.* (2017) 'Galectin-1: A Jack-of-All-Trades in the Resolution of Acute and Chronic Inflammation.', *Journal of immunology (Baltimore, Md. : 1950)*. American Association of Immunologists, 199(11), pp. 3721–3730. doi: 10.4049/jimmunol.1701172.

Széles, L. *et al.* (2009) ',25-Dihydroxyvitamin D 3 Is an Autonomous Regulator of the Transcriptional Changes Leading to a Tolerogenic Dendritic Cell Phenotype 1,2', *The Journal of Immunology*, 182, pp. 2074–2083. doi: 10.4049/jimmunol.0803345.

Széles, L. *et al.* (2010) 'Research Resource: Transcriptome Profiling of Genes Regulated by RXR and Its Permissive and Nonpermissive Partners in Differentiating Monocyte-Derived Dendritic Cells', *Molecular Endocrinology*, 24(11), pp. 2218–2231. doi: 10.1210/me.2010-0215.

Tagliani, E. and Erlebacher, A. (2011) 'Dendritic cell function at the maternal–fetal interface', *Expert Review of Clinical Immunology*, 7(5), pp. 593–602. doi: 10.1586/eci.11.52.

Takeuchi, O. and Akira, S. (2010) 'Pattern recognition receptors and inflammation.', *Cell*. Elsevier, 140(6), pp. 805–20. doi: 10.1016/j.cell.2010.01.022.

Tas, S. W. *et al.* (2007) 'Noncanonical NF-κB signaling in dendritic cells is required for indoleamine 2,3-dioxygenase (IDO) induction and immune regulation', *Blood*, 110(5), pp. 1540–1549. doi: 10.1182/blood-2006-11-056010.

Theocharidis, A. *et al.* (2009) 'Network visualization and analysis of gene expression data using BioLayout Express3D', *Nature Protocols*. Nature Publishing Group, 4(10), pp. 1535–1550. doi: 10.1038/nprot.2009.177.

Théry, C. and Amigorena, S. (2001) 'The cell biology of antigen presentation in dendritic cells', *Current Opinion in Immunology*. Elsevier Current Trends, 13(1), pp. 45–51. doi: 10.1016/S0952-7915(00)00180-1.

Torri, A. *et al.* (2010) 'Gene Expression Profiles Identify Inflammatory Signatures in Dendritic Cells', *PLoS ONE*. Edited by P. T. Bozza. Public Library of Science, 5(2), p. e9404. doi: 10.1371/journal.pone.0009404.

Toulon, A. *et al.* (2009) 'A role for human skin-resident T cells in wound healing', *Journal of Experimental Medicine*. The Rockefeller University Press, 206(4), pp. 743–750. doi: 10.1084/jem.20081787.

Traag, V. A., Waltman, L. and van Eck, N. J. (2019) 'From Louvain to Leiden: guaranteeing well-connected communities', *Scientific Reports*. Nature Publishing Group, 9(1), pp. 1–12. doi: 10.1038/s41598-019-41695-z.

Turvey, S. E. and Broide, D. H. (2010) 'Innate immunity', *Journal of Allergy and Clinical Immunology*, 125(2 SUPPL. 2). doi: 10.1016/j.jaci.2009.07.016.

Valladeau, J. and Saeland, S. (2005) 'Cutaneous dendritic cells', *Seminars in Immunology*. Academic Press, 17(4), pp. 273–283. doi: 10.1016/j.smim.2005.05.009.

Vallejo, A. F. *et al.* (2019) 'Resolving cellular systems by ultra-sensitive and economical single-cell transcriptome filtering', *bioRxiv*. Cold Spring Harbor Laboratory, p. 800631. doi: 10.1101/800631.

Vendelova, E. *et al.* (2018) 'Tolerogenic transcriptional signatures of steady-state and pathogen-induced dendritic cells', *Frontiers in Immunology*. Frontiers Media S.A., p. 333. doi: 10.3389/fimmu.2018.00333.

Villani, A.-C. *et al.* (2017) 'Single-cell RNA-seq reveals new types of human blood dendritic cells, monocytes, and progenitors', *Science*, 356(6335). Available at: http://science.sciencemag.org/content/356/6335/eaah4573 (Accessed: 22 July 2017).

Wakkach, A. *et al.* (2003) 'Characterization of dendritic cells that induce tolerance and T regulatory 1 cell differentiation in vivo', *Immunity*. Cell Press, 18(5), pp. 605–617. doi: 10.1016/S1074-7613(03)00113-4.

Wang, Siwen *et al.* (2018) 'S100A8/A9 in inflammation', *Frontiers in Immunology*. Frontiers Media S.A., p. 1298. doi: 10.3389/fimmu.2018.01298.

Wculek, S. K. *et al.* (2019) 'Metabolic Control of Dendritic Cell Functions: Digesting Information', *Frontiers in immunology*. NLM (Medline), p. 775. doi: 10.3389/fimmu.2019.00775.

Weaver, C. T. *et al.* (2013) 'The Th17 Pathway and Inflammatory Diseases of the Intestines, Lungs, and Skin', *Annual Review of Pathology: Mechanisms of Disease*, 8(1), pp. 477–512. doi: 10.1146/annurev-pathol-011110-130318.

West, H. C. and Bennett, C. L. (2018) 'Redefining the Role of Langerhans Cells As Immune Regulators within the Skin', *Front. Immunol*, 8, p. 1941. doi: 10.3389/fimmu.2017.01941.

Wieczorek, M. *et al.* (2017) 'Major histocompatibility complex (MHC) class I and MHC class II proteins: Conformational plasticity in antigen presentation', *Frontiers in Immunology*. Frontiers Research Foundation, p. 1. doi: 10.3389/fimmu.2017.00292.

Williams, J. W. *et al.* (2013) 'Transcription factor IRF4 drives dendritic cells to promote Th2 differentiation', *Nature Communications*. Nat Commun, 4. doi: 10.1038/ncomms3990.

de Witte, L. *et al.* (2007) 'Langerin is a natural barrier to HIV-1 transmission by Langerhans cells', *Nature Medicine*. Nature Publishing Group, 13(3), pp. 367–371. doi: 10.1038/nm1541.

Wolf, F. A. *et al.* (2019) 'PAGA: graph abstraction reconciles clustering with trajectory inference through a topology preserving map of single cells', *Genome Biology*. BioMed Central, 20(1), pp. 1–9. doi: 10.1186/s13059-019-1663-x.

Wolf, F. A., Angerer, P. and Theis, F. J. (2018) 'SCANPY: Large-scale single-cell gene expression data analysis', *Genome Biology*. BioMed Central Ltd., 19(1), p. 15. doi: 10.1186/s13059-017-1382-0.

Wolk, K. and Sabat, R. (2006) 'Interleukin-22: A novel T- and NK-cell derived cytokine that regulates the biology of tissue cells', *Cytokine and Growth Factor Reviews*. Pergamon, pp. 367–380. doi: 10.1016/j.cytogfr.2006.09.001.

Worthington, J. J. *et al.* (2012) 'Regulation of TGFβ in the immune system: An emerging role for integrins and dendritic cells', *Immunobiology*. Urban & Fischer, 217(12), pp. 1259–1265. doi: 10.1016/J.IMBIO.2012.06.009.

Xue, J. *et al.* (2014) 'Resource Transcriptome-Based Network Analysis Reveals a Spectrum Model of Human Macrophage Activation'. doi: 10.1016/j.immuni.2014.01.006.

Yamazaki, S. *et al.* (2003) 'Direct Expansion of Functional CD25 CD4 Regulatory T Cells by Antigen-processing Dendritic Cells', *The Journal of Experimental Medicine J. Exp. Med. The*. Rockefeller University Press, 198(2), pp. 235–247. doi: 10.1084/jem.20030422.

Yasmin, N. *et al.* (2013) 'Identification of bone morphogenetic protein 7 (BMP7) as an instructive factor for human epidermal Langerhans cell differentiation', *Journal of Experimental Medicine*. The Rockefeller University Press, 210(12), pp. 2597–2610. doi: 10.1084/jem.20130275.

Yoshiki, R. *et al.* (2010) 'The Mandatory Role of IL-10–Producing and OX40 Ligand-Expressing Mature Langerhans Cells in Local UVB-Induced Immunosuppression', *The Journal of Immunology*. The American Association of Immunologists, 184(10), pp. 5670–5677. doi: 10.4049/jimmunol.0903254.

Yoshino, M. *et al.* (2006) 'Constant rate of steady-state self-antigen trafficking from skin to regional lymph nodes', *International Immunology*, 18(11), pp. 1541–1548. doi: 10.1093/intimm/dxl087.

Zhan, Y. *et al.* (2017) 'Life and death of activated T cells: How are they different from naïve T Cells?', *Frontiers in Immunology*. Frontiers Media S.A., p. 1809. doi: 10.3389/fimmu.2017.01809.

Zhang, X. *et al.* (2019) 'Comparative Analysis of Droplet-Based Ultra-High-Throughput Single-Cell RNA-Seq Systems', *Molecular Cell*. Cell Press, 73(1), pp. 130-142.e5. doi: 10.1016/j.molcel.2018.10.020.

Zheng, G. X. Y. *et al.* (2017) 'Massively parallel digital transcriptional profiling of single cells', *Nature Communications*. Nature Publishing Group, 8, p. 14049. doi: 10.1038/ncomms14049.

Zheng, Y. *et al.* (2004) 'CD86 and CD80 Differentially Modulate the Suppressive Function of Human Regulatory T Cells', *The Journal of Immunology*. The American Association of Immunologists, 172(5), pp. 2778–2784. doi: 10.4049/jimmunol.172.5.2778.

Zhou, Z. *et al.* (2011) 'HIV-1 Efficient Entry in Inner Foreskin Is Mediated by Elevated CCL5/RANTES that Recruits T Cells and Fuels Conjugate Formation with Langerhans Cells', *PLoS Pathogens*. Edited by G. Silvestri. Public Library of Science, 7(6), p. e1002100. doi: 10.1371/journal.ppat.1002100.